T.C.
REPUBLIC OF TURKEY
HACETTEPE UNIVERSITY
INSTITUTE OF HEALTH SCIENCES

ISOLATION OF POTENTIAL DRUG CANDIDATE MOLECULES FROM *RUMEX ACETOSELLA* L. AND *IN SILICO*, *IN VITRO* RESEARCHES ON THOSE MOLECULES

Dr. Pharm. Nadire ÖZENVER

Program of Pharmacognosy
DOCTOR OF PHILOSOPHY THESIS

ANKARA
2018

T.C.
REPUBLIC OF TURKEY
HACETTEPE UNIVERSITY
INSTITUTE OF HEALTH SCIENCES

ISOLATION OF POTENTIAL DRUG CANDIDATE MOLECULES FROM *RUMEX ACETOSELLA* L. AND *IN SILICO*, *IN VITRO* RESEARCHES ON THOSE MOLECULES

Dr. Pharm. Nadire ÖZENVER

Program of Pharmacognosy
DOCTOR OF PHILOSOPHY THESIS

ADVISOR OF THE THESIS
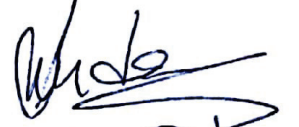**Prof. Dr. L. Ömür DEMİREZER**

ANKARA
2018

Isolation of Potential Drug Candidate Molecules from *Rumex acetosella*
L. and *In silico*, *In vitro* Researches on Those Molecules
Nadire ÖZENVER

This study has been approved and accepted as a PhD dissertation in the program of "Pharmacognosy" by the examining committee, whose members are listed below, on 19.01.2018.
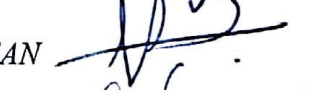
Chairman of the Committee :   *Prof. Dr. Funda N. YALÇIN*
(Hacettepe University)

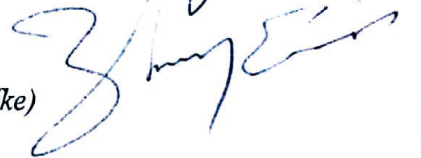**Member :**   *Prof. Dr. L. Ömür DEMİREZER*
(Hacettepe University)

Member :   *Prof. Dr. H. Gülçin SALTAN İŞCAN*
(Ankara University)

Member :   *Prof. Dr. İclal SARAÇOĞLU*
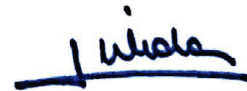*(Hacettepe University)*

Member :   *Prof. Dr. Tayfun ERSÖZ*
(European University of Lefke)

This dissertation has been approved by the committee above in conformity to the regulations and by laws of Hacettepe University Graduate Programs.

1 2 Şubat 2018

Prof. Dr. Diclehan ORHAN
Institute Director

YAYIMLAMA VE FİKRİ MÜLKİYET HAKLARI BEYANI

Enstitü tarafından onaylanan lisansüstü tezimin/raporumun tamamını veya herhangi bir kısmını, basılı (kağıt) ve elektronik formatta arşivleme ve aşağıda verilen koşullarla kullanıma açma iznini Hacettepe Üniversitesine verdiğimi bildiririm. Bu izinle Üniversiteye verilen kullanım hakları dışındaki tüm fikri mülkiyet haklarım bende kalacak, tezimin tamamının ya da bir bölümünün gelecekteki çalışmalarda (makale, kitap, lisans ve patent vb.) kullanım hakları bana ait olacaktır.

Tezin kendi orijinal çalışmam olduğunu, başkalarının haklarını ihlal etmediğimi ve tezimin tek yetkili sahibi olduğumu beyan ve taahhüt ederim. Tezimde yer alan telif hakkı bulunan ve sahiplerinden yazılı izin alınarak kullanılması zorunlu metinlerin yazılı izin alınarak kullandığımı ve istenildiğinde suretlerini Üniversiteye teslim etmeyi taahhüt ederim.

o **Tezimin/Raporumun tamamı dünya çapında erişime açılabilir ve bir kısmı veya tamamının fotokopisi alınabilir.**
(Bu seçenekle teziniz arama motorlarında indekslenebilecek, daha sonra tezinizin erişim statüsünün değiştirilmesini talep etseniz ve kütüphane bu talebinizi yerine getirse bile, teziniz arama motorlarının önbelleklerinde kalmaya devam edebilecektir)

x **Tezimin/Raporumun 14.02.2021 tarihine kadar erişime açılmasını ve fotokopi alınmasını (İç kapak, Özet, İçindekiler ve Kaynakça hariç) istemiyorum.**
(Bu sürenin sonunda uzatma için başvuruda bulunmadığım takdirde, tezimin/raporumun tamamı her yerden erişime açılabilir, kaynak gösterilmek şartıyla bir kısmı veya tamamının fotokopisi alınabilir)

o **Tezimin/Raporumun.................tarihine kadar erişime açılmasını istemiyorum ancak kaynak gösterilmek şartıyla bir kısmı veya tamamının fotokopisinin alınmasını onaylıyorum.**

o **Serbest Seçenek/Yazarın Seçimi**

14/02/2018

Nadire ÖZENVER

ETHICAL DECLARATION

In this thesis study, I declare that all the information and documents have been obtained in the base of the academic rules and all audio-visual and written information and results have been presented according to the rules of scientific ethics. I did not do any distortion in data set. In case of using other works, related studies have been fully cited in accordance with the scientific standards. I also declare that my thesis study is original except cited references. It was produced by myself in consultation with supervisor (Prof. Dr. L. Ömür DEMİREZER) and written according to the rules of thesis writing of Hacettepe University Institute of Health Sciences.

Nadire ÖZENVER

ACKNOWLEDGEMENTS

ABSTRACT

Ozenver, N., Isolation of Potential Drug Candidate Molecules From *Rumex acetosella* L. and *In Silico*, *In Vitro* Researches on Those Molecules, Hacettepe University, Institute of Health Sciences, Pharmacognosy Program, Doctor of Philosophy Thesis, Ankara, 2018. In this thesis, biological activity studies on the extracts of *R. acetosella* as well as its compounds were conducted. Some extracts of the title plant and some isolated substances were investigated against diabetes and cancer, hence *R. acetosella* is traditionally used in diabetes and cancer. Initially, antioxidant studies were performed as preliminary researches so that oxidative stress may have a role in the etiology of these diseases, which indicated alcoholic extracts as good antioxidants. Then, isolation studies were conducted to view phytochemical profile of *R. acetosella*. Isolated compounds and the main anthraquinone aglycones were tested for their cytotoxicities by resazurin reduction and protease viability marker assays. Aloe-emodin was detected as the most cytotoxic compound and the mechanisms behind its cytotoxicity were further investigated. Inducement of cell cycle distribution, apoptosis and necrosis, reactive oxygen species, mitochondrial membrane potential breakdown, DNA damage were detected. Microarray hybridization revealed deregulated genes in aloe-emodin-treated cells, validating by qPCR analysis. Motif analysis pointed out NF-κB as a transcriptional regulator. Molecular docking and reporter cell assays revealed the aloe-emodin/NF-κB relation. Antidiabetic effects of the extracts and some of their chemical constituents were investigated by means of α-amylase and α-glucosidase inhibition assays, which emphasized the ethanol extracts as antidiabetic, confirming the traditional use of *R. acetosella*. All findings pointed out that *R. acetosella* and aloe-emodin may have potentials for the development of new drugs in the treatment of both diabetes and cancer.

Key Words: *Rumex acetosella*, aloe-emodin, cancer, diabetes, phytochemistry.

ÖZET

Özenver, N., *Rumex acetosella* **L. Bitkisinden Potansiyel İlaç Adayı Moleküllerin İzolasyonu ve Moleküller Üzerinde** *İn Siliko***,** *İn Vitro* **Araştırmalar, Hacettepe Üniversitesi Sağlık Bilimleri Enstitüsü Farmakognozi Programı, Doktora Tezi, Ankara, 2018.** Bu tezde *R. acetosella* ekstreleri ve içerdiği maddeler üzerinde biyolojik aktivite çalışmaları gerçekleştirilmiştir. *R. acetosella* geleneksel olarak diyabet ve kansere karşı kullanılması nedeniyle, bazı ekstreler ve bunlardan izole edilen bazı maddelerin antidiyabetik ve sitotoksik etkileri araştırılmıştır. Oksidatif stresin bu hastalıkların etiyolojisinde rol alması nedeniyle, başlangıçta ön araştırma olarak antioksidan çalışmalar yapılmış ve etanollü ekstrelerin en iyi antioksidanlar olduğu görülmüştür. Daha sonra, bitkinin fitokimyasal profilini belirlemek için izolasyon çalışmaları yürütülmüştür. İzole edilen maddelerin ve temel antrakinon aglikonlarının sitotoksisiteleri "resazurin redüksiyon" ve "proteaz viability marker" yöntemleri ile araştırılmıştır. Aloe-emodin en yüksek sitotoksik etkiyi göstermiş ve sitotoksisitesinin altında yatan mekanizmalar da ayrıca araştırılmıştır. Hücre döngüsünün bozulmasının, apoptozun, nekrozun, reaktif oksijen türlerinin, mitokondri zar potansiyelinin bozulmasının ve DNA zararının indüklendiği görülmüştür. Mikrodizi hibridizasyonu, aloe-emodin ile muamele edilen CCRF-CEM hücrelerinin gen profillerini ortaya çıkarmış ve qPCR ile doğrulanmıştır. Motif analizi ile NF-κB transkripsiyonal bir düzenleyici olarak gösterilmiştir. Moleküler doking ve reporter hücre yöntemleri ile aloe-emodin/NF-κB ilişkisi gösterilmiştir. Ekstreler ve antrakinon aglikonlarının antidiyabetik etkileri, α-amilaz ve α-glukozidaz inhibisyonu yöntemleri ile araştırılmış; etanollü ekstrelerin bitkinin geleneksel kullanımını doğrulayacak şekilde antidiyabetik etkili olabileceği gösterilmiştir. Tüm bulgular, *R. acetosella* ve aloe-emodinin diyabet ve kanserde yeni ilaçların geliştirilmesinde potansiyel olabileceklerini göstermiştir.

Anahtar Kelimeler: *Rumex acetosella*, aloe-emodin, kanser, diyabet, fitokimya.

TABLE OF CONTENTS

LIST OF SYMBOLS AND ABBREVIATIONS

α	Alpha
ABC transporter	ATP-binding cassette transporter
ABTS	2,2'-azino-bis(3-ethylbenzothiazoline-6-sulphonic acid)
Ara	Arabinose
ATR	Attenuated Total Reflection
AV	Annexin V
β	Beta
br	Broad
CC	Column Chromatography
CCRF-CEM	Drug-sensitive leukemia cell lines
cDNA	Cyclic DNA
CD$_3$OD	Deuterated methanol
CEM/ADR5000	P-glycoprotein (P-gp) overexpressing, multidrug-resistant CEM/ADR5000 leukemia cells
CHCl$_3$	Chloroform
CH$_2$Cl$_2$	Dichloromethane
CH$_3$OH	Methanol
C$_2$H$_5$OH	Ethanol
C$_2$H$_5$COOCH$_3$	Ethyl acetate
cm	Centimeter
^{13}C NMR	^{13}C Nuclear Magnetic Resonance
COSY	Two-dimensional (2D) ^{1}H-^{1}H homonuclear correlation spectrum
d	Doublet
dd	Doublet doublet
ddd	Doublet doublet doublet
DEPT	Distortionless Enhancement by Polarization Transfer
DM	Diabetes mellitus
DMSO	Dimethyl sulfoxide
DN	Diabetic Neuropathy

DPPH	2,2-diphenyl-1-picrylhydrazyl
DTP	Developmental Therapeutics Program of the National Cancer Institute
EGFR	Epidermal Growth Factor Receptor
ESI-MS	Electrospray ionisation mass spectrometry
FBS	Fetal Bovine Serum
FDA	Food and Drug Administration
Fr	Fraction
gal	Galactose
GF-AFC	Glyxyl-phenylalanyl-aminoflourocoumarin
glu	Glucose
HMBC	Heteronuclear Multiple Bond Correlation
HMQC	Heteronuclear Multiple Quantum Correlation
^{1}H NMR	^{1}H Nuclear Magnetic Resonance
HPLC	High Performance Liquid Chromatography
H_2O	Water
H_2O_2	Hydrogen peroxide
H_2SO_4	Sulfuric acid
Hz	Hertz
IκK	Inhibitor of kappa B
IARC	International Agency for Research on Cancer
IC$_{50}$	The concentration required for 50% inhibition
IPA	Ingenuity Pathway Analysis
IR	Infrared
J	Coupling constant
KOH	Potassium hydroxide
man	Mannose
m	Multiplet
MDR	Multi-drug resistance
mg	Milligram
MHz	Megahertz
mL	Mililiter

mM	Milimolar
MMP	Mitochondrial membrane potential
MPLC	Medium Pressure Liquid Chromatography
mRNA	Messenger RNA
MS	Mass spectrometry
µM	Micromolar
µg	Microgram
µL	Microliter
NCI	National Cancer Institute
NEMO	NF-Kappa-B Essential Modulator
NF- κB	Nuclear factor-kappa B
NO	Nitric oxide
PBS	Phosphate buffered saline
PCR	Polymerase chain reaction
PDB	Protein Data Bank
PI	Propidium iodide
PMNC	The human peripheral mononuclear cells
***p*-NP**	*para*-Nitrophenol
ppm	Parts per million
PS	Phosphatidylserine
p50	Nuclear Factor Kappa B Subunit 1
p65	NF-Kappa-B Transcription Factor P65
rham	Rhamnose
ROS	Reactive oxygen species
RT-PCR	Real time polymerase chain reaction
rut	Rutinose
s	Singlet
SARs	Structure-Activity Relationships
SEAP	Secreted Embryonic Alkaline Phosphatase
SPH	Sephadex column chromatography
SK	Silica gel column chromatography
t	Triplet

TEAC	Trolox Equivalent Antioxidant Capacity
TLC	Thin Layer Chromatography
TMS	Tetramethylsilane
TÜBİTAK	The Scientific and Technological Research Council of Turkey
UV	Ultra violet
ν	Wave number (cm^{-1})
VLC	Vacuum Liquid Chromatography
WHO	World and Health Organization

LIST OF FIGURES

LIST OF TABLES

1. INTRODUCTION

Nature is an unique source of model compounds for the development of new drugs (1).

Plants constitute a significant part of natural resources utilizing in traditional medicine as well as obtaining pure drug molecules and their semi-synthetic derivatives.

Oxidative stress, caused by excessive ROS (reactive oxygen species) or RNS (reactive nitrogen species) accumulation in the body, has a pivotal role in the development of such diseases like cancer and diabetes. The human body has diverse rules to neutralize oxidative stress to prevent damages or diseases caused by ROS or RNS, which are naturally produced or outwardly supplied antioxidants and known as "free radical scavengers"(2-5).

Rumex acetosella L. is a member of *Rumex* genus widely distributed over the world from Polygonaceae family, which has a wide scale of usage in traditional medicine worldwide. Leaves of *R. acetosella* are consumed as food (6-10) and used as analgesic and diuretic in Turkey (11). Steamed leaves are used for the treatment of warts and bruises in North America (Indians) and Romania (8, 12). Chewed fresh leaves are used as stomach aid in North America (Indians) (8) as well as aerial parts and seeds to be applied against diarrhoea in Hungary (13, 14). Aerial parts are used against jaundice and fever as decoction in Iran (15). In American traditional medicine, it is reported to be applied for the treatment of different kinds of tumors (16) and have a long traditional usage in folk medicine for the treatment of cancer (13, 17, 18), *e.g.* as component of Essiac tea (19) in different regions in the world.

R. acetosella has an anthraquinone-rich phytochemical content. Anthraquinones characterized by wide structural diversity and low toxicity have an important place among the phytochemicals (20). They are mostly present in the families of Fabaceae, Liliaceae, Polygonaceae, Rhamnaceae, Rubiaceae, and Scrophulariaceae (21). Anthraquinones were previously shown to inhibit proliferation or tumor growth in several cell lines such as breast (22-24), lung (23), cervix (25), prostate (26), colon, central nervous system as well as of glioma (23, 27), hepatoma (28) and leukemia (29, 30).

Natural compounds (*e.g.* anthracyclines, *Vinca* alkaloids, taxanes, camptothecins etc.) are very important substances used in cancer treatment. Evidently, 69% of the anticancer drugs approved between 1980s and 2002 are originated from nature and usually improved in the light of knowledge obtained from natural sources (31). Natural compounds are also assumed as important precursors in the development of novel targeted chemotherapeutics with improved antitumor activity and fewer side effects (32).

Structural similarities of anthraquinone aglycones to anthracyclines allow to speculate on their possible anticancer activities.

Cancer is one of the leading cause of death worldwide. In 2012, 14.1 million patients were diagnosed (33) and new cases with cancer are predicted to increase by 70% over the next 20 years (34).

Despite notable improvements in cancer research in the past few decades, many cancer patients still cannot be cured due to the development of drug resistance. Even worse, tumors frequently develop resistance not only to a single drug, but also to many drugs at the same time. This phenomenon has been termed as multidrug resistance (MDR) and reduces the success of chemotherapy, which is the mainstay in cancer treatment (35). The response of tumor cells to cytotoxic agents is frequently determined by multiple factors (36, 37).

R. acetosella has a long tradition in folk medicine for the treatment of cancer (13, 17-19). The traditional use of *R. acetosella* extracts were confirmed by *in vitro* studies (38). The plant contains anthraquinones (39), flavonoids (39) and other phenolics (40). These components of the plant may be associated with the cytotoxicity. The main anthraquinone aglycones (emodin, aloe-emodin, physcion, rhein), reported to be present in *R. acetosella* in previous researches (13, 39, 41), were investigated for their cytotoxicity as they have structural similarity to clinically established anticancer agents like Doxorubicin.

One of the other uses of *Rumex* species is diabetes (42, 43). Fresh leaves of *R. acetosella* were reported to have a traditonal usage in diabetes by local people in Elazığ district of Turkey (44-47). Ethnobotanical information indicates that more than 800 plants are used for the treatment of diabetes throughout the world (48).

Diabetes mellitus (DM) is a disease caused by abnormal metabolism of carbohydrate, characterized by increased blood sugar level. Insulin disturbance occurred in the disease causes imbalances in carbohydrate, fat and protein metabolism, affecting the vital organs in the body such as eyes, kidney, heart, nervous system etc. and leading morbidity and mortality. These can be both macrovascular and microvascular originated such as coronary artery disease, myocardial infarction, hypertension, peripheral vascular disease, retinopathy and neuropathy (49, 50). According to World and Health Organization (WHO) reports, patients with DM has been 422 million nearly quadrupling since 1980 and inclined 1.5 milllion deaths in 2012 (51). Therefore, glycemic control has a prominent role to preclude worse complication outcomes and diabet-regarded deaths.

Pancreatic alpha (α)-amylase and intestinal alpha (α)-glucosidases as starch hidrolyzing enzymes cause increased glucose levels in blood (52). A therapeutic approach to treat diabetes and prevent complications is to reduce postprandial hyperglycemia, which can be achieved through the inhibition of α-amylase and α-glucosidase involved in carbohydrate hydrolysis (53-56). Inhibitors of these enzymes delay carbonhydrate digestion and interrupt the increase in postprandial glucose in plasma (53), indicating that they are important agents in the discovery of new drugs in diabetes (57).

R. acetosella are used in traditional medicine against cancer and diabetes in many countries, from this point of view, the aims of the present thesis are:

(1) To measure the antioxidant capacities of various *R. acetosella* extracts as preliminary studies since the oxidative stress takes part in the etiology of many diseases such as cancer and diabetes mellitus,

(2) To isolate possible drug candidate molecules from *R. acetosella* and elucidate their structures,

(3) To determine the cytotoxicities of all isolated molecules from *R. acetosella* and commercial main anthraquinone aglycones. It is also planned to identify the mode of action of the most active compound via detection of reactive oxygen species (ROS), DNA damage, cell cycle arrest, apoptosis and necrosis. Besides, inherent resistance of the most active compound was planned to be investigated by microarray-based mRNA profiling. Because tumor cells can be

unresponsive to cytotoxic compounds, even if they have never been exposed to drugs before,

     (4) To investigate the α-amylase and α-glucosidase inhibition potentials of the extracts prepared from *R. acetosella* and the main anthraquinone aglycones of the title plant.

2. GENERAL INFORMATION

2.1   Botanical Information

Botanical knowledge of Polygonaceae family, *Rumex* genus and *Rumex acetosella* L. were separately indicated below.

2.1.1   Polygonaceae Family

Kingdom: Plantae
Subkingdom: Tracheobionta
Superdivision: Spermatophyta
Division: Magnoliophyta
Class: Magnoliopsida
Subclass: Caryophyllidae
Order: Polygonales
Family: Polygonaceae

Polygonaceae family members are seen as herbs, shrubs, rarely vines or trees with jointed stems and with alternate, opposite, whorle, hastate or sagittate leaves in nature. Stipulas when represent are merged and sheathing. Flowers are exact on pedicels. Calyx is 2-6 parted or dissected. Sepals are constant without any petals. Stamens are 2-9, situated near the base of the calyx whereas pistil individually free from the calyx, ovary as superior 1 celled including ovule solitary, orthotropous, erect or hanging. Styles are 2-3 or 4 exact or partly united. Fruits are lentiform, 3 or 4 angled achene usually invested by the persistent calyx. Embriyo direct within the endosperm or curved around it (58, 59).

Polygonaceae family is mostly prevalent in Northern hemisphere with thirty two genus and around eight hundred species worldwide as well as eight genus and seventy four species including fourteen endemic species in Turkey (59).

The identification key for the genera of the plants in Polygonaceae family grown in Turkey:

1. Woody branches

    2. Stamens 10-16, the fruit is covered with hard, lumpy, thorns on.

<div align="right">

3. Calligonum
</div>

    2. Stamens 6-8, fruit is without thorn

        3. Stamens attach to the mouth part of the parts of perianth, the fruit has 2 lobes, 3 wings

<div align="right">

2. Pteropyrum
</div>

        3. Stamens attach to the base of the parts of perianth, the fruit is wingless

<div align="right">

1. Atraphaxis
</div>

2. Sometimes weeds bearing woody branches

    4. Perianths 4-segmented, leaves mostly completely grounded, from reniform to triangular cord, long adjustable

<div align="right">

5. Oxyria
</div>

    4. Perianths 5-6-segmented, leaves not like the above

        5. Flowers unisexual

            6. Leaves hastate or sagittate, the end of perianth parts fruity, not bushy

<div align="right">

7. *Rumex*
</div>

            6. Leaves cordate, the ends of perianth parts are bushy,

<div align="right">

8. Emex
</div>

        5. Flowers hermaphrodite

            7. Stamens 9, fruit winged, leaves palmat-nerved

<div align="right">

4. Rheum
</div>

            7. Stamens 6-8, fruit not winged, leaves pennat nerved

                8. Perianths 6-segmented, inner ones bigger than the outer ones, stamens 6

<div align="right">

7. *Rumex*
</div>

                8. Perianths 5-segmented, all equal in size, stamens usually 8

<div align="right">

6. Polygonum
</div>

2.1.2 The Genus *Rumex*

Rumex as the second most extensive genus in Polygonaceae family is distributed in Europe, Asia, Africa and North America-substantially in Northern hemisphere with approximately 200 species (13).

Plants in *Rumex* genus are annuals, biennials or perennials as mostly herbs seldomly shrubs. Roots are frequently long and strong, occasionally rhizomatous. Leaves are alternate, hastate, sagittate and ochreae tubular. Flowers may be organized in simple whorls or branched inflorescens as unisexual and hermaphrodites. Fruits are trigonous nuts (13, 60, 61). 31 taxa -8 of whom are subspecies and 27 different *Rumex* species including 6 endemic ones are growing in Turkey (61, 62).

Rumex species growing in Turkey and their distribution are shown in (**Table 2.1**.).

Table 2.1. *Rumex* species growing in Turkey and their distribution.

Plant species	City	Region
Rumex acetosella L.	Edirne, Canakkale, Istanbul, Bolu, Kastamonu, Amasya, Ordu, Rize, Coruh, Izmir, Kutahya, Ankara, Artvin, Giresun, Kayseri, Kahramanmaras, Tunceli, Bitlis, Agrı, Isparta,	A1, A2, A3, A4, A5, A6, A7, A8, A9, B1, B2, B4, B5, B6, B7, B9, B10, C3, C6
Rumex scutatus L.	Adana, Kastamonu, Ankara, Antalya, Bursa, Gumushane, Izmir, Konya, Kahramanmaras, Mugla, Mus, Rize, Sivas, Van	A2, A3, A4, A7, A8, B2, B3, B4, B5, B6, B7, B9, C2, C3, C6, C9, C10
Rumex tuberosus L.	Adana, Bolu, Istanbul, Karabuk, Antalya, Bursa, Canakkale, Denizli, Hatay, Icel, Izmir, Kutahya, Samsun	A1, A2, A3, A4, A5, B1, B2, B5, C2, C3, C4, C6
Rumex arifolius ALL.	Sivas	A6, A7
Rumex tmoleus Boiss. (Endemic)	Izmir, Antalya	B2, C2
Rumex alpinus L.	Bursa, Bolu, Gumushane, Coruh, Rize, Erzincan, Erzurum, Bitlis	A2, A3, A7, A8, B7, B8
Rumex gracilescens Rech. (Endemic)	Agrı, Kastamonu, Kars	A4, A9, B9
Rumex olympicus Boiss. (Endemic)	Bursa	A2

8

Table 2.1. *Rumex* species growing in Turkey and their distribution (continued).

Plant species	City	Region
Rumex patientia L.	Kars, Izmir, Kahramanmaras, Sivas, Izmir, Antalya, Adana, Mardin, Diyarbakir	A9, B1, B6, B9, C3, C5, C8
Rumex caucasicus Rech.	Rize	A8
Rumex cristatus DC.	Canakkale, Kocaeli, Izmir, Denizli,	A1, A2, B2, C2
Rumex ponticus E.H.L. Krause (Endemic)	Gumushane, Erzurum, Erzincan, Bitlis, Hakkari	A7, A8, B7, B8, C10
Rumex angustifolius Campd.	Gumushane, Usak, Kutahya, Kayseri, Sivas, Tunceli, Antalya, Konya, Hakkari, Kahramanmaras, Erzincan, Bitlis, Nigde	A7, B2, , B5, B6, B7, C2, C3, C4, C5, C9,
Rumex crispus L.	Canakkale, Istanbul, Bolu, Kastamonu, Coruh, Kars, Izmir, Ankara, Tunceli, Diyarbakir, Gaziantep	A1, A2, A5, A8, A9, B2, B4, B7, B9, C4, C6
Rumex conglomeratus Murray	Adana, Istanbul, Karabuk, Bitlis, Çanakkale, Isparta, Konya, Mugla	A1, A2, A4, B8, C1, C3, C4, C5
Rumex palustris SM.	Izmir	B1, B2
Rumex maritimus L.	Samsun	A6
Rumex sanguineus L.	Gaziantep, Istanbul	A2, C6
Rumex hydrolapathum Huds.	Bolu	A3
Rumex obtusifolius L.	Istanbul, Bursa, Bolu, Kastamonu, Sinop, Gumushane, Coruh	A2, A3, A4, A5, A7, A8
Rumex chalepensis Miller	Gaziantep	C6
Rumex pulcher L.	Canakkale, Istanbul, Kocaeli, Trabzon, Izmir, Kutahya, Ankara, Aydin, Denizli, Antalya, Icel, Diyarbakir	A1, A2, A7, B1, B2, B4, B5, C1, C2, C3, C4, C8
Rumex bithynicus Rech. Fil. (Endemic)	Bursa	A2
Rumex amanus Rech. (Endemic)	Hatay	C6
Rumex nepalensis Sprengel	Bursa, Bolu, Zonguldak, Gumushane, Balikesir, Izmir, Bilecik, Tunceli, Hatay	A2, A3, A4, A7, B1, B2, B3, B7, C6
Rumex dentatus L.	Kastamonu, Eskısehir, Ankara, Konya, Hatay	A5, B3, B6, B4, C4, C6
Rumex bucephalophorus L.	Istanbul, Antalya, Aydin, Balikesir, Icel, Izmir, Mugla	A2, B1, C1, C2, C3, C4, C5

2.1.3 *Rumex acetosella* L.

Rumex acetosella (**Figure 2.1.**) (Syn: *Acetosella vulgaris* (W.D.J. Koch) Fourr., *Rumex acetoselloides* Bal.) is a perennial and slight plant with 15-40 cm hairless or delicately papillose stems, hastate leaves with central lobes from lanceolate to oblanceolate, more splitted lateral lobes and unisexual flowers as dioecious plants. Outer sepals can reach to 1.5 mm long and lanceolate whereas inner sepals can reach to 2 mm long as obovate in the staminate flower with 6 stamen and mostly ovate in the pistillate flower. Three angular and gold brown achene can reach to 1.5 mm long. Permanent calyx is not broadened. It blooms from April to August and bear fruits until October (61, 63).

Figure 2.1. *Rumex acetosella* L. deposited as a voucher specimen in the Herbarium of Faculty of Pharmacy, Hacettepe University, Ankara, Turkey (HUEF: 13005).

Vernacular Names
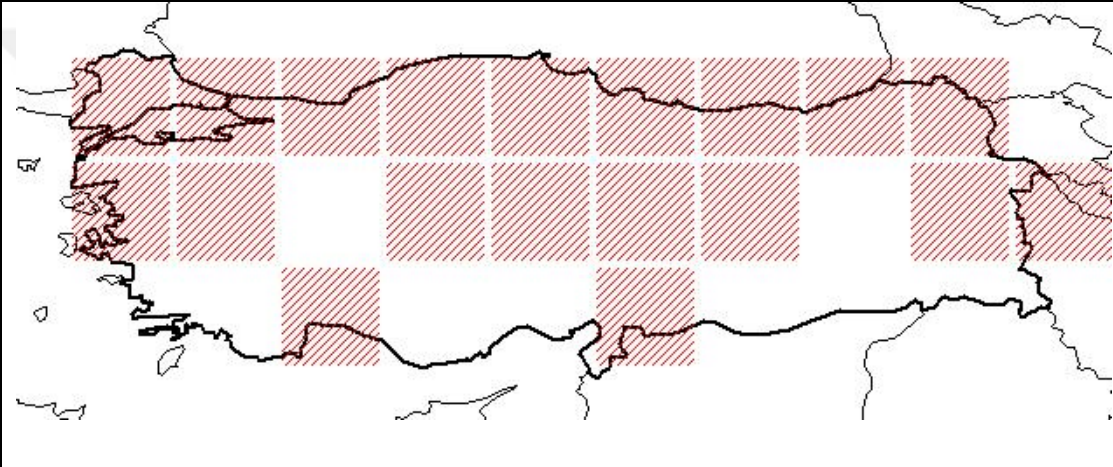
R. acetosella is locally named as "kuzukulagı, ebeneksisi, egsikulak, egsimene, eksice, eksikulak, eksilik, eksimcik, eksimelek, eksimen, eksimenek,

guzugulagı, guzukulagı, oglakkulagı, seytankulagı, tursu otu" (62) in Turkey and "sour dock, red sorrel, sheep sorrel, common sheep sorrel, field sorrel, reti/mezei soska, juhsoska" in different countries and regions in the World (11, 13, 64-66).

Range and Habitat

It grows on the fields, roadsides and waste areas with acidic soils. It ranges from Europa and Asia to United States and Canada (63, 67). It's also widely distributed in Turkey (**Table 2.2.**) (62, 68).

Table 2.2. Distribution of *R. acetosella* over Turkey based on grids.

A1(E) Edirne: 20 km E of Edirne, *Sorger* T-63-58-7 **A1(A)** Canakkale: Dardanelles, Saradschik, *Sint.*1883:861 **A2(E)** Istanbul: Belgrad forest, Kayacik 84 **A2(A)** Istanbul; Alemdag, 3 vi 1895, *Azn*. **A3** Bolu: Ala Da., Kartal Kaya Tepe, 2100-2200 m, *D*. 37303 **A4** Kastamonu: N side of Ilgaz Da., 1500 m, *D*. 38287 **A5** Amasya: Amasya, Abaci Da., 1300- 1500 m, *Bornm*. 1889:1256 **A6** Ordu: 10 km from Unye, *Jardine* 426a **A7** Giresun: Tamdere to Yavuzkemal, 1500 m, *D*. 20725 **A8** Rize: Khavia De. nr. Miracalo, *Bal*. 1477 **A9** Coruh: Kordevan Da., 2200 m, *D*. 30234 **B1/2** Izmir: Izmir and Bozdag, *Bal*. 351 **B2** Kutahya: Demirci to Simav, 1340-1390 m, *Demiriz* 2082 **B4** Ankara: Ankara, *Bornm.* 1892:3120 **B5** Kayseri: Talasse, 7 km SE of Kayseri, 1300 m, *Bal.* 1105 **B6** Maras: Goksun to Elbistan, 1400 m, *Stn & Hend.* 5578 **B7** Tunceli: S of Ovacik, 1750 m, D. 31557 **B9** Bitlis: Bitlis to Tatvan, 1800 m, *D.* 22363 **B10** Agri: Great Ararat (Agri Da.), *B. Post* 1910: 2104 **C3** Isparta: Dedegol Da., 1400 m, Sorger T-65-43-109 **C6** Maras: 3 miles N of Andirin,

Table 2.2. Distribution of *R. acetosella* over Turkey based on grids (continued).

1000 m, *Coode & Jones* 1202 **A4** Ankara: Camlidere, along road sides 1 km behind the Camkoru Lake, 1450 m (HUEF 13005!), **B6** Sivas to Tokat, Camlibel location, 1934m (HUEF 92205!), **A2(A)** Istanbul: Pasakoy Omerli Dam Lake, 200 m (ANK 3649!), **A(5)** Corum: Bayat, Kurudag location, 1800 m (ANK 3931!), **B3** Eskisehir: Turkmen Mountain, 1300 m (ANK 5280!), **B7** Tunceli: S of Ovacik, 1750 m (ANK 31557!), **A4** near by Karabuk location: Ardıc duzu location, 1300 m (ANK 1764!), **A4** Kastamonu: Ilgaz Mountains, 1600 m (ANK 11771!), **A4** Summit of Isık Mountain, 2000 m (ANK 6467!), **A4** Ankara: Kizilcahamam- Kargasekmez location, 1100 m (ANK 208!), **A8**: Murgul-Damar location, 1165 m (ANK 708!), **A4**: Road Kastamonu to Kure, 1100 m (ANK 1415!), **A5** Yozgat: Cekerek, Koyunculu Village, Fakı Mountain, 1350 m (ANK 935!), **B5** Kayseri: Erciyes Mountain, Derin dere location, 2570 m (ANK 3957!).

2.2   Substances in *Rumex* Species

Primary and secondary metabolites from *Rumex* genus identified by phytochemical studies were shown in tables (**Tables 2.3.-2.16.**) below.

2.2.1   Anthranoids
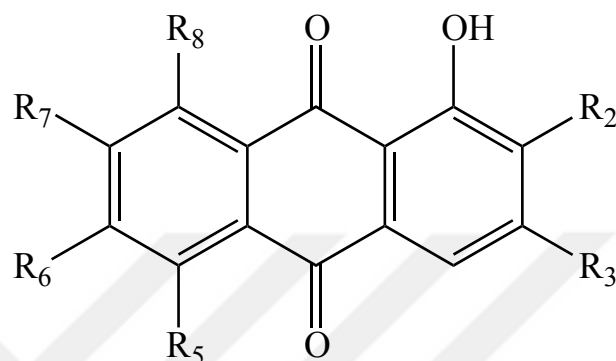
Table 2.3. Antraquinone aglycones in *Rumex* species.

Compound	R_2	R_3	R_5	R_6	R_7	R_8	Plant	Reference
Alizarin	OH	H	H	H	H	H	*R. abyssinicus*	(69)
							R. alpinus	(70)
							R. chalepensis	(70)
Aloe-emodin	H	CH_2OH	H	H	H	OH	*R. acetosa*	(13, 41, 71, 72)
							R. acetosella	(13, 41, 71)
							R. alpinus	(41, 73)
							R. angustifolius	(73)
							R. arifolius	(41)
							R. chalepensis	(74)
							R. confertus	(13, 41, 71)
							R. conglomeratus	(41)
							R. crispus	(13, 71, 73)
							R. cristatus	(74)
							R. dentatus	(73)
							R. gracilescens	(73)
							R. hydrolapathum	(13, 71)
							R. japonicus	(75)
							R. maritimus	(41)
							R. nepalensis	(41)
							R. obtusifolius	(13, 41, 71)
							R. palustris	(41)
							R. patientia	(41)
							R. sanguineus	(73)
							R. scutatus	(41, 76)
ω-acetoxy-aloe-emodin	H	CH_2O-$COCH_3$	H	H	H	OH	*R. acetosa*	(77)

Table 2.3. Antraquinone aglycones in *Rumex* species (continued).

Compound	R$_2$	R$_3$	R$_5$	R$_6$	R$_7$	R$_8$	Plant	Reference
Chrysophanol	H	CH$_3$	H	H	H	OH	*R. abyssinicus*	(42, 78, 79)
							R. acetosa	(13, 41, 71, 72, 80)
							R. acetosella	(41, 71, 74)
							R. alpinus	(41, 81)
							R. altissimus	(41)
							R. angustifolius	(73)
							R. aquaticus	(13)
							R. arifolius	(41)
							R. bequaertii	(79)
							R. britannicus	(13)
							R. brownii	(41)
							R. bucephalopherus	(82)
							R. chalepensis	(83)
							R. confertus	(41, 71)
							R. conglomeratus	(41)
							R. crispus	(41, 71)
							R. cristatus	(74)
							R. cyprius	(74, 84)
							R. dentatus	(85)
							R. dictyocarpus	(74, 86)
							R. domesticus	(82)
							R. lanceolatus	(13)
							R. ginii	(82)
							R. gracilescens	(87)
							R. hastatus	(13, 88, 89)
							R. hydrolapathum	(41, 71)
							R. hymenosepalus	(13, 90)
							R. japonicus	(13, 74, 91)
							R. luminiastrum	(13, 74, 92)
							R. maritimus	(41)
							R. nepalensis	(13, 41, 88, 89)
							R. obtusifolius	(41, 71)
							R. palustris	(41)
							R. paulsenianus	(41, 74, 93)
							R. patientia	(13, 41, 94-97)
							R. pictus	(13, 84)
							R. pulcher	(41)
							R. ruwenzoriensis	(79)
							R. sanguineus	(41)
							R. scutatus	(41, 76)
							R. stenophyllus	(41)
							R. tingitanus	(74, 98)
							R. thyrsiflorus	(99)
							R. usambarensis	(74, 79)
							R. vesicarius	(100, 101)

Table 2.3. Antraquinone aglycones in *Rumex* species (continued).

Compound	R_2	R_3	R_5	R_6	R_7	R_8	Plant	Reference
Chrysophanol (continued)	H	CH_3	H	H	H	OH	*R. wallichii*	(74, 102)
Citreoresin	H	CH_2OH	H	OH	H	OH	*R. acetosella*	(74)
							R. hastatus	(13, 88, 89)
							R. nepalensis	(13, 88, 89)
							R. patientia	(13, 89)
Emodin	H	CH_3	H	OH	H	OH	*R. abyssinicus*	(42, 78, 79)
							R. acetosa	(41, 71, 72, 80, 103)
							R. acetosella	(41, 71)
							R. aegyptiacus	(84)
							R. alpinus	(41, 73, 81)
							R. altissimus	(41)
							R. angustifolius	(73)
							R. aquaticus	(104)
							R. arifolius	(41)
							R. bequaertii	(79)
							R. britannicus	(104)
							R. brownii	(41)
							R. bucephalophorus	(105)
							R. chalepensis	(74)
							R. confertus	(41, 71, 106)
							R. conglomeratus	(41, 104)
							R. crispus	(41, 71, 106)
							R. cristatus	(70, 74, 107)
							R. cyprius	(84)
							R. dentatus	(106)
							R. dictyocarpus	(74)
							R. domesticus	(82)
							R. lanceolatus	(13)
							R. gmelini	(108)
							R. gracilescens	(87)
							R. hastatus	(88, 109)
							R. hydrolapathum	(13, 41, 71)
							R. hymenosepalus	(13)
							R. japonicus	(75, 91, 110, 111)
							R. luminiastrum	(13, 92)
							R. maritimus	(41)
							R. nepalensis	(41)
							R. obtusifolius	(41, 70, 71, 106)
							R. palustris	(41)
							R. patientia	(13, 41)
							R. pictus	(13, 84)
							R. pulcher	(41)
							R. rechingerianus	(84)
							R. ruwenzoriensis	(79)

Table 2.3. Antraquinone aglycones in *Rumex* species (continued).

Compound	R₂	R₃	R₅	R₆	R₇	R₈	Plant	Reference
Emodin (continued)	H	CH₃	H	OH	H	OH	*R. sanguineus*	(13, 41)
							R. scutatus	(13, 41)
							R. simpliciflorus	(13, 84)
							R. stenophyllus	(13, 41)
							R. thyrsiflorus	(13)
							R. usambarensis	(79)
							R. vesicarius	(13, 84, 101)
							R. wallichii	(102)
Endocrocin	COOH	CH₃	H	OH	H	OH	*R. dentatus*	(112)
							R. nepalensis	(113)
Physcion	H	CH₃	H	OCH₃	H	OH	*R. abyssinicus*	(42, 78, 79)
							R. acetosa	(41, 71, 72, 79, 80, 83)
							R. acetosella	(41, 71)
							R. alpinus	(41, 81)
							R. altissimus	(41)
							R. angustifolius	(73)
							R. arifolius	(41)
							R. bequaertii	(79)
							R. brownii	(41)
							R. chalepensis	(83)
							R. confertus	(41, 71)
							R. conglomeratus	(41)
							R. crispus	(41, 71, 79, 83)
							R. cristatus	(74, 107)
							R. dentatus	(73, 114)
							R. domesticus	(82)
							R. gmelini	(83)
							R. gracilescens	(73)
							R. hastatus	(84, 89)
							R. hydrolapathum	(41, 71)
							R. hymenosepalus	(90)
							R. japonicus	(83)
							R. luminiastrum	(92)
							R. maritimus	(41)
							R. nepalensis	(41, 83, 89, 113)
							R. obtusifolius	(41, 71)
							R. palustris	(41)
							R. patientia	(41, 83, 89)
							R. pulcher	(41)
							R. ruwenzoriensis	(79)
							R. sanguineus	(41)
							R. scutatus	(41, 76)
							R. stenophyllus	(41)
							R. usambarensis	(79)
							R. vesicarius	(100)

Table 2.3. Antraquinone aglycones in *Rumex* species (continued).

Compound	R$_2$	R$_3$	R$_5$	R$_6$	R$_7$	R$_8$	Plant	Reference
Przewalsqui-none B	H	OCH$_3$	OH	H	CH$_3$	H	*R. crispus*	(115, 116)
Rhein	H	COOH	H	H	H	OH	*R. abyssinicus* *R. acetosa* *R. acetosella* *R. andreaeanum* *R. confertus* *R. conglomeratus* *R. cristatus* *R. crispus* *R. hydrolapathum* *R. obtusifolius* *R. palustris* *R. vesicarius*	(69) (13, 71) (13, 71) (117) (13, 71) (41) (74, 107) (13, 71) (13, 71) (13, 71) (41) (74, 101)
Ziganein	H	CH$_3$	OH	H	H	H	*R. crispus*	(13, 115)
1,3,5-trihydroxy-6-hydroxymet-hylanthraqui-none	H	OH	OH	CH$_2$OH	H	OH	*R. crispus*	(13, 115)
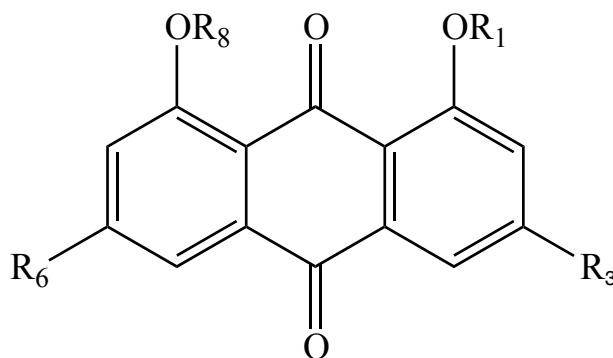
Table 2.4. Antraquinone glycosides in *Rumex* species.

Compound	R$_1$	R$_3$	R$_6$	R$_8$	Plant	Reference
Emodin-1-*O*-*β* -D-glucopyranoside	glu	CH$_3$	OH	H	*R. gmelini*	(118)
Emodin-6-*O*-*β*-D-glucopyranoside	H	CH$_3$	*O*-*β*-D-glu	H	*R. patientia*	(13, 97)
Emodin-8-*O*-*β*-D-(6′-O-acetyl)glucopyranoside	H	CH$_3$	OH	*β*-D- (6′-O-acetyl) glu	*R. nepalensis* *R. hastatus*	(88, 113) (88)
Emodin-8-*O*-*β*-D-glucopyranoside	H	CH$_3$	OH	*β*-D-glu	*R. abyssinicus* *R. acetosa* *R. acetosella* *R. alpinus* *R. angustifolius* *R. aquatica* *R. confertus* *R. conglomeratus* *R. crispus* *R. dentatus* *R. hastatus* *R. japonicus* *R. gracilescens* *R. hymenosepalus* *R. luminiastrum* *R. nepalensis* *R. patientia* *R. sanguineus* *R. scutatus*	(78) (71, 80) (119) (119) (119) (13, 120) (121) (119) (119, 122) (119) (13, 88) (13, 91, 123) (119) (13, 90) (92) (88, 113) (13, 97) (119) (119)
Chrysophanol-8-*O*-*β*-D-galactopyranoside	H	CH$_3$	H	gal	*R nepalensis*	(124)

Table 2.4. Antraquinone glycosides in *Rumex* species (continued).

Compound	R_1	R_3	R_6	R_8	Plant	Reference
Chrysophanol-1-*O*-*β*-D-glucopyranoside	glu	CH_3	H	H	*R. acetosa* *R. confertus* *R. gmelini*	(125) (121) (118, 126)
Chrysophanol-8-*O*-*β*-D-(6′O-acetyl)glucopyranoside	H	CH_3	H	*β*-D-(6′-O-acetyl) glu	*R. gmelini* *R. nepalensis* *R. hastatus*	(127) (88) (88)
Chrysophanol-8-*O*-*β*-D-glucopyranoside	H	CH_3	H	*β*-D-glu	*R. abyssinicus* *R. acetosa* *R. aquaticus* *R. confertus* *R. crispus* *R. dentatus* *R. gmelini* *R. gracilescens* *R. hastatus* *R. japonicus* *R. nepalensis* *R. patientia*	(78) (71) (128) (106) (122) (106) (127) (87) (88) (91, 123) (88, 113) (94, 97)
Physcion-1-*O*-*β*-D-glucopyranoside	Glu	CH_3	OCH_3	H	*R. acetosa*	(71)
Physcion-8-*O*-*β*-D-glucopyranoside	H	CH_3	OCH_3	*β*-D-glu	*R. acetosa* *R. crispus* *R. patientia* *R. japonicus*	(71) (122) (96) (123, 129)
Nepalenside A					*R. nepalensis*	(89, 130)
Nepalenside B					*R. nepalensis*	(89, 130)
Reocrisin	glu	OCH_3	H	H	*R. abyssinicus* *R. acetosa* *R. alpinus* *R. bequaertii* *R. chalepensis* *R. crispus* *R. cristatus* *R. hymenosepalus* *R. japonicus*	(74) (74) (74) (74) (74) (74) (74) (74) (74)

Table 2.4. Antraquinone glycosides in *Rumex* species (continued).

Compound	R$_1$	R$_3$	R$_6$	R$_8$	Plant	Reference
Reocrisin	glu	OCH$_3$	H	H	*R. maritimus*	(74)
					R. nepalensis	(74)
					R. obtusifolius	(74)
					R. patientia	(74)
					R. stenophyllus	(74)
					R. tingitanus	(74)
					R. usambarensis	(74)
					R. vesicarius	(74)

Table 2.5. Anthrone derivatives in *Rumex* species.
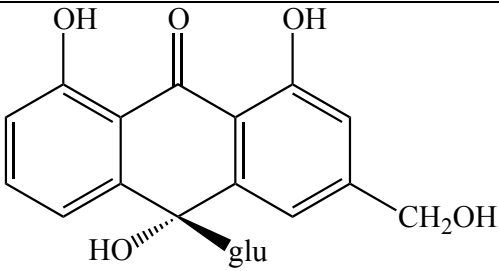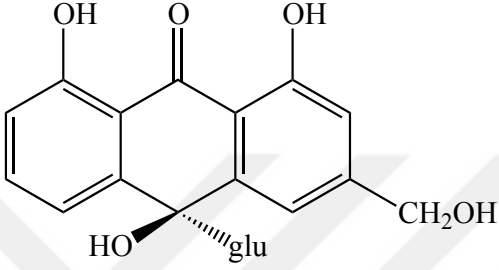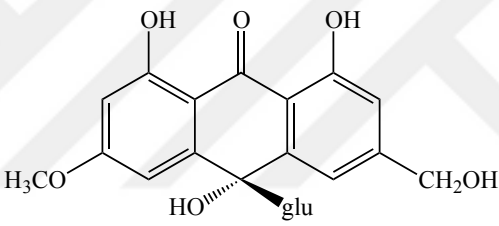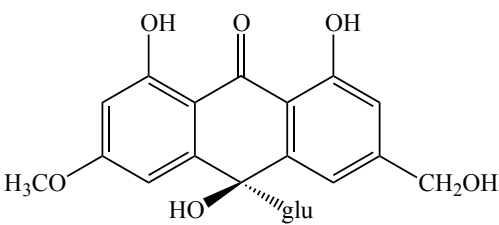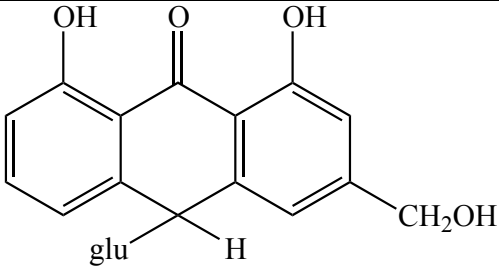
Compound	Structure	Plant	Reference
10-hydroxyaloin A		*R. gmelini*	(17)
10-hydroxyaloin B		*R. gmelini*	(17)
6-methoxyl-10-hydroxyaloin A		*R. gmelini*	(108)
6-methoxyl-10-hydroxyaloin B		*R. gmelini*	(108)
Barbaloin		*R. acetosa* *R. acetosella* *R. confertus* *R. crispus* *R. hydrolapathum* *R. obtusifolius*	(71) (71) (71) (71) (71) (71)

Table 2.5. Anthrone derivatives in *Rumex* species (continued).

Compound	Structure	Plant	Reference
Cassialoin	OH O OH ... CH₃ glu OH	*R. dentatus* *R. patientia*	(131) (89)
Chrysophanol anthrone	OH O OH ... CH₃	*R. acetosa* *R. crispus* *R. hydrolapathum*	(72) (132) (133)
Emodin anthrone	OH O OH ... HO CH₃	*R. acetosa* *R. hydrolapathum*	(72) (133)
Physcion anthrone	OH O OH ... H₃CO CH₃	*R. acetosa* *R. hydrolapathum*	(72) (133)
Rumejaposide A	OH O OH O ... OH H glu OH CH₃ (10R)	*R. japonicus*	(13, 110)
Rumejaposide B	OH O OH O ... OH H glu OH CH₃ (10S)	*R. japonicus*	(13, 110)

Table 2.5. Anthrone derivatives in *Rumex* species (continued).
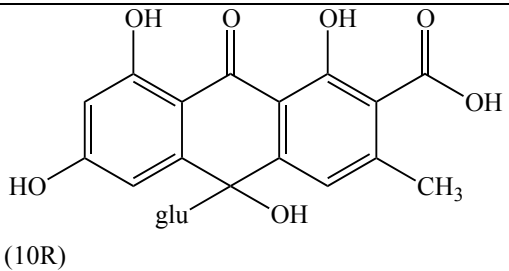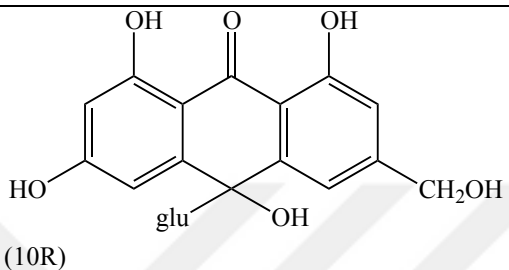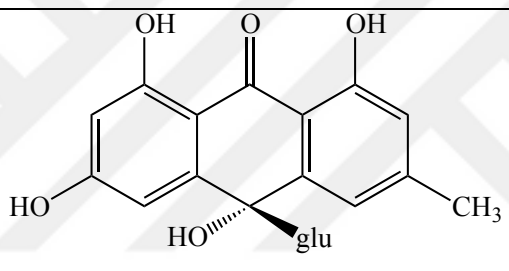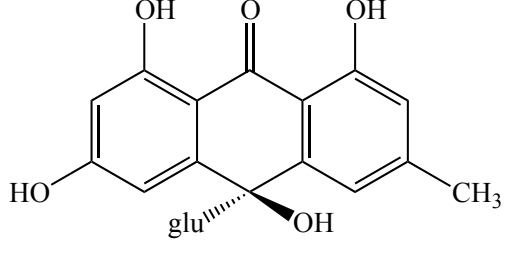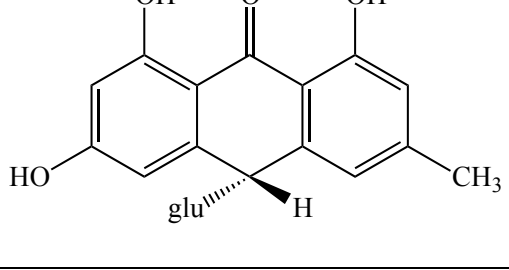
Compound	Structure	Plant	Reference
Rumejaposide C	 (10R)	*R. japonicus*	(13, 110)
Rumejaposide D	 (10R)	*R. japonicus*	(13, 110)
Rumejaposide E		*R. japonicus* *R. dentatus* *R. patientia*	(13, 110) (131) (13, 89)
Rumejaposide F		*R. dentatus* *R. patientia*	(13, 131) (89)
Rumejaposide G		*R. dentatus* *R. patientia*	(13, 131) (89)

Table 2.5. Anthrone derivatives in *Rumex* species (continued).
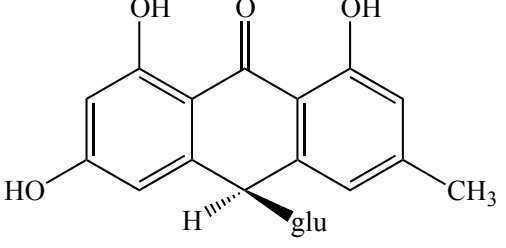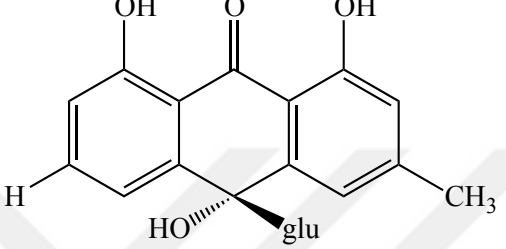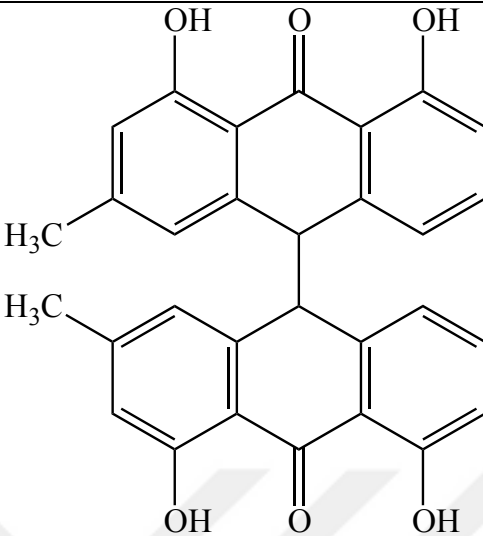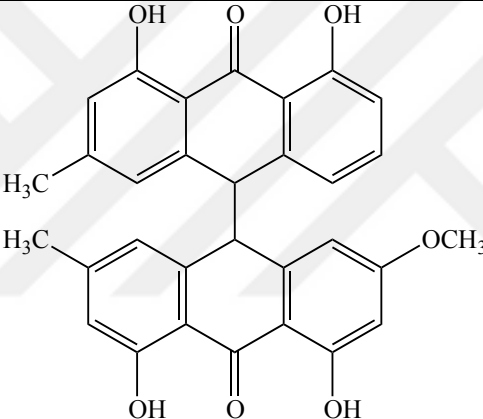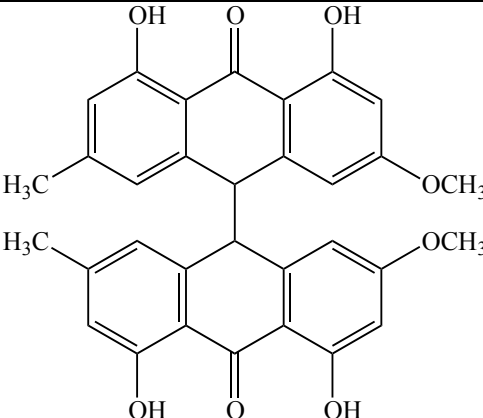
Compound	Structure	Plant	Reference
Rumejaposide H		*R. dentatus* *R. patientia*	(13, 131) (89)
Rumejaposide I		*R. dentatus* *R. patientia*	(13, 131) (89)

Table 2.6. Dianthrone derivatives in *Rumex* species.

Compound	Structure	Plant	Reference
Chrysophanol dianthrone		*R. alpinus*	(81)
Chrysophanol-physcion heterodianthrone		*R. alpinus*	(81)
Physcion dianthrone		*R. alpinus*	(81)

Table 2.6. Dianthrone derivatives in *Rumex* species (continued).

Compound	Structure	Plant	Reference
Sennoside A		*R. acetosa* *R. acetosella* *R. confertus* *R. crispus* *R.* *hydrolapathum* *R. obtusifolius*	(71) (71) (71) (71) (71) (71)
Sennoside B		*R. acetosa* *R. acetosella* *R. confertus* *R. crispus* *R.* *hydrolapathum* *R. obtusifolius*	(71) (71) (71) (71) (71) (71)

2.2.2 Flavonoids
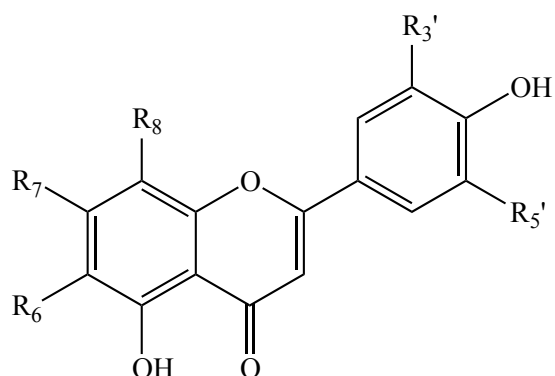
Table 2.7. Flavone derivatives in *Rumex* species.

Compound	R$_6$	R$_7$	R$_8$	R$_3$'	R$_5$'	Plant	Reference
Apigenin	H	OH	H	H	H	*R. acetosella*	(134)
						R. cyprius	(84)
						R. pictus	(135)
						R. scutatus	(136)
						R. simpliciflorus	(84)
						R. vesicarius	(84)
Apigenin-6-*C*-glucoside	C-glu	OH	H	H	H	*R. nervosus*	(137)
						R. induratus	(138)
Apigenin-6-*C*-glucoside-7-*O*-glucoside	C-glu	O-glu	H	H	H	*R. nervosus*	(137)
Apigenin-8-*C*-glucoside	H	OH	C-glu	H	H	*R. nevosus*	(137)
						R. vesicarius	(139)
Isoorientin	C-glu	OH	H	H	OH	*R. acetosa*	(140, 141)
						R. cyprius	(84)
						R. pictus	(84)
						R. simpliciforus	(84)
						R. vesicarius	(142-144)
Isovitexin	C-glu	OH	H	H	H	*R. acetosa*	(84, 141)
						R. cyprius	(84)
						R. pictus	(84)
						R. simpliciforus	(84)
						R. vesicarius	(142-144)
Luteolin	H	OH	H	OH	H	*R. acetosella*	(134)
						R. cyprius	(84)
						R. nervosus	(137)
						R. pictus	(84)
						R. scutatus	(136)
						R. simpliciflorus	(84)
						R. vesicarius	(135)
Luteolin-6-*C*-glucoside	C-glu	OH	H	OH	H	*R. nervosus*	(137)
						R. induratus	(138)

Table 2.7. Flavone derivatives in *Rumex* species (continued).

Compound	R_6	R_7	R_8	R_3'	R_5'	Plant	Reference
Luteolin-7-*O*-glucoside	H	O-glu	H	H	OH	*R. acetosella*	(134)
Luteolin-8-*C*-glucoside	H	OH	H	OH	C-glu	*R. vesicarius* *R. induratus*	(139) (138)
Orientin	H	OH	C-glu	OH	H	*R. acetosa* *R. cyprius* *R. luminiastrum* *R. pictus* *R. simpliciforus* *R. vesicarius*	(140, 141) (84) (92) (84) (84) (142-144)
Vitexin	H	OH	C-glu	H	H	*R. acetosa* *R. cyprius* *R. pictus* *R. simpliciforus* *R. vesicarius*	(141, 145) (84) (84) (84) (142-144)

In addition to the flavones indicated above, 6-*C*-glucosyl-quercetin, 8-*C*-glucosyl-luteolin, *C*-glucosyl-luteolin, 6-*C*-glucosyl-apigenin from *R. induratus* (138), 2″,6″-di-*O*-acetyl-isoorientin, 2″,6″-di-*O*-acetyl-orientin, 2″-*O*-acetyl-orientin from *R. acetosa* (140), and 3,5-dihydroxy-6,7,3c,4c-tetramethoxyflavone from *R. patientia* (146) were also reported.

Table 2.8. Flavonol derivatives in *Rumex* species.

Compound	R₃	R₇	R₈	R₃'	R₅'	Plant	Reference
Astragalin	glu	OH	H	H	H	*R. confertus*	(147)
						R. japonicus	(111)
						R. obtusifolius	(148)
						R. rechingerianus	(149)
Avicularin	ara	OH	H	OH	H	*R. acetosa*	(140)
						R. alpinus	(150, 151)
						R. hymenosepalus	(150, 151)
						R. salicifolius	(150, 151)
Hyperoside	gal	OH	H	OH	H	*R. acetosa*	(140, 152)
						R. acetosella	(153)
						R. aquaticus	(154)
						R. arifolius	(150, 151)
						R. confertus	(150, 151)
						R. crispus	(150, 151)
						R. dentatus	(155)
						R. domesticus	(150, 151)
						R. hastatus	(151, 156)
						R. heterophyllus	(150, 151)
						R. hydrolapathum	(150, 151)
						R. hymenosepalus	(150, 151)
						R. longifolius	(150, 151)
						R. maritimus	(157)
						R. obtusifolius	(150, 151, 155)
						R. patientia	(150, 151)
						R. rechingerianus	(158)
						R. salicifolius	(150, 151)
						R. scutatus	(150, 151)
						R. thyrsiflorus	(159)
Isoquercetin	glu	OH	H	OH	H	*R. obtusifolius*	(148)
						R. rechingerianus	(149)

Table 2.8. Flavonol derivatives in *Rumex* species (continued).

Compound	R$_3$	R$_7$	R$_8$	R$_3$'	R$_5$'	Plant	Reference
Isoquercitrin	glu	OH	H	OH	H	*R. confertus* *R. longifolius* *R. japonicus*	(147) (141) (123)
Isorhamnetin	H	OH	H	O-CH$_3$	H	*R. hastatus*	(160)
3-*O*-rutinosyl-isorhamnetin	rut	OH	H	O-CH$_3$	H	*R. induratus*	(161)
Kaempferol	H	OH	H	H	H	*R. acetosa* *R. acetosella* *R. crispus* *R. maritimus*	(162, 163) (162, 163) (122) (157)
Kaempferol-3-*O*-α-L-rhamnopyranosyl-(1→6)-*β*-D-galactopyranoside	rham-(1→6) gal	OH	H	H	H	*R. chalepensis*	(164)
Kaempferol-7-*O*-α-L-rhamnopyranosyl(1→6)-*β*-D-galactopyranoside	H	*O*-rham (1→6) gal	H	H	H	*R. luminiastrum*	(92)
Kaempferol-3-*O*-*β*-D-glucopyranoside	glu	OH	H	H	H	*R. aquaticus* *R. japonicus*	(120) (123)
Kaempferol-3-*O*-glucuronide	glucuro-nopyranoside	OH	H	H	H	*R. dentatus*	(84)
Myricetin	H	OH	H	OH	OH	*R. crispus* *R. obtusifolius*	(165) (165)
Rumarin	ara (1→6) gal	OH	H	OH	H	*R. maritimus*	(166)
Rutin	rham (1→6)-glu	OH	H	OH	H	*R. acetosa* *R. acetosella* *R. alpinus* *R. arifolius* *R. chalepensis* *R. confertus* *R. crispus* *R. dentatus* *R. domesticus* *R. gmelini* *R. hastatus* *R. heterophyllus* *R. hydrolapathum* *R. hymenosepalus*	(167) (150) (150, 151) (150, 151) (164) (150, 151) (150) (168) (150, 151) (127) (169) (150, 151) (150, 151) (150)

Table 2.8. Flavonol derivatives in *Rumex* species (continued).

Compound	R₃	R₇	R₈	R₃'	R₅'	Plant	Reference
Rutin (continued)	rham (1→6)-glu	OH	H	OH	H	*R. japonicus* *R. longifolius* *R. obtusifolius* *R. patientia* *R. rechingerianus* *R. scutatus* *R. vesicarius*	(110) (150, 151) (148) (167) (149) (150, 151) (139)
Sexangularetin	OH	OH	OCH₃	H	H	*R. acetosa* *R. acetosella*	(163) (163)
Quercetin	H	OH	H	OH	H	*R. acetosa* *R. acetosella* *R. confertus* *R. cyprius* *R. dentatus* *R. dictyocarpus* *R. japonicus* *R. obtusifolius* *R. rechingerianus* *R. thyrsiflorus* *R. vesicarius*	(163) (163) (147) (74) (170, 171) (86) (123, 172) (155) (84) (159) (100)
Quercetin-3-*O*-arabinoside	ara	OH	H	OH	H	*R. aquaticus*	(154, 173)
Quercetin-3-*O*-*β*-D-galactopyranoside	gal	OH	H	OH	H	*R. rossicus*	(99)
Quercetin-3-*O*-*β*-glucuronopyranoside	glucu-ronopy-ranosi-de	OH	H	OH	H	*R. aquaticus* *R. aegyptiacus* *R. conglomeratus* *R. crispus* *R. dentatus* *R. obtusifolius* *R. pulcher*	(13, 174) (84) (141) (141) (84, 168) (141) (84)
Quercetin-3-*O*-*β*-D-glucopyranoside	glu	OH	H	OH	H	*R. aquaticus* *R. induratus* *R. nervosus*	(120) (137)
Quercetin-3-*O*-*β*-D-glucopyranosyl (1→4)-*β*-D-galactoside	glu (1→4) gal	OH	H	OH	H	*R. chalepensis*	(164)
Quercetin-3-*O*-rutinoside	glu-rham	OH	H	OH	H	*R. nervosus* *R. induratus*	(137) (138, 161)
Quercetin-*O*-pentoside	C₅H₉O₄	OH	H	OH	H	*R. nervosus*	(137)
Quercetin-3-acetlyrhamnoside	acetyl-rham	OH	H	OH	H	*R nervosus*	(137)
Quercetin-3-galactoside	gal	OH	H	OH	H	*R. vesicarius*	(135)

Table 2.8. Flavonol derivatives in *Rumex* species (continued).

Compound	R₃	R₇	R₈	R₃'	R₅'	Plant	Reference
Quercitrin	rham	OH	H	H	OH	*R. acetosa*	(145, 162)
						R. alpinus	(162)
						R. aquaticus	(120)
						R. chalepensis	(164)
						R. crispus	(141)
						R. dentatus	(175)
						R. dictyocarpus	(86)
						R. domesticus	(150, 151)
						R. japonicas	(123)
						R. heterophyllus	(150, 151)
						R. hydrolapathum	(150, 151)
						R. longifolius	(141)
						R. nervosus	(137)
						R. obtusifolius	(141)
						R. patientia	(150, 151)
						R. rechingerianus	(149)
Quercimetrin	H	O-glu	H	H	OH	*R. luminiastrum*	(92)
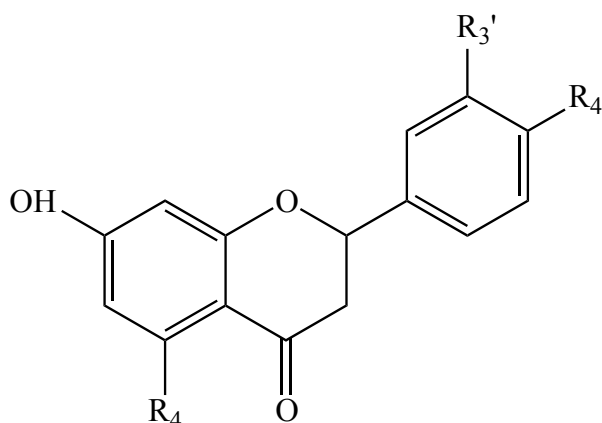
Table 2.9. Flavanone derivatives in *Rumex* species.

Compound	R$_4$	R$_3$'	R$_4$'	Plant	Reference
Eriodictyol	OH	OH	OH	*R. scutatus*	(136)
Hesperetin	OH	OH	OCH$_3$	*R. nervosus*	(137)
Liquiritin	H	H	O-glu	*R. nervosus*	(137)
Naringenin	OH	H	OH	*R. conglomeratus*	(137)
				R. nervosus	(137)

Exceptionally, 7-*O*-hexosyl-diosmetin from *R. induratus* (161), naringin, from *R. nervosus* (137), 5,7,3'- trihydroxy- 4'- methoxy- 8- (3"- methyl- 5"-methylene) hexenylflavanone (vesicariaflavanone A) and 5,7,3',4'-tetrahydroxy-6-methoxy-8- (3"-methylene)-hexenylflavanone (vesicariaflavone B) and (2a,3a-trans)-3a(β),5a,7a,3'a,4'a-pentahydroxyflavanolyl-(8a-2')-5,7,3'-trihydroxy-4'-methoxy-8-n-but-3"-enyl-flavanone and 5,7,3',4',5'-pentahydroxy-8-(cis-1"α,2"β-dihydroxyhept-4"- enyl- 7"- oicacid) - flavanoyl - (2'-8a) - 5a,7a,3'a,5'a- tetrahydroxy- 4'a - methoxyflavanone from *R. vesicarius* (176, 177) and mikanin from *R. patientia* (146) were also reported as the constituents of those plants.

2.2.3   Naphthalenes

Table 2.10. Naphthalene derivatives in *Rumex* species.

Compound	Plant	Reference
Aloesin	*R. nepalensis*	(130)
3-acetyl-2-methyl-1,5-dihydroxy-2,3-epoxynaphtoquinol	*R. japonicus*	(178)
3-acetyl-2-methyl-1,4,5-trihydroxy-2,3-epoxynaphtoquinol	*R. japonicus*	(110)
Hastatuside A	*R. hastatus*	(169)

Table 2.10. Naphthalene derivatives in *Rumex* species (continued).
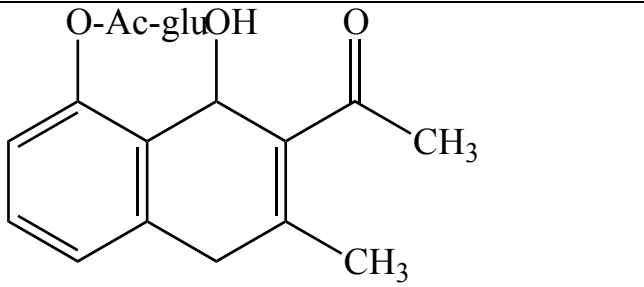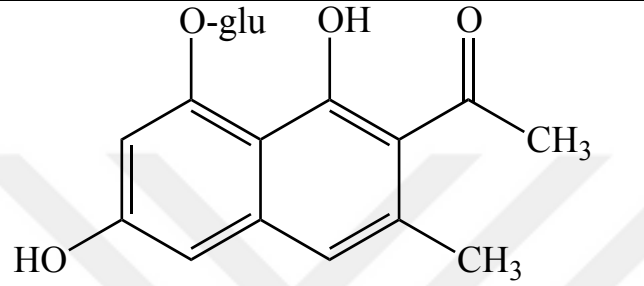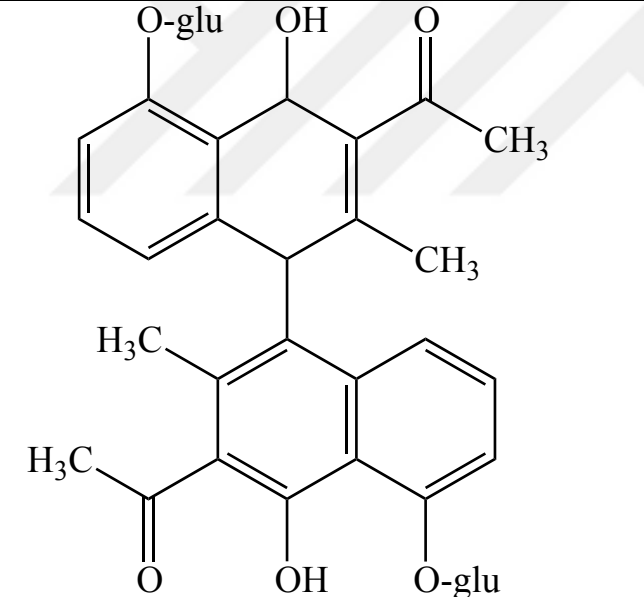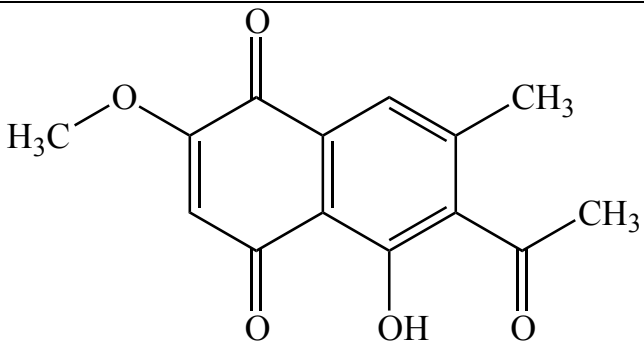
Compound	Plant	Reference
 Hastatuside B	*R. hastatus*	(169)
 6-hydroxynepodin-8-*O*-glucoside	*R. hastatus*	(151, 160)
 Labadoside	*R. patientia*	(97, 179)
 2-methoxystypandrone	*R. aquaticus* *R. japonicus*	(128) (180)

Table 2.10. Naphthalene derivatives in *Rumex* species (continued).
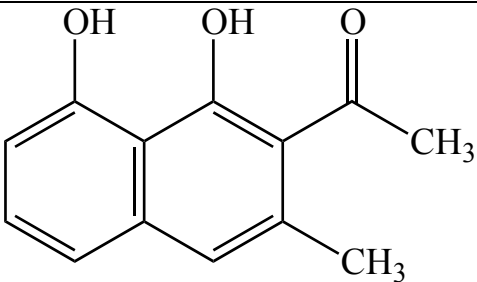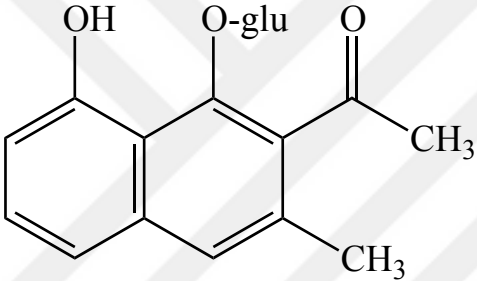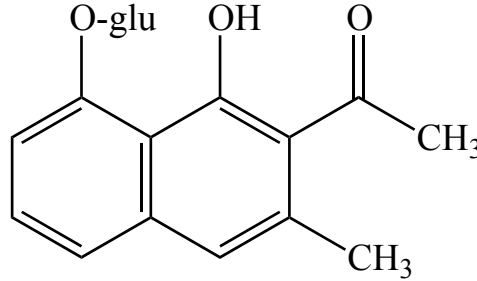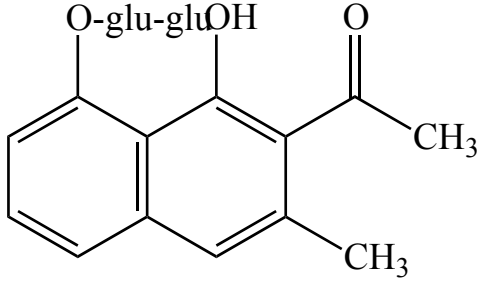
Compound	Plant	Reference
OH OH O CH₃ CH₃ Nepodin	*R. acetosa* *R. alpinus* *R. aquaticus* *R. bequaertii* *R. chalepensis* *R. crispus* *R. confertus* *R. gmelini* *R. hastatus* *R. japonicus* *R. nepalensis* *R. obtusifolius* *R. orientalis* *R. patientia* *R. ruwenzoriensis* *R. stenophyllus*	(74) (74, 81) (128) (74, 79) (74) (74, 181, 182) (121) (17) (169) (74, 183) (184) (74) (74, 185) (74) (79) (74)
OH O-glu O CH₃ CH₃ Nepodin-1-*O*-glucoside	*R. acetosa* *R. alpinus* *R. confertus* *R. crispus* *R. nepalensis*	(151, 186) (151, 186) (151, 186) (151, 186) (124, 151)
O-glu OH O CH₃ CH₃ Nepodin-8-*O*-glucoside	*R. aquaticus* *R. confertus* *R. gmelini* *R. japonicus* *R. nepalensis* *R. obtusifolius* *R. patientia*	(128) (121) (17) (187) (88, 184) (188) (189, 190)
O-glu-glu OH O CH₃ CH₃ Orientaloside	*R. hastatus* *R. nepalensis* *R. patientia*	(169) (130) (97, 179)

Table 2.10. Naphthalene derivatives in *Rumex* species (continued).
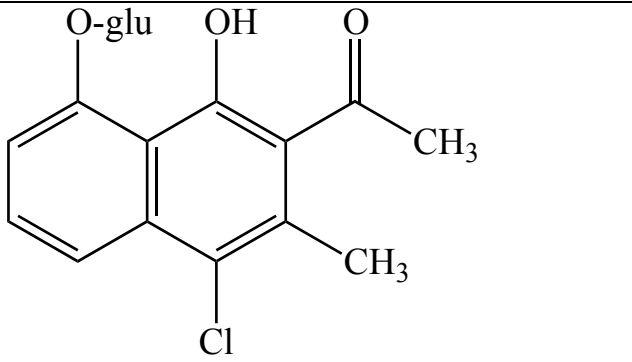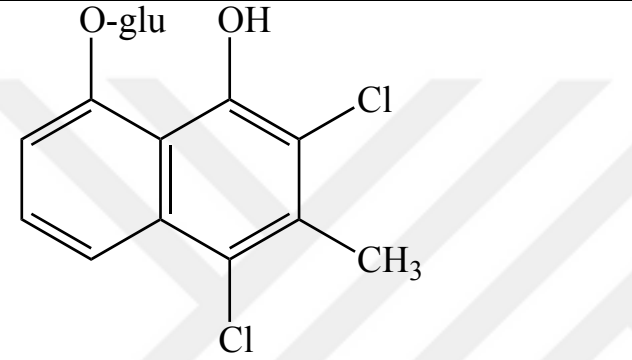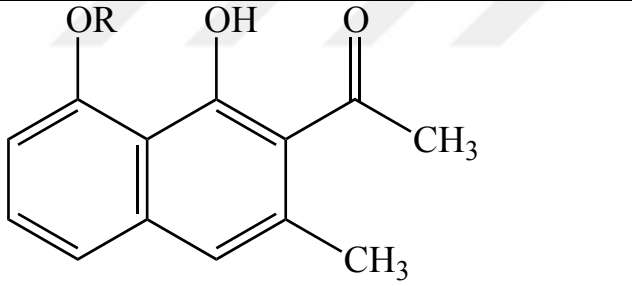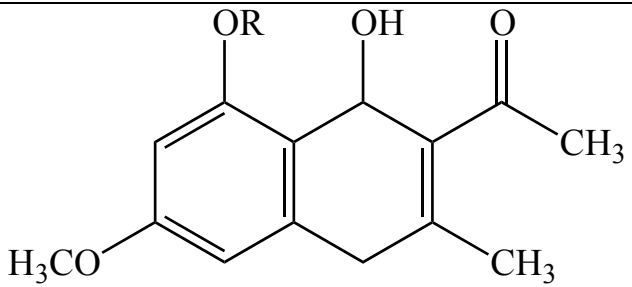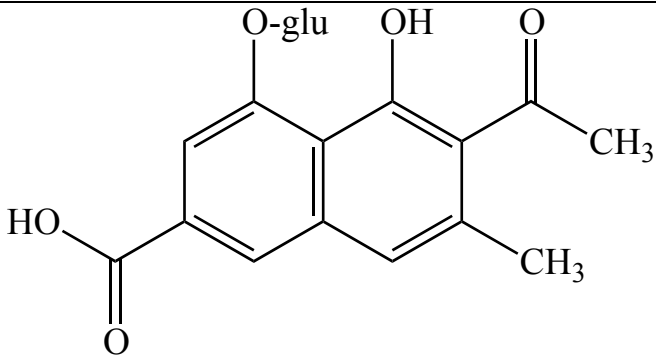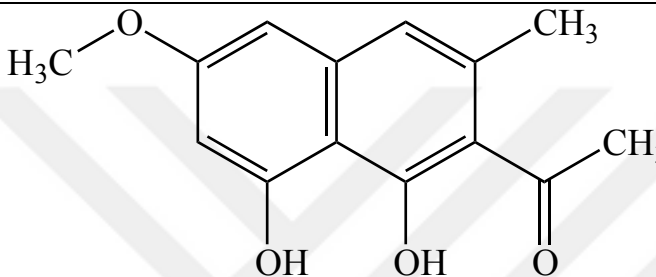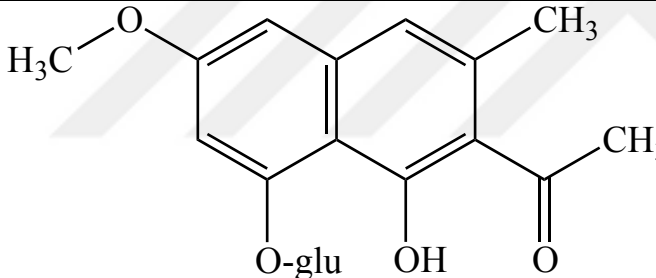
Compound	Plant	Reference
 Patientoside A	*R. patientia*	(94, 191)
 Patientoside B	*R. patientia*	(94, 191)
 (R = 6-*O*-[(2*E*)-1-oxo-2-buten- 1-il]-*β*-D-glucopyranoside) Rumexneposide A	*R. nepalensis*	(88)
 (R = 6-*O*-[acetyl]-*β*-D-glucopyranoside) Rumexneposide B	*R. nepalensis*	(88)

Table 2.10. Naphthalene derivatives in *Rumex* species (continued).

Compound	Plant	Reference
Rumexoside	*R. hastatus* *R. nepalensis* *R. patientia*	(169) (130) (97, 179)
Torachrysone	*R. alpinus* *R. japonicus* *R. nepalensis*	(81) (180) (130)
Torachrysone-8-*O*-glucoside	*R. confertus* *R. hastatus* *R. nepalensis* *R. patientia*	(121) (169) (88) (189, 190)

In additon the compounds indicated above, 2-acetyl-1,8-dihydroxy-3-methyl-6-methoxynaphthalene from *R. japonicus* (110), 6-methyl-7-acetyl-1,8-dihydroxy-3-methoxy naphthalene-1-*O-β-D*(L)-glucoside and 6-methyl-7-acetyl-1,8-dihydroxy naphthalene-1-*O-β-D*(L)-glucoside from *R. dentatus* (85) and 2-acetyl-3-methyl-6-carboxy-1,8-dihydroxynaphthalene-8-*O-β*-D-glucopyranoside, 4,4"-binaphthalene-8,8"-*O,O*-di-*β*-D-glucopyranoside and 2-acetyl-3-methyl-1,8-dihydroxynaphthalene-8-*O-β*-D-glucopyranosyl (1→3)-*β*-D-glucopyranoside from *R. patientia* (190) were isolated.

2.2.4 Tannins

Table 2.11. Monomer tannins in *Rumex* species (flavan-3-ol-derivatives).
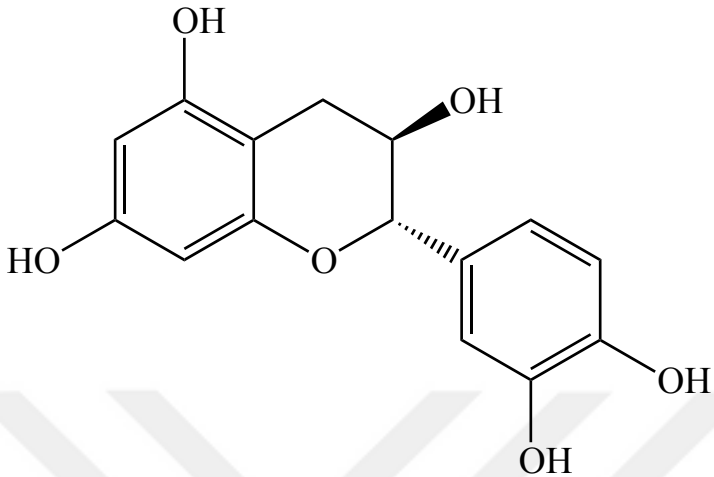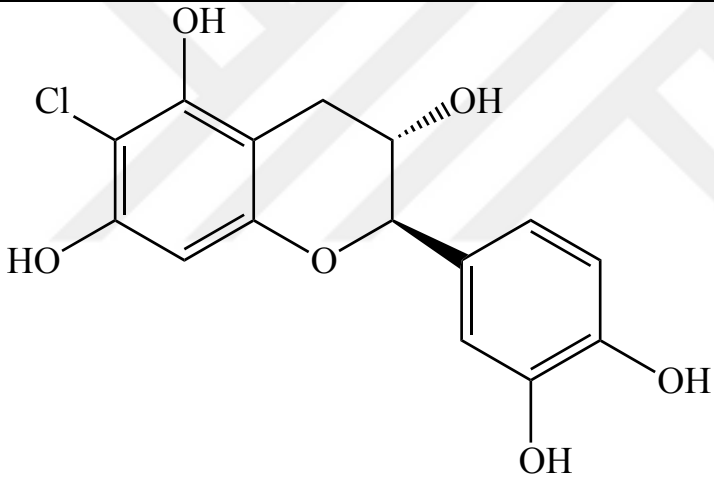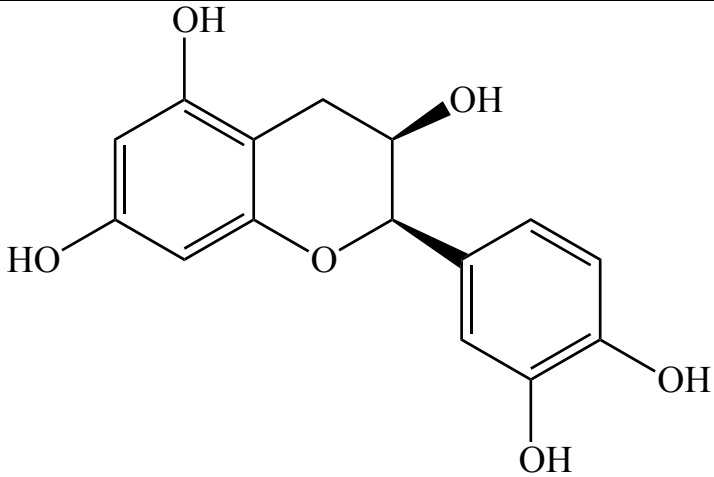
Compound	Plant	Reference
 Catechin	*R. acetosa* *R. aquaticus* *R. crispus* *R. dentatus* *R. japonicus* *R. nervosus* *R. patientia* *R. rechingerianus* *R. scutatus* *R. vesicarius*	(192, 193) (128) (122) (194) (111) (195) (94, 95) (158) (136) (139)
 6-chlorocatechin	*R. patientia*	(97)
 Epicatechin	*R. acetosa* *R. dentatus* *R. hymenosepalus* *R. japonicus* *R. scutatus* *R. vesicarius*	(192, 193, 196) (194) (90) (197) (136, 137) (139)

Table 2.11. Monomer tannins in *Rumex* species (flavan-3-ol-derivatives) (continued).
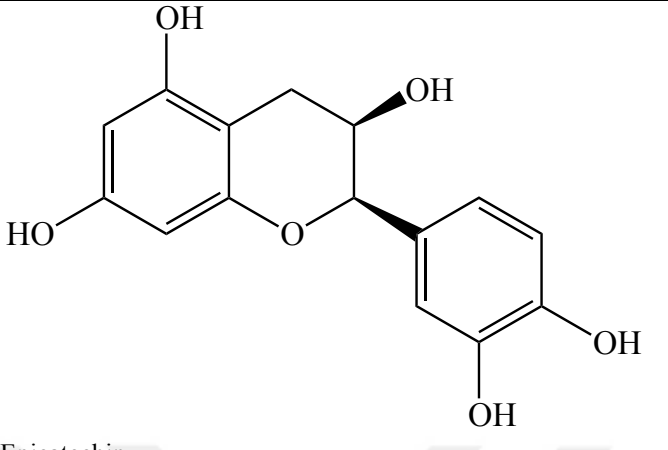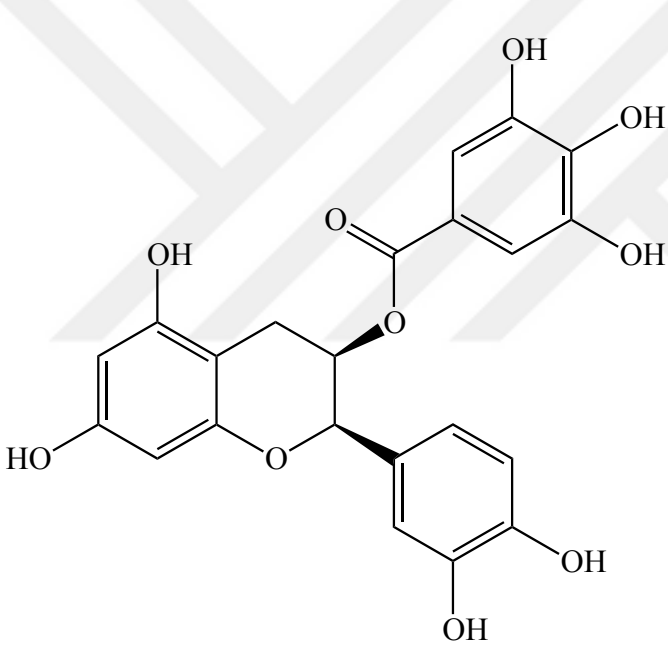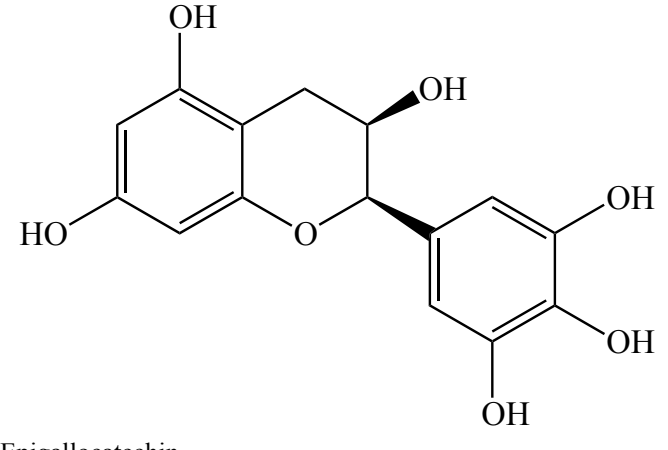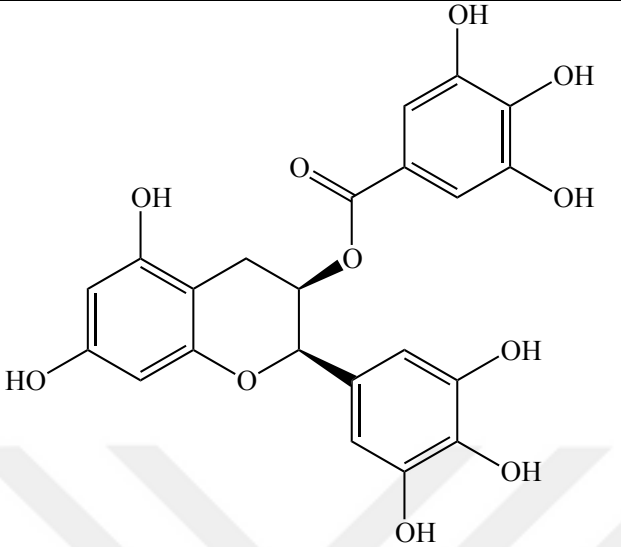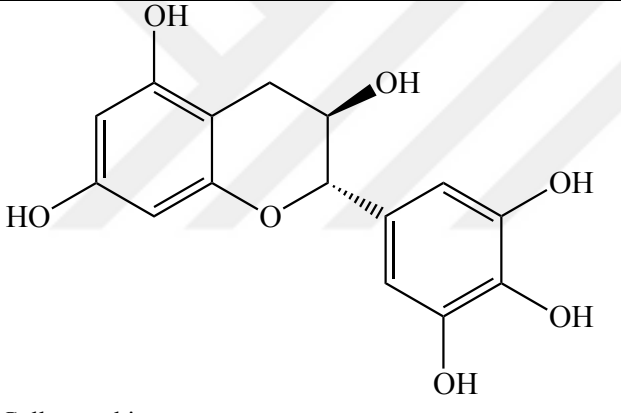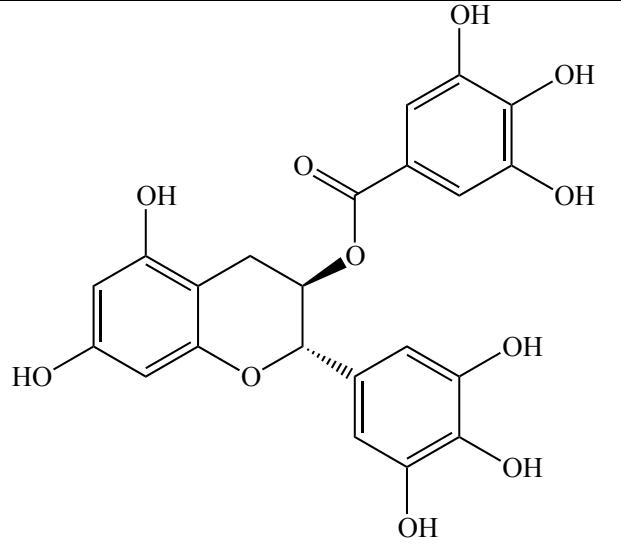
Compound	Plant	Reference
Epicatechin	*R. acetosa* *R. dentatus* *R. hymenosepalus* *R. japonicus* *R. scutatus* *R. vesicarius*	(192, 193, 196) (194) (90) (197) (136, 137) (139)
Epicatechin gallate	*R. acetosa* *R. nervosus* *R. vesicarius*	(192, 196) (137) (139)
Epigallocatechin	*R. acetosa* *R. acetosella* *R. alpinus* *R. confertus*	(196) (198) (198) (198)

Table 2.11. Monomer tannins in *Rumex* species (flavan-3-ol-derivatives) (continued).

Compound	Plant	Reference
 Epigallocatechin gallate	*R. acetosa* *R. alpinus* *R. confertus* *R. vesicarius*	(196) (198) (198) (139)
 Gallocatechin	*R. acetosa*	(196)
 Gallocatechin gallate	*R. acetosa* *R. alpinus* *R. confertus*	(198) (198) (198)

In addition to the monomer tannins indicated above, A- and B-type procyanidins and propelargonidins (15 dimers, 7 trimers, 2 tetramers) from *R. acetosa* (192), 6-*C*-glucosyl-catechin from *R. vesicarius* (139), and pyrocatechin from *R. japonicus* (197) were isolated. Furthermore, various *Rumex* species such as *R. thyrsiflorus, R. pamiricus, R. pseudonatronatus, R. aquaticus, R. marschallianus, R. rossicus, R. maritimus* (99), *R. acetosa* (74, 192, 199), *R. lunaria* (200), *R. patientia* (74, 97), *R. alpinus, R. confertus, R. conglomeratus, R. hastatus, R. hydrolapathum, R. maderensis, R. nervosus, R. odontocarpus, R. palustris, R. pictus, R. pulcher, R. sanguineus, R. tianschanicus*, (74), R. *nepalensis* (201), *R. vesicarius* (74, 202), *R. hymenosepalus* (203, 204), *R. obtusifolius* (205), *R. crispus* (74, 206), *R. acetosella* (207, 208), *R. alpinus, R. angustifolius, R. tmoleus, R. gracilescens* (208), *R. chalepensis* (209) were shown to have tannins in their phytochemical compositions in previous researches.

2.2.5 Simple Phenols and Phenolic Acids

Table 2.12. Simple phenols and phenolic acids in *Rumex* species.
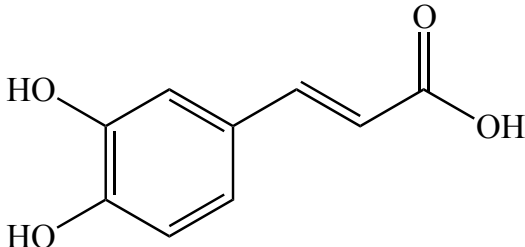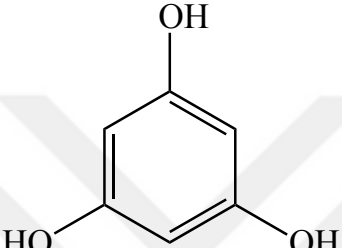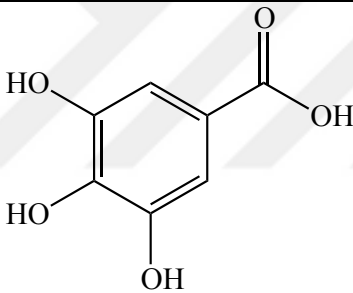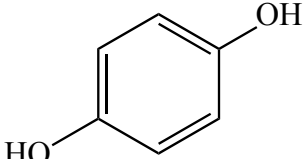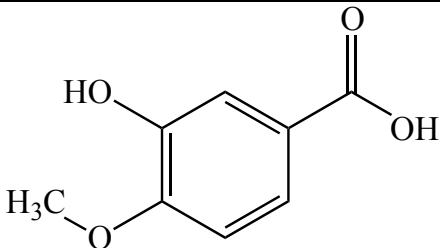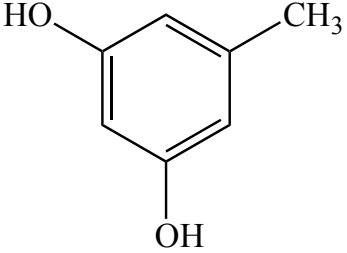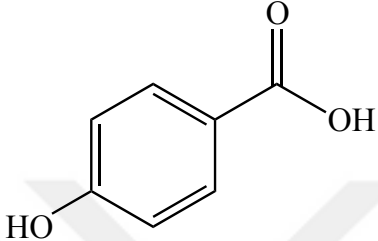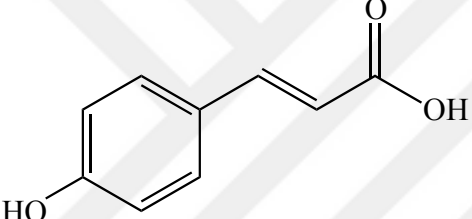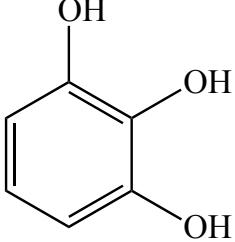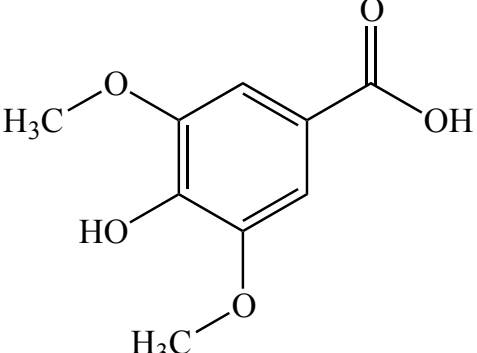
Compound	Plant	Reference
Caffeic acid	*R. thyrsiflorus*	(99)
Floroglucinol	*R. thyrsiflorus*	(99)
Gallic acid	*R. thyrsiflorus* *R. dentatus*	(99) (170)
Hydroquinone	*R. thyrsiflorus*	(99)
Isovanillic acid	*R. dentatus*	(170)

Table 2.12. Simple phenols and phenolic acids in *Rumex* species (continued).

Compound	Plant	Reference
Orcinol	*R. patientia*	(94)
p-hydroxybenzoic acid	*R. japonicus* *R. thyrsiflorus*	(197) (99)
p-hydroxysinnamic acid	*R. dentatus*	(170)
Pyrogallol	*R. japonicus* *R. thyrsiflorus*	(197) (99)
Syringic acid	*R. japonicus* *R. marschallianus*	(197) (99)

2.2.6 Anthocyanidin and Leucoanthocyanidins

Table 2.13. Anthocyanidin and leucoanthocyanidin derivatives in *Rumex* species.
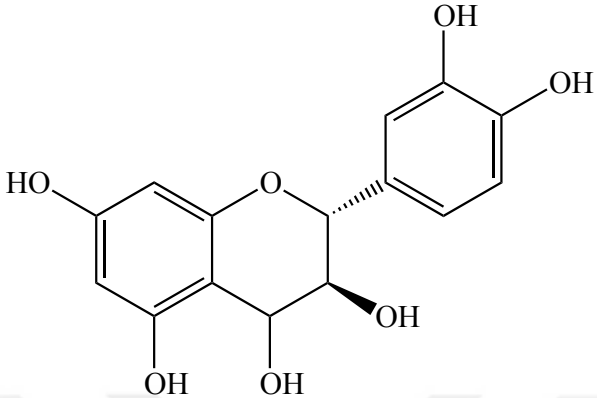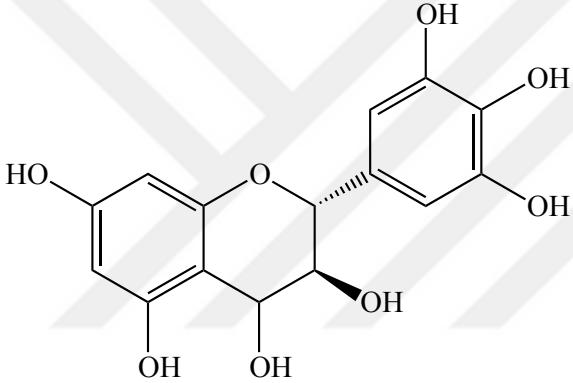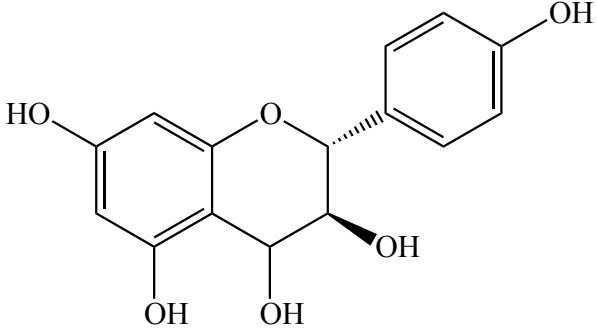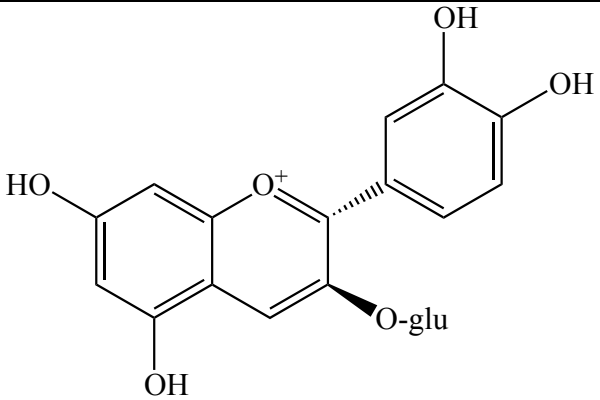
Compound	Plant	Reference
Leucoanthocyanidol	*R. confertus* *R. crispus* *R. hastatus* *R. hymenosepalus*	(210) (211) (156) (204)
Leucodelphinidol	*R. confertus*	(210)
Leucopelargonidol	*R. confertus*	(210)

Table 2.13. Anthocyanidin and leucoanthocyanidin derivatives in *Rumex* species (continued).

Compound	Plant	Reference
 Cyanidol-3-glucoside	*R. acetosa* *R. acetosella* *R. arifolius* *R. crispus* *R. obtusifolius* *R. thyrsiflorus*	(212) (212) (212) (212) (212) (159)

2.2.7 Coumarins
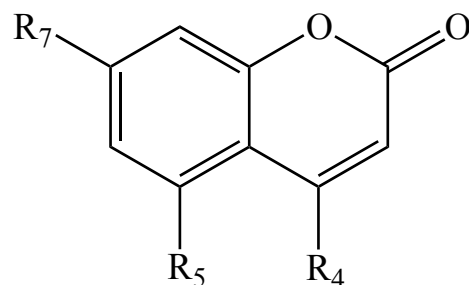
Table 2.14. Coumarin derivatives in *Rumex* species.

Substance	R_4	R_5	R_7	Plant	Reference
5,7-dhydroxycoumarin	H	OH	OH	*R. conglomeratus*	(213)
7-hydroxy-5-methyl-coumarin-4-*O-β*-D-glucopyranoside	O-glu	CH$_3$	OH	*R. hastatus*	(169)

In addition to the coumarins indicated above, the presence of coumarin derivatives in *Rumex acetosella* were also reported in previous studies (207, 208).

2.2.8 Saponins

Various *Rumex* species like *R. alpinus* (208)*, R. angustifolius* (208), *R. chalepensis* (214)*, R. conglomeratus* (208), *R. crispus* (208)*, R. gracilescens* (208)*, R. hastatus* (215), *R. nervosus* (216, 217), *R. patientia* (208)*, R. sanguineus* (208) and *R. vesicarius* (214), *R. sagittatus* (218) were reported to have saponins in their phytochemical composition.

2.2.9 Stilbene Derivatives
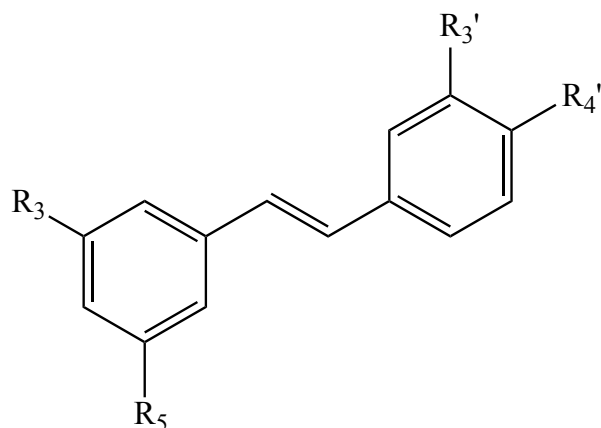
Table 2.15. Stilbene derivatives in *Rumex* species.

Compound	R$_3$	R$_5$	R$_3$'	R$_4$'	Plant	Reference
5-[(*E*)-2-(4-hydroxyphenyl)ethenyl]-1,3-benzenediol	OH	OH	H	OH	*R. hymenosepalus*	(90)
4-[(*E*)-2-(3,5-dihydroxyphenyl)ethenyl]-1,2-benzenediol	OH	OH	OH	OH	*R. hymenosepalus*	(90)
4-[(*E*)-2-(3,5-dihydroxyphenyl)ethenyl]-phenylhexopyranoside	OH	OH	H	O-glu	*R. hymenosepalus*	(90)
4-[(*E*)-2-(3,5-dihydroxyphenyl)ethenyl]-2-hydroxyphenylhexopyrano-side	OH	OH	OH	O-glu	*R. hymenosepalus*	(90)
3,5-dihydroxy-4'-methoxystilbene	OH	OH	H	OCH$_3$	*R. bucephalophorus*	(219)
5,4'-dihydroxy-3-methoxystilbene	OCH$_3$	OH	H	OH	*R. bucephalophorus*	(219)
Piceid	O-glu	OH	H	OH	*R. aquaticus* / *R. bucephalophorus* / *R. gmelini*	(128) / (220) / (127)
Rhapontin	O-glu	OH	OH	OCH$_3$	*R. crispus* / *R. gmelini* / *R. japonicus* / *R. nepalensis* / *R. patientia* / *R. obtusifolius*	(221) / (221) / (221) / (221) / (221) / (221)
Resveratrol	OH	OH	H	OH	*R. aquaticus* / *R. bucephalophorus* / *R. gmelini* / *R. hastatus*	(128) / (219, 220) / (74) / (169)
Rumexoid	O-α-ara	OH	H	OH	*R. bucephalophorus*	(220)

2.2.10 Sterol Derivatives

Table 2.16. Sterol derivatives in *Rumex* species.
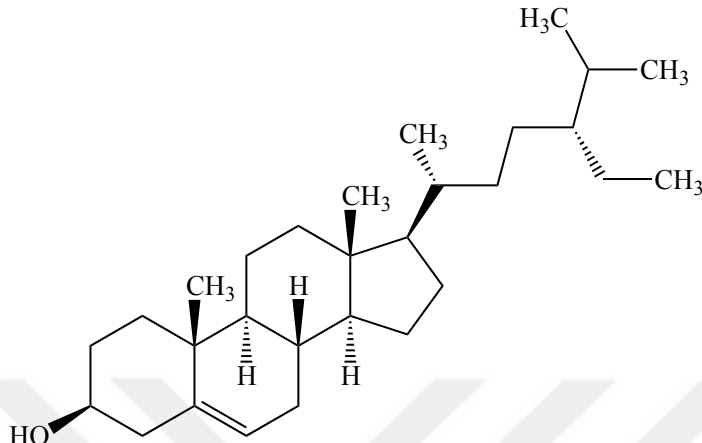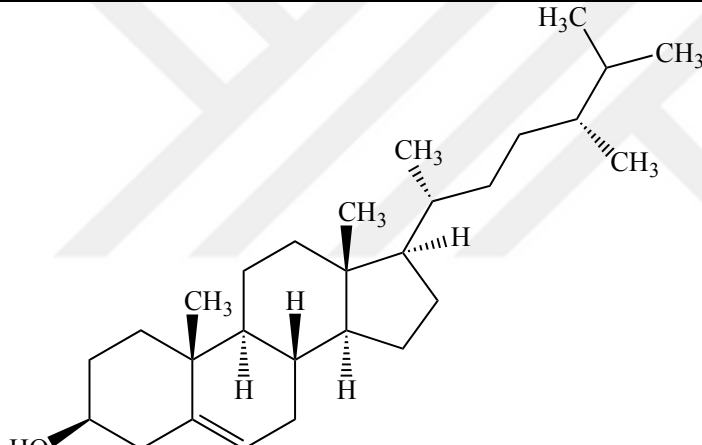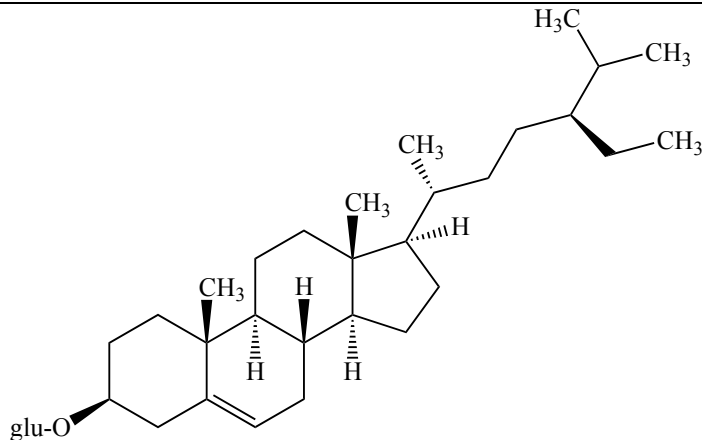
Compound	Plant	Reference
β-sitosterol	*R. crispus* *R. dentatus* *R. hastatus* *R. hymenosepalus* *R. maritimus* *R. orientalis* *R. japonicus* *R. maritimus* *R. nepalensis* *R. patientia* *R. paulsenianus* *R. pictus* *R. vesicarius* *R. thyrsiflorus*	(122) (170, 171) (156) (74) (222) (74, 185) (74) (74) (74) (74) (74, 223) (224) (224) (225)
Campesterol	*R. paulsenianus* *R. pictus* *R. vesicarius*	(223) (224) (224)
Daucosterol	*R. dentatus* *R. patientia*	(170) (146)

Table 2.16. Sterol derivatives in *Rumex* species (continued).
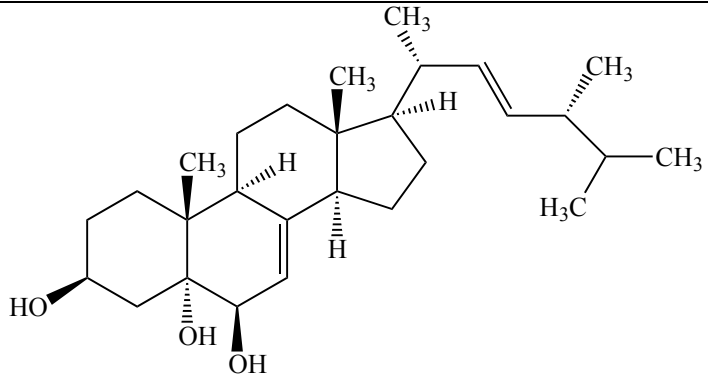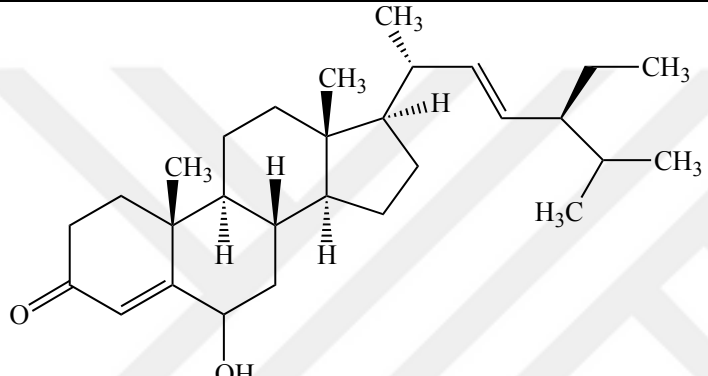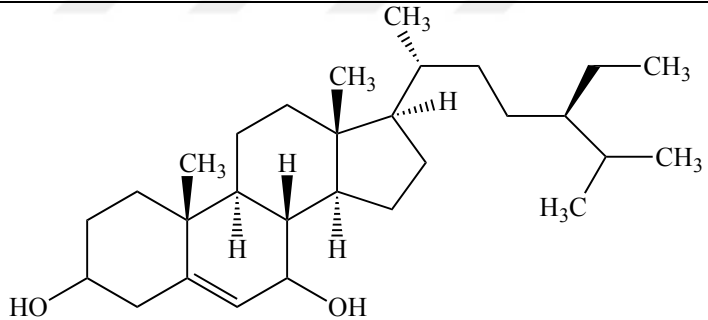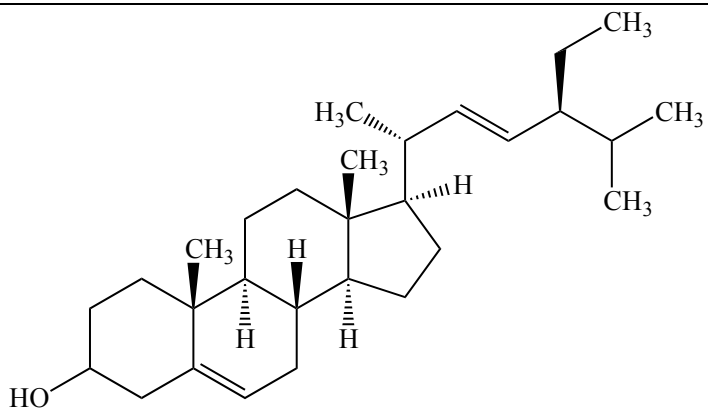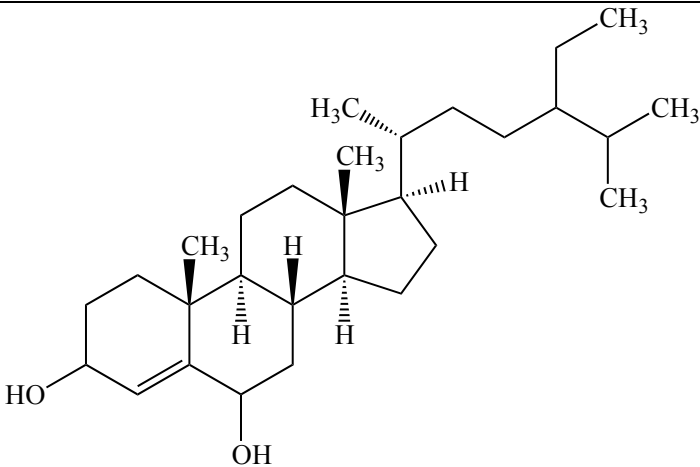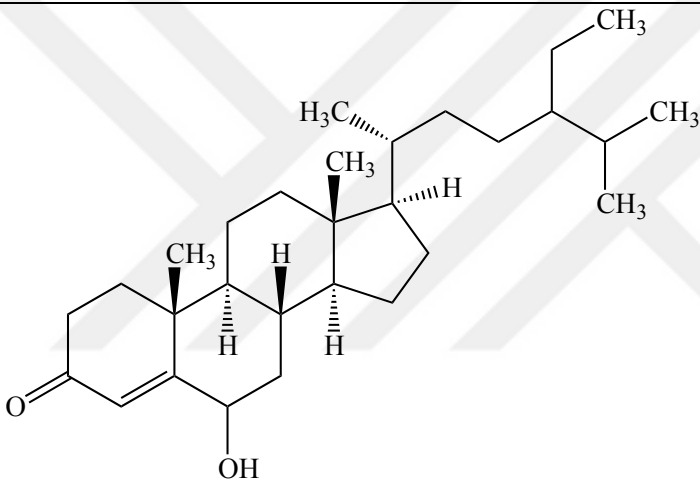
Compound	Plant	Reference
(22*E*,24R)-ergosta-7,22-dien-3*β*,5*α*,6*β* -triol	*R. patientia*	(146)
6-hydroxystigmasta-4,22-dien-3-on	*R. patientia*	(146)
7-hydroxysterol	*R. patientia*	(146)
Stigmasterol	*R. paulsenianus* *R. pictus* *R. vesicarius*	(223) (224) (177, 224)

Table 2.16. Sterol derivatives in *Rumex* species (continued).

Compound	Plant	Reference
Stigmast-4-en-3β,6β-diol	*R. patientia*	(146)
Stigmast-4-en-6α-ol-3-one	*R. patientia*	(146)

In addition to the sterol derivatives indicated above, a steroidal diglucoside stigmasta-5-en-3-ol-3-*O*-β-D-glucopyranosido-(4→1")-*O*-β-D-glucopyranoside, α- and β-amyrin from *R. vesicarius* (177, 224), β-sitosterol-β-D-glucoside from *R. maritimus* (74) and α- and β-amyrin and taraxasterol from *R. pictus* (224) were isolated.

2.2.11 Fixed and Essential oils

Lipids from *Rumex acetosa* (74, 226)*,* the fatty acid glycerides and essential oil compositions from *R. vesicarius* (177, 227, 228), essential oil from *R. japonicus* (229)*,* essential oil from *R. hastatus* (230), fatty acid and essential oil compositions from *R. dentatus* (227)*,* lipids from *R. confertus* (231), fatty acids from *R. pseudonatronatus* (232), fats and oils from *R. nervosus* (217), essential oils from *R. crispus* and *R. cristatus* (233), lipids from *R. pauselnianus* (223), and essential oil from *R. chalepensis* (234) were reported in previous studies.

2.2.12 Alkaloids

The presence of alkaloids in *Rumex nervosus* (217), *R. vesicarius* (235), *R. dentatus* (236), *R. sagittatus* (218), *R. obtusifolius* (237) and *R. pictus* (238), were reported in previous studies.

2.2.13 Other Substances

Rumex thyrsiflorus, R. pamiricus, R. pseudonatronatus, R. aquaticus, R. marschallianus, R. rossicus, R. maritimus were shown to include aminoacids (phenylalanine, proline, alanine, threonine, tryptophan, glutamine, arginine, serine, glutamic acid, histidine, lysine) (99) and essential aminoacids (226).

R. thyrsiflorus was reported to have carbonhydrates as glucose, galactose, rhamnose, fructose, saccharose (99).

$2\alpha,3\alpha,19\alpha$-trihydroxy-24-norurs-4(23),12-dien-28-oic acid, myrianthic acid, tormentic acid and 4(R),23-epoxy-$2\alpha,3\alpha,19\alpha$-trihydroxy-24-norurs-12-en-28-oic acid, as ursane-type triterpenoids with and ethyl gallate as a phenolic compound were reported in *R. japonicus* (239).

Oxalic acid from *R. acetosa* (67, 240, 241), *R. induratus* (138), *R. crispus* (242), *R. acetosella* (67, 241), *R. obtusifolius* (243), were reported. Shikimic, malic, ascorbic and citric acids in *R. induratus* (161), malic and citric acids in *R. papillaris* and *R. pulcher* (244), high concentration of malic acid and other organic acids in *R. obtusifolius* (243) were identified.

Chlorophyl, *β*-carotene, lycopene in *R. vesicarius* (202), anhydrolutein I (all-*E*,3R,6'R)-3',4'-didehydro-beta,gamma-caroten-3-ol) and anhydrolutein II (all-*E*, 3R,6'S)-2',3'-didehydro-beta,epsilon-caroten-3-ol) in *R. rugosus* (245), orcinol in *R. patientia* (190), 2-acetylorcinol and its monoglucoside in *R. alpinus* (81), caffeic acid, 1-methylcaffeic acid, rumexin and 1-*O*-caffeoyl-*β*-D-glucopyranoside in *R. aquaticus* (120), vanillic acid, 2,6-dihydroxybenzoic acid, 4-hydroxybenzoic acid and 2,6-dimethoxy-4-hydroxybenzoic acid in *R. japonicus* (110), vanillic acid and sinapic acid in *R. acetosa* (246), 6-*O*-malonyl-*β*-methyl-D-glucopyranoside and ascorbalamic acid in *R. obtusifolius* (247), caffeoyl-hexoside, sinapoyl-hexoside, *p*-coumaroyl-hexoside isomers, feruloyl-hexoside in *R. induratus* (138), ascorbic acid in *R. maderensis* (172) and *R. papillaris* and *R. pulcher* (244), vitamins C with calcium mineral and *β*-carotene in *R. dentatus* (248), lyoniresinol 3*α*-*O*-*β*-D-glucopyranoside as a lignan derivative with orcinol-glucoside in *R. nepalensis* (130), ascorbic acid, tocopherol, mineral, protein, lipid, organic acid in *R. vesicarius* and *R. acetosella* (249-251), iron, sodium, calcium, potassium, magnesium in *R. acetosa* (226, 252), fatty acids with 22 and 24 carbon-chain lengths in *R. obtusifolius* (253), fatty acids having high polyunsaturated/saturated ratio in *R. pulcher* (254), lectins in *R. crispus* (255), polysaccharides in *R. acetosa* (256), phytoestrogens (257) and cytokines (258, 259) in *R. acetosella* were detected.

2.3   Utilisation of *Rumex* Species

2.3.1   *Rumex* Species as Foods

Various ethnobotanical and ethnopharmacological researches associated with *Rumex* genus reported that *R. acetosa* (260-262)*, R. acetosella* (260-263), *R. confertus* (261), *R. conglomeratus* (264) *, R. crispus* (263), *R. patientia* (263), *R. obtusifolius* (263), *R. scutatus* (264), *R. thyrsiflorus* (262), *R. tuberosus* (264), *R. vesicarius* (265) are consumed as green vegetables as well as, *R. acetosa* (266) as herbal tea and *R. hymenosepalus'*s roots as chewing gum (65) by local people.

The seeds of *R. hymenosepalus* (65) and *R. crispus* (267) crushes into flour to make pancakes.

Exceptionally, few species like *R. abyssinicus* and *R. hymenosepalus* may be used as colouring agents for foods (65, 268).

2.3.2   *Rumex* Species in Traditional Medicine

The leaves of *Rumex nepalensis* and *R. obtusifolius* are used to cover affected skin following injury (113, 269).

In Hungary and Romania, *R. acetosa, R. acetosella, R. confertus, R. obtusifolius, R. crispus*, and *R. alpinus* are applied for the treatment of constipation, diarrhoea, swellings, kidney disorders, sores, ringworm, rashes and wounds and as an astringent (12, 13, 270).

In Britain and Ireland, *R. conglomeratus*, *R. hydrolapathum* and *R. palustris* are used in scurvy, rashes and sunburn to bath and cancer cure. Furthermore the seeds of *R. obtusifolius* are applied to treat bronchitis, coughs and colds (66). *R. obtusifolius* is used as tonic, astringent, laxative and to treat sores and cancer in Ireland (271).

In Austria *R. alpinus* is used against viral infections (272), whereas *R. nervosus* as an ophthalmic antiseptic and a hypoglycaemic agent (43).

In Turkey, *R. scutatus* were reported to be used against fewer, *R. tuberosus* against hypertension, diuresis and constipation, as well as *R. tuberosus* for wound treatment, *R. acetosella* as analgesic and diuretic (11, 273-275) and *R. crispus* against constipation (116).

In Africa, *R. abyssinicus, R. usambarensis* and *R. bequaertii* are used for the treatment of stomach disorder, whereas *R. abyssinicus* is used to control diabetes, additionally as a diuretic, analgesic, antihypertensive agent (42, 268). In Ethiopia, *R. steudelii* is used as an antifertility agent as well as for healing several disorders (276). *R. nepalensis* is recorded to be used against stomach ache in Ethiopia (13) and *R. vesicarius* for the treatment of several diseases in Egypt (139).

In China, some *Rumex* species are used as herbal drugs, such as *R. dentatus* an as antibacterial and antifungal agent (85), *R. hastatus* against cough and fever (169), *R. dentatus* for the treatment of skin disorders, diarrhoea and constipation (131), *R. nepalensis* as purgative and for the treatment of colic and ulcers (113), *R. japonicus* against constipation and jaundice (178), *R. aquaticus* against infections, constipation and fever (277), *R. acetosa* as purgative and for the healing of cutaneous diseases (80), *R. maritimus* against burns and as tonic and aphrodisiac (278), *R. crispus* against skin problems and as tonic, astringent and cholagogue (267, 279), *R. dentatus* and *R. hastatus* against several diseases (280).

In American traditional medicine several *Rumex* species have been used for the treatment of different tumors types (16). Moreover, *Rumex* species were listed with their diverse effects in the Native American Ethnobotany (8).

R. acetosella has diverse traditional usage worldwide. Leaves of *R. acetosella* are eaten as vegetables (6-8), raw (8-10) or boiled (8, 10). They are freshly consumed by children (8, 281) as food, as well. The leaves of *R. acetosella* are used as analgesic and diuretic in Turkey (11). Plaster of steamed leaves are used for the treatment of warts and bruises in North America (Indians) and Romania (8, 12). Chewed fresh leaves are used as stomach aid in North America (Indians) (8), and aerial parts and seeds of the plant are used against diarrhoea in Hungary (13, 14). Aerial parts of the plant are also used against jaundice and fever as decoction in Iran (15). In American traditional folk medicine *R. acetosella* is reported to be applied for the treatment of different kinds of tumors (16). Furthermore, it is reported to have a long tradition in folk medicine for the treatment of different types of cancer (13, 17, 18), *e.g.* as component of Essiac tea (19) in different regions in the world. Leaves are published to be utilized in diabetes as raw or decoction in Turkey (44-47).

Traditional usages of *Rumex* species from different countries and regions are

summarized in **Table 2.17**. (13).

Table 2.17. Traditional usages of *Rumex* species from different countries and regions.

Plant	Plant parts	Traditional uses	Region	Reference
R. abyssinicus	Root	Stomach disorders	East Africa	(42)
	No data	Mild diabetes, analgesic, antihypertensive, diuretic, cancer	Ethiopia, Cameroon	(268, 282)
R. acetosa	No data	Mild purgative, jaundice, warts, cutaneous diseases, sore throat	Britain, Ireland and Korea	(66, 80)
	Root	Kidney disease, tenesmus, gonorrhoea dysentery, fever, skin itch, ulcer, scabies	Britain and Ireland	(66, 283)
	Leaf	Lack of appetite, fever, diarrhoea, worm, "blood cleanser"	Hungary and Romania	(12, 270)
	Leaf	Abscesses	South Africa	(64)
	Leaf	Bruises wounds, diarrhoea, warts,	North America	(8, 66)
R. acetosella	Leaf	Antidiabetic	Turkey	(44)
	Leaf	Analgesic, diuretic	Turkey	(11)
	Leaf	Warts, bruises	North America and Romania	(8, 12)
	Leaf	Stomach aid	North America	(8)
	Aerial part, seed	Diarrhoea	Hungary	(13, 14)
	Aerial part	Jaundice, fever	Iran	(15)
	Seed	Diarrhoea, dysentery	Hungary	(13)
	Whole plant	Cancer	America, Canada	(13, 17, 18)
R. alpinus	Root	Constipation	Hungary	(13)
	No data	Stomach problems	Bulgaria and Ukraine	(284)
	No data	Eczema, constipation, diarrhoea	Turkey	(284)
R. aquaticus	No data	Infections, diarrhoea, oedema, jaundice, constipation, fever	Far East	(285)

Table 2.17. Traditional usages of *Rumex* species from different countries and regions (continued).

Plant	Plant parts	Traditional uses	Region	Reference
R. bequaertii (syn. Rumex nepalensis Spreng.)	Root	Stomach disorder, cancer	East Africa and Cameroon	(42, 282)
R. chinensis (R. trisetifer Stokes)	Root, leaf	Acne, scalp scabies, constipation, vulvitis, contusion, eczema, prurigo, inflammation, scalp scabies,	Vietnam	(286)
R. confertus	Seed	Diarrhoea	Hungary	(13)
R. crispus	Root	Laxative, icterus, "blood cleanser", skin diseases, swellings, gastrointestinal tract ailments, bruises, rashes, burns, gonorrhea, venereal diseases, sores	Turkey, Britain, Ireland, Hungary and Indian tribes	(8, 13, 66, 116, 287, 288)
	Root	Swellings, sores	North America	(8)
	No data	Astringent, anthrax, purgative	South Africa	(13, 64)
	No data	Dysentery	North America	(8)
	Leaf	Eye infections, vermicide, antipyretic, expectorant, constipation, dizziness, antitussive	Taiwan	(13)
	Seed	Diarrhoea, wounds	Romania	(13)
	No data	Skin diseases, constipation, rheumatism, tonic, cough	Pakistan	(279)
R. dentatus	Root	Eczema, constipation, bacterial and fungal infections, diarrhoea	China	(85, 131)

Table 2.17. Traditional usages of *Rumex* species from different countries and regions (continued).

Plant	Plant parts	Traditional uses	Region	Reference
R. ecklonianus	No data	Astringent	India	(248)
	Root	Sterility, purgative, washing wounds and bruises	Southern Africa	(13, 64)
R. hastatus	Root, whole plant	Laxative, skin diseases, tonic agent, diuretic, bleeding of the lungs, against rheumatism, piles,	China	(169, 289)
	No data	AIDS, cough, headache, fever Astringent	India	(248)
R. hydrolapathum	Root	Scurvy, "blood purifier", astringent	Britain and Ireland	(66)
R. hymenosepalus	Leaf	Fever, cold, gastrointestinal disturbances sore	-	(8, 90)
	Root	Astringent, "purify the blood", wounds, skin irritation, cough, diarrhoea		(8, 13, 90)
R. japonicus	No data	Uterine haemorrhage, constipation, jaundice, haematemesis	China	(178)
R. madarensis	No data	Diuretic, dermatosis, "blood depurative"	-	(172)
R. maritimus	Leaf	Burns	-	(278)
	No data	Purgative	India	(248)
	Seed	Tonic, aphrodisiac , analgetic for the back and the lumbar region	India	(248, 278)
	Root	Purgative	India	(248)

Table 2.17. Traditional usages of *Rumex* species from different countries and regions (continued).

Plant	Plant parts	Traditional uses	Region	Reference
R. nepalensis	Root	Dysentery, Stomach ache, haemostasis, tinea, purgative	Ethiopia, China	(130)
	Root	Purgative	South Africa, India	(13, 248)
	Leaf	Syphilic ulcers, colic, skin disorders	North India, India, Afghanistan	(113, 248, 290)
	Leaf	Bilharziasis	South Africa	(13)
R. nervosus	No data	Wounds, acne, typhus, diabetes, ophthalmic antiseptic, eczema, rabies	-	(43)
R. obtusifolius	Aerial parts	Constipation	Hungary	(13)
	No data	Tonic, astringent, laxative, burns, antidote to nettle, blisters, sores, cancer, tumour	Ireland	(271)
	Root	Jaundice, skin eruption, blood purifier, contraceptive	Britain, Ireland and North America	(8, 66)
	Seed	Cough, colds, bronchitis	Britain and Ireland	(66)
R. patientia	Root	Constipation, dysentery	Hungary, North India, North America and Afghanistan	(8, 290)
	Root	Skin problems	North America	(8)
	Leaf	Wounds	Hungary	(8)
	Leaf	Anaemia	Serbia	(291)
	Leaf	Backache, rheumatism, fever, respiratory disorders, throat sores, skin diseases	North India, North America and Afghanistan	(8, 290)
	Shoot	Backache, rheumatism, skin diseases, fever	Afghanistan, North India	(290)
R. scutatus	No data	Antipyretic	Turkey	(11)
	Plant, leaf	Antiscorbutic, refrigerant, astringent	India	(248)
R. stenophyllus	Seed	Cough	Romania	(13)

Table 2.17. Traditional usages of *Rumex* species from different countries and regions (continued).

Plant	Plant parts	Traditional uses	Region	Reference
R. steudelii	Root	Haemorrhoids, antifertility, rectal prolapse, eczema, wounds, swelling, leprosy, tinea nigra, abdominal colic	Ethiopia	(276)
R. tuberosus	Leaf	Constipation, antihypertensive, wound healing	Turkey	(273, 274)
R. usambarensis	Root	Stomach disorders	East Africa	(13)
R. verticillatus	No data	Jaundice	North America	(292)
R. vesicarius	No data	Tonic, analgesic, constipation, hepatic diseases, bronchitis, dyspespsia, poor digestion, spleen disorders, flatulence, asthma, vomiting, alcoholism, piles	Egypt, India	(139)
	No data	Antidote to scorpion stings	Suudi Arabia	(142)
	Seed	Dysentery	India	(248)
R. woodii	No data	Diarrhoea	South Africa	(64)

2.4   Biological Activity Studies on *Rumex* Species

2.4.1   Cytotoxic, Antitumor and Anticancer Activities

The cytotoxicities of ethanol extracts of the roots, leaves and fruits of few *Rumex* species were examined against 1301 and EOL-1 as two human leukemic cell lines and the normal H9 as a derivative of T lymphoblastic cells. Roots of *R. confertus*, leaves of *R. obtusifolius* and fruits of *R. hydrolapathum* displayed the best cytotoxicity in their counterparts, which were [0.22mg/mL (1301) and 0.23 mg/mL (EOL-1)], [0.47 mg/mL (1301) and 0.44 mg/mL (EOL-1)] and [0.42mg/mL (1301) and 0.17 mg/mL (EOL-1)], respectively (38).

The absolute methanol and 80% methanol extracts of roots of *R. crispus* was shown to led to apoptosis on HT-29 cells in dose dependent manner and inhibited cell growth 40.1% ± 0.87 and 10.2% ± 1.03, respectively at 400 μg/mL (287).

27 species in Polygonaceae family growing in the Carpathian Basin were searched against human tumor cells in a previous study. The chloroform and n-hexane extracts of *R. acetosa* were shown to inhibit HeLa cells at 10 and 30 μg/mL as 77.7% and 97.0%, respectively. The chloroform and n-hexane extracts of *R. aquaticus* and *R. scutatus* were exhibited to inhibit cell growth of HeLa cells as 60.9% and 51.2%, respectively and of MCF7 cells as 69.3% and 56.2%, respectively at 30 μg/mL. Furthermore, *R. thyrsiflorus* was presented to induce growth inhibition on A431 cells as 96.2% and on MCF7 cells as 88.55% at 30 μg/mL (293).

Another study associated with the evaluation of cytotoxic activities of Cameroonian plants used in folk medicine revealed that *R. abyssinicus* and *R. bequaertii* exerted moderate cytotoxicity on melanoma WM35 (4.615 μg/mL and 22.29 μg/mL, respectively), ovary carcinoma A2780 (12.55 μg/mL and 14.44 μg/mL, respectively), cisplatin- resistant ovary carcinoma A2780cis (8.014 μg/mL and 29.31 μg/mL, respectively) and epidermal carcinoma A431 cells (6.715 μg/mL and 3.615 μg/mL, respectively) (282).

The alcoholic extract of *R. hymenosepalus'* roots were reported to exert antitumour activity in Walker 256 and sarcoma 180 test models in mice (203, 204).

R. acetosa polysaccharide (RA-P) was tested on female mice implanted with sarcoma 180 solid tumor to evaluate its antitumor activity, which revealed RA-P to

exert 88.1% inhibition at 100 mg/kg on the tumor via the complement system's activation, hepatic drug-metabolising enzymes' inhibition and the reticuloendothelial system's stimulation (256).

Kucekova et al. conceived the methanol extract of *R. acetosa* flowers to inhibit cell proliferation in a dose dependent manner on HaCaT human non-tumourigenic keratinocyte cells by MTT assay (246).

Lee et al. investigated the cytotoxicity of dicholoromethane extract of the aerial parts of *R. acetosa* with four anthraquinones yielded from the bioactivity guided fractionation of the extract. They tested cytotoxicity of those compounds and two synthetic derivatives against A549 (non-small cell lung), XF498 (central nervous system), SK-MEL-2 (melanoma), SK-OV-3 (ovary) and HCY15 (colon) human tumor cell lines. Emodin exerted a strong cytotoxicity with IC_{50} values of 3.32 μg/mL, 2.94 μg/mL, 3.64 μg/mL, 2.98 μg/mL and 3.10 μg/mL for A549, SK-OV-3, SK-MEL-2, XF498 and HCT15, respectively. The antimutagenic effect was also evaluated with SOS chromotest and Ames test on *Salmonella typhimurium* strains. Emodin further exerted the highest activity indicating its antigenotoxic effect (80).

Demirezer et al. searched the cytotoxicity of the compounds isolated from *R. patientia* towards HM02 (human melanoma), MCF (human breast carcinoma) and HEPG2 (human epidermoid carcinoma) cell lines. The compounds were anthraquinone derivatives, flavan derivatives and orcinol. None was shown to inhibit the growth of the cells (97). In a former study, Demirezer and Kuruuzum investigated the cytotoxicity of several *Rumex* species with brine shrimp assay and observed methanolic extract of *R. scutatus* as getting the best cytotoxicity. A further fractionation process yielded an containing emodin, chrysophanol, physcion and aloe emodin, which were shown to be active agents with the LC_{50} values of 0.01, 0.05, 0.15 μg/mL, respectively (76).

Zhang et al. investigated the cytotoxicities of chrysophanol with two naphthalene derivatives isolated from *R. dentatus* towards MCF-7 (breast cancer), A375 (melanoma), 7901 (gastric cancer) and SKOV-3 (oophoroma) cell lines. The study indicated that chrysophanol revealed a better antiproliferation activity than those of the other two naphthalene compounds (85).

Harshaw et al. researched the cytotoxicity of *R. obtusifolius* extract by brine shrimps lethality assay. Dichloromethane (1 mg/mL) and methanol (>1 mg/mL) extracts of the plant exhibited low cytotoxicity by comparison with podophyllotoxin as positive control (LD_{50}=2.80 10^{-3} mg/mL) (271).

R. acetosella containing Essiac tea used in homeopathic treatment of cancer was shown to inhibit the growth of cancerous prostate cells (LNCaP), Jurkat leukemia cells, MCF7 and MDA-MB-468 breast cancer cells in previous studies (294, 295).

Liang et al. conducted a research to detect cytotoxicity of several compounds isolated from *R. nepalensis* and *R. hastatus* towards five cell lines by MTT method, which were A549, H522 (lung cancer), MCF-7, MCF-10A and SKBR3 (breast cancer). Generally, the compounds didn't exhibit any cytotoxicity towards those cells except rumexneposide A, which presented extensive activity against lung and breast cancer cells. Furthermore, MCF-10A was shown to be sensitive to rumexneposide A, resveratrol, chrysophanol-8-*O*-*β*-D-(6′-*O*-acetyl)glucopyranoside and orientaloside (88).

Ahmad et al. researched the cytotoxicity of several solvent fractions of *R. hastatus* towards HeLa and NIH/3T3 cell lines. Chloroform fraction was observed as the best cytotoxic in all with IC_{50} values of 151.52 and 53.37 μg/mL against HeLa and NIH/3T3 respectively (296).

Kamal et al. conducted a study to determine the cytotoxicity of *R. hastatus* against brine shrimps. Saponins of *R. hastatus* were observed to have superb cytotoxicity against brine shrimps with the LC_{50} of 10 μg/mL as well as chloroform fractions having significant cytotoxicity with LC_{50} of 65 μg/mL. Furthermore, ethyl acetate and methanol extracts were shown to exhibit similar lethality with LC_{50} of 90 μg/mL, whereas aqueous and n-hexane fractions were evaluated as moderate with LC_{50} of 100 μg/mL and 390 μg/mL, respectively (297).

Wang et al. tested the cytotoxicity of physcion-8-*O*-*β*-glucopyranoside (298) from *R. japonicus* Houtt towards HCC (human hepatocellular carcinoma) by MTT assay. PG was found to inhibit growth of HCC cells via downregulation of DNA methyltransferase 1 (DNMT1) (299).

R. hastatus and its fractions were analyzed for their cytotoxic and antitumor activity by means of brine shrimp assay and potato disc assay, respectively. The cytotoxicity of *R. hastatus* were determined in the following order: BRR (n-butanol fraction) > MRR (methanol fraction) > CRR (chloroform fraction) > ARR (aqueous fraction) > ERR (ethyl acetate fraction) > HRR (*n*-hexane fraction). Antitumor activity of the roots of *R. hastatus* were stated in the following order: MRR > BRR > ARR > CRR > ERR > HRR.

2.4.2 Antidiabetic Activities

Degirmenci et al. conducted an investigation to detect antidiabetic potential of 2% decoction of *Rumex patientia* grain. The glucose and HbA1c levels of wistar albino rats injected with streptozotocin (STZ) were observed to be decreased by the decoction of the plant indicating its antidiabetic potential (300). Sedaghat et al. also investigated hypoglycemic effect of seeds of *R. patientia* on STZ-diabetic rats, which indicated serum glucose levels to be decreased in *R. patientia* treated cells at 2nd and 4th weeks by comparison with the untreated diabetics ($p< 0.05$ and $p< 0.01$, respectively) (301).

Shiwani et al. revealed absolute and 80% methanol extracts of the roots of *R. crispus* to inhibit α-glucosidase and α-amylase significantly ($p< 0.01$) by comparison with positive control acarbose (287).

Ahmed et al. conceived that methanol extract of *R. acetosella* and various fractions of the extract with diverse polarities (*n*-hexane, chloroform, ethyl acetate, *n*-butanol and residual water) exhibited better inhibition than acarbose ($IC_{50}= 1.20$ mg/mL) on α-amylase with the lowest IC_{50} value of 0.85 mg/mL of aqueous fraction (302) in all. Çakılcıoglu et al. investigated the plants decreasing blood sugar in Elazığ central district and reported *R. acetosella* to be used in folk medicine in the region (44, 45).

Yang et al. investigated the activities of anthraquinones from *R. patientia*, *R. nepalensis* and *R. hastatus* against diabetic nephropathy (DN). Chrysophanol, emodin, physcion, aloe-emodin, chrysophanol-8-*O*-β-D-glucopyranoside, emodin-8-*O*-β-D-(6)-*O*-acetyl)glucopyranoside, emodin-8-*O*-β-D-glucopyranoside, nepalenside A**,** patientoside A and patientoside B were shown to inhibit IL-6 secretion remarkably at 10 μM. Chrysophanol, emodin, physcion, nepalenside A**,** rumejaposide E and patientoside A were presented to inhibit extracellular matrix production at 10 μM, as well. Furthermore, all the compounds were expressed to be non-toxic at 10 μM indicating they might be good candidates as anti-DN drugs (89).

Kerem et al. investigated α-glucosidase inhibition potential of trans-resveratrol, piceid and rumexoid from *R. bucephalophorus*. *Trans*- resveratrol (58% at 0.1 mM) and rumexoid (57% 0.5 mM) were presented to inhibit α-glucosidase better than acarbose as positive control (35% at 0.5 mM). However, piceid was

observed to have no activity (220).

Reddy et al. performed a research based on determination of antihyperglycemic activity of ethanol extracts of *R. vesicarius*, which indicated that *R. vesicarius* notably dampen blood glucose level of streptozotocin induced rats. This was further confirmed by histopathological evaluation of pancreas (303).

Ha et al. researched the antidiabetic effect of nepodin from the roots of *R. japonicus*. Nepodin was conceived to supress enhancement of blood glucose levels during fasting and ameliorate glucose intolerance in a type 2 diabetic model of mice, (304).

2.4.3 Other Activity Studies

Rumex species were shown to have diverse biological activities in previous studies. The biological activities of *Rumex* genus are summarized in **Table 2.18.** below.

Table 2.18. Biological activities of *Rumex* species.

Biological activity	Plant	Reference
Analgesic	*R. abyssinicus*	(268)
	R. crispus	(305)
	R. madaio	(306)
	R. maritimus	(307)
	R. patientia	(308)
Antiallergic	*R. acetosa*	(309)
	R. crispus	(310)
Antiangiogenic	*R. hastatus*	(215)
Antibacterial	*R. aquaticus*	(311)
	R. crispus	(94)
	R. chalepensis	(312)
	R. confertus	(313)
	R. hymenosepalus	(90)
	R. japonicus	(197)
	R. obtusifolius	(271, 314)
	R. patientia	(315)
	R. thyrsiflorus	(311)
	R. vesicarius	(316)
Anticancer	*R. abyssinicus*	(282)
	R. acetosa	(293)
	R. bequaertii	(282)
Anticholinesterase	*R. hastatus*	(230)
	R. patientia	(43)
Antidiabetic	*R. acetosella*	(45, 302)
	R. crispus	(287)
	R. patientia	(300, 301, 317)
Antidiarrheal	*R. maritimus*	(278)
Antifungal	*R. acetosa*	(318, 319)
	R. andreaeanus	(318)
	R. crispus	(182, 320)
	R. cyprius	(321)
	R. japonicus	(318, 320)
	R. maritimus	(222)
Antihelmentic	*R. abyssinicus*	(322, 323)
	R. dentatus	(324)
Antihistaminic	*R. nepalensis*	(325, 326)
Antihyperlipidemic	*R. patientia*	(301)

Table 2.18. Biological activities of *Rumex* species (continued).

Biological activity	Plant	Reference
Antiinflamatory	*R. abyssinicus*	(43, 327)
	R. alpinus	(272)
	R. crispus	(305)
	R. hastatus	(328)
	R. nervosus	(43, 137)
	R. nepalensis	(113)
	R. obtusifloius	(329)
	R. patientia	(315, 330, 331)
	R. vesicarius	(298, 332)
Antimalarial	*R. abyssinicus*	(333)
	R. crispus	(334)
Antimicrobial	*R. abyssinicus*	(43)
	R. acetosa	(335)
	R. acetosella	(335, 336)
	R. crispus	(335, 337-339)
	R. confertus	(335)
	R. dentatus	(340)
	R. hydrolapathum	(335)
	R. abyssinicus	(43)
	R. bequaertii	(282)
	R. dentatus	(236, 341)
	R. japonicus	(180)
	R. nervosus	(43)
	R. obtusifolius	(335)
	R. scutatus	(136)
	R. vesicarius	(342)
Antimutagenic	*R. acetosa*	(80)
Antinociceptive	*R. hastatus*	(328)
Antioxidant	*R. abyssinicus*	(282)
	R. acetosa	(343-345)
	R. acetosella	(346-349)
	R. crispus	(287, 338, 339, 350, 351)
	R. confertus	(313)
	R. conglomeratus	(352)
	R. cyprius	(353)
	R. dentatus	(354)
	R. hastatus	(230, 355)
	R. japonicus	(172, 183, 197)
	R. nepalensis	(113)
	R. obtusifolius	(271)
	R. palustris	(356)
	R. patientia	(331, 347, 357, 358)
	R. scutatus	(136)
	R. thyrsiflorus	(359, 360)
	R. vesicarius	(139, 142, 202, 316, 361)

Table 2.18. Biological activities of *Rumex* species (continued).

Biological activity	Plant	Reference
Antipyretic	*R. madaio*	(306)
	R. patientia	(308)
	R. hastatus	(328)
Antitumoral	*R. abyssinicus*	(362)
	R. confertus	(13, 38)
	R. crispus	(13, 38)
	R. hastatus	(215)
	R. hydrolapathum	(13, 38)
	R. hymenosepalus	(204)
	R. obtusifolius	(13, 38)
Antiulcerogenic	*R. patientia*	(363)
Antiviral	*R. acetosa*	(196)
	R. bequaertii	(364)
	R. cyprius	(365)
	R. dentatus	(354)
	R. hastatus	(366)
	R. obtusifolius	(367)
	R. nervosus	(43)
	R. usambarensis	(368)
Capillary permeability inhibitor	*R. patientia*	(369)
Chemopreventor	*R. abyssinicus*	(69)
Collagenous tissue restorative activity	*R. crispus*	(151)
Cytotoxic	*R. acetosa*	(38, 80, 345)
	R. acetosella	(38)
	R. angustifolius	(76)
	R. crispus	(38, 76, 287, 370)
	R. confertus	(38)
	R. hydrolapathum	(38)
	R. obtusifolius	(38, 367)
	R. patientia	(76)
	R. scutatus	(76)
Diuretic	*R. abyssinicus*	(268)
	R. vesicarius	(371)
DNA protection ability	*R. crispus*	(287)
Gastroprotective effect	*R. acetosa*	(372)
	R. aquaticus	(277, 373, 374)
	R. patientia	(363, 375)
Hematologic	*R. acetosa*	(376)
	R. crispus	(255)
	R. japonicus	(377, 378)
Hepatoprotective effect	*R. crispus*	(305)
	R. dentatus	(175)
	R. patientia	(175)
	R. vesicarius	(139)

Table 2.18. Biological activities of *Rumex* species (continued).

Biological activity	Plant	Reference
Laxative	*R. alpinus*	(379)
	R. chalepensis	(379)
	R. crispus	(379)
	R. cristatus	(379)
	R. obtusifolius	(379)
	R. pulcher	(379)
	R. sanguineus	(379)
Neuroprotective	*R. aquaticus*	(173)
Psychopharmacological effect	*R. nepalensis*	(380)
Vasoconstructor	*R. confertus*	(381)
Vasorelaxant	*R. acetosa*	(382)
Xantine oxidase inhitor	*R. acetosella*	(383)

2.4.4 Biological Activities of *R. acetosella*

Ethanol extract of *Rumex acetosella* was shown to have strong antioxidant capacity by phosphomolybdenum, *β*-carotene bleaching, radical scavenging (DPPH, ABTS and NO radicals), reducing power (CUPRAC and FRAP) and metal chelating assays. Total flavonol content of *R. acetosella* was 338.10 mg (QAEs/g extract), implying a potent correlation between the phytochemical profile and antioxidant activity. Acetyl cholinesterase (mg galantamine equivalent/g extract), butyryl cholinesterase (mg galantamine equivalent/g extract), *α*-amylase (mmol acarbose equivalent/g extract) and *α*-glucosidase inhibitory effect (mmol acarbose equivalent/g extract) of the extract followed as 4.84 ± 0.12, 15.27 ± 1.93, 0.77 ± 0.06 and 3.40 ± 0.04, respectively and flavonol content was detected as 338.10 mg quercetin equivalent/ g extract (347). In another study, antioxidant capacities of the edible plants in the Black Sea Region of Turkey were investigated. *R acetosella* was shown as a great source of antioxidants with 15000 μmol *α*-tocopherol equivalent/g extract (349). Furthermore, ethanol extracts of wild and cultivated *R. acetosella* were investigated to detect phenolic content with antiradical and antioxidant effects in a previous study. Wild *R. acetosella* was observed to have higher phenolic content (69.21 ± 8.5 gallic acid equivalent/g extract) than its cultivated form (57.57 ± 1.8 mg gallic acid equivalent/g extract), better antiradical activity (wild type inhibited lipid peroxidation and DPPH radical with the EC_{50} values of 0.02 and 3.67 mg/mL, respectively, whereas cultivated type inhibited them with the EC_{50} values of 0.76 and 21.94 mg/mL, respectively) and better antioxidant activity (for wild and cultivated type of *R. acetosella,* the reduction potentials were detected as 59.4% and 56.2%, respectively at 1 mg/mL) (346).

Methanol-water and *n*-hexane extracts of *R. acetosella* were tested for their antimicrobial activity against Gram negative, Gram positive bacteria strains and fungal strains. Both extracts were displayed 64 μg/mL of MIC values against ATCC 1045 of *P. aeruginosa*, RSSK 02026 of *A. baumannii* and RSKK 538 of *S. enterititis* and ≥ 256 μg/mL of MIC values against isolated strains of each as Gram negative strains. Furthermore, both extracts presented 64 μg/mL of MIC values against 25923 of *S. aureus*, ATCC 29212 of *E. faecalis*, ATCC 6633 of *B. subtilis* and ≥ 256 μg/mL

of MIC values against isolated strains of each as Gram positive strains. MIC values of methanol-water and *n*-hexane extract of *R. acetosella* were determined for both as 16 μg/mL for ATCC 10231 of *C. albicans* and 32 and 64 μg/mL for ATCC 6258 of *C. krusei*, respectively, indicating antimicrobial activity of the plant (336). In another study, ethanol extract of the fruits of *R. acetosella* was shown to possess no activity against *T. menthagrophytes* and *A. niger* whereas anticandidal effects of some extracts were observed at 500 μg/mL (335).

In a previous study, xanthine oxidase (XO) inhibitory effects of Polygonaceae plants in Carpathian Basin were researched. Among the plants investigated, *R. acetosella* was shown to display notable XO inhibitory activity as 21.45 ± 4.02 μg/mL (*n*-hexane partition from 50% methanol extract of whole plant), 83.29 ± 2.01 μg/mL (chloroform partition from 50% methanol extract of whole plant), 61.03 ± 2.15 μg/mL (the residual 50% methanol extract of the whole plant), 33.13 ± 1.75 μg/mL (water extract of the main methanol extract of whole plant) at 400 μg/mL. Particularly the chloroform partition of the plant displayed high activity against XO with the IC_{50} value of 19.3 μg/mL (383).

The ethanol extracts of roots, leaves and fruits of *R. acetosella* were investigated against 1301 and H-9 cell lines to determine their cytotoxicity. The extracts were exhibited low cytotoxicity against 1301 cells (IC_{50}= 1.56-2.56 mg/mL), whereas the root, leave and fruit extracts have better apoptotic activity on H-9 cells (IC_{50}= 0.99, 1.83, 1 mg/mL, respectively) (38).

Ethanol extract of the roots of *R. acetosella* was shown to exhibit moderate inhibition on CYP3A4 ve CYP19 enzymes, which are important for drug metabolism (384).

R. acetosella was presented to have notable phytotoxicity and inhibit germination of Scots pine due to high contents of phenolic compounds. Shoots and roots extracts of *R. acetosella* of the 2-year-old clear-cuts decreased mean germination by 70% and 82%, respectively, indicating *R. acetosella* to affect the action of natural reforestation (385).

2.5 General Information About Cancer

World and Health Organization describes cancer as "Cancer is a generic term for a broad group of diseases characterized by the growth of abnormal cells beyond their usual boundaries that can then invade adjoining parts of the body and/or spread to other organs". Cancers can be named as malignant tumors or neoplasms (386).

Cancer is one of the leading cause of death worldwide. In 2012, 14.1 millon people were diagnosed with cancer (33) and new cases with cancer is predicted to ascend by 70% over the next 20 years (34).

According to the statistics published by IARC (International Agency for Research on Cancer)/WHO, cancer incidence is higher in Australia/New Zeland, Northern America and Europe than that of other regions of the world shown in **Figure 2.2.** (33). Among men, lung, prostate, colorectal, stomach and liver cancers were monitored as the most common cancers, while breast, colorectal, lung, cervix and stomach cancers were substantially common in women (386).

Age, alcohol, cancer-causing substances, chronic inflammation, diet, hormones, immunosuppression, infectious agents, tobacco, obesity, sunlight and radiation were identified as the most known or suspected risk factors for development of cancer in previous studies (387). Genes also have significant role in development of cancer. Genetic alterations and mutations in tumor suppressor genes or oncogenes are considered to responsible for cancer development (388).

Despite notable improvements in cancer research in the past few decades, many cancer patients still cannot be cured due to the development of drug resistance, which decreases the success of chemotherapy- a mainstay for cancer treatment (35). The response of tumor cells to cytotoxic agents is frequently determined by multiple factors (36, 37). To gain deeper insight into the multifactorial nature of cellular response to drugs is a significant approach to overcome cancer.

Figure 2.2. Worldwide cancer incidence.

2.6 Cancer Treatment

Surgery, chemotheraphy, radiotheraphy, cancer drugs, hormone theraphy, biological theraphy, bisphosphonates, bone marrow and stem cell transplants, complementary and alternative therapies, palliative treatment and other treatments are main treatment regimes for cancer.

2.6.1 Surgery

Surgery is a way to remove tumor entirely or partly from the patient's body by surgeons with thin knives called scalpels. Cryosurgery, lasers, hyperthermia and photodynamic theraphy are additionally alternative approaches to eradicate tumors from the body without scalpels. Cryosurgery (cryotheraphy) is a technic based on destruction of abnormal tissue by excessive cold caused by liquid nitrogen or argon. Lasers are strong beams of light cutting tumors from tissue and shrinking or destroying tumors. Hyperthermia is a method exposing small areas of body to high temperatures that causes destruction of tumor or makes tumors more sensitive to chemotheraphy or radiotheraphy. Photodynamic theraphy utilizes drugs which becomes active by a certain types of light. When tumors are subjected to that light, drugs turn to active form and kill abnormal tissue around (389).

2.6.2 Radiotheraphy (Radiation Treatment)

Radiotherapy is a way to cure cancer via radiation that kills cells with cancer or causes tumors to shrink. High doses radiation theraphy damages DNA of cancer cells, thus leading cells to stop growth and dividing and to die. Adequate DNA damage for cancer cells to die takes days or weeks of the treatment. Following the ending of treatment, death of cancer cells occupies time from several weeks to months. External beam and internal radiotheraphy are two types of radiation theraphy. External beam radiation theraphy cures the specific part of the body with tumor directing radiation from a machine to outside of the body, while internal radiotheraphy put solid or liquid radiation source inside the body. Application of solid radiotherapeutic in internal radiotheraphy is named brachytheraphy and a kind

of local treatment, whereas internal radiation theraphy with a liquid radiotherapeutic is called systemic theraphy (390).

2.6.3 Chemotheraphy

Chemotheraphy is a way to cure cancer by using drugs, thus laeding death of cancer cells (391). Detailed knowledge is indicated below under the title of "Chemotheraphy".

2.6.4 Immunotheraphy

Immunotheraphy as a kind of biological theraphy assist immun system to fight with cancer. It comprises substances like white blood cells and tissues or organs of lymph system. Types of immunotheraphy include monoclonal antibodies, adoptive cell transfer, cytokines, treatment vaccines and BCG (392).

Monoclonal Antibodies

Monoclonal antibodies specifically bind to a certain target causing immune response to fight with cancer cells. In targeted theraphy as a type of theraphy with monoclonal antibodies, other types of monoclonal antibodies mark cancer cells so that immune system can easily identicate and destroy them (392).

Adoptive Cell Transfer

Adoptive cell transfer is a way promoting natural ability of T cells to cope with cancer. Researchers exclude the most active T cells against the cancer from the tumor or modify the gene in them to make them stronger to demolish cancer cells. Following researches may grow these T lines in the laboratories (392).

Cytokines

Cytokines are proteins produced in the body taking a part to present immune response against cancer cells. Interferons and interleukins are two principal cytokines used in cancer treatment (392)

Treatment Vaccines

The vaccines are applied to combat against cancer by boosting immune response to cancer cells (392).

BCG

BCG (Bacillus Calmette-Guerin) is a weakened form of the bacteria causing tubeculosis and used for the treatment of bladder cancer inducing immune response (392).

2.6.5 Targeted Theraphy

Targeted theraphy is a kind of cancer treatment targeting differences in cancer cells and other cells around cancer cells that help them grow and thrive (393). Further information is provided under the title of "Chemotheraphy- Targeted cancer theraphy".

2.6.6 Hormone Theraphy

Hormone theraphy (hormonal theraphy, hormone treatment) is a way to fight with cancer that damps or ceases growth of cancer cells standing hormones for their growth. It may be referred not only for the treatment but also for easing cancer symptoms in patients with prostate cancer who can't have a chance to have a surgery or radiation theraphy (394).

2.6.7 Stem Cell Transplant

Stem cell transplants are operations to regenerate blood-forming stem cells in people with destroyed blood-forming stem cells as a result of chemotheraphy or radiotheraphy. Mainly blood-forming stem cells form white blood cells, red blood cells as well as platelets. Stem cell transplant can work either indirectly to recover patient's ability to produce blood-forming stem cells or directly in multiple myeloma and leukemia as an effect of graft-versus-tumor to attack the tumor in the body (395).

2.6.8 Precision Medicine

Precision medicine (Personalized medicine) is a way to cure patients based on genetics of their tumors. Researchers are still going on the patients who were treated by the drugs targeting cancer-causing genetic alterations in their tumors. These drugs mostly known as targeted therapies some of which were approved by FDA (Food and Drug Administration). Though developments in this field go further everyday, it hasn't taken the place of routine theraphy applied for many patients. Since most of the drugs have been in clinical trials and needed time to be approved by an official agency as effective against a genetic change of a tumor (396). Further information is indicated under the title of "Targeted Cancer Theraphy" in the next page.

2.7 Chemotheraphy

Chemotheraphy (chemo) is a way to cure cancer by using drugs, thus leading death of cancer cells. Chemotheraphy is both used to treat cancer or ease cancer symptoms and performed as a single treatment or combinations of other treatments such as surgery, radiotheraphy and biological theraphy.

Chemotheraphy can be applied before surgery to make the tumor smaller (neoadjuvant theraphy), after surgery to remove debris of the tumor (adjuvant theraphy) or in case of metastasis. Chemotherapy may be given by mouth, injection, or infusion, or on the skin, depending on the type and stage of the cancer being treated (391).

2.7.1 Targeted Cancer Theraphy

Targeted theraphy is a kind of cancer treatment targeting differences in cancer cells and other cells around cancer cells that help them grow and thrive. Targeted theraphy comprises small molecule drugs and monoclonal antibodies. Small molecule drugs have ability to enter inside of the cells, since they are small enough, while monoclonal antibodies interact with the targets outer surface of the cancer cells. Targeted theraphy work against cancer by assisting immune system to demolish cancer cells, ending the growth of cancer cells, ending signals forming blood vessels, presenting cell-killing substances to cancer cells, causing cancer cell

death, preventing delivery of hormones to cancer cells, which need them to grow. There might be obstacles of application of targeted theraphy, since it can not be possible to develop drugs for each targets or cancer cells can gain resistance towards those drugs. Therefore other treatments such as chemotheraphy and radiotheraphy should be applied together with targeted theraphy as combination theraphy (393).

Targeted therapies (molecularly targeted drugs, molecularly targeted therapies, precision medicines) are drugs or substances preventing growth of cancer by interacting with special targets of the cancer cells, which are associated with growth, progression and spread of the cells.

Targeted therapies inventionally selected to interact with their specialized targets and mostly cytostatic, whereas others are cytotoxic to tumor cells. Drugs perform on their targets in targeted theraphy, while they act on both normal and cancerous cells in chemotheraphy. Targeted theraphy is a way to treat people in accordance with their genes and proteins as a basis of a precision medicine. There are several ways to detect targets for the application of targeted therapies. Quantity of genes or proteins in both normal and cancer cells is an approach. In case a gene or protein is high quantity in cancer cells, that may take into consideration as a possible target, particularly as for that they are associated with cell dividing and growth. Checking abnormalities in chromosomes and altered proteins in cancer cells may be other approaches for targeted theraphy (397).

2.7.2   Drug Resistance and Resistance Theraphy

Despite notable improvements in cancer research in the past few decades, many cancer patients still cannot be cured due to the development of drug resistance. Even worse, tumors frequently develop resistance not only to single drugs, but also to many drugs at the same time. This phenomenon was termed as multidrug resistance, which decreases the success of chemotherapy- a mainstay for cancer treatment. Drug resistance may grow during repeated treatment cycles after initially successful therapy (acquired or secondary resistance). Or else, tumors may gain resistance from the beginning (inherent or primary resistance) (35).

The mechanisms of secondary metabolism might be both genetic and non-genetic-welded (398, 399). Tumor cell heterogeneity is the main factor for genetic-

welded secondary resistance that genome gain resistance due to the fact that their genes have rapidly increasing mutations under drug treatment. This change results in mutation in drug targets and activation or inhibition of signaling components, which cause drug resistance. The mechanisms of non-genetic-welded secondary resistance were less examined than genetic-welded ones. Possible role of epigenetics, RNA splicing, metabolic alterations and certain protein modifications which are not induced via mutations may be substantial cause of non-genetic-welded secondary resistance (399).

One of the most important mechanisms having a significant role in drug resistance is increased number of drug efflux pumps. ATP binding cassette (ABC) transporters are mainly responsible for drug efflux. Numerous different anticancer drugs like taxanes, epidermal growth factor receptor inhibitors and topoisomerase inhibitors are recognized (400) and pumps out of the cells by ATP transporters (398), which are considered as a fundamental cause of MDR (401).

In human, at least 48 members of ABC transporter family were reported (402, 403) and 12 of whom were identified as possible drug transporters (403, 404). P-glycoprotein (MDR1/ABCB1), breast cancer resistance protein (BCRP/ABCG2) and MDR- associated protein 1 (MRP1/ABCC1) are known ABC transporters (403, 405). Oncogenes and tumor suppressor genes also confer drug resistance (406).

Drug resistance mechanisms are summarized in detail in **Figure 2.3.** (403) in addition to **Figure 2.4.** illustrating several of those mechanisms (407).
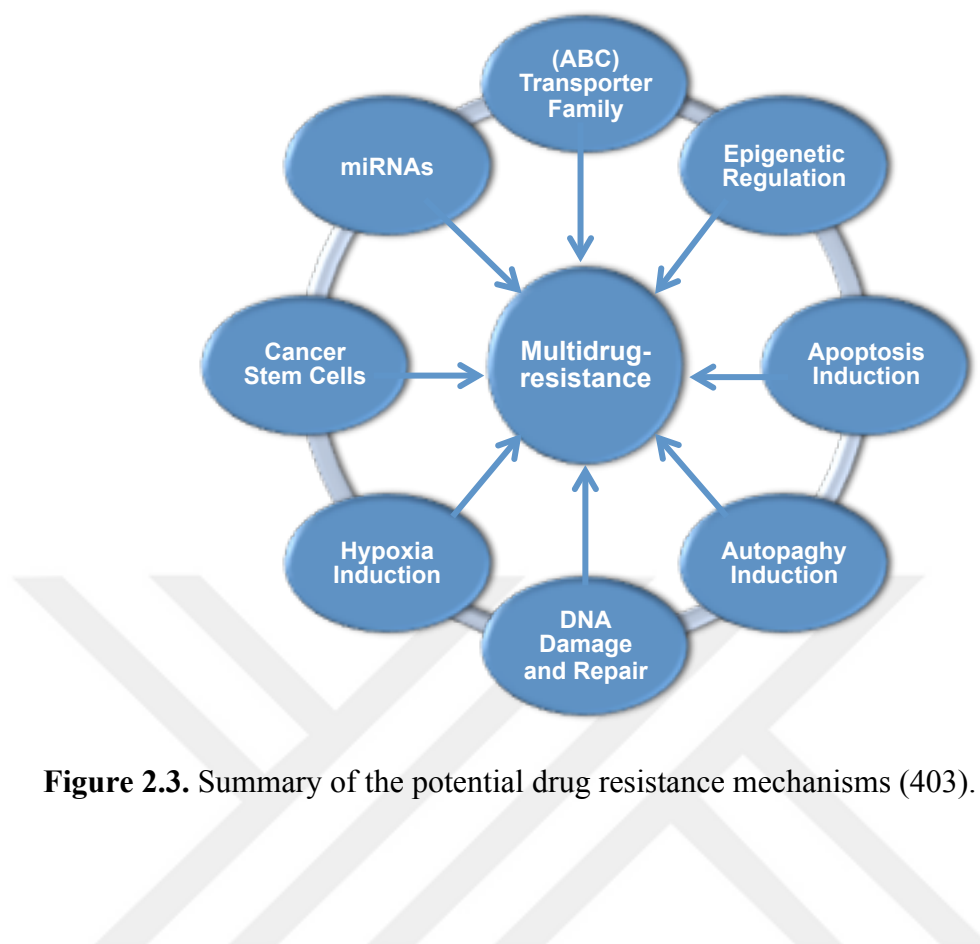
Figure 2.3. Summary of the potential drug resistance mechanisms (403).
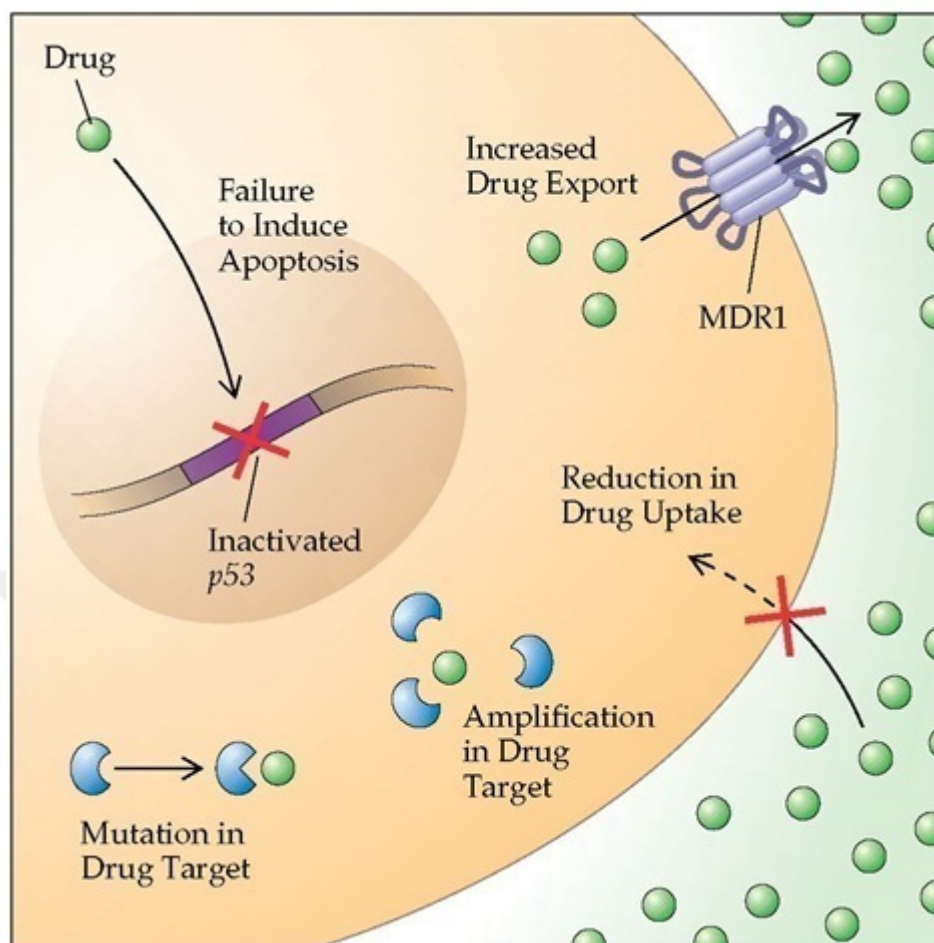
Figure 2.4. Illustration of several drug resistance mechanisms including mutations in the p53 gene, decreased drug uptake, enhanced drug export by MDR1-related proteins, a mutation or amplification in drug target (407).

Because cancer is a multifactorial disease and to overcome MDR, utilization of two or more drugs for the treatment (rational combination theraphy) is the best approach. Drugs with diverse mechanisms widen target range and improve therapeutic effectiveness and lessen possibility of drug resistance (408).

2.7.3 Natural Sources for Cancer Theraphy

Nature is an attractive source to get natural products or a substance in cancer. Naturally occurring chemical substances are generated by living organisms (409). The compounds involved in metabolism are generally the same, called primary metabolism products. Additionally, a broad spectrum of biochemical pathways may be indigenous for one or few species of organisms, even they might be only special for a particular level of differentiation of a specific cell, which is called as secondary metabolism and the compounds formed by secondary metabolism are known as secondary products (410). Secondary metabolism products have evolved depending on the ecological habitat secondary metabolism occurred so that they can protect themselves from challengers, herbivores and pathogens (411), which is also expressed as natural version of combinatorial chemistry (412).

Natural sources might have importance as potential drug candidates. Evidently, 69% of anticancer drugs approved between the 1980s and 2002 are either natural products or developed based on knowledge gained from natural substances (31) as natural compounds are indispensable not only as chemically established anticancer drugs (*e.g.* anthracyclines, *Vinca* alkaloids, taxanes, camptothecins etc.), but also as lead compounds for the development of novel targeted chemotherapeutics with improved antitumor efficacy and fewer side effects (32).

Anticancer effects of the compounds are numerous and varied due to the wide range of divereness of natural substances (409). As example, vinblastine as a destabilizing agent inhibits microtubule polymerization, while taxol as a stabilizing agent enhance microtubule polymerization, which means both suppress microtubule dynamics (413). Furthermore, camptothecin and podophyllotoxin derivatives act as topoisomerase inhibitors (414, 415). Several pathways affected by drugs are further associated with cancer development as we see in curcumin. Curcumin was reported to antagonize epidermal growth factor receptor (EFGR) on cell surface and incline apoptosis in human melanoma cells via Fas receptor and caspase-8 activation, targeting several pathways rather than only one target in a previous study (416). A natural product-derived drug temsirolimus was also reported to be approved as not only a cytotoxic drug, but also molecularly targeting agent and a mTOR protein

83

kinase inhibitor (417). As reported in previous studies, natural substances or derived products may show their effects on different targets, which is quite significant for natural sources to be advanced as a drug for the treatment of cancer, which is a multifactorial disease.

2.8 Anthraquinones and Their Derivatives

2.8.1 Sources, Structures and Biological Activities

An anthraquinone molecule is an aromatic organic compound and anthracene derivative with the chemical formula of $C_{14}H_8O_2$. Anthraquinones are seen as solid crystalline powder in nature with the colours ranged from yellow or light grey to grey-green. They melt at 286 °C and boil at 379.8 °C. Usually they are insoluble in water and alcohol while soluble in nitrobenzene and aniline being quite stable under normal conditions. Due to aglycon moieties, they can be observed as anthraquinone, anthranol, anthrone, dimers of anthrones or their derivatives (**Figure 2.5.)** (418).

anthranol   anthrone   dianthrone   anthraquinone
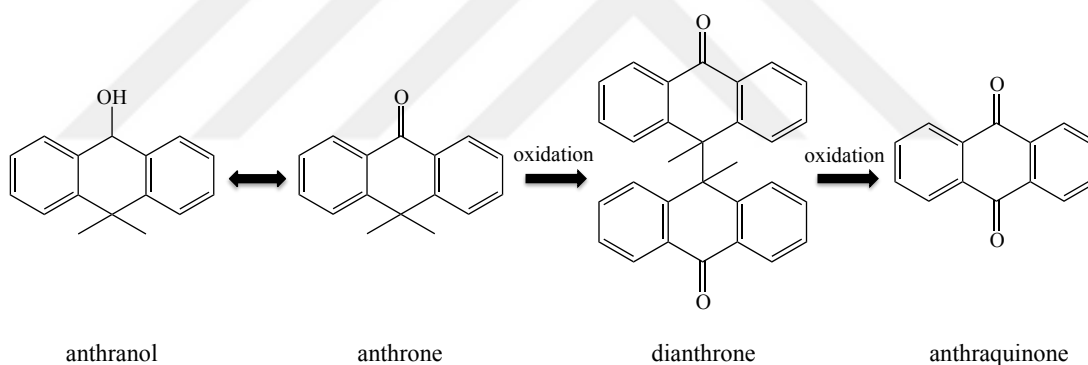
Figure 2.5. Oxidation steps of anthraquinones.

Borntraeger test is used to test the presence of anthracene glycosides. Generally, they are in the form of *O*-glycosides or *S*-glycosides. Their hydrolysis derivatives are obtained as 1,8-dihydroxy anthraquinones, anthranols, anthrones and dianthrones (418).

The main anthraquinone aglycones are chrysophanol, aloe-emodin, emodin, rhein (**Table 2.19**) and physcion which may prevail as anthranols, anthrones and anthraquinones. Glucose, arabinose and rhamnose are the sugars, for the anthroquinone derivatives which substantially observed in the glycosylated forms (418).
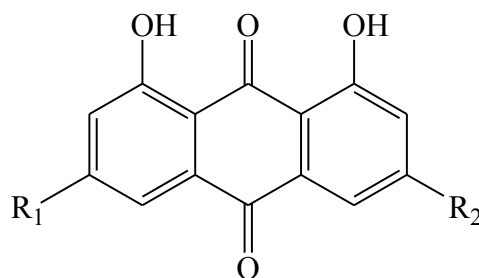
Table 2.19. The main anthraquinone aglycones.

Substance	R_1	R_2
Chrysophanol	CH_3	H
Aloe-emodin	CH_2OH	H
Rhein	COOH	H
Emodin	CH_3	OH
Physcion	CH_3	OCH_3

Naturally antraquinone derivatives generally have laxative effects, which are also colour pigments. Reduced anthraquinones are biologically more active and glycosidic derivatives are more active than oxidized aglycones, as well (418). Among the various chemical classes of natural products, anthraquinones are characterized by their large structural diversity, pronounced biological activity and low toxicity (20). Anthraquinones may occur in fungi, lichens, insects, and plants (418), recorded in the families of Fabaceae, Liliaceae, Polygonaceae, Rhamnaceae, Rubiaceae, and Scrophulariaceae (21).

Anthraquinones have diverse biological activities. They can be natural dyes (419) as well as they possess laxative (420, 421), anti-inflammatory and antiarthritic (422, 423), antioxidant (424, 425), virucidal (426-428), antileishmanial and antimalarial (429), antiosteoporotic (430), antimicrobial (428, 431-433), estrogenic (434), molluscicidal (435), phytoalexin (436), antifeedant (437) and photodynamic (438) properties. Furthermore, they were also reported to inhibit aldose reductase (439), RNA polymerase (440), DNA topoisomerase II (441), xanthine oxidase (442) enzyme activities and platelet aggregation (443) in previous studies.

2.8.2 Cytotoxic, Antitumor and Anticancer Effects

Anthraquinones were shown to inhibit proliferation or tumor growth of breast (22-24), lung (23), cervical (25), prostate (26), colon, central nervous system, glioma (23, 27), hepatoma (28) and leukemia cancers (29, 30) in previous studies. Furthermore, the structural similarity of anthraquinone aglycons to anthracyclines as well established anticancer drugs allows to speculate on their possible activities against cancer.

2.9   General Information About Diabetes Mellitus (DM)

According to World Health Organization (WHO), the global prevalence of diabetes was around 9% among adults in 2014 (444). WHO also asserts diabetes to be the 7th leading cause of death in 2030 (445).

DM may be otoimmmun-origined or idiopatic (Type I DM) as well as caused by insulin resistance or relative insulin deficiency (Type II DM). There are also specific types of diabet such as gestational diabetes, which comprises only small proportion of the disease. Patients with type II DM comprises large majority of the people (90-95%), while the rest are suffering from type I DM. Eyes, kidneys, hearts and vital organs of people living with long-lasting hyperglycemia are under risk (50).

Diabetes mellitus is a condition arising from abnormal metabolism of carbohydrate, which causes defects in insulin secretion, insulin action, or both. Various complications occur due to the metabolic imbalances by diabetes, affect all the vital organs in the body such as heart, kidneys, eyes, nerves and cause coronary artery disease, myocardial infarction, hypertension, peripheral vascular disease, retinopathy, neuropathy (446). Many studies emphasized the importance of glycemic control, which may intercept worse complication outcomes. Therefore, to monitore and control hyperglycemia is a significant approach to cope with related outcomes.

Treatment of type I diabet depends on insulin uptake, while type II diabet requires oral medication, foot care and insulin uptake in case of necessity (50). From this point of view, drugs preventing hyperglycemia may have importance.

Pancreatic α-amylase and intestinal α-glucosidases are starch hidrolyzing enzymes and cause hyperglycemia (52). Inhibitors of these enzymes delay carbonhydrate digestion and interrupt the increase in postprandial glucose in plasma (53), which indicates their potentials as antidiabetic agents (57).

α-amylase and α-glucosidase inhibitors may be significant agents for the development of new drugs in DM.

3. MATERIAL AND METHODS

3.1 Plant Material

Rumex acetosella was collected from Camlidere (Ankara, Turkey) in May 2013. A voucher specimen has been deposited in the Herbarium of Faculty of Pharmacy, Hacettepe University, Ankara, Turkey (HUEF: 13005).

3.2 Chemicals and Equipment

Anthraquinones were purchased from commercial sources to have adequate amounts for mechanistic studies. Aloe-emodin (purity (HPLC): min. 97 area %) was obtained from TCI Deutschland GmbH (Eschborn, Germany) and was dissolved in DMSO. Emodin (purity after HPLC ≥ 90%), physcion (purity after TLC ≥ 98% TLC) and rhein (technical grade) (Sigma, Turkey) were also dissolved in DMSO. TNF-α was obtained from Biotrend Chemikalien GmbH (Köln, Germany). Doxorubicin was provided by the University Hospital of Johannes Gutenberg University (Mainz, Germany).

DMEM medium (Life Technologies, Germany), RPMI 1640 medium (Life Technologies, Germany), Fetal Bovine Serum (FBS) (Life Technologies, Germany), Penicillin (10000 U/mL)/ Streptomycin (10000 μg/mL) (Life Technologies, Germany), Geneticin (Sigma Aldrich, Germany) were purchased for cytotoxicity researches.

α-amylase (Sigma, Turkey), α-glucosidase (Sigma, Turkey), acarbose (Sigma, Turkey), 2,2-diphenyl-1-picrylhydrazyl (Sigma, Turkey), sodium nitroprusside dihydrate (Sigma, Turkey), sulfanilamide (Sigma, Turkey), N-(1-naphthyl) ethylenediamine (Sigma, Turkey), 2,2-azino-bis (3-ethylbenzothiazoline-6-sulfonic acid) (Sigma, Turkey), potassium persulfate (Sigma, Turkey), 6-hydroxy-2,5,7,8-tetramethylchromane-2-carboxylic acid (Trolox) (Sigma, Turkey), ascorbic acid (Sigma, Turkey), ammonium molybdate (Sigma, Turkey), sodium phosphate (Sigma, Turkey) were purchased for enzyme assays.

n-Hexane (Sigma, Merck, Turkey), dichloromethane (Sigma, Merck, Turkey), *n*-butanol (Merck, Turkey), *t*-butanol (Carlo Erba, Turkey), ethylacetate

(Sigma, Merck, Turkey), chloroform (Sigma, Merck, Turkey), methanol (Merck, Riedel-De Haen, Turkey), sulfuric acid (Merck, Turkey), ethanol (Sigma, Merck, Turkey), phosphoric acid (Merck, Turkey) were purchased for purification of the compounds by chromatographic techniques.

Nuclear magnetic resonance (NMR) spectra were recorded on an Avance III 600 (Bruker) using 5 mm probe heads at a temperature of 23 °C. The ^{1}H and ^{13}C chemical shifts were referenced to the residual/deuterated solvent (*e.g.*, for MeOD, Sigma, Germany, δ = 3.31 and 49.00 ppm for ^{1}H and ^{13}C NMR, respectively) and reported in parts per million (ppm, δ) relative to tetramethylsilane (TMS, δ = 0.00 ppm). Coupling constants (*J*) are reported in Hz, and the splitting abbreviations used were: s, singlet; d, doublet; t, triplet; m, multiplet; br, broad; and combinations thereof. High-resolution masses (ESI) were recorded on a Q-ToF-Ultima 3 instrument (Waters) with LockSpray^{TM} interface and a suitable external calibrant. Optical rotations were measured with a Perkin–Elmer 241 polarimeter at 589 nm. Infrared spectra were recorded as FT-IR spectra on a Tensor 27 spectrometer (Bruker) using a diamond ATR unit and are reported in terms of frequency of absorption (v, cm^{-1}).

Normal phase column chromatography and reverse phase column chromatography were run on silica gel 60 (0.063-0.200 mm, Merck, Darmstadt, Germany) and RP-18 silica gel (40-63 μM, Merck, Darmstadt, Germany), respectively. Sephadex LH-20 (Sigma, Sweden) was used for separation of the compounds based on their molecular size. Thin layer chromatography (TLC) was applied on silica gel 60 F$_{254}$ precoated plates (Merck, Darmstadt, Germany). The spots were observed using an UV lamp at 254 and 365 nm, sprayed with 1% Vanilin/H$_2$SO$_4$ and then heated at 100-110 °C for detection.

Spraying Reagents for the Detection of Spots in TLC:

1% Vanilin/H$_2$SO$_4$: Solution of 1% of vanilin in 95-98% H$_2$SO$_4$ as (w/v). Following spraying, plate is heated at 110 °C for 1 to 2 minutes.

5% KOH: Solution of 5% of KOH in 50% (v/v) methanol solution as (w/v). Following spraying, plate is heated at 110 °C for 5 minutes. It is used for the detection of anthranoids.

3.3 Extraction

3.3.1 Extraction Procedures for Isolation of Pure Compounds

Roots of *Rumex acetosella* (529.68 g) were air dried, grinded and extracted with methanol (10 L × 7) at 40 °C under reflux for 72 h. The extract was filtered and evaporated under vacuum and 83.26 g crude extract was gained.

Normal phase silica gel column chromatography, reverse phase column chromatography including vacuum liquid chromatography (VLC) or medium pressure liquid chromatography (MPLC) and Sephadex column chromatography with isocratic CH_3OH elution were performed to isolate the pure substances.

3.3.2 Extraction Procedures for Enzyme Assays and Radical Scavenging Capacity Studies

Preparation of the Ethanol, Methanol, 70% Ethanol, 70% Methanol Extracts of Herbs and Roots of *Rumex acetosella*:

5 g of dried powdered roots and herbs were individually extracted twice with 50 mL of methanol, ethanol, 70% methanol and 70% ethanol, respectively for six hours stirring in a water bath at 40 °C to get the required extracts. The extracts were then filtered, and evaporated to dryness *in vacuo*. In addition, the herbal extracts were seperated from their lipids and pigments with petroleum ether extraction. Then, the extracts were dissolved in buffer solution to prepare the required concentrations for enzymatic and radical scavenging capacity studies.

Preparation of the Chloroform Extract of *Rumex acetosella* Herbs:

5 g of dried powdered herbs were extracted twice with 50 mL petroleum ether for six hours stirring in a water bath at 40 °C for removing chlorophylles. Then, the residue was extracted twice with 50 mL chloroform for six hours stirring in a water bath at 40 °C. The extract was then filtered, evaporated to dryness *in vacuo* and then dissolved in DMSO: buffer mixture to prepare the required concentrations for enzymatic and radical scavenging capacity studies.

Preparation of the Chloroform Extract of *Rumex acetosella* Roots:

5 g of dried powdered roots were extracted two times with 50 mL chloroform for six hours stirring in a water bath at 40 °C. The extract was then filtered, evaporated to dryness *in vacuo* and dissolved in DMSO: buffer mixture to prepare the required concentrations for enzymatic and radical scavenging capacity studies.

3.4   Antioxidant Capacity Assays

3.4.1   DPPH Radical Scavenging Activity

DPPH radical scavenging activity was conducted using a previously described method (447, 448). DPPH radical scavenging effect of the extracts were determined spectrophotometrically by the decolorization of a methanol solution of 2,2-diphenyl-1-picrylhydrazyl (DPPH). DPPH is a radical and in case of reacting with an antioxidant agent donating hydrogen, it is reduced to its nonradical form. A MeOH solution (200 µL) of the samples at various concentrations was added to a DPPH−MeOH solution. The absorbance of the remaining DPPH was measured at 520 nm after 30 min. The radical scavenging activity was determined by comparing the absorbance with that of blank (100%) containing only DPPH and solvent.

Radical scavenging activity (%)= ((A$_{control}$ −A$_{sample}$)/A$_{control}$)) x 100

A: Absorbance

3.4.2   ABTS Radical Scavenging Activity (TEAC)

Trolox equivalent antioxidant capacity (TEAC) assay was conducted using a previously described method (449, 450) with slight modifications. TEAC assay was used to determine the ability of the samples to scavenge the ABTS$\cdot$+ radical. ABTS is a chemical compound and converts into its radical cation form via addition of potassium persulfate, which gives blue colour and absorbs the light at 734 nm. In the presence of antioxidants such as phenolics, thiols ...etc., the radical cation converts back to its nonradical neutral form which is colourless. In this way, radical scavenging activity of such antioxidants may be tested spectrophotometrically. Primarily, 7 mM (2 mL) 2,2'-azino-bis(3-ethylbenzothiazoline-6-sulphonic acid)

(ABTS) and 2.45 mM (2 mL) $K_2S_2O_8$ were mixed and incubated 16 hours in the dark. After incubation $ABTS^+$ occurred was diluted with ethanol till absorbance was measured 0.700± 0.050 at 734 nm. After preparation of ABTS working solution ($ABTS^+$), 130 µL of that was added on 50 µL ethanol extracts and mixed properly. Then, the absorbance was measured at 734 nm after an exact reaction time of 6 min at 24 °C. Each extract was investigated in triplicate.

3.4.3   NO Scavenging Activity

Na nitroprusside generates nitric oxide radical interacting with oxygen which is detected by use of Griess reagent. NO_2^- scavenging agents competes with oxygen leading to reduced production of nitric oxide. The absorbance of the chromophore formed following the addition of Griess reagent is measured spectrophotometrically. Nitric oxide (NO) scavenging activity is carried out on the extracts with slight modifications on a previously desccribed method (451). Na nitroprusside was prepared by dissolving in phosphate buffered saline (PBS). Prepared concentrations of the extracts and Na nitroprusside solution were added into the well and incubated at room temperature for 150 min. At the same time, Griess reagent (0.100 g sulfanilamide, 0.010 g naphthyl ethylenediamine dihydrochloride, 250 µL H_3PO_4, 10 mL distilled water) was prepared freshly. After the addition of the reagent and waiting for 10 min, the absorbances of wells were measured at 577 nm. Radical scavenging activities of the extracts were determined by comparison with the blind absorbance.

Radical scavenging activity (%)= ((Acontrol −Asample)/Acontrol)) x 100

A: Absorbance

3.4.4   The Phosphomolybdate Antioxidant Assay

The phosphomolybdate antioxidant assay was carried out according to the procedure reported by Prieto et al. (452) with slight modifications. Phosphomolybdate reagent was prepared by mixing 0.6 M sulfuric acid (100 mL), 4 mM ammonium molybdate (100 mL) and 28 mM sodium phosphate (100 mL) solution. In a well of 24-well plate, 1 mL of phosphomolybdate reagent was mixed with 100 µL of the plant extract, standard solution or methanol. The plates were

capped with silver foil and incubated in water bath at 95 °C for 90 min. After the contents of the plates were cooled down, the absorbances were measured at 765 nm against a blank. The total antioxidant capacity was expressed as μg equivalents of ascorbic acid by using the standard ascorbic acid graph.

3.5   Phytochemical Studies

3.5.1   Isolation Studies

We used various chromatography techniques to view phytochemical profile of *Rumex acetosella*. We performed normal phase, reverse phase, sephadex column chromatographies for isolation of compounds and thin layer chromatography (TLC) to monitor the results of column chromatographies.

Solvent systems used in chromatographic separations were presented in **Table 3.1.**.

Phytochemical studies were performed on methanol extract of the roots of *R. acetosella* and 12 compounds were isolated from this point of view (**Figure 3.1.**).

Table 3.1. Solvan systems used in chromatographic techniques.

Solvent systems	Chromatographic techniques
$CHCl_3$: CH_3OH (95:5)	Preparative TLC
CH_2Cl_2: CH_3OH (95:5)	Silica gel CC
CH_2Cl_2: CH_3OH (90:10)	Silica gel CC
CH_2Cl_2: CH_3OH (80:20)	Silica gel CC
CH_2Cl_2: CH_3OH (70:30)	Silica gel CC
CH_2Cl_2: CH_3OH (60:40)	Silica gel CC
$CHCl_3$: CH_3OH: H_2O (90:10:1)	Silica gel CC, TLC
$CHCl_3$: CH_3OH: H_2O (80:20:2)	Silica gel CC, TLC, preparative TLC
$CHCl_3$: CH_3OH: H_2O (70:30:3)	Silica gel CC, TLC, preparative TLC
$CHCl_3$: CH_3OH: H_2O (60:40:4)	Silica gel CC, TLC
$CHCl_3$: CH_3OH: H_2O (61:32:7)	Silica gel CC, TLC, preparative TLC
$C_2H_5COOCH_3$: CH_3OH: H_2O (100:5:2)	Silica gel CC, TLC
$C_2H_5COOCH_3$: CH_3OH: H_2O (100:10:5)	Silica gel CC, TLC
$C_2H_5COOCH_3$: CH_3OH: H_2O (100:17:13)	Silica gel CC, TLC
CH_3OH	Sephadex CC, VLC, MPLC
CH_3OH: H_2O (20:80)	VLC, MPLC
CH_3OH: H_2O (30:70)	VLC, MPLC, RP TLC
CH_3OH: H_2O (40:60)	VLC, MPLC, RP TLC
CH_3OH: H_2O (50:50)	VLC, MPLC, RP TLC
CH_3OH: H_2O (60:40)	VLC, MPLC, RP TLC
CH_3OH: H_2O (70:30)	VLC, MPLC, RP TLC
CH_3OH: H_2O (80:20)	VLC, MPLC
CH_3OH: H_2O (90:10)	VLC, MPLC
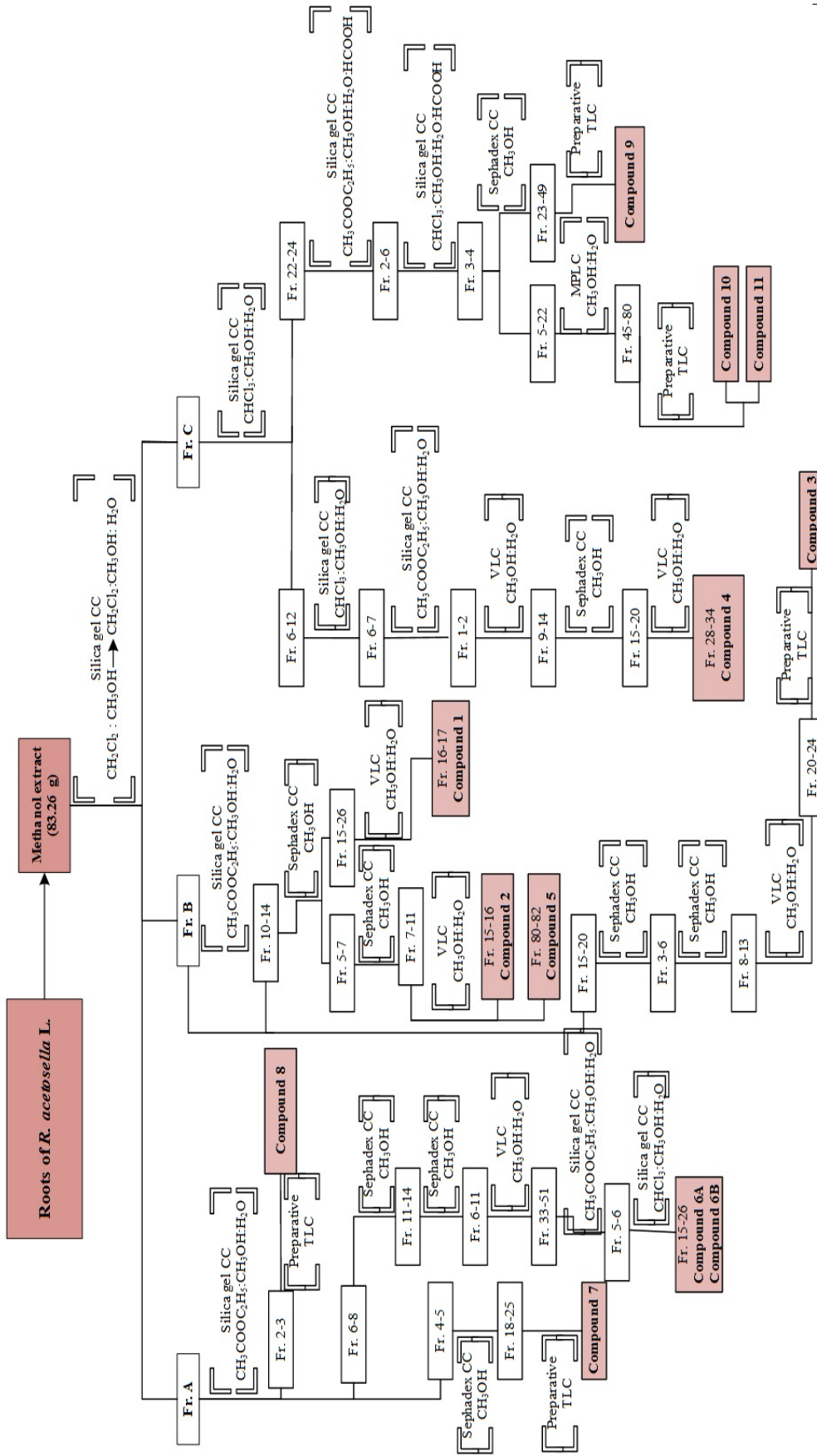
Figure 3.1. Isolation procedure of the compounds from the roots of *Rumex acetosella*.

Initially, the most appropriate solvent system was determined by testing various kinds of solvent systems for thin layer chromatography (TLC) to view phytochemical profile of the crude extract in the best way. That solvent system was found to be $CH_2Cl_2:CH_3OH$. Thus, we began phytochemical studies with normal phase silica gel column chromatography (CC) by using $CH_2Cl_2:CH_3OH$ gradient elution. The crude extract (83.26 g) was processed by SK-1 (silica gel CC-1) with a gradient elution of from $CH_2Cl_2:CH_3OH$ (95:5 → 60:40:4) to get the SK-1 fractions (**Figure 3.2.**).
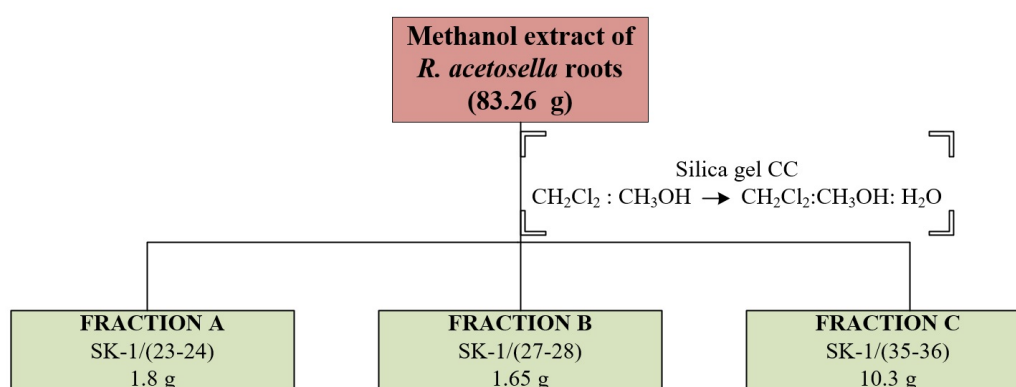
Figure 3.2. Main fractions obtained from the methanol extract of roots of *Rumex acetosella* used for the isolation of compounds.

Isolation Processes of Compounds 1-3 and 5

Fraction B [Fr. (27-28)] of SK-1 was further processed on SK accompanied by $CH_3COOC_2H_5:CH_3OH:H_2O$ gradient elution from (100:5:2) to (100:17:13). Fraction (10-14) of SK was then subjected to SPH. The obtained fraction (13-16) was re-conducted on SPH to get fraction (15-26), which was enriched in compound **1**. This fraction was subsequently applied to vacuum liquid chromatography (VLC) consecutively to get a pure compound (**Compound 1**, 21.3 mg).

Similar purification steps applied for compound **1** were performed, until we obtained the fractions of SPH. SPH (5-7) was then applied to SPH, again. Fraction (7-11) from SPH was combined and subjected to VLC to obtain **Compound 2** (10 mg) in pure form.

Fraction (15-20) obtained from SK was run on successive SPH columns to get the fraction (8-13) from SPH. Subsequently, this fraction was then processed by

VLC with $CH_3OH:H_2O$ (20:80) isocratic elution. Then, the fraction (20-24) from VLC being virtually pure was finally applied to preparative TLC to yield **Compound 3**, (12.4 mg).

The identical protocol applied for compound 2 was conducted until getting fractions from VLC. VLC (80-82) was the pure compound (**Compound 5**, 3.6 mg).

Isolation processes of compounds 1-3 and 5 were shown in **Figure 3.3.**.
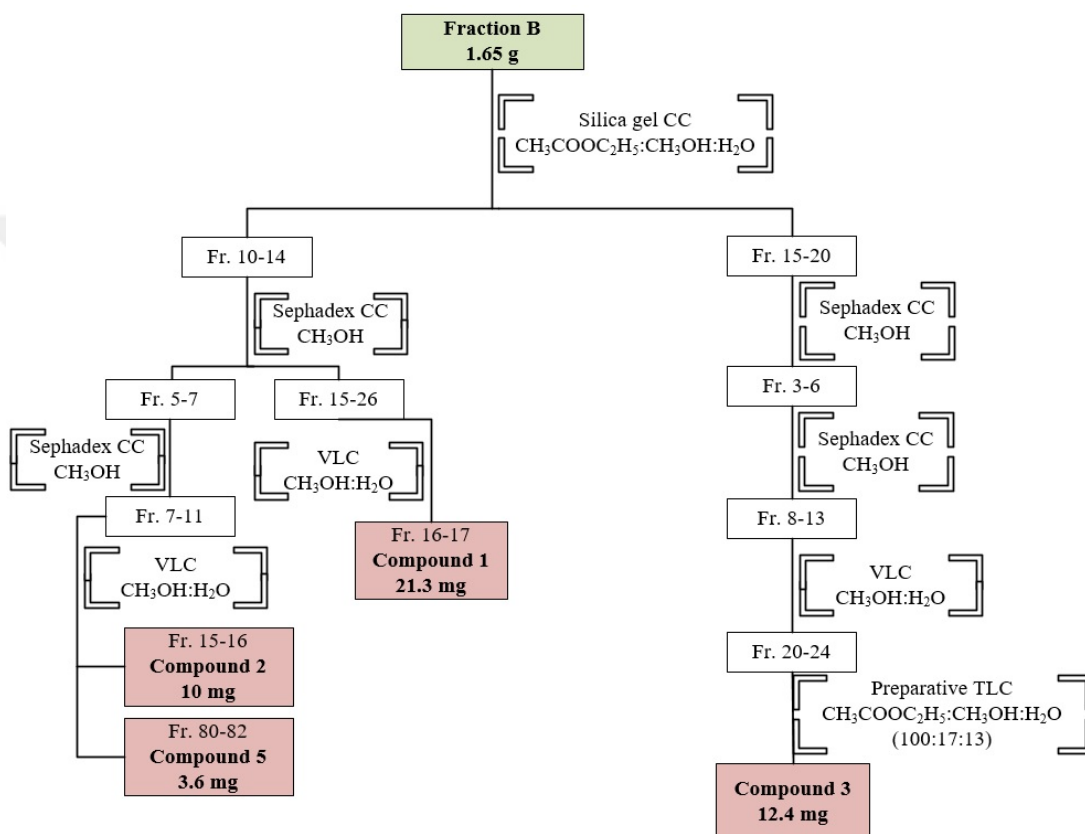
Figure 3.3. Isolation processes of compounds 1-3 and 5.

Isolation Processes of Compounds 4, 9, 10 and 11

Fraction C [SK-1/(35-36)] was run on SK with the gradient elution of CHCl$_3$:CH$_3$OH:H$_2$O from (80:20:2) to (61:32:7). SK (6-12) was repeatedly applied to silica gel column chromatographies until the fraction SK (1-2) was obtained. After subjecting this fraction to VLC with CH$_3$OH:H$_2$O (60:40) isocratic elution, we gained fraction (9-14) and applied the fraction to SPH. Fraction (15-20) from SPH was applied on VLC with CH$_3$OH:H$_2$O from (40:60) to (50:50) isocratic elution, and VLC (28-34) was gained as a pure compound (**Compound 4**, 13.5 mg).

Fraction (35-36) of SK-1 (Fr. B) was applied to SK accompanied by gradient elution of CHCl$_3$:CH$_3$OH:H$_2$O from (80:20:2) to (61:32:7) and SK fraction (22-24) was subjected to SK with CH$_3$COOC$_2$H$_5$:CH$_3$OH:H$_2$O:HCOOH (100:17:13:0.5) isocratic elution. SK (2-6) was then run on SK accompanied with CHCl$_3$:CH$_3$OH:H$_2$O:HCOOH gradient elution from (70:30:3:0.5) to (61:32:7:0.5). SK (3-4) was applied to SPH and fraction (23-49), which was almost pure, was applied to preparative TLC to obtain the completely pure compound (**Compound 9**, 13.5 mg).

The same procedure performed to isolate compound **9** were also conducted to obtain fraction (5-22) from SPH. SPH (5-22) was then applied to MPLC followed by CH$_3$OH:H$_2$O gradient elution from (45:55) to (100:0). Fraction (45-80) obtained from VLC was applied to preparative TLC and compounds **10+11** (12 mg) were obtained.

Isolation procedures of compounds **4**, **9-11** were shown in **Figure 3.4.**.
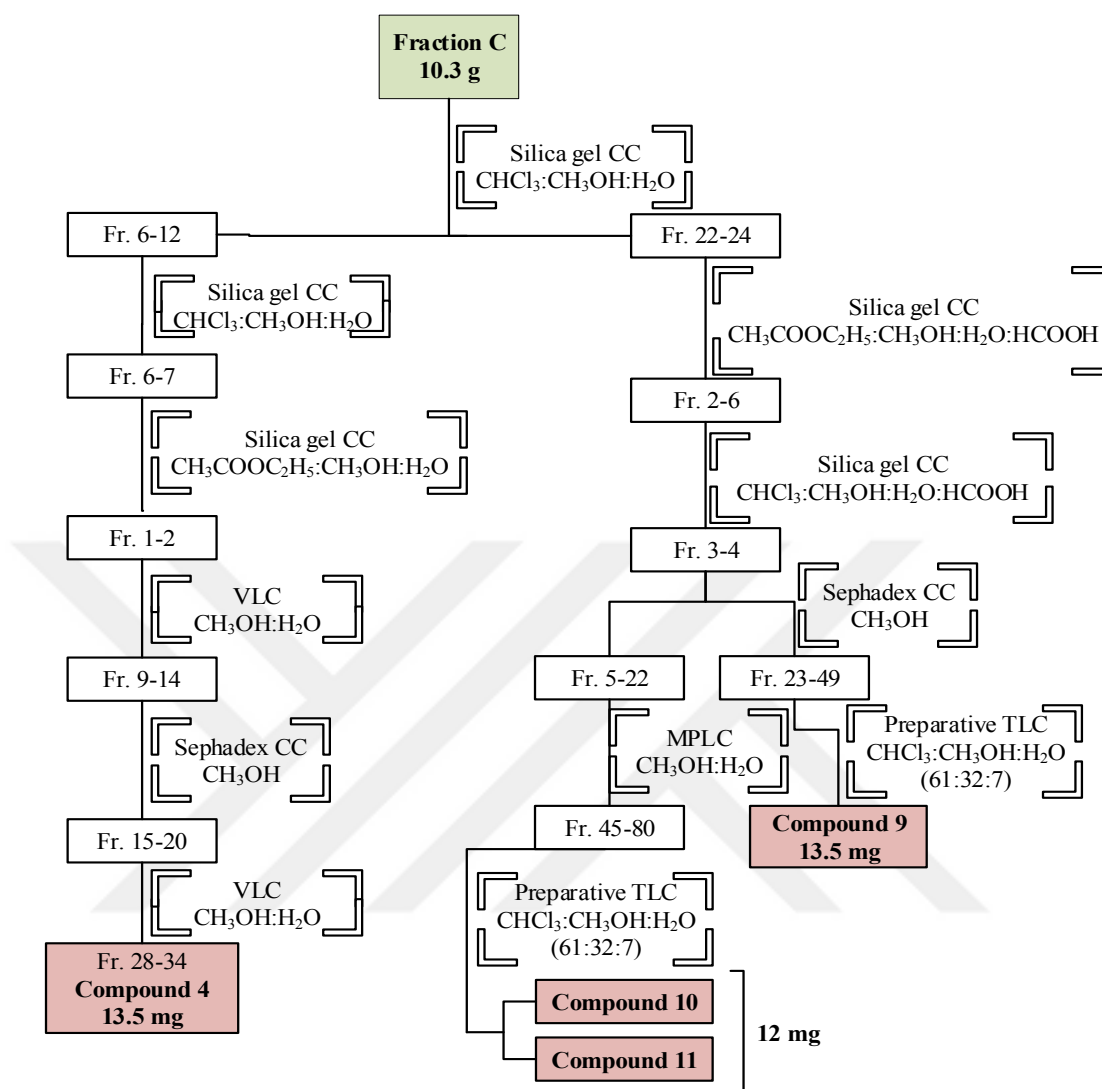
Figure 3.4. Isolation processes of compounds **4**, **9-11.**

Isolation Processes of Compounds 6 (6A and 6B), 7 and 8

The fraction SK-1/(23-24) as one of the first column fractions of the crude extract was applied on SK accompanied with $CH_3COOC_2H_5:CH_3OH:H_2O$ (100:17:13) isocratic elution. Fraction (6-8) from SK was repeatedly applied to Sephadex (SPH) column chromatography until fraction (6-11) was obtained from SPH. After subjecting this fraction to VLC accompanied by $CH_3OH:H_2O$ gradient elution from (40:60) to (55:45), a yielded fraction (33-51) from VLC was then subjected to another silica gel column chromatographies by using gradient elutions of $CH_3COOC_2H_5:CH_3OH:H_2O$ and $CHCl_3:CH_3OH:H_2O$, respectively in order to

isolate SK (15-26) as pure compounds (**Compound 6A**, **compound 6B** 13 mg).

The fraction SK-1/(23-24) was applied to SK accompanied by CH₃COOC₂H₅:CH₃OH:H₂O (100:17:13) isocratic elution. Fraction (4-5) obtained from SK was run on SPH to get fraction (18-25), which was almost pure. Fraction (18-25) from SPH, was then applied to preparative TLC to obtain a pure compound (**Compound 7**, 17.8 mg).

The fraction SK-1/(23-24) was applied to SK accompanied by CH₃COOC₂H₅:CH₃OH:H₂O (100:17:13) isocratic elution. Fraction (2-3) of SK was applied to preparative TLC to get the pure compound (**Compound 8**, 6 mg).

Isolation procedures for compounds **6A**, **6B**, **7** and **8** were shown in **Figure 3.5.**.
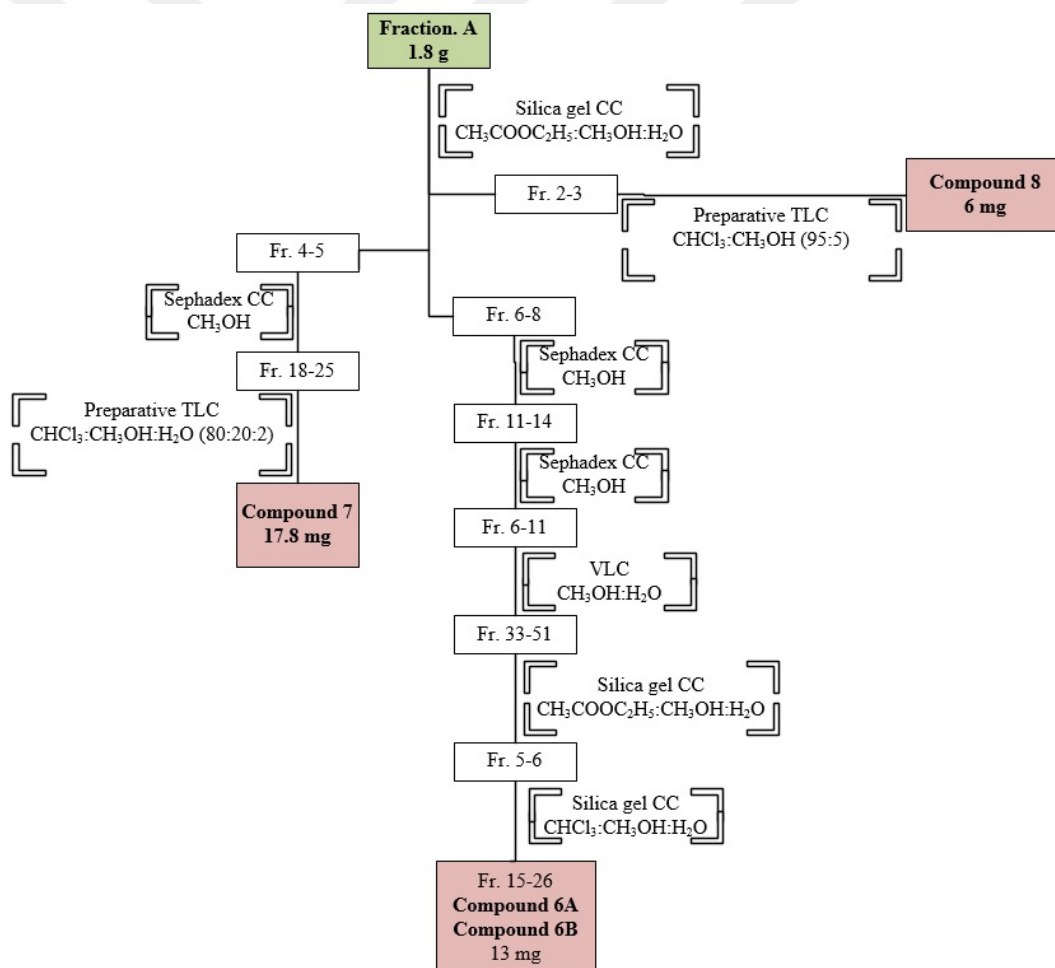
Figure 3.5. Isolation processes of compounds **6A**, **6B**, **7** and **8**.

Thin Layer Chromatography (TLC)

TLC was applied on silica gel 60 F_{254} precoated plates, 0.2 mm (Merck, Darmstadt, Germany) or reverse phase silica gel (RP-18) F_{254} precoated plates, 0.2 mm (Merck, Darmstadt, Germany) to observe phytochemical profiles of the fractions for the next purification steps. The spots of substances were detected by using an UV lamp at 254 and 365 nm, followed by spraying with 1% Vanilin/H_2SO_4 or 5% KOH and then heating at 100 to 110 °C.

Preparative Thin Layer Chromatography

A few of the fractions, which were enriched with major substances, were purified by using preparative thin layer chromatography. We used Silica gel 60 F_{254} precoated plates, 0.2 mm (Merck, Darmstadt, Germany). Various solvent systems were experienced to select appropriate solvent system for the best possible separation. Determining the best solvan system for the separation, each fraction to be purified was dissolved in the minimum amount of the solvent system in which it can completely be dissolved and applied on TLC plate (20×20 cm) by using a Pasteur pipette. After development process, spots were marked under 254 and 366 nm, scraped from plate, dissolved in the suitable solvent system and filtrated with filter paper, respectively to gain pure substances.

Silica Gel Column Chromatography

Silica gel column chromatography as a convenient and common method for purification of compounds based on their polarity. We used Silica gel 60 (0.063-0.200 mm, Merck, Darmstadt, Germany) as the polar stationary phase (adsorbant) in normal phase column chromatography, while silica gel derivatized with octadecyl (C18) (RP-18 silica gel, 40-63 μM, Merck, Darmstadt, Germany) was used in reverse phase column chromatography.

For preparation of normal phase column chromatography system, desired amount of silica gel was weighed, mixed with the initial solvent system and poured into the appropriately sized column of which having about 1 cm of cotton at the bottom to prevent from silica gel leakaging. Following silica gel to be packed tightly

and excluded any air bubbles, sample is applied on the system by dry method or as solution. 1 cm of cotton to the top of the silica gel is placed and elution is started.

For reverse phase column chromatography systems, diverse sized of columns are usually ready to use in MPLC and HPLC, which are filled with silica gel derivatized with octadecyl (C18). In case of need, similar steps for picking the column are followed as in normal phase column chromatography with different adsorbent and solvent systems.

Sephadex Column Chromatography

Sephadex LH-20 (Sigma, Sweden) was used for separation of the compounds based on their molecular size. For picking the column, desired amount of Sephadex is weighed and mixed with methanol to make the sephadex slurry. Similar picking steps are followed as in normal phase column chromatography. Methanol is used as a mobile phase.

Vacuum Liquid Chromatography (VLC)

Vacuum liquid chromatography is a kind of reversed-phase chromatography technique. The adsorbent is applied in dry form into a sintered glass funnel. The sample is introduced as a solution or preadsorbed on the packing material. Then, the mobile phase is added portion by portion and vacuum is applied after each portion to collect the fraction(s).

Medium Pressure Liquid Chromatography (MPLC)

Medium Pressure Liquid Chromatography (MPLC) is a kind of reversed-phase chromatography technique. The pressure required is in the range of 5-20 bar. Various volume proportions of the mixtures of methanol (MeOH) and water (H_2O) were used as mobile phase and the compounds eluted from the column were detected by means of a UV detector. MPLC data were indicated as follows:

Stationary phase: LiChroprep C-18 (40-63 μm, Merck)

Column: Buchi (3 x 45 cm)

Fraction collector: Buchi Fraction Collector C-660

Fraction volume: 25 mL

Injection: Rheodyne (Loop 2 mL)

Pump: Buchi (C-605)

Flow rate: 5 mL/min

Pressure: 5-15 bar

Mobile phase: 20% MeOH →90% MeOH, 100% MeOH

3.5.2 Structure Determination

Structures of the isolated compounds were determined by the utilization of spectroscopic data such as IR, NMR (1D- and 2D-NMR), MS and of the measurement of optical rotations.

3.6 Cell Culture

The cell lines were prolonged in a humidified environment at 37 °C with 5% CO_2 and splitted twice per week. Adherent cells except for HEK cells were detached by trypsine treatment. HEK cells were detached harvesting gently by cell scrapers. All experiments were conducted on the cells in the logarithmic phase of growth. The cells were counted by the utilization of Z2 Coulter Counter (Beckman Coulter).

3.6.1 Leukemia Cell Lines

CCRF-CEM and its resistant counterpart- P-glycoprotein (P-gp) overexpressing, multidrug-resistant CEM/ADR5000 leukemia cells were cultured in RPMI 1640 medium (Invitrogen/Life Technologies, Darmstadt, Germany) with 10% fetal bovine serum (Life Technologies, Germany) and 1% penicillin and

streptomycin (Life Technologies, Germany). To maintain multidrug-resistance, quality of CEM/ADR5000 cells, 5000 ng/mL doxorubicin is added biweekly.

3.6.2   Breast Cancer Cell Lines

Breast cancer cells including MDA-MB-231-pcDNA cells and a multidrug-resistant subline transfected with a *BCRP* cDNA (MDA-MB-231-BCRP clone 23) were cultivated in DMEM medium (Life Technologies, Germany) supplemented with 10% fetal bovine serum (Life Technologies, Germany) and 1% penicillin and streptomycin (Life Technologies, Germany). Drug resistance in MDA-MB-231-BCRP clone 23 was sustained by the supplementation of geneticin (Sigma-Aldrich) once a week.

3.6.3   Glioblastoma Cell Lines

Brain tumor cells as wild type U87.MG and a subline transfected with a deletion-activated *EGFR* cDNA (U87.MGΔEGFR) were cultivated in DMEM medium (Invitrogen) supplemented with 10% fetal bovine serum (Life Technologies, Germany) and 1% penicillin and streptomycin (Life Technologies, Germany). Drug resistance in U87.MGΔEGFR was hold by the addition of geneticin (Sigma-Aldrich, Germany) once a week.

3.6.4   Colon Cancer Cell Lines

HCT116 cells with wild-type TP53 tumor supressor gene (HCT116($p53^{+/+}$)) or HCT116 knockout cells (HCT116($p53^{-/-}$)) as colon cancer cells were cultivated in DMEM medium (Life Technologies, Germany) supplemented with 10% fetal bovine serum (Life Technologies, Germany) and 1% penicillin and streptomycin (Life Technologies, Germany). Drug resistance in HCT116 ($p53^{-/-}$) was maintained by the addition of geneticin (Sigma-Aldrich, Germany) once a week.

3.6.5   Human Embriyonic Kidney Cell Lines

Embryonic kidney cells concerning wild type drug-sensitive HEK293 cells and a multidrug-resistant subline transfected with an *ABCB5* cDNA (HEK293-ABCB5) were cultivated in DMEM medium (Life Technologies, Germany)

supplemented with 10% fetal bovine serum (Invitrogen) and 1% penicillin and streptomycin (Life Technologies, Germany).

3.6.6 Human Peripheral Mononuclear Cells (PMNC)

The human peripheral mononuclear cells (PMNC) were isolated from fresh blood samples of a healthy donor by using Histopaque® (Sigma-Aldrich, St. Louis, MO, USA).

3.7 Cytotoxicity Assays

3.7.1 Resazurin Reduction Assay

Resazurin reduction assay was performed to detect cytotoxicity. The assay depends on the reduction of resazurin to resorufin by viable cells (453). Non-viable cells lost their metabolic capacity which prevents transition of resazurin to resorufin and formation a blue staining. Briefly, aliquots of 0.5×10^4 adherent cells being allowed to attach overnight and 1×10^4 suspension cells per well were seeded in 96-well-plates with or without the inclusion of varying concentrations of the drug to get a final volume of 200 µL/well. Following 72 h drug treatment of the cells with drugs, resazurin (Sigma-Aldrich, Taufkirchen, Germany) was put on the cells for 4 h and staining was measured by an Infinite M2000 ProTM plate reader (Tecan, Germany) using an excitation wavelength of 544 nm and an emission wavelength of 590 nm. Each assay was independently performed for at least three times, with six parallel replicates each. The protocol has been recently reported (454). Fifty percent inhibition concentrations (IC_{50}) represent the drug concentrations required to inhibit 50% of cell proliferation, which were fitted with nonlinear regression using GraphPad® Prism7.

3.7.2 Protease Viability Marker Assay

Protease viability marker assay was further performed to determine the cytotoxicity of aloe-emodin to eliminate any cross talk, since we observed aloe-emodin to induce excessive ROS production in our researches and thus, it might affect the results of resazurin assay, which relies on redox system. The assay

measures the protease activity within living cells, the protease activity is restricted to intact viable cells and is measured using a flourogenic, cell permeant, peptide substrate (glyxyl-phenylalanyl-aminoflourocoumarin; GF-AFC). The substrate enters intact cells where it is cleaved by the live-cell protease activity to generate a fluorescent signal proportional to the number of living cells. Briefly, CCRF-CEM cells (2×10^4 cells/well) were seeded in 96-well plate. Aloe-emodin was added in a concentration dependent manner (0.001 – 100 μM). After 72 hours, 100 μl of GF-AFC substrate (Promega, Madison, USA) was added to each well, cells were incubated for 30 minutes at 37 °C. Using Infinite M2000Pro™ plate reader (Tecan, Crailsheim, Germany), the fluorescent intensity was measured at excitation wavelength 400 nm, and emitted light was collected at 505 nm.

3.8   Toxicity of Aloe-emodin in Normal Cells

Using Histopaque® (Sigma-Aldrich, St. Louis, MO, USA), the human peripheral mononuclear cells (PMNC) were isolated from fresh blood samples of a healthy donor. In brief, six mL blood was layered with six mL Histopaque® and centrifuged ($400 \times g$) for 30 min at 4 °C. The opaque interface, containing lymphocytes and other mononuclear cells, was transferred into a new tube and washed several times. Isolated PMNCs were kept in Panserin 413 medium (PAN-Biotech, Aidenbach, Germany) supplemented with 2% phytohemagglutinin M (PHA-M, Life Technologies, Darmstadt, Germany).

3.9   mRNA Microarray Gene Expression Profiling

3.9.1   RNA Isolation

CCRF-CEM cells were treated with IC_{50} value of aloe-emodin or DMSO for 48 h. Total RNA was isolated by InviTrap Spin Universal RNA Mini kit (Stratec Molecular, Berlin, Germany) according to the manufacturer's instructions. RNA concentrations were detected by the nanodrop spectrophotometer (Thermo Fisher).

3.9.2   Probe Labeling, Hybridization, Scanning and Data Processing

The quality control of total RNA, probe labeling, hybridization, scanning and

data analysis was performed in the Genomics and Proteomics Core Facility at the German Cancer Research Center (DKFZ, Heidelberg, Germany). Details have been previously described (455).

3.9.3 Data Analysis

Chipster Analysis

Chipster software for analyzing high-throughput data filtered microarray gene expression data. The Chipster software was used to filter the set of differentially expressed genes obtained from microarray hybridization (http://chipster.csc.fi/) by using Bayes t-test with a *p* value lower than 0.05.

Ingenuity Pathway Analysis

The filtered genes with fold-changes of more than 1-fold were selected for Ingenuity Pathways Analysis (IPA) Software (http://www.ingenuity.com/ Ingenuity Systems, Redwood City, CA, USA) to obtain profiles of genetic networks and signaling pathways.

3.10 Real-time RT-PCR

Primer sequences of *HHEX*, *MCMDC2* and *CRCP* were designed using NCBI and GenScript Real Time PCR Primer Design (https://www.genscript.com/ssl-bin/app/primer) websites. *DUSP6*, *HHEX*, *MCMDC2* and *CRCP* primers were synthesized by Eurofins MWG Operon (Ebersberg, Germany) and their sequence specificities were checked by NCBI Primer-Blast. The reaction properties of primers were calculated by Eurofins genomics. The primer sequences were as follows: *DUSP6*, forward (5′–3′): CCTGAGGCCATTTCTTTCATAGA, reverse (5′–3′): GTCACAGTGACTGAGCGGCTAAT (456); *HHEX*, forward: TCTACTCTGGAGCCCCTTCT, reverse: GGTTTTGACCTGTCTCTCGC; *MCMDC2*, forward: TGCGGCTTCTAGACAGTTCA, reverse: GAGCTTGTTCTGATTCTGCG; *CRCP*, forward: GGGGAGAAGAAACATGGTGA, reverse: CCGTGGAGGAAATCTTTCAA. Total RNA was isolated by InviTrap Spin Universal RNA Mini kit (Stratec

Molecular) according to the manufacturer's instruction. One microgram RNA was converted to cDNA using RevertAid H Minus First Strand cDNA Synthesis Kit (Thermo Scientific). The mRNA levels were analyzed by using of 5Hot Start Tag EvaGreen® qPCR Mix (Axon Labortechnik, Kaiserslautern, Germany) and CFX384™ Real-Time PCR Detection System (Bio-Rad, Munich, Germany). RT-PCR was performed with an initial denaturation at 95 °C for 10 seconds followed by 40 cycles including strand separation at 95 °C for 15 s, annealing at 62 °C for 30 s and extension at 95 °C for 1 min. The *GAPDH* gene was used for normalization. Forward and reverse primer sequences of *GAPDH* were TGAAGGTCGGAGTCAACGGATTTGGT for forward and CATGTGGGCCATGAGGTCCACCAC for reverse, respectively (457).

The quantification method was done as follow:

Delta Ct = Ct gene test − Ct endogenous control

Delta Delta Ct = ΔCt sample1 − ΔCt calibrator

RQ = Relative quantification = 2-ΔΔCt

The RQ is your fold change compared to the calibrator (untreated sample, time zero, etc.). The calibrator has a RQ value of 1. All samples are compared to the calibrator. (A RQ of 10 means that this gene is 10 times more expressed in sample x then in the calibrator sample. A RQ of 0,1 means that the gene is 10 times less expressed).

3.11   Detection of Reactive Oxygen Species by Flow Cytometry

2′,7′-Dichlorofluorescin diacetate (H_2DCFH-DA, Sigma-Aldrich) is a cell-permeable non-fluorescent probe used to detect cellular ROS levels. In the presence of ROS, the compound is de-esterified intracellularly and converts into the highly fluorescent 2′,7′-dichlorofluorescein upon oxidation. Thus, it can be measured by flow cytometry (458). CCRF-CEM cells were re-suspended in PBS and incubated for 30 min with H_2DCFH-DA at a concentration of 2 μM. After washing with PBS, the cells were treated with DMSO as negative control, H_2O_2 and doxorubicin as positive controls or varying concentrations of aloe-emodin (0.5-, 1-, 2- and 4-fold IC_{50}) for 1 h. The results were assessed by a BD Accuri™ C6 flow cytometer (Becton

Dickinson) using FL-1 the channel (488 nm excitation). For each sample, 10^4 cells were counted. The protocol has been previously reported (459).

3.12 Comet Assay

The OxiSelect^{TM} Comet Assay Kit (Cell Biolabs/Biocat, Heidelberg, Germany) was used to detect DNA damage according to the manufacturer's instructions. CCRF-CEM cells treated with IC_{50}, $2\times IC_{50}$ and $4\times IC_{50}$ concentration of aloe-emodin in the culture medium for 24 h. Then, the cells were mixed with agarose and applied to OxiSelect^{TM} Comet Assay slides. These slides including the embedded cells were treated with lysis buffer and alkaline solution. Subsequently, electrophoresis was performed on the slide with a voltage of 22 V for 30 min corresponding to 1 V/cm of the electrophoresis chamber. These slides were washed with distilled water. After fixation with 70% ethanol, the slides were stained with by a fluorescent DNA binding dye.

Then, the slides were photographed by a fluorescence microscope (EVOS^S FL Cell Image System, Thermo Fisher Scientific Waltham, USA) using a FITC filter with an excitation wavelength of 490 nm and emission at 520 nm. At least 50 cells per image were randomly selected and analyzed with the OpenComet software (http://www.cometbio.org). Percentages of tail DNA, tail moment and olive moment were assessed as parameters for DNA damage. The statistical significance was determined by one-way ANOVA with Tukey's multiple comparison test.

3.13 Cell Cycle Analysis by Flow Cytometry

CCRF-CEM cells (2×10^4) were treated with 0.5-, 1-, 2- and 4-fold IC_{50} values of aloe-emodin, respectively for 6, 24, 48 or 72 h. The cells were collected, washed in PBS and fixed with ice-cold 96% ethanol. After washing the cells with PBS again, the cells were dissolved in PBS and stained with propidium iodide (PI, Sigma-Aldrich) at a final concentration of 50 μg/mL for 15 min in the dark. Cell cycle analyses were performed using a BD Accuri^{TM} C6 Flow cytometer (Becton-Dickinson, Heidelberg, Germany) at 488 nm excitation wavelength and emission was measured by a 610/20 nm band pass filter. All experiments were performed at least in triplicates. The protocol has been previosly reported (460).

3.14 Detection of Mitochondrial Membrane Potential by Flow Cytometry

The JC-1 Mitochondrial Membrane Potential Assay Kit (Cayman Chemical, Ann Arbor, MI, USA) was applied for the detection of MMP by flow cytometry according to the manufacturer's instructions. The cationic dye, 5, 5', 6, 6'-tetrachloro- 1, 1', 3, 3'- tetraethylbenzimidazolylcarbocyanine iodide (JC-1) enters the mitochondria and changes its fluorescent properties based on the aggregation of the probe. In healthy cells having high MMP, JC-1 forms complexes known as J-aggregates with intense red fluorescence. On the other hand, in cells with low MMP, JC-1 remains in its monomeric form showing green fluorescence (461). Aliquots of 5×10^5 cells/ml were treated with DMSO as negative control, doxorubicin as positive control or IC_{50}, $2 \times IC_{50}$ and $4 \times IC_{50}$ concentrations of aloe-emodin for 24 and 48 h. A LSR-Fortessa FACS analyzer (Becton–Dickinson) was used to detect the J-aggregate form of JC-1 with an excitation wavelength of 535 ± 20 nm and an emission wavelength of 590 ± 20 nm as well as the monomeric form of JC-1 at excitation and emission wavelengths of 485 and 535 nm, respectively. The results were analyzed by the FlowJo software (Celeza, Olten, Switzerland). 2×10^4 cells were counted for each experiment which were repeated in triplicate.

3.15 Annexin V (AV) and Propidium Iodide (PI) Double Staining by Flow Cytometry

A commercial annexin V/PI detection apoptosis kit was used to detect early apoptosis and necrosis according to the manufacturer's instructions (Life Technologies, Carlsbad, CA, USA). Annexin V is a calcium-dependent phospholipid-binding protein, which binds to phosphatidylserine (PS). PS is predominantly located at the inner side of the plasma membrane under normal conditions and moves to outer surface of the membrane upon the onset of early apoptosis. This can be detected FITC-labeled annexin V. PI is a marker of late apoptosis and necrosis. We treated aliquots of 1×10^6 CCRF-CEM cells with 0.5-, 1-, 2- and 4-fold IC_{50} values of aloe-emodin for 48, 72 or 96 h, respectively. After washing the cells with PBS, they were stained with annexin V/FITC at room temperature for 10-15 min. Subsequently, cells were washed again and stained with

PI in the dark. Then, the results were analyzed by a BD Accuri^{TM} C6 flow cytometer at excitation wavelength 488 nm and emission wavelength 530 nm to record annexin V/FITC signals. The fluorescence of PI was detected at 488 nm excitation and was measured by a 610/20 nm band pass filter. At least three independent experiments were performed.

3.16 COMPARE and Hierarchical Cluster Analyses of Transcriptome-Wide mRNA Expression in Untreated Cell Lines

A panel of 60 cell lines from the National Cancer Institute (NCI), USA were used to perform COMPARE. Logarithmic IC_{50} values ($\log_{10}IC_{50}$) of As_2O_3 have been deposited at the NCI database (http://dtp.cancer.gov/databases_tools/default.htm). The mRNA expression values of the NCI cell lines were determined via microarray analyses were deposited at the NCI website (http://dtp.cancer.gov/databasestools/default.htm) as well. These data were used to generate rank ordered lists of genes expressed in the NCI cell lines panel using COMPARE analyses (462). Briefly, the selected genes of the NCI microarray database were ranked for similarity of its mRNA expression values to the $\log_{10}IC_{50}$ values for aloe-emodin.

Objects were categorized by determination of distances with regard to the closeness of between-individual distances to conduct hierarchical cluster analysis. All objects were assembled into dendrograms. Grouping of objects with similar properties provokes cluster formation. Distances of subordinate cluster branches to superior cluster branches serve as criteria for the closeness of clusters. Thus, objects with tightly related features were clustered closely, while separation of objects in the dendrogram increased with progressive dissimilarity. We applied the WARD method using the WinSTAT program (Kalmia, Cambridge, MA, USA). The protocol has been previously reported (463).

The distribution of cell lines sensitive or resistant to the drug was calculated using the χ^2 test. The χ^2-test was performed to determine bivariate frequency distributions of pairs of nominal scaled variables. It was used to calculate significance values (*p*-values) and rank correlation coefficients (*R*-values) as relative measure for the linear dependency of two variables. This test was implemented into

the WinSTAT program (Kalmia Co.). The χ^2-test determines the difference between each observed and theoretical frequency for each possible outcome, squaring them, dividing each by the theoretical frequency, and taking the sum of the results. To perform the χ^2-test, the median $\log_{10}IC_{50}$ value of all cell lines tested for the drug was used as cut-off to separate tumor cell lines as being ''sensitive'' or ''resistant''.

3.17 Gene Promoter Binding Motif Analysis

Binding motifs for transcription factors in the promoter sequences of genes were analyzed by the Cistrome analysis software (464). Briefly, genes of interest were retrieved in BED format from http://genome.ucsc.edu/cgi-bin/hgTables. SeqPos (http://cis- trome.org), was used to screen for enriched transcription factor binding motifs in gene promoter sequences. The screening was performed for motifs deposited in JASPAR database. The protocol has been previously reported (460).

3.18 NF-κB Reporter Assay

HEK293 cells stably expressing HEK-Blue-Null1 vector and SEAP (Secreted Embryonic Alkaline Phosphatase) on a NF-κB promoter were obtained from Invivogen (San Diego, CA, USA). The cells were cultured according to manufacturer's recommendations and treated with various concentrations of aloe-emodin (10, 50, 75, 100 μM), triptolide (1 μM) as positive control and DMSO as negative control for 24 h. NF-κB activation was detected by measuring SEAP spectrophotometrically at 630 nm upon Quanti Blue addition (Invivogen). The protocol has been previously reported (465).

3.19 Molecular Docking

Molecular docking was performed by Autodock4 and with AutodockTools-1.5.7rc1 using lamarckian algorithm (466, 467). The three-dimensional structures of aloe-emodin and control drug triptolide were prepared as a PDB format by using Corina online Demo (https://www.mn-am.com/online_demos/corina_demo). The X-ray crystallography-based structure of the targets were obtained from (PDB) (http://www.rcsb.org/pdb/home/home.do, PDB code: 3DO7, 1VKX, 3BRT, 3RZF). Initially, we conducted blind docking to identify possible pharmacophores.

Afterwards, defined docking was performed by setting a grid box based around the pharmacophores. Three independent docking calculations were examined with 250 runs and 2.500.000 energy calculations. Lamarckian Genetic Algorithm was chosen for the docking calculations. Docking log (dlg) file ensured information of the lowest binding energy, the number of clusters and predicted inhibition constant (pKi). Mean ± SD of binding energies were calculated from the independent dockings. AutoDock Tools and Visual Molecular Dynamics (VMD) were used to visualize docking results.

3.20   Enzyme Inhibition Assays

3.20.1 *α*-Amylase Enzyme Inhibition Assay

Preliminary experiments on *α*-amylase activity were performed according to previously described methods (468) with slight modifications. For subsequent assays, equal volumes (100 μL) of extract and 100 μL of porcine pancreatic *α*-amylase enzyme solution (25 U/mL) were incubated in plates at 25 °C for 10 min. Following, 1% starch solution in 20 mM sodium phosphate buffer (pH 6.9 with 6 mM sodium chloride) was also added and incubated at 25 °C for a further 10 min. The reaction was stopped with the addition of 200 μL dinitrosalicyclic acid colour reagent. They all were incubated at 100 °C in a water bath for 5 min. Once samples had cooled to room temperature, 50 μL was removed from each well and transferred to the wells of 96-well microplate. The reaction mixture was diluted by adding 200 μL of water to each well and absorbance was measured at 540 nm. Blank readings (i.e. no enzyme) were subtracted from each well and results were compared to the control. The pharmacological inhibitor, acarbose, was included as a positive control. The results were expressed as % inhibition of enzyme activity and calculated according to the following equation:

% Inhibition= [(Acontrol-Asample)/ Acontrol] x 100

3.20.2 α-Glucosidase Enzyme Inhibition Assay

α-glucosidase inhibitory activity was determined as previously described method (469) with slight modifications using a 96-well plate. Briefly, α-glucosidase was dissolved in 0.1 M potassium phosphate buffer (pH 6.9) (1 Unit/mL). This was used as the enzyme solution. The substrate, 3 mM of p-nitrophenyl-α-D-glucopyranoside (pNPG) was prepared in the same buffer (pH 6.9). 10 μL enzyme solution and 50 μL phosphate buffer (0.1 M, PH 6.9) were added to each well, respectively. Following that, each sample (20 μL) were also added to the plate. The reaction was initiated by adding 20 μL substrate. The reaction mixture was incubated at 37 °C for 30 min. After incubation, 50 μL (0.1 M) sodium carbonate in 0.1 M potassium phosphate buffer (pH 6.9) was added to each well to quench the reaction. The amount of p-nitrophenol (pNP) released was quantified using a 96-well reader at 405 nm. The control experiment contained the same reaction mixture, but the sample solution was replaced with the same volume of phosphate buffer. Acarbose was used as a positive control. Each assay was done at least twice with three replicate each. The percentage inhibition (%) was calculated by using the following equation:

% Inhibition= -[(Acontrol- Asample)/ Acontrol] x 100, where Acontrol is the absorbance of the control and Asample is the absorbance of the sample. The IC_{50}, which is the concentration of the sample required to inhibit the enzyme was determined for each sample.

3.21 Statistical Analysis

Data were shown as mean ± standard deviation. Each results were obtained from at least three independent experiments. In Comet assay, the statistical significance was determined by one-way ANOVA with Tukey's multiple comparison test.

4. RESULTS

4.1 Antioxidant Capacity Assays

4.1.1 DPPH Radical Scavenging Activity

Reducing activity of several root and herb extracts of *Rumex acetosella* were investigated against DPPH radical as well as ascorbic acid as a positive control. DPPH radical scavenging activities of chloroform, methanol, 70% methanol, ethanol and 70% ethanol extracts of both roots and herbs of *R. acetosella* in the concentration ranges of 25 to 500 μg/mL as well as ascorbic acid in the concentration ranges of 5 to 100 μg/mL were searched (**Tables 4.1.-4.3.; Figures 4.1.-4.3.**) and then evaluated based on their RC_{50} values (**Table 4.4.**). The methanol extract of the roots presented the best reducing activity with $RC_{50}= 67.94$ μg/mL, while the herbal ethanol extract displayed the best reducing activity with $RC_{50}= 59.66$ μg/mL against DPPH. In general, we observed herbal extracts were found to have better radical scavenging activity than those of root extracts in all concentrations.

Table 4.1. DPPH radical scavenging activity % of various root extracts of *R. acetosella*.

Concentration (µg/mL)	Root extracts of *R. acetosella*				
	CHCl$_3$	CH$_3$OH	70% CH$_3$OH	C$_2$H$_5$OH	70% C$_2$H$_5$OH
25	3.5 ± 3.39	23.10 ± 2.21	16.70 ± 3.33	31.07 ± 2.12	22.63 ± 2.72
50	8.55 ± 3.89	38.87 ± 2.34	30.80 ± 3.91	40.85 ± 3.43	23.35 ± 3.38
100	12.1 ± 3.96	69.90 ± 3.35	54.07 ± 5.77	63.02 ± 0.15	41.97 ± 4.20
200	17.5 ± 3.25	92.13 ± 0.42	81.43 ± 4.76	89.89 ± 0.36	84.24 ±2.41
500	37.65 ± 0.21	93.07 ± 0.40	91.13 ± 0.55	92.14 ± 0.05	92.10 ± 0.10
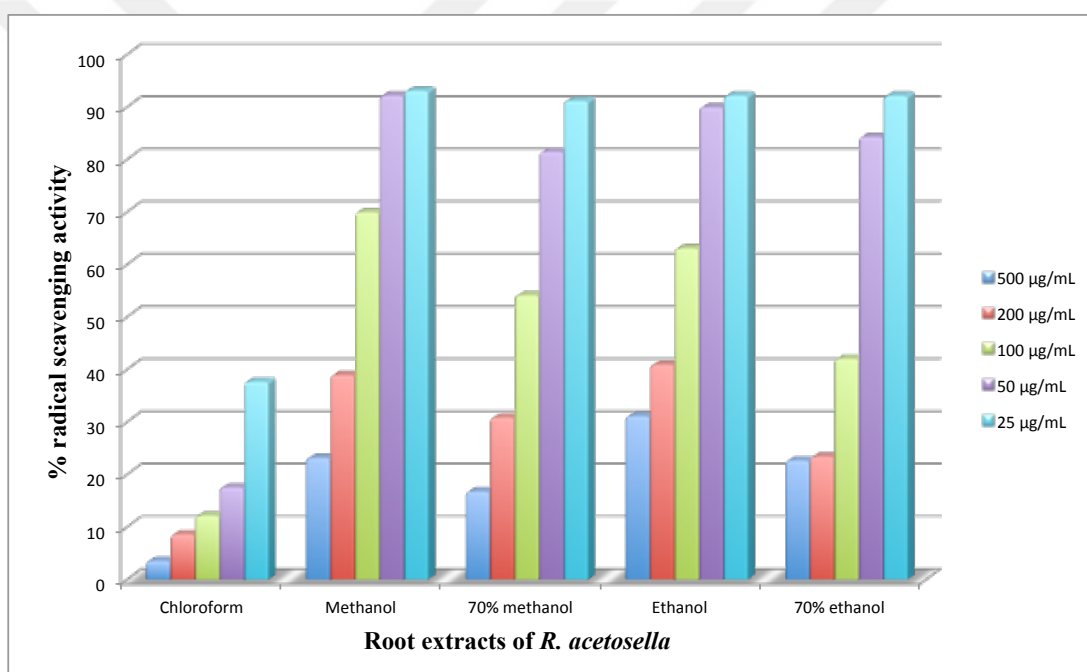
Figure 4.1. DPPH radical scavenging activity % of various root extracts of *R. acetosella*.

Table 4.2. DPPH radical scavenging activity % of various herbal extracts of *R. acetosella.*

Concentration (μg/mL)	Herbal extracts of *R. acetosella*				
	$CHCl_3$	CH_3OH	70% CH_3OH	C_2H_5OH	70% C_2H_5OH
25	9.0 ± 4.34	21.57 ± 4.42	14.93 ± 1.90	19.58 ± 4.61	21.47 ± 2.91
50	12.9 ± 4.11	38.57 ± 5.42	30.10 ± 1.75	42.98 ± 0.46	34.36 ± 2.48
100	21.7 ± 2.82	65.93 ± 5.26	58.73 ± 4.87	79.28 ± 0.41	56.75 ± 0.61
200	37.5 ± 3.32	90.03 ± 1.98	86.50 ± 3.96	91.74 ± 0.31	87.21 ± 1.38
500	62.0 ± 2.90	93.30 ± 0.26	92.37 ± 0.15	92.71 ± 0.10	92.03 ± 0.20
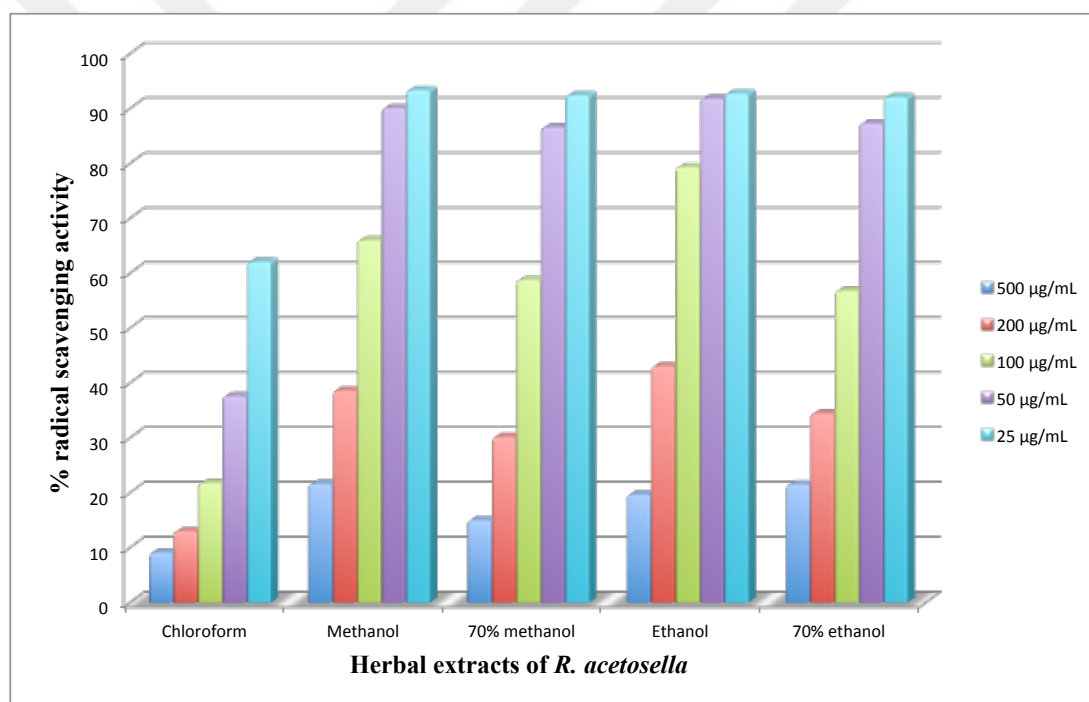
Figure 4.2. DPPH radical scavenging activity % of various herbal extracts of *R. acetosella.*

Table 4.3. DPPH radical scavenging activity % of ascorbic acid as a positive control.

Ascorbic acid	Concentration				
	5 µg/mL	10 µg/mL	25 µg/mL	50 µg/mL	100 µg/mL
% radical scavenging activity	15.60 ± 0.42	29.95 ± 4.17	81.05 ± 1.06	94.24 ± 0.15	94.35 ± 0.10
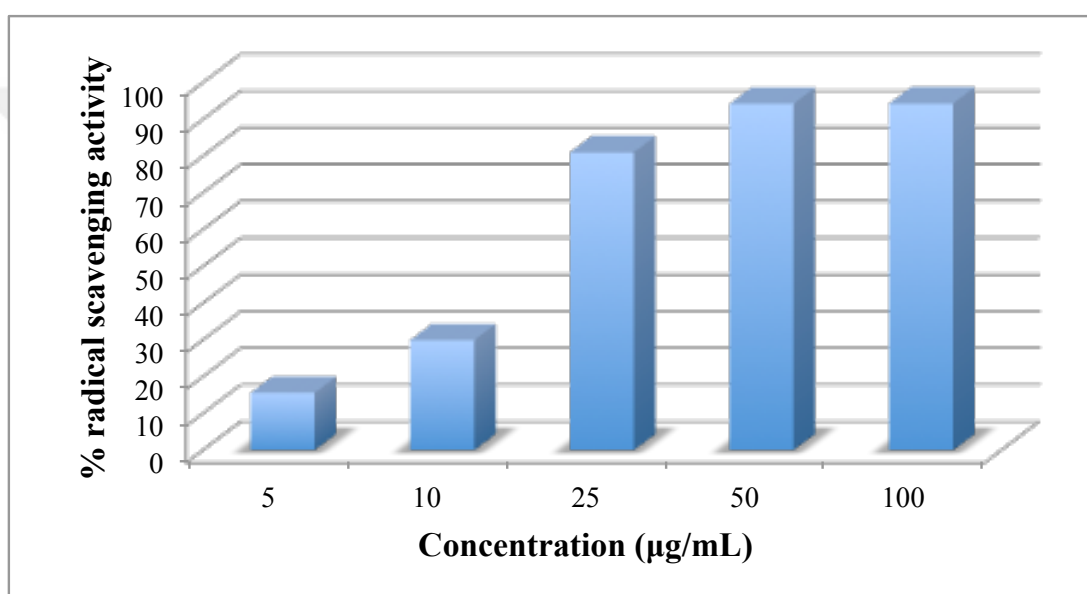
Figure 4.3. DPPH radical scavenging activity % of ascorbic acid.

Table 4.4. The concentration of *R. acetosella* extracts and ascorbic acid required for 50% reduction (RC_{50}) against DPPH radicals.

Extracts	RC_{50} values of extracts and ascorbic acid (µg/mL)		
	Roots	Herbs	Ascorbic acid
CHCl$_3$	-	352.86	
CH$_3$OH	67.94	70.90	
70% CH$_3$OH	91.26	84.75	15.89
C$_2$H$_5$OH	70.64	59.66	
70% C$_2$H$_5$OH	118.99	84.92	

4.1.2 ABTS Radical Scavenging Activity

ABTS+ radical scavenging activity of various root and herb extracts of *Rumex acetosella* with the concentration ranges of 50 to 800 μg/mL and trolox as a positive control with the concentration ranges of 0.78 to 25 μg/mL were investigated (**Tables 4.5.-4.7.; Figures 4.4.-4.6.**). The concentration of *R. acetosella* extracts and trolox required for 50% reduction (RC_{50}) against ABTS radicals and are given in **Table 4.8.**. According to these results, methanol extracts of both roots and herbs of *R. acetosella* showed the best radical scavenging activity with the RC_{50} values of 70 and 65.57 μg/mL, respectively among all studied extracts. In conclusion, herbal extracts displayed better ABTS scavenging activity than those of root extracts; however Trolox, used as a positive control, displayed the best radical scavenging activity in all in all with RC_{50}= 6.21 μg/mL (**Table 4.7.** and **Figure 4.6.**).

Table 4.5. ABTS radical scavenging activitiy % of various root extracts of *R. acetosella*.

Concentration (µg/mL)	Root extracts of *R. acetosella*				
	CHCl$_3$	CH$_3$OH	70% CH$_3$OH	C$_2$H$_5$OH	70% C$_2$H$_5$OH
50	8.80 ± 3.11	42.51 ± 1.82	28.05 ± 4.60	3.86 ± 0.00	11.67 ± 2.21
100	22.65 ± 4.07	61.24 ± 2.44	47.15 ± 3.61	41.08 ± 6.35	52.08 ± 4.83
200	36.55 ± 4.00	80.21 ± 4.47	82.95 ± 4.88	76.43 ± 2.95	77.19 ± 4.49
400	44.40 ± 5.52	88.30 ± 2.30	87.00 ± 2.40	89.40 ± 1.08	89.90 ± 0.07
800	54.85 ± 5.13	90.10± 1.20	87.50 ± 2.12	90.59 ± 0.12	90.73 ± 0.66
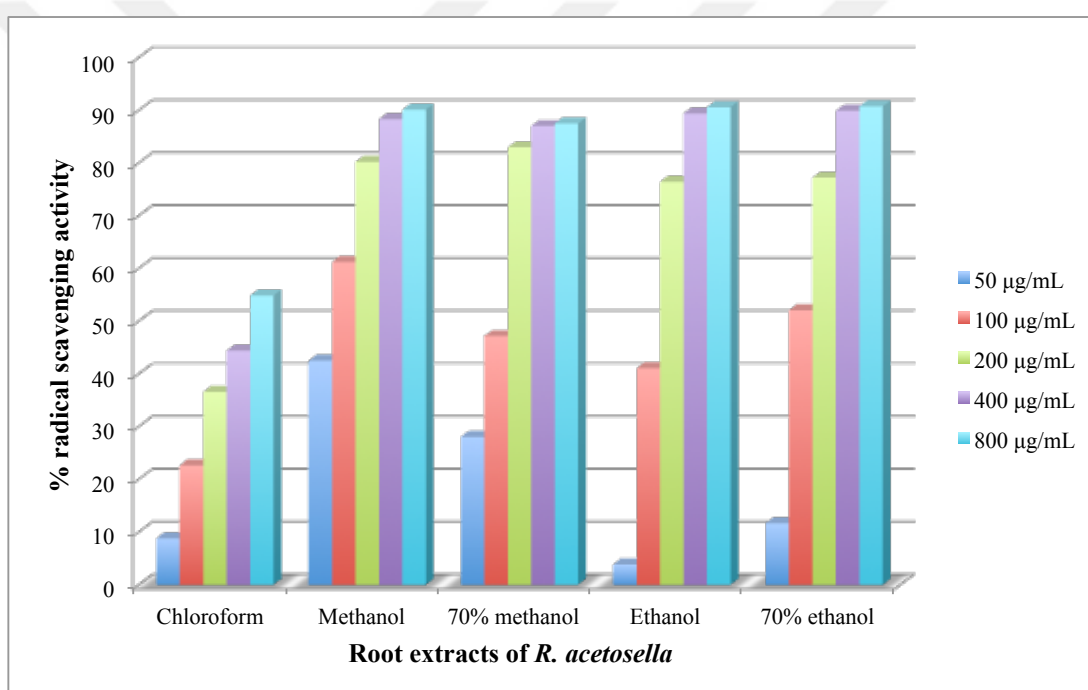
Figure 4.4. ABTS radical scavenging activity % of various root extracts of *R. acetosella*.

Table 4.6. ABTS radical scavenging activitity % of various herbal extracts of *R. acetosella.*

Concentration (µg/mL)	Herb extracts of *R. acetosella*				
	CHCl₃	CH₃OH	70% CH₃OH	C₂H₅OH	70% C₂H₅OH
50	10.67 ± 4.65	41.63 ± 2.75	24.75 ± 3.04	17.92 ± 0.30	33.65 ± 1.99
100	20.97 ± 5.66	68.50 ± 2.51	53.15 ± 3.18	77.71 ± 0.29	73.13 ± 3.98
200	32.53 ± 1.96	86.97 ± 1.97	83.10 ± 1.98	86.04 ± 0.27	88.54 ± 1.03
400	61.63 ± 1.59	89.77 ± 2.87	89.40 ± 0.85	90.21 ± 0.29	90.63 ± 0.00
800	83.57 ± 3.21	89.70 ± 2.55	90.60 ± 1.56	90.52 ± 0.15	90.63 ± 0.00
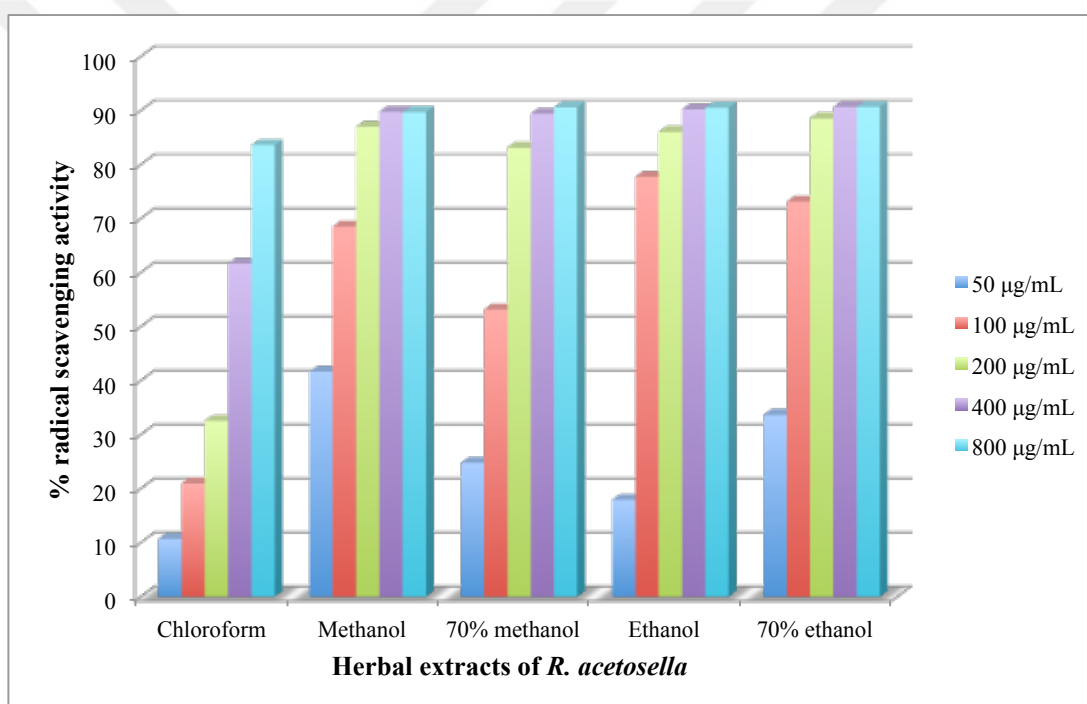
Figure 4.5. ABTS radical scavenging activity % of various herbal extracts of *R. acetosella.*

Table 4.7. ABTS radical scavenging activity % of trolox as a positive control.

Trolox	Concentration (µg/mL)					
	0.78 µg/mL	1.56 µg/mL	3.125 µg/mL	6.25 µg/mL	12.5 µg/mL	25 µg/mL
% radical scavenging activity	35.43 ± 1.77	37.58± 3.98	42.32 ± 4.57	50.07 ± 0.88	64.49 ± 4.57	91.28 ± 0.10
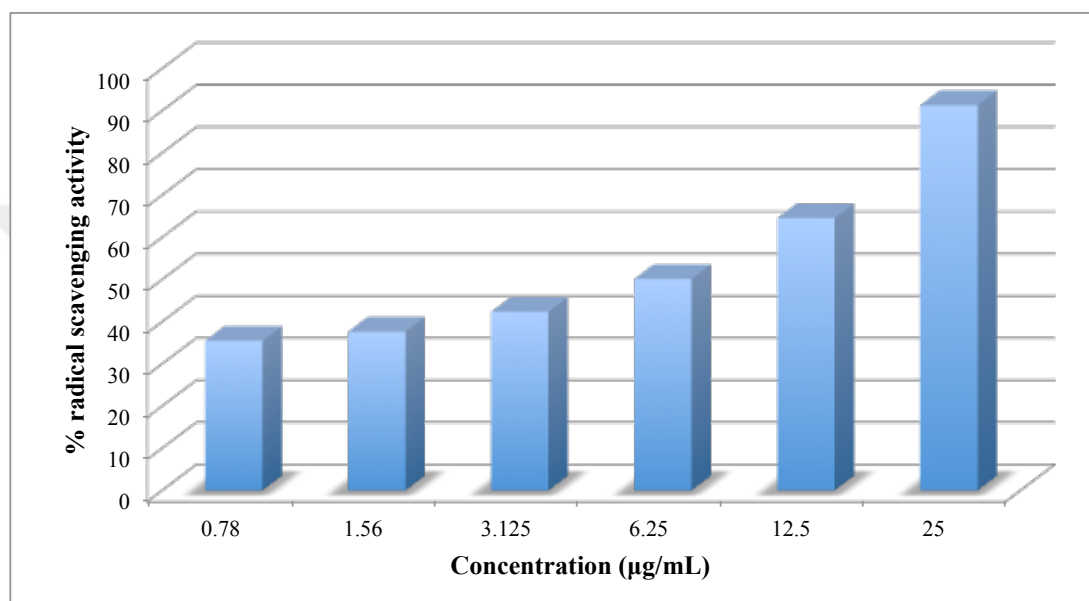
Figure 4.6. ABTS radical scavenging activity of trolox.

Table 4.8. The concentration of *R. acetosella* extracts and trolox required for 50% reduction (RC$_{50}$) against ABTS radicals.

Extracts	RC$_{50}$ values of extracts and trolox (µg/mL)		
	Roots	Herbs	Trolox
CHCl$_3$	614.35	320.04	
CH$_3$OH	70	65.57	
70% CH$_3$OH	107.96	94.45	6.21
C$_2$H$_5$OH	125.24	76.83	
70% C$_2$H$_5$OH	97.43	70.71	

4.1.3   NO Scavenging Activity

NO$_2^-$ scavenging activity of various root and herb extracts of *Rumex acetosella* and ascorbic acid with the concentration ranges of 50 to 800 µg/mL were investigated Chloroform extracts of the roots did not scavenge NO$_2^-$. Hoowever the the remaining extracts showed scavenging effects in a dose dependent manner and displayed better activity than positive control ascorbic acid (**Tables 4.9.-4.11.**; **Figures 4.7.-4.9.**). Specificially, ethanol extract of the herbs showed the best scavenging activity with RC$_{50}$= 208.61 µg/mL among all and the ethanol extract of the roots followed with the RC$_{50}$ value of 280 µg/mL (**Table 4.12.**).

Table 4.9. NO radical scavenging activity % of various root extracts of *R. acetosella.*

Concentration (µg/mL)	Root extracts of *R. acetosella*				
	CHCl$_3$	CH$_3$OH	70% CH$_3$OH	C$_2$H$_5$OH	70% C$_2$H$_5$OH
50	-	2.95 ± 0.34	1.40 ± 0.10	13.28 ± 1.14	-
100	-	9.68 ± 2.60	8.81 ±0.75	28.80 ± 0.91	30.70 ± 0.60
200	-	29.86 ± 1.16	22.89 ± 0.17	44.42 ± 1.06	45.12 ± 0.10
400	-	50.73 ± 0.00	38.82 ± 0.27	58.36 ± 1.48	54.81 ± 0.57
800	-	56.82 ± 1.10	39.45 ± 0.17	69.00 ± 1.01	62.25 ± 0.13
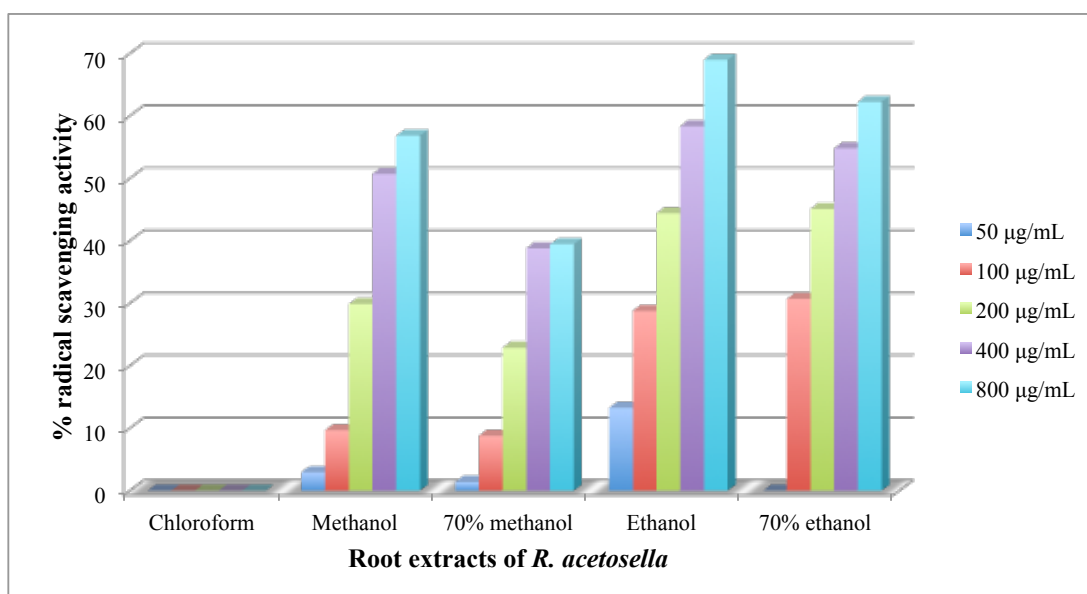
Figure 4.7. NO radical scavenging activity % of various root extracts of *R. acetosella.*

Table 4.10. NO radical scavenging activities % of various herbal extracts of *R. acetosella.*

Concentration (μg/mL)	Herbal extracts of *R. acetosella*				
	CHCl$_3$	CH$_3$OH	70% CH$_3$OH	C$_2$H$_5$OH	70% C$_2$H$_5$OH
50	9.50 ± 2.12	12.90 ± 2.55	11.75 ± 2.47	4.48 ± 0.83	3.30 ± 3.53
100	12.60 ± 1.56	22.25 ± 1.34	20.10 ± 0.99	17.61 ± 3.11	22.52 ± 1.25
200	19.10 ± 5.52	37.70 ± 3.82	33.55 ± 3.61	49.23 ± 3.01	43.69 ± 2.02
400	20.20 ± 6.08	54.00 ± 0.00	53.05 ± 1.34	67.13 ± 1.56	54.11 ± 1.61
800	21.05 ± 2.47	54.50 ± 0.99	55.20 ± 1.98	75.28 ± 0.31	71.46 ± 1.04
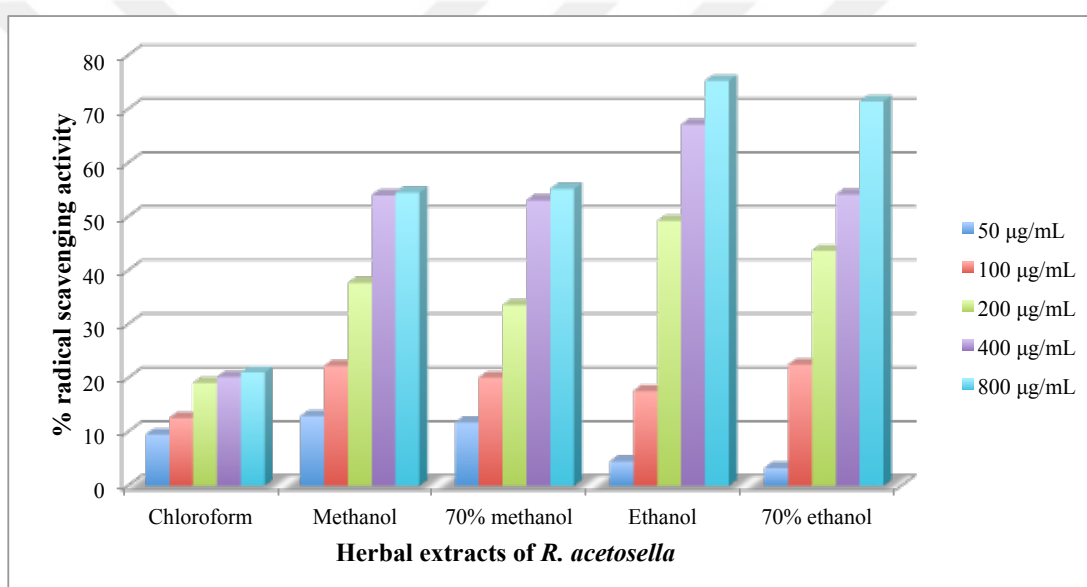
Figure 4.8. NO radical scavenging activity % of various herbal extracts of *R. acetosella.*

Table 4.11. NO radical scavenging activity % of ascorbic acid as a positive control.

Ascorbic acid	Concentration				
	50 µg/mL	100 µg/mL	200 µg/mL	400 µg/mL	800 µg/mL
% radical scavenging activity	8.98 ± 5.23	13.95 ± 4.38	23.40 ± 0.15	41.82 ± 5.95	46.49 ± 2.97
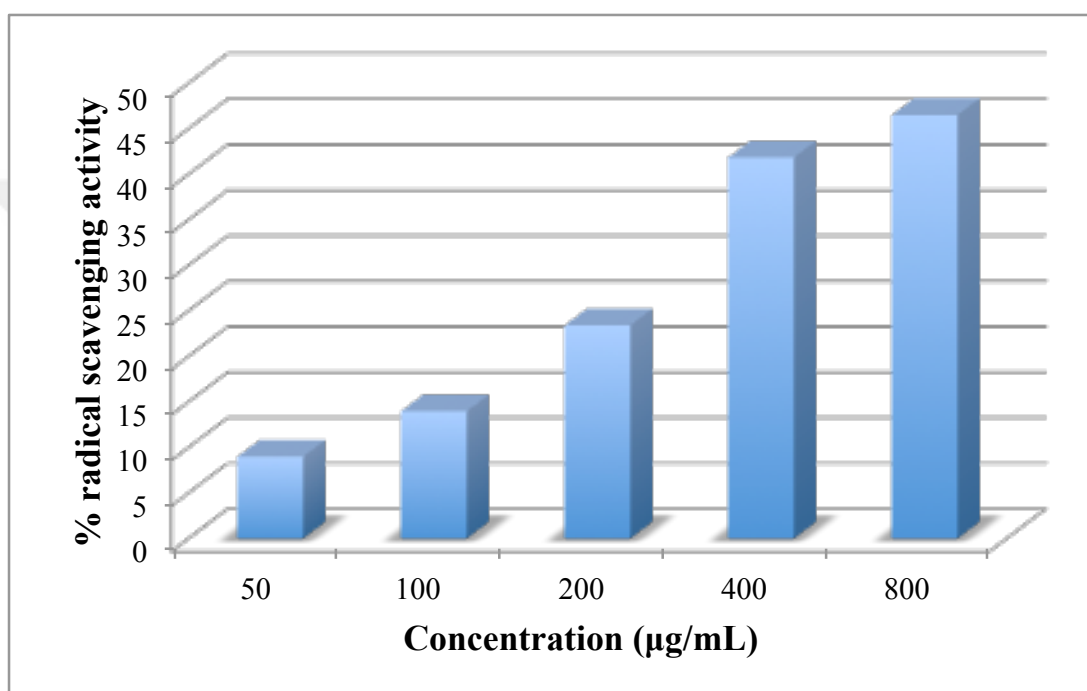
Figure 4.9. NO radical scavenging activity % of ascorbic acid.

Table 4.12. The concentrations of *R. acetosella* extracts and ascorbic acid required for 50% reduction (RC_{50}) against NO radicals.

Extracts	RC_{50} values of extracts and ascorbic acid (µg/mL)		
	Roots	Herbs	Ascorbic acid
CHCl$_3$	-	>800	
CH$_3$OH	393.04	350.92	
70% CH$_3$OH	>800	368.72	>800
C$_2$H$_5$OH	280	208.61	
70% C$_2$H$_5$OH	300	321.13	

4.1.4 The Phosphomolybdate Antioxidant Assay

The total antioxidant assay is based on reduction of phosphate-molybdenum (VI) to phosphate-molybdenum (V). The incubation of extracts with the molybdenum (VI) will tell us the presence of antioxidant components in the extract, which can be assessed by recording the absorbance at 765 nm to detect the reduced green molybdenum complex. Absorbances of root and herb extracts of *Rumex acetosella* as well as ascorbic acid increased in a dose dependent manner (**Tables 4.13.-4.15.**), indicating accelerating total antioxidant capacity.

Total antioxidant capacity was evaluated based on ascorbic acid (**Figure 4.10.**) and as an expression of ascorbic acid equivalent (AEE) each extract presented. In roots, 70% ethanol extracts presented the highest ascorbic acid equivalent (422.6 mg AEE/g extract) (**Table 4.16.**, **Figure 4.11.**), while in herbs methanol extracts presented 324.03 AEE/g extract (**Table 4.17.**, **Figure 4.12.**).

Table 4.13. Absorbances of various root extracts of *R. acetosella* at 765 nm.

Concentration (µg/mL)	Root extracts of *R. acetosella*				
	$CHCl_3$	CH_3OH	70% CH_3OH	C_2H_5OH	70% C_2H_5OH
50	0.1345 ± 0.01	0.182 ± 0.01	0.2065 ± 0.01	0.172 ± 0.12	0.2835 ± 0.00
100	0.148 ± 0.00	0.196 ± 0.01	0.24 ± 0.01	0.182 ± 0.08	0.2925 ± 0.00
200	0.28 ± 0.01	0.218 ± 0.02	0.262 ± 0.02	0.206 ± 0.04	0.3425 0.02
400	0.285 ± 0.01	0.373 ± 0.07	0.2795 ± 0.01	0.2835 ± 0.01	0.419 ± 0.02
800	0.301 ± 0.00	0.393 ± 0.06	0.394 ± 0.01	0.438 ± 0.02	0.5375 ± 0.01

Table 4.14. Absorbances of various herbal extracts of *R. acetosella* at 765 nm.

Concentration (µg/mL)	Herbal extracts of *R. acetosella*				
	$CHCl_3$	CH_3OH	70% CH_3OH	C_2H_5OH	70% C_2H_5OH
50	0.209 ± 0.10	0.2005 ± 0.07	0.1925 ± 0.09	0.1495 ± 0.01	0.138 ± 0.01
100	0.2245 ± 0.01	0.2225 ± 0.05	0.225 ± 0.10	0.1525 ± 0.00	0.151 ± 0.01
200	0.31 ± 0.14	0.2975 ± 0.04	0.2625 ± 0.05	0.154 ± 0.00	0.185 ± 0.02
400	0.345 ± 0.03	0.348 ± 0.07	0.2775 ± 0.01	0.2275 ± 0.00	0.2555 ± 0.01
800	0.355 ± 0.02	0.3615 ± 0.11	0.3795 ± 0.15	0.339 ± 0.00	0.347 ± 0.01

126

Table 4.15. Absorbance of ascorbic acid at 765 nm.

Ascorbic acid	Concentration				
	50 µg/mL	100 µg/mL	200 µg/mL	400 µg/mL	800 µg/mL
Absorbance at 765 nm	0.1792 ± 0.06	0.375 ± 0.10	0.511 ± 0.11	0.6804 ± 0.08	1.6054 ± 0.12
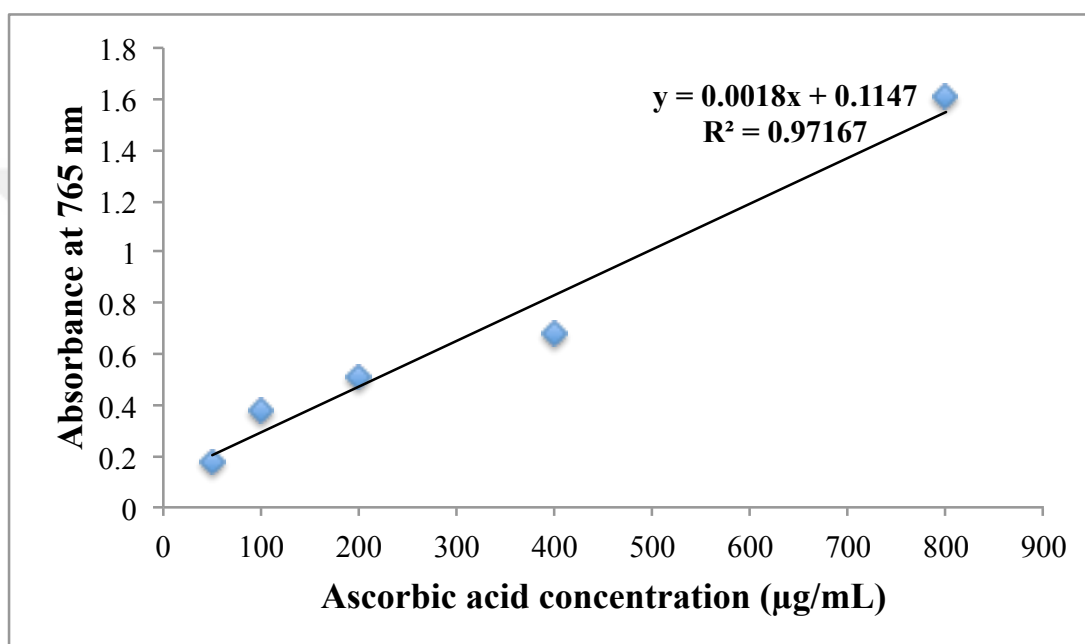
Figure 4.10. Total antioxidant capacity of ascorbic acid.

Table 4.16. Total antioxidant capacities of various root extracts of *R. acetosella* equivalent to ascorbic acid.

mg AEE/g extract	Root extracts of *R. acetosella*				
	CHCl$_3$	CH$_3$OH	70% CH$_3$OH	C$_2$H$_5$OH	70% C$_2$H$_5$OH
	236.5	359.2	228.9	234.4	422.6
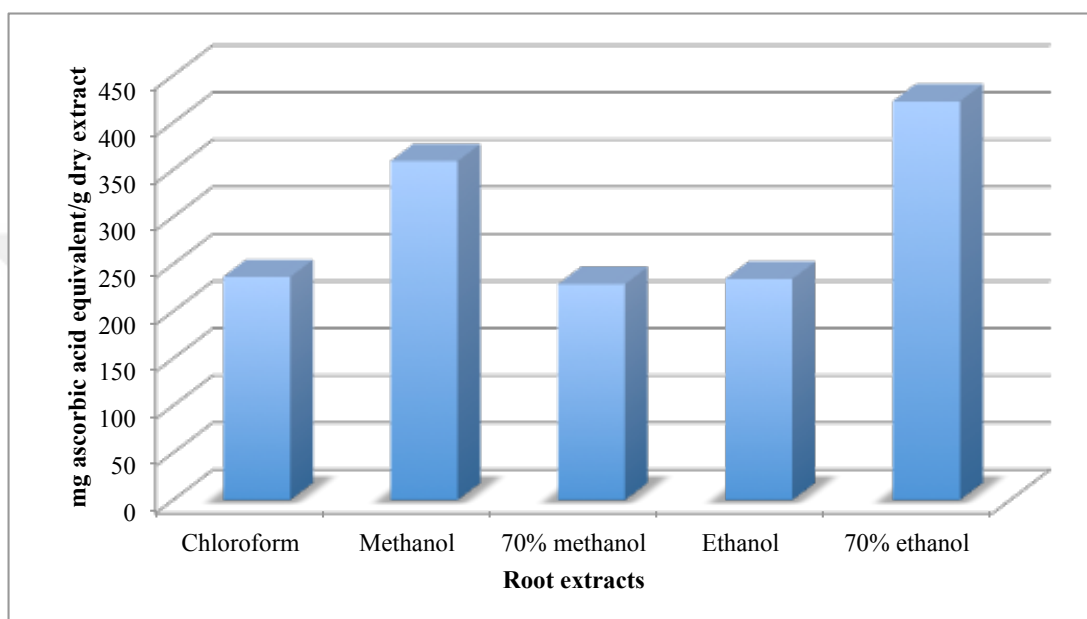
Figure 4.11. Total antioxidant capacities of various root extracts of *R. acetosella* equivalent to ascorbic acid (mg AEE/g extract).

Table 4.17. Total antioxidant capacities of various herbal extracts of *R. acetosella* equivalent to ascorbic acid.

mg AEE/g extract	Herb extracts of *R. acetosella*				
	$CHCl_3$	CH_3OH	70% CH_3OH	C_2H_5OH	70% C_2H_5OH
	319.9	324.03	226.1	156.7	195.6
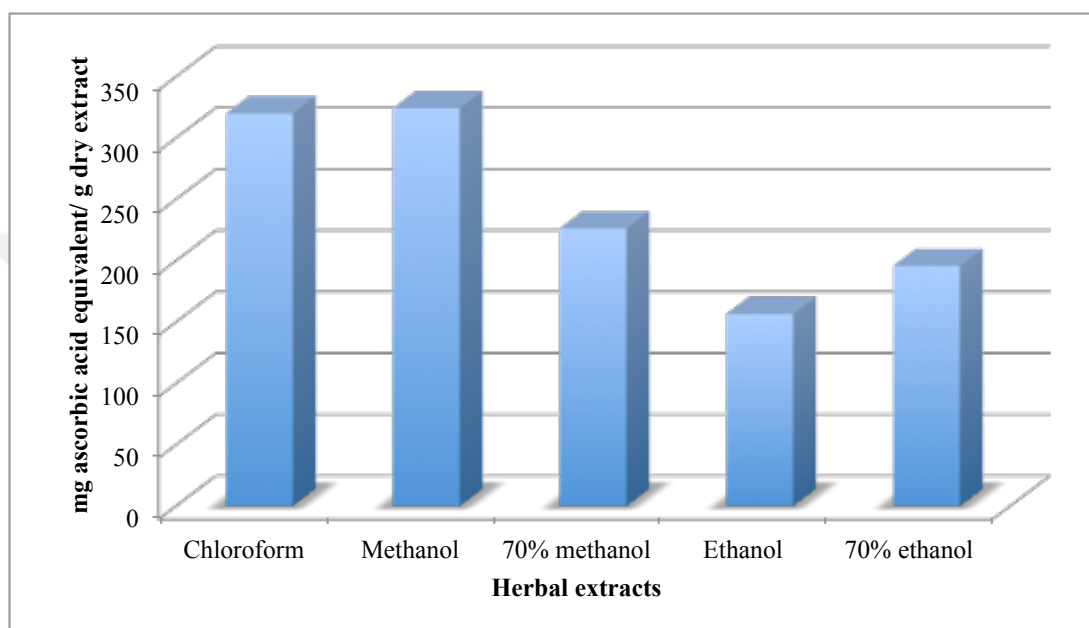
Figure 4.12. Total antioxidant capacities of various herbal extracts of *R. acetosella* equivalent to ascorbic acid (mg AEE/g extract).

4.2   Structural Determination of The Isolated Phytochemicals

4.2.1   (*E*)-Piceid
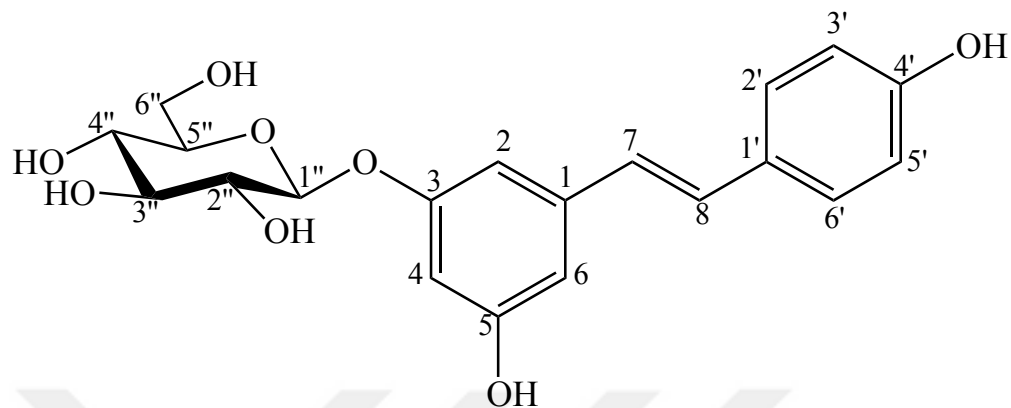
Figure 4.13. Structure of (*E*)-Piceid.

The data about (*E*)-piceid was expressed in **Table 4.18.** in the next page.

Table 4.18. The data about (*E*)-Piceid.

Molecular formula	$C_{20}H_{22}O_8$
Synonyms	3,4',5-trihydroxystilbene-3-*β*-glucoside 3-hydroxy-5-(p-hydroxystyryl)phenyl glucoside 3-hydroxy-5-[(*E*)-2-(4-hydroxyphenyl) ethenyl]phenyl *β*-D-glucopyranoside 3-Hydroxy-5-[(*E*)-2-(4-hydroxyphenyl) vinyl]phenyl *β*-D-glucopyranoside 3-Hydroxy-5-[(*E*)-2-(4-hydroxyphenyl) vinyl]phenyl-*β*-D-glucopyranoside 3-Hydroxy-5-[2-(4-hydroxyphenyl) ethenyl]phenyl-*β*-D-glucopyranoside Piceid Polydatin Resveratrol-3-*β*-mono-D-glucoside *trans*-piceid *β*-D-glucopyranoside-3-hydroxy-5-[(*E*)-2-(4-hydroxyphényl)vinyl]phényle *β*-D-glucopyranoside, 3-hydroxy-5-(2-(4 hydroxyphenyl)ethenyl)phenyl *β*-D-glucopyranoside, 3-hydroxy-5-[(*E*)-2-(4-hydroxyphenyl)ethenyl]phenyl
Molecular weight	390.384 g/mol
IR (ATR) ν (cm^{-1})	3533 – 3050, 2928, 1620, 1513, 1433, 1173, 1076, 1023, 944
MS (ESI) *m/z*	[M+Na]$^+$ 413.1213
[α]$_D^{22}$	–39.3° (MeOH, c = 0.54)
^{1}H NMR	**Figure 4.14.** **Table 4.19.**
^{13}C NMR	**Figure 4.15.** **Table 4.19.**
COSY	**Figure 4.16.**
HMQC	**Figure 4.17.** **Table 4.19.**
HMBC	**Figure 4.18.** **Table 4.19.**

Compound **1** was isolated as an amorphous and white powder. In case of application to TLC plate, no colour was observed before reagent spraying; but floresans inhibiting zones under UV 254 nm and blue floresans under UV 366 nm were monitored. Following Vanilin/H_2SO_4 reagent spraying and Vanilin/H_2SO_4 sprayed-plate to be heated up to 110 °C, dark blue/ purple spots were detected. The substance was elucidated on the basis of spectroscopic data such as IR, NMR and mass spectrometry.

IR spectrum of the compound **1** pointed out presence of aromatic C=C (1513, 1433 cm^{-1}), aromatic C-H (3050-3100 cm^{-1}), alkene C=C (1620 cm^{-1}), alkene C-H (3080-3140 cm^{-1}), C-H (2928 cm^{-1}), C-C (944, 1023 cm^{-1}), O-H (3300-3533 cm^{-1}) and C-O (1076, 1173 cm^{-1}) functions.

^{1}H-NMR indicated number of H signals and chemical shifts of H atoms in the molecule based on their different magnetic environments and gave information about their magnetic environments. When ^{1}H-NMR spectrum was analysed, H atom signals in the aromatic field of the spectrum integrating 1 H in their carbons were detected as follows at 7.42 (d, 1H, H-2'), 7.37 (d, 1H, H-6'), 6.78 (d, 1H, H-3'), 6.73 (d, 1H, H-5'), 6.72 (d, 1H, J = 1.8 Hz, H-2), 6.55 (d, 1H, H-6), 6.32 (d, 1H, J = 1.8 Hz, H-4) ppm (**Table 4.19**, **Figure 4.14.**).

A proton signal at 4.79 ppm splitting into two peaks as doublet with 7.7 Hz coupling constant (J) is an anomeric proton. 7.7 Hz of J value indicated that sugar molecule is in β configuration. The other proton signals in the sugar molecule were ranged from δ_H 3.15 to δ_H 3.72 ppm. H atoms bounded with O atoms (-OH) were also detected in NMR spectrum, which were observed at 5.04 (s, OH-4"), 5.11 (s, OH-3"), 5.29 (d, J = 4.8 Hz, OH-2"), and 4.64 (t, J = 5.8 Hz, OH-6") ppm. δ_H of H atoms in sugar molecule were detected at 4.79 (d, J = 7.7 Hz, H-1"), 3.20 (td, J = 8.4, 4.8 Hz, H-2"), 3.26 (t, J = 8.9 Hz, H-3"), 3.15 (t, J = 9.4 Hz, H-4"), 3.31 (ddd, J = 9.4, 5.8, 2.1 Hz, H-5"), 3.72 (dd, J = 11.8, 2.1 Hz, H-6"α) and 3.48 (dd, J = 11.8, 5.8 Hz, H-6"β). H-6" protons with J = 11.8, 2.1 Hz (H-6"α) and 11.8, 5.8 Hz (H-6"β) coupling constants as well as H-1" at 4.79 ppm with J = 7.7 Hz coupling constant give rise to thought the structure to include β-glucose. Signals of H atoms bounded with O atoms in the aromatic rings were displayed at 9.49 (s, -OH-5) and 9.56 (s, -OH-4') ppm, as well.

^{13}C-NMR spectrum (**Table 4.19**; **Figure 4.15.**) showed the presence of 6 carbon atoms in the sugar molecule as well as other carbon atoms in the molecule. δ_C of C atoms in the sugar molecule were detected as 100.7 (anomeric C, C-1″), 73.3 (C-2″), 76.7 (C-3″), 69.8 (C-4″), 77.2 (C-5″) and 60.7 ppm (C-6″). Both δ_C and δ_H values for sugar molecule indicated that the sugar moiety is a hexose and a comparison with previous data, identified the hexose unit as *β*-glucose (401, 473). 7.42 (d, H-2′), 6.78 (d, H-3′), 6.73 (d, H-5′) and 7.37 (d, H-6′) are assigned to a AA′XX′ system of a 1-4 disubstituted aromatic ring; three doublets at δ 6.72, 6.32, 6.55 are assigned to three *meta* related protons of a 1, 3, 5-trisubstituted aromatic ring and two doublets (δ 6.86 and 7.03) with a large coupling constant (*J*= 16.3 Hz) show a trans olefinic proton system. These signals are consistent with a *trans* stilbene system substituted by a glucoside.

δ_C of alkene carbon signals were detected at 125.2 (C-7) and 128.6 ppm (C-8), respectively. δ_C of aromatic C atoms' signals were ranged from 102.7 to 158.9 ppm. δ_C of C-5 (158.4 ppm) and C-4′ (157.4 ppm) revealed that they may be connected with OH groups due to their chemical shifts in high frequencies.

Based on Cosy (COrrelation SpectroscopY) spectrum, all H signals coupling with each other in glucose molecule were displayed based on anomeric H at C-1″. Furthermore, ^{1}H-^{1}H couplings in aromatic rings were clearly detected (**Figure 4.16.**).

^{1}H-^{13}C heteronuclear multiple-quantum correlation (HMQC) spectrum pointed out protons attaching to their relating carbon atoms. H atoms in hexose molecule and aglycone connected with their relating carbons were shown in **Figure 4.17..**

^{1}H-^{13}C heteronuclear multiple-bond correlation (HMBC) spectrum gave information about the relationships between protons and carbons in a structure. As seen in HMBC spectrum (**Figure 4.18.**), there was a long range coupling between the anomeric proton of *β*-glucose H-1″ and C-3, indicating the linkage of the glucose unit on C-3. Furthermore, the relationships between H-2′ and H-6′ with C-4′, H-8 with C-1, C-2′ and C-6′, H-7 with C-6, C-1, C-2, C-2′ and C-6′, H-3′ and H-5′ with C-2′ and C-6′, H-2 with C-4, C-5, C-6, C-7, H-6 with C-2, C-4, C-5 and C-7, H-4 with C-2, C-3, C-5 and C-6, H-5″ with C-1″, H-3″ with C-2″ and C-4″, H-2″ with C-1″, C-3″ and C-5″, H-4″ with C-3″, C-5″ and C-6″ were also observed (**Figure 4.18.**). The

long range coupling of H-7 and H-8 with their relating C atoms pointed their linked aromatic rings.

Following the analysis of NMR spectra, molecular formula of the compound was detected as $C_{20}H_{22}O_8$, which was further confirmed by HR-MS (ESI) *m/z* as $[M+Na]^+$ 413.1213 (**Table 4.18.**).

Our spectroscopic data (**Table 4.19.**) were in consistent with those previously indicated in the literature (401, 473). Therefore, based on the spectroscopic data and literature comparison, compound **1** was elucidated as (*E*)-piceid (**Figure 4.13.**).

Table 4.19. ^{1}H- and ^{13}C-NMR spectroscopic data of (*E*)-piceid (DMSO-*d₆*, ^{1}H: 600 MHz, ^{13}C: 151 MHz).

C/H		δ_H (ppm), *J* (Hz)	δ_C (ppm)	HMBC (H➔C)
1	C	-	139.4	-
2	CH	6.72 (d, 1.8)	104.7	C-4, C-5, C-7
3	C	-	158.9	-
4	CH	6.32 (d, 1.8)	102.7	C-2, C-3, C-5, C-6
5	C	-	158.4	-
6	CH	6.55 (d, 1.8)	107.2	C-2, C-4, C-5, C-7
7	CH	6.86 (d, 16.3)	125.2	C-1, C-2, C-6, C-2', C-6'
8	CH	7.03 (d, 16.3)	128.6	C-1, C-2', C-6'
1'	C	-	-	-
2'	CH	7.42 (d)	128.0	C-8, C-4'
3'	CH	6.78 (d)	115.6	C-4'
4'	C	-	157.4	-
5'	CH	6.73 (d)	115.6	C-4'
6'	CH	7.37 (d)	128.0	C-8, C-4'
1"	CH	4.79 (d, 7.7)	100.7	C-3
2"	CH	3.20 (td, 8.4, 4.8)	73.3	C-1", C-3", C-5"
3"	CH	3.26 (t, 8.9)	76.7	C-2", C-4"
4"	CH	3.15 (t, 9.4)	69.8	C-3", C-5", C-6"
5"	CH	3.31 (ddd, 9.4, 5.8, 2.1)	77.2	C-1"
6"	CH₂	3.72 (dd, 11.8, 2.1) 3.48 (dd, 11.8, 5.8)	60.7	C-2", C-3", C-4", C-5"
5	OH	9.49 (s)	-	-
4'	OH	9.56 (s)	-	-
2"	OH	5.29 (d, 4.8)	-	-
3"	OH	5.11 (s)	-	-
4"	OH	5.04 (s)	-	-
6"	OH	4.64 (t, 5.8)	-	-
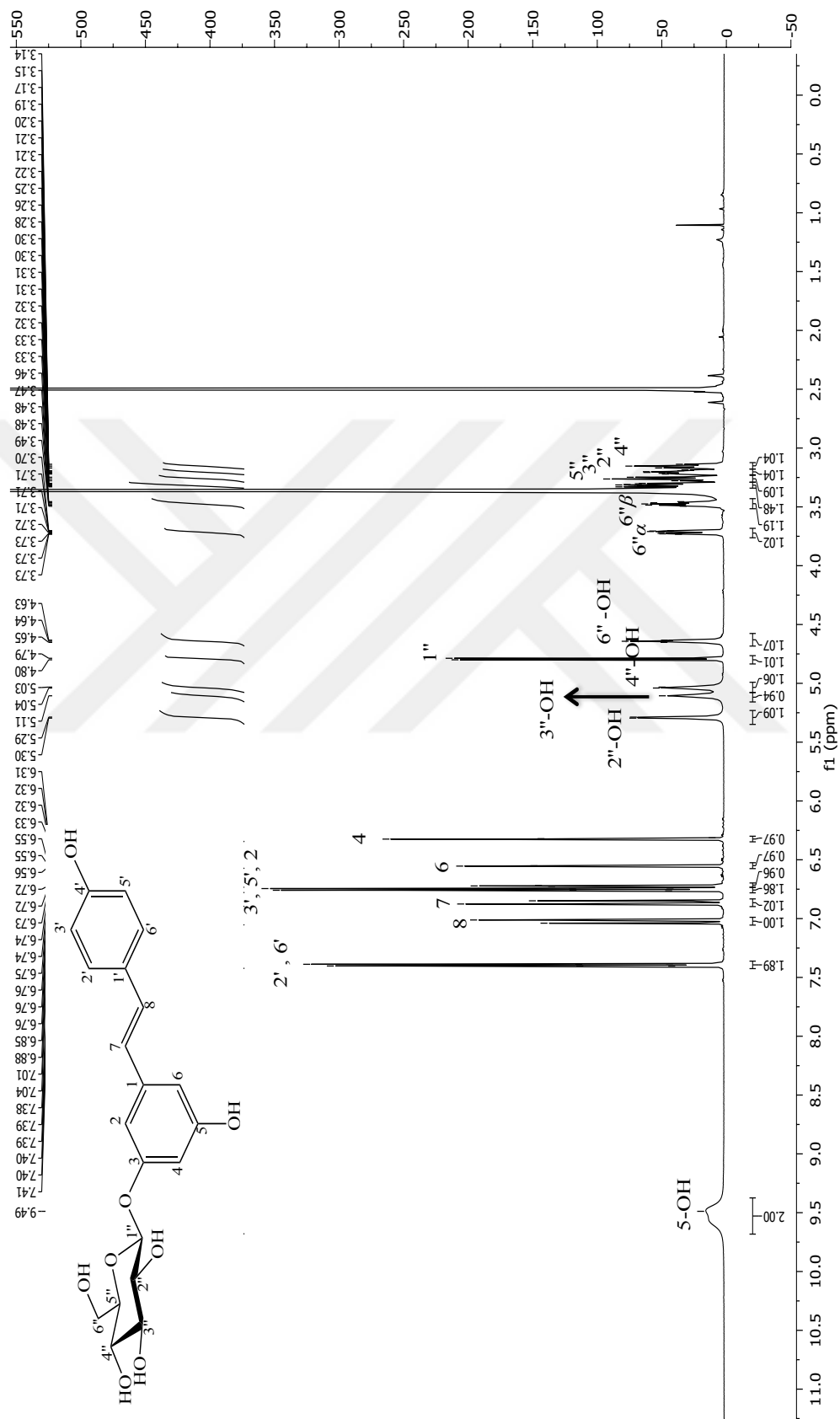
Figure 4.14. ¹H-NMR spectrum of (*E*)-piceid (Compound **1**) (DMSO-*d₆*, ¹H: 600 MHz).
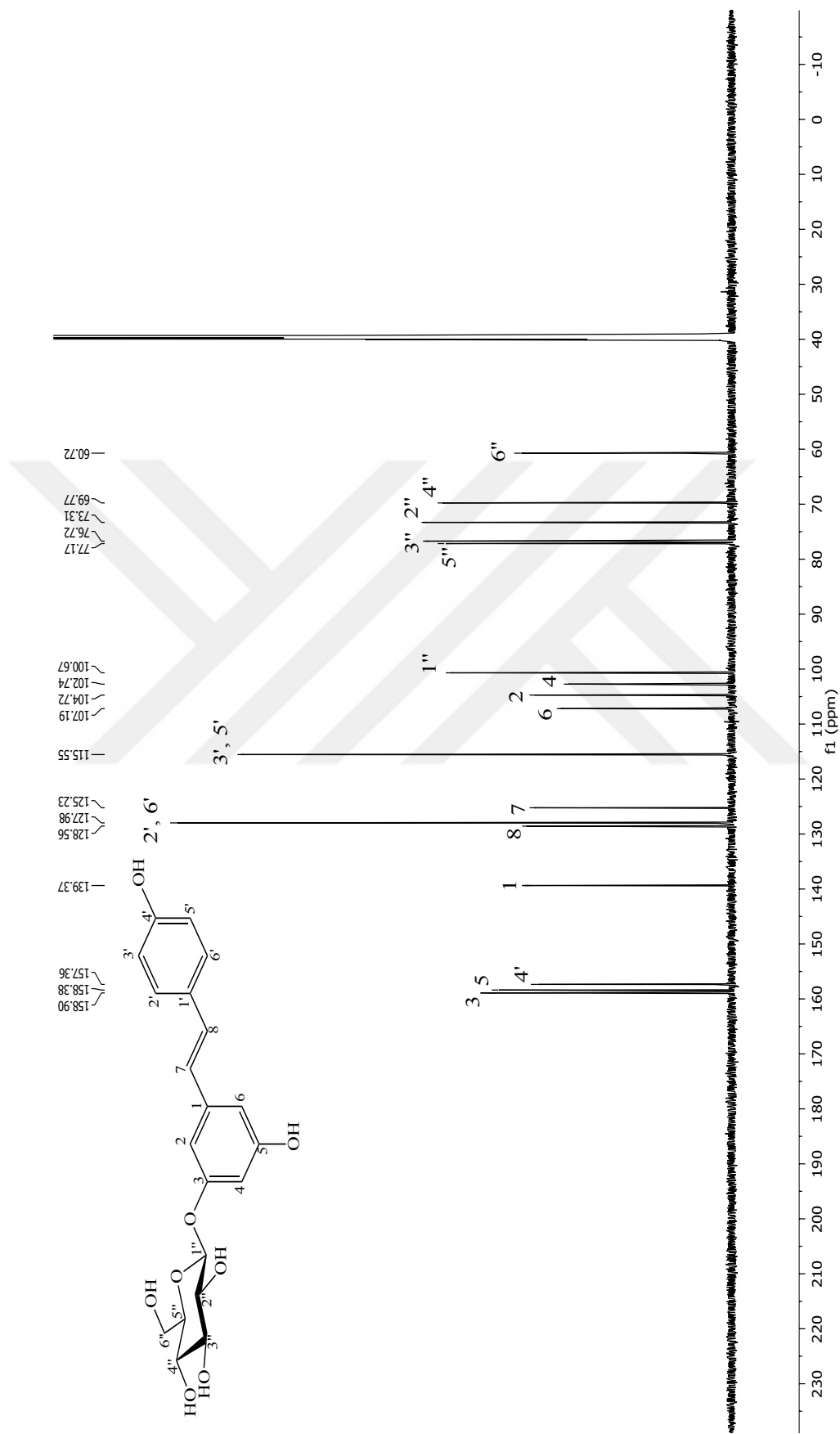
Figure 4.15. ^{13}C-NMR spectrum of (*E*)-piceid (Compound **1**) (DMSO-*d*$_6$, ^{13}C: 151 MHz).
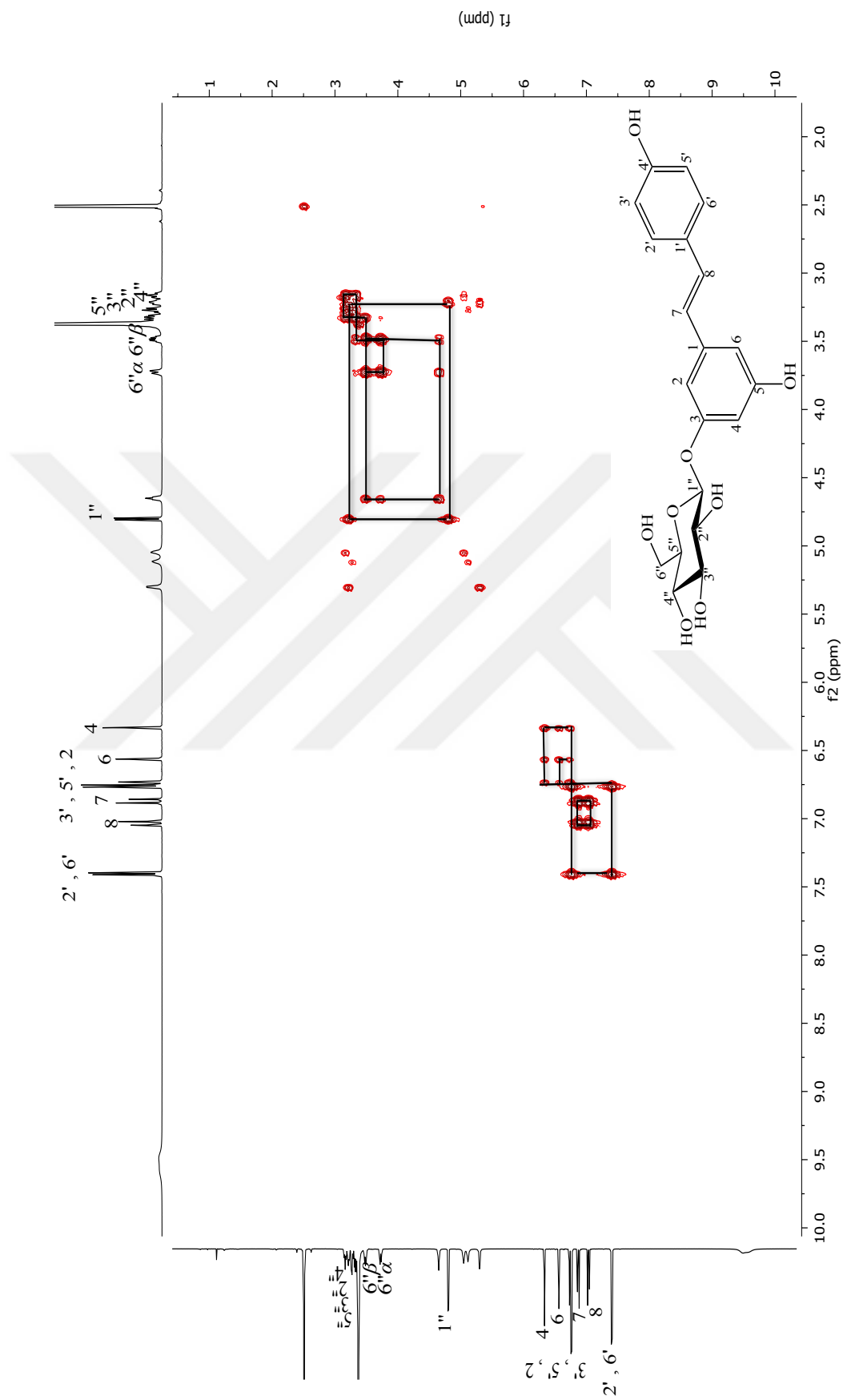
Figure 4.16. ¹H-¹H homonuclear correlation spectrum (COSY) of (*E*)-piceid (Compound **1**).
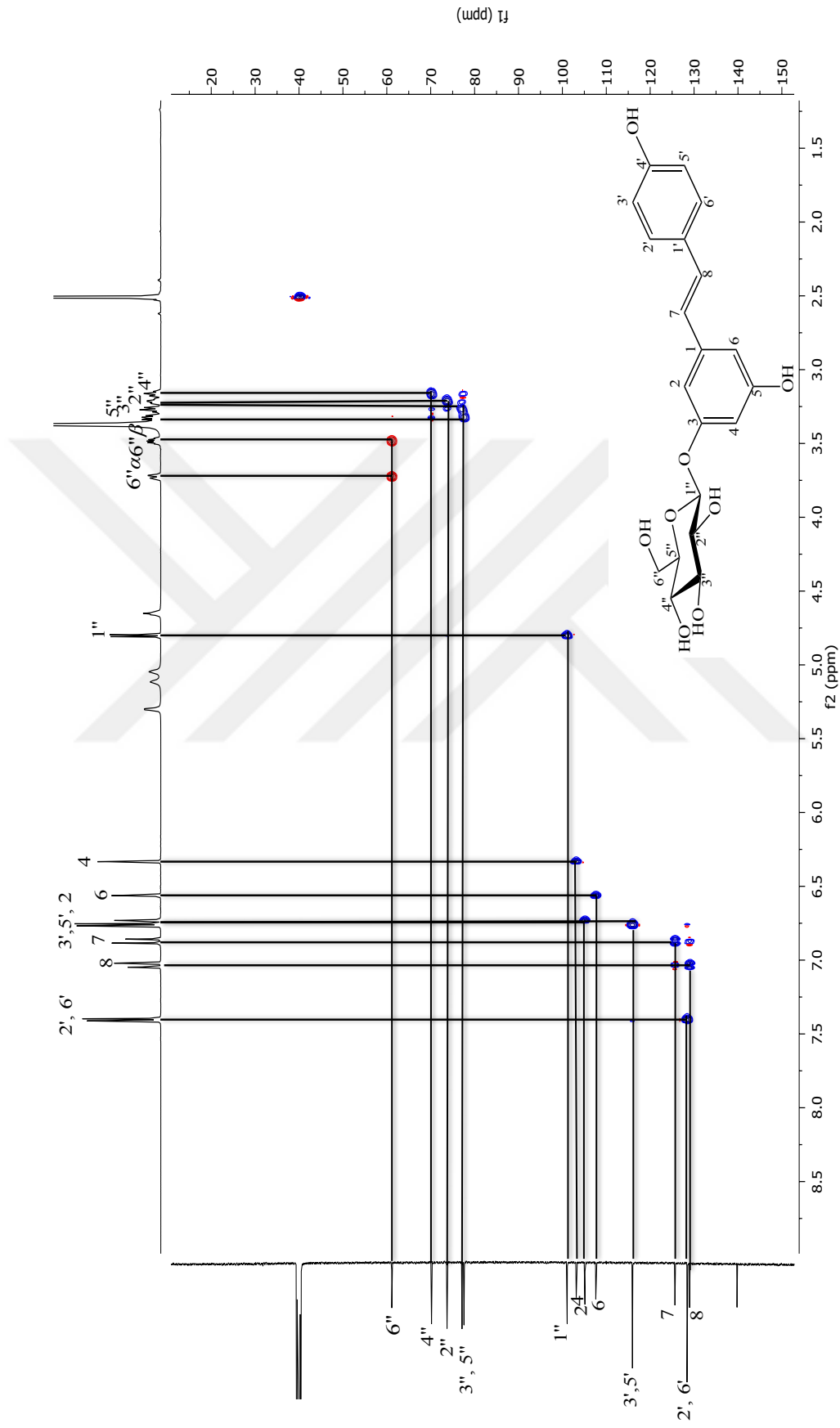
Figure 4.17. ^{1}H-^{13}C heteronuclear multiple-quantum correlation (HMQC) spectrum of (*E*)-piceid (Compound **1**).
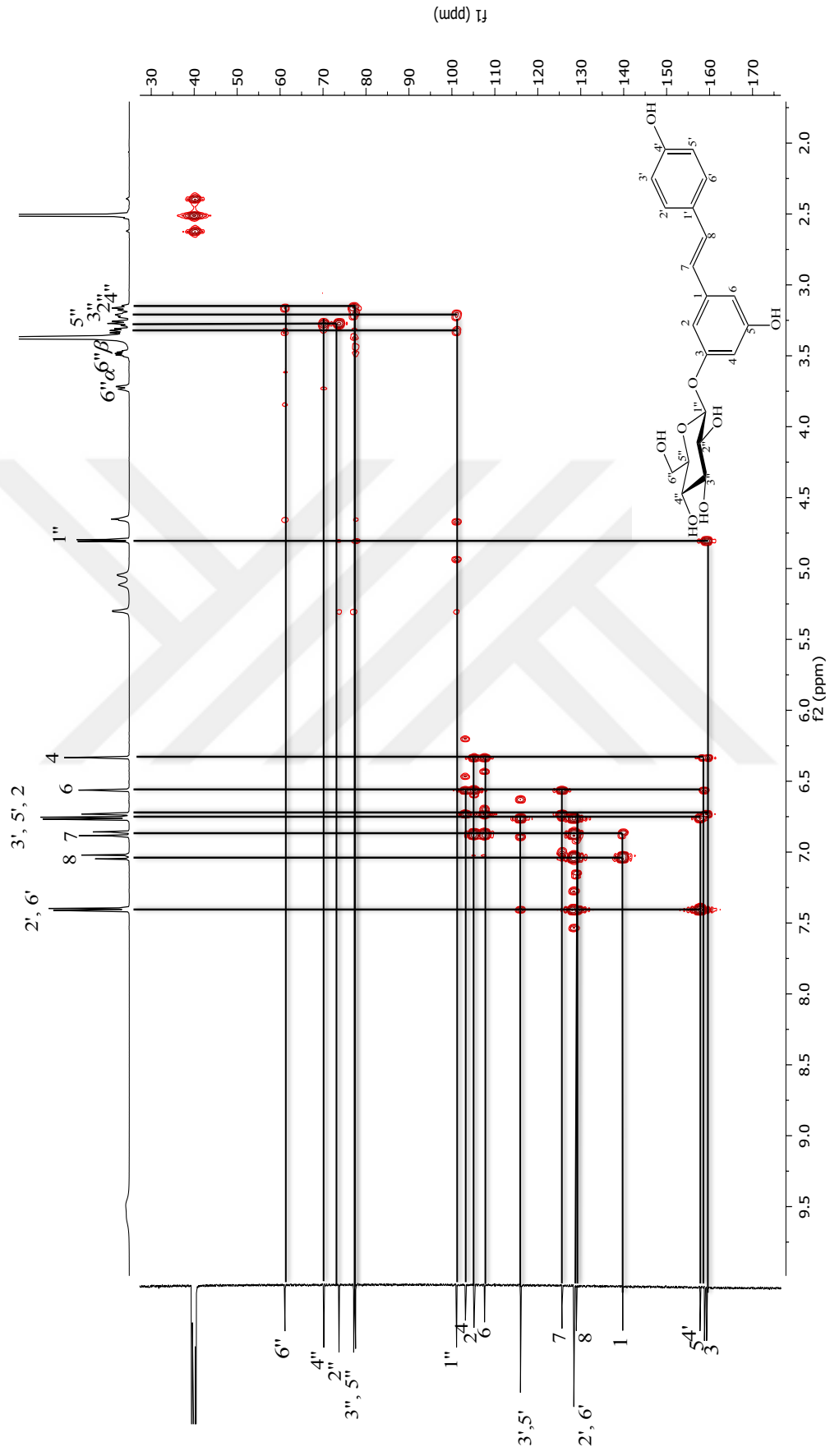
Figure 4.18. ^1H-^{13}C heteronuclear multiple-bond correlation (HMBC) spectrum of (*E*)-piceid (Compound **1**).

4.2.2 Ethanone,1-[2-(*β*-glucopyranosyloxy)-4-hydroxy-6-methylphenyl)] (Compound 2, named as acetoselloside)
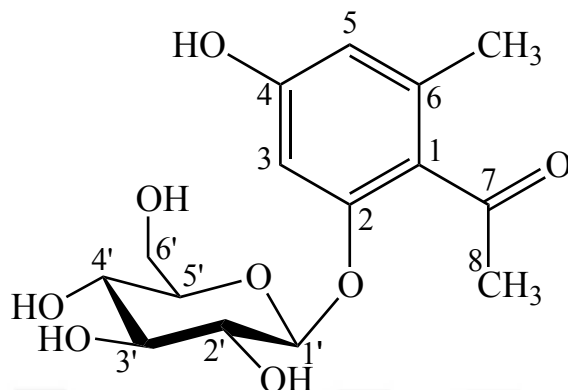
Figure 4.19. Structure of acetoselloside (ethanone, 1-[2-(*β*-glucopyranosyloxy)-4-hydroxy-6-methylphenyl]).

The data about acetoselloside was expressed in **Table 4.20.** below.

Table 4.20. The data about acetoselloside.

Molecular formula	$C_{15}H_{20}O_8$
Molecular weight	328 g/mol
MS (ESI) *m/z*:	$[M+Na]^+$ 351.1047
IR (ATR) ν (cm^{-1})	3650 – 3000, 2928, 1654, 1605, 1464, 1328, 1258, 1173, 1077
^{1}H NMR	**Figure 4.20.** **Table 4.21.**
^{13}C NMR	**Figure 4.21.** **Table 4.21.**
COSY	**Figure 4.22.**
HMQC	**Figure 4.23.** **Table 4.21.**
HMBC	**Figure 4.24.** **Table 4.21.**

Compound **2** was isolated as an amorphous and colourless solid. When applied to TLC plate, light yellow spot was observed at daylight before reagent spraying. Additionally, the spot having fluorescence inhibiting zones under UV 254 nm and blue fluorescence under UV 366 nm were monitored. After Vanilin/H_2SO_4 sprayed and the plate to be heated up to 110 °C, a dark blue spot was detected. The structure of the substance was identified based on the spectroscopic data (IR, NMR and mass spectroscopy).

IR spectrum of the compound **2** pointed out the presence of aromatic C=C (1464, 1605 cm^{-1}), aromatic C-H (3000-3100 cm^{-1}), alkane C-H (1328, 2928 cm^{-1}), C-C (944, 1023 cm^{-1}), O-H (3300-3650 cm^{-1}), C-O (1077, 1173 cm^{-1}), and C=O (1654 cm^{-1}) functions.

Based on the data obtained from ^{1}H-NMR spectrum (**Figure 4.20.**), H atoms in the aromatic field of the spectrum with their integrating proton signals were detected at δ_H 6.42 (d, J = 2.0 Hz, 1H, H-3) and 6.27 (d, J = 2.0 Hz, 1H, H-5), while other proton signals were detected at δ_H 5.29 (d, J = 5.4 Hz, 1H, H of OH in C-2'-OH), 5.11 (s, 1H, H of OH in C-3'-OH), 5.05 (s, 1H, H of OH in C-4'-OH), 4.83 (d, J = 7.7 Hz, 1H, H-1'), 4.56 (s, 1H, H of OH in C-6'-OH), 3.68 (dd, J = 11.9, 2.1 Hz, 1H, H-6'), 3.48 (dd, J = 11.9, 5.4 Hz, 1H, H-6'), 3.31 – 3.23 (2H, for both H-3' and H-5'), 3.23 – 3.15 (2H, for both H-2' and H-4'), 2.43 (s, 3H, H-8), 2.08 (s, 3H, H atoms of Me in C-6-Me).

A proton signal at 4.83 ppm splitting into two peaks as doublet with 7.7 Hz coupling constant (J) is an anomeric proton. 7.7 Hz of J value indicated that sugar molecule is in β configuration. The other protons' signals in the sugar molecule were ranged from δ_H 3.15 to δ_H 3.68 ppm. Signals of the H atoms connecting to O atoms (-OH) were also detected in the NMR spectrum as indicated above. H atom signals in the aromatic ring were detected at 6.27 and 6.42 ppm.

^{13}C-NMR spectrum (**Table 4.21**; **Figure 4.21.**) showed the presence of 15 carbon atoms in the structure, 6 of which belong to a sugar molecule. δ_C of the signals of the C atoms in the sugar molecule were noted at 100.5 (anomeric C, C-1'), 73.3 (C-2'), 76.8 (C-3'), 69.5 (C-4'), 77.1 (C-5') and 60.6 ppm (C-6'), which was quite similar to the data of a glucose molecule indicated in the literature (400, 470, 471). δ_C and δ_H values pointed out that the sugar unit is a hexose and a literature survey

revealed that its structure is identical to β-glucose. IR spectrum supported the proposed the structure of **2** expressing the signals indicating the presence of an aromatic ring, and broad OH signals as well as signals attributed to carbonyl and alkane groups, thus it was assumed that the structure of compound **2** might be a member of ethanone derivative. δ_C of the aromatic C atom signals were ranged from 99.9 to 159.2. δ_C of the C signals at 1st, 2nd, 4th and 6th positions in the aromatic ring were observed at downfield region indicating that the aromatic ring carries substitutions at those C atoms. Particularly C-4 and C-2 signals with higher chemical shifts pointed that that they might be connected with O-containing groups such as OH and O-glucoside.

In the COSY spectrum, all H signals coupled with each other in glucose molecule were clearly displayed following with the detection of anomeric proton at C-1'. Furthermore, ^{1}H-^{1}H couplings in the aromatic rings were clearly observed. Couplings of H-3 with H-5, H-3 with H atoms of Me in C-6-Me, H-5 with H atoms of Me in C-6-Me were also detected (**Figure 4.22.**).

HMQC spectrum indicating H atoms and their binding carbons in the structure were shown in **Figure 4.23.**.

HMBC showing the relationships between protons and carbons pointed out a long-range coupling between anomeric proton of β-glucose and C-2 indicating β-glucose substitution at C-2 in the aromatic ring. Furthermore, the relationships of H-3 with C-1, C-2, C-4 and C-5, H-5 with C-1, C-3, C-4 and C of Me in C-6-Me, H-6' with C-4', H-5' with C-2', C-3' and C-4', H-3' with C-1', C-2', C-4' and C-5', H-2' with C-1', H-4' with C-3', C-5' and C-6', H-8 with C-7, H atoms of Me in C-6-Me with C-1, C-2, C-5 and C-6 were also detected (**Figure 4.24.**).

Following the analysis of NMR spectra, molecular formula of the compound was detected as $C_{15}H_{20}O_8$, which was further confirmed by HR-MS (ESI) *m/z* as $[M+Na]^+$ 351.1047 (**Table 4.20.**).

Spectroscopic data (**Table 4.21.**) of compound **2** were checked in the literature, however not any substance with those data was found. Therefore, compound **2** was identified as a new compound and named as acetoselloside (**Figure 4.19.**).

Table 4.21. ^{1}H- and ^{13}C-NMR spectroscopic data of acetoselloside (DMSO-d_6, ^{1}H: 600 MHz, ^{13}C: 151 MHz).

C/H		δ_H (ppm), J (Hz)	δ_C (ppm)	HMBC (H→C)
1	C	-	122.5	-
2	C	-	156.4	-
3	CH	6.42 (d, 2.0)	99.9	C-1, C-2, C-4, C-5
4	C	-	159.2	-
5	CH	6.27 (d, 2.0)	111.0	C-1, C-3, C-4, C6-Me
6	C	-	137.1	-
7	C	-	203.4	-
8	CH$_3$	2.43 (s)	32.7	C-7
1'	CH	4.83 (d, 7.7)	100.5	C-2
2'	CH	3.23 – 3.15†	73.3	C-1'
3'	CH	3.31 – 3.23†	76.8	C-1', C-2', C-4', C-5'
4'	CH	3.23 – 3.15†	69.5	C-3', C-5', C-6'
5'	CH	3.31 – 3.23†	77.1	C-2', C-3', C-4'
6'	CH$_2$	3.68 (dd, 11.9, 2.1)	60.6	C-4'
		3.48 (dd, 11.9, 5.4)		
2'-OH	OH	5.29 (d, 5.4)	-	-
3'-OH	OH	5.11 (s)	-	-
4'-OH	OH	5.05 (s)	-	-
6'-OH	OH	4.56 (s)	-	-
C-6-Me	CH$_3$	2.08 (s)	19.6	C-1, C-2, C-5, C-6

†: Coupling constant (J) were not calculated due to overlap of signals.
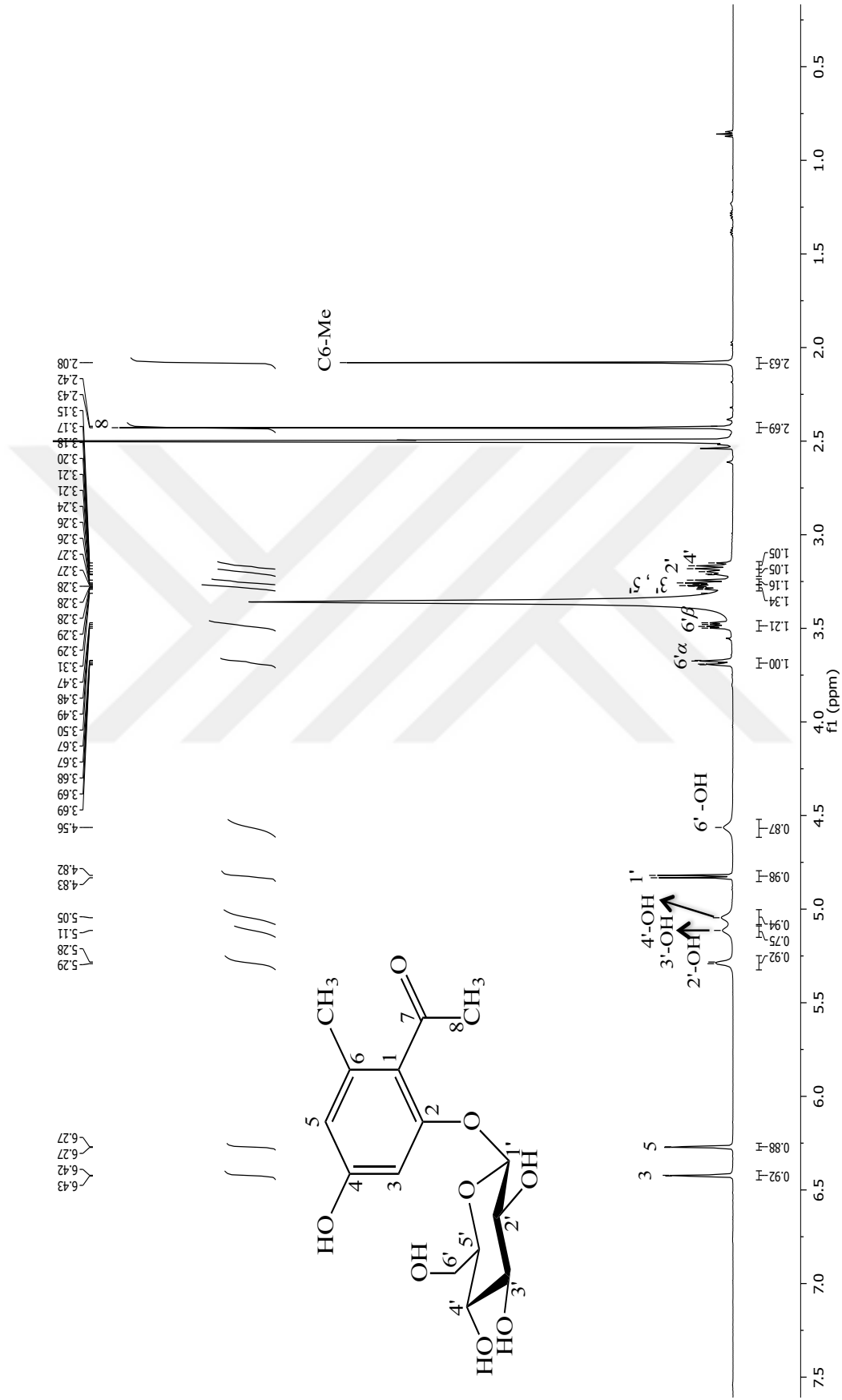
Figure 4.20. ^{1}H-NMR spectrum of acetoselloside (Compound **2**) (DMSO-d_6, ^{1}H: 600 MHz).

145
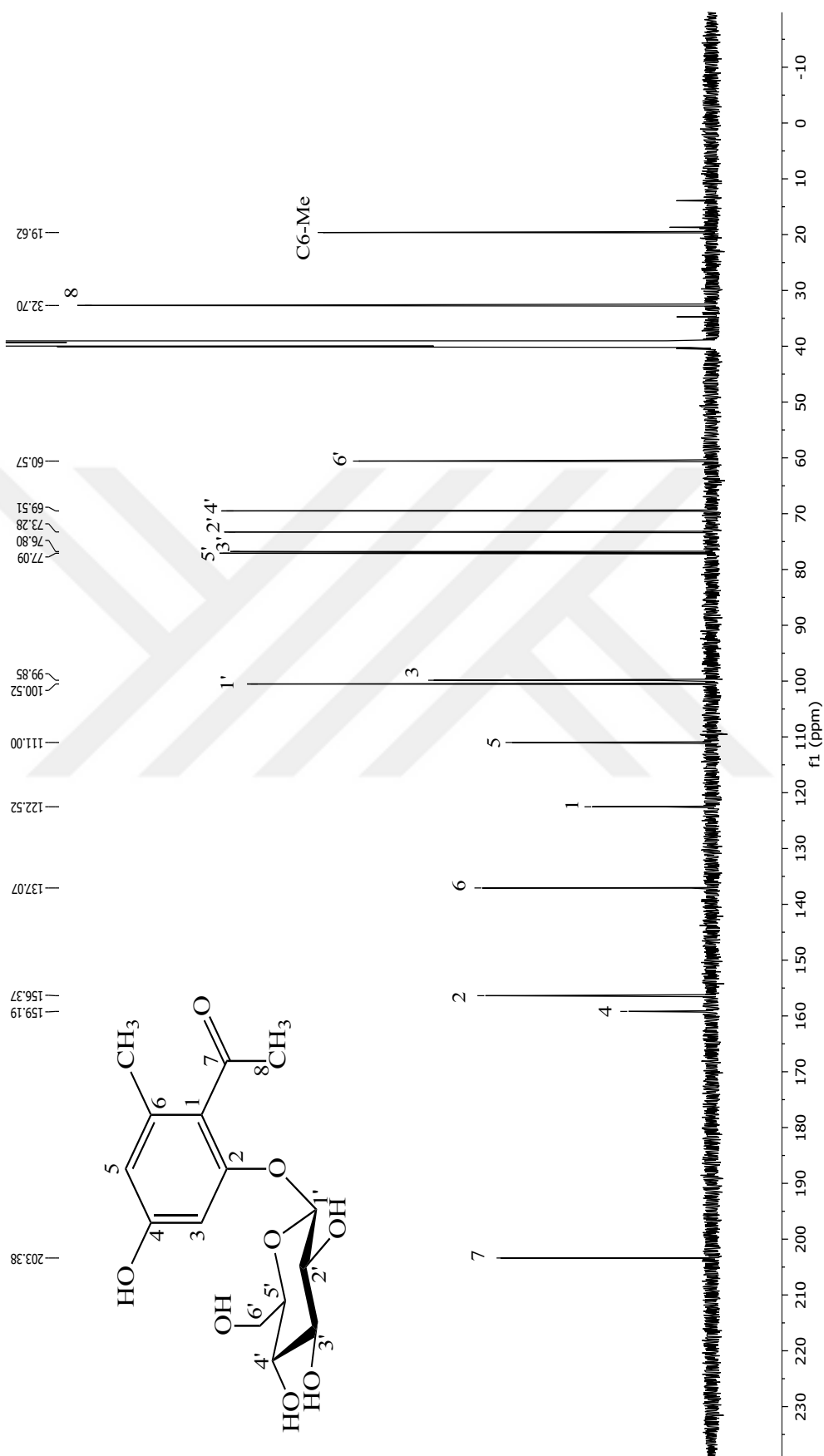
Figure 4.21. ^{13}C-NMR spectrum of acetoselloside (Compound **2**) (DMSO-d_6, ^{13}C: 151 MHz).
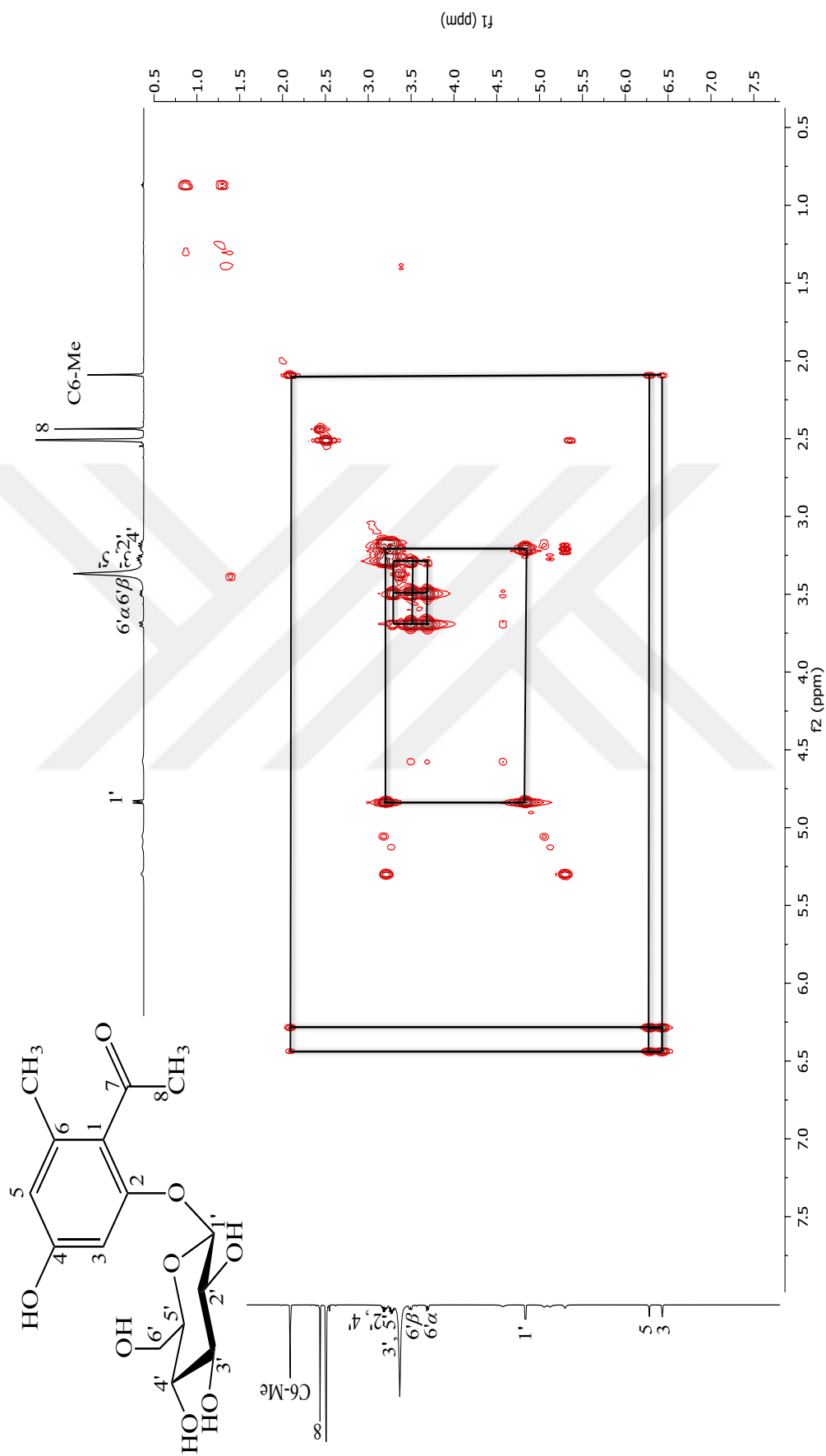
Figure 4.22. ^{1}H-^{1}H homonuclear correlation spectrum (COSY) of acetoselloside (Compound **2**).
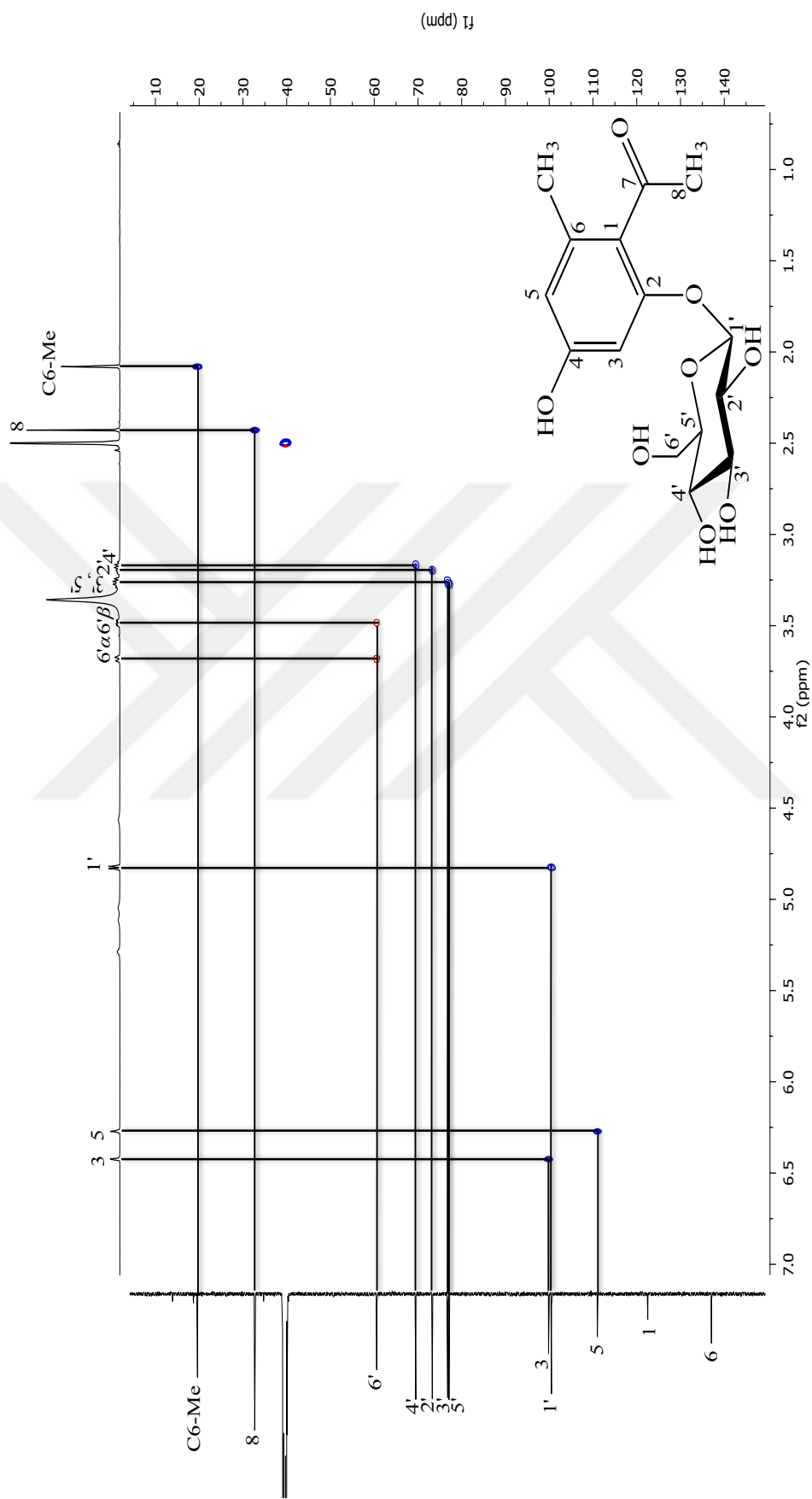
Figure 4.23. ^{1}H-^{13}C heteronuclear multiple-quantum correlation (HMQC) spectrum of acetoselloside (Compound **2**).
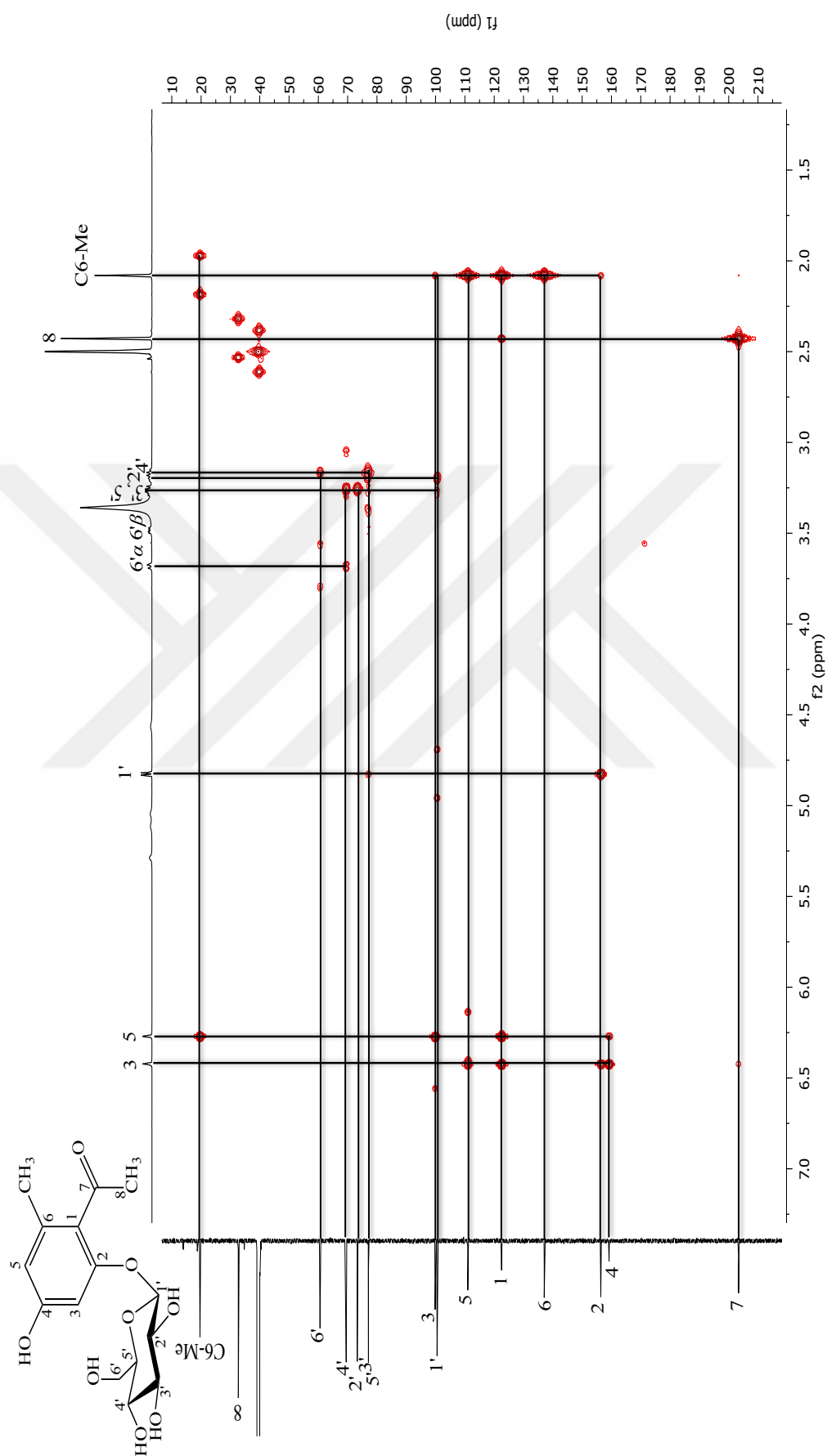
Figure 4.24. ^{1}H-^{13}C heteronuclear multiple-bond correlation (HMBC) spectrum of acetoselloside (Compound **2**).

4.2.3 Lyoniside
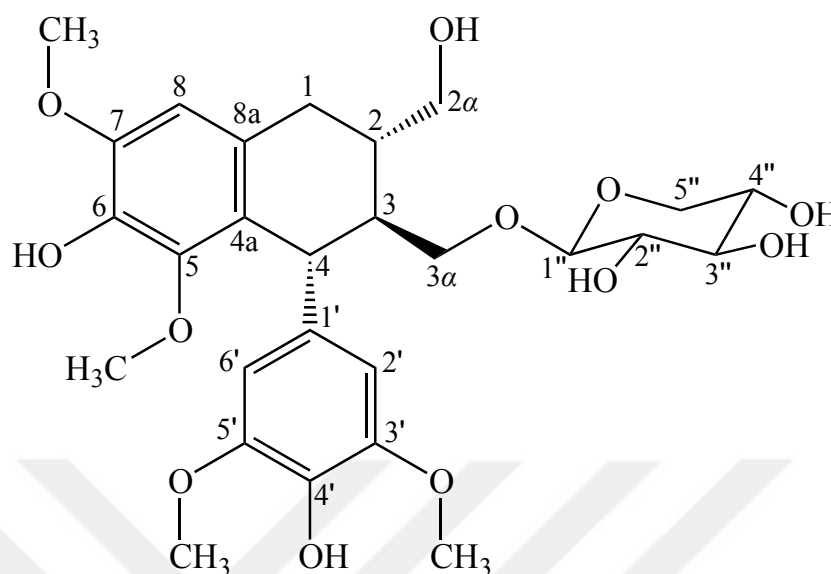
Figure 4.25. Structure of lyoniside.

The data about lyoniside was expressed in **Table 4.22.** below.

Table 4.22. The data about lyoniside.

Molecular formula	$C_{27}H_{36}O_{12}$
Synonyms	(+)-Lyoniside
Molecular weight	552.6 g/mol
IR (ATR) ν (cm^{-1})	3550 –3050, 2934, 2851, 1611, 1515, 1462, 1324, 1221, 1113, 1047, 1025, 994
MS (ESI) *m/z*:	$[M+Na]^+$ 575.2093
^{1}H NMR	**Figure 4.26.** **Table 4.23.**
^{13}C NMR	**Figure 4.27.** **Table 4.23.**
COSY	**Figure 4.28.**
HMQC	**Figure 4.29.** **Table 4.23.**
HMBC	**Figure 4.30.** **Table 4.23.**

Compound **3** was isolated as an amorphous and yellow solid. Following TLC application, a dark spot under UV 254 nm and blue floresans under UV 366 nm were monitored. After Vanilin/H_2SO_4 sprayed and Vanilin/H_2SO_4 sprayed-plate heated up to 110 °C, a dark blue spot was detected. The structure of the substance was identified based on the spectroscopic data (IR, NMR and mass spectroscopy).

IR spectrum of the compound **3** pointed out the presence of aromatic C=C (1462, 1515, 1611 cm^{-1}), aromatic C-H (3050-3100 cm^{-1}), alkane C-H (2934, 2851 cm^{-1}), alkane C-C (994, 1025 cm^{-1}), O-H (3200-3550 cm^{-1}), C-O (1047, 1113 cm^{-1}), and ether C-O-C (1221 cm^{-1}) functions.

In the analysis of ^{1}H-NMR spectrum, H atom signals in the aromatic field integrating 1 H were detected at 6.53 (s, H-8) and 6.32 ppm (s, 1H for both H-2' and H-6'). The other proton signals were detected at d_H 5.20 (d, $J = 4.9$ Hz, 1H, H of OH in C-2''-OH), 5.06 (d, $J = 4.3$ Hz, 1H, H of OH in C-4''-OH), 5.00 (d, $J = 4.9$ Hz, 1H, H of OH in C-3''-OH), 4.48 (t, $J = 5.1$ Hz, 1H, H of OH in CH$_2$-OH), 4.25 (d, $J = 6.6$ Hz, 1H, H-4), 4.10 (d, $J = 7.7$ Hz, 1H, H-1''), 3.76 (s, 3H, H atoms of Me in C-7-OMe), 3.73 − 3.64 (2H, H-3α), 3.53 (s, 3H for both H atoms in C-3'-OMe and C-7'-OMe), 3.52 − 3.44 (2H, H-2α), 3.22 (s, 3H, H atoms of Me in C-5-OMe), 3.30 − 3.24 (1H, H-3''), 3.13 − 3.08 (1H, H-4''), 3.04 − 2.98 (1H for both H-2'' and H-5''), 2.65 − 2.57 (1H, H-1), 1.94 − 1.86 (1H, H-3), 1.50 ppm (dt, $J= 11.4, 7.7$ Hz, 1H, H-2). (**Table 4.23 and Figure 4.26.**).

A proton signal at 4.10 ppm splitting into two peaks as doublet with 7.7 Hz coupling constant (J) is an anomeric proton. 7.7 Hz of J value indicated that sugar molecule is in β configuration. The other proton signals in the sugar molecule were ranged from δ_H 2.98 to δ_H 3.73 ppm. Signals belonging H atoms in OH groups of sugar molecule were also detected in the NMR spectrum as indicated above. H atom signals in aromatic rings were detected at 6.53 (H-8) and 6.32 (H-2'/6') ppm at high frequency, while –OMe groups were detected at lower frequency following as 3.76 (s, 3H, H atoms of Me in C-7-OMe), 3.53 (s, 3H for both H atoms in C-3'-OMe and C-7'-OMe) and 3.22 ppm (s, 3H, H atoms of Me in C-5-OMe).

^{13}C-NMR spectrum (**Figure 4.27.**) presented 27 carbon atom signals in the structure, 5 of which belong to the sugar molecule (pentose). δ_C of C atoms in the sugar molecule were monitored at 104.10 (anomeric C, C-1''), 73.31 (C-2''), 69.61

(C-3"), 76.85 (C-4") and 65.68 (C-5") ppm, which were quite similar to the data of xylose indicated in the literature (472-474). Therefore based on the δ_C and δ_H values pentose unit was identified as β-xylose. IR spectrum confirmed the structure to include aromatic rings, alkane groups. δ_C of aromatic C atoms were ranged from 105.86 to 147.5. C atom signals at the position of C-5, 6, 7, 1', 3', 4' and 5' in aromatic rings were observed at downfield region indicating aromatic rings are to be substituted at those C atoms. In addition due to 2D-NMR spectra (COSY, HMQC and HMBC), the structure of compound **3** was assumed to be a member of lignan derivative as explained in details below.

According to COSY spectrum, all H signals coupling with each other in the xylose molecule were displayed following the detection of anomeric proton at C-1". ^{1}H-^{1}H couplings of H-1 with H-2, H-2 with H-3 and H-3 with H-4 were clearly monitored. Furthermore, couplings of H-3 with H-3α, H-2 with H-2α were also detected (**Figure 4.28.**).

HMQC spectrum showing C atoms with their relating H atoms was indicated in **Figure 4.29.**

HMBC spectrum showing the relationships between protons and long range coupling carbons pointed out the correlation between anomeric proton H-1" of β-xylose and C-3α supporting the linkage of the xylose unit to C-3α. Furthermore, the relationship of H-4 with C-1', H-2α with C-1, H-3α with C-1" were also shown in addition to other correlations like in xylose molecule (**Figure 4.30.**).

Following analysis of NMR spectra, molecular formula of the compound was detected as $C_{27}H_{36}O_{12}$, which was further confirmed by HR-MS (ESI) *m/z* as [M+Na]$^+$ 575.2093 and IR spectrum (**Table 4.22.**).

Spectroscopic data (**Table 4.23.**) of compound **3** were checked in the literature and found to be quite similar to the data given for lyoniside (474). Therefore, compound **3** was identified as lyoniside (**Figure 4.25.**).

Table 4.23. ^{1}H- and ^{13}C-NMR spectroscopic data of lyoniside (DMSO-d_6, ^{1}H: 600 MHz, ^{13}C: 151 MHz).

C/H		δ_H (ppm), J (Hz)	δ_C (ppm)	HMBC (H➜C)
1	CH$_2$	2.65 – 2.57	32.67	C-2, C-3, C-4, C-8, C-4a, C-8a
2	CH	1.50 (dt, 11.4, 7.7)	38.81	-
3	CH	1.94 – 1.86	44.65	-
4	CH	4.25 (d, 6.6)	41.03	C-2, C-3, C-1', C-C-3α, C-4a, C-8a
5	C	-	146.52	-
6	C	-	137.27	-
7	C	-	146.90	-
8	CH	6.53 (s)	106.65	C-1, C-5, C-6, C-7, C-4a, C-8a
2α	CH$_2$	3.52 – 3.44	63.65	C-1
3α	CH$_2$	3.73 – 3.64	68.86	C-1'
4a	C	-	124.94	-
8a	C	-	128.34	-
1'	C	-	137.63	-
2'	CH	6.32 (s)	105.86	C-4, C-6'
3'	C	-	147.50	-
4'	C	-	133.24	-
5'	C	-	147.50	-
6'	CH	6.32 (s)	105.86	C-4, C-2'
1"	CH	4.10 (d, 7.7)	104.10	C-2", C-3", C-5", C-3α
2"	CH	3.04 – 2.98	73.31	C-1", C-3", C-4"
3"	CH	3.30 – 3.24	69.61	C-1"
4"	CH	3.13 – 3.08	76.85	C-2", C-3"
5"	CH$_2$	3.73 – 3.64 3.04 – 2.98	65.78	C-3", C-4"
5-OMe	CH$_3$	3.22 (s)	58.62	C-5
7-OMe	CH$_3$	3.76 (s)	55.65	C-7
3'-OMe	CH$_3$	3.63 (s)	56.07	C-3'
5'-OMe	CH$_3$	3.63 (s)	56.07	C-5'

Table 4.23. ^{1}H- and ^{13}C-NMR spectroscopic data of lyoniside (DMSO-d_6, ^{1}H: 600 MHz, ^{13}C: 151 MHz) (continued).

C/H		δ_H (ppm), J (Hz)	δ_C (ppm)	HMBC (H→C)
2"-OH	OH	5.20 (d, 4.9)	-	-
3"-OH	OH	5.00 (d, 4.9)	-	-
4"-OH	OH	5.06 (d, 4.3)	-	-
CH$_2$-OH	OH	4.48 (t, 5.1)	-	-
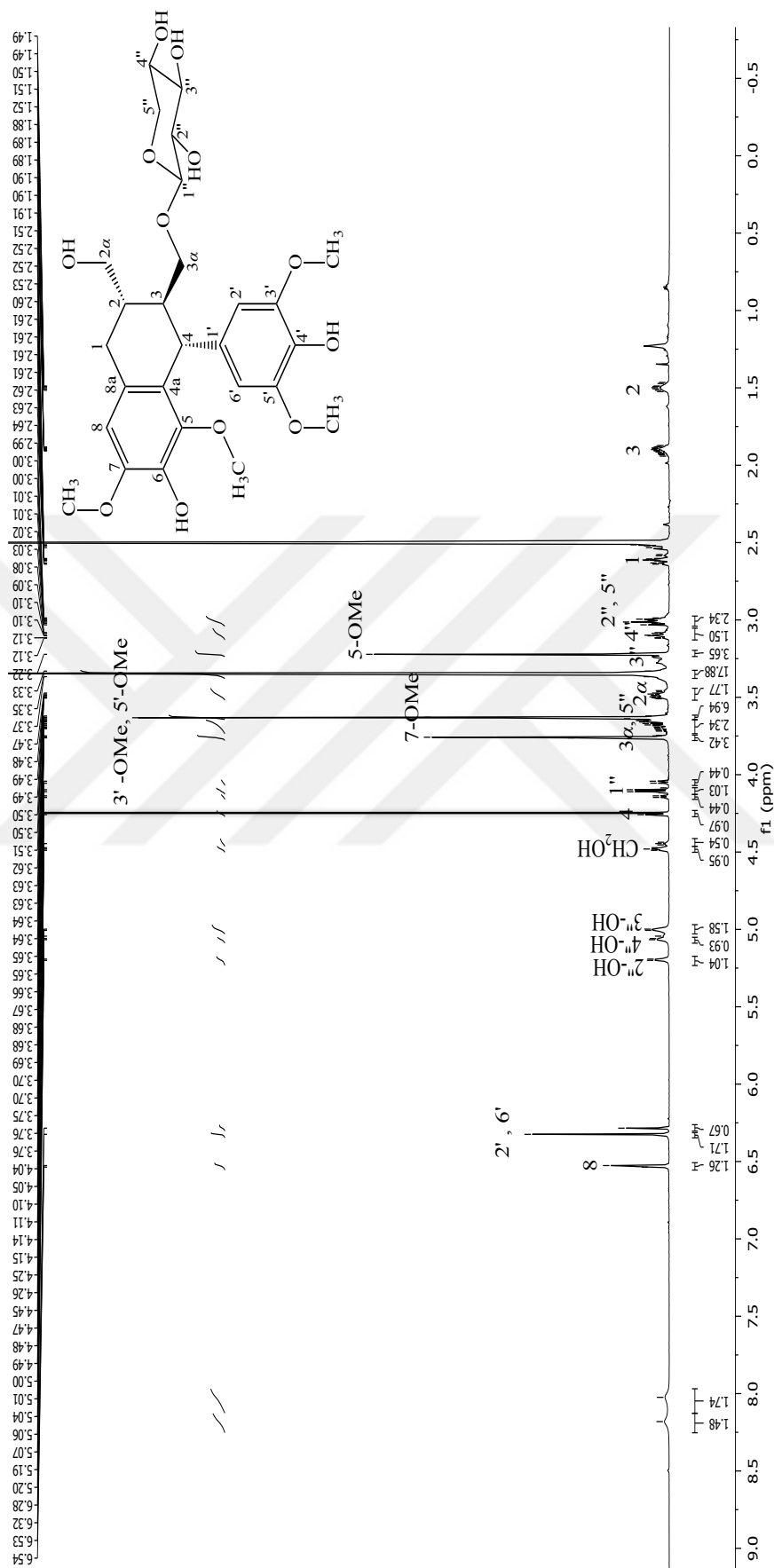
Figure 4.26. ^{1}H-NMR spectrum of lyoniside (Compound **3**) (DMSO-d_6, ^{1}H: 600 MHz).
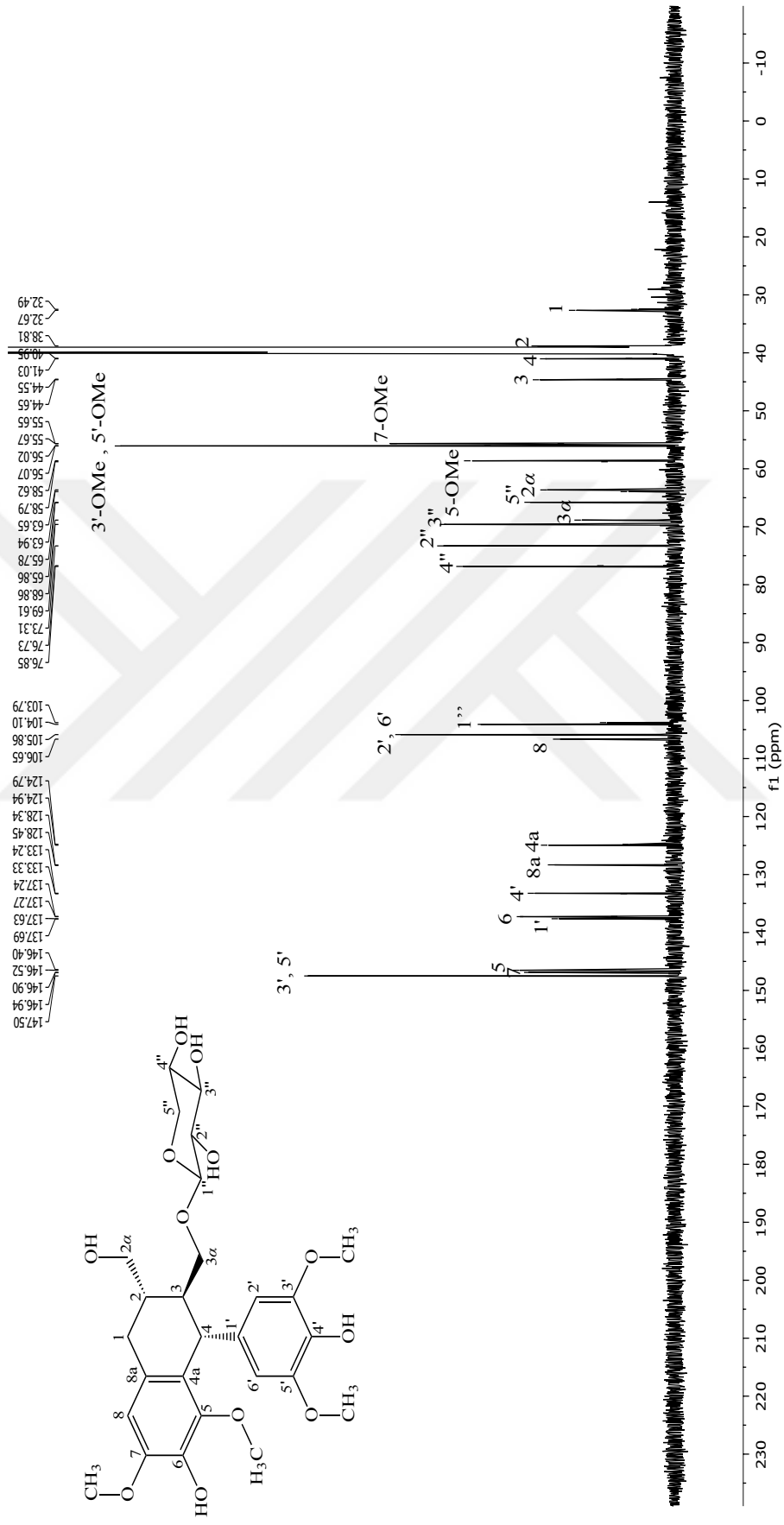
Figure 4.27. ^{13}C-NMR spectrum of lyoniside (Compound **3**) (DMSO-d_6, ^{13}C: 151 MHz).
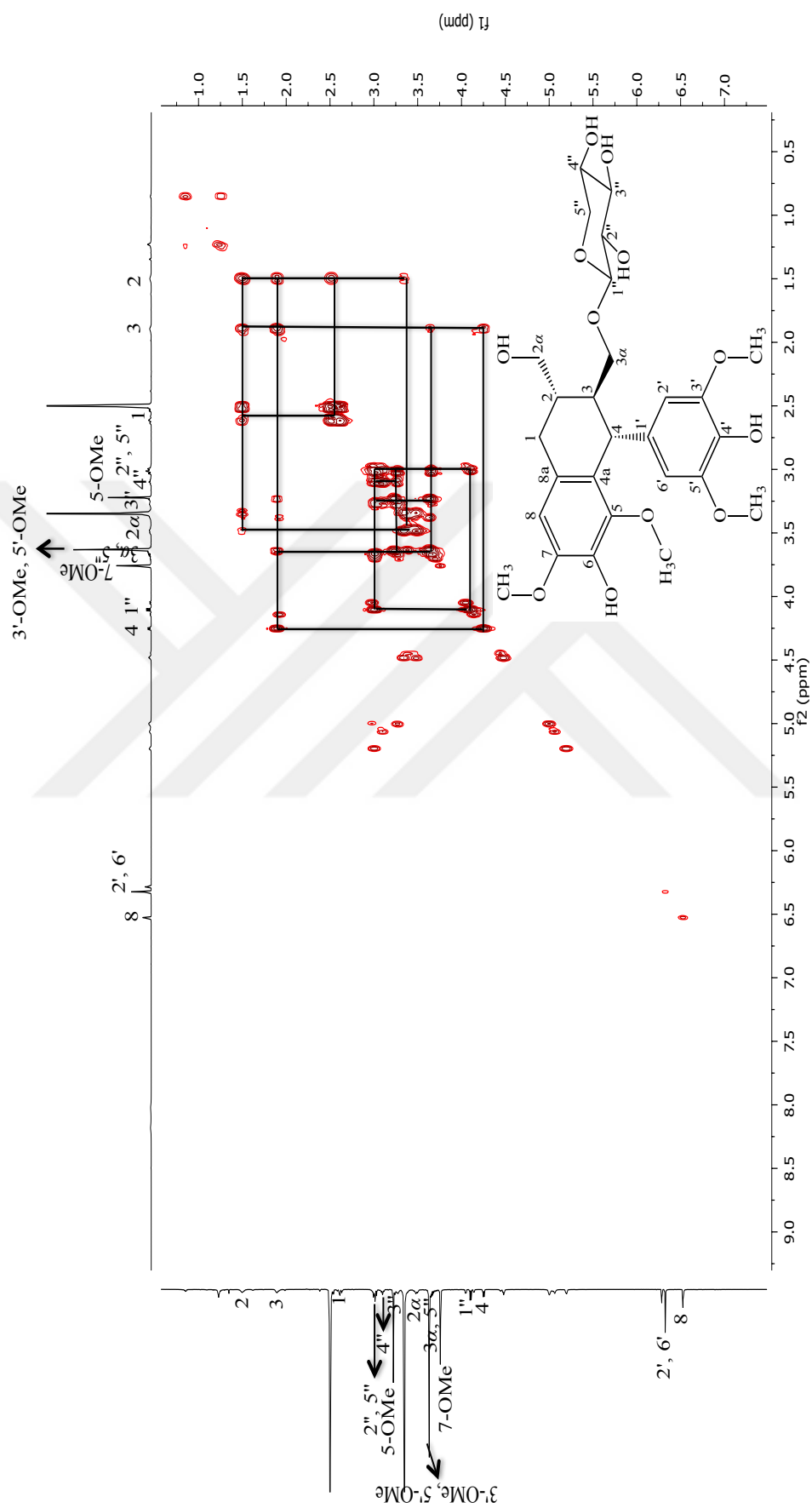
Figure 4.28. ^{1}H–^{1}H homonuclear correlation spectrum (COSY) of lyoniside (Compound **3**).
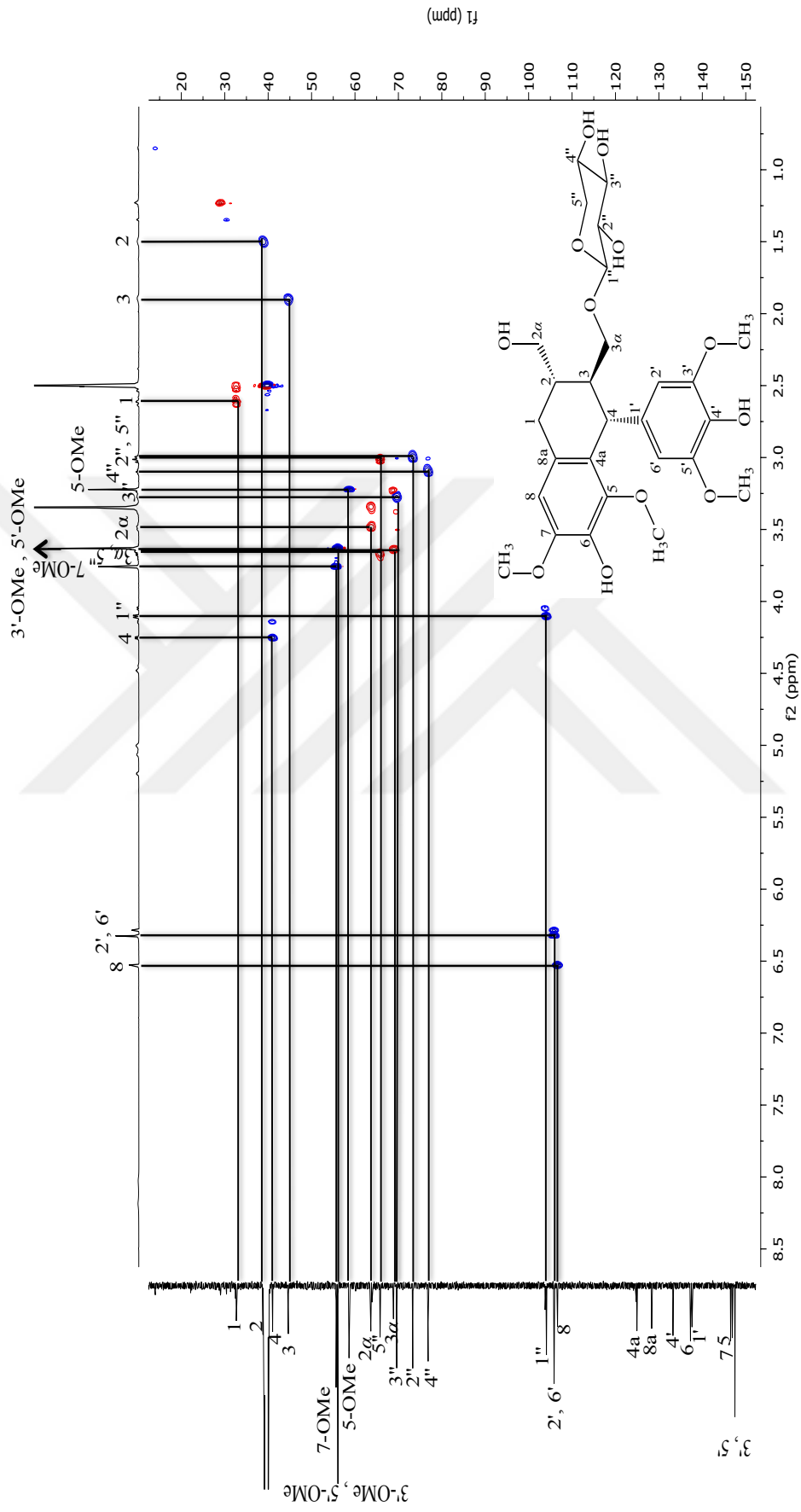
Figure 4.29. ^1H-^{13}C heteronuclear multiple-quantum correlation (HMQC) spectrum of lyoniside (Compound **3**).
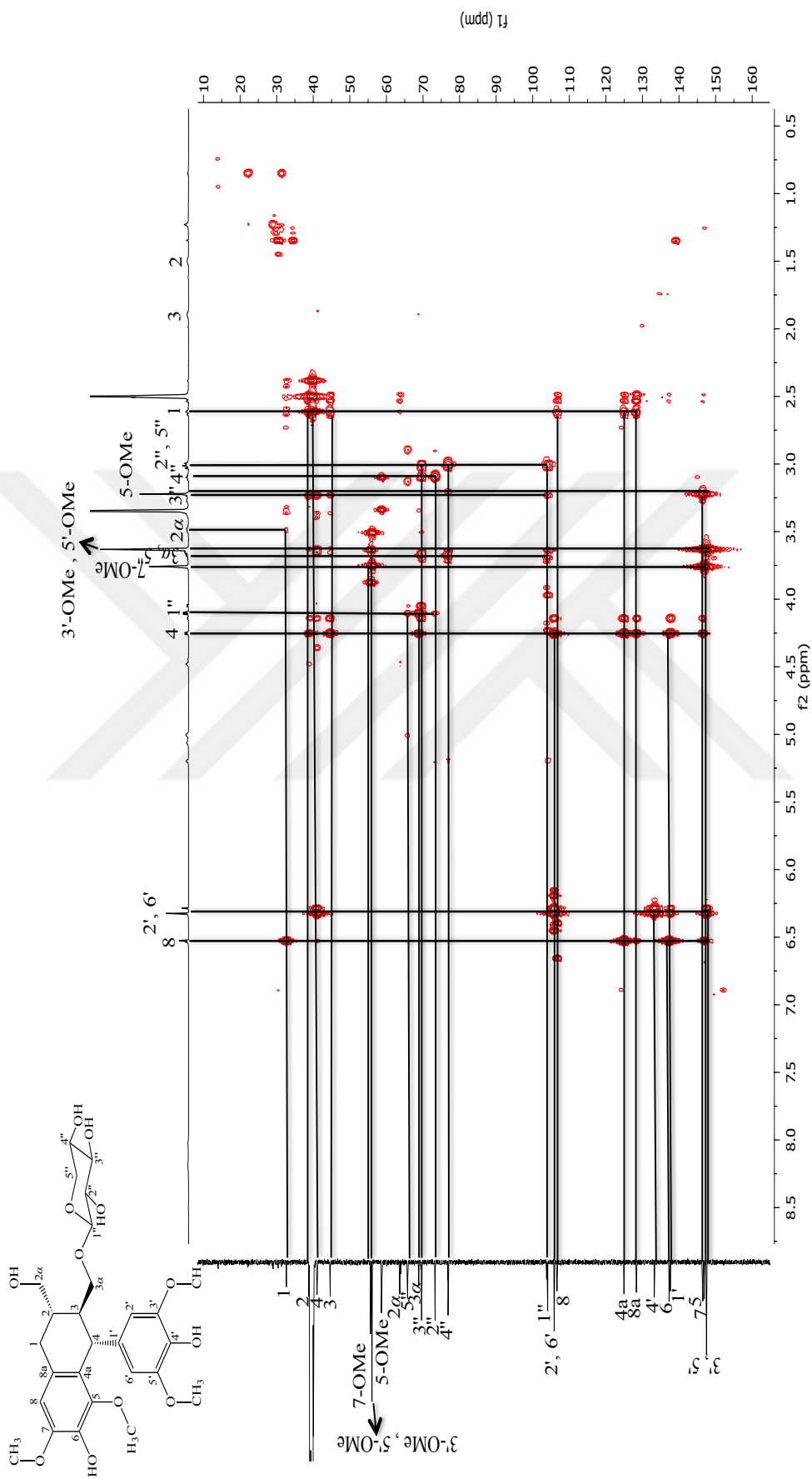
Figure 4.30. ^{1}H-^{13}C heteronuclear multiple-bond correlation (HMBC) spectrum of lyoniside (Compound **3**).

4.2.4 Nepodin-8-*O*-*β*-glucoside
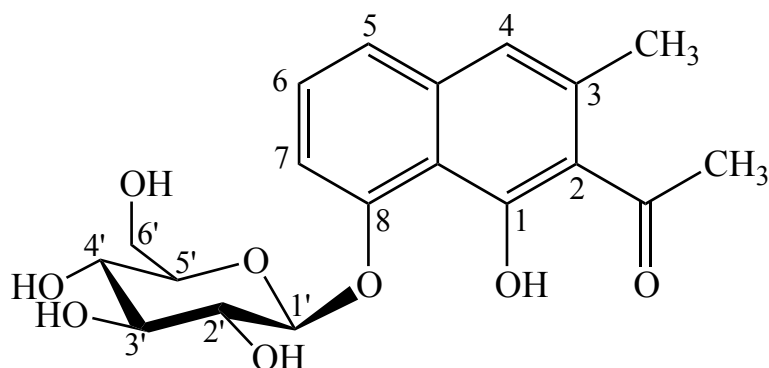
Figure 4.31. Structure of nepodin-8-*O*-*β*-glucoside.

The data about nepodin-8-*O*-*β*-glucoside was expressed in **Table 4.24.** below.

Table 4.24. The data about nepodin-8-*O*-*β*-glucoside.

Molecular formula	$C_{19}H_{22}O_8$
Synonyms	Musizin-8-*O*-*β*-D-glucopyranoside
Molecular weight	378 g/mol
IR (ATR) ν (cm^{-1})	3385, 3298, 2964, 2925, 1670, 1578, 1354, 1079
MS (ESI) *m/z*:	[M+Na]$^+$ 401.1201
^{1}H NMR	**Figure 4.32.** **Table 4.25.**
^{13}C NMR	**Figure 4.33.** **Table 4.25.**
DEPT 90 and DEPT 135	**Figure 4.34.**
COSY	**Figure 4.35. and Figure 4.36.**
HMQC	**Figures 4.37.-4.39.** **Table 4.25.**
HMBC	**Figures 4.40.-4.42** **Table 4.25.**

Compound **4** was isolated as an amorphous and brown solid. In TLC, a light yellow spot was observed at daylight before reagent spraying. Additionally, the spot exhibited fluorescence inhibiting zones under UV 254 nm and blue fluorescence under UV 366 nm. After Vanilin-H_2SO_4 sprayed and Vanilin-H_2SO_4 sprayed-plate to be heated up to 110 °C, dark blue spots were detected. The structure of the substance was identified based on spectroscopic data (IR, NMR and mass spectroscopy).

IR spectrum of the compound **4** pointed out the presence of aromatic C=C (1568 cm^{-1}), aromatic C-H (3000-3100 cm^{-1}), alkane C-H (1354 cm^{-1}, 2925, 2964 cm^{-1}), O-H (3298, 3385 cm^{-1}), C-O (1079 cm^{-1}) and C=O (1670 cm^{-1}) functions.

^{1}H-NMR spectrum revealed the presence of H atom signals in the aromatic field at d_H 7.44 (dd, $J = 7.9$, 1.5 Hz, 1H, H-5), 7.39 (t, $J = 7.8$ Hz, 1H, H-6), 7.35 (dd, $J = 8.2$, 1.5 Hz, 1H, H-7) and 7.17 (s, 1H, H-4). Other proton signals were detected at 5.13 (d, $J = 7.2$ Hz, 1H, H-1'), 3.98 (dd, $J = 12.1$, 2.16 Hz, 1H, H-6'α), 3.77 (dd, $J = 12$, 5.7 Hz, 1H, H-6'β), 3.59 (dd, 1H, H-2'), 3.55 (dd, 1H, H-5'), 3.53 (dd, 1H, H-3'), and 3.45 (d, 1H, H-4') (**Table 4.25**; **Figure 4.32.**).

A proton signal at 5.13 ppm splitting into two peaks as doublet with 7.8 Hz coupling constant (J) is an anomeric proton. 7.8 Hz of J value indicated that sugar molecule is in β configuration. The other proton signals in the sugar molecule were ranged from δ_H 3.45 to δ_H 3.98 ppm. H atoms' signals in the aromatic ring were observed at around 7 ppm, while H atoms in C-OCH$_3$ and 3-CH$_3$ displayed signals observed at 2.3 (s) and 2.59 (s) ppm, respectively.

^{13}C-NMR and DEPT spectra (**Figures 4.33. and 4.34.**) showed the presence of 19 carbon atoms in the structure, 6 of which belong to a sugar molecule. δ_C of the signals of the C atoms in the sugar molecule were detected at 102.92 (anomeric C, C-1'), 73.59 (C-2'), 76.77 (C-3'), 69.90 (C-4'), 77.43 (C-5') and 61.08 ppm (C-6'), which were quite similar to the data of β-glucose indicated in the literature before (400, 470, 471). IR spectrum pointed out that the structure of **4** contain an aromatic ring as well as carbonyl and alkane groups. The ^{1}H-NMR data as well as total number of C atoms determined by means of ^{13}C-NMR proposed that the structure might be a member of naphthalene derivatives. δ_C values of aromatic C atom signals in the aromatic ring were ranged from 110.47 to 154.75 ppm. C-1 and C-8 having higher chemical shifts indicated that those carbons are substituted with O-containing groups

such as OH and O-glucoside.

According to COSY spectrum, H signals coupling with each other in the glucose molecule were displayed. Furthermore, couplings of H-5 with H-6, H-6 with H-7, H-5 with H-7 and H-4 with H-6 in the aromatic ring were shown (**Figures 4.35. and 4.36**).

HMQC spectrum indicating C atoms with their binding H atoms were shown in **Figures 4.37.-4.39.**.

HMBC spectrum showing the relationships between protons and their multiple bond correlating carbons pointed out a long range coupling between anomeric proton of β-glucose H-1' and C-8 indicating β-glucose substitution at C-8 in the aromatic ring. Furthermore, the relationship of H-1' with C-3' and C-5', H atoms of Me in C-3-Me with C-1, C-2, C-4, C-4a and C-8a, H-4' with C-3', C-5' and C-6', H-3' with C-2', C-4', C-5' and C-6', H-5' with C-2' and C-4', H-2' with C-3', C-4' and C-5', H-6' with C-2', C-3', C-4' and C-5', H-7 with C-4a, C-8a, C-5 and C-8, H-6 with C-4a, C-8a, C-5, C-7 and C-8, H-5 with C-4a, C-8a, C-4, C-7 and C-8 were also displayed (**Figures 4.40.-4.42.**).

Following analysis of NMR spectra, molecular formula of the compound was detected as $C_{19}H_{22}O_8$, which was further confirmed by HR-MS (ESI) *m/z* as $[M+Na]^+$ 401.1201 (**Table 4.24.**).

Spectroscopic data (**Table 4.25.**) of compound **4** were checked in the literature, which were quite similar to the data for nepodin-8-*O*-β-glucoside published previously (94, 151). Therefore, compound **4** was elucidated as nepodin-8-*O*-β-glucoside (**Figure 4.31.**).

Table 4.25. ^{1}H- and ^{13}C-NMR spectroscopic data of nepodin-8-*O*-β-glucoside (Methanol-d_4, ^{1}H: 400 MHz, ^{13}C: 100 MHz).

C/H		δ$_H$ (ppm), *J* (Hz)	δ$_C$ (ppm)	HMBC (H➔C)
1	C	-	151.45	-
2	C	-	124.72	-
3	C	-	133.23	-
4	CH	7.17 (s)	119.57	C-1, C-2, C-5, C-6, C-8, C-4a, C-8a
5	CH	7.44 (dd, 7.9, 1.5)	122.49	C-4, C-7, C-8, C-4a, C-8a
6	CH	7.39 (t, 7.8)	127.18	C-5, C-7, C-8, C-4a, C-8a
7	CH	7.35 (dd, 8.2, 1.5)	110.47	C-5, C-8, C-4a, C-8a
8	C	-	154.75	-
4a	C	-	136.70	-
8a	C	-	113.55	-
1'	CH	5.13 (d, 7.2)	102.92	C-8, C-3', C-5'
2'	CH	3.59 (d, †)	73.59	C-3', C-4', C-5'
3'	CH	3.55 (dd, †)	76.77	C-2', C-4', C-5', C-6'
4'	CH	3.45 (d, †)	69.90	C-3', C-5', C-6'
5'	CH	3.53 (dd, †)	77.43	C-2', C-4'
6'	CH$_2$	3.98 (dd, 12.1, 2.16) 3.77 (dd, 12, 5.7)	61.08	C-2', C-3', C-4', C-5'
C=O	C	-	207.00	
C-OMe	CH$_3$	2.59 (s, 3H)	31.02	
3-Me	CH$_3$	2.3 (s, 3H)	18.46	C-1, C-2, C-4, C-4a, C-8a

†: Coupling constant (*J*) were not calculated due to overlap of signals.
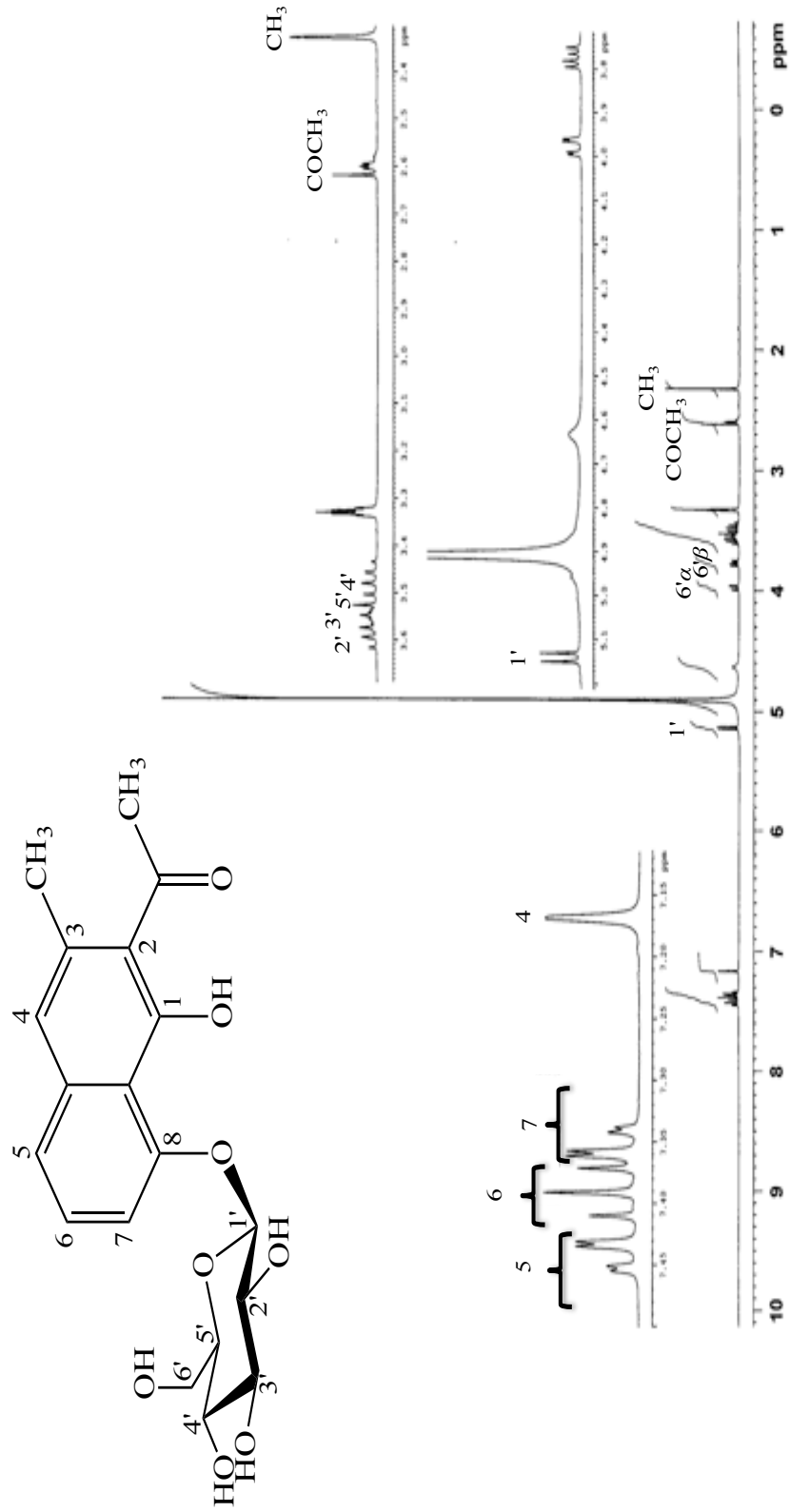
Figure 4.32. ¹H-NMR spectrum of nepodin-8-*O*-*β*-glucoside (Compound **4**) (Methanol-*d₄*, ¹H: 400 MHz).
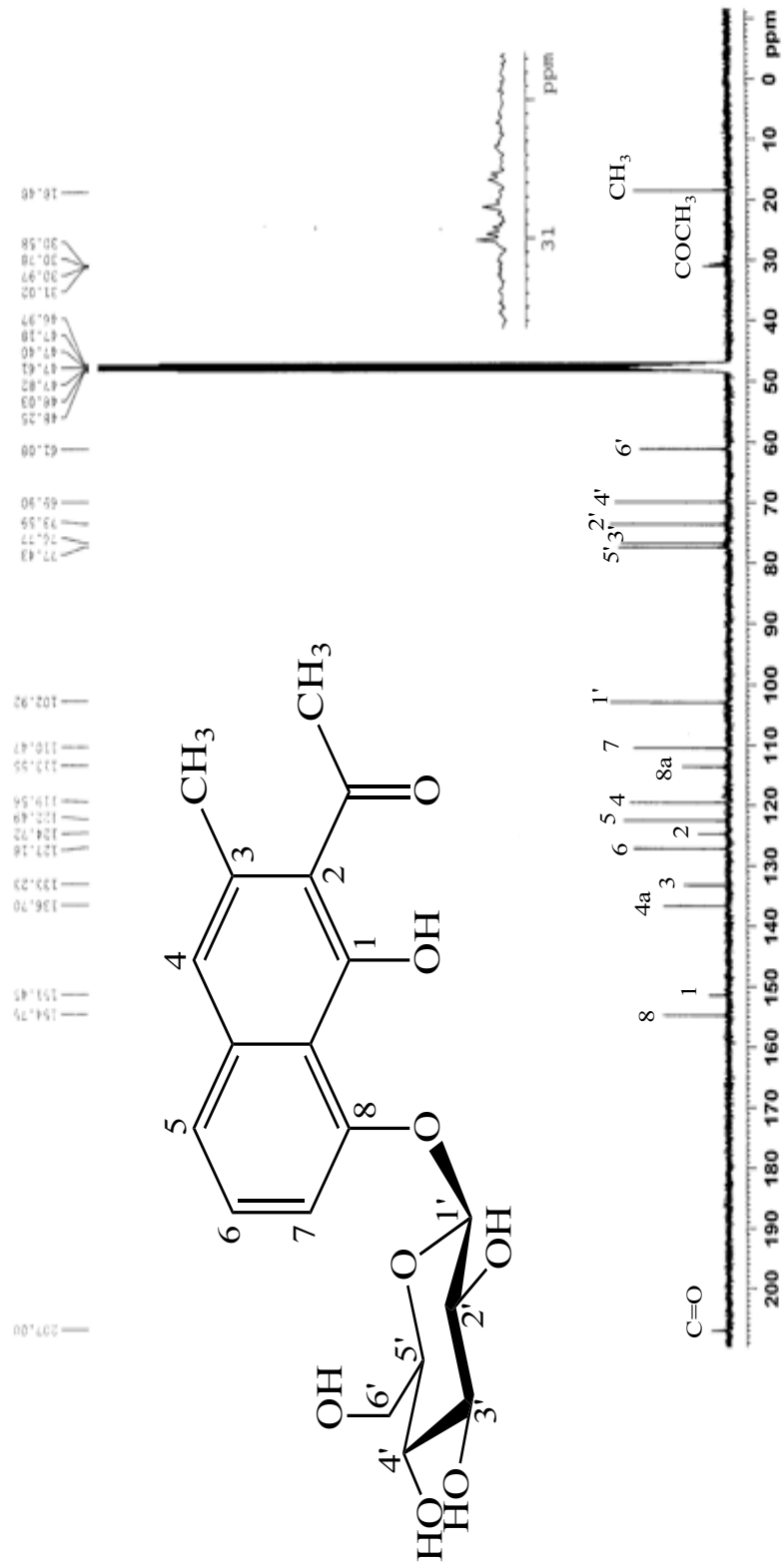
Figure 4.33. ^{13}C-NMR spectrum of nepodin-8-O-β-glucoside (Compound **4**) (Methanol-d_4, ^{13}C: 100 MHz).
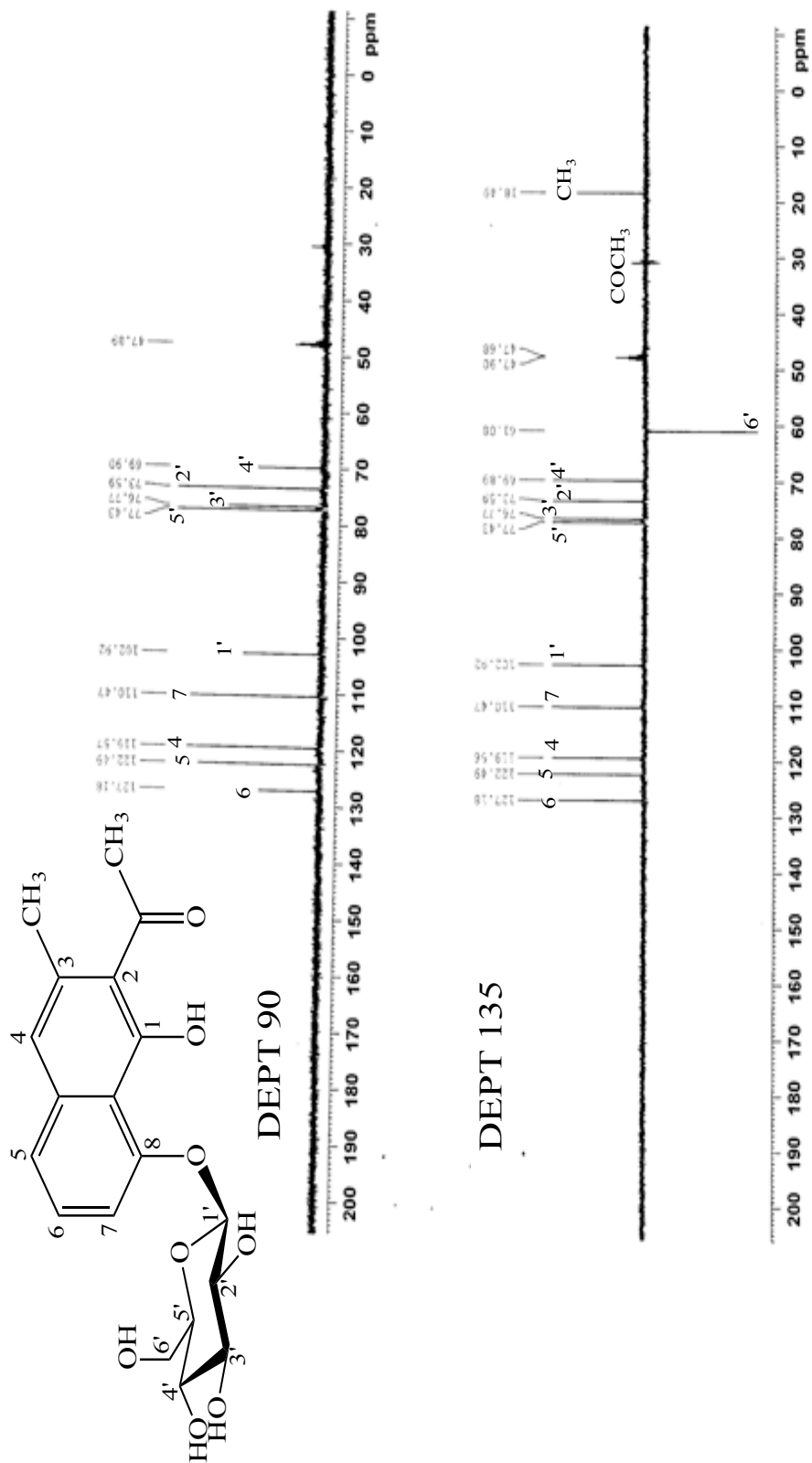
Figure 4.34. DEPT 90 and DEPT 135 spectra of nepodin-8-*O*-*β*-glucoside (Compound **4**).
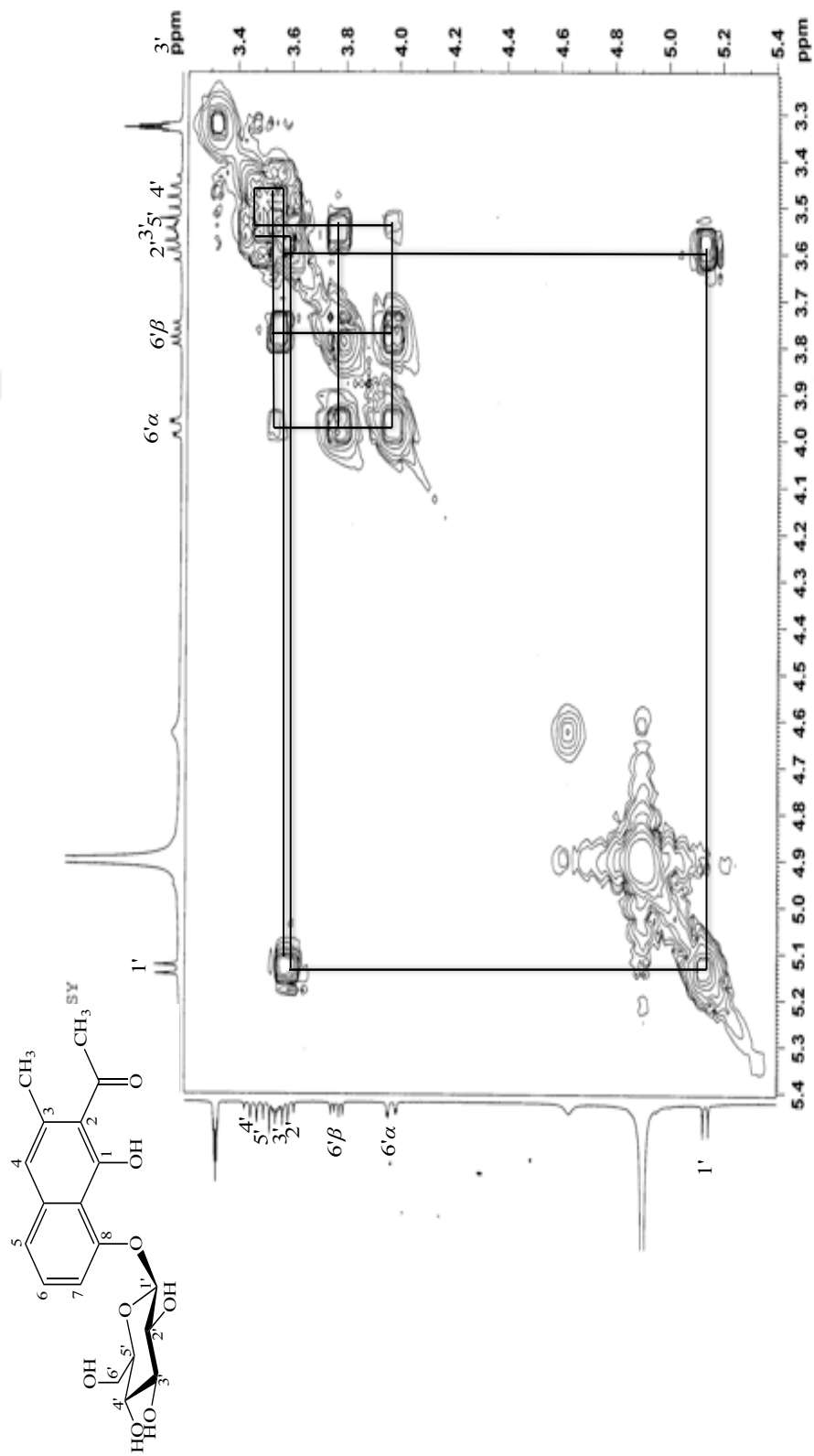
Figure 4.35. ^{1}H-^{1}H homonuclear correlation spectrum (COSY) of nepodin-8-*O*-*β*-glucoside (Compound **4**).
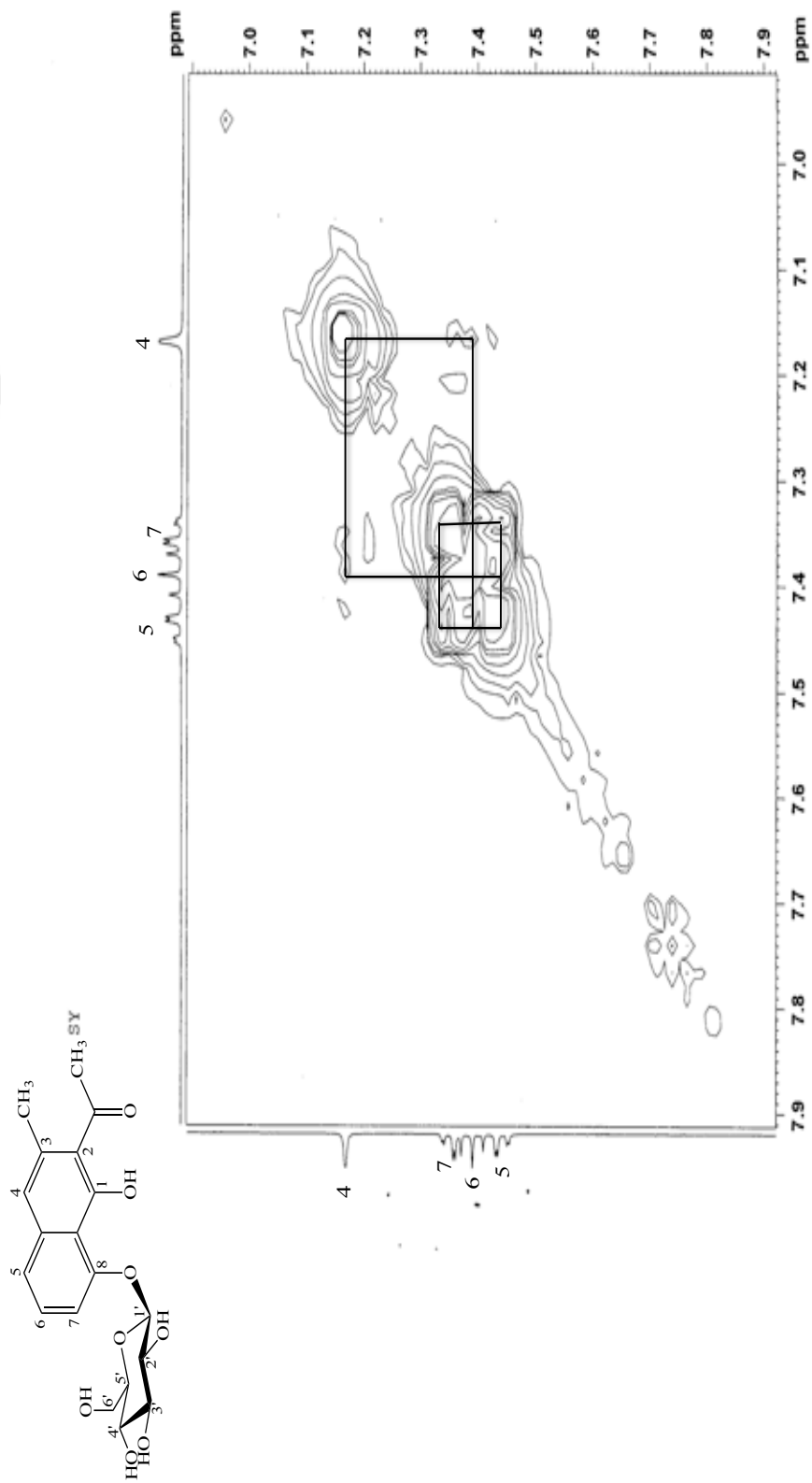
Figure 4.36. ^{1}H-^{1}H homonuclear correlation spectrum (COSY) of nepodin-8-*O*-*β*-glucoside (Compound **4**).
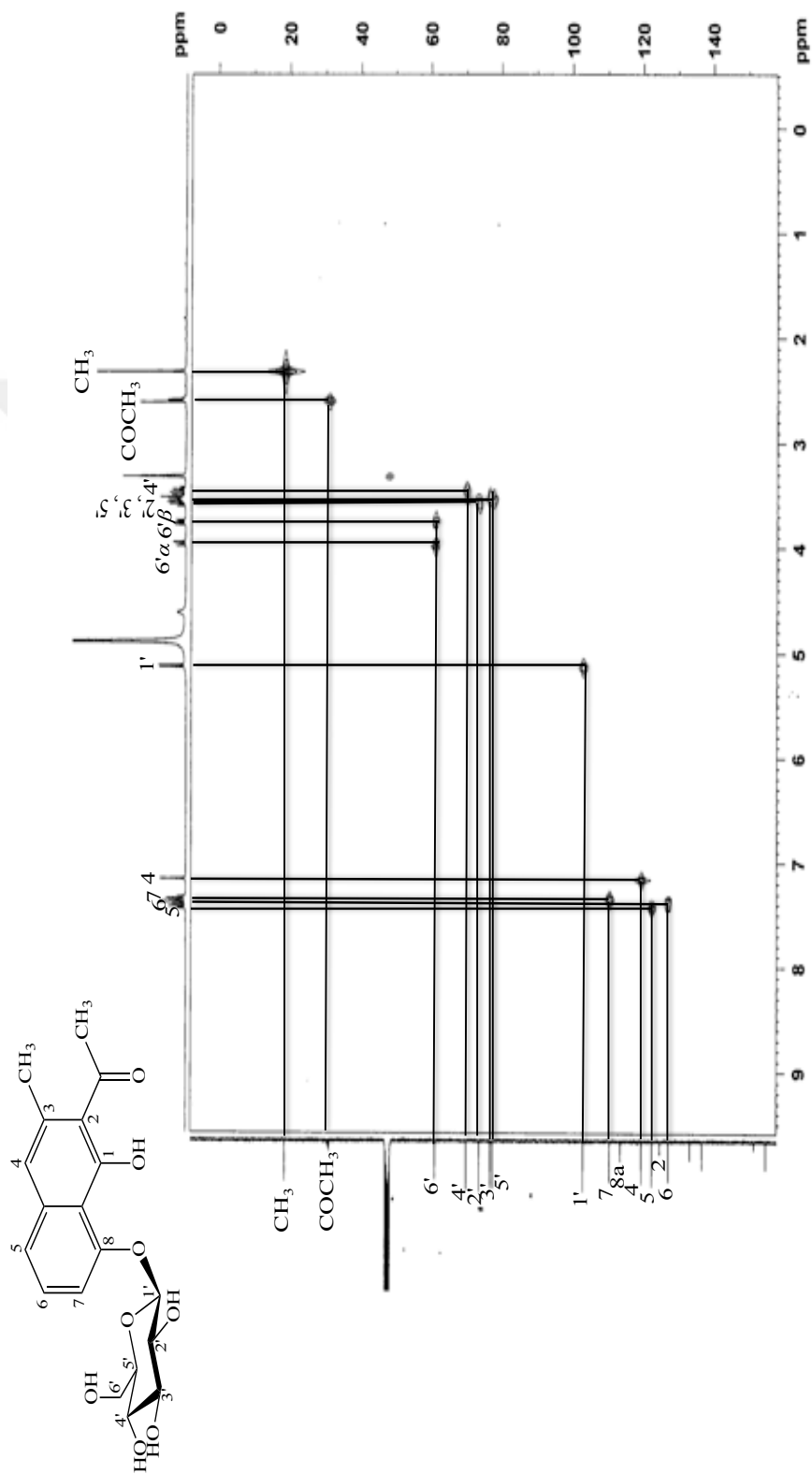
Figure 4.37. ^{1}H-^{13}C heteronuclear multiple-quantum correlation (HMQC) spectrum of nepodin-8-*O*-*β*-glucoside (Compound **4**).
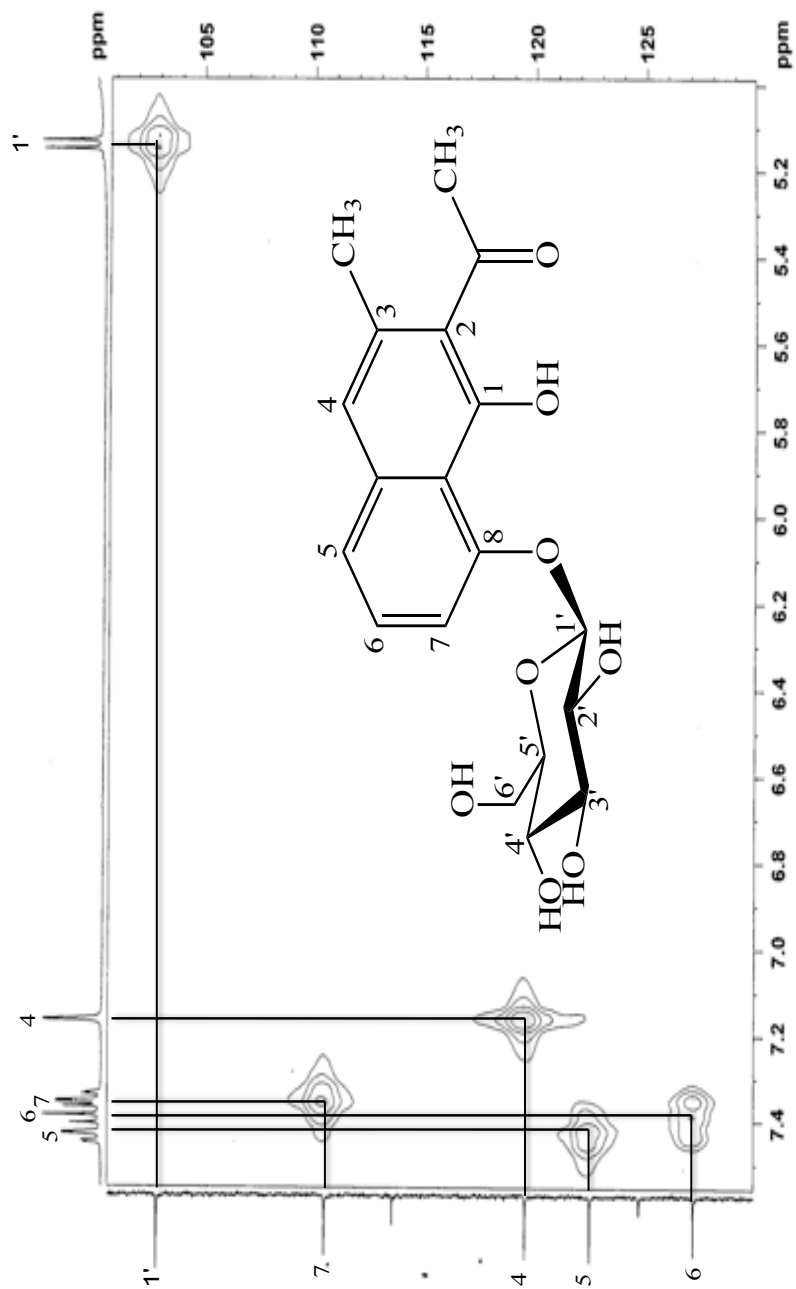
Figure 4.38. ^{1}H-^{13}C heteronuclear multiple-quantum correlation (HMQC) spectrum of nepodin-8-*O*-*β*-glucoside (Compound **4**).
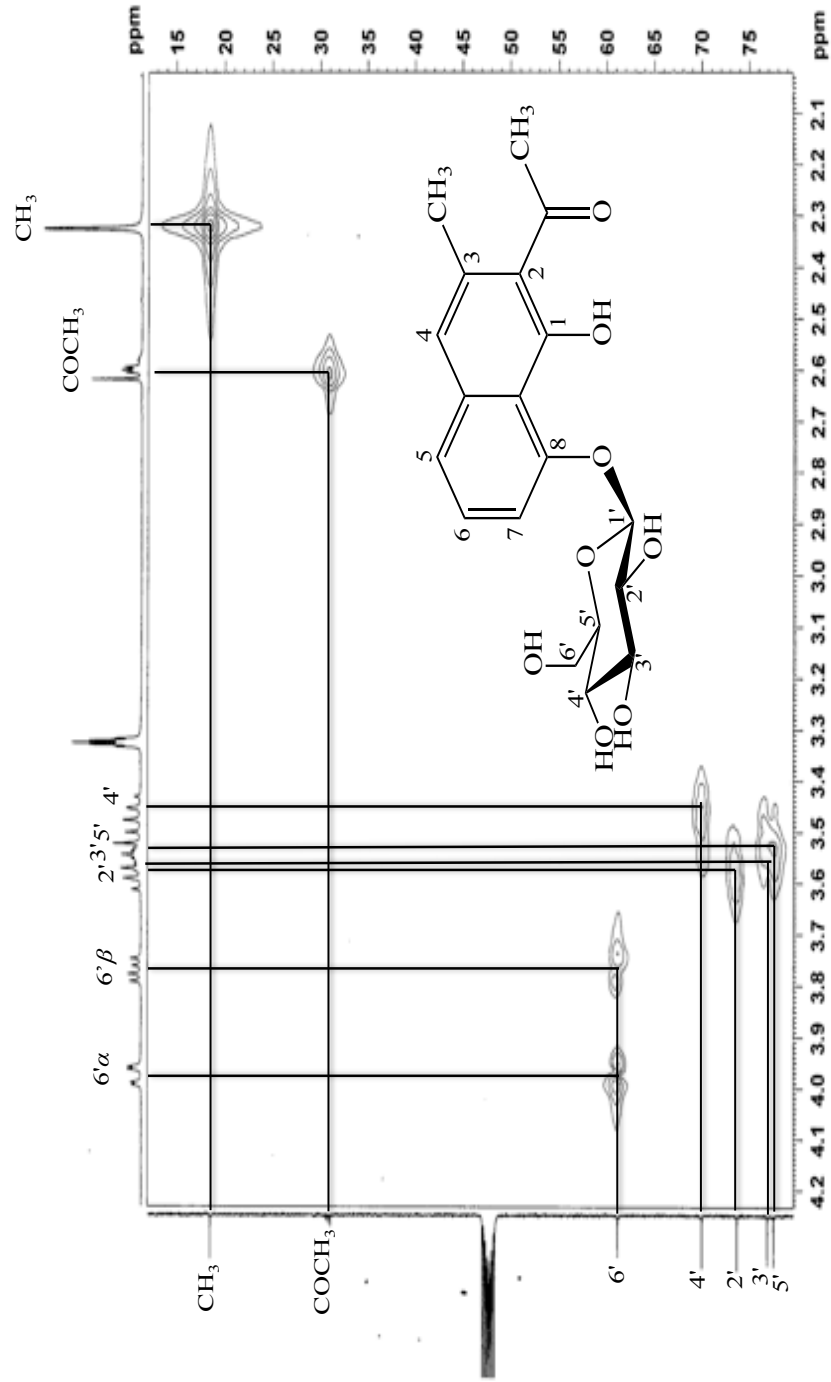
Figure 4.39. ^{1}H-^{13}C heteronuclear multiple-quantum correlation (HMQC) spectrum of nepodin-8-O-β-glucoside (Compound **4**).
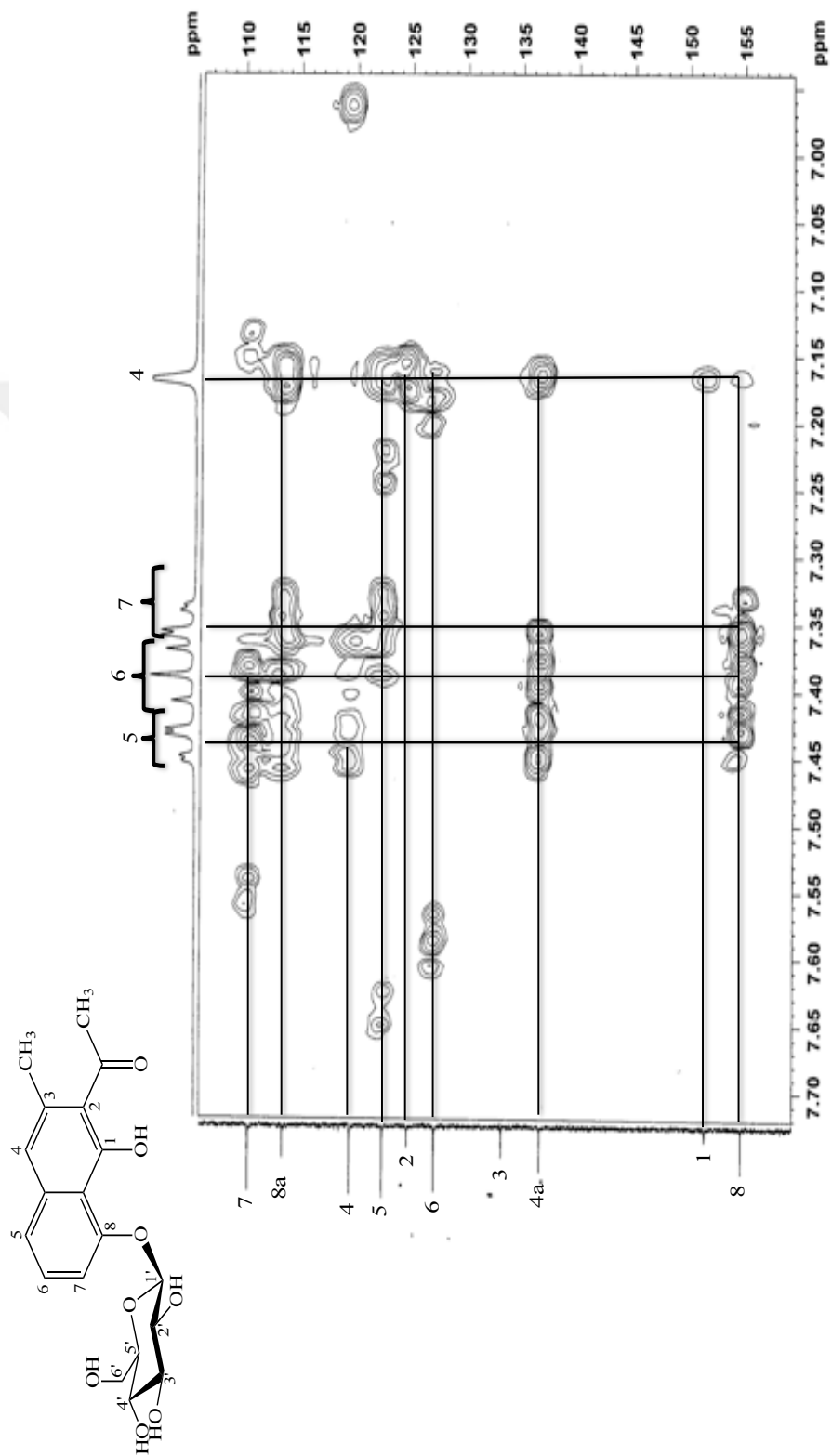
Figure 4.40. ^{1}H-^{13}C heteronuclear multiple-bond correlation (HMBC) spectrum of nepodin-8-*O*-β-glucoside (Compound **4**).
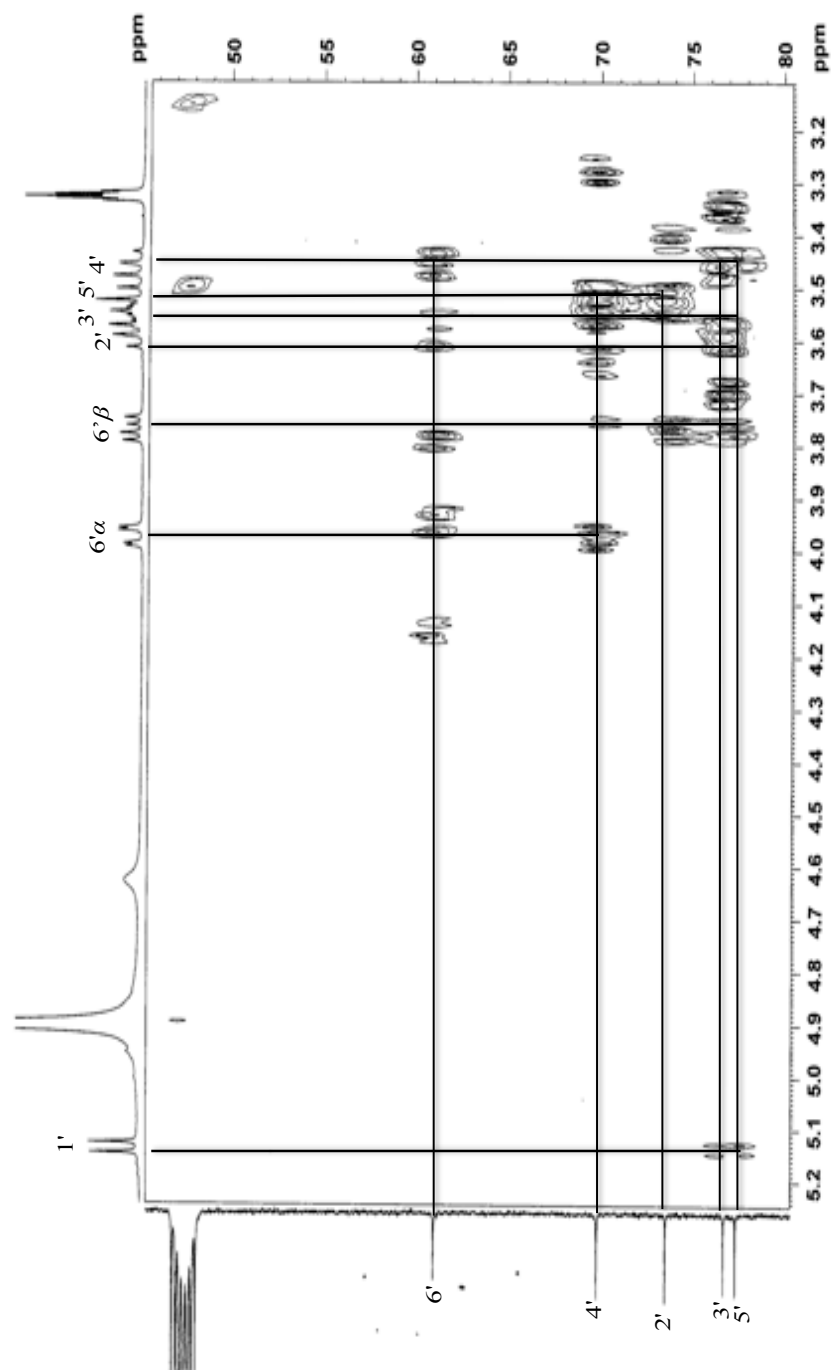
Figure 4.41. ^{1}H-^{13}C heteronuclear multiple-bond correlation (HMBC) spectrum of nepodin-8-O-β-glucoside (Compound **4**).
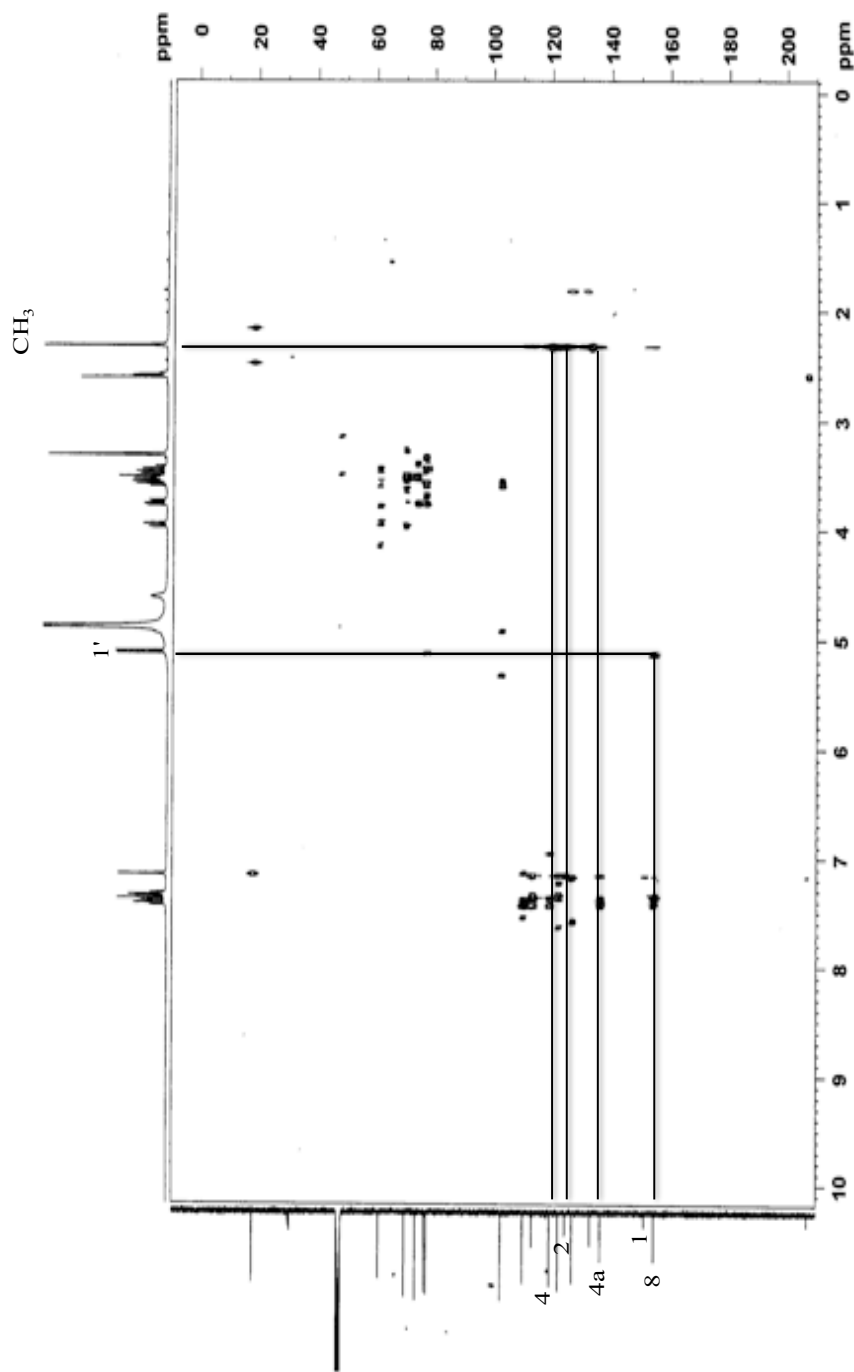
Figure 4.42. ^{1}H-^{13}C heteronuclear multiple-bond correlation (HMBC) spectrum of nepodin-8-*O-β*-glucoside (Compound **4**).

4.2.5   (+)-Isolariciresinol-9-*O*-β-xyloside
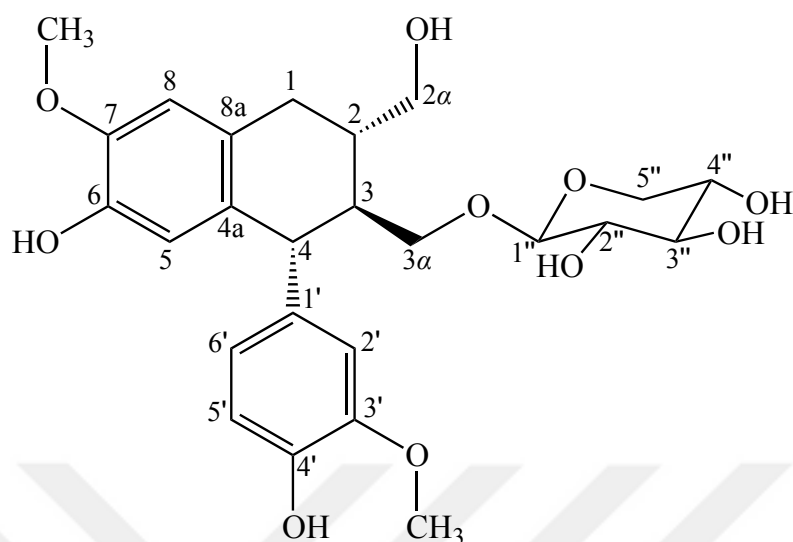
Figure 4.43. Structure of isolariciresinol-9-*O*-β-xyloside.

The data about isolariciresinol-9-*O*-β-xyloside was expressed in **Table 4.26.** below.

Table 4.26. The data about isolariciresinol-9-*O*-β-xyloside.

Molecular formula	$C_{25}H_{32}O_{10}$
Synonyms	Schisandriside, Schizandriside
Molecular weight	492 g/mol
IR (ATR) ν (cm^{-1})	3550 – 3050, 1620, 1481, 1368, 1284, 1150, 1025, 992
MS (ESI) *m/z*:	[M+Na]$^{+}$ 515.1904
[α]$_D^{22}$	+16.9° (MeOH, c = 0.19)
^{1}H NMR	**Figure 4.44.** **Table 4.27.**
^{13}C NMR	**Figure 4.45.** **Table 4.27.**
COSY	**Figure 4.46.**
HMQC	**Figure 4.47.** **Table 4.27.**
HMBC	**Figure 4.48.** **Table 4.27.**

Compound **5** was isolated as an amorphous and colourless solid. Following TLC application, dark spot under UV 254 nm and blue fluorescence under UV 366 nm were monitored. After Vanilin/H_2SO_4 sprayed and Vanilin/H_2SO_4 sprayed-plate was heated up to 110 °C, a purple spot was detected. The structure of the substance was identified based on spectroscopic data (IR, NMR and mass spectroscopy).

IR spectrum of compound **5** pointed out the presence of aromatic C=C (1481 cm^{-1}), aromatic C-H (3050-3100 cm^{-1}), alkane C-H (1368 cm^{-1}), alkane C-C (992 cm^{-1}), O-H (3200, 3550 cm^{-1}) and C-O (1150 cm^{-1}) functions.

When ^{1}H-NMR spectrum was analysed, H atom signals in the aromatic field were detected at 6.79 (d, J = 2.0 Hz, 1H, H-2'), 6.68 (d, J = 8.0 Hz, 1H, H-5'), 6.59 (s, 1H, H-8), 6.47 (dd, J = 8.1, 1.9 Hz, 1H, H-6'), and 6.06 ppm (s, 1H, H-5) Other proton signals were detected at 8.74 (s, 1H, H of OH in C-4'-OH), 8.44 (s, 1H, H of OH in C-6-OH), 5.24 (d, J = 4.7 Hz, 1H, H of OH in C-2"-OH), 4.99 (d, J = 4.8 Hz, 1H, H of OH in C-3"-OH), 4.95 (d, J = 5.0 Hz, 1H, H of OH in C-4"-OH), 4.41 (t, J = 5.1 Hz, 1H, H of OH in C-2α-OH), 4.02 (d, J = 10.9 Hz, 1H, H-4), 3.90 (d, J = 7.6 Hz, 1H, H-1"), 3.84 (dd, J = 9.6, 2.4 Hz, 1H, H-3α), 3.71 (s, 3H, H atoms of Me in C-3'-OMe), 3.70 (s, 3H, H atoms of Me in C-7-OMe), 3.64 (dd, J = 11.3, 5.4 Hz, 1H, H-5"), 3.57 (dt, J = 10.5, 4.2 Hz, 1H, H-2α), 3.46 (dt, J = 11.0, 5.9 Hz, 1H, H-2α), 3.26 (ddt, J = 10.4, 8.8, 5.2 Hz, 1H, H-4"), 3.07 (td, J = 8.8, 4.8 Hz, 1H, H-3"), 3.00 − 2.94 (1H for each H-3α, H-2" and H-5"), 2.73 − 2.70 (2H, H-1), 1.86 (ddd, J = 13.1, 6.2, 3.5 Hz, 1H, H-2), and 1.68 (tt, J = 10.7, 2.7 Hz, 1H, H-3) ppm (**Figure 4.44.**).

A proton signal at 3.90 ppm splitting into two peaks as doublet with 7.9 Hz coupling constant (J) is an anomeric proton. 7.6 Hz of J value indicated that sugar molecule is in β configuration. The other proton signals in the sugar molecule were ranged from δ_H 2.94 to δ_H 3.64 ppm. H atoms in aromatic ring were displayed signals at around 7 ppm at higher frequency, while H atom signals in C-3α, C-2α, Me of C-3'-OMe and Me of C-7-OMe were observed at lower frequencies.

^{13}C-NMR spectrum (**Figure 4.45.**) presented 25 carbon atom signals including the signals of a sugar molecule with 5 C (pentose). δ_C of C atom signals in the sugar molecule were observed at 104.59 (anomeric C, C-1"), 73.37 (C-2"), 76.59 (C-3"), 69.58 (C-4") and 65.70 (C-5") ppm, which were quite similar to the data of β-

xylose indicated in the literature (472-474). IR and NMR spectra revealed the structure to include aromatic rings, alkane groups as well as a β-xylose unit. δ_C of aromatic C atom signals were ranged from 111.76 to 147.14 ppm. δ_C of C atom signals at the position of 6, 7, 1', 3' and 4' in aromatic rings were observed at higher chemical shifts indicating that the aromatic ring has to be substituted at those C atoms. Based on the data in COSY, HMQC and HMBC spectra, the structure of compound **5** was assumed to be a lignan derivative as explained in details below.

COSY spectrum, displayed the couplings of H of OH in C-2"-OH with H-2", H of OH in C-3"-OH with H-3" as well as H-4", H of OH in 2α-OH with H-2α, H-4 with H-3, H-1" with H-2", H-3α with H-3 as well as the other H-3α, H-5" with H-4" as well as H-5", H-2α with H-2, H-2 with H-3, H-1 as well as H-2α, H-3 with H-3α, H-4 as well as H-2 and H-2' with H-6' (**Figure 4.46.**).

HMQC spectrum indicating C atoms with their binding H atoms were shown in **Figure 4.47**.

HMBC spectrum pointed out a long range coupling between the anomeric proton H-1" of β-xylose and C-3α, which indicates a β-xylose substitution at C-3α. Furthermore, the long range couplings of H-2' with C-1', C-3', C-4' and C-6', H-5' with C-3' and C-4', H-8 with C-7, C-4a and C-8a, H-6' with C-4, C-2' and C-4', H of OH in C-2"-OH with C-1" and C-3", H of OH in C-3"-OH with C-2", C-3", C-4" and C-5", H-5 with C-4, C-6, C-7 and C-8a, H of OH in C-2α-OH (CH$_2$-OH) with C-2, H-4 with C-3, C-3α, C-4a, C-8a, C-1', C-2', C-6' and C-1", H-1" with C-4 and C-3α, H-3α with C-4, C-2, C-3 and C of Me in C-3'-OMe, H-5" with C-1", C-3" and C-4", H atoms of Me in C-3'-OMe with C-3' and C-4', H atoms of Me in C-7-OMe with C-6 and C-7, both H-5" and H-2" with C-3" and C-4", H-3" with C-2" and C-4", H-4" with C-3", H-2α with C-1, H-1 with C-2, C-3, C-8, C-4a, C-8a and C-2α, H-2 with C-1, C-3, C-2α, H-3 with C-4, H of OH in C-6-OH with C-5, H of OH in C-4'-OH with C-5' were also displayed (**Figure 4.48.**).

Following the analysis of NMR spectra, the compound was found to have the molecular formula $C_{25}H_{32}O_{10}$ which was later confirmed by HR-MS (ESI) at *m/z* 515.1904 [M+Na]$^+$ (**Table 4.26.**).

Spectroscopic data of compound **5** (**Table 4.27.**) were checked in the literature, and found to be quite similar to the data for isolariciresinol-9-*O*-β-xyloside

(475). Therefore, compound **5** was elucidated as isolariciresinol-9-*O*-*β*-xyloside (**Figure 4.43.**).

Table 4.27. ^{1}H- and ^{13}C-NMR spectroscopic data of isolariciresinol-9-O-β-xyloside (DMSO-d_6, ^{1}H: 600 MHz, ^{13}C: 151 MHz).

C/H		δ_H (ppm), J (Hz)	δ_C (ppm)	HMBC (H→C)
1	CH$_2$	2.73 – 2.70	32.63	C-2, C-3, C-8, C-4a, C-8a, C-2α
2	CH	1.86 (ddd, 13.1, 6.2, 3.5)	37.56	C-1, C-3, C-2α
3	CH	1.68 (tt, 10.7, 2.7)	44.11	C-4
4	CH	4.02 (d, 10.9)	45.64	C-3, C-3α, C-4a, C-8a, C-1', C-2', C-6', C-1"
5	C	6.06 (s)	116.27	C-4, C-6, C-7, C-8a
6	C		144.03	-
7	C		145.50	-
8	CH	6.59 (s)	111.76	C-7, C-4a, C-8a
2α	CH$_2$	3.57 (dt, 10.5, 4.2) 3.46 (dt, 11.0, 5.9)	62.60	C-1
3α	CH$_2$	3.84 (dd, 9.6, 2.4) 3.00 – 2.94	67.23	C-4, C-2, C-3, C-3'-OMe
4a	C	-	132.62	-
8a	C	-	127.02	-
1'	C	-	136.91	-
2'	CH	6.79 (d, 2.0)	113.86	C-1', C-3', C-4', C-6'
3'	C	-	147.14	-
4'	C	-	144.47	-
5'	C	6.68 (d, 8.0)	115.48	C-3', C-4',
6'	CH	6.47 (dd, 8.1, 1.9)	121.05	C-4, C-2', C-4'
1"	CH	3.90 (d, 7.6)	104.59	C-3α, C-4
2"	CH	3.00 – 2.94	73.37	C-3", C-4"
3"	CH	3.07 (td, 8.8, 4.8)	76.59	C-2", C-4"
4"	CH	3.26 (ddt, 10.4, 8.8, 5.2)	69.58	C-3"
5"	CH$_2$	3.64 (dd, 11.3, 5.4) 3.00 – 2.94	65.70	C-1", C-3", C-4"

Table 4.27. ^{1}H- and ^{13}C-NMR spectroscopic data of isolariciresinol-9-O-β-xyloside (DMSO-d_6, ^{1}H: 600 MHz, ^{13}C: 151 MHz) (continued).

C/H		δ_H (ppm), J (Hz)	δ_C (ppm)	HMBC (H➔C)
7-OMe	CH$_3$	3.70 (s)	55.57	C-6, C-7
3'-OMe	CH$_3$	3.71 (s)	55.48	C-3', C-4'
6-OH	OH	8.44 (s)	-	C-5
4'-OH	OH	8.74 (s)	-	C-5'
2"-OH	OH	5.24 (d, 4.7)	-	C-1", C-3"
3"-OH	OH	4.99 (d, 4.8)	-	C-2", C-3", C-4", C-5"
4"-OH	OH	4.95 (d, 5.0)	-	-
CH$_2$OH	OH	4.41 (t, 5.1)	-	C-2
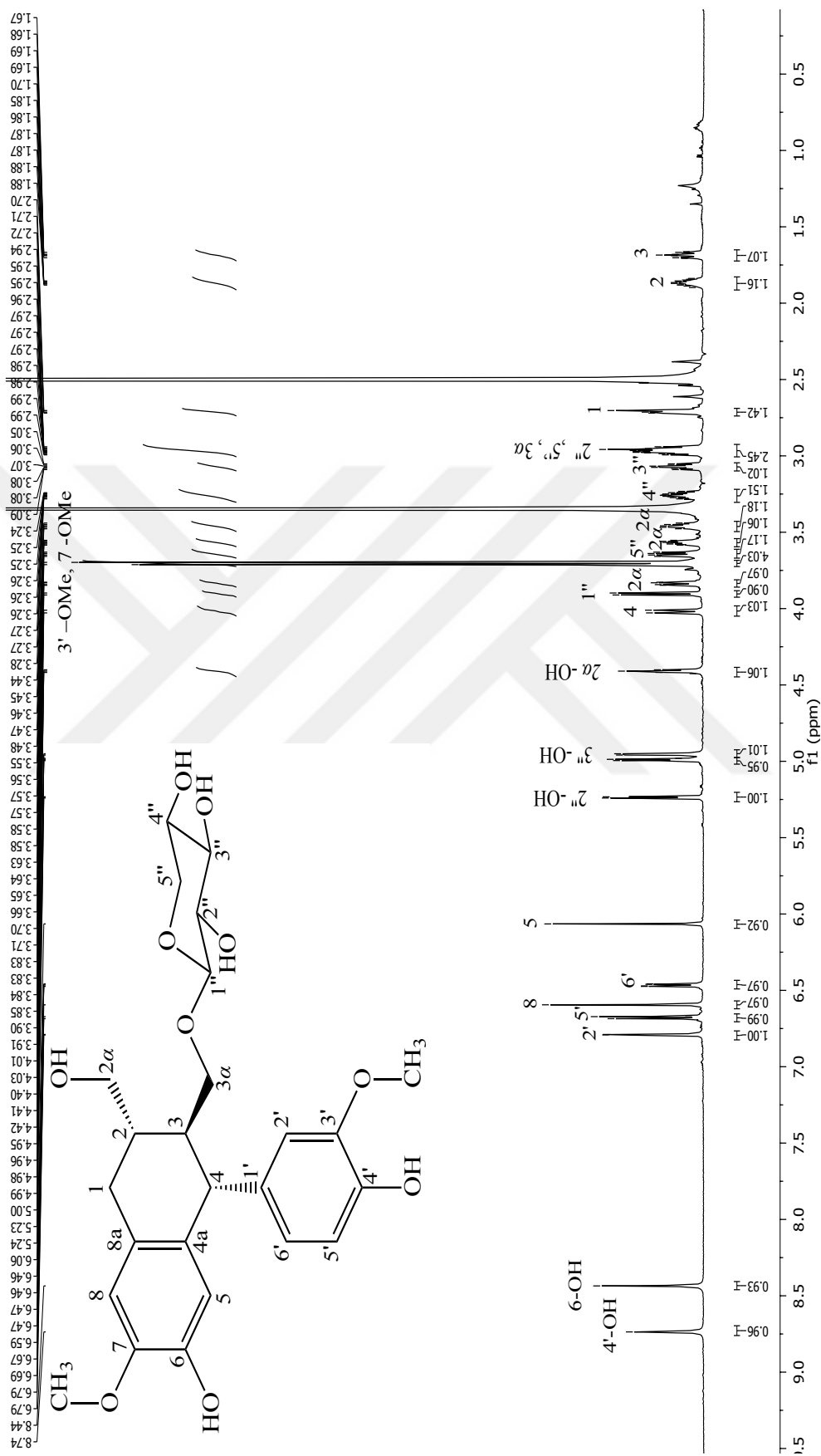
Figure 4.44. ^{1}H-NMR spectrum of isolariciresinol-9-O-β-xyloside (Compound **5**) (DMSO-d_6, ^{1}H: 600 MHz).
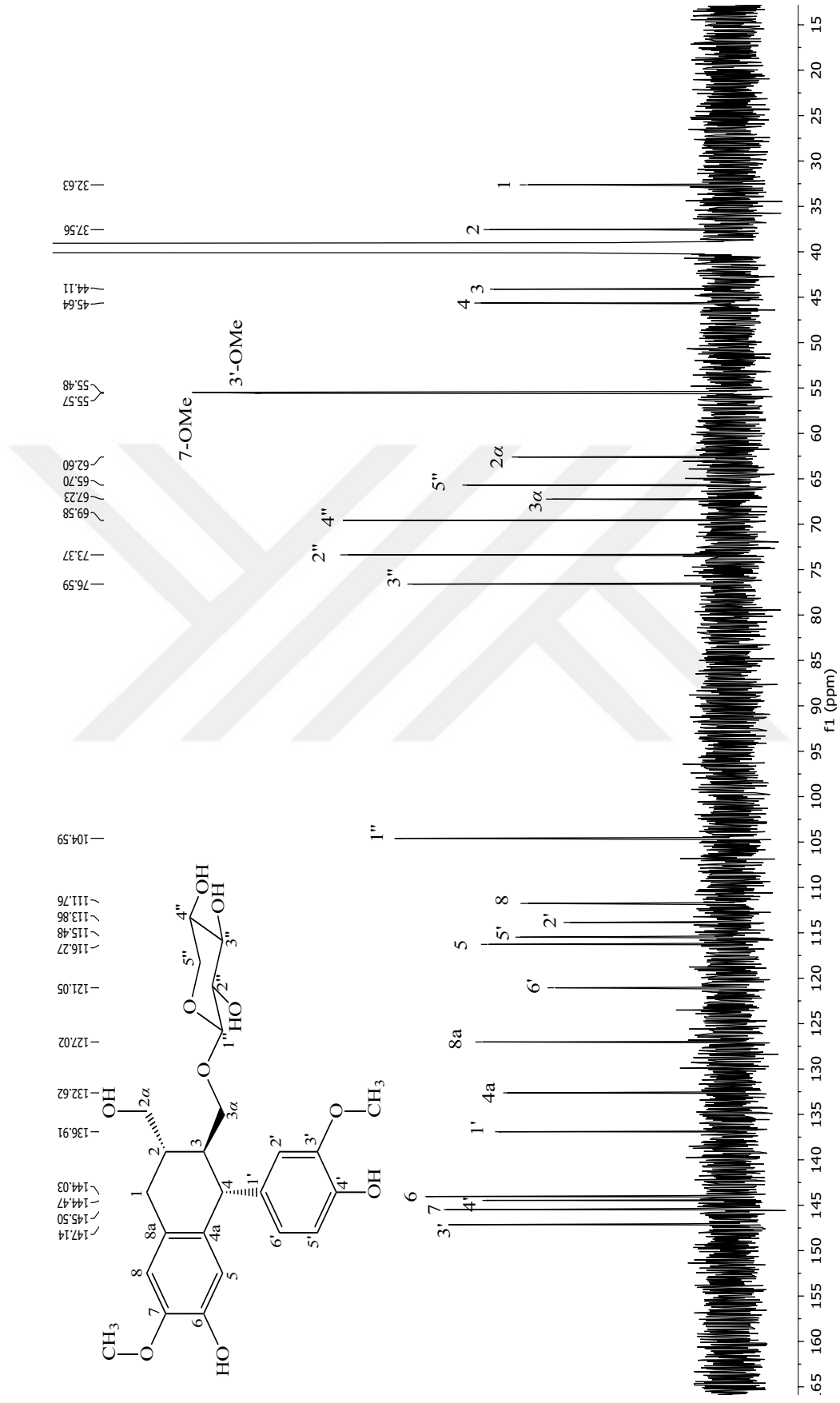
Figure 4.45. ^{13}C-NMR spectrum of isolariciresinol-9-*O*-β-xyloside(Compound **5**) (DMSO-*d6*, ^{13}C: 151 MHz).
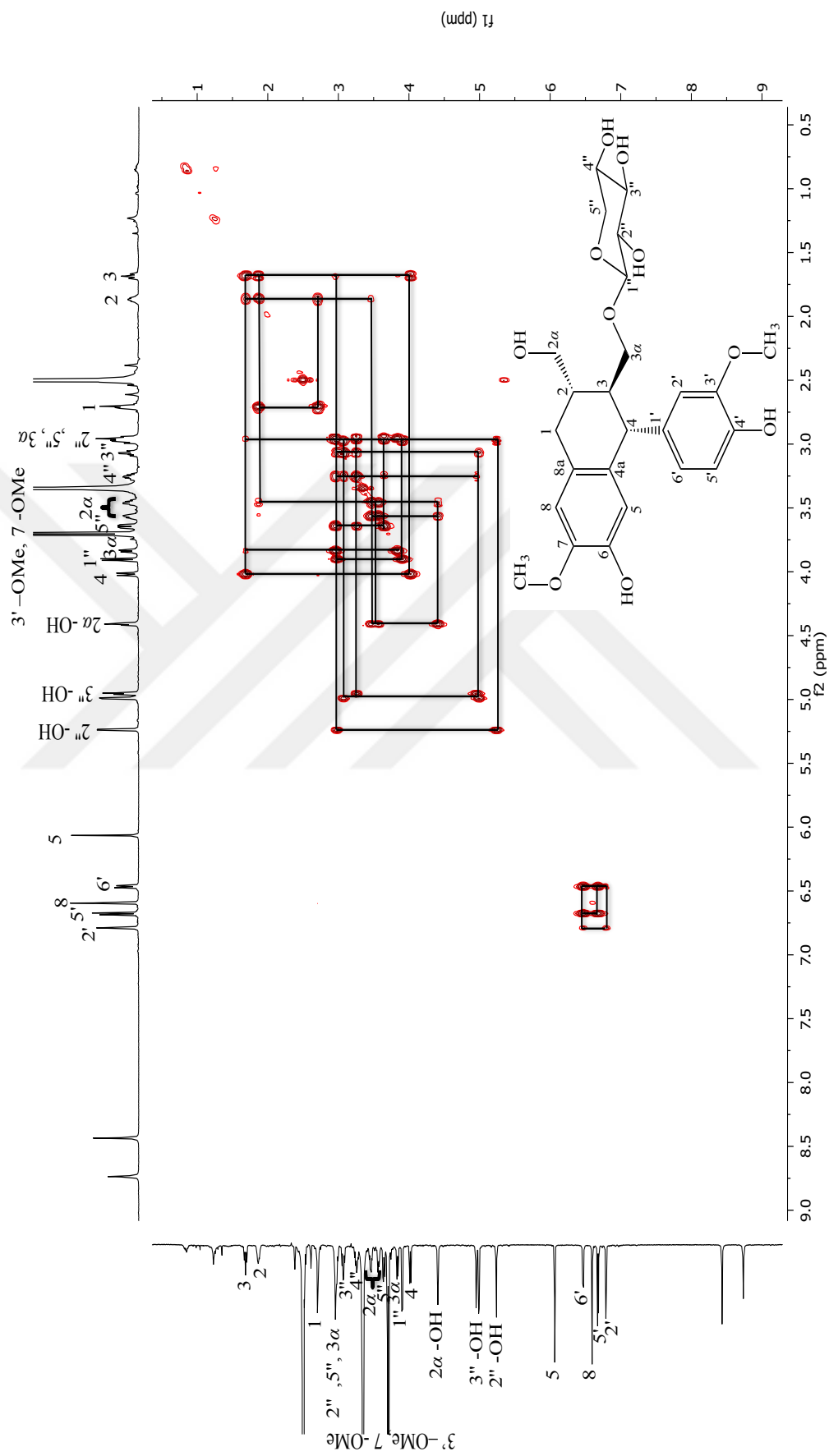
Figure 4.46. ^{1}H-^{1}H homonuclear correlation spectrum (COSY) of isolariciresinol-9-O-β-xyloside (Compound **5**).
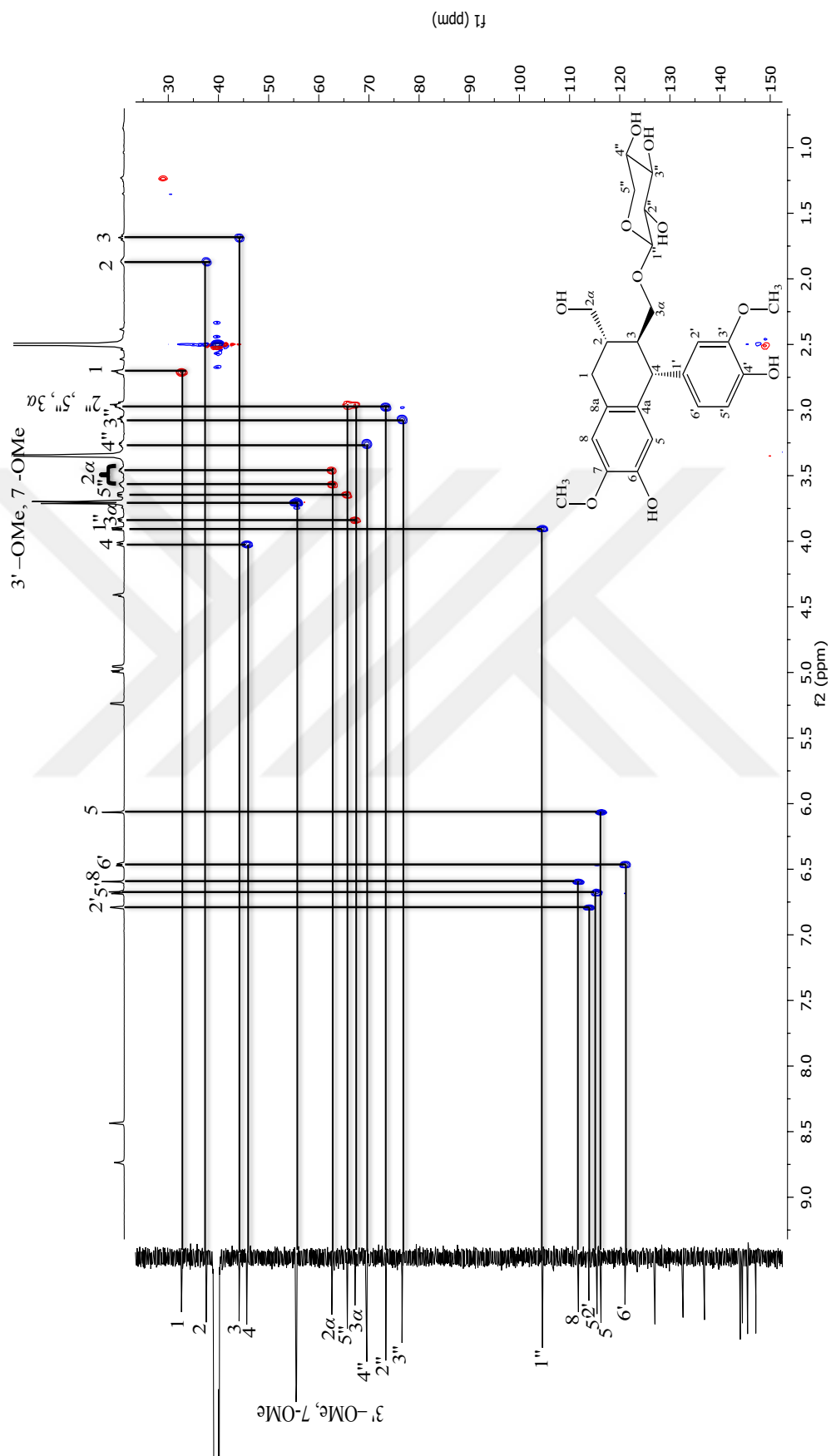
Figure 4.47. ^{1}H-^{13}C heteronuclear multiple-quantum correlation (HMQC) spectrum of isolariciresinol-9-*O*-β-xyloside (Compound **5**).
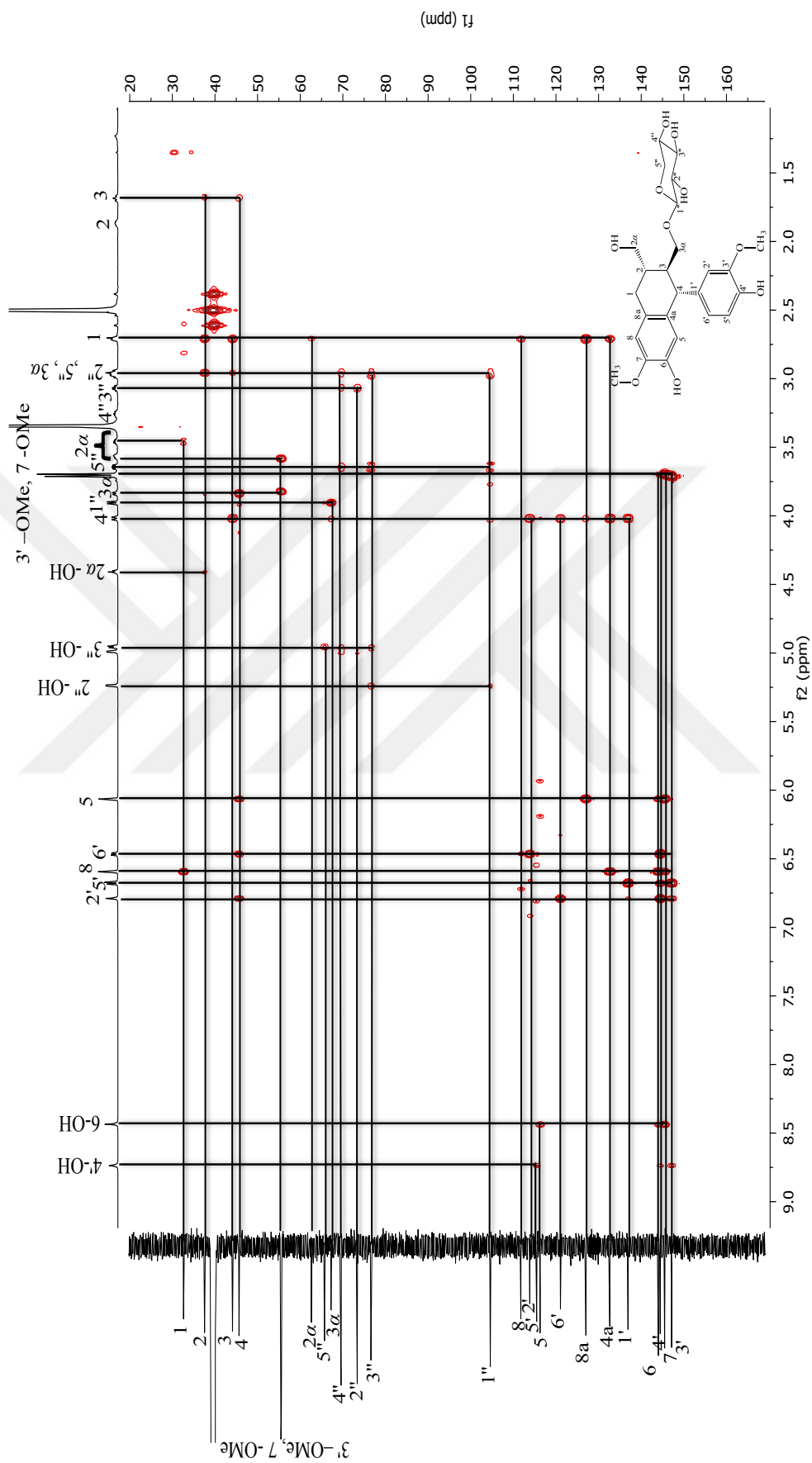
Figure 4.48. ^{1}H-^{13}C heteronuclear multiple-bond correlation (HMBC) spectrum of isolariciresinol-9-*O*-β-xyloside (Compound **5**).

185

4.2.6 Rumejaposide G/H diastereomeric mixture
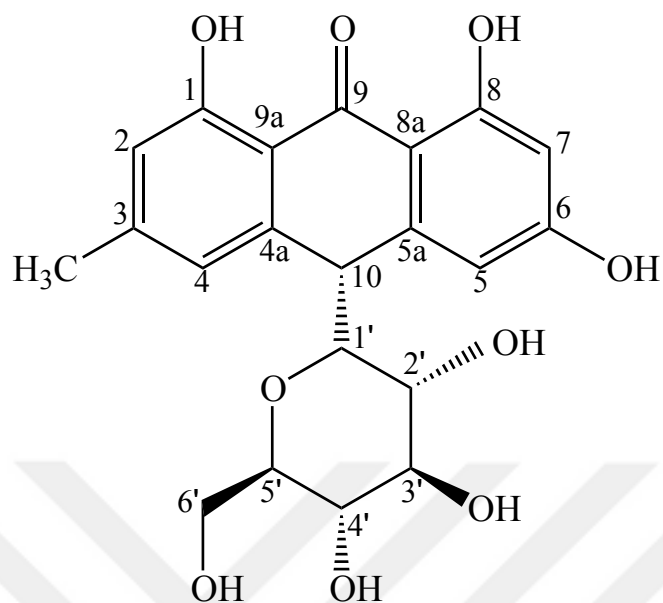
Rumejaposide G (Compound **6A**)
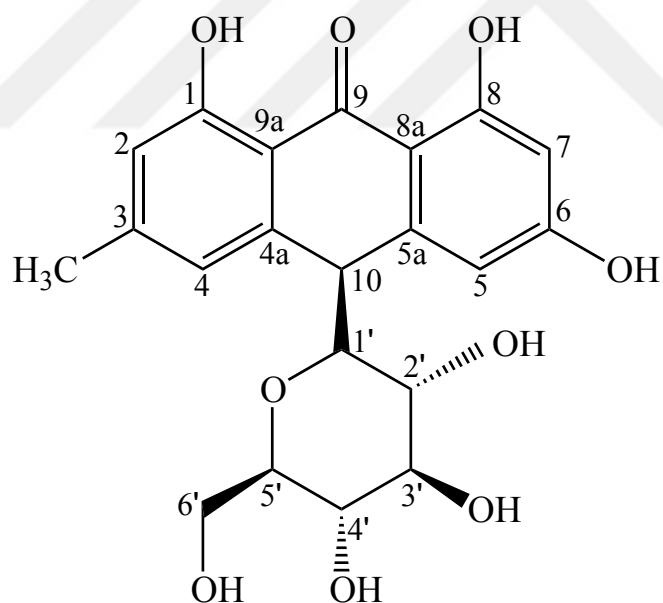
Rumejaposide H (Compound **6B**)

Figure 4.49. Structure of rumejaposide G/H diastereomers.

The data about rumejaposide G/H diastereomers were expressed in the following pages.

Table 4.28. The data about rumejaposide G/H diastereomers.

Molecular formula	$C_{21}H_{22}O_9$
Synonyms	-
Molecular weight	418 g/mol
IR (ATR) ν (cm^{-1})	3550 – 3050, 1620, 1481, 1368, 1284, 1150, 1025, 992
MS (ESI) *m/z*:	[M+Na]$^+$ 441.1169
$[\alpha]_D^{22}$	–3.2° (MeOH, c = 0.22)
^{1}H NMR	**Figures 4.50. and 4.55.** **Tables 4.29. and 4.30.**
^{13}C NMR	**Figures 4.51. and 4.56.** **Tables 4.29. and 4.30.**
COSY	**Figures 4.52. and 4.57.**
HMQC	**Figures 4.53. and 4.58.** **Tables 4.29. and 4.30.**
HMBC	**Figures 4.54. and 4.59.** **Tables 4.29. and 4.30.**

Compound **6** was isolated as an amorphous and yellow solid. In case of application to TLC plate, light yellow spot was observed at daylight before reagent spraying. Additionally, the spots having fluorescence inhibiting zones under UV 254 nm and red/orange fluorescence under UV 366 nm were monitored. After Vanilin/H_2SO_4 sprayed and Vanilin/H_2SO_4 sprayed-plate was heated up to 110 °C, an orange spot was detected. The structure of the substance was identified based on its spectroscopic data (IR, NMR and mass spectroscopy).

IR spectrum of the compound **6** pointed out the presence of aromatic C=C (1481 cm^{-1}), aromatic C-H (3050-3100 cm^{-1}), alkane C-H (1368 cm^{-1}), alkane C-C (992 cm^{-1}), O-H (3200, 3550 cm^{-1}) and C-O (1150 cm^{-1}) functions.

Mass spectrum pointed out $[M+Na]^+$ peaks at *m/z* 441.1169. ^{13}C spectrum pointed out presence of 42 C atoms in the structure. Therefore, we assumed that the compound 6 may consist of two diastereomers, which were expressed as compound **6A** and compound **6B**. NMR spectra of the mixture of the compounds **6A** and **6B** were recorded and spectroscopic data of the both compounds were shown in the same spectra, separately (**Figures 4.50-4.59**). 2D spectra (COSY, HMQC and HMBC) also supported the presence of two diastereomers.

^1H-NMR spectrum displayed signals in the aromatic field at 6.88 (d, *J* = 1.4 Hz, 1H, H-4), 6.68 (s, 1H, H-2), 6.47 (d, *J* = 2.3 Hz, 1H, H-5), 6.22 ppm (d, *J* = 2.3 Hz, 1H, H-7) for compound **6A** and 6.84 (s, 1H, H-4), 6.67 (s, 1H, H-2), 6.52 (d, *J* = 2.2 Hz, 1H, H-5), 6.20 ppm (d, *J* = 2.2 Hz 1H, H-7) for compound **6B**. Furthermore, ~~the~~ other proton signals in the structure were detected at 12.17 (s, C-8-OH), 12.00 (s, C-1-OH), 10.74 (s, C-6-OH), 5.19 (d, *J* = 5.9 Hz, C-2'-OH), 4.92 (d, *J* = 4.9 Hz, C-3'-OH), 4.79 – 4.76 (H, C-4'-OH), 4.41 (d, *J* = 2.1 Hz, H-10), 3.89 (pseudo-q, *J* = 5.5 Hz, C-6'-OH), 3.42 – 3.36 (H, H-6'), 3.27 (dd, *J* = 9.2, 2.2 Hz, H-1'), 3.19 – 3.13 (H, H-6'), 3.13 – 3.06 (H-2, H-3'), 2.84 (td, *J* = 9.2, 5.9 Hz, H-2'), 2.79 (ddd, *J* = 9.8, 5.8, 2.2 Hz, H-5'), 2.74 – 2.68 (H, H-4'), and 2.34 ppm (s, 3H, H atoms of Me in C-3-Me) for compound **6A** and 12.16 (s, C-8-OH), 12.00 (s, C-1-OH), 10.74 (s, C-6-OH), 5.14 (d, *J* = 5.9 Hz, C-2'-OH), 4.94 (d, *J* = 5.0 Hz, C-3'-OH), 4.79 – 4.76 (H, C-4'-OH), 4.42 (d, *J* = 2.1 Hz, H-10), 3.89 (pseudo-q, *J* = 5.5 Hz, C-6'-OH), 3.42 – 3.36 (H, H-6'), 3.26 (dd, *J* = 9.2, 2.2 Hz, H-1'), 3.19 – 3.13 (H, H-6'), 3.13 – 3.06 (H-2, H-3'), 2.92 (td, *J* = 9.2, 5.9 Hz, H-2'), 2.74 – 2.68 (H, H-5'), 2.74 – 2.68 (H, H-4'), 2.33

(s, 3H, H atoms of Me in C-3-Me) ppm for compound **6B** (**Figures 4.50. and 4.55.**).

Proton signals at 3.27 (d, J = 9.2 Hz) and 3.26 ppm (d, J = 9.2 Hz) were attributed to the anomeric protons for compounds **6A** and compound **6B**, respectively. A J value of 9.2 Hz indicated that the sugar molecule is in β configuration for both compounds. The other proton signals in the sugar molecule were ranged from δ_H 2.68 to δ_H 3.42 ppm for compound **6A** and from 2.68 to 3.42 ppm for compound **6B**. H atom signals in aromatic rings were observed at around 7 ppm at higher frequency, while H atom signals in the sugar molecules and 3-Me were observed at lower frequency. H atom signals of the substituted OH groups in the 1st, 6th and 8th positions of the molecules were additionally detected at 12.00, 10.74 and 12.17 ppm for compound **6A** and 12.00, 10.74 and 12.16 ppm for compound **6B**, respectively.

^{13}C-NMR spectrum (**Figures 4.51. and 4.56.**) presented the substances to have totally 42 carbon atom signals, each having sugar molecules with 6 carbons and totally containing 21 carbons in their structures. δ_C of C atom signals in the sugar molecule were detected at 86.33 (anomeric C, C-1'), 70.53 (C-2'), 78.64 (C-3'), 70.71 (C-4'), 81.28 (C-5') and 61.78 ppm (C-6') for compound 6A and 86.15 (anomeric C, C-1'), 70.31 (C-2'), 78.68 (C-3'), 70.74 (C-4'), 81.38 (C-5') and 61.87 ppm (C-6') for compound 6B. IR spectrum supported the structure to include aromatic rings, alkane groups, -OH groups. δ_C of the aromatic C atom signals were ranged from 101.64 to 164.84 ppm for compound 6A and from 101.55 to 164.32 ppm for compound 6B. δ_C of C atom signals at the 1st, 3rd 6th, 8th, and 9th positions of aromatic rings were observed at higher chemical shifts indicating aromatic ring to be substituted with polar groups at those C atoms. Furthermore, δ_C of C atom signals at the 10th positions of aromatic rings pointed out the presence of a e$^-$ withdrawing groups ~~in~~ at those positions with deshielding effects, which may indicate a C-glucosylation. Based on the data from ^{1}H and ^{13}C NMR spectra as well as 2D spectra (COSY, HMQC and HMBC), it was assumed that compound **6** might be member of antranoid derivatives as a mixture of two diastereomeric compounds as explained in details below.

According to COSY spectrum, H signals coupling with each other were displayed, the couplings of H-4 with H-2, H-10 and H of Me in C-3-Me, H-5 with H-10 as well as H-7, H-7 with H-5 and H-4, H of OH in C-2'-OH with H-2', H of OH in

C-3'-OH with H-3', H of OH in C-4'-OH with H-4', H of OH in C-6'-OH with H-6' and H-1', H-6' with H-6', H-1' with H-3' and H-10', H-3' with H-2', H-4' with H of OH in C-4'-OH, H of Me in C-3-Me with H-4 (**Figures 4.52. and 4.57.**).

HMQC spectrum indicating C atoms with their relating H atoms were shown in **Figures 4.53. and 4.58.**

In the HMBC spectrum, the long range couplings of H-4 with C of Me in C-3-Me, C-10 and C-2, H-2 with C of Me in C-3-Me, C-4, C-9a and C-1, H-5 with C-10, C-7 and C-8a, H-7 with C-5, C-6 and C-8a, H-1' with C-3', C-5', C-4a and C-5a, H of Me in C-3-Me with C-2, C-3 and C-4, H-10 with C-6', H-3' with C-2' and C-4', H-2' with C-1' and C-3', H-4' with C-3' and C-5', H-5' with C-3', H of OH in C-6'-OH with C-1', C-3, C-4, C-5, C-4a, C-5a and C-8a, H of OH in C-2'-OH with C-1', H of OH in C-3'-OH with C-2' and C-4', H of OH in C-4'-OH with C-2', C-4' and C-5' were shown for both diastereomers (**Figures 4.54. and 4.59.**).

Following the analysis of NMR spectra, the compound was detected as a mixture of two diastereomers and were found to have the molecular formula of $C_{21}H_{22}O_9$, which was also confirmed by HR-MS (ESI) at *m/z* 441.1169 $[M+Na]^+$ (**Table 4.28.**).

Spectroscopic data of compound **6** (**Tables 4.29. and 4.30.**) were found to be identical for rumejaposide G and rumejaposide H (131) published before. Therefore, the compound **6** was elucidate as a mixture of two diastereomer, which are rumejaposide G and rumejaposide H (**Figure 4.49.**).

Table 4.29. ^{1}H- and ^{13}C-NMR spectroscopic data of rumejaposide G (Compound **6A**, DMSO-d_6, ^{1}H: 600 MHz, ^{13}C: 151 MHz).

C/H		δ$_H$ (ppm), J (Hz)	δ$_C$ (ppm)	HMBC (H→C)
1	C	-	161.32	
2	CH	6.68 (s)	116.20	C-3-Me, C-4, C-9a, C-1
3	C	-	146.11	
4	CH	6.88 (d, 1.4)	121.58	C-3-Me, C-10, C-2
5	CH	6.47 (d, 2.3)	107.96	C-10, C-7, C-8a
6	C	-	164.84	
7	CH	6.22 (d, 2.3)	101.64	C-5, C-6, C-8a
8	C	-	164.15	
10	CH	4.41 (d, 2.1)	44.44	C-6'
4a	C	-	148.51	
5a	C	-	142.06	
8a	C	-	110.54	
9a	C	-	115.18	
3-Me	CH$_3$	2.34 (s, 3H)	22.12	C-2, C-3, C-4
1'	CH	3.27 (d, 9.2)	86.33	C-3', C-5', C-4a, C-5a
2'	CH	2.84 (td, 9.2, 5.9)	70.53	C-1', C-3'
3'	CH	3.13 – 3.06	78.64	C-2', C-4'
4'	CH	2.74 – 2.68	70.71	C-3', C-5'
5'	CH	2.79 (ddd, 9.8, 5.8, 2.2)	81.28	C-3'
6'	CH$_2$	3.42 – 3.36 3.19 – 3.13	61.78	
1-OH	OH	12.00 (s)	-	
6-OH	OH	10.74 (s)	-	
8-OH	OH	12.17 (s)	-	
2'-OH	OH	5.19 (d, 5.9)	-	C-1'
3'-OH	OH	4.92 (d, 4.9)	-	C-2', C-4'
4'-OH	OH	4.79 – 4.76	-	C-2', C-4', C-5'
6'-OH	OH	3.89 (pseudo-q, 5.5)	-	C-1', C-3, C-4, C-5, C-4a, C-5a, C-8a
C=O	C	-	191.86	

191
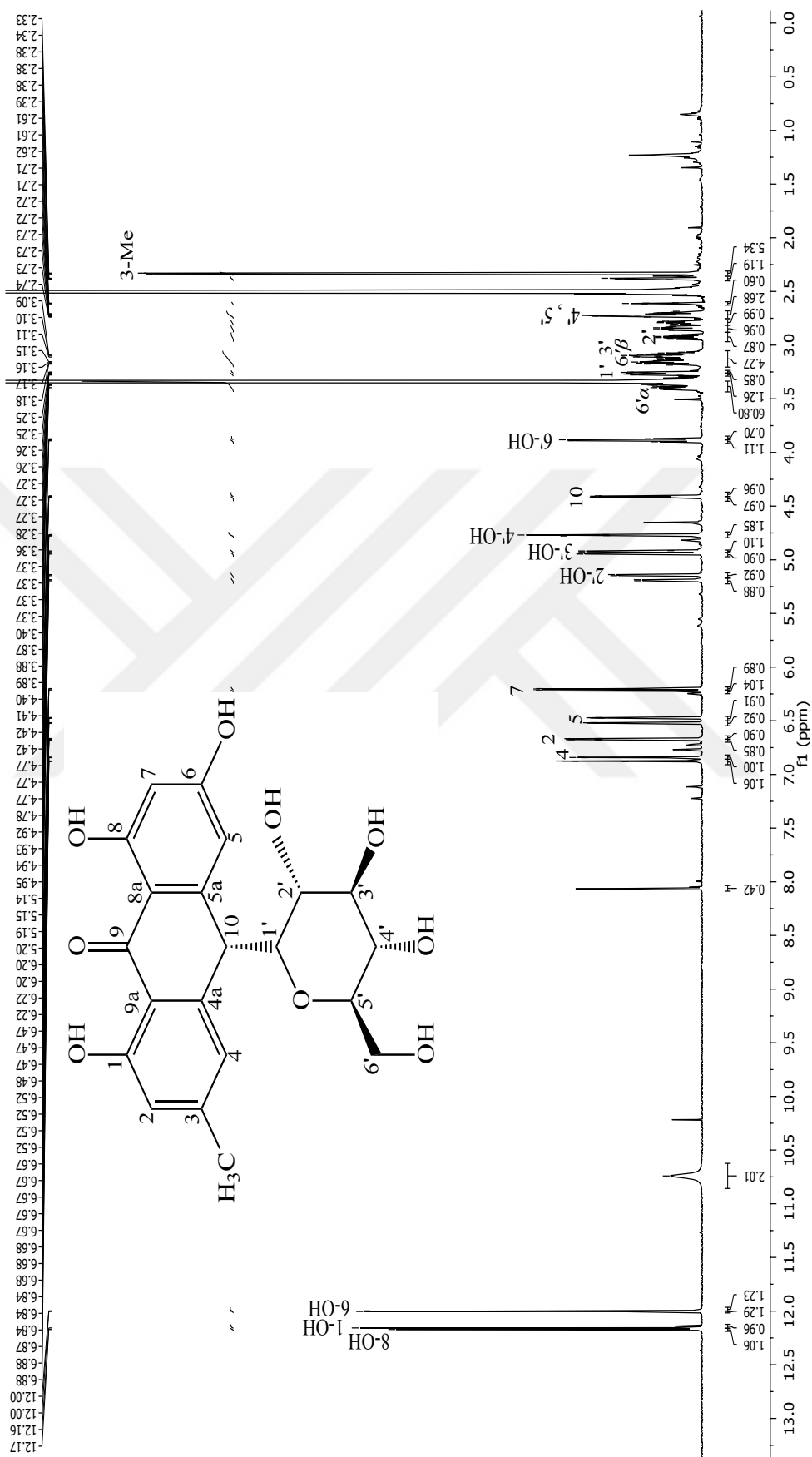
Figure 4.50. ¹H-NMR spectrum of rumejaoposide G (Compound **6A**) (DMSO-d_6, ¹H: 600 MHz).
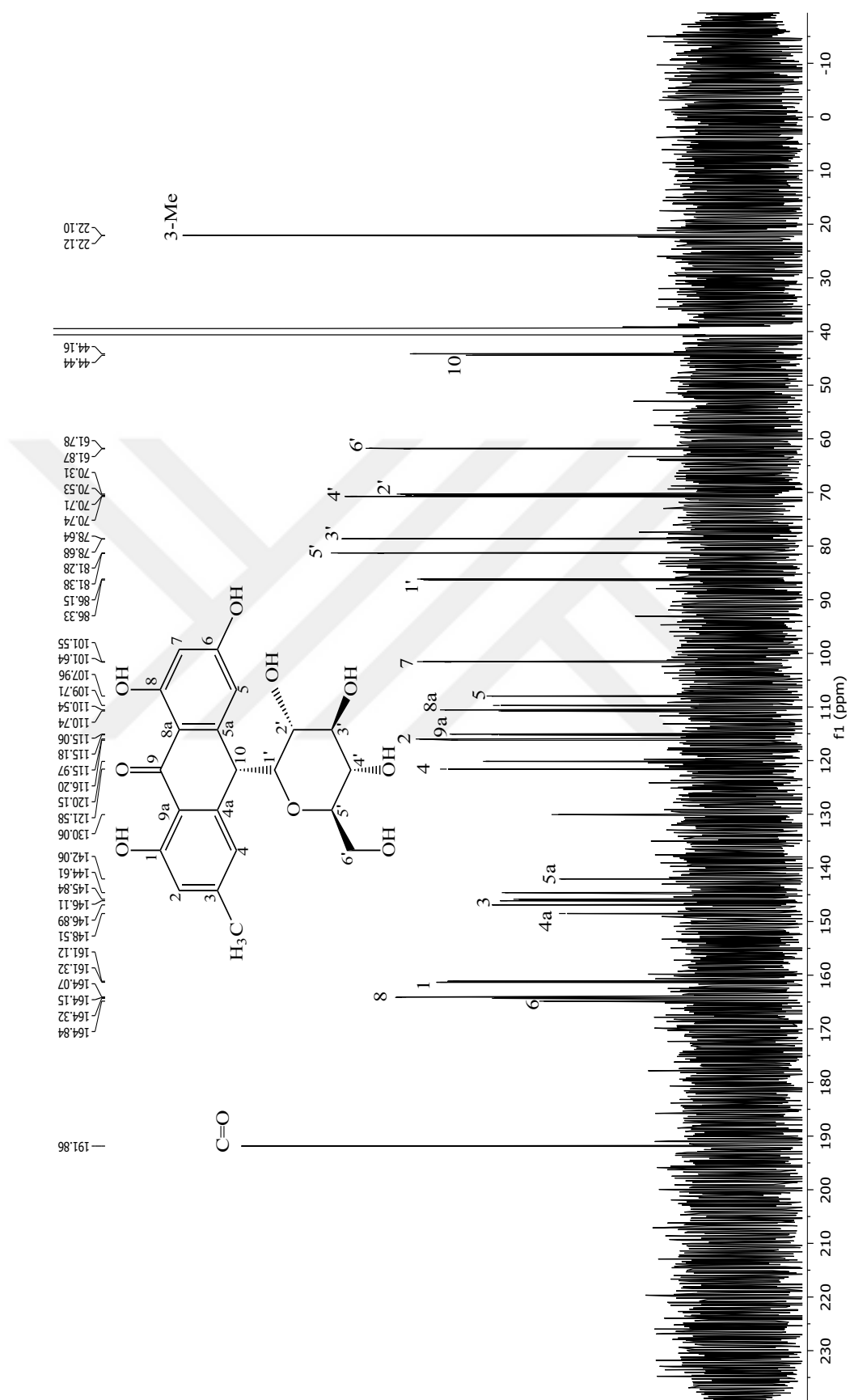
Figure 4.51. ^{13}C-NMR spectrum of rumejaposide G (Compound **6A**) (DMSO-d_6, ^{13}C: 151 MHz).
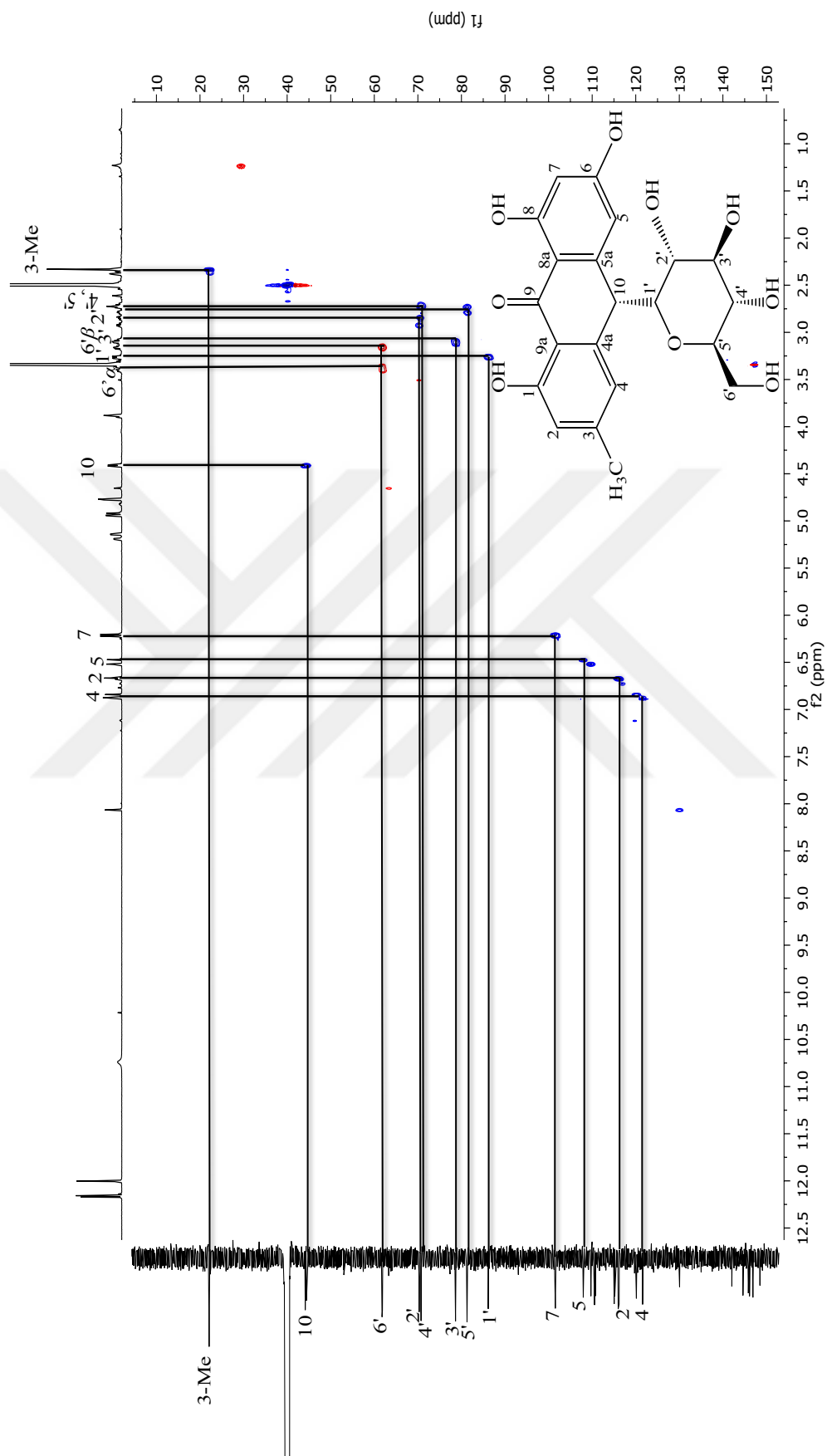
Figure 4.52. ^{1}H-^{1}H homonuclear correlation spectrum (COSY) of rumejaposide G (Compound **6A**).
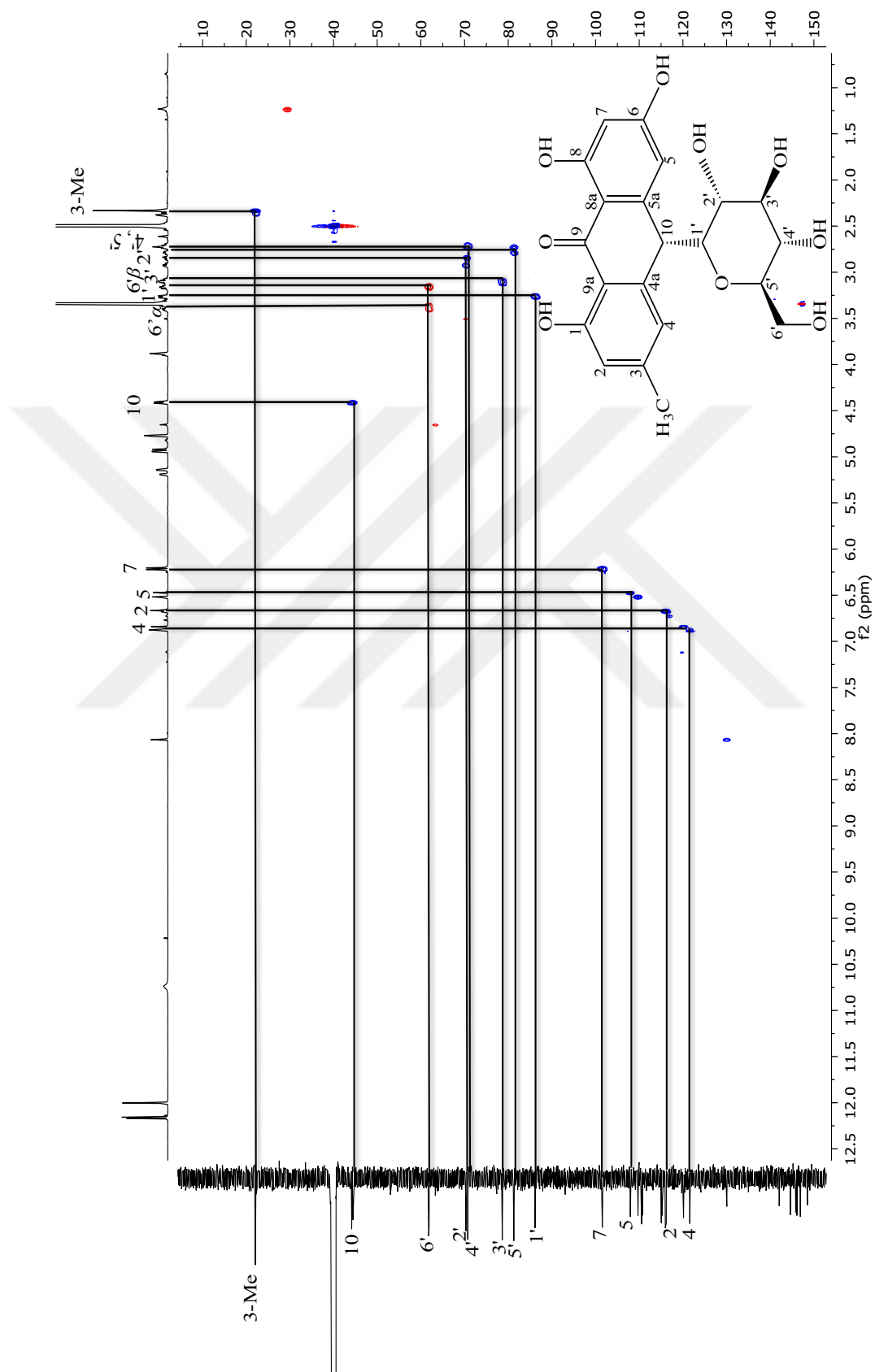
Figure 4.53. ^{1}H-^{13}C heteronuclear multiple-quantum correlation (HMQC) spectrum of rumejaposide G (Compound **6A**).
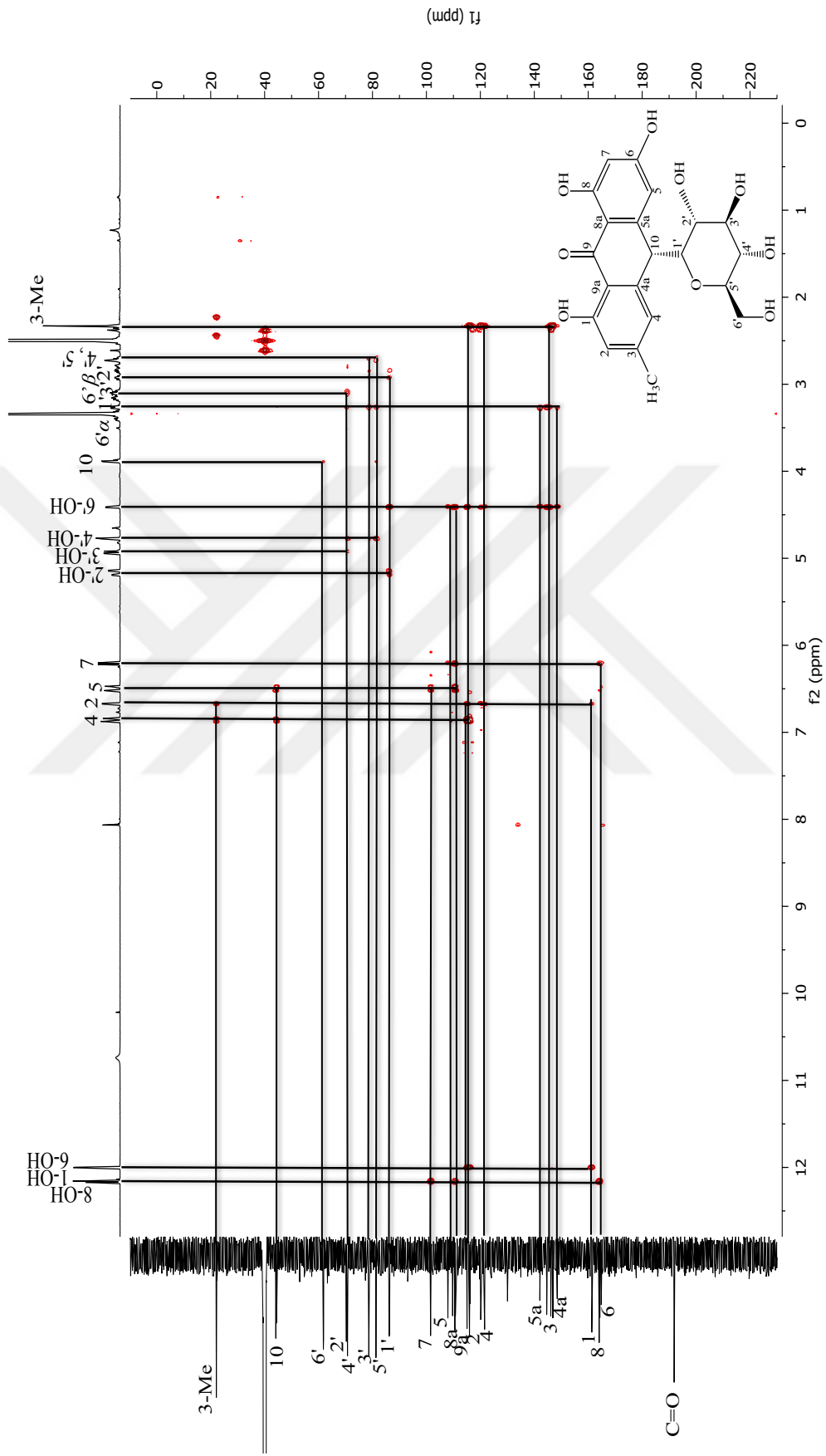
Figure 4.54. ^{1}H-^{13}C heteronuclear multiple-bond correlation (HMBC) spectrum of rumejaposide G (Compound **6A**).

Table 4.30. ^{1}H- and ^{13}C-NMR spectroscopic data of rumejaposide H (Compound **6B**, DMSO-d_6, ^{1}H: 600 MHz, ^{13}C: 151 MHz).

C/H		δ_H (ppm), J (Hz)	δ_C (ppm)	HMBC (H➔C)
1	C	-	161.12	
2	CH	6.67 (s)	115.97	C-3-Me, C-4, C-9a, C-1
3	C	-	146.89	
4	CH	6.84 (s)	120.15	C-3-Me, C-10, C-2
5	CH	6.52 (d, 2.2)	109.71	C-10, C-7, C-8a
6	C	-	164.32	
7	CH	6.20 (d, 2.2)	101.55	C-5, C-6, C-8a
8	C	-	164.07	
10	CH	4.42 (d, 2.1)	44.16	C-6'
4a	C	-	148.51	
5a	C	-	144.61	
8a	C	-	110.74	
9a	C	-	115.06	
3-Me	CH$_3$	2.33 (s, 3H)	22.10	C-2, C-3, C-4
1'	CH	3.26 (d, 9.2)	86.15	C-3', C-5', C-4a, C-5a
2'	CH	2.92 (td, 9.2, 5.9)	70.31	C-1', C-3'
3'	CH	3.13 – 3.06	78.68	C-2', C-4'
4'	CH	2.74 – 2.68	70.74	C-3', C-5'
5'	CH	2.74 – 2.68	81.38	C-3'
6'	CH$_2$	3.42 – 3.36 3.19 – 3.13	61.87	
1-OH	OH	12.00 (s)	-	
6-OH	OH	10.74 (s)	-	
8-OH	OH	12.16 (s)	-	
2'-OH	OH	5.14 (d, 5.9)	-	C-1'
3'-OH	OH	4.94 (d, 5.0)	-	C-2', C-4'
4'-OH	OH	4.79 – 4.76	-	C-2', C-4', C-5'
6'-OH	OH	3.89 (pseudo-q, 5.5)	-	C-1', C-3, C-4, C-5, C-4a, C-5a, C-8a
C=O	C	-	191.86	

197
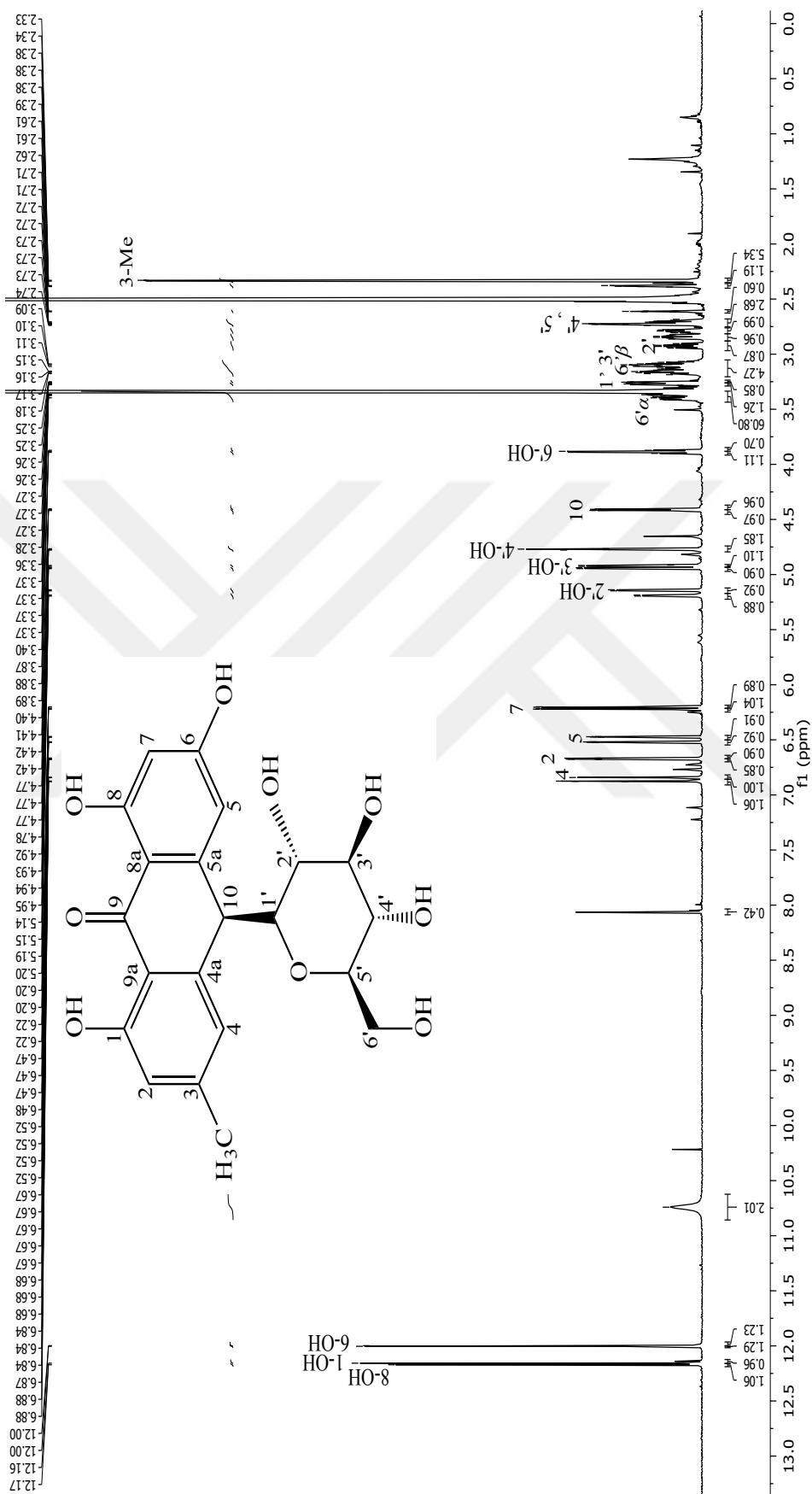
Figure 4.55. ¹H-NMR spectrum of rumejaposide H (Compound **6B**) (DMSO-d_6, ¹H: 600 MHz).

Figure 4.56. ^{13}C-NMR spectrum of rumejaposide H (Compound **6B**) (DMSO-d_6, ^{13}C: 151 MHz).
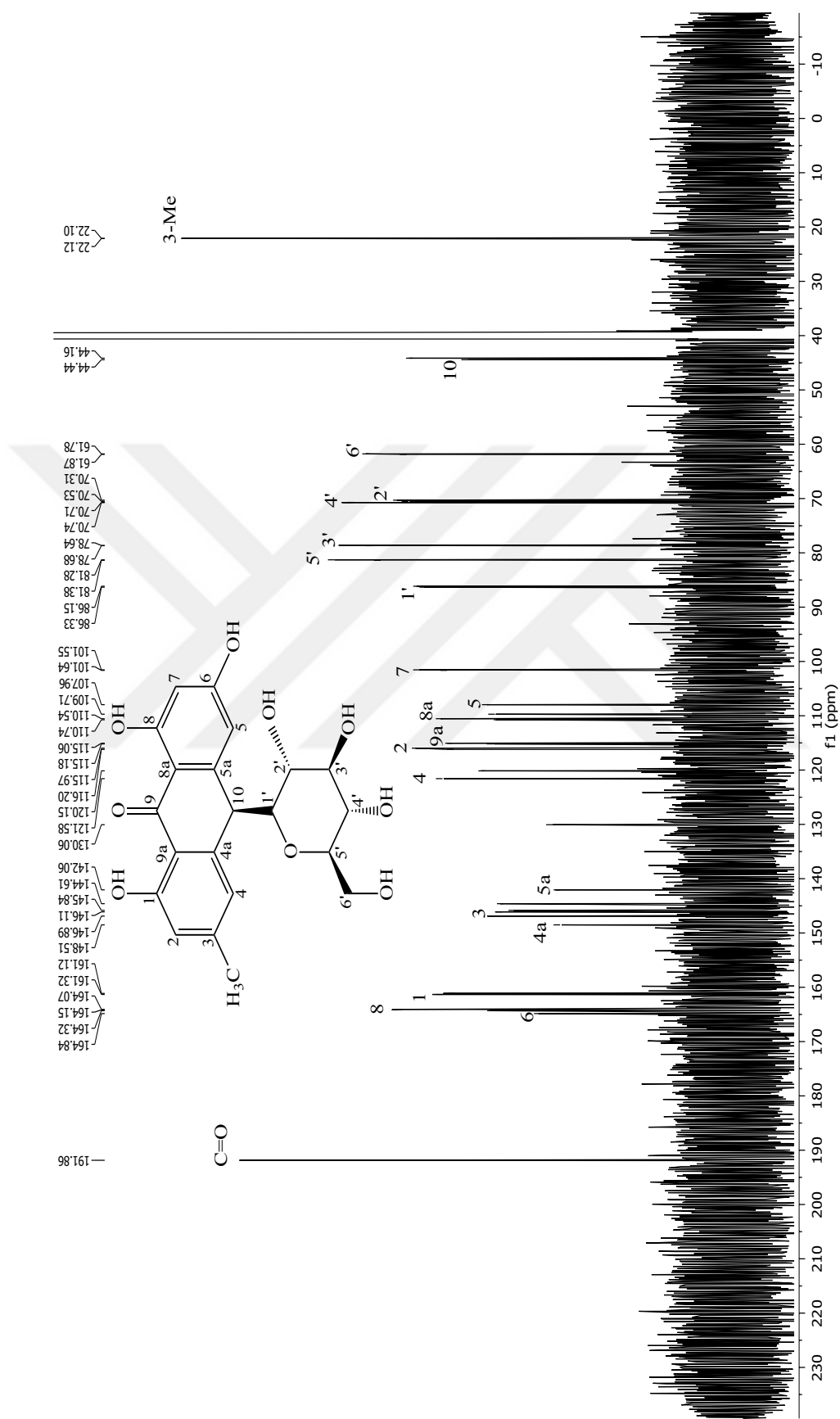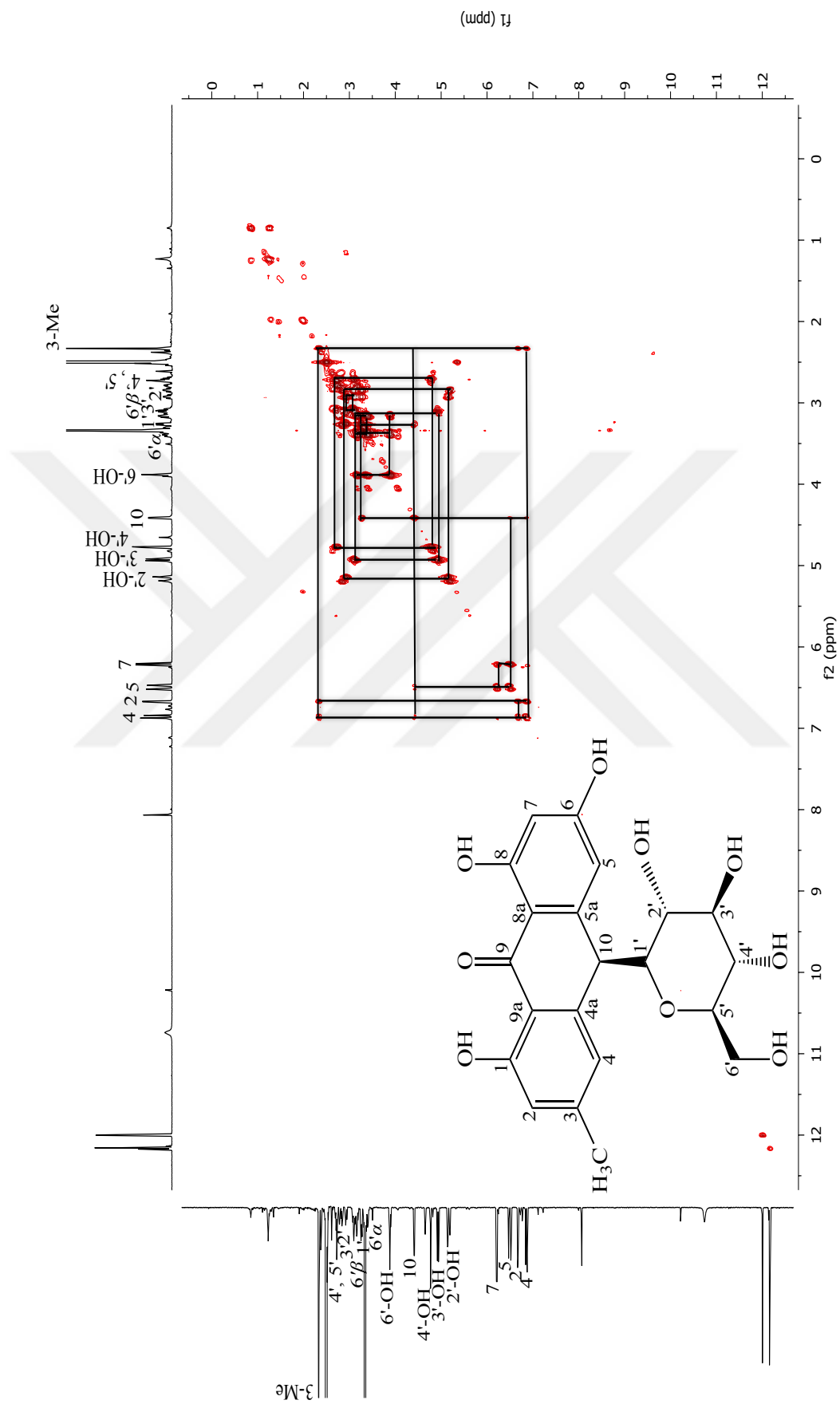
Figure 4.57. ^{1}H–^{1}H homonuclear correlation spectrum (COSY) of rumejaposide H (Compound **6B**).
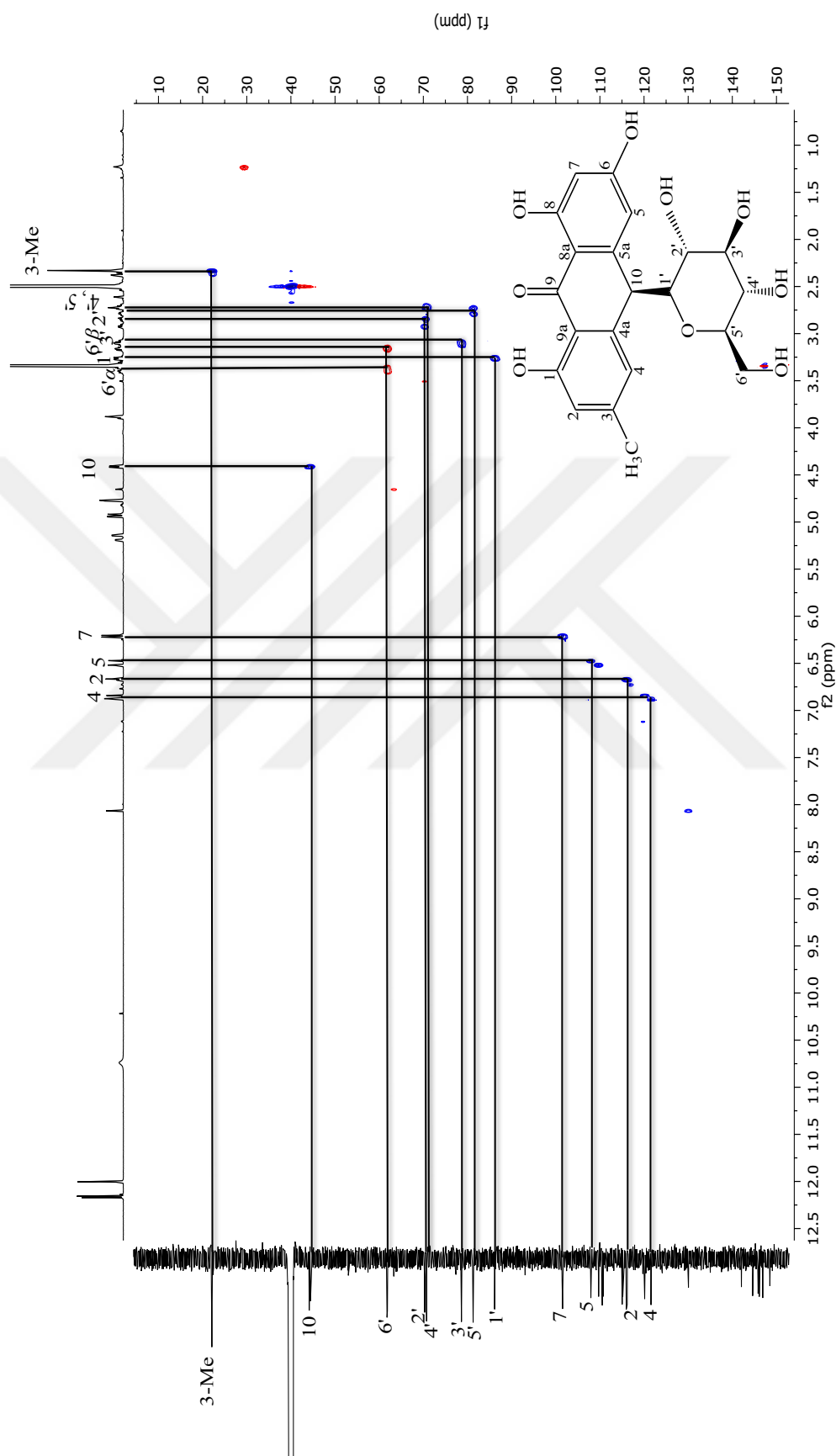
Figure 4.58. ^{1}H-^{13}C heteronuclear multiple-quantum correlation (HMQC) spectrum of rumejaposide H (Compound **6B**).

Figure 4.59. ^{1}H-^{13}C heteronuclear multiple-bond correlation (HMBC) spectrum of rumejaposide H (Compound **6B**).
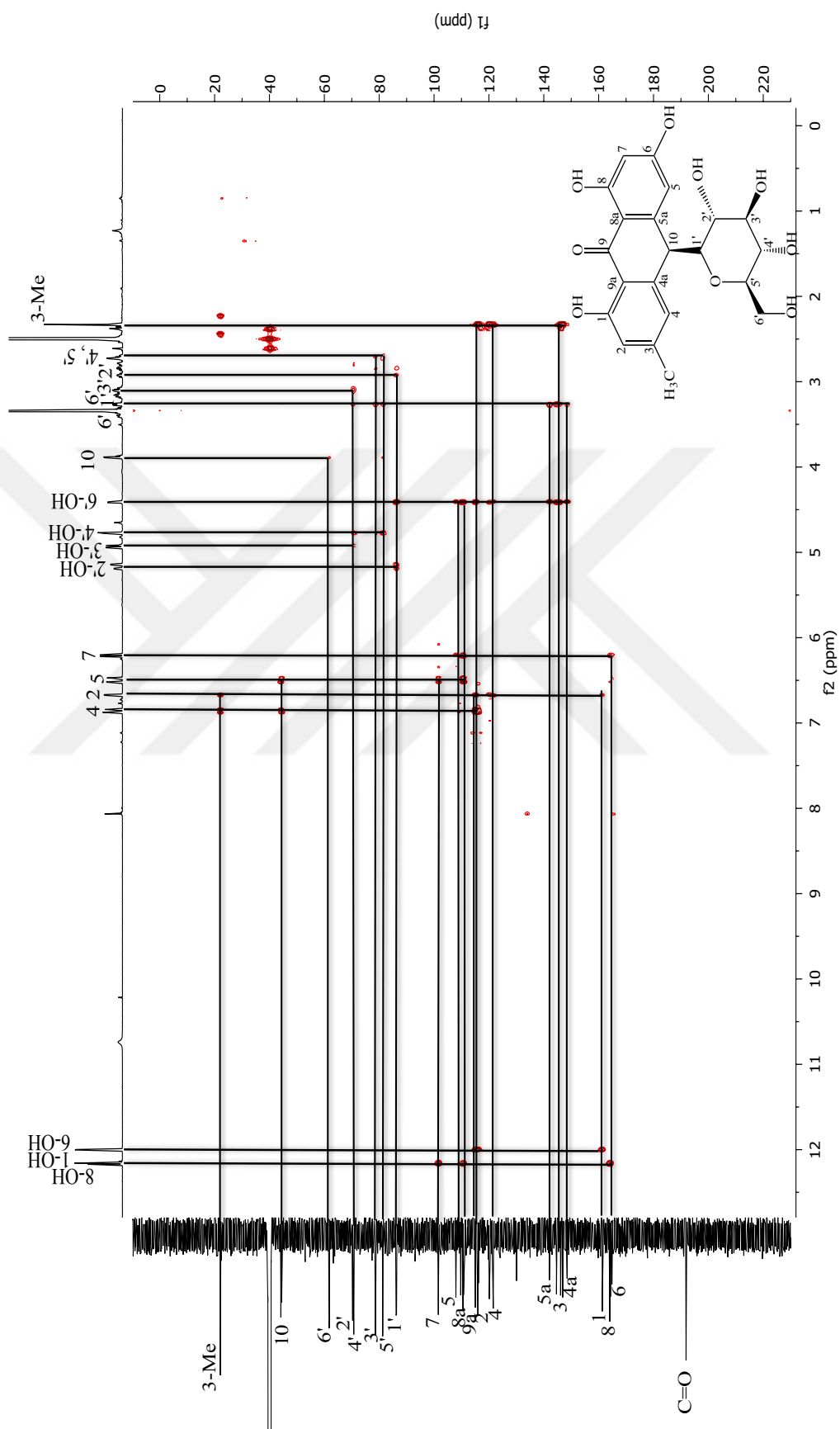
4.2.7   (–)-Catechin
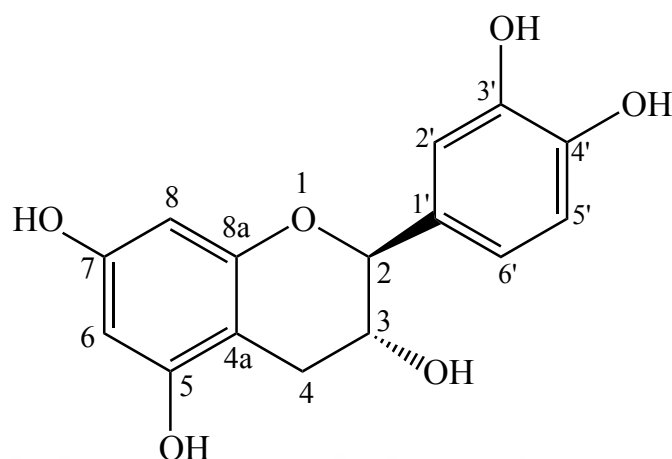
Figure 4.60. Structure of catechin.

The data about catechin were expressed in **Table 4.31.** below.

Table 4.31. The data about catechin.

Molecular formula	$C_{15}H_{14}O_6$
Synonyms	Catechol Catechin, alpha (2S,3R)-2-(3,4-dihydroxyphenyl) chroman-3,5,7-triol
Molecular weight	290.27 g/mol
IR (ATR) ν (cm^{-1})	3571 – 3050, 2965, 1626, 1605, 1468, 1284, 1147, 1024, 911
MS (ESI) *m/z*:	$[M+H]^+$ 291.1
$[\alpha]_D^{22}$	–12.6° (MeOH, c = 0.32)
^{1}H NMR	**Figure 4.61.** **Table 4.32.**
^{13}C NMR	**Figure 4.62.** **Table 4.32.**
COSY	**Figure 4.63.**
HMQC	**Figure 4.64.** **Table 4.32.**
HMBC	**Figure 4.65.** **Table 4.32.**

Compound **7** was isolated as an amorphous and beige solid. Following TLC application and Vanilin/H_2SO_4 spraying, a characteristic red coloured spot was observed. The structure of the substance was identified based on its spectroscopic data of IR, NMR and mass spectroscopy.

IR spectrum of compound **7** pointed out the presence of aromatic C=C (1468, 1605 cm^{-1}), aromatic C-H (3050-3100 cm^{-1}), alkane C-H (2965 cm^{-1}), alkane C-C (911 cm^{-1}), O-H (3200, 3571 cm^{-1}) and ether C-O-C 1024, 1147, 1284 cm^{-1}) functions.

^{1}H-NMR spectrum indicated the H atom signals in the aromatic field at 6.88 (d, $J = 1.9$ Hz, 1H, H-2'), 6.66 (d, $J = 8.1$ Hz, 1H, H-5'), and 6.63 ppm (dd, $J = 8.1$, 1.9 Hz, 1H, H-6'). Further, other proton signals were detected at d_H 9.14 (s, 1H, Ar-OH), 8.92 (s, 2H, 2x Ar-OH), 8.85 (s, 1H, Ar-OH), 5.89 (d, $J = 2.3$ Hz, 1H, H-6), 5.71 (d, $J = 2.3$ Hz, 1H, H-8), 4.72 (s, 1H, H-2), 4.68 (s, 1H, H of OH in C-3-OH), 3.99 (s, 1H, 3), 2.67 (dd, $J = 16.3$, 4.5 Hz, 1H, H-4), and 2.49 − 2.45 (1H, H-4) (**Figure 4.61.**).

The distinctive signals of the B-ring aromatic protons are of the ABX-type. The methine proton H-2' was split by H-6' in a meta position resulting in a doublet at δ_H 6.88 (d, 1.9 Hz), H-5' was split by H-6' in an ortho position yielding a doublet at 6.66 (d, 8.1 Hz) and H-6' was split by H-2' and H-5' given a doublet of doublet at 6.63 (dd, 8.1, 1.9 Hz).

The ring A aromatic protons also showed H-6 and H-8 coupling, with each yielding a doublet at δ_H 5.89 and 5.71 (d, 2.3 Hz, each). The basic structure of this compound was therefore deduced as 3, 3', 4', 5, 7-pentahydroxyflavan.

The ^{1}H NMR spectrum showed that the protons at H-4 were split by H-3, giving a doublet of doublet at δ_H 2.67 and around δ_H 2.49-2.45. The position of the H-2 chemical shift (δ_H 4.72) suggests that the flavan structure possesses the trans-2,3 stereochemistry. These signals are attributed to ring C.

^{13}C-NMR spectrum (**Figure 4.62.**) presented totally 15 carbon atoms. IR and ^{1}H-NMR spectra revealed that the structure of compound **7** includes aromatic rings as well as alkane groups. δ_C of aromatic C atom signals were ranged from 94.06 to 156.56 ppm. Downfield chemical shifts of C atom signals at the positions of 5, 7, 8a, 3' and 4' indicated that the aromatic ring has to be substituted at those C atoms.

Based on the data obtained from COSY, HMQC and HMBC analysis, the structure of compound **7** was supposed to be a flavanol derivative. The presence of the proton signals attributed to H-2 at δ_H 4.72 and H-3 at δ_H 3.99 as well as their chemical shifts in the ^{13}C NMR spectrum (δ_C 78.08 and 64.93, resp.) and the chemical shifts of the signals atrributed to H-4 (δ_H 2.67, 2.49-2.45) and C-4 (δ_C 28.26) clearly supported the predicted flavanol structure.

COSY spectrum, indicated the couplings of H-2" with H-6", H-6 with H-8, H-2 with H-3 as well as H-4, H-3 with H-4, H-4 with H-4 (**Figure 4.63.**).

HMQC spectrum indicating C atoms with their binding H atoms were shown in **Figure 4.64.**

HMBC spectrum pointed out the long range couplings of H-2 with C-1', C-2', C-6' and C-4, H-3 with C-4a, H-4 with C-2, C-3, C-5, C-4a and C-8a, H-6 with C-5, C-7, C-8 and C-4a, H-8 with C-6, C-4a and C-8a, H-5' with C-1', C-3' and C-4' as well as H-6' with C-2, C-3' and C-4' (**Figure 4.65.**).

Following the analysis of NMR spectra, the compound were shown to have a molecular formula as $C_{15}H_{14}O_6$ which was also supported by HR-MS (ESI) at *m/z* $[M+H]^+$ 291.1 (**Table 4.31.**).

Spectroscopic data of the compound (**Table 4.32.**) were checked in the literature, and found to be quite similar to the data for catechin (94, 476) and therefore, compound **7** was elucidated as catechin (**Figure 4.60.**).

Table 4.32. ^{1}H- and ^{13}C-NMR spectroscopic data of catechin (DMSO-d_6, ^{1}H: 600 MHz, ^{13}C: 151 MHz).

C/H		δ_H (ppm), J (Hz)	δ_C (ppm)	HMBC (H➔C)
1	-	-	-	-
2	CH	4.72 (s)	78.08	C-4, C-1', C-2', C-5', C-6'
3	CH	3.99 (s)	64.93	C-4a
4	CH$_2$	2.67 (dd, 16.3, 4.5)	28.26	C-2, C-3, C-5, C-4a, C-8a
		2.49 – 2.45		
5	C	-	156.25	-
6	CH	5.89 (d, 2.3)	95.05	C-8, C-4a, C-8a
7	C	-	156.56	-
8	CH	5.71 (d, 2.3)	94.06	C-6, C-4a, C-8a
4a	C	-	98.47	-
8a	C	-	155.79	-
1'	C	-	130.58	-
2'	CH	6.88 (d, 1.9)	114.90	C-2, C-3', C-4', C-6'
3'	C	-	144.52	-
4'	C	-	144.55	-
5'	CH	6.66 (d, 8.1)	114.76	C-2, C-1', C-3', C-4'
6'	CH	6.63 (dd, 8.1, 1.9)	117.93	C-2, C-1', C-3', C-4'
Ar-OH	OH	9.14 (s)	-	-
Ar-OH	OH	8.85 (s)	-	-
2 ×Ar-OH	OH	8.92 (s)	-	-
3-OH	OH	4.68 (s)	-	-
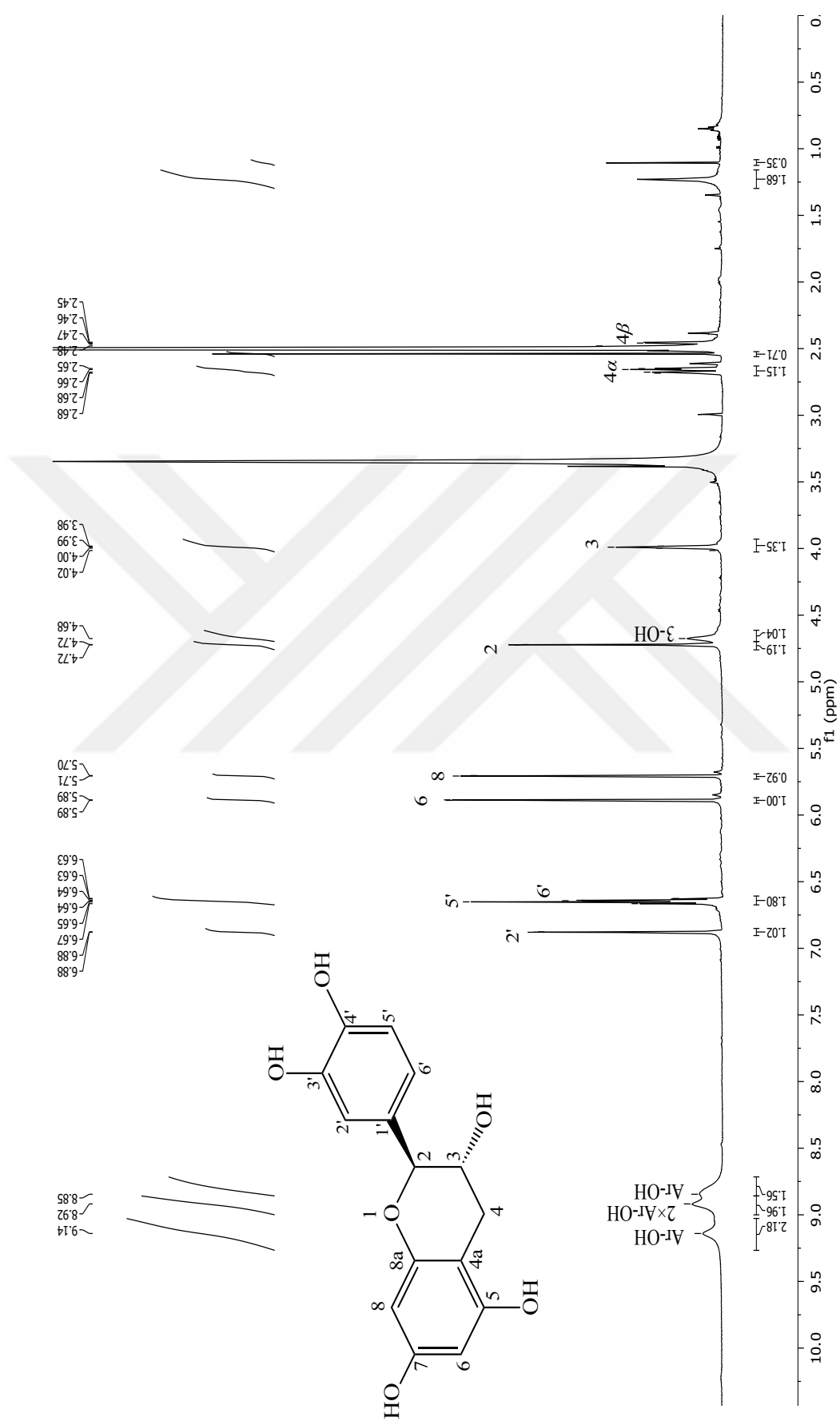
Figure 4.61. ^{1}H-NMR spectrum of catechin (Compound **7**) (DMSO-d_6, ^{1}H: 600 MHz).
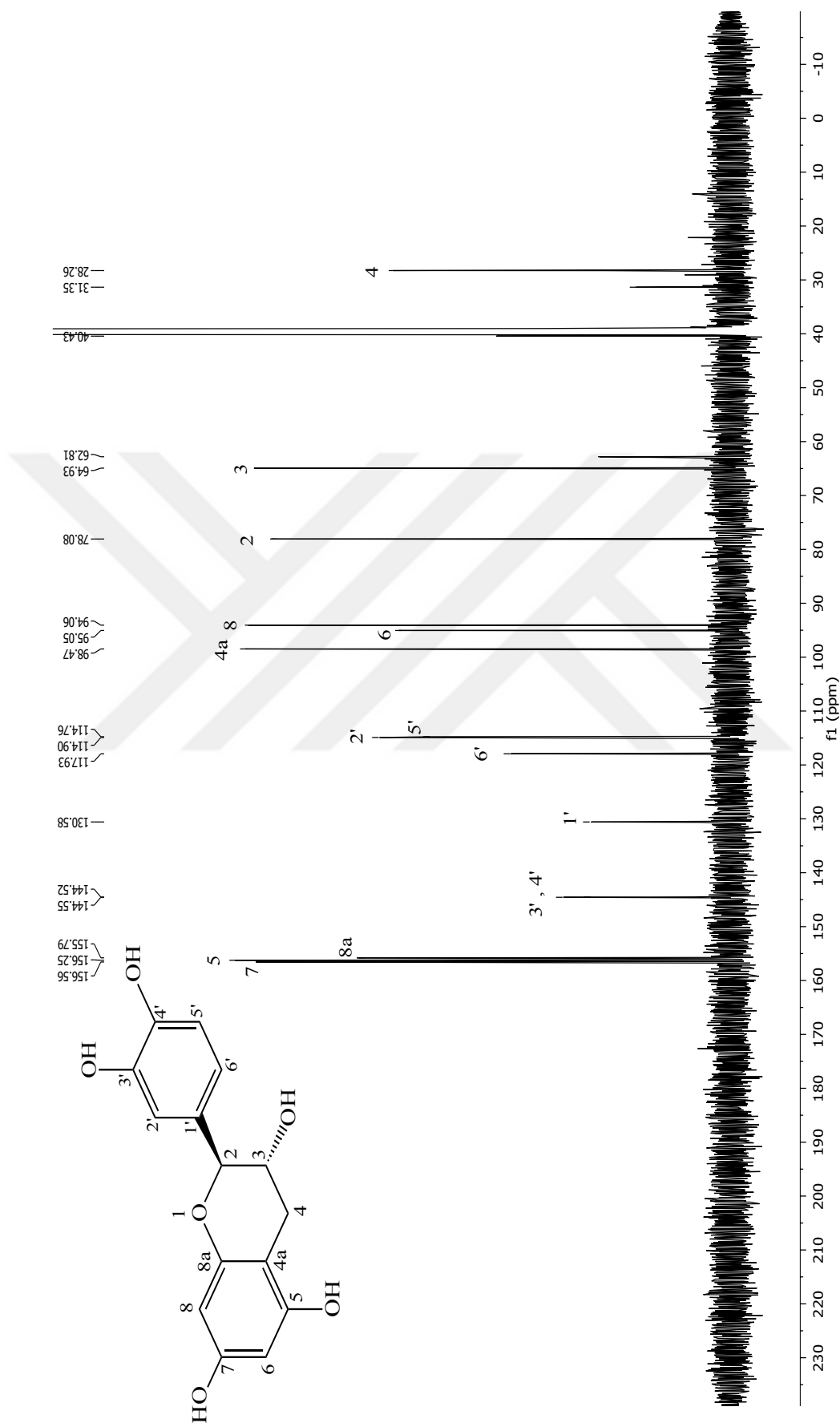
Figure 4.62. ^{13}C-NMR spectrum of catechin (Compound **7**) (DMSO-d_6, ^{13}C: 151 MHz).
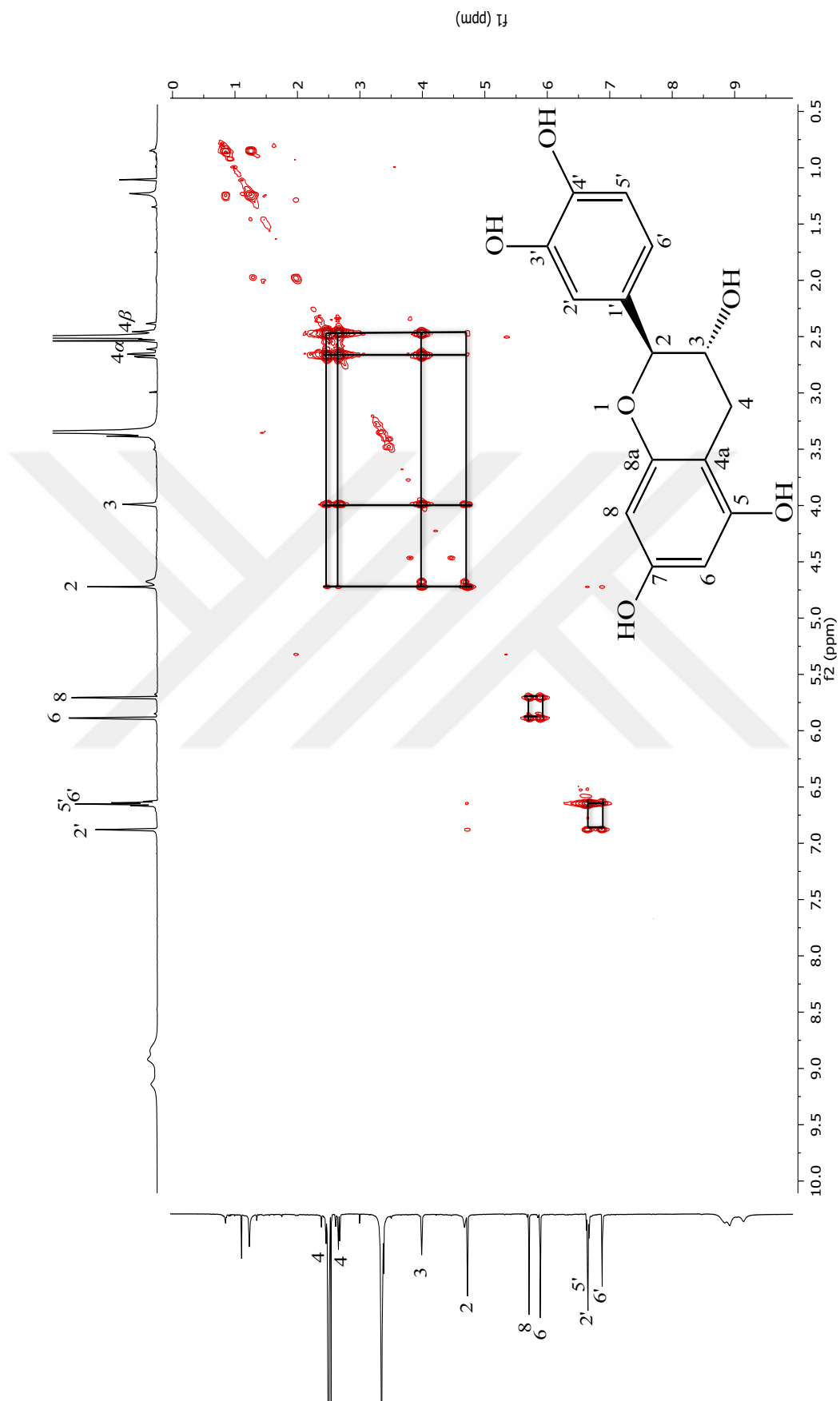
Figure 4.63. ^{1}H-^{1}H homonuclear correlation spectrum (COSY) of catechin (Compound **7**).
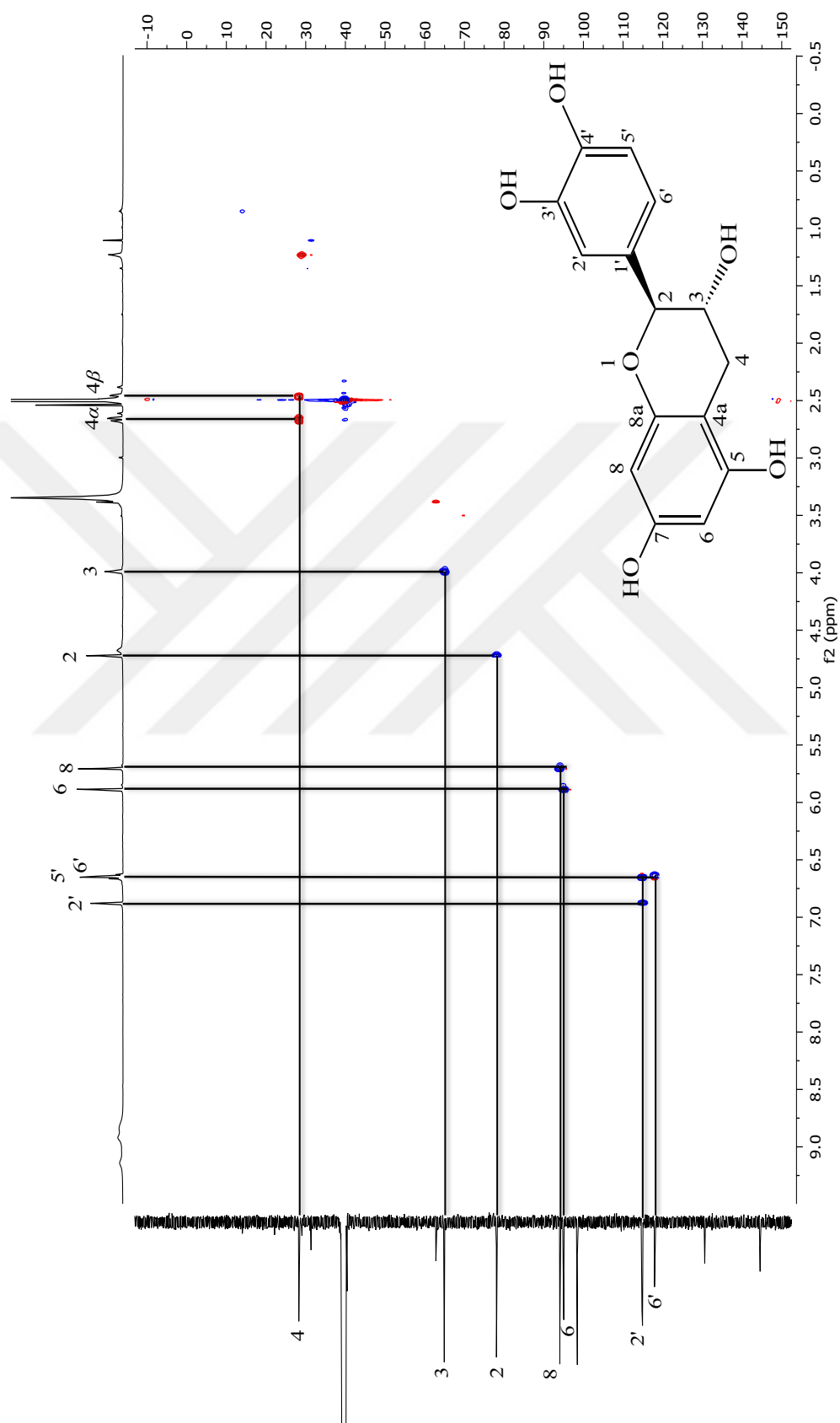
Figure 4.64. ^{1}H-^{13}C heteronuclear multiple-quantum correlation (HMQC) spectrum of catechin (Compound **7**).
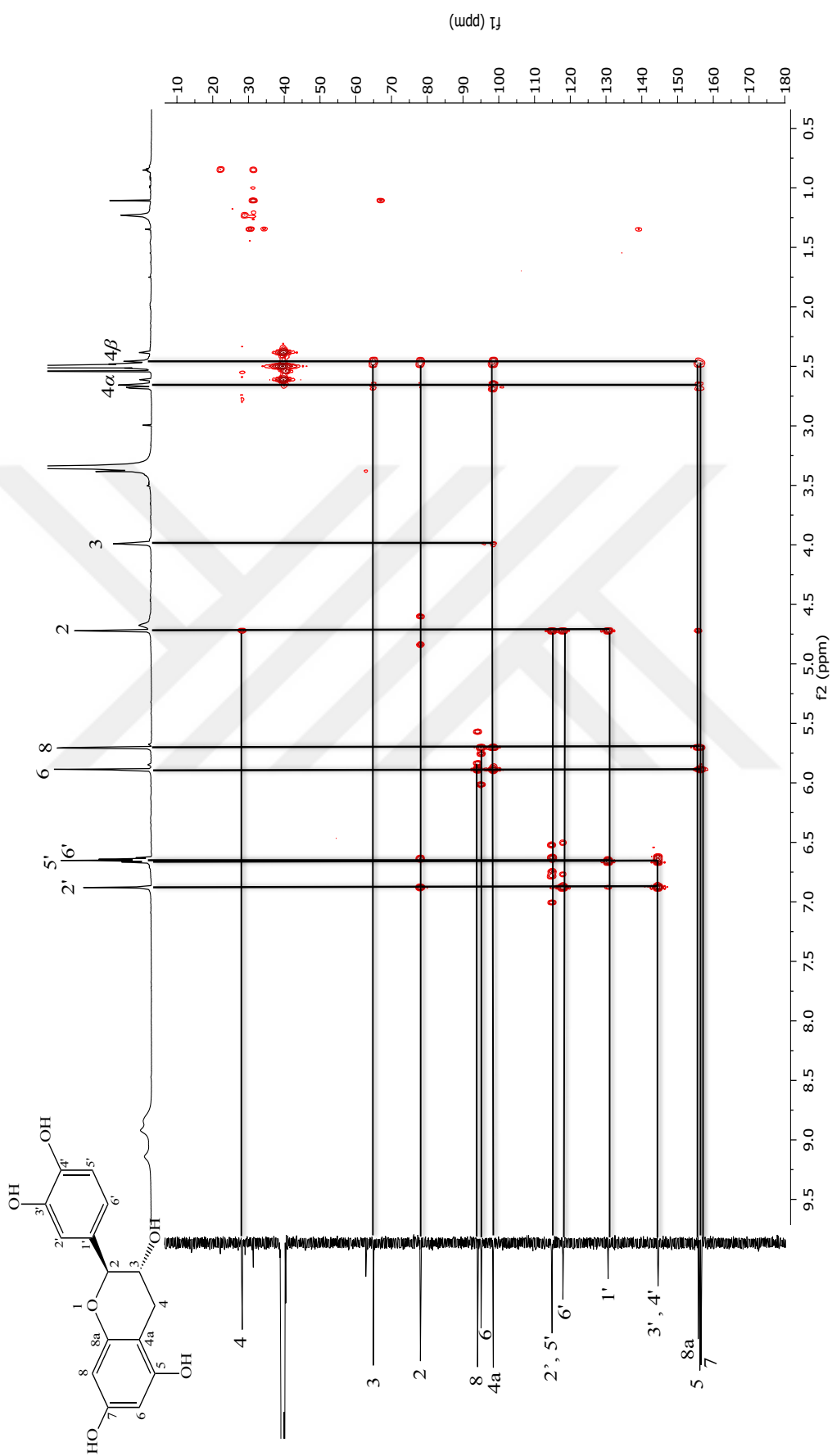
Figure 4.65. ^{1}H-^{13}C heteronuclear multiple-bond correlation (HMBC) spectrum of catechin (Compound **7**).

4.2.8 Emodin
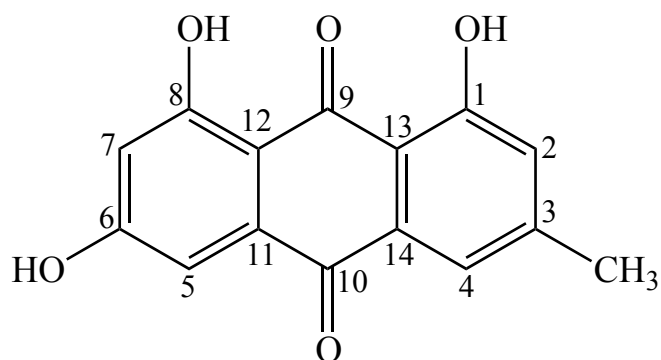
Figure 4.66. Structure of emodin.

The data about emodin were expressed in **Table 4.33.** below.

Table 4.33. The data about emodin.

Molecular formula	$C_{15}H_{10}O_5$
Synonyms	Emodol 3-Methyl-1,6,8-trihydroxyanthraquinone Frangulic acid Archin 1,3,8-Trihydroxy-6-methyl-9,10-anthraquinone 1,3,8-Trihydroxy-6-methyl-9,10-anthracenedione
Molecular weight	270.24 g/mol
IR (ATR) ν (cm^{-1})	1683, 1653, 1478, 758
MS (ESI) *m/z*:	[M+H]$^+$ 271.2
^{1}H NMR	**Figure 4.67.** **Table 4.34.**
^{13}C NMR	**Table 4.34.**

Compound **8** was isolated as a red solid. In TLC, analysis a light yellow spot was observed at daylight before reagent spraying. In addition, spots having fluorescence inhibiting zones under UV 254 nm and red floresans under UV 366 nm were also monitored. After Vanilin/H_2SO_4 sprayed and Vanilin/H_2SO_4 sprayed-plate was heated up to 110 °C, a yellow/ orange spot was detected. The structure of the substance was identified based on the IR, NMR and mass spectroscopic data.

IR spectrum of the compound **8** pointed out the presence of aromatic C=C (1478 cm^{-1}), carbonyl C=O (1653, 1683 cm^{-1}), OH (758 cm^{-1}) functions.

^{1}H-NMR spectrum (**Table 4.34; Figure 4.67**) indicated, the signals of H atoms in the aromatic field detected at 7.36 (s, H-4), 7.00 (s, H-2), 6.52 (d, J = 2.3 Hz, H-5) and 5.62 (d, J = 2.3 Hz, H-7) ppm. Further, proton signals were detected at 13.15 (H of OH in C-6-OH), 12.41 (H of OH in C-8-OH) and 2.35 (s, 3H, H atoms of CH$_3$ in C-3-CH$_3$) ppm.

δ_C of the aromatic C atom signals were ranged from 101.64 to 184.48 ppm. C atom signals observed at higher chemical shifts indicating aromatic ring to be substituted with polar groups at those carbons ~~such as the~~ (C atoms at the 1st, 6th, 8th, 9th and 10th positions in structure.

Following the analysis of the NMR spectra data, the compound was shown to have the molecular formula of $C_{15}H_{10}O_5$ as established by HR-MS (ESI) at *m/z* 270.24 g/mol [M+Na]$^+$ (**Table 4.33.**). IR spectrum pointed out the structure to include aromatic ring, carbonyl (C=O) and OH groups, confirming the NMR data and mass measurement.

Spectroscopic data were found to be quite similar to the data published for emodin (477). Therefore, compound **8** was clarified as emodin (**Figure 4.66.**).

Table 4.34. ^{1}H- and ^{13}C-NMR spectroscopic data of emodin (DMSO-d_6, ^{1}H: 600 MHz, ^{13}C: 151 MHz).

C/H		δ_H (ppm), J (Hz)	δ_C (ppm)
1	C	-	161.22
2	CH	7.00 (s)	123.90
3	C	-	144.93
4	CH	7.36 (s)	119.40
5	CH	6.52 (d, 2.3)	119.40
6	C	-	166.55
7	CH	5.62 (d, 2.3)	107.92
8	C	-	166.44
9	C	-	181.52
10	C	-	184.48
11	C	-	134.35
12	C	-	101.64
13	C	-	115.34
14	C	-	133.37
3-CH$_3$	CH$_3$	2.35 (s, 3H)	21.76
OH	OH	13.15	-
OH	OH	12.41	-
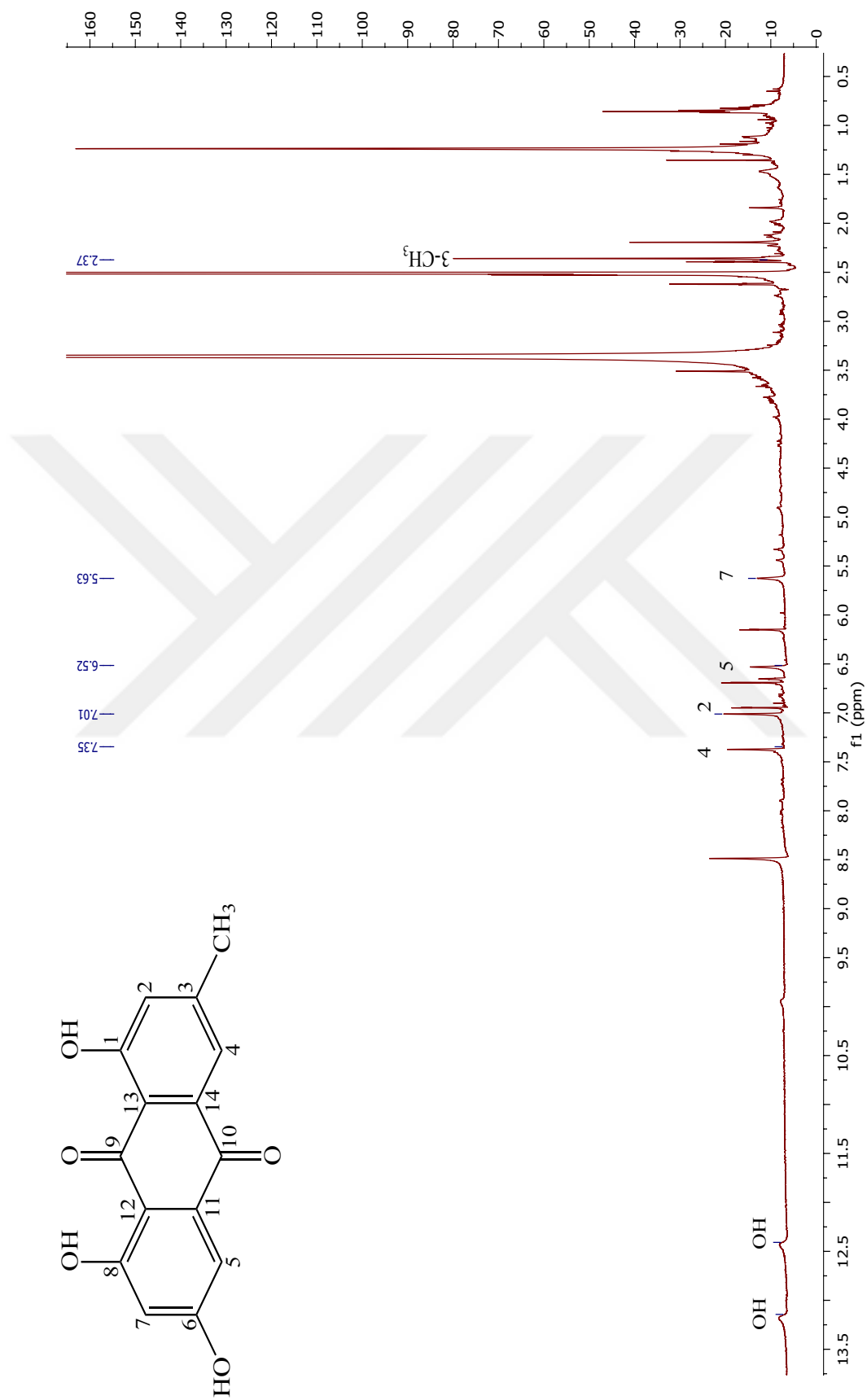
Figure 4.67. ^{1}H-NMR spectrum of emodin (Compound **8**) (DMSO-d_6, ^{1}H: 600 MHz).

4.2.9   Emodin-8-*O-β*-glucoside
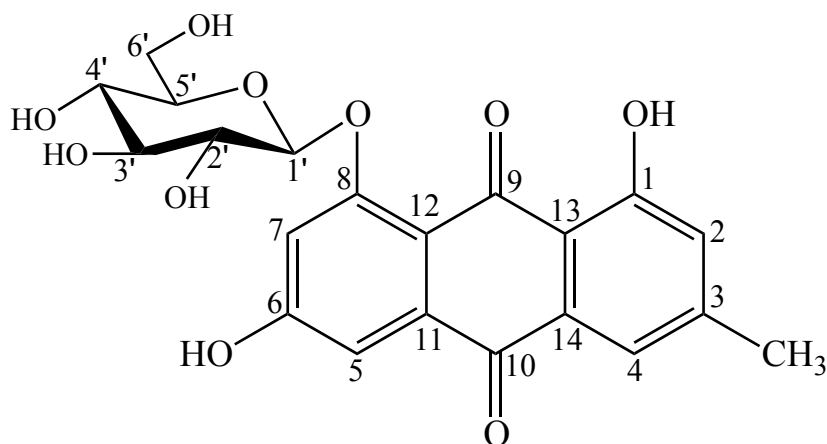
Figure 4.68. Structure of emodin-8-*O-β*-glucoside.

The data about emodin-8-*O-β*-glucoside was expressed in **Table 4.35.** below.

Table 4.35. The data about emodin-8-*O-β*-glucoside.

Molecular formula	$C_{21}H_{20}O_{10}$
Synonyms	3,8-dihydroxy-6-methyl-1-anthraquinonyl-beta-D-glucopyranoside Emodin-8-beta-D-glucoside
Molecular weight	432.3 g/mol
IR (ATR) ν (cm^{-1})	3550 – 3050, 1629, 1480, 1366, 1266, 1074, 1025, 991
^{1}H NMR	**Figure 4.69.** **Table 4.36.**
^{13}C NMR	**Figure 4.70.** **Table 4.36.**
DEPT 90 and DEPT 135	**Figure 4.71.** **Table 4.36.**
COSY	**Figure 4.72.**
HMQC	**Figures 4.73.-4.75.** **Table 4.36.**
HMBC	**Figures 4.76.-4.78.** **Table 4.36.**

Compound **9** was isolated as a red solid. In TLC, a light yellow spot was observed at daylight before reagent spraying. Additionally, the spot exhibited fluorescence inhibiting zones under UV 254 nm and red fluorescence under UV 366 nm were monitored. After Vanilin/H_2SO_4 sprayed and Vanilin/H_2SO_4 sprayed-plate was heated up to 110 °C, a yellow/orange spot was detected. The structure of the compound was identified based on the spectroscopic data (IR, NMR and mass spectroscopy).

IR spectrum of compound **9** pointed out the presence of aromatic C=C (1480 cm^{-1}), aromatic C-H (3050-3100 cm^{-1}), alkane C-H (1366 cm^{-1}), alkane C-C (991 cm^{-1}), O-H (3200, 3550 cm^{-1}) and C-O (1025, 1074, 1266 cm^{-1}) groups (**Table 4.35.**).

^{1}H-NMR spectrum exhibited the H atom signals in the aromatic field at 7.83 (d, J =14.40 Hz, 1H, H-5), 7.69 (d, J = 6.9 Hz, 1H, H-7), 7.45 (s, 1H, H-4) and 7.15 (s, 1H, H-2) ppm, while other proton signals were detected at d_H 12.79 (s, H of OH in C-6-OH), 5.16 (d, J = 7.6 Hz, H-1'), 3.70 (d,†, H-6'), 3.45 (dd, J = 14.2 Hz, H-2', H-6'), 3.36 – 3.21 (H-3', H-5'), 3.23 (t, H-4'), 2.35 ppm (s, 3H, H atoms of CH_3 in C-3-CH_3) (**Figure 4.69.**).

A proton signal at 5.16 ppm splitted into two peaks as doublet with 7.6 Hz coupling constant (J) is attributed to an anomeric proton. 7.6 Hz of J value of the compound indicated that sugar molecules is in β configuration. The remaining proton signals in sugar molecule were ranged from δ_H 3.70 to δ_H 3.23. H atom signals in the aromatic rings were observed at around 7 ppm, while the signals of H atoms in sugar molecule and Me of C-3-Me (2.35 ppm) were observed at lower frequencies.

^{13}C-NMR spectrum (**Figure 4.70.**) presented chemical shifts of C atom signals in the molecule, as well as DEPT (Distortionless Enhancement by Polarization Transfer) 90 spectrum showed -CH_2 (**Figure 4.71.**) groups, whereas DEPT 135 spectrum indicated the presence of CH_3, CH_2 and CH groups (**Figure 4.71.**). δ_C of C atom signals in the sugar molecule were detected at 100.97 (anomeric, C-1'), 73.71 (C-2'), 76.88 (C-3'), 70.00 (C-4'), 77.63 (C-5') and 61.08 (C-6') ppm., which were quite similar to the data of glucose indicated in the literature (400, 470, 471). δ_H values as well as the J value of H-1' (7.6 Hz) pointed out that the hexose unit has to be a β-glucose, as well. NMR and IR spectra pointed out that the structure include aromatic rings, alkane groups as well as a β-glucose moiety. δ_C of aromatic C

atom signals were ranged from 115.13 to 187.96 ppm. Higher chemical shifts of the aromatic carbon atom signals indicated that aromatic rings were supposed to be substituted with polar groups at those C atoms. In addition, the data obtained from COSY, HMQC and HMBC, the structure of compound **9** was supposed to be an anthraquinone derivative as explained in details below.

COSY spectrum displayed the couplings between H-1'/H-2', 2' with 4' as well as 5 with 7 (**Figure 4.72.**).

HMQC spectrum pointed out C atoms with their relating H atoms on, which were shown in **Figures 4.73-4.75.**

HMBC spectrum pointed out a long range coupling between the anomeric proton (H-1') of β-glucose and C-8, which indicates a β-glucose substitution at C-8. Furthermore, the long range couplings of H-5 with C-7, C-8, C-10, C-13, and C-14, H-7 with C-8, C-10 and C-13, H-4 with C atom of CH_3 in C-3-CH_3, C-10, H atoms of CH_3 in C-3-CH_3 with C-2, C-3 and C-4, H-4 with C-2, H-2 with C of CH_3 in C-3-CH_3, C-4 and C-12, H-2' with C-3' and C-5', H-3' and H-5' with C-6', H-4' with C-5', H-6' with C-5' as well as H-6' with C-4' were also displayed (**Figures 4.76-4.78).**

Following the analysis of NMR spectra, the compound was shown to have the molecular formula of $C_{21}H_{20}O_{10}$ (**Table 4.35.).**

Spectroscopic data (**Table 4.36.)** of the compound **9** were then checked in the literature, and were found to be quite similar to the data given for emodin-8-*O*-β-glucoside (94) detected before. Therefore, compound **9** was clarified as emodin-8-*O*-β-glucoside (**Figure 4.68.**).

Table 4.36. ^{1}H- and ^{13}C-NMR spectroscopic data of emodin-8-O-β-glucoside (DMSO-d_6, ^{1}H: 400 MHz, ^{13}C: 100 MHz).

C/H		δ_H (ppm), J (Hz)	δ_C (ppm)	HMBC (H→C)
1	C	-	162.04	-
2	CH	7.15 (s)	124.55	3-CH$_3$, C-4, C-12
3	C	-	148.20	-
4	CH	7.45 (s)	119.84	C-2, 3-CH$_3$, C-10
5	CH	7.83 (d, 14.40)	121.14	C-7, C-8, C-10, C-13, C-14
6	C	-		
7	CH	7.69 (d, 6.9)	122.99	C-8, C-10, C-13
8	C	-	158.59	-
9	C	-	187.96	-
10	C	-	182.56	-
11	C	-	132.51	-
12	C	-	115.13	-
13	C	-	120.97	-
14	C	-	135.13	-
3-CH$_3$	CH$_3$	2.35 (s, 3H)	21.82	C-2, C-3, C-4
1'	CH	5.16 (d, 7.6)	100.97	C-8
2'	CH	3.45 (dd, 14.2)	73.71	C-3', C-5'
3'	CH	3.36 – 3.21	76.88	-
4'	CH	3.23 (t)	70.00	-
5'	CH	3.36 – 3.21	77.63	C-6'
6'	CH$_2$	3.45 (dd, 14.2)	61.08	C-4', C-5'
		3.70 (d,†)		
6-OH	OH	12.79	-	-

†: Coupling constant (J) were not calculated due to overlap of signals.

219
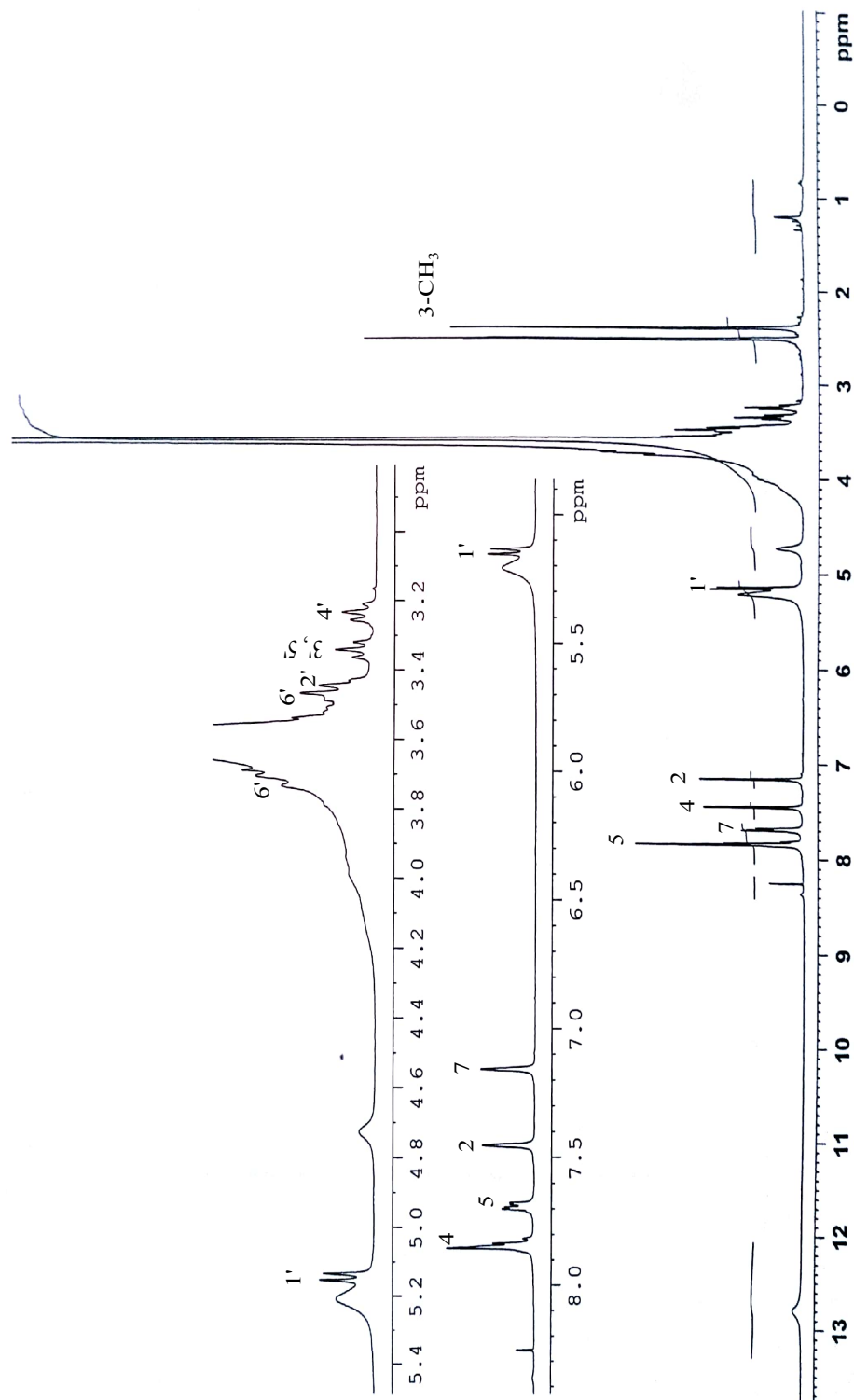
Figure 4.69. ^{1}H-NMR spectrum of emodin-8-O-β-glucoside (Compound **9**) (DMSO-d_6, ^{1}H: 400 MHz).
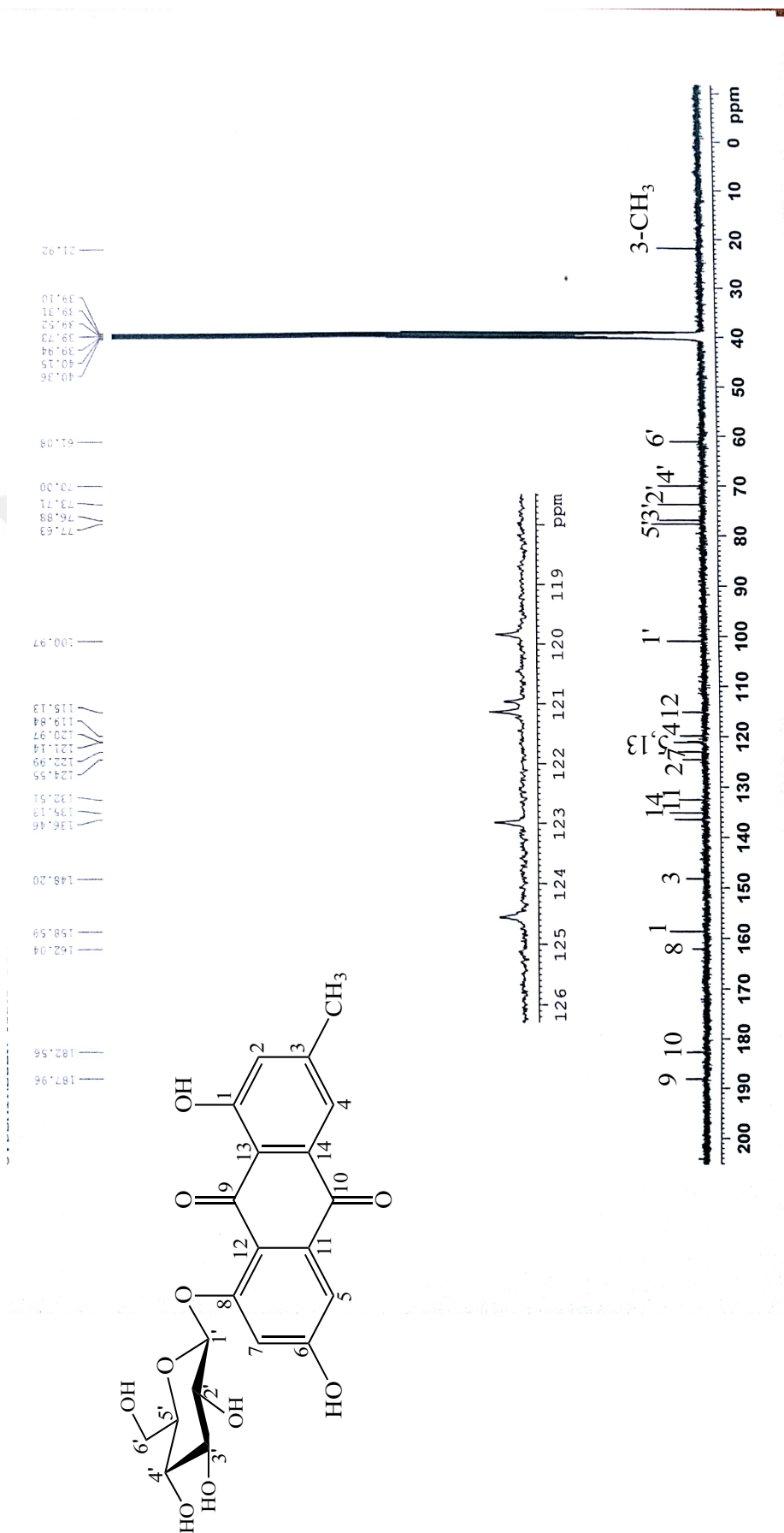
Figure 4.70. ^{13}C-NMR spectrum of emodin-8-O-β-glucoside (Compound **9**) (DMSO-d_6, ^{13}C: 100 MHz).

221

Figure 4.71. DEPT 90 and DEPT 135 spectra of emodin-8-*O*-*β*-glucoside (Compound **9**).
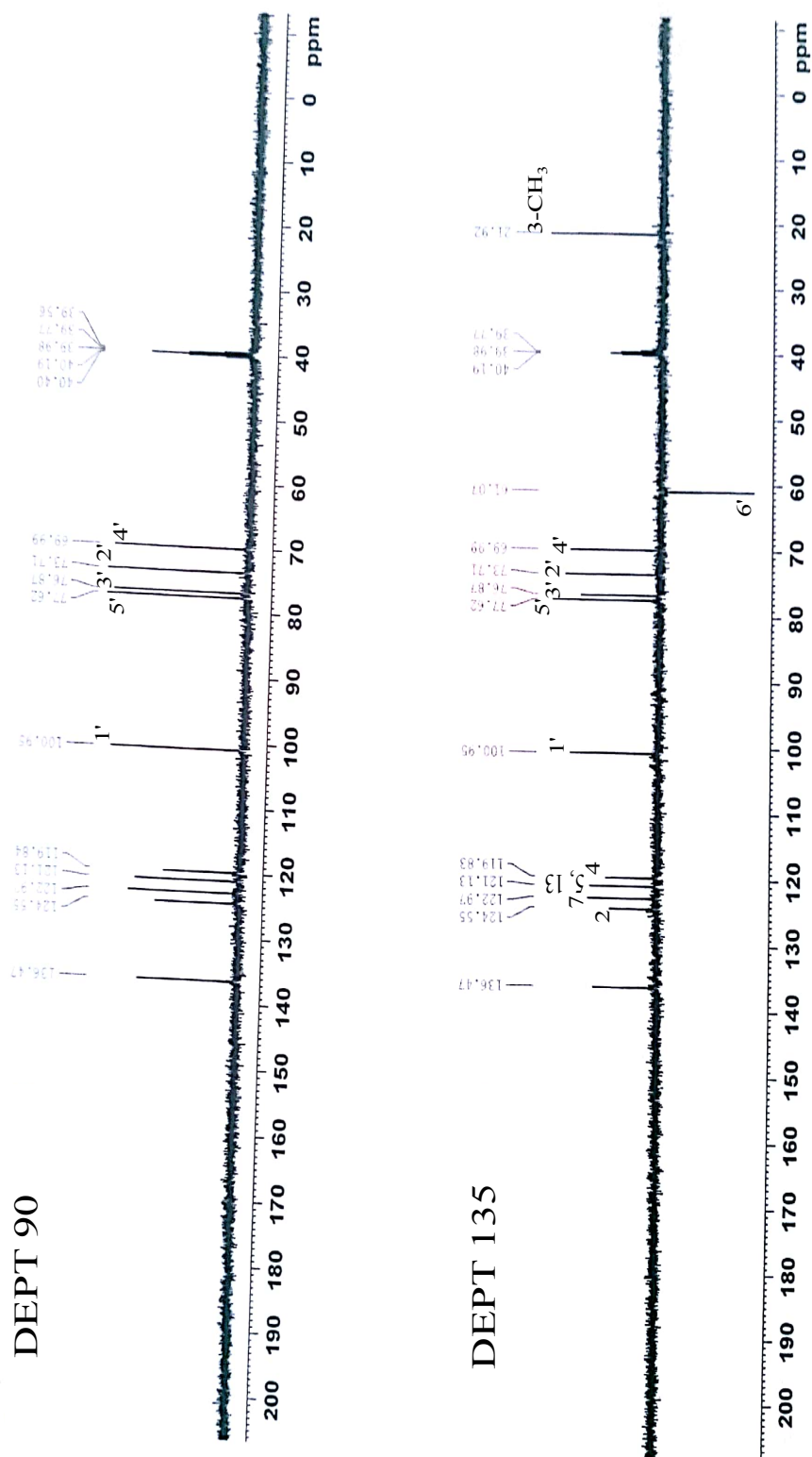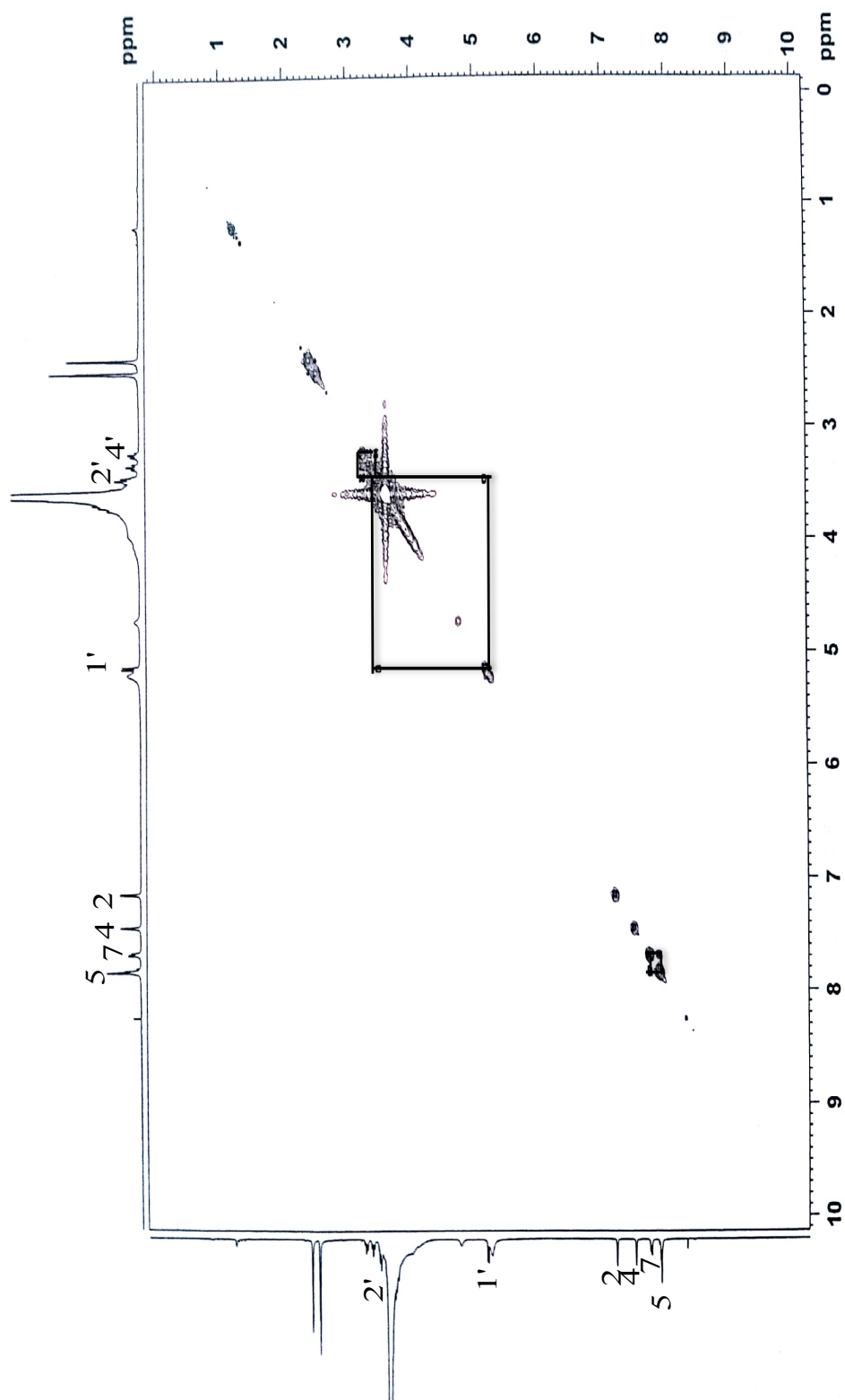
Figure 4.72. ^{1}H-^{1}H homonuclear correlation spectrum (COSY) of emodin-8-O-β-glucoside (Compound **9**).
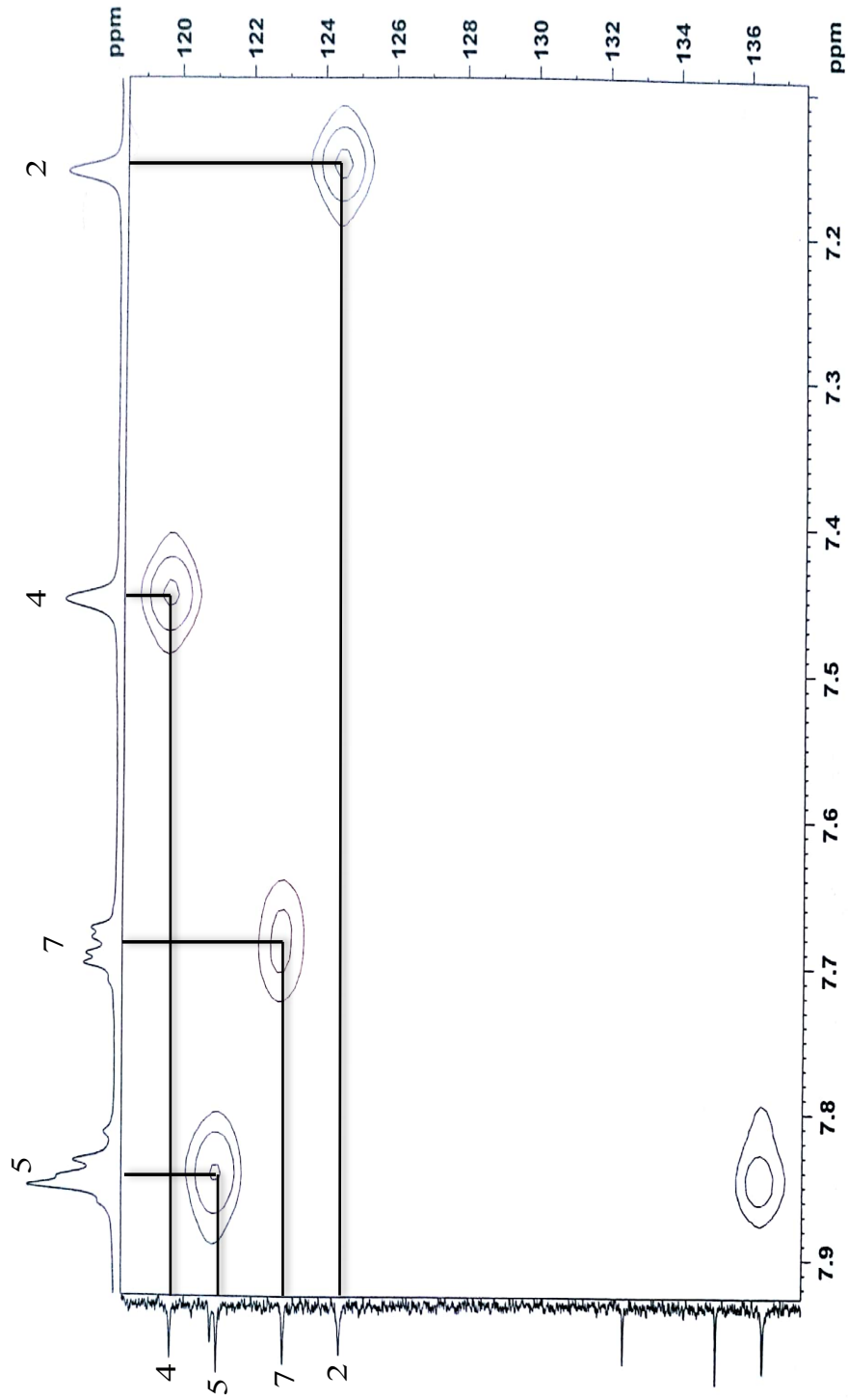
Figure 4.73. ^{1}H-^{13}C heteronuclear multiple-quantum correlation (HMQC) spectrum of emodin-8-*O*-*β*-glucoside (Compound **9**).
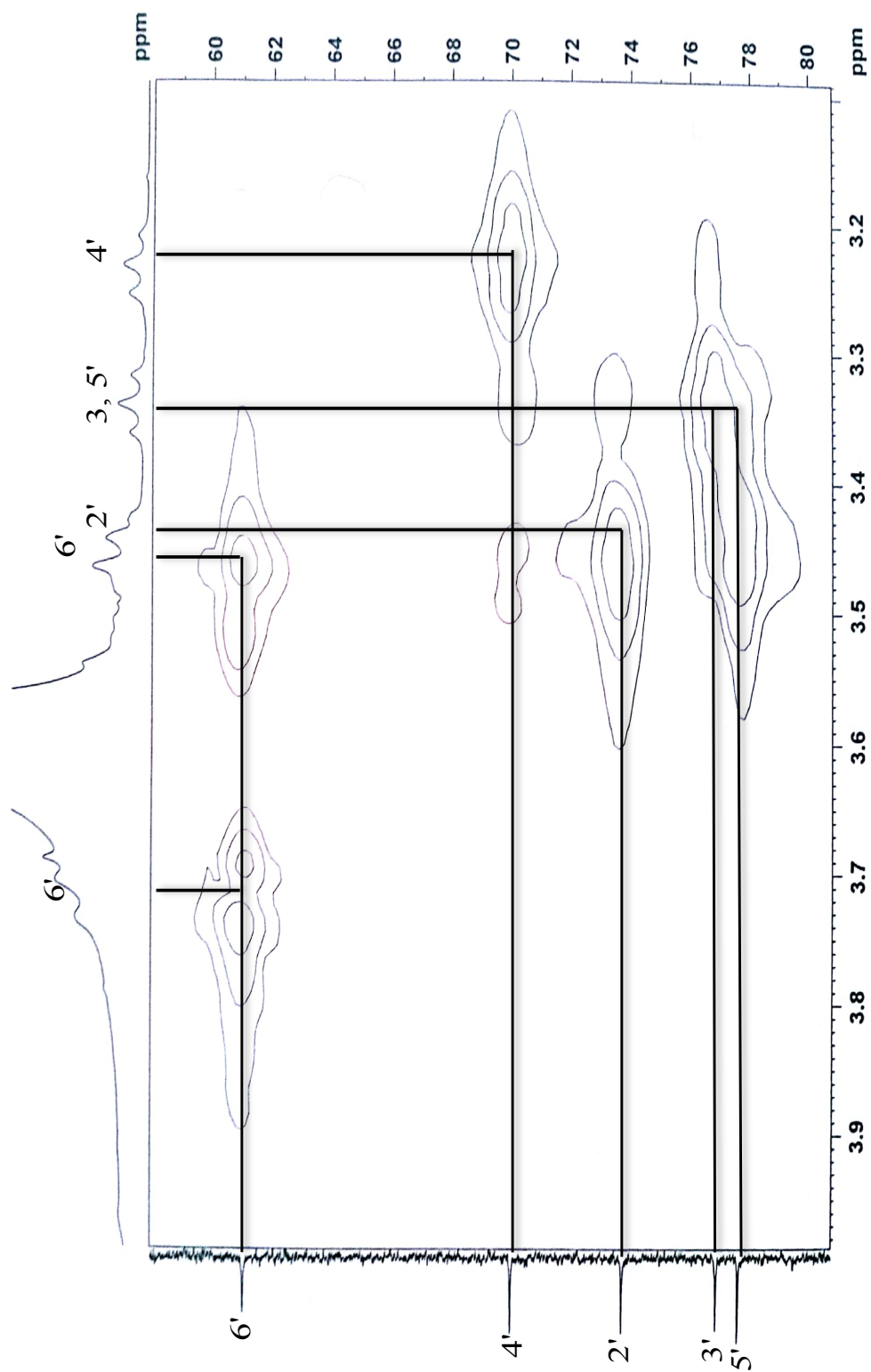
Figure 4.74. ^{1}H-^{13}C heteronuclear multiple-quantum correlation (HMQC) spectrum of emodin-8-*O*-*β*-glucoside (Compound **9**).
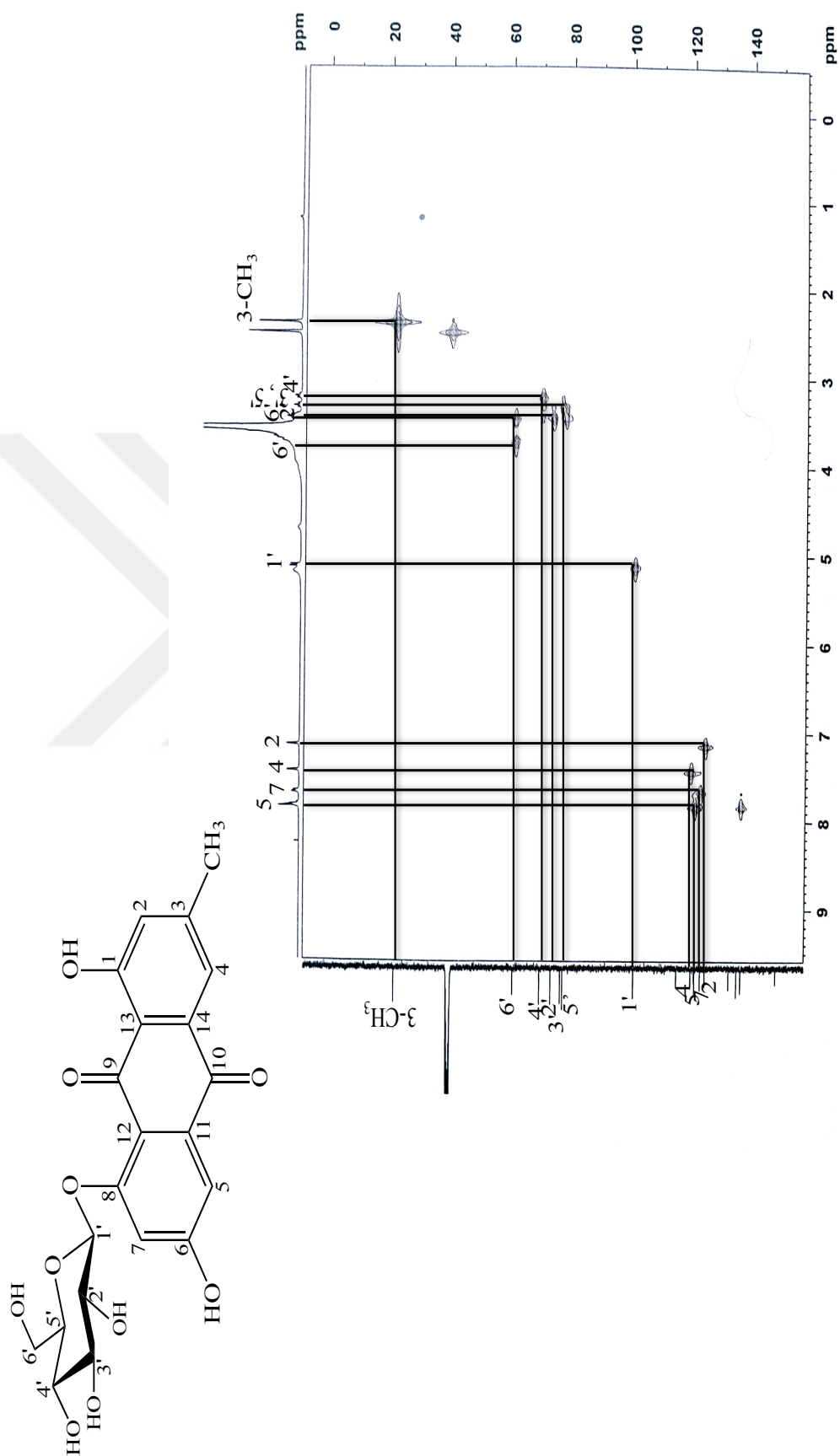
Figure 4.75. ^{1}H-^{13}C heteronuclear multiple-quantum correlation (HMQC) spectrum of emodin-8-*O*-*β*-glucoside (Compound **9**).
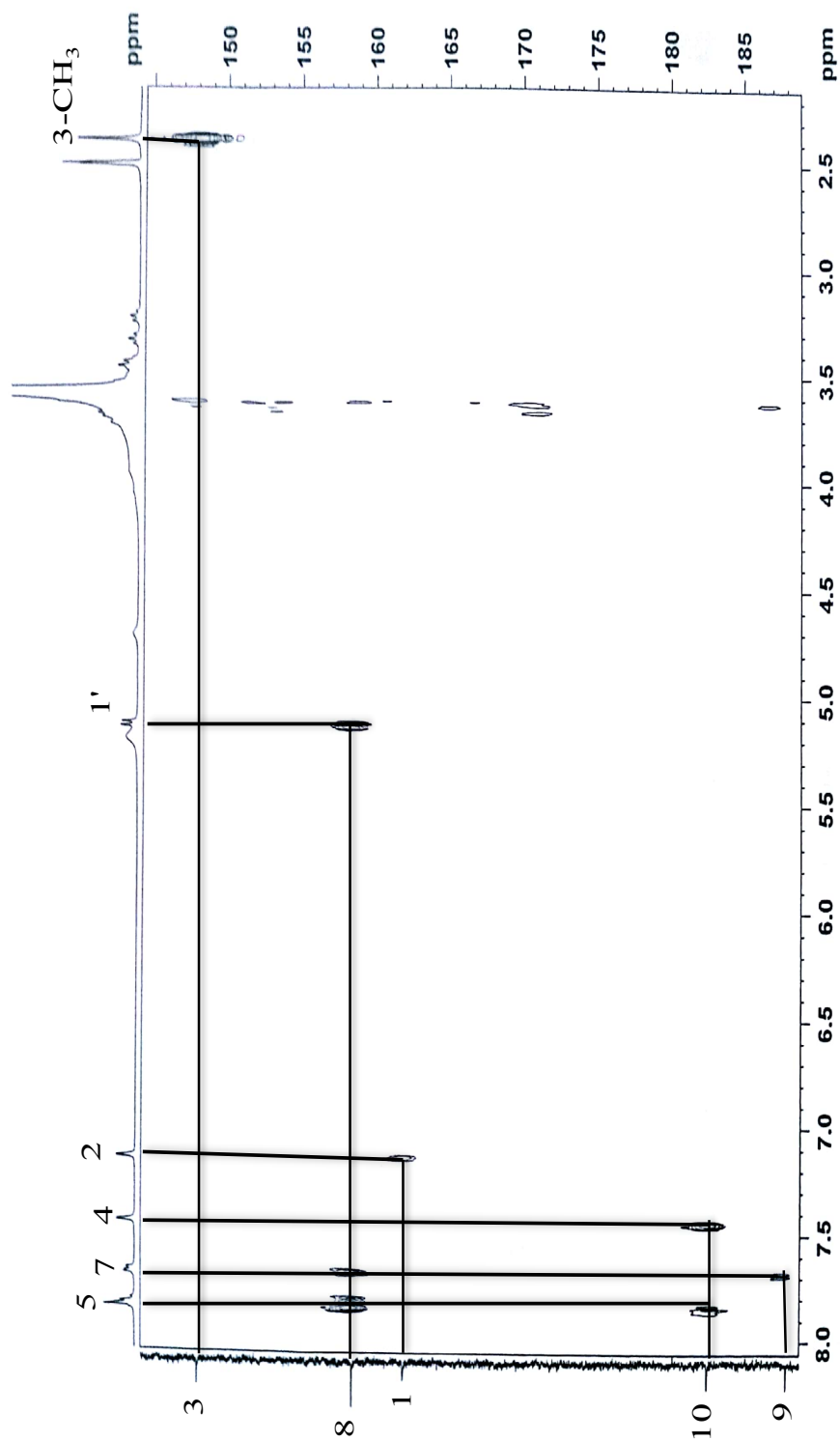
Figure 4.76. ^1H-^{13}C heteronuclear multiple-bond correlation (HMBC) spectrum of emodin-8-O-β-glucoside (Compound **9**).
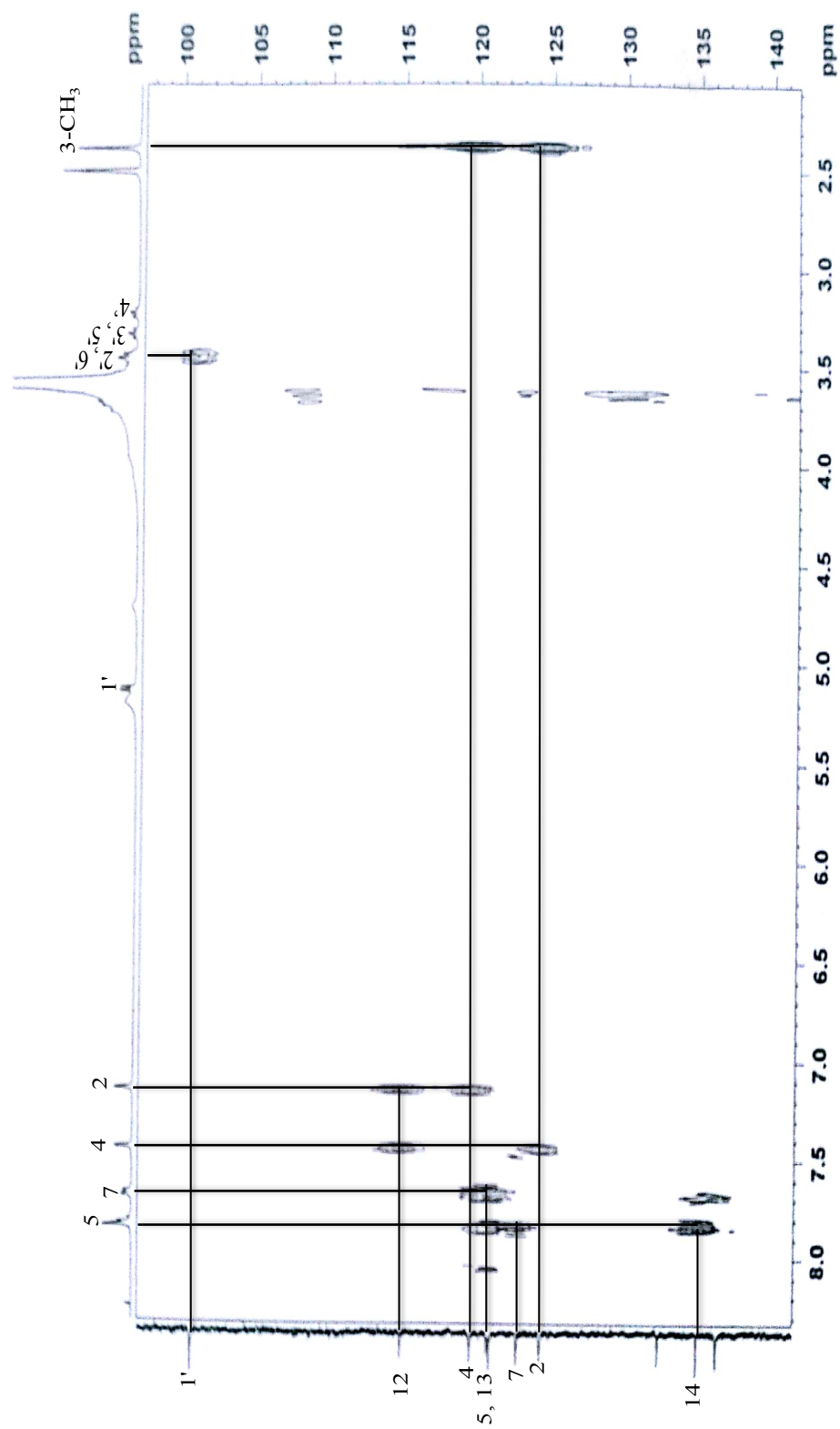
Figure 4.77. ^{1}H-^{13}C heteronuclear multiple-bond correlation (HMBC) spectrum of emodin-8-O-β-glucoside (Compound **9**).
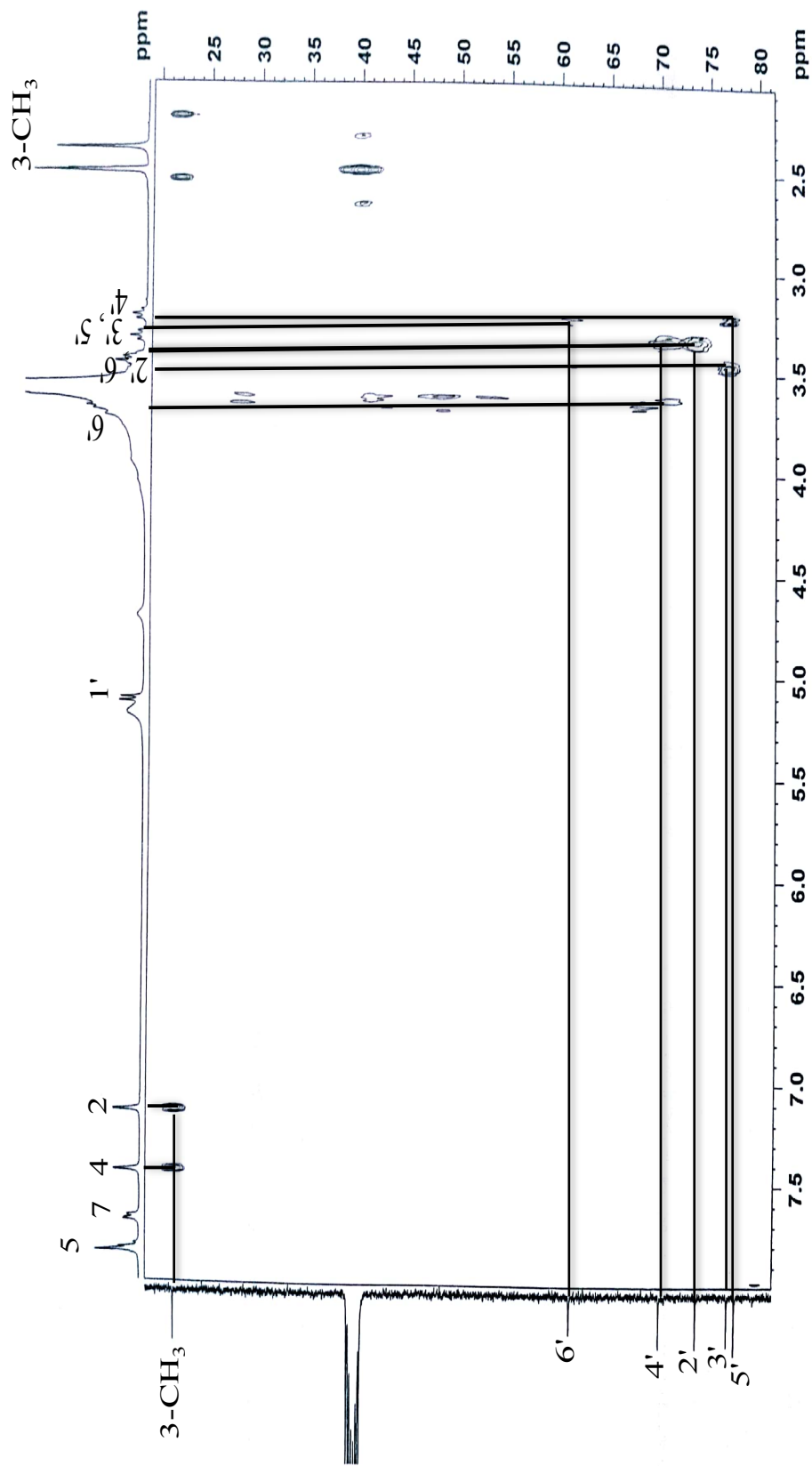
Figure 4.78. ^1H-^{13}C heteronuclear multiple-bond correlation (HMBC) spectrum of emodin-8-O-β-glucoside (Compound **9**).

4.2.10 Chrysophanol-8-*O*-*β*-glucoside and physcion-8-*O*-*β*-glucoside
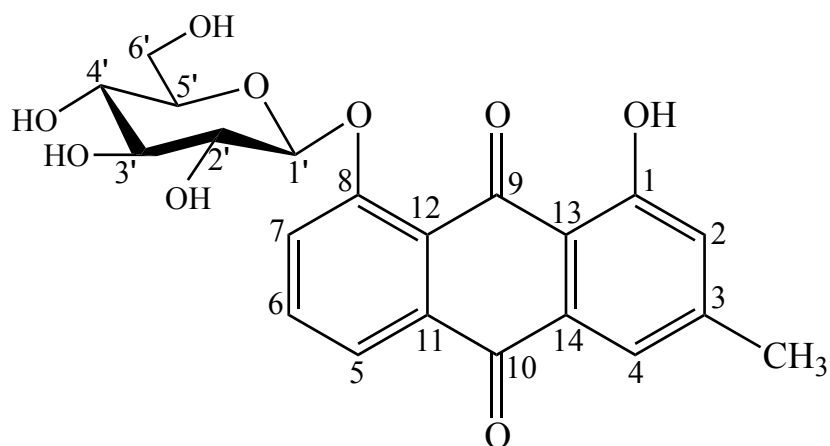
Compound **10** (Chrysophanol-8-*O*-*β*-glucoside)
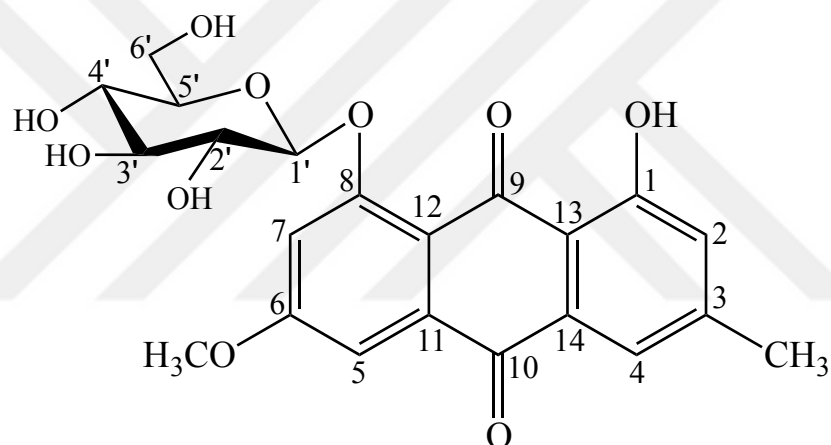
Compound **11** (Physcion-8-*O*-*β*-glucoside)

Figure 4.79. Structures of chrysophanol-8-*O*-*β*-glucoside and physcion-8-*O*-*β*-glucoside.

The data about chrysophanol-8-*O*-*β*-glucoside and physcion-8-*O*-*β*-glucoside were expressed in **Table 4.37.** in the following page.

Table 4.37. The data about chrysophanol-8-*O*-*β*-glucoside and physcion-8-*O*-*β*-glucoside.

Molecular formula	$C_{21}H_{20}O_9$ **(10)** and $C_{22}H_{22}O_{10}$ **(11)**
Synonyms	**(10)** Pulmatin, Chrysophanol 8-glucoside, 8-(beta-D-glucopyranosyloxy)-1-hydroxy-3-methyl-9,10-anthraquinone, 1-hydroxy-3-methyl-8-[(2S,3R,4S,5S,6R)-3,4,5-trihydroxy-6-(hydroxymethyl)oxan-2-yl]oxyanthracene-9,10-dione **(11)** Physcion 8-glucoside, 1-hydroxy-3-methoxy-6-methyl-8-(((2S,3R,4S,5S,6R)-3,4,5-trihydroxy-6-(hydroxymethyl)tetrahydro-2H-pyran-2-yl)oxy)anthracene-9,10-dione, 1-hydroxy-3-methoxy-6-methyl-8-[(2S,3R,4S,5S,6R)-3,4,5-trihydroxy-6-(hydroxymethyl)oxan-2-yl]oxyanthracene-9,10-dione
Molecular weight	416.378 g/mol and 446.4 g/mol
MS (ESI) *m/z*:	$[M+Na]^+$ 439.1 and 469.1
$[\alpha]_D^{22}$	-21.8° (MeOH, c=0.17)
¹H NMR	**Figures 4.80. and 4.85.** **Tables 4.38. and 4.39.**
¹³C NMR	**Figures 4.81. and 4.86.** **Tables 4.38. and 4.39.**
COSY	**Figures 4.82. and 4.87.**
HMQC	**Figures 4.83. and 4.88.** **Tables 4.38. and 4.39.**
HMBC	**Figures 4.84. and Figure 4.89.** **Tables 4.38. and 4.39.**

Compounds **10** and **11** were isolated as a mixture of an amorphous and orange solid. In TLC, light yellow spots with different retention factors were observed at daylight before reagent spraying. Additionally, the spots having fluorescence inhibiting zones under UV 254 nm and revealed red fluorescence under UV 366 nm were monitored. After Vanilin/H_2SO_4 sprayed and Vanilin/H_2SO_4 sprayed-plate was heated up to 110 °C, yellow/orange spots were detected. The structure of the substance was identified as a mixture of two compounds depending on NMR and mass spectroscopy as explained below.

Following TLC, Mass spectrum pointed out presence of two compounds with $[M+Na]^+$ peaks at *m/z* 439.1 and 469.1 in the mixture, which were expressed as compound **10** and compound **11**, respectively. NMR spectra of the mixture were recorded and spectroscopic data of the both compounds were shown in the same spectra, separately (**Figures 4.80-4.89**).

^{1}H-NMR spectrum displayed H atom signals in the aromatic field of the spectrum at 7.85 (d, *J* = 8.0 Hz, 1H, H-5, Comp. 10), 7.81 (t, *J* = 8.0 Hz, 1H, H-6, Comp. 10), 7.67 (d, *J* = 8.0 Hz, 1H, H-7, Comp. 10), 7.35 (d, *J* = 2.5 Hz, 1H, H-5, Comp. 11), 7.17 (d, *J* = 2.5 Hz, 1H, H-7, Comp. 11), while other protons were detected at 5.16 (d, *J* = 7.7 Hz, 1H, H-1', Comp. 11), 5.12 (d, *J* = 7.7 Hz, 1H, H-1', Comp. 10), 3.95 (s, 3H, H atoms of Me in C-6-OMe, Comp. 11), 3.73 – 3.68 (2H, H-6', H-6', Comp. 10 and Comp. 11), 3.50 (t, *J* = 6.0 Hz, 2H, H-6', H-6', Comp. 10 and Comp. 11), 3.49 – 3.31 (6H, H-2', H-2', H-3', H-3', H-5', H-5', Comp. 10 and Comp. 11), 3.22 (t, *J* = 9.3 Hz, 1H, H-4', Comp. 10), 3.18 (t, *J* = 9.0 Hz, 1H, H-4', Comp. 11), 2.40 (s, 3H, H atoms of Me in C-3-Me, Comp. 11), 2.38 (s, 3H, H atoms of Me in C-3-Me, Comp. 10) (**Figures 4.80. and 4.85.**).

Two proton signals at 5.16 and 5.12 ppm, both splitting into two peaks as doublets with 7.7 Hz coupling constants (*J*), were attributed to the anomeric protons of the sugar units in compound 11 and compound 12, respectively. 7.7 Hz of *J* values of both proton signals indicated that sugar molecules both *β* configurations. The remaining proton signals in the sugar molecules were ranged from δ_H 3.73 to δ_H 3.18 ppm and δ_H 3.73 to δ_H 3.22 ppm for compound 11 and compound 10, respectively. H atom signals in the aromatic rings were observed at around 7 ppm at high frequency, while H atoms in the sugar molecules, Me of C-6-OMe (3.95 ppm, Comp. 11), Me of

C-3-Me (2.40, Comp. 11) and Me of C-3-Me (2.38, Comp. 10) were observed at lower frequencies.

^{13}C-NMR spectrum (**Figures 4.81. and 4.86.**) presented. δ_C of C atom signals in the sugar molecule at 100.64 (anomeric C, C-1'), 73.24 (C-2'), 76.45 (C-3'), 69.54 (C-4') and 77.34 (C-5') and 60.60 (C-6') for compound 10 and 100.68 (anomeric C, C-1'), 73.24 (C-2'), 76.60 (C-3'), 69.79 (C-4'), 77.51 (C-5') and 60.76 (C-6') for compound 11 which were quite similar to the data of glucose indicated in the literature (400, 470, 471). δ_H values pointed out that the hexose units of both compounds as have to be β-glucose units. NMR spectra revealed the presence of aromatic carbons, alkane groups as well as β-glucose units. δ_C of aromatic C atom signals were ranged from 118.17 to 182.54 ppm for compound 10 and from 106.31 to 182.14 ppm for compound 11. δ_C of C atom signals at the 3rd and 6th positions in the aromatic rings for compounds 10 and 11, respectively were observed at higher chemical shifts indicating aromatic rings have to be substituted at those C atoms. In addition COSY, HMQC and HMBC, data proposed that compounds **10** and **11** are both anthranoid derivatives and obtained as a mixture as explained in details below.

According to COSY spectrum, couplings of H-1' with H-2', H-3' with H-4', H-5' with H-4', H-6' with H-6', and H-6 with H-7 for compound 10 and H-1' with H-2', H-3' with H-4', H-5' with H-4', H-6' with H-6', and H-5 with H-7 for compound 11 were displayed (**Figures 4.82 and 4.87.**).

HMQC spectrum indicating C atoms on which their binding H atoms were shown in **Figures 4.83. and 4.88.**.

HMBC spectrum pointed out a long range couplings between anomeric proton (H-1') of β-glucose units and C-8 atoms, indicating a β-glucose substitutions at C-8 for both compounds 10 and 11. Furthermore, long range couplings of H-5 with C-6 and C-8, H-6 with C-8, H-7 with C-6 and C-8 for compound 10, H-5 with C-7, H-7 with C-5 and C-6 for compound 11 and H-1' with C-8, H-6' with C-4' as well as H-6' with C-4', C-5' and C-1', H-2' with C-3' and C-4', H-3' with C-2', C-4' and C-5', H-5' with C-3' and C-4' for both compound 10 and compound 11 were also displayed (**Figures 4.84. and 4.89.**).

Following analysis of NMR spectra, the compounds were shown to have the molecular formulas $C_{21}H_{20}O_9$ (**10**) and $C_{22}H_{22}O_{10}$ (**11**) as established by HR-MS

(ESI) at *m/z* 439.1 and 469.1 $[M+Na]^+$ for compound 10 and compound 11, respectively (**Table 4.37.**).

       Spectroscopic data (**Tables 4.38 and 4.39.**) were found to be quite similar to the previously published data for chrysophanol-8-*O*-*β*-glucopyranoside (94) and physcion-8-*O*-*β*-glucopyranoside (471). Therefore, compounds 10 and compound 11 were elucidated as chrysophanol-8-*O*-*β*-glucopyranoside and physcion-8-*O*-*β*-glucopyranoside, respectively (**Figure 4.79.**).

Table 4.38. ^{1}H- and ^{13}C-NMR spectroscopic data of chrysophanol-8-O-β-glucoside (DMSO-d_6, ^{1}H: 600 MHz, ^{13}C: 151 MHz).

C/H		δ_H (ppm), J (Hz)	δ_C (ppm)	HMBC (H➔C)
1	C			-
2	CH			
3	C		146.83	-
4	CH		118.17	
5	CH	7.85 (d, 8.0)	120.35	C-6, C-8
6	CH	7.81 (t, 8.0)	135.37	C-8
7	CH	7.67 (d, 8.0)	122.42	C-6, C-8
8	C	-	158.09	-
9	C	-		-
10	C	-	182.54	-
11	C	-		-
12	C	-		-
13	C	-	121.62	-
14	C	-	134.79	-
3-CH$_3$	CH$_3$	2.38 (s, 3H)	21.48	-
1'	CH	5.12 (d, 7.7)	100.64	C-8
2'	CH	3.49 – 3.31	73.24	C-3', C-4'
3'	CH	3.49 – 3.31	76.45	C-2', C-4', C-5'
4'	CH	3.22 (t, 9.3)	69.54	C-4'
5'	CH	3.49 – 3.31	77.34	C-3', C-4'
6'	CH$_2$	3.73 – 3.68 3.50 (t, 6.0)	60.60	C-1', C-4', C-5'
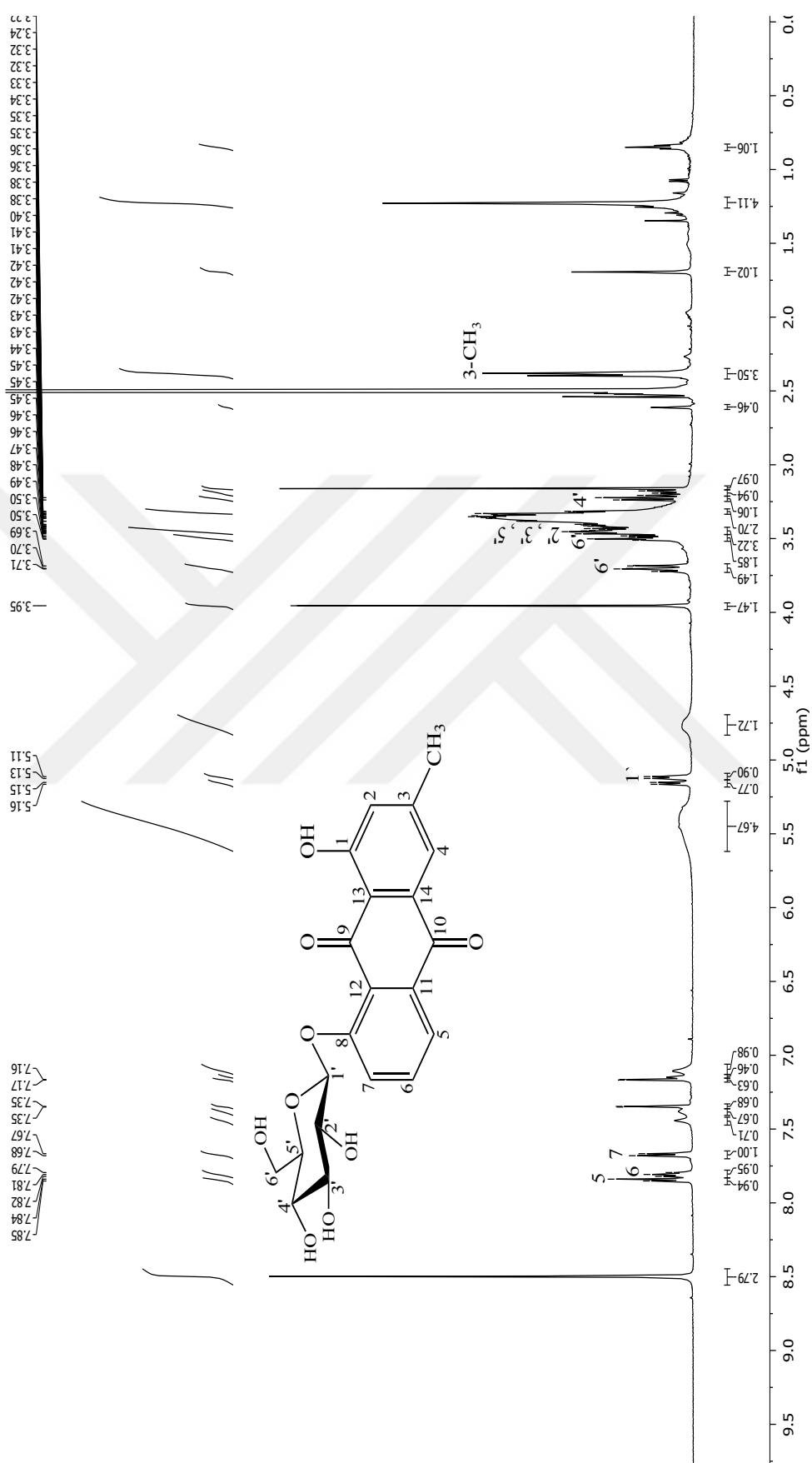
Figure 4.80. ^{1}H-NMR spectrum of chrysophanol-8-O-β-glucoside (Compound **10**) (DMSO-d_6, ^{1}H: 600 MHz).
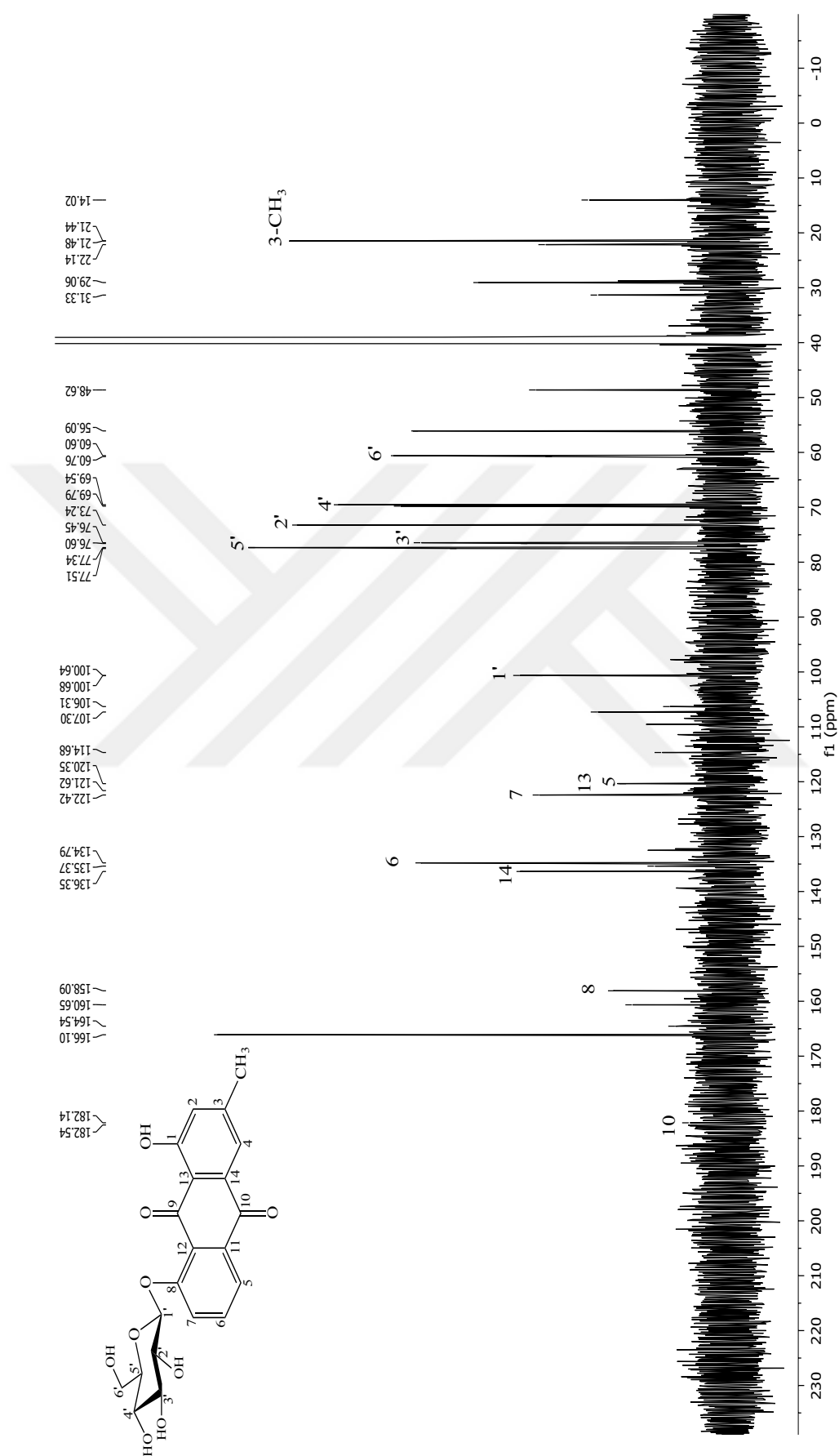
Figure 4.81. ^{13}C-NMR spectrum of chrysophanol-8-*O*-*β*-glucoside (Compound **10**) (DMSO-*d₆*, ^{13}C: 151 MHz).
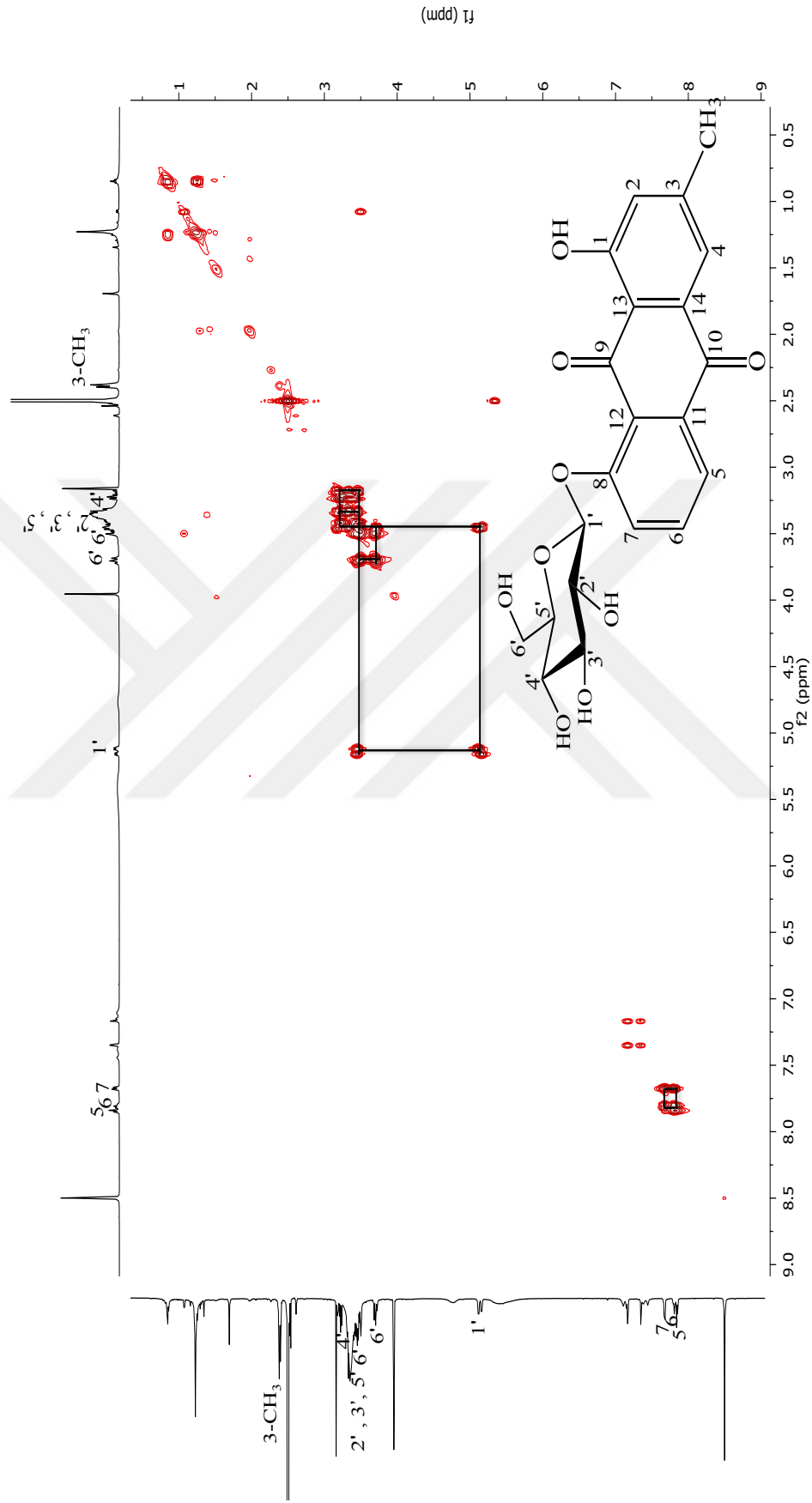
Figure 4.82. ^{1}H-^{1}H homonuclear correlation spectrum (COSY) of chrysophanol-8-*O*-*O*-*β*-glucoside (Compound **10**).
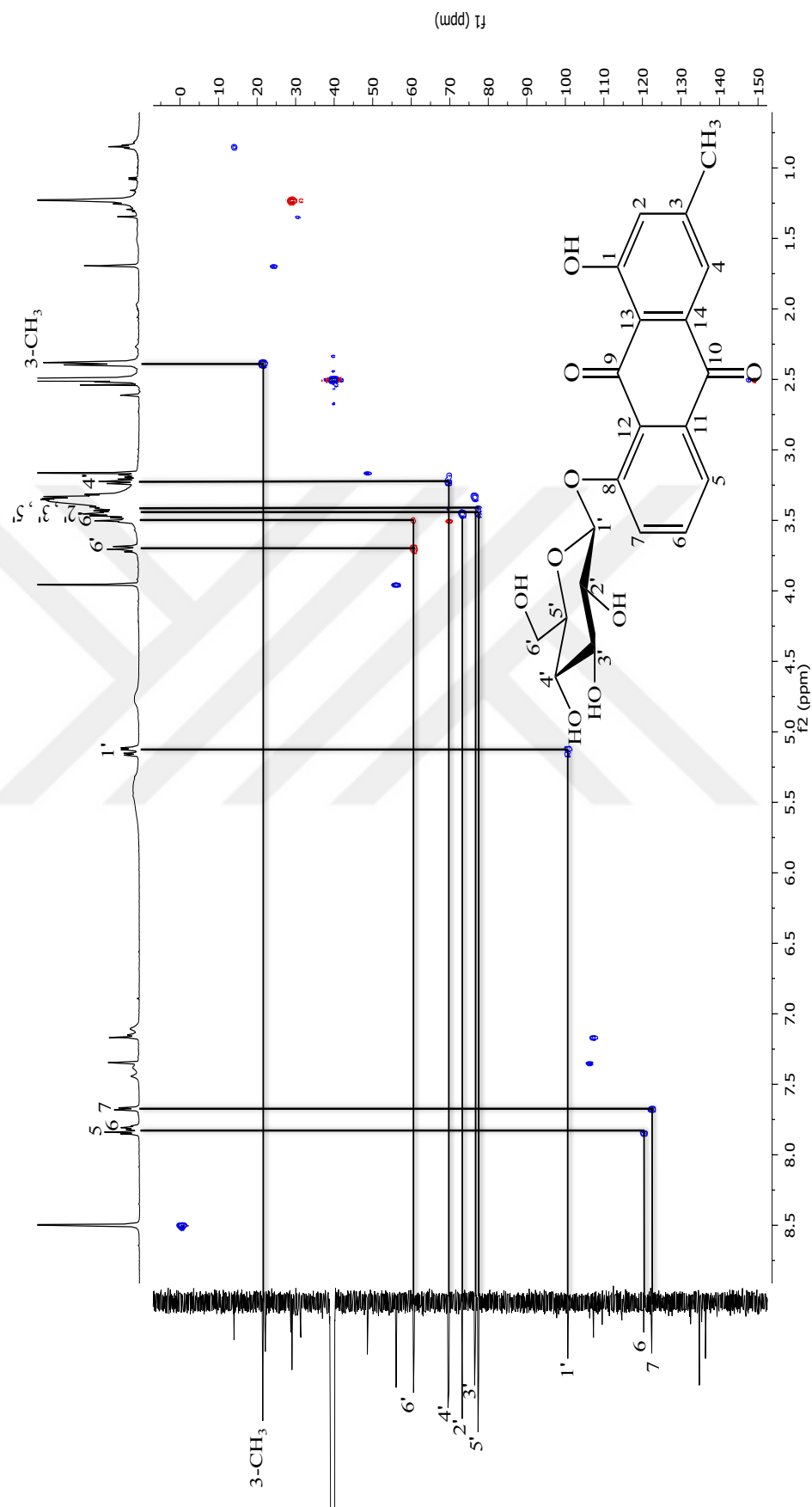
Figure 4.83. ^{1}H-^{13}C heteronuclear multiple-quantum correlation (HMQC) spectrum of chrysophanol-8-*O*-*β*-glucoside (Compound **10**).

239
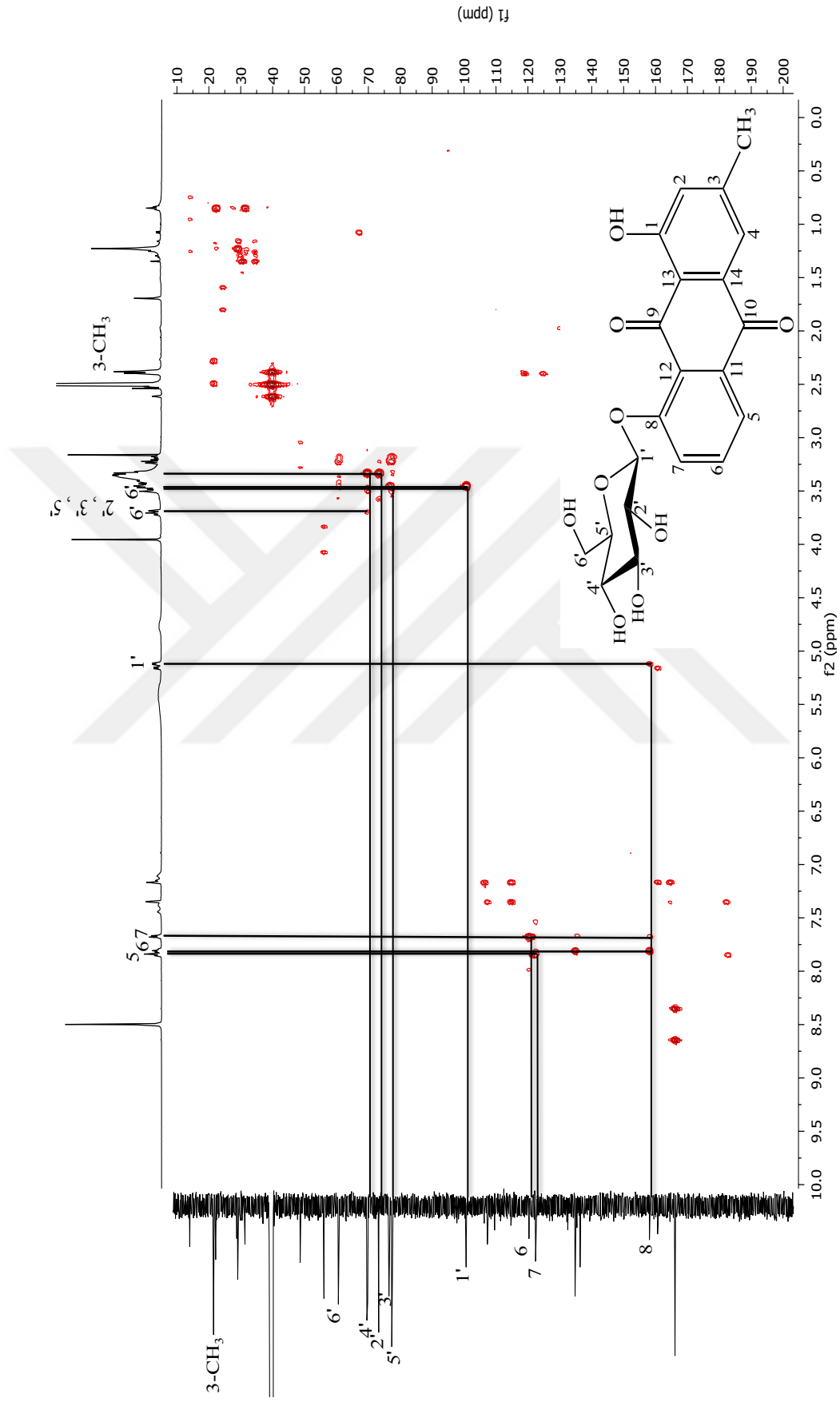
Figure 4.84. ^1H-^{13}C heteronuclear multiple bond correlation (HMBC) spectrum of chrysophanol-8-*O*-*β*-glucoside (Compound **10**).

Table 4.39. ^{1}H- and ^{13}C-NMR spectroscopic data of physcion-8-O-β-glucoside (DMSO-d_6, ^{1}H: 600 MHz, ^{13}C: 151 MHz).

C/H		δ_H (ppm), J (Hz)	δ_C (ppm)	HMBC (H→C)
1	C	-		-
2	CH		124.82	
3	C	-		-
4	CH		118.82	
5	CH	7.35 (d, 2.5)	106.31	C-7
6	CH		164.54	
7	CH	7.17 (d, 2.5)	107.30	C-5, C-6
8	C	-	160.65	-
9	C	-		-
10	C	-	182.14	-
11	C	-		-
12	C	-		-
13	C	-	114.68	-
14	C	-	136.35	-
3-CH$_3$	CH$_3$	2.40 (s, 3H)	21.44	
6-O-CH$_3$	CH$_3$	3.95 (s, 3H)	56.09	
1'	CH	5.16 (d, 7.7)	100.68	C-8
2'	CH	3.49 – 3.31	73.24	C-3', C-4'
3'	CH	3.49 – 3.31	76.60	C-2', C-4', C-5'
4'	CH	3.18 (t, 9.0)	69.79	
5'	CH	3.49 – 3.31	77.51	C-3', C-4'
6'	CH$_2$	3.73 – 3.68 3.50 (t, 6.0)	60.76	C-1', C-4', C-5'

241
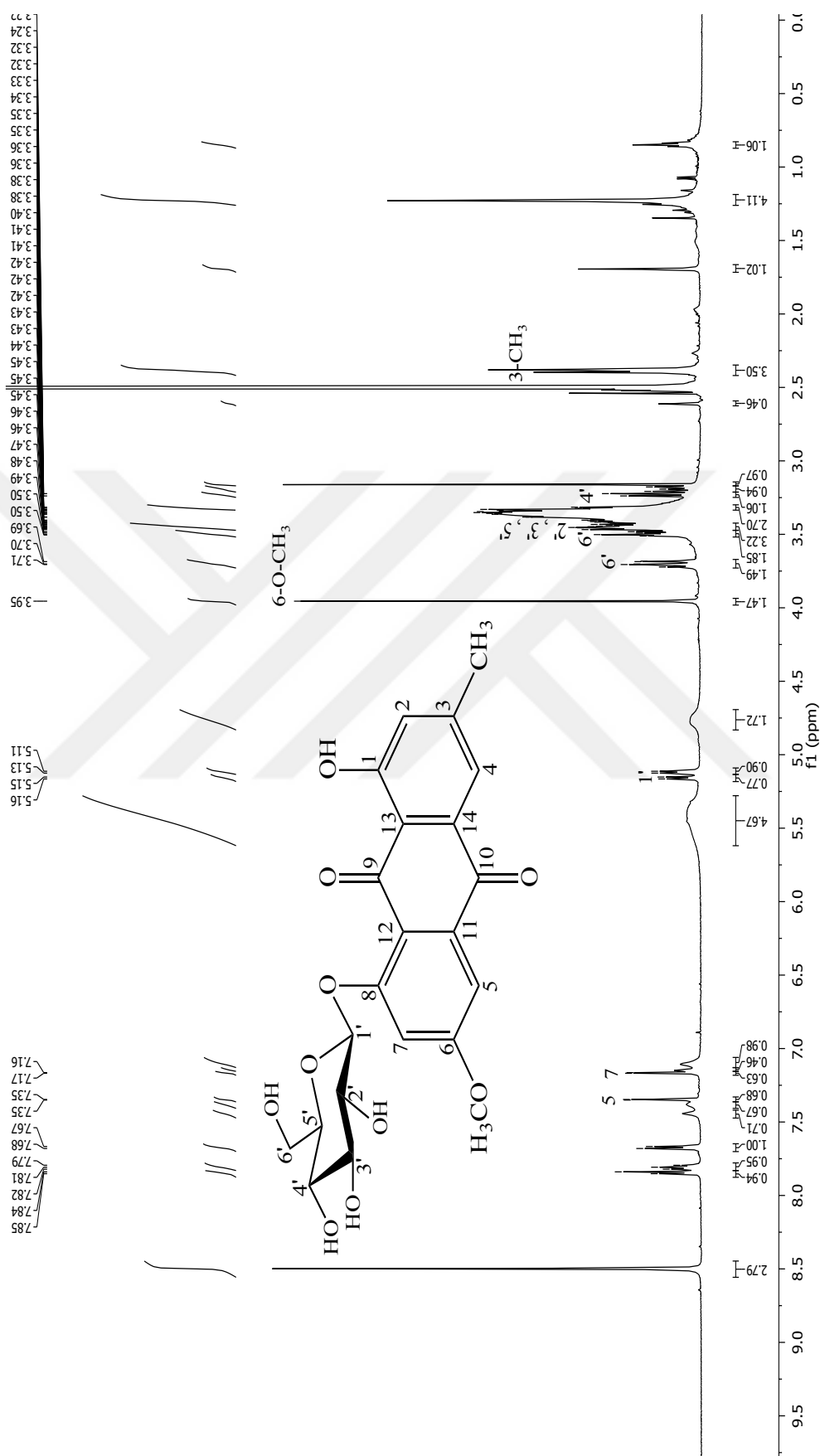
Figure 4.85. ^{1}H-NMR spectrum of physcion-8-*O*-*β*-glucoside (Compound **11**) (DMSO-*d$_6$*, ^{1}H: 600 MHz).
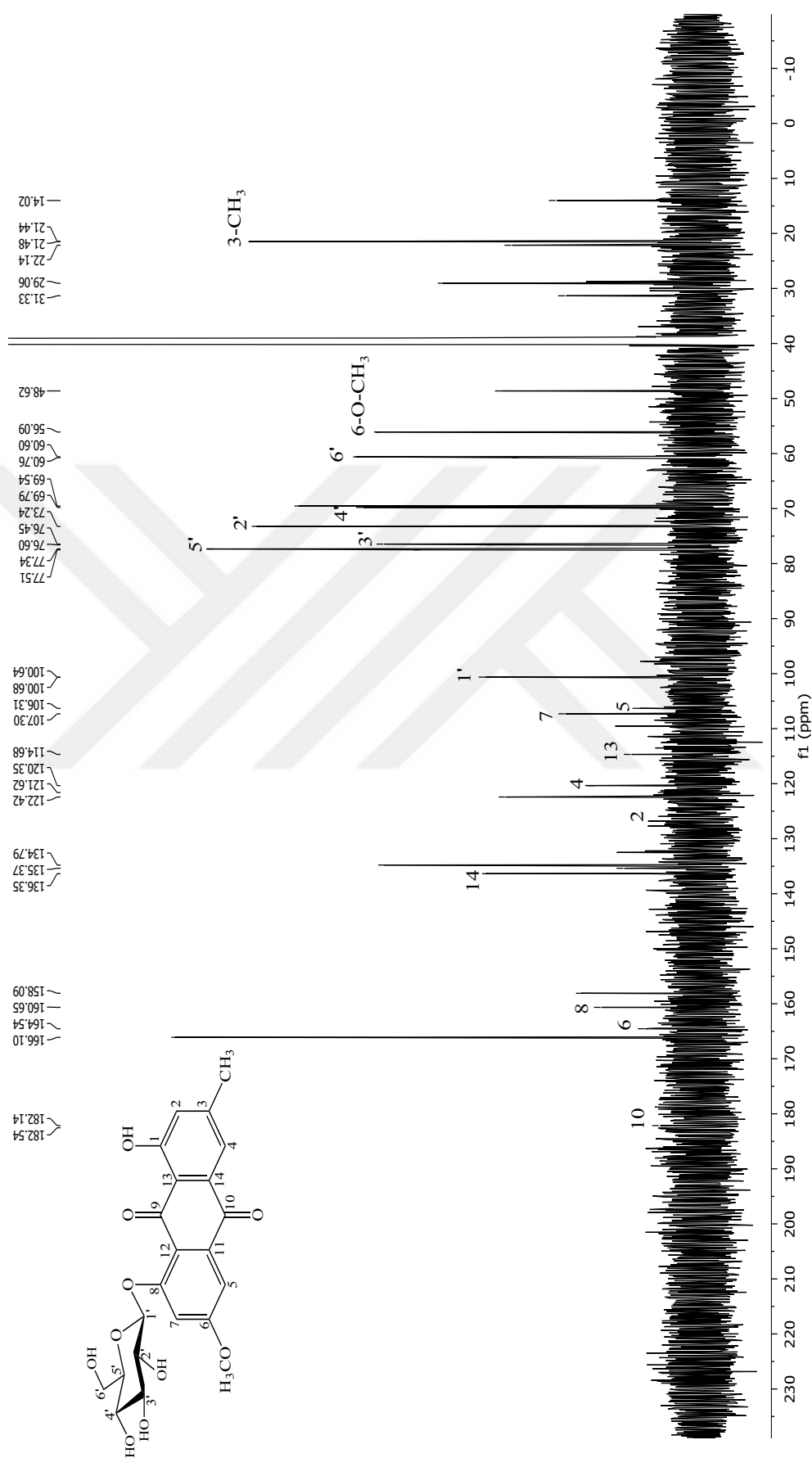
Figure 4.86. ^{13}C- NMR spectrum of physcion-8-O-β-glucoside (Compound **11**) (DMSO-d_6, ^{13}C: 151 MHz).
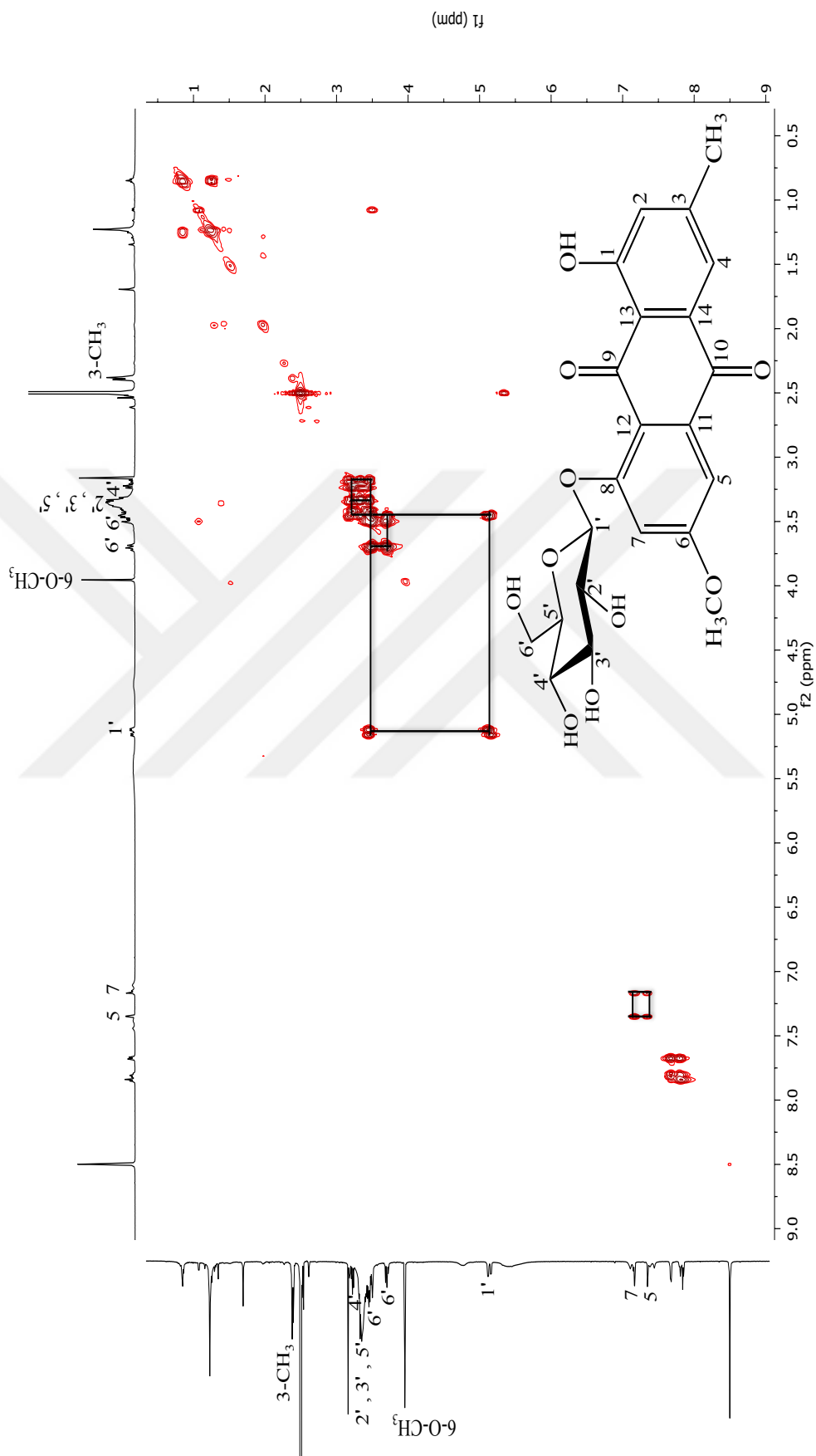
Figure 4.87. ^{1}H–^{1}H homonuclear correlation spectrum (COSY) of physcion-8-O-β-glucoside(Compound **11**).
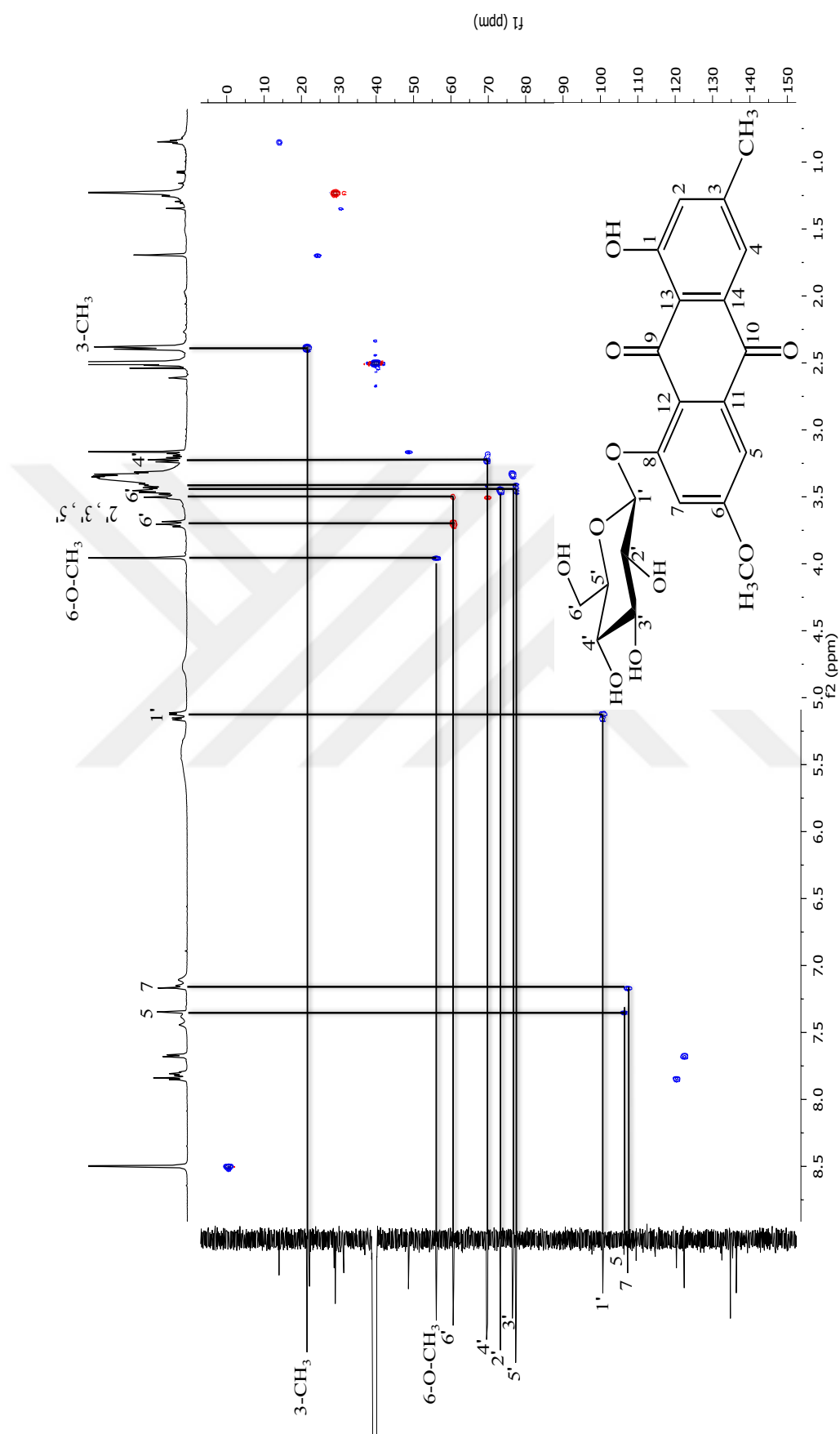
Figure 4.88. ^{1}H-^{13}C heteronuclear multiple-quantum correlation (HMQC) spectrum of physcion-8-O-β-glucoside (Compound **11**).
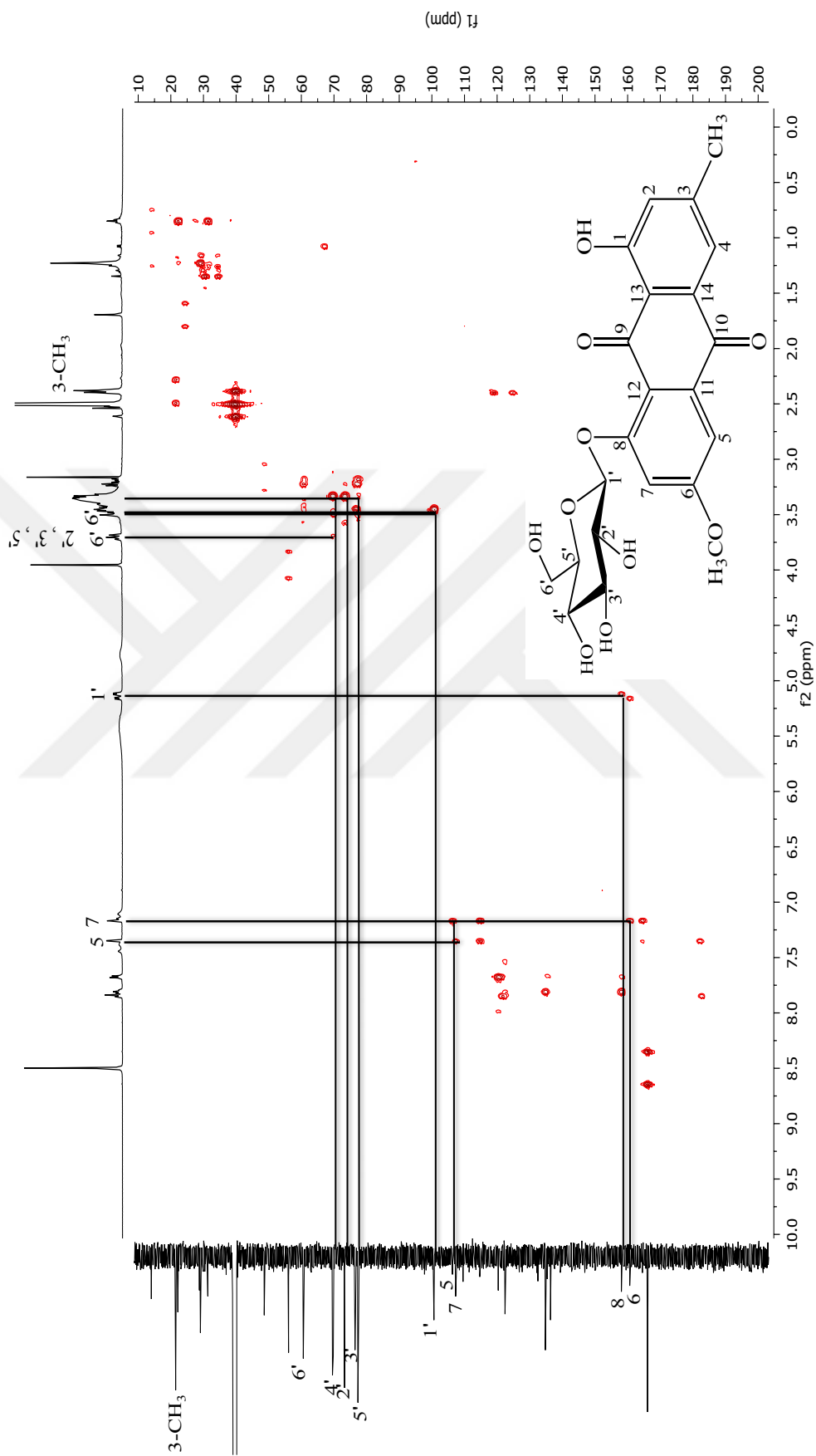
Figure 4.89. ^{1}H-^{13}C heteronuclear multiple-bond correlation (HMBC) spectrum of physcion-8-O-β-glucoside (Compound **11**).

4.3   Cytotoxicity

4.3.1   Cytotoxicity of Anthraquinones towards Sensitive and Drug-Resistant Cancer Cells

As a first step, cytotoxicities of main anthraquinone aglycons in *Rumex acetosella* were investigated towards drug-sensitive CCRF-CEM and multidrug-resistant P-glycoprotein-overexpressing CEM/ADR5000 leukemia cells by means of resazurin assay, since those cells were more sensitive than other cell lines.

The cytotoxicities of the main anthraquinone aglycons were determined and presented in the graphs (**Figures 4.90.-4.93.**). The IC_{50} values of emodin, aloe-emodin, rhein and physcion were 35.62 µM, 9.872 µM, 34.42 µM and 123.5 µM, respectively for CCRF-CEM cells and 35.27 µM, 12.85 µM, 46.87 µM and 74.79 µM, respectively for CEM/ADR5000 cells. The degrees of resistance were calculated by dividing the IC_{50} values of CEM/ADR5000 cells by the IC_{50} values of CCRF-CEM. Compared to their corresponding sensitive cell lines, collateral sensitivity (hypersensitivity) of CEM/ADR5000 cells towards physcion (0.61-fold) was observed. Aloe-emodin was the most cytotoxic compound among four anthraquinones with IC_{50} values of 9.872 µM (CCRF-CEM) and 12.85 µM (CEM/ADR5000) (**Figure 4.91.**). We observed clinically used doxorubicin to have IC_{50} values as 0.0007 µM and 10.98 µM towards CCRF-CEM and CEM/ADR5000, respectively. It is worth noting that the IC_{50} value of aloe-emodin was nearly as comparable as that of doxorubicin towards CEM/ADR5000 cells (**Figure 4.94.**).
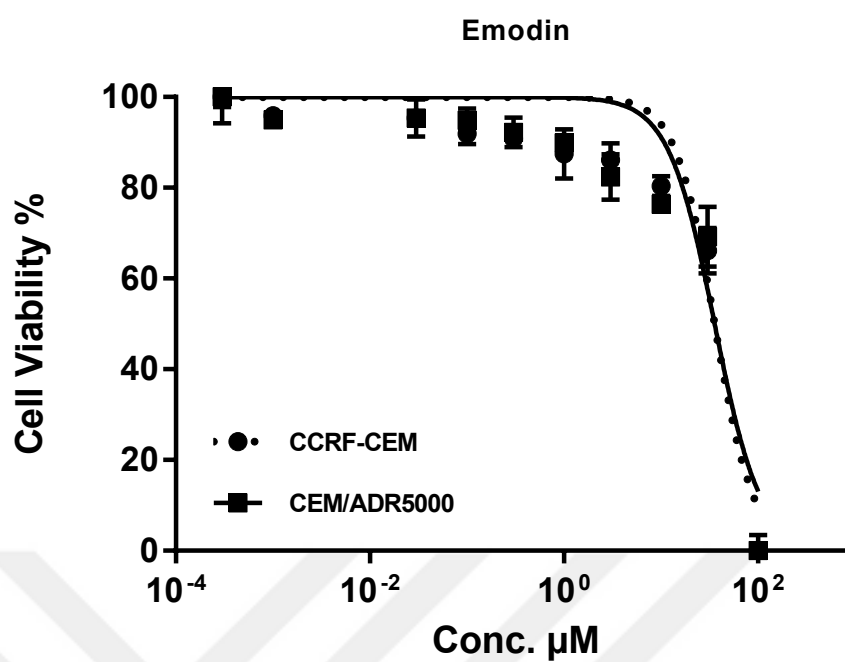
Figure 4.90. Dose response curve of leukemia cells treated by emodin.

(CCRF/CEM IC_{50}: 35.62 μM, CEM/ADR5000 IC_{50}: 35.27 μM)
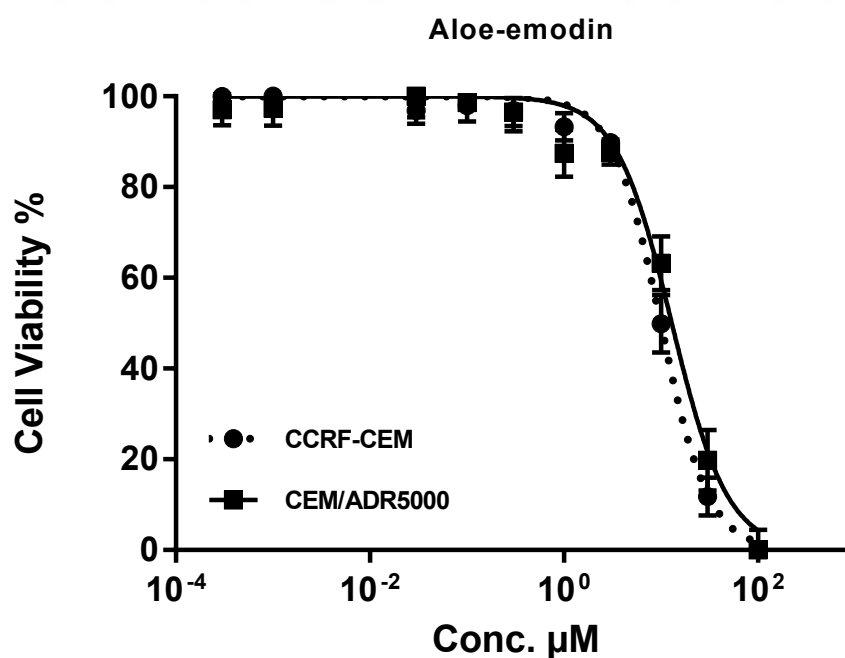
Figure 4.91. Dose response curve of leukemia cells treated by aloe-emodin.

(CCRF/CEM IC_{50}: 9.872 μM, CEM/ADR5000 IC_{50}: 12.85 μM)
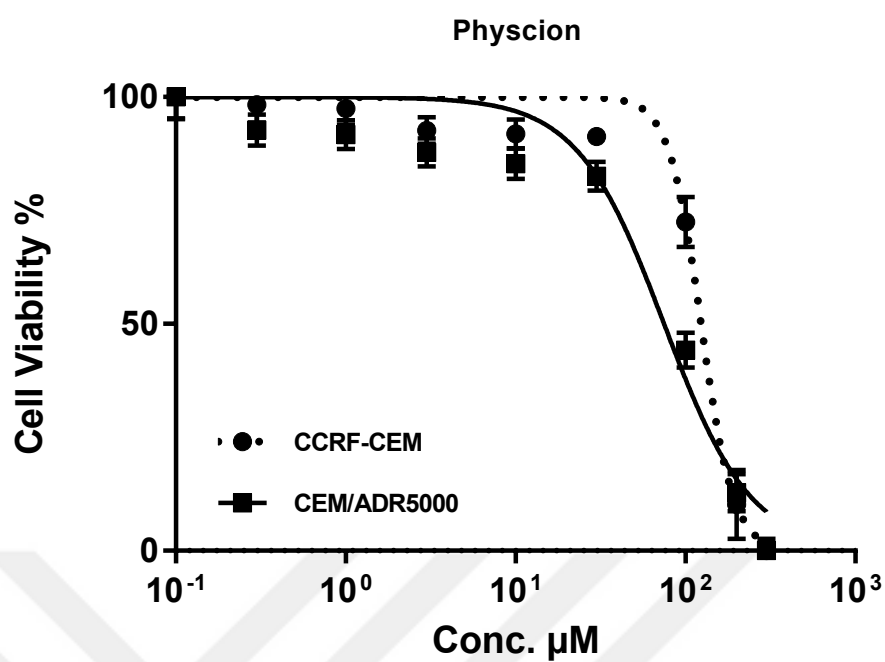
Figure 4.92. Dose response curve of leukemia cells treated by physcion.

(CCRF/CEM IC$_{50}$: 123.5 μM, CEM/ADR5000 IC$_{50}$: 74.79 μM)
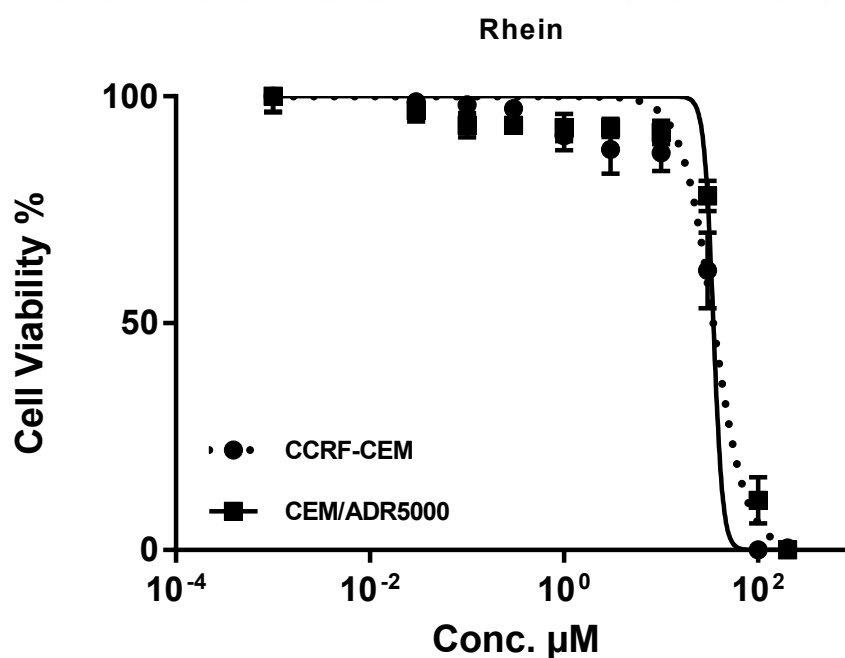
Figure 4.93. Dose response curve of leukemia cells treated by rhein.

(CCRF/CEM IC$_{50}$: 34.42 μM, CEM/ADR5000 IC$_{50}$: 46.87 μM)
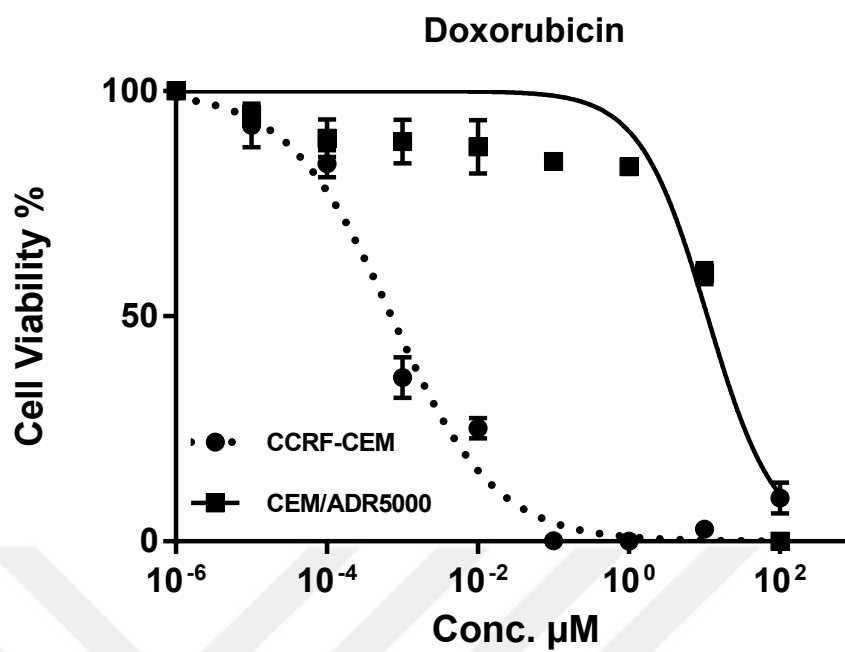
Figure 4.94. Dose response curve of leukemia cells treated by doxorubicin.

(CCRF/CEM IC$_{50}$: 0.0007 μM, CEM/ADR5000 IC$_{50}$: 10.98 μM)

We further conducted preliminary cytotoxicity studies for the compounds isolated from *R. acetosella*. Cytotoxic effects of the compounds except for the compounds **3** and **5** (since the isolated amounts for both were too small for dose response curves and IC_{50} determination) were investigated towards CCRF-CEM and CEM/ADR5000. None revealed notable cytotoxicity at 10 μg/mL (To evaluate a compound as cytotoxic, cell viability must be less than 30% at 10 μg/mL). Therefore, we moved to further researches only regarding aloe-emodin, since that revealed the most profound cytotoxicity in our pair of sensitive and multidrug-resistant leukemia cell lines.

Cell viabilities of isolated compounds towards CCRF-CEM and CEM/ADR5000 leukemia cells at 10 μg/mL as preliminary cytotoxicity researches were shown in **Table 4.40.**.

Table 4.40. Cell viabilities of isolated compounds towards CCRF-CEM and CEM/ADR5000 leukemia cells at 10 μg/mL.

Compound	Cell viability%	
	CCRF-CEM	**CEM/ADR5000**
(*E*)-piceid	86.2 ± 1.3	91.6 ± 1.2
Nepodin-8-*O*-*β*-glucoside	84.9 ± 2.8	81.3 ± 1.8
Emodin	86.2 ± 3.7	84.8 ±3.9
Emodin-8-*O*-*β*-glucoside	83.4 ± 2.5	79.6 ± 2.8
Catechin	71.33 ± 6.9	81.12 ± 3.5
Rumejaposide G and Rumejaposide H	80.72 ± 2.9	79.03 ± 2.8
Chrysophanol-8-*O*-*β*-glucoside Physcion-8-*O*-*β*-glucoside	48.74 ± 1.7	78.9 ± 2.9
Acetoselloside	90.2 ± 2.3	93 ± 3.5

As a next step, we tested the cytotoxicity of aloe-emodin towards pairs lines from different tumor types and different drug resistant mechanisms. The following cell lines were treated with aloe-emodin and measured by the resazurin assay:

(1) Breast cancer cells: MDA-MB-231-pcDNA cells and a multidrug-resistant subline transfected with a *BCRP* cDNA (MDA-MB-231-BCRP clone 23).

(2) Embryonic kidney cells: wild type HEK293 cells and a multidrug-resistant subline transfected with an *ABCB5* cDNA (HEK293-ABCB5).

(3) Colon cancer cells: HCT116 cells with wild-type TP53 tumor supressor gene (HCT116(p53$^{+/+}$)) and HCT116 knockout cells (HCT116(p53$^{-/-}$)).

(4) Brain tumor cells: wild type U87.MG and a subline transfected with a deletion-activated *EGFR* cDNA (U87.MGΔEGFR).

As shown in **Figures 4.95.-4.98.**, we determined aloe-emodin's cytotoxicity towards pairs lines from different tumor types and different drug resistant mechanisms. IC$_{50}$ values ranged from 16.47 μM to 22.3 μM for drug-sensitive and wild-type cell lines and from 11.19 μM to 33.76 μM for drug-resistant and transfected sublines. The IC$_{50}$ values of aloe-emodin towards HCT116(p53$^{+/+}$), U87.MG, MDA-MB-231-pcDNA and HEK293 were 16.47 μM, 21.73 μM, 22.3 μM and 16.9 μM, respectively. For resistant cell lines the IC$_{50}$ values were detected as 11.19 μM (HCT116(p53$^{-/-}$)), 33.76 μM (U87.MGΔEGFR), 26.95 μM (MDA-MB-231-BCRP clone 23) and 25.92 μM (HEK293-ABCB5), respectively. Collateral sensitivity (hypersensitivity) to aloe-emodin was observed in HCT116 (*p53$^{-/-}$*) knockout cells (0.68-fold). Aloe-emodin was taken into the further researchers towards CCRF-CEM cells, since it displayed the best cytotoxicity on these cells.
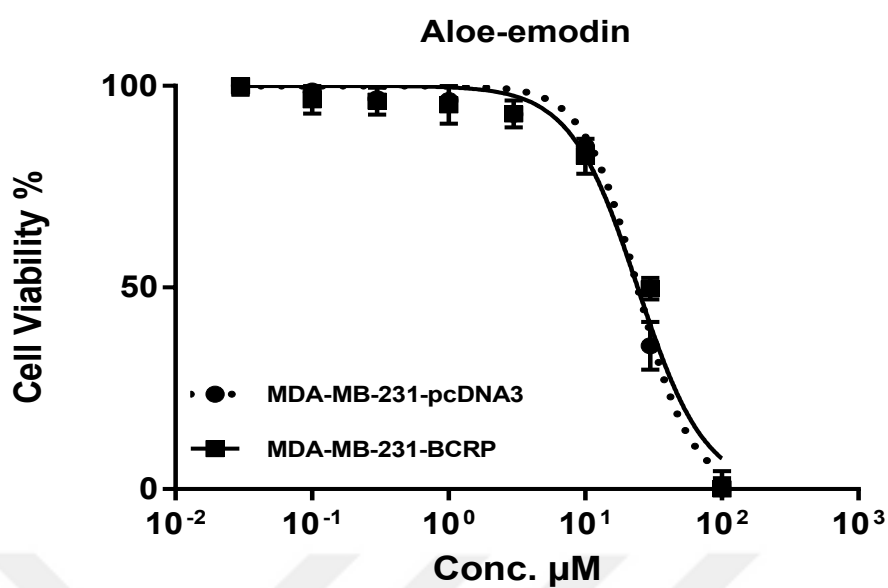
Aloe-emodin

Figure 4.95. Dose response curve of breast cancer cells treated by aloe-emodin.

(MDA-MB-231-pcDNA IC$_{50}$: 22.3 μM, MDA-MB-231-BCRP clone 23 IC$_{50}$: 26.95 μM)
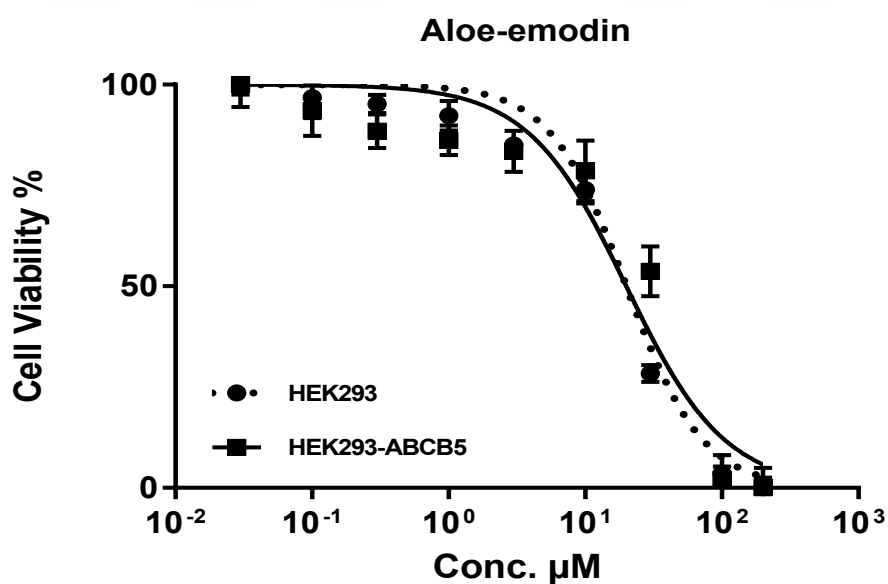
Aloe-emodin

Figure 4.96. Dose response curve of human embryonic kidney cells treated by aloe-emodin.

(HEK293 IC$_{50}$: 16.9 μM, HEK293-ABCB5 IC$_{50}$: 25.92 μM)
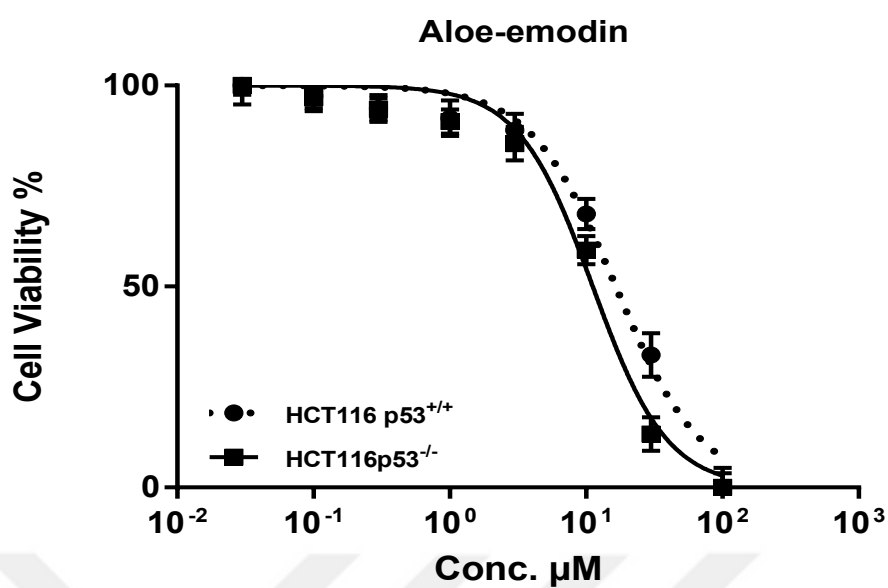
Figure 4.97. Dose response curve of colon cancer cells treated by aloe-emodin.

(HCT116(p53$^{+/+}$) IC$_{50}$: 16.47 μM, HCT116(p53$^{-/-}$) IC$_{50}$: 11.19 μM)
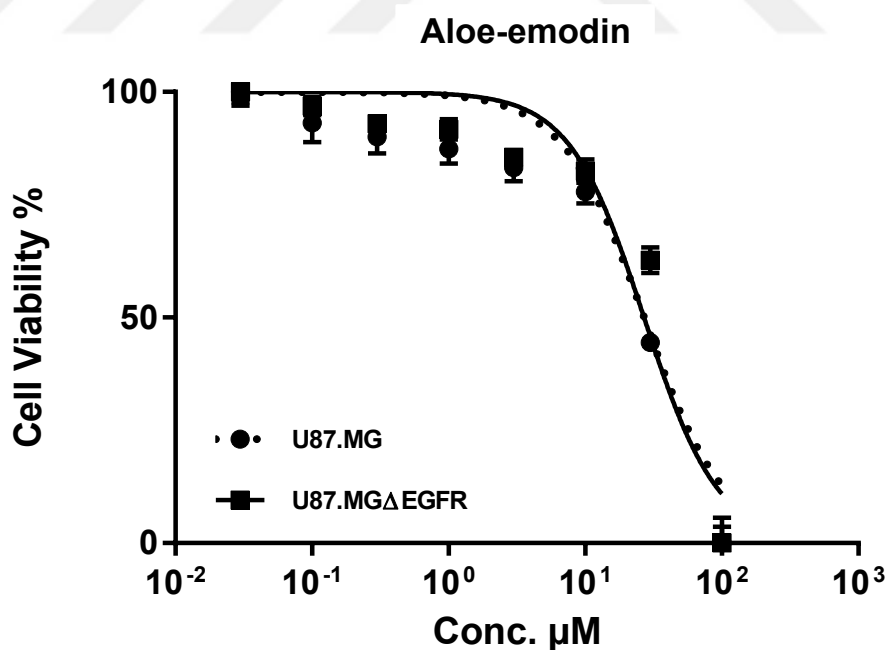
Figure 4.98. Dose response curve of brain tumor cells treated by aloe-emodin.

(U87.MG IC$_{50}$: 21.73 μM, U87.MGΔEGFR IC$_{50}$: 33.76 μM)

4.3.2 Cytotoxicity of Aloe-emodin towards CCRF-CEM cells by means of Protease Viability Marker Assay

The cytotoxicity of aloe-emodin was futher investigated by means of protease viability marker assay in order to rule out any cross-talk or reciprocal interdependence with resazurin assay, which depends on redox system. Since, we detected aloe-emodin to induce excessive ROS production in our advancing studies, which might affect the resuts of resazurin assay. Therefore, we performed protease viability marker assay by measuring the protease activity within living cells. Aloe-emodin presented strong cytotoxicity towards CCRF-CEM cells with the IC_{50} value of 13.8 μM, which was quite similar to the data gained by resazurin assay (**Figure 4.99.**).
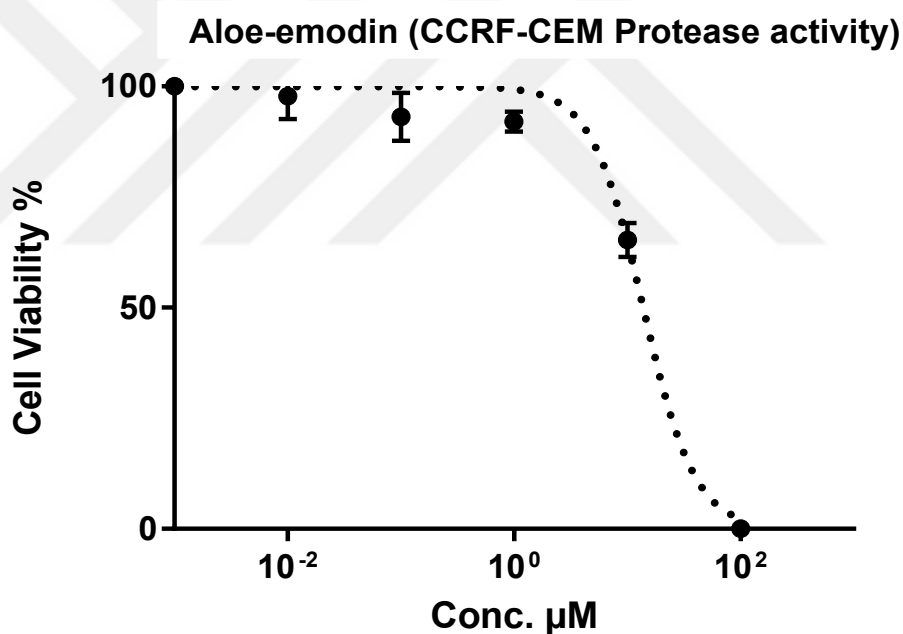
Figure 4.99. Cytotoxicity of aloe-emodin towards CCRF-CEM cells by means of protease viability marker assay.

4.3.3 Toxicity of Aloe-emodin in Normal Cells

We also investigated aloe-emodin's toxicity towards normal cells, as well. The human peripheral mononuclear cells (PMNC) were isolated from fresh blood samples of a healthy donor and tested against various concentrations of aloe-emodin ranging from 0.001-100 µM. Interestingly, aloe-emodin did not show any cytotoxic activity towards the normal cells at all concentrations tested (**Figure 4.100.**).
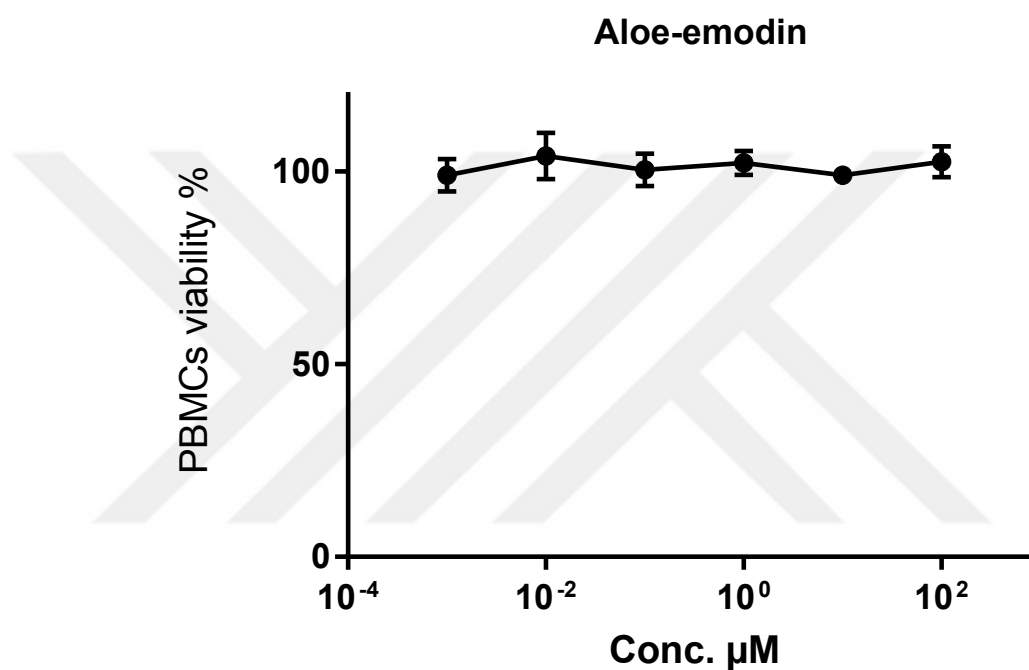
Figure 4.100. Toxicity of aloe-emodin in normal cells.

4.4 Differential Transcriptome-wide mRNA Expression upon Aloe-emodin Treatment

We performed microarray hybridization experiments to find clues on the possible mechanisms of action of aloe-emodin and to generate testable hypothesis. CCRF-CEM cells were treated with IC_{50} concentration of aloe-emodin or DMSO for 48 h. Using Chipster software, 1712 genes were found to be deregulated upon aloe-emodin treatment in comparison with DMSO treatment as control. These genes were subsequently subjected to IPA (Ingenuity Pathway Analysis) to obtain profiles of possibly affected signaling pathways. The most pronounced molecular and cellular functions identified by IPA were: cell death and survival, cellular growth and proliferation, cellular development, gene expression, cellular function and maintenance (**Figure 4.101.**). NF-κB pathway was seen to be downregulated via pathways shown in **Figures 4.102** and **4.103.**.

Figure 4.101. Microarray-based mRNA expression profiling and the impression of the most upregulated and downregulated genes of CCRF-CEM cells treated with aloe-emodin for 48 h identified by Ingenuity Pathway Analysis.
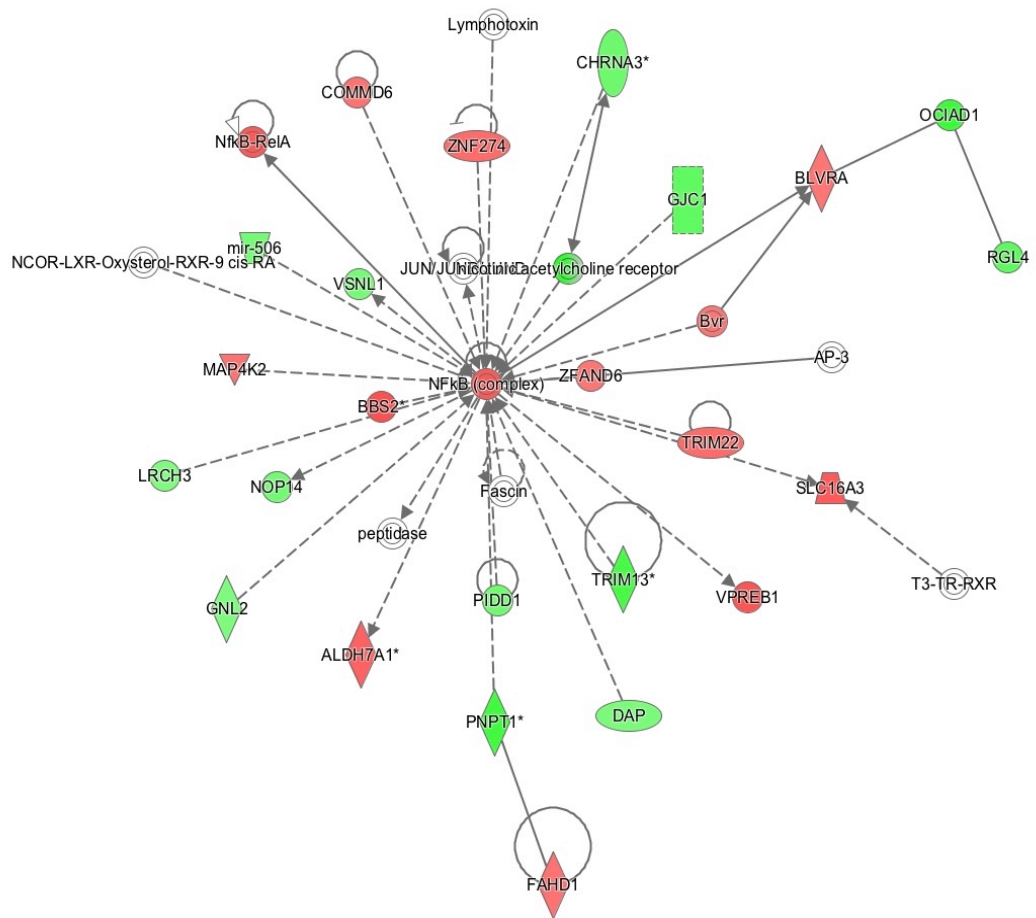
Figure 4.102. Signaling networks regulated by deregulated genes (A).
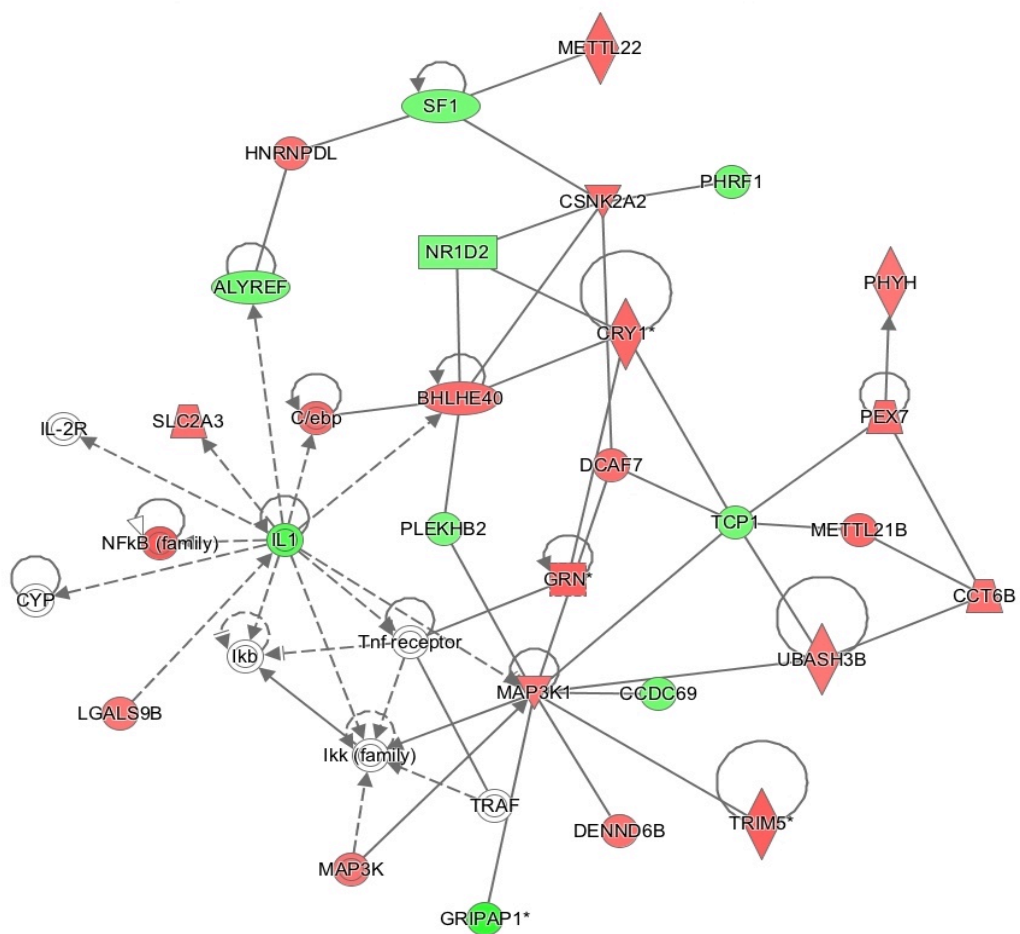
Figure 4.103. Signaling networks regulated by deregulated genes (B).

4.5   Validation of Microarray Data by qPCR

As a result of pathway analysis of microarray data, the most deregulated genes were additionally shown in **Figure 4.104.**. Two up- or down-regulated genes were selected for qPCR analysis (*DUSP6*, *HHEX*, *MCMDC2*, *CRCP*). Their expression was normalized to *GAPDH*. Then, the fold-change values of aloe-emodin-treated and untreated samples obtained from microarray hybridization and qPCR were subjected to Pearson correlation test. We obtained a correlation coefficient R-value of 0.989, indicating a high consistency of microarray and qPCR data (**Table 4.41.**).
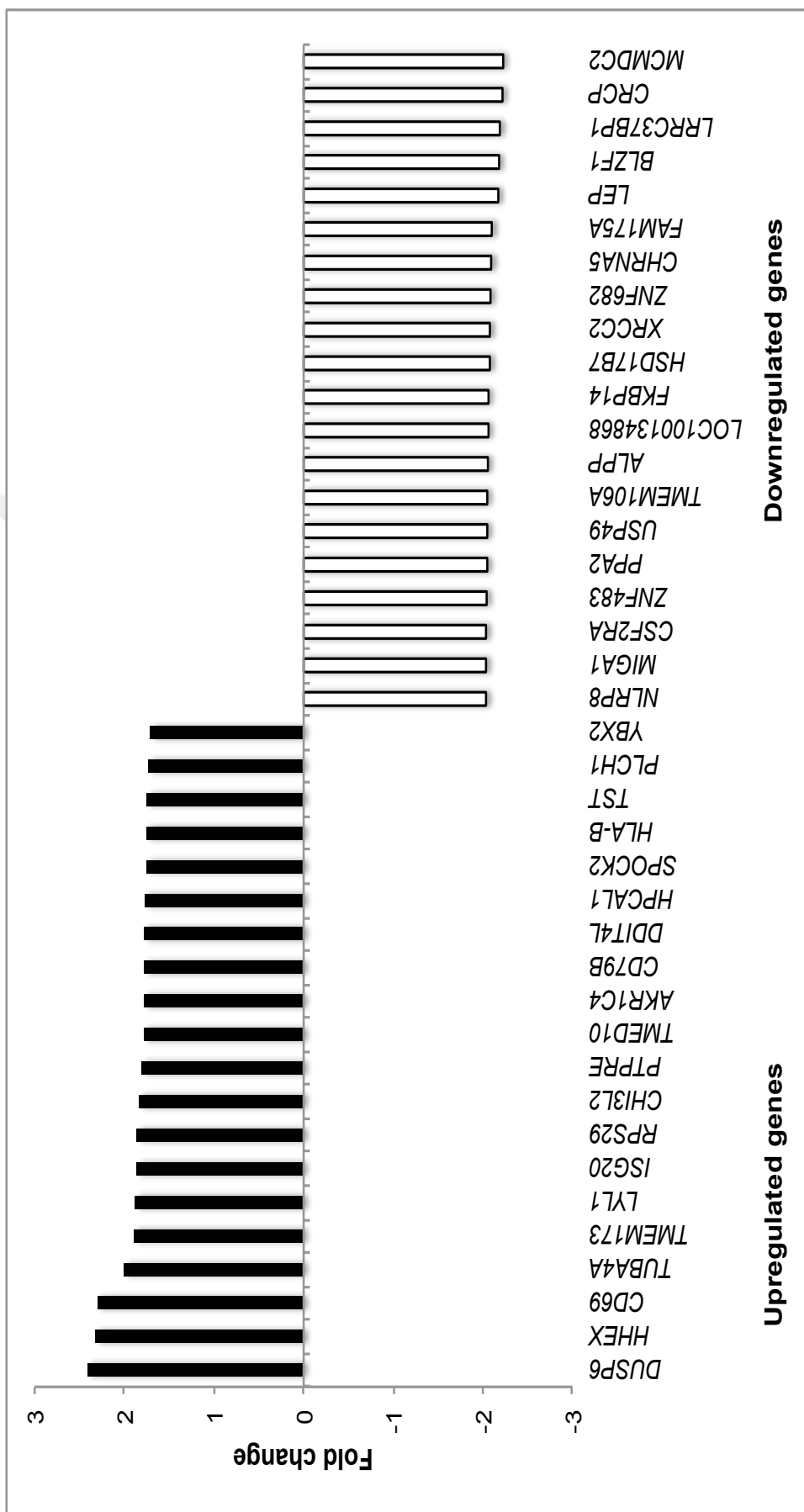
Figure 4.104. The most deregulated genes at the treatment with IC_{50} value of aloe-emodin for 48 h.

Table 4.41. Validation of microarray-based gene expressions by real-time reverse transcription-PCR.

Gene name	Microarray data (FC)*	qPCR data (FC)
DUSP6	2.403	1.40
HHEX	2.321	2.23
MCMDC2	-2.227	-2.47
CRCP	-2.219	-2.63

R value= 0.989 (Correlation coefficient of mRNA expression values between microarray and qPCR was determined by Pearson correlation test).

- FC: Fold change.

4.6   Detection of Reactive Oxygen Species (ROS)

IPA revealed that the deregulated genes were correlated with substantially apoptosis as well as other cellular functions including DNA replication, recombination and repair. Therefore, we assumed that oxidative stress generated in cells might be a reason for DNA damage; thus leading the cells to go apoptosis.

CCRF-CEM cells were treated with 0.5-, 1-, 2- and 4- fold IC_{50} values of aloe-emodin, respectively for 1 h. As expected, aloe-emodin stimulated ROS production in a dose dependent manner with the fold changes ≥ 1.5. Remarkably, aloe-emodin induced even higher ROS generation in all studied than doxorubicin (1 μM) and H_2O_2 (250 μM) as positive controls (**Figure 4.105.**).
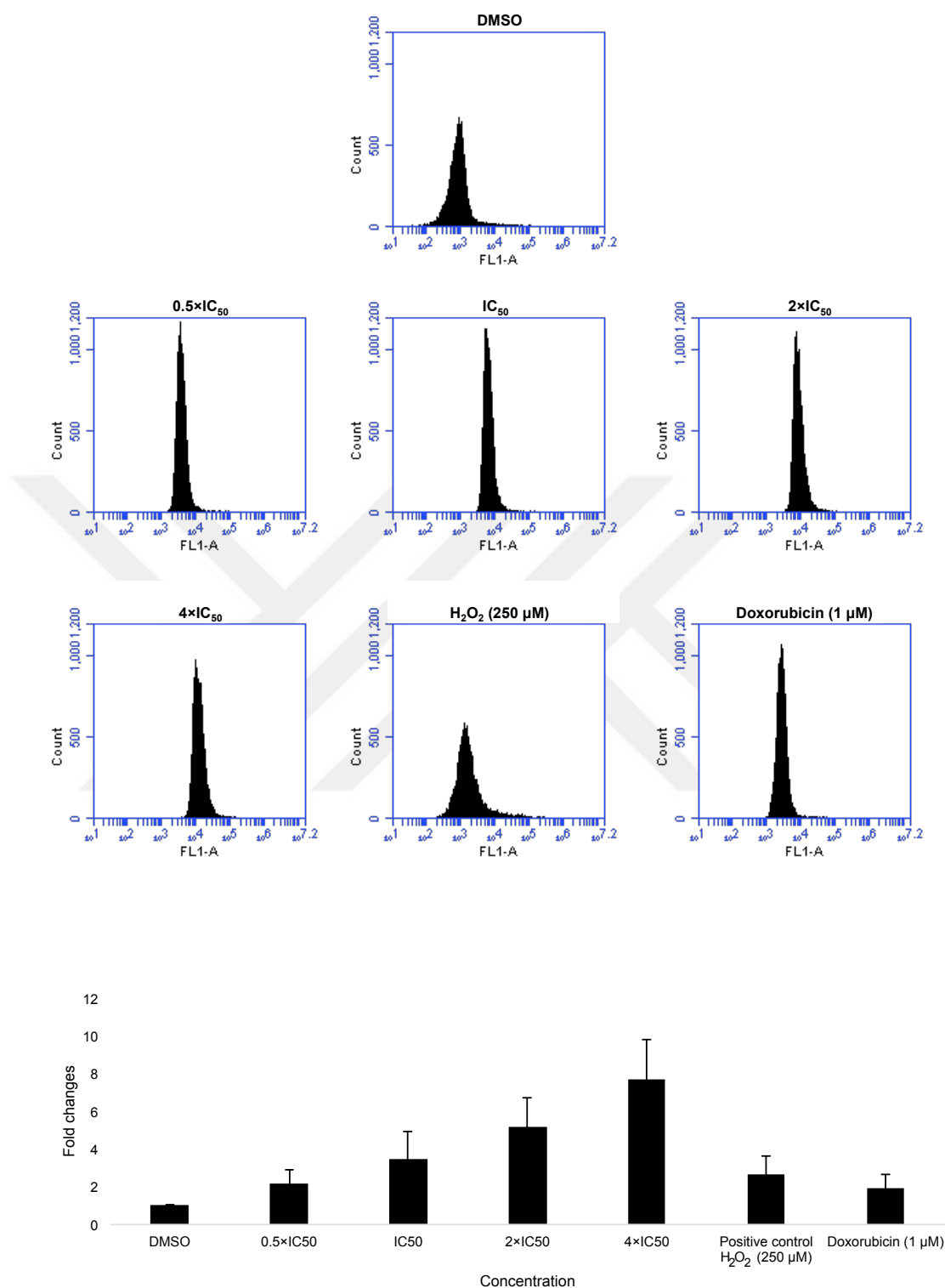
Figure 4.105. Induction of ROS level in CCRF-CEM cells after treatment with 0,5-, 1-, 2- and 4-fold IC_{50} values of aloe-emodin, DMSO as control, doxorubicin (1 μM) and H_2O_2 (250 μM) as positive control for 1 h and statistical quantification of ROS level. Mean values ± SD of three independent experiments are shown.

Excessive ROS production is known to evoke DNA damage in cells (478, 479). Pathway analysis of microarray results also showed that genes associated with DNA metabolism, replication, recombination and repair were deregulated (Figure 3A). This may imply that aloe-emodin could induce DNA damage. For this reason, we performed alkaline comet assay to detect single and double-stranded DNA damage.

4.7   Comet Assay

In the light of the pahway analysis, DNA metabolism comprising DNA replication, recombination and repair was observed to be deregulated. Therefore we tested aloe-emodin's effect on the DNA of CCRF-CEM cells by treating the cells with 1-, 2- or 4-fold IC_{50} of aloe-emodin for 24 h. We compared the DNA of aloe-emodin-treated cells with the DNA of DMSO-treated cells as negative control. Aloe-emodin indeed induced comet tails indicating DNA damage and increased percentages of tail DNA. We additionally monitored DNA migration with tail and olive tail movements and accomplished aloe-emodin to induce DNA damage in a dose-dependent manner (**Figures 4.106.-4.108.**).
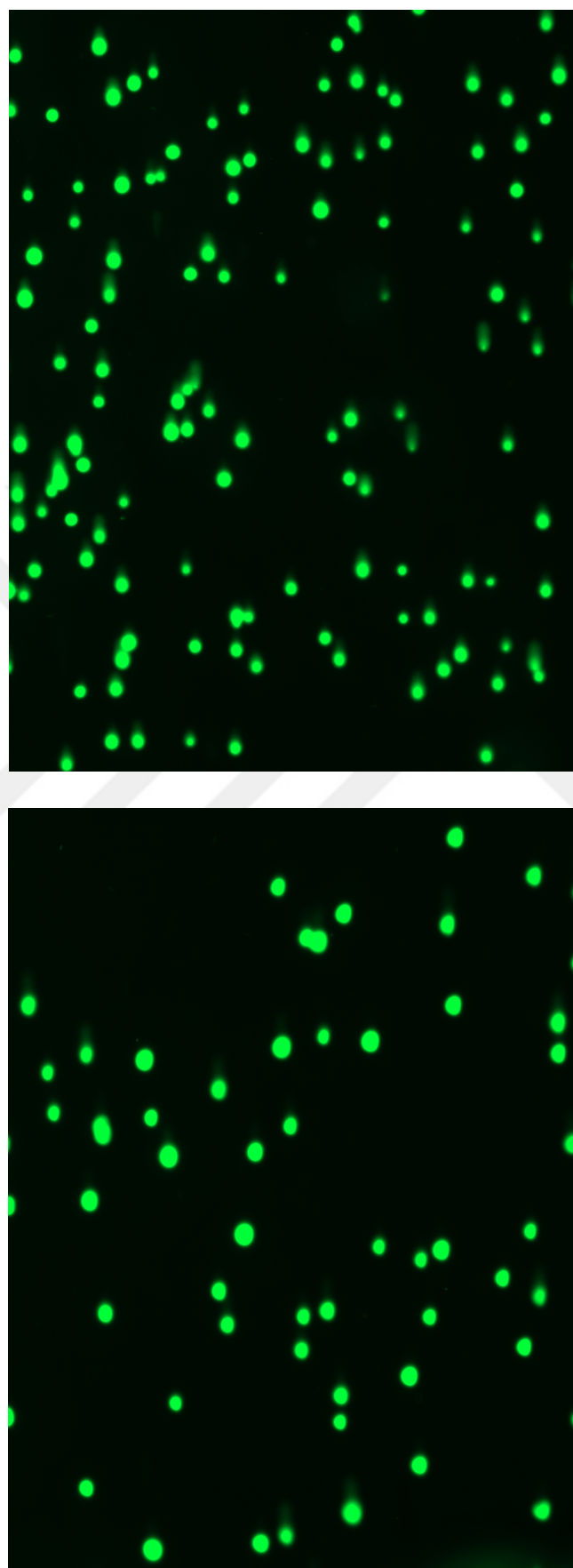
Figure 4.106. Induction of DNA damage by aloe-emodin in CCRF-CEM cells. Cells were incubated with various concentration of aloe-emodin for 24 h. DNA damage was measured by Comet assay. Representative pictures of C group and IC_{50} –treated group by aloe-emodin were shown above.
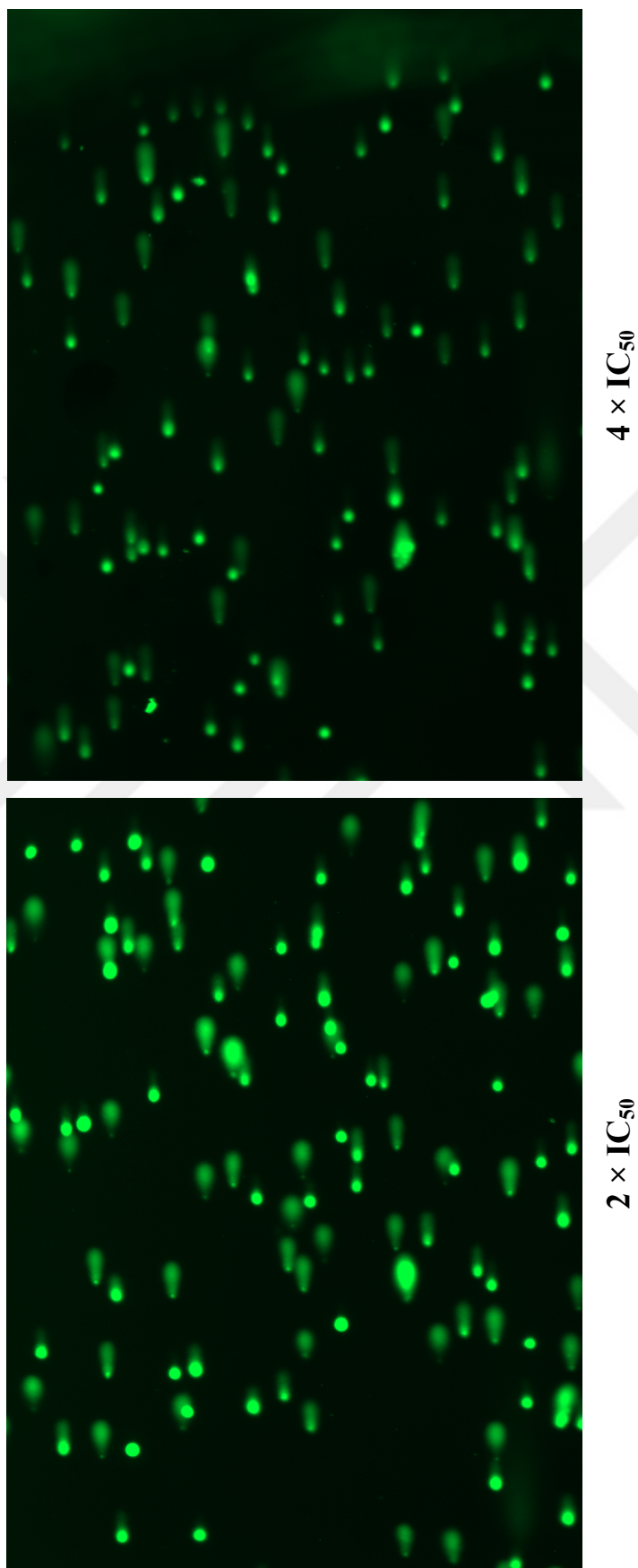
2 × IC$_{50}$

4 × IC$_{50}$

Figure 4.107. Induction of DNA damage by aloe-emodin in CCRF-CEM cells. Cells were incubated with various concentration of aloe-emodin for 24 h. DNA damage was measured by Comet assay. Representative pictures of $2 \times IC_{50}$- and $4 \times IC_{50}$ –treated groups by aloe-emodin were shown above.
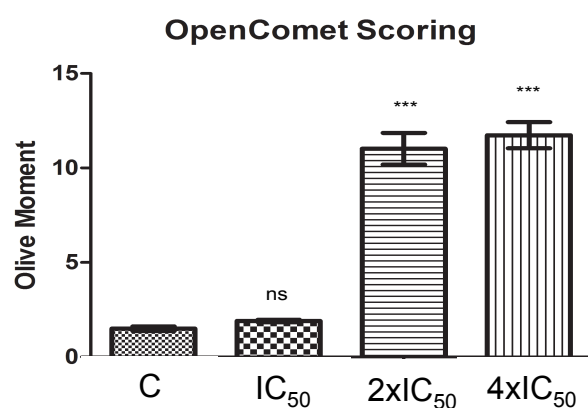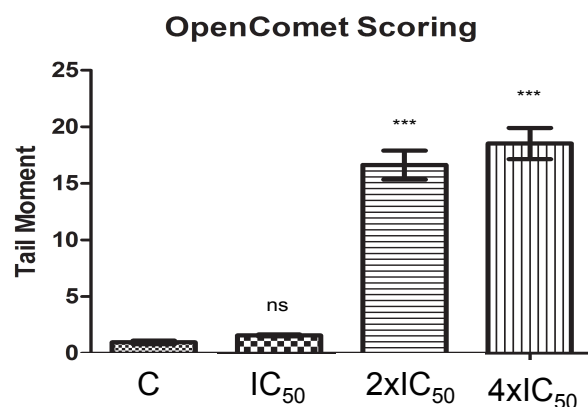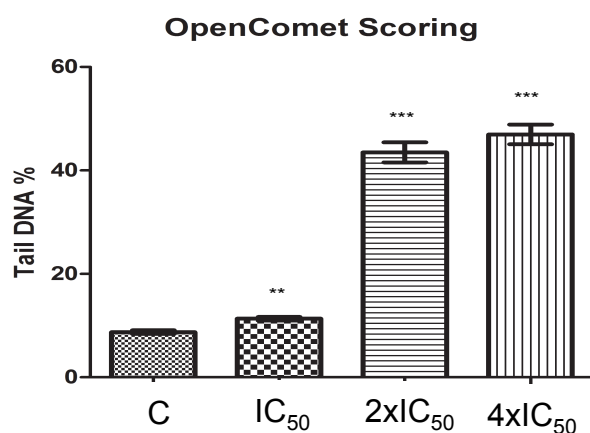
Figure 4.108. Three parameters of Comet assay were detected including tail DNA %, tail moment and olive moment. Tail and olive tail movement were presented in arbitrary units. Results were presented as mean ± SEM of at least 50 cells for each. *ns* not significant, **$p < 0.005$; ***$p < 0.0001$ as compared to control cells. *$p < 0.05$ compared with DMSO. Mean values ± SEM of three independent experiments are shown.

4.8   Cell Cycle Analysis

Pathway analysis of microarray data indicated that genes associated with cell cycle progression were deregulated by aloe-emodin. Therefore, we investigated whether aloe-emodin causes cell cycle arrest or not. We treated CCRF-CEM cells with 0.5-, 1-, 2- and 4- fold IC_{50} of aloe-emodin for 6, 24, 48 and 72 h, respectively. Indeed, the cells showed a clear arrest on S-phase of the cell cycle upon the treatment with 4- fold IC_{50} of aloe-emodin for 24 h (**Figure 4.109**.). Doxorubicin was used as a positive control and the cells treated with 0.01 μM and 0.1 μM Doxorubicin for 24 h revealed S and G2/M arrest (**Figure 4.110.**).
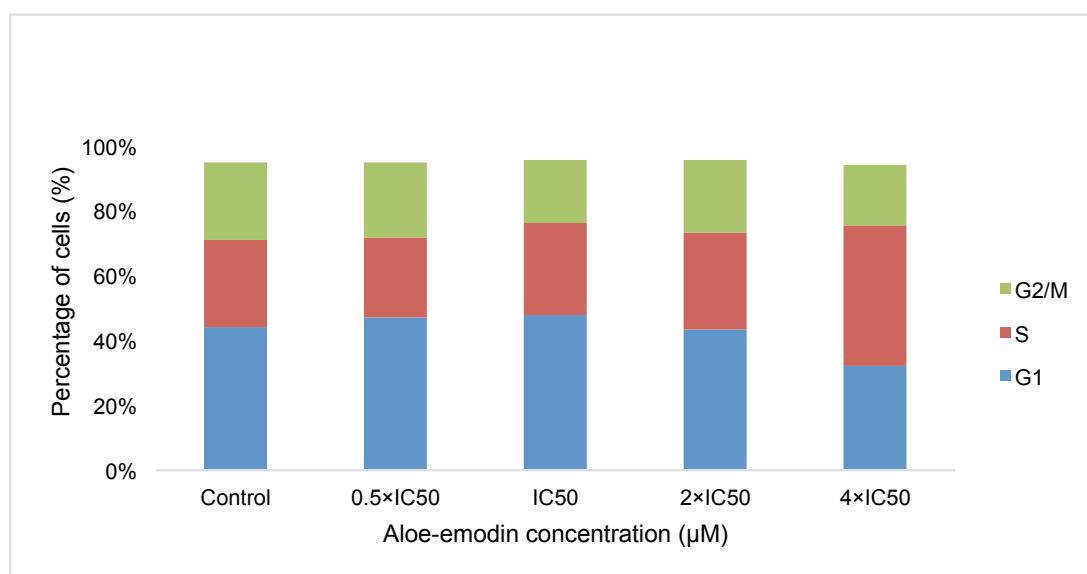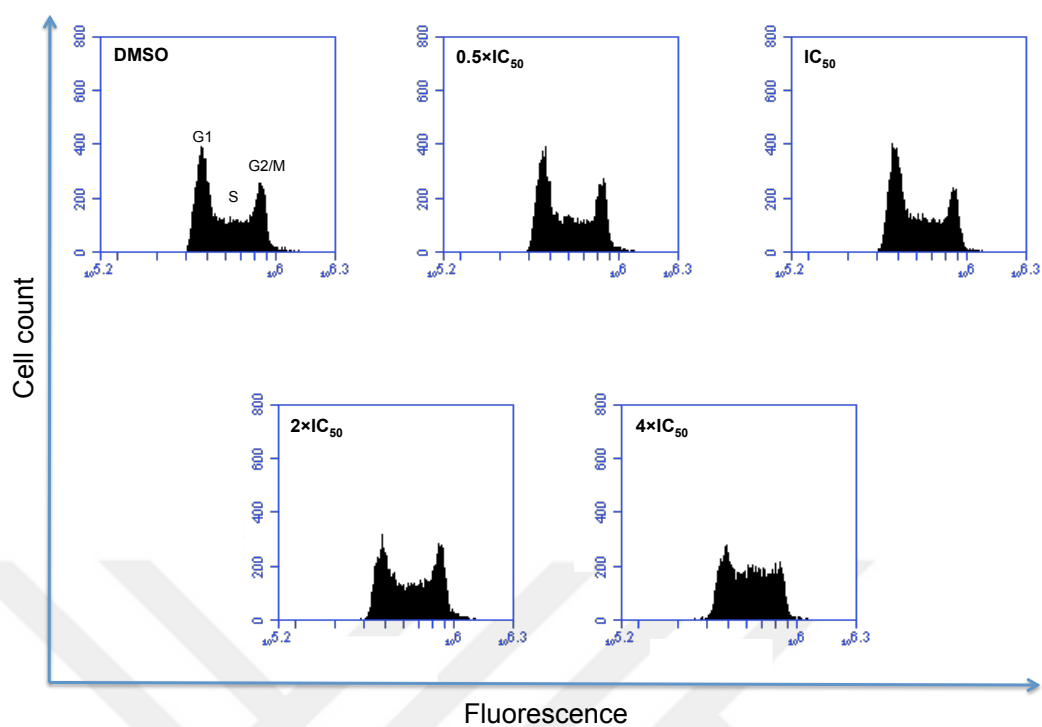
Figure 4.109. DNA histograms and cell cycle distribution of CCRF-CEM cells treated with indicated concentrations of aloe-emodin for 24 h.
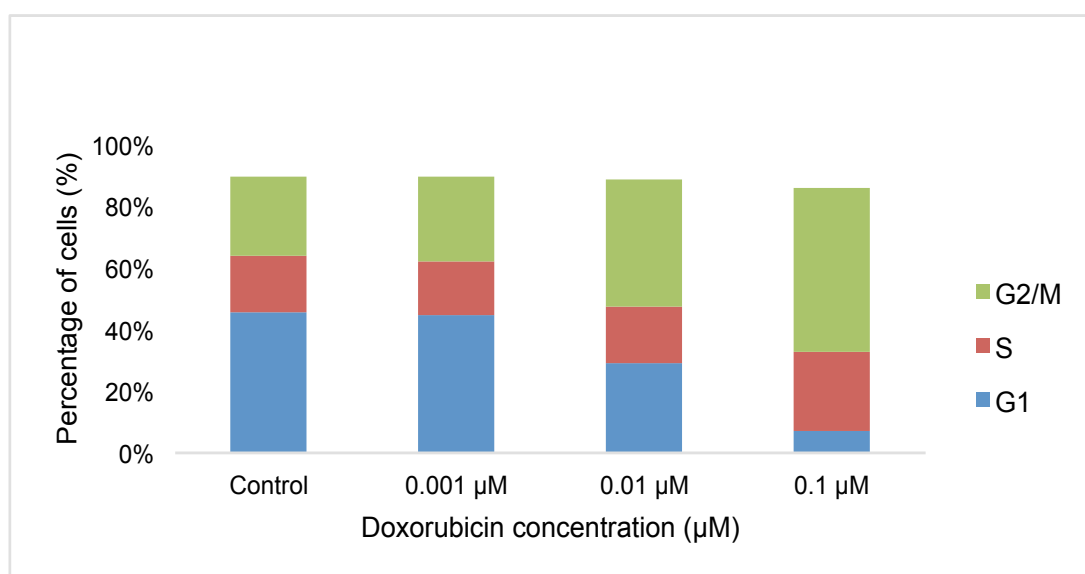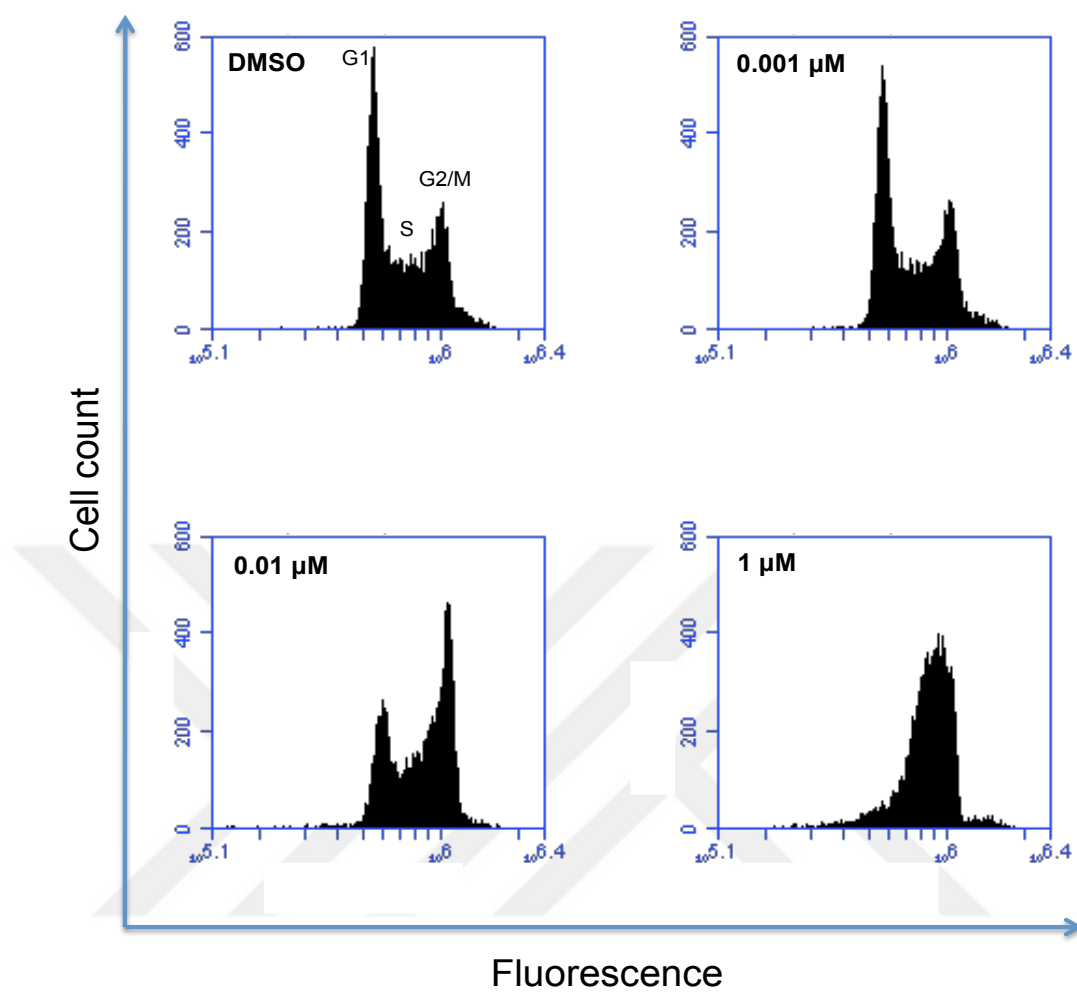
Figure 4.110. DNA histograms and cell cycle distribution of CCRF-CEM cells treated with indicated concentrations of doxorubicin, respectively for 24 h.

Aloe-emodin-induced S phase arrest can be taken as a hint that the cell cycle disturbance is a consequence of oxidative stress and DNA damage. Pathway analysis of microarray data also pointed out this hypothesis. Therefore, we investigated this hypothesis in details.

4.9 Measurement of Mitochondrial Membrane Potential

DNA damage causes apoptosis (479). Numerous apoptosis-regulating genes were deregulated according to Ingenuity Pathway Analysis of microarray data, which represents another clue for apoptosis induction following aloe-emodin exposure. An early event in mitochondria-driven apoptosis is MMP breakdown (480, 481). Mitochondria control cell death by releasing cytochrome *c* to the cytosol and followed by activating caspases (482).

We analyzed possible alterations of MMP in CCRF-CEM cells. Therefore, we treated the cells with 1-, 2- and 4-fold IC_{50} of aloe-emodin, respectively and incubated for 24 and 48 h. Doxorubicin was further tested as a positive control at 0.001, 0.01, 0.1 and 1 μM for 48 h. JC-1-stained CCRF-CEM cells revealed a shift from red to green fluorescence following 2- and 4-fold IC_{50} treatment of aloe-emodin (**Figures 4.111.** and **4.112.**) and 0.01, 0.1, 1 μM treatment of doxorubicin for 48 h (**Figure 4.113.**), indicating MMP depolarization.
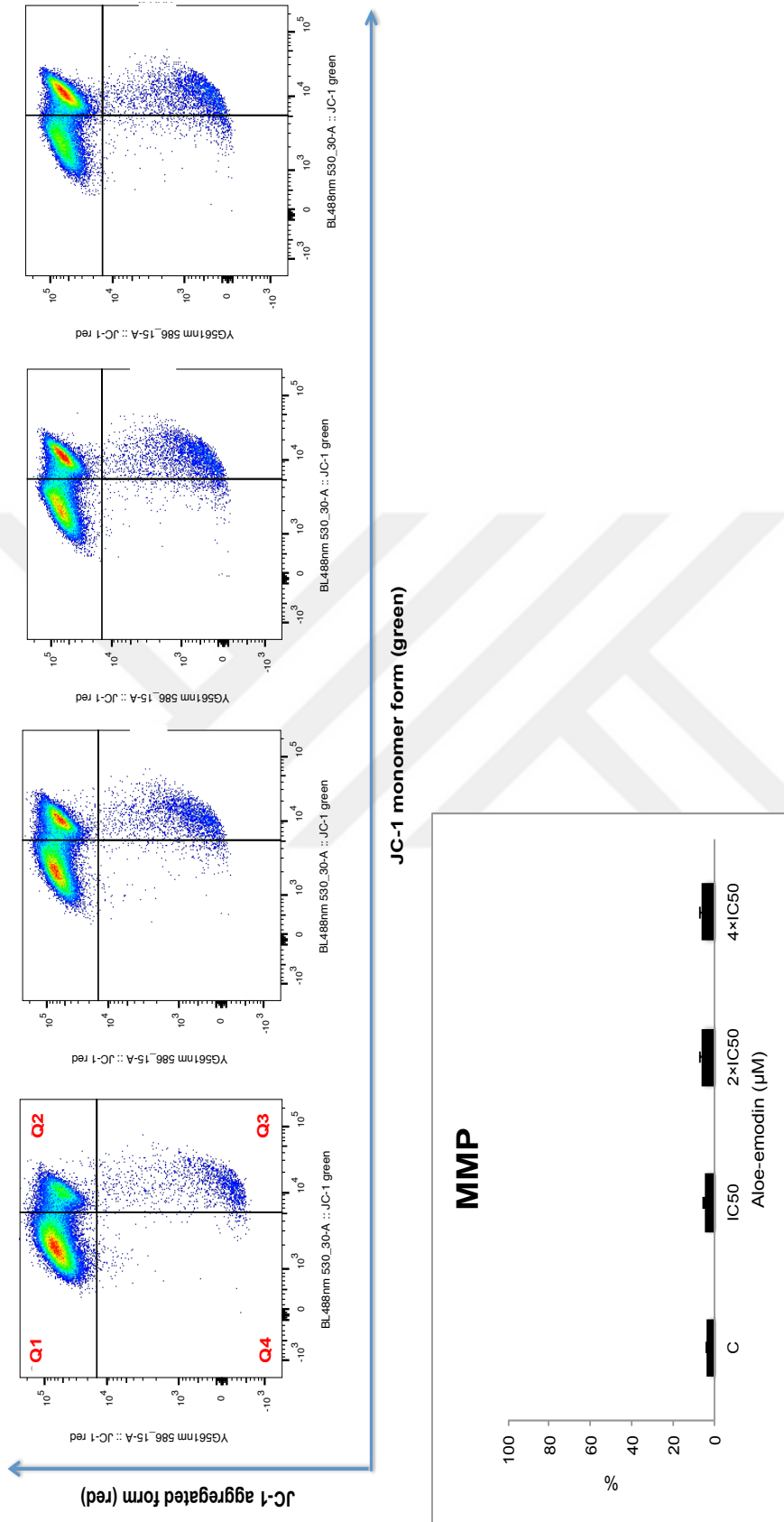
Figure 4.111. MMP disruption by aloe-emodin in CCRF-CEM cells. Cells were treated with or without DMSO as negative control and 1-, 2- and 4- fold IC_{50} values of aloe-emodin for 24 h and stained by JC-1. Healthy cells mainly displayed the J-aggregated form with red fluorescence (Q1) and cells with loss of MMP showed JC-1 monomers with green fluorescence (Q3). Statistical results of the cell population in Q3, which was defined as disruption of mitochondrial membrane potential with aloe-emodin treatment for 24 h. Mean values ± SD of three independent experiments are shown.
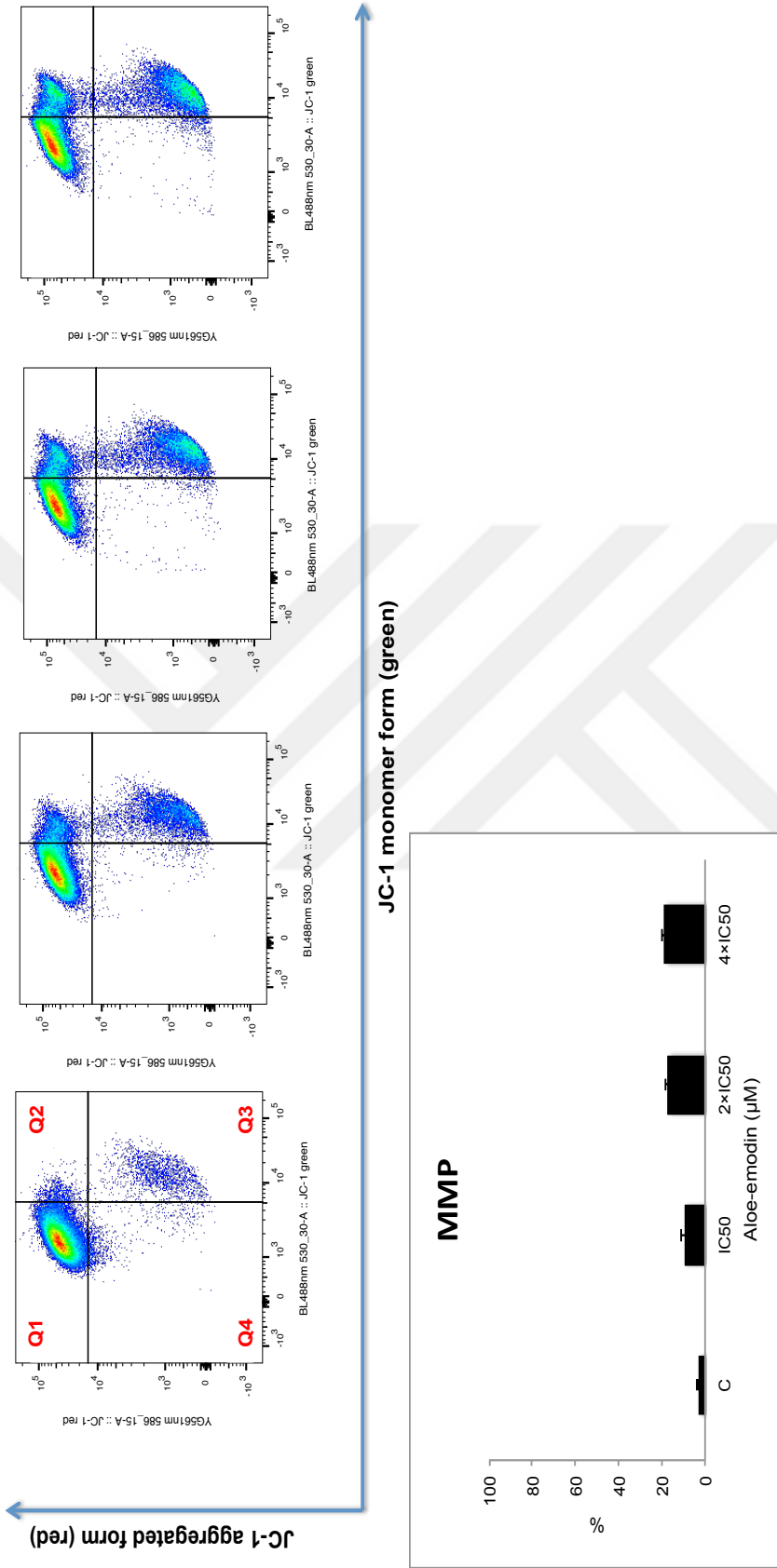
Figure 4.112. MMP disruption by aloe-emodin in CCRF-CEM cells. Cells were treated with or without DMSO as negative control and 1-, 2- and 4- fold IC_{50} values of aloe-emodin for 48 h and stained by JC-1. Healthy cells mainly displayed the J-aggregated form with red fluorescence (Q1) and cells with loss of MMP showed JC-1 monomers with green fluorescence (Q3). Statistical results of the cell population in Q3, which was defined as disruption of mitochondrial membrane potential with aloe-emodin treatment for 48 h. Mean values ± SD of three independent experiments are shown.
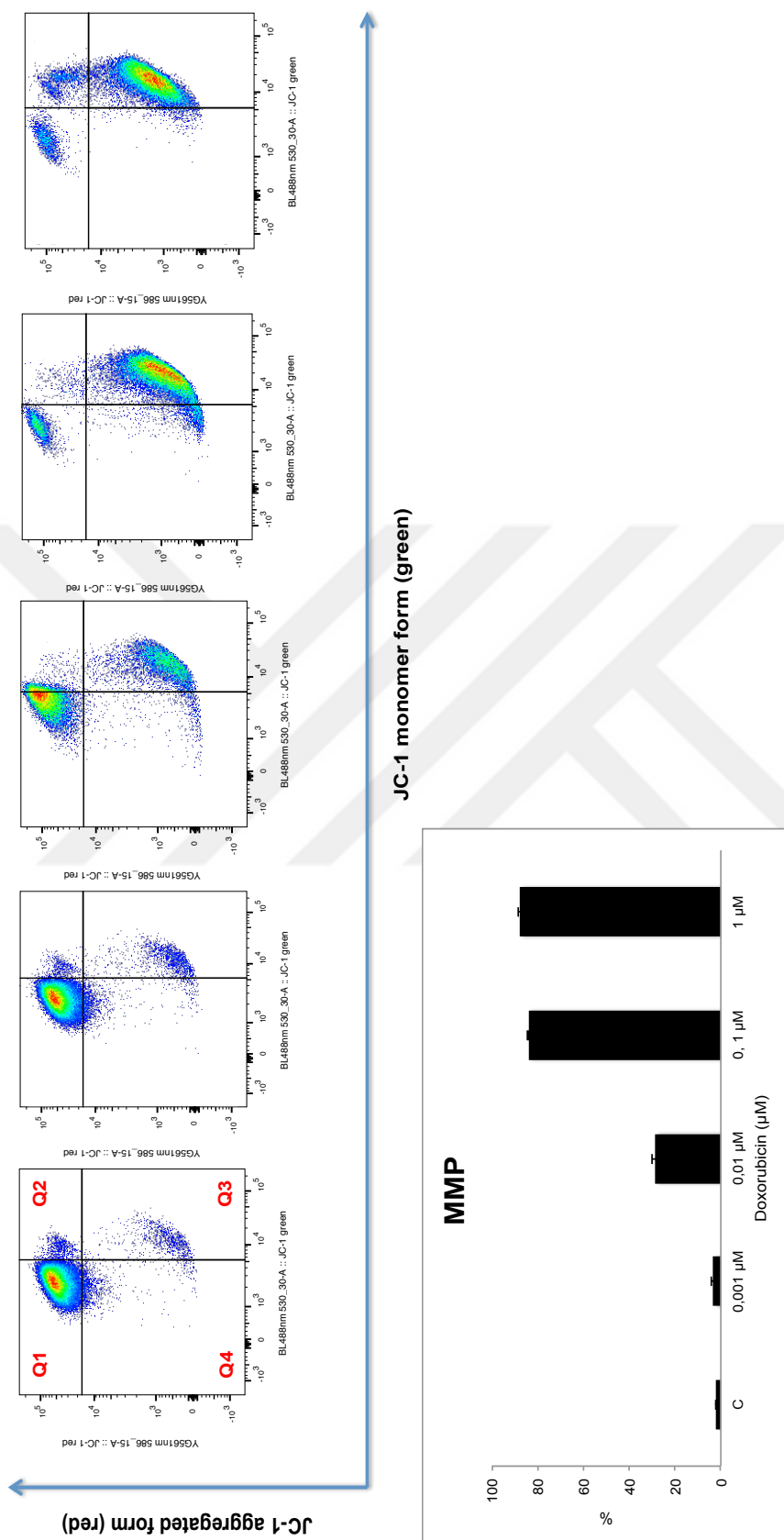
Figure 4.113. MMP disruption by doxorubicin in CCRF-CEM cells. Cells were treated with or without DMSO as negative control or with 0.001, 0.01, 0.1 and 1 μM Doxorubicin as positive control for 48 h and stained by JC-1. Healthy cells mainly displayed the J-aggregated form with red fluorescence (Q1) and cells with loss of MMP showed JC-1 monomers with green fluorescence (Q3). Statistical results of the cell population in Q3, which was defined as disruption of mitochondrial membrane potential by doxorubicin for 48 h. Mean values ± SD of three independent experiments are shown.

4.10   Detection of Early Apoptosis and Necrosis

We performed annexin V/PI staining to detect apoptotic or necrotic cell death on CCRF-CEM cells. The gated cells show the populations corresponding to viable and non-apoptotic (Annexin V^-PI^-), early (Annexin V^+PI^-), and late apoptotic and early necrotic (Annexin V^+PI^+), late necrotic (Annexin V^-PI^+) cells. Aloe-emodin induced early, late apoptosis and early, late necrosis with the treatment of 47.8 μM corresponding to its $4\times IC_{50}$ for 72h or early, late apoptosis and early, late necrosis with the treatment of 23.9 μM, 47.8 μM corresponding to its $2\times IC_{50,}$ $4\times IC_{50,}$ respectively, for 96 h (**Figures 4.114.** and **4.115.**), whereas clinically used doxorubicin inclined late apoptosis and early necrosis at 0.1 μM or late necrosis at 1 μM for 72 h treatment (**Figure 4.116.**).
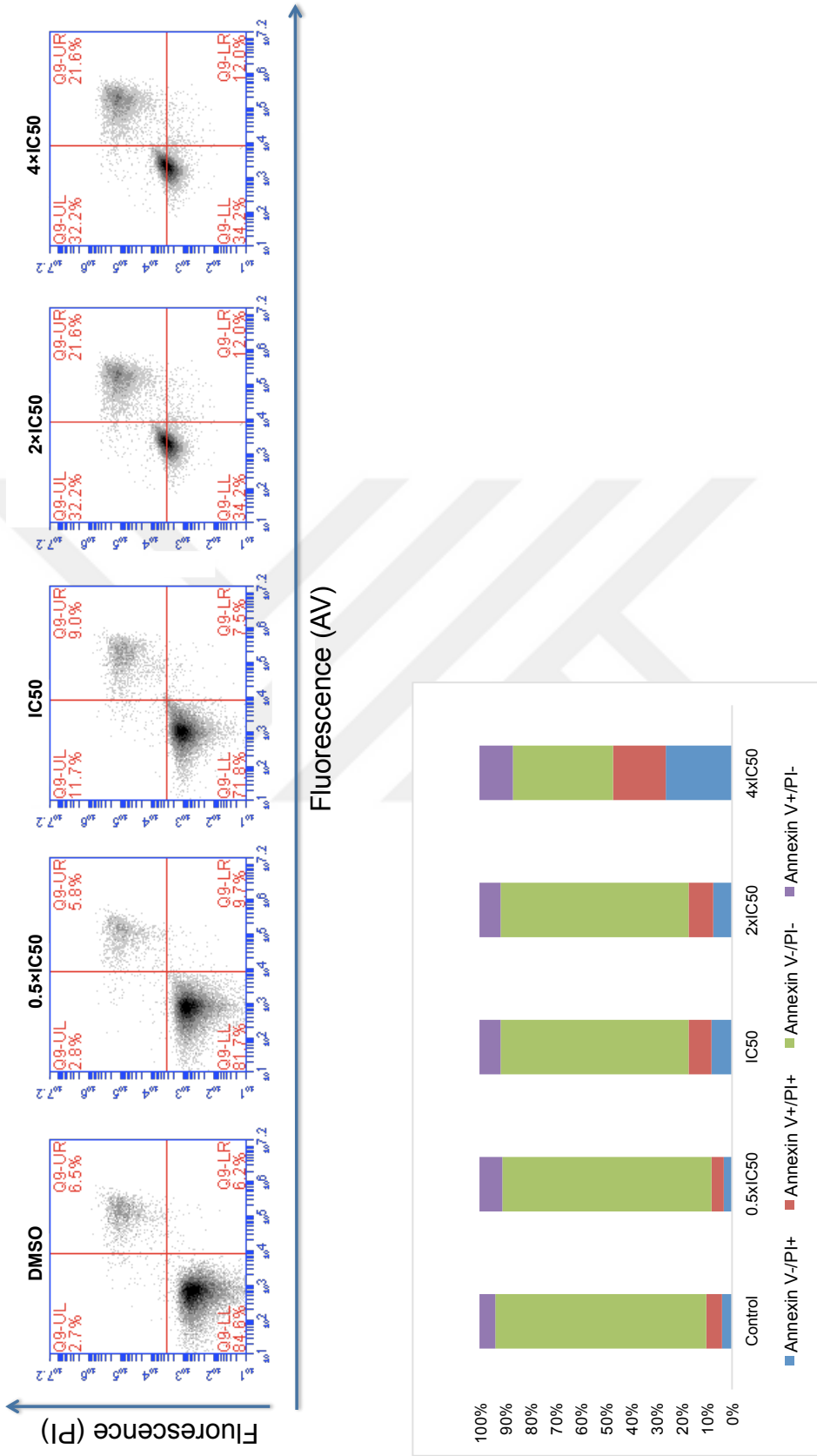
Figure 4.114. Apoptosis effect in CCRF-CEM cells of aloe-emodin for 72 h.
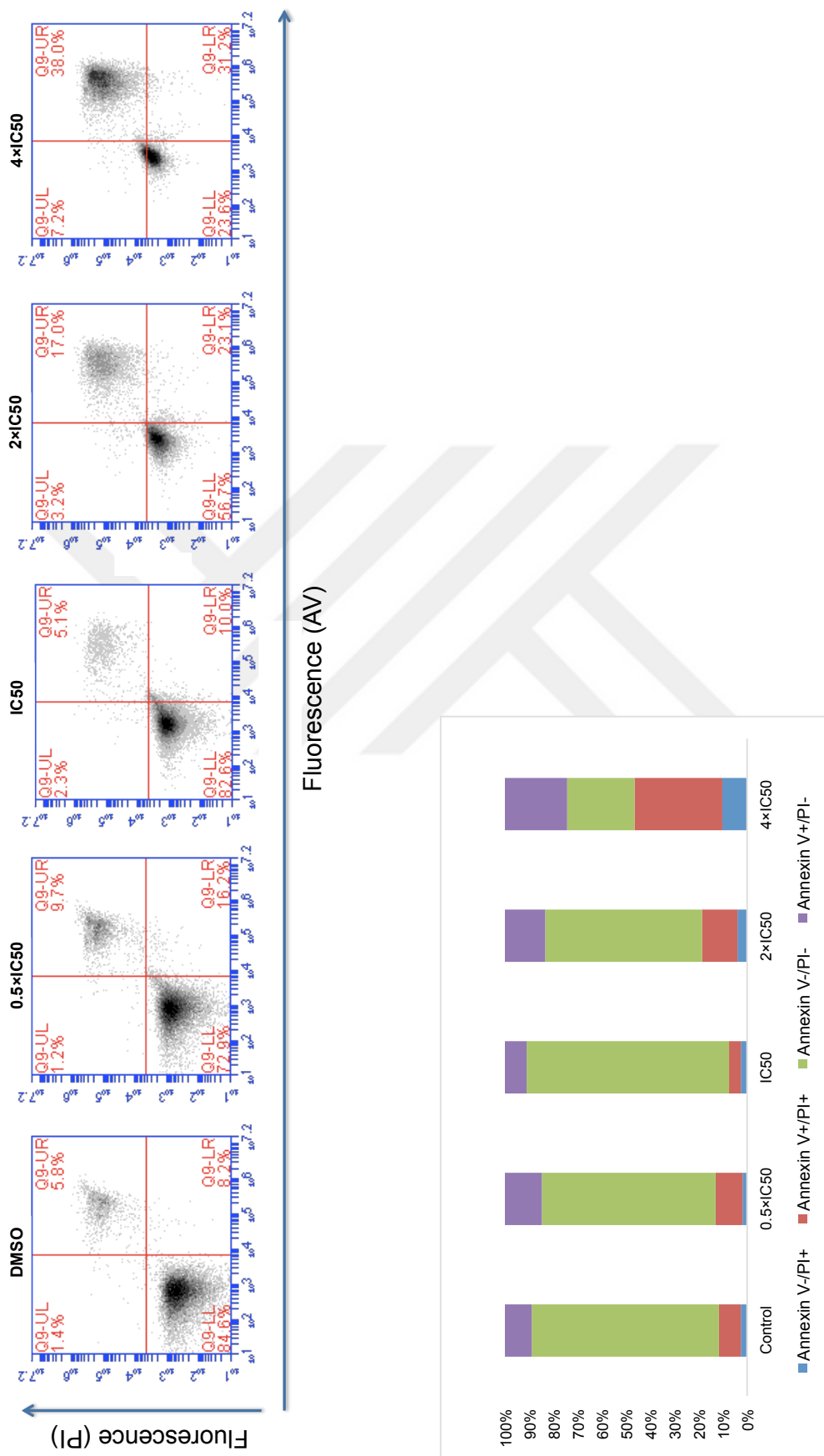
Figure 4.115. Apoptosis effect in CCRF-CEM cells of aloe-emodin for and 96 h.
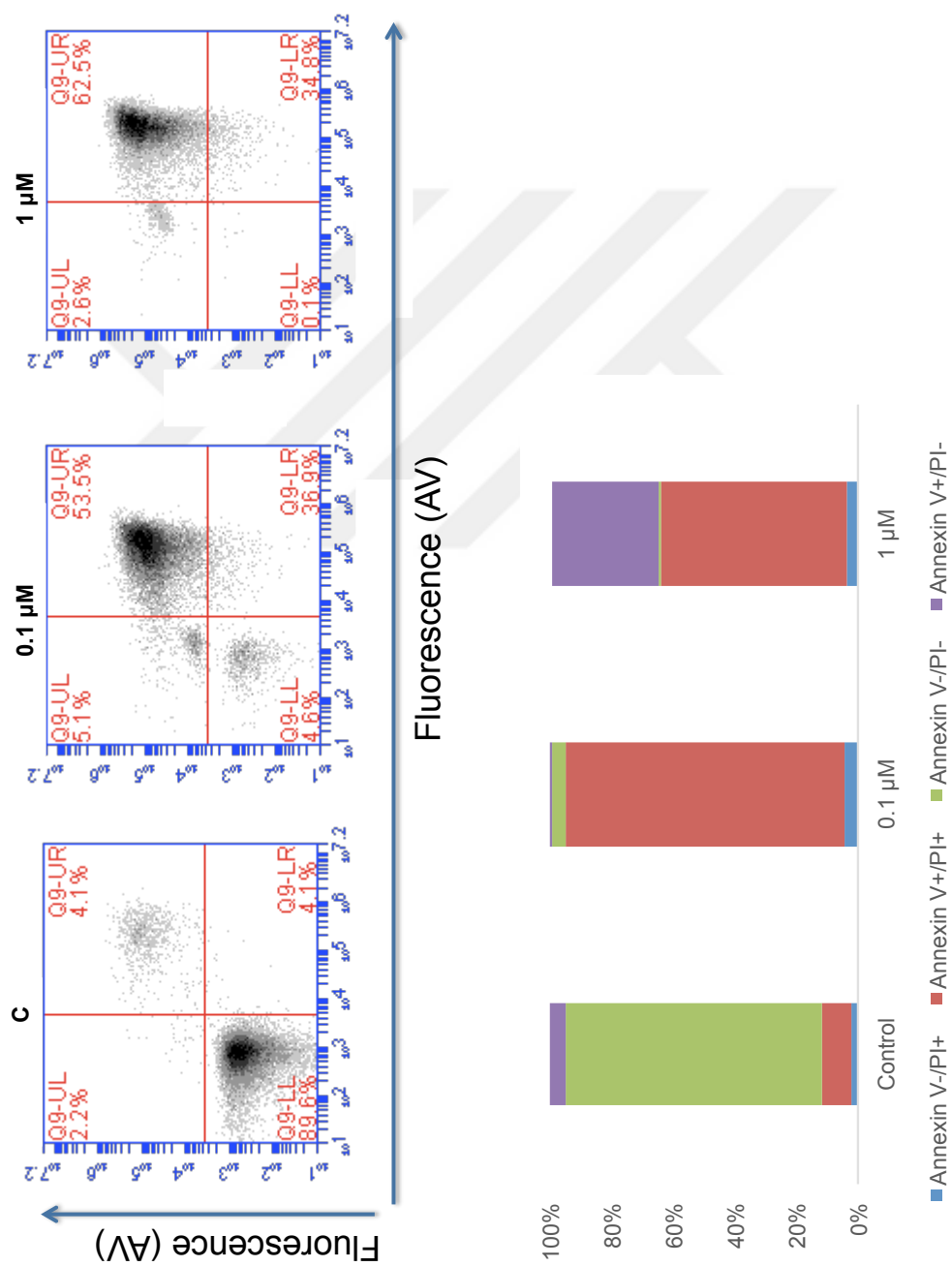
Figure 4.116. Apoptosis effect in CCRF-CEM cells of doxorubicin for 72 h.

4.11 COMPARE and Hierarchical Cluster Analysis of Transcriptome-Wide mRNA Expression in Untreated Cell Lines

The mRNA microarray data of the NCI tumor cell lines has been reported and deposited at the NCI website. COMPARE analyses were applied to generate rank-ordered lists of genes expressed in the NCI cell lines as previously described (462, 483). Briefly, every gene of the NCI microarray database was ranked for similarity of its mRNA expression to the $\log_{10}IC_{50}$ values for aloe-emodin. To derive COMPARE rankings, a scale index of correlation coefficients (R-values) was created (**Table 4.42.**).

The mRNA expression data of the cell lines were submitted to hierarchical cluster analyses. Each three main cluster branches appeared in the dendrogram for aloe-emodin (**Figure 4.117.**). We examined the distribution of sensitive or resistant cells to aloe-emodin by using the chi-square (χ^2) test.

To perform the χ^2-test, we defined the cell lines as being sensitive or resistant to Aloe-emodin. The $\log_{10}IC_{50}$ value of Aloe-emodin for all cell lines (−4.35 M) served as cut-off threshold. Cell lines with $\log_{10}IC_{50}$ values below this threshold were defined as sensitive while, cell lines above this threshold as resistant. Cluster 1 and cluster 3 contained mainly sensitive and resistant cell lines, respectively, whereas cluster 2 was of a mixed type. This distribution of sensitive and resistant cell lines was statistically significant (χ^2 test, $P = 5.90 \times 10^{-7}$; **Table 4.43.**). This implies that the expression of this set of genes caused dendrogram branching in a way that gene expression predicted the inherent cellular responsiveness to Aloe-emodin in a statistically significant manner.

The analysis of microarray data showed that, genes involved in signal transduction, apoptosis, nucleic acid metabolism etc. seemed to have a role for inherent resistance responsiveness of tumor cells towards aloe-emodin.

Table 4.42. Correlation of constitutive mRNA expression of genes identified by COMPARE analyses with the $\log_{10}IC_{50}$ values of aloe-emodin for the NCI tumor cell lines.

COMPARE coefficient	Experimental ID	GeneBank Accession	Gene Symbol	Name	Function
0.641	29457	Y00978	DLAT	Dihydrolipoamide S-acetyltransferase	Transferase activity; links the glycolytic pathway to the tricarboxylic cycle
0.614	23142	D50929	EIF3A	Eukaryotic translation initiation factor 3, subunit A	Involved in apoptosis of synovial fibroblasts
0.613	31751	AF047042	CS	Citrate synthase	Poly(A) RNA binding and citrate (Si)-synthase activity; mitochondrial targeting
0.584	25141	D21851	LARS2	Leucyl-tRNA synthetase 2, mitochondrial	Nucleotide binding and aminoacyl-tRNA editing activity
0.581	31188	AF081280	NPM3	Nucleophosmin/nucleoplasmin 3	Poly(A) RNA binding
0.57	24945	S79522	RPS27A	Ribosomal protein S27a	Poly(A) RNA binding and structural constituent of ribosome
0.561	22197	AB011136	KIAA0564	KIAA0564	ATPase activity
0.558	25753	AB018307	SUPT7L	Suppressor of Ty 7 (S. cerevisiae)-like	Transcription coactivator activity and histone acetyltransferase; role in chromatin activation, transcriptional regulation, and DNA damage repair
0.551	31083	D50925	PASK	PAS domain containing serine/threonine kinase	Transferase activity; protein tyrosine kinase activity
0.545	28659	D26488	WDR43	WD repeat domain 43	Poly(A) RNA binding and binding
0.533	22297	X79563	RPS21	Ribosomal protein S21	Poly(A) RNA binding and protein N-terminus binding

Table 4.42. Correlation of constitutive mRNA expression of genes identified by COMPARE analyses with the $\log_{10}IC_{50}$ values of aloe-emodin for the NCI tumor cell lines (continued).

COMPARE coefficient	Experimental ID	GeneBank Accession	Gene Symbol	Name	Function
0.524	30065	U94703	POLG2	Polymerase (DNA directed), γ2, accessory subunit	Identical protein binding and DNA-directed DNA polymerase activity
0.523	23131	AI541050	NDUFB8	NADH dehydrogenase (ubiquinone) 1 β subcomplex, 8, 19 kDa	NADH dehydrogenase (ubiquinone) activity and NADH dehydrogenase activity
0.521	30499	X16396	MTHFD2	Methylenetetrahydrofolate dehydrogenase (NADP$^+$ dependent) 2, methenyltetrahydrofolate cyclohydrolase	Magnesium ion binding and formate-tetrahydrofolate ligase activity
0.516	29266	D79989	AGAP2	ArfGAP with GTPase domain, ankyrin repeat and PH domain 2	GTP binding and GTPase activator activity mediates anti-apoptotic effects of nerve growth factor is overexpressed in cancer cells, and promotes cancer cell invasion
0.515	32195	M92439	LRPPRC	Leucine-rich PPR-motif containing	Poly(A) RNA binding and ubiquitin protein ligase binding
0.514	25646	AF067139	NDUFS3	NADH dehydrogenase (ubiquinone) Fe-S protein 3, 30kDa (NADH-coenzyme Q reductase)	Poly(A) RNA binding and ubiquitin protein ligase binding; transcriptional regulation of both nuclear and mitochondrial genes
0.506	25108	D80007	PDCD11	Programmed cell death 11	Nucleic acid binding and transcription factor binding; required for rRNA maturation and generation of 18S rRNA

Table 4.42. Correlation of constitutive mRNA expression of genes identified by COMPARE analyses with the $\log_{10}IC_{50}$ values of aloe-emodin for the NCI tumor cell lines (continued).

COMPARE coefficient	Experimental ID	GeneBank Accession	Gene Symbol	Name	Function
0.506	31640	L49380	*SF1*	Splicing factor 1	Nucleic acid binding and RNA binding; plays a role in nuclear pre-mRNA retention and transcriptional repression
0.502	32348	U66615	*SMARCC1*	SWI/SNF related, matrix associated, actin dependent regulator of chromatin, subfamily c, member 1	Chromatin binding and RNA polymerase II core promoter proximal region sequence-specific DNA binding
-0.606	27140	AL096739	*GALNT10*	UDP-N-acetyl-α-D-galactosamine:polypeptide N-acetylgalactosaminyltransferase 10 (GalNAc-T10)	Carbohydrate binding and polypeptide N-acetylgalactosaminyltransferase activity
-0.581	24659	AB023175	*POFUT2*	Protein O-fucosyltransferase 2	Fucosyltransferase activity and peptide-O-fucosyltransferase activity
-0.547	28663	AB020689	*TBC1D9*	TBC1 domain family, member 9 (with GRAM domain)	Calcium ion binding and GTPase activator activity
-0.546	24243	AI547262	*ATP6V0E1*	ATPase, H$^+$ transporting, lysosomal 9 kDa, V0 subunit e1	Transporter activity and proton-transporting ATPase activity, rotational mechanism; encodes a component of vacuolar ATPase (V-ATPase) which is necessary for diverse intracellular processes

Table 4.42. Correlation of constitutive mRNA expression of genes identified by COMPARE analyses with the $\log_{10}IC_{50}$ values of aloe-emodin for the NCI tumor cell lines (continued).

COMPARE coefficient	Experimental ID	GeneBank Accession	Gene Symbol	Name	Function
-0.545	32200	Z47087	*SKP1*	S-phase kinase-associated protein 1	Ubiquitin-protein transferase activity; encodes an essential component of SCF complex which mediates ubiquitination of proteins involved in cell cycle progression, signal transduction and transcription
-0.542	31737	AA477898	*ITM2B*	Integral membrane protein 2B	β-amyloid binding plays a regulatory role in processing of β-amyloid A4 precursor protein (APP); inhibitor of β-amyloid peptide aggregation and fibrils deposition
-0.538	23424	L07738	*CACNG1*	Calcium channel, voltage-dependent, γ subunit 1	Voltage-gated calcium channel activity; role in excitation-contraction coupling
-0.536	29496	M88458	*KDELR2*	KDEL (Lys-Asp-Glu-Leu) endoplasmic reticulum protein retention receptor 2	ER (endoplasmic reticulum) retention sequence binding and KDEL (Endoplasmic Reticulum Protein Retention Receptor 2) sequence binding.
-0.532	22897	AF063002	*FHL1*	Four and a half LIM domains 1	Ion channel binding
-0.531	24272	AB007144	*DAPK3*	Death-associated protein kinase 3	Protein homodimerization activity and transferase activity; role in induction of apoptosis

Table 4.42. Correlation of constitutive mRNA expression of genes identified by COMPARE analyses with the $\log_{10}IC_{50}$ values of aloe-emodin for the NCI tumor cell lines (continued).

COMPARE coefficient	Experimental ID	GeneBank Accession	Gene Symbol	Name	Function
-0.531	30005	AB020640	*CAMTA1*	Calmodulin binding transcription activator 1	Transcriptional activator; may act as tumor suppressor
-0.527	29746	D86983	*PXDN*	Peroxidasin homologue (*Drosophila*)	Heme binding and peroxidase activity; involved in extracellular matrix formation; may function in the physiological and pathological fibrogenic response in fibrotic kidney
-0.526	29587	AL049957	*CD59*	CD59 molecule, complement regulatory protein	Complement binding; encodes a cell surface glycoprotein that regulates complement-mediated cell lysis; involved in lymphocyte signal transduction
-0.524	22562	M83088	*PGM1*	Phosphoglucomutase 1	Magnesium ion binding and phosphoglucomutase activity; participates in both breakdown and synthesis of glucose
-0.523	20761	L25081	*RHOC*	Ras homolog gene family, member C	GTP binding and signal transducer activity; overexpression is associated with tumor cell proliferation and metastasis
-0.522	30218	D63475	*AP2M1*	Adaptor-related protein complex 2, μ 1 subunit	Transporter activity and low-density lipoprotein particle receptor binding

Table 4.42. Correlation of constitutive mRNA expression of genes identified by COMPARE analyses with the $\log_{10}IC_{50}$ values of aloe-emodin for the NCI tumor cell lines (continued).

COMPARE coefficient	Experimental ID	GeneBank Accession	Gene Symbol	Name	Function
-0.522	26170	H93123	VAMP3	Vesicle-associated membrane protein 3 (cellubrevin)	SNARE binding and syntaxin-1 binding
-0.516	20862	L77886	PTPRK	Protein tyrosine phosphatase, receptor type, K	Protein kinase binding and protein tyrosine phosphatase activity; regulation of processes involving cell contact and adhesion (growth control, invasion, and metastasis)
-0.511	32199	AL096879	TMEM184B	Transmembrane protein 184B	May activate the MAP kinase signaling pathway
-0.51	27189	Z24727	TPM1	Tropomyosin 1 (α)	Actin binding and cytoskeletal protein binding; suppresses anchorage-independent growth

Positive correlation coefficients indicate direct correlations to $\log_{10}IC_{50}$ values, negative ones indicate inverse correlations. Information on gene functions was taken from the OMIM database (NCBI, Bethesda, MD, USA) (484) and from the GeneCards database of the Weizman Institute of Science (Rehovot, Israel) (485).

Table 4.43. Separation of clusters of NCI cell line panel obtained by hierarchical cluster analysis shown in **Figure 4.111.** in comparison to drug sensitivity[a].

	Partition	Cluster 1	Cluster 2	Cluster 3
Sensitive	< -4.35 M	0	8	12
Resistant	> -4.35 M	16	5	0
chi-square test: p= 5.90 ×10^{-7}				

[a]The median $\log_{10} IC_{50}$ value (-4.35 M) for each compound was used as a cutoff to separate tumor cell lines as being "sensitive" or "resistant".
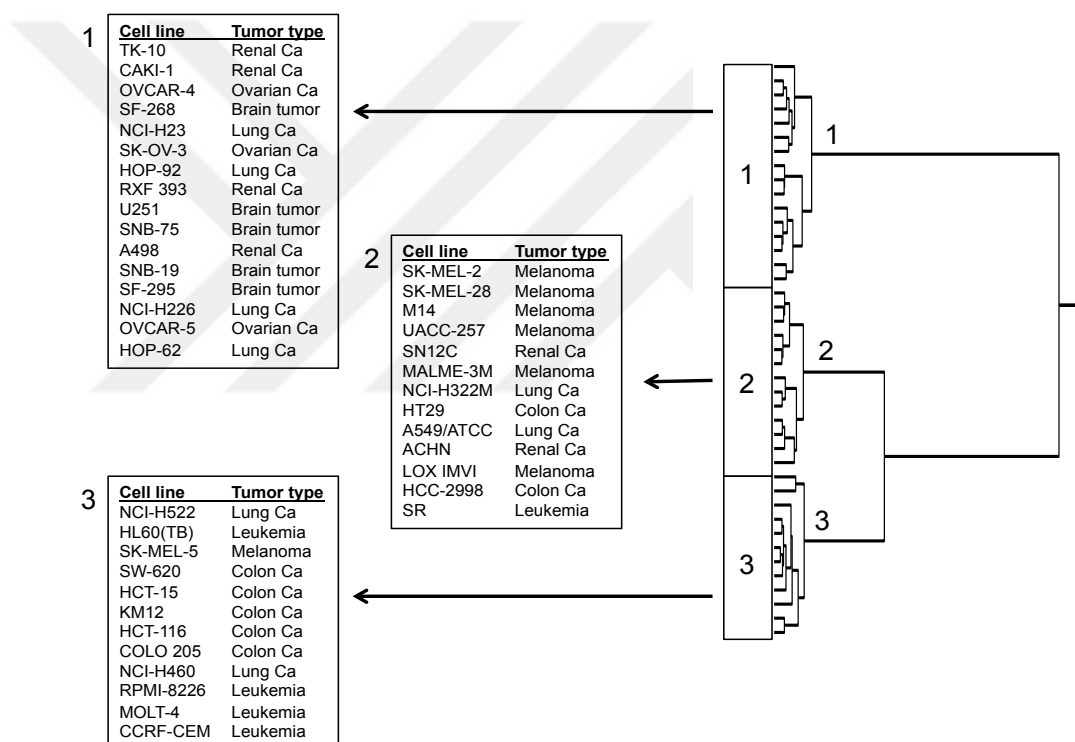
Figure 4.117. Hierarchical cluster analysis of microarray-based mRNA expression of genes for aloe-emodin. The dendrograms show the clustering of the NCI cell line panel according to the degrees of relatedness between cell lines.

4.12 Gene Promoter Binding Motif Analysis

The genes identified by COMPARE analysis (**Table 4.42.**) were subjected to gene promoter binding motif analysis to evaluate their regulation at transcription level. We hypothesized that genes with high frequency of binding motifs in their promoters for NF-κB may be tightly regulated by this transcription factor. Cistrome analysis recognizes binding sites for transcription factors in DNA promoter regions. Therefore, we investigated the DNA promoter sequences of 40 genes identified by COMPARE analysis for NF-κB which were screened 75 kb upstream of the transcription start site of the genes of interest and significantly associated with cellular responsiveness to aloe-emodin. All 40 genes identified by COMPARE analysis was observed to have NF-κB binding motifs being remarkably enriched (with a log p-value of -18.92) with 50 hits (**Figure 4.118.**, **Table 4.44.**), which showed NF-κB elements including NF-κB may have a notable function for the regulation of genes associated with cellular response to aloe-emodin

Table 4.44. Binding motifs for NF- κB in the promoter region of 40 genes, which were significantly associated with cellular responsiveness to aloe-emodin in the NCI cell line panel.

Gene symbol	Chromosome	Start	End	Binding sequence
1. DLAT	chr11	111997749	111997763	TTGTGCATATATAG
2. RPS21	chr10	119113652	119113666	TTTTTGTGCGTGAA
3. CS	chr12	56344136	56344150	CTGGATACCCAAAG
4. LARS2	chr3	45350094	45350108	TGTTGCCTTGATGG
5. NPM3	chr10	101825017	101825031	GTGAAGCTTAGTCA
6. RPS27A	chr2	55215906	55215920	CTATCTCAACATCT
7. KIAA0564	chr13	41999752	41999766	TCTATCTCTGCACT
8. SUPT7L	chr2	27701145	27701159	ACTTTTACTACTA
9. PASK	chr2	241219240	241219254	CTAATGTTGGAGCA
10. WDR43	chr2	28863756	28863770	TAGATAATATTCAT
11. RPS21	chr20	62386554	62386568	GAATTTCTCCTCTG
12. POLG2	chr17	64562714	64562728	AAGCAATGGGTTTC
13. NDUFB8	chr10	100572948	100572962	ATTTGAGGACTTGT
14. MTHFD2	chr2	74172271	74172285	GTCACAGACCACAA
15. AGAP2	chr12	57797085	57797099	AGGTGCTCTGCAGT
16. LRPPRC	chr2	44045417	44045431	GAATGTCTGCTAAA
17. NDUFS3	chr11	47542435	47542449	GAGATCCATTAGGT
18. PDCD11	chr10	103353129	103353143	AGGGGTGGTAGCTC
19. SF1	chr9	124552393	124552407	GCACAGCAGTGTAA
20. SMARCC1	chr3	47813678	47813692	CCTGATTGTGTCTT
21. GALNT10	chr5	154161773	154161787	TCTATAAAGTGAC
22. POFUT2	chr21	45345205	45345219	CTGGATTTTCAACA
23. *TBC1D9*	chr4	140798131	140798145	GGTGAGCACGGAGT
24.ATP6V0E1	chr5	172939868	172939882	ACGTACACACACGG
25. SKP1	chr5	134228623	134228637	TAAGGAATGAATTC
26. *ITM2B*	chr13	48212117	48212131	AGAACGTCCCTGTT
27. *CACNG1*	chr17	67002469	67002483	AAGAACTGTTCTCA
28. *KDELR2*	chr7	6519981	6519995	ATGCTGCAGGTGGG
29. FHL1	chrX	136106408	136106422	GAGAGTTATTAAGA
30. DAPK3	chr19	4007477	4007491	CCCACCTGCGCAGG
31. CAMTA1	chr1	6746269	6746283	AGGCAGCTCCCTAC
32. PXDN	chr2	1810469	1810483	TGTGTTTATTCTCT
33. *CD59*	chr11	33780595	33780609	ATTGGCCTGTTTTG
34. *PGM1*	chr1	63566587	63566601	CCTCTTTGGTTGAA
35. RHOC	chr1	112758006	112758020	TGCAGCAGGGCTGA
36. *AP2M1*	chr3	184140611	184140625	CTGAGGTCAGCCTG
37. VAMP3	chr1	7737258	7737272	TGGGCGTGTGCCCT
38. PTPRK	chr6	128573205	128573219	NNCCAGGGCTTTT
39. TMEM184B	chr22	38310244	38310258	ATGAGTCAGACACA
40. TPM1	chr15	63000315	63000329	ATTCATAGCACCTG
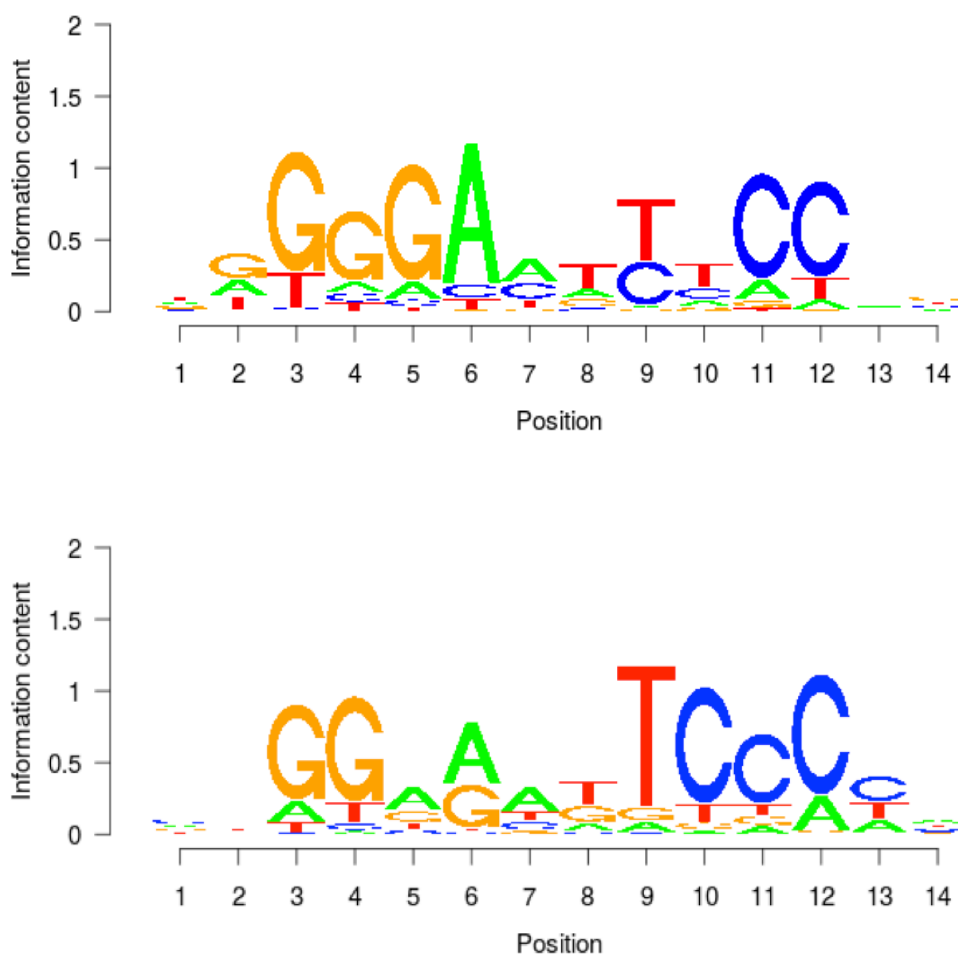
Figure 4.118. Motif analysis of 75 kb upstream regions of 40 genes identified by COMPARE analysis revealing the presence of NF-κB binding motif. NFκB1 (id M00194); DBD: RHR (Rel homology region); cutoff: 7.186; z-score: -5.697; -10log (p-value): 189.155.

4.13   NF-κB Reporter Assay

NF-κB plays not only an important role in inflammation and immunity, but also in cancer initiation, progression and inhibition of programmed cell death (486-488), indicating that it is a crucial target for cancer theraphy.

Based on IPA of microarray data and gene promoter binding motif analysis, NF-κB may be an important target and act as transcriptional regulator of genes associated with cellular responsiveness to aloe-emodin. Therefore, it was assumed that NF-κB could be important for aloe-emodin's effect towards CCRF-CEM cells. The microarray data indicated that NF-κB was shown to be downregulated by aloe-emodin in CCRF-CEM cells by several pathways (**Figure 4.102. and 4.103.**) Additionally, *TNF*, *CD48*, *HLA-B*, *CD44*, *ALOX5AP*, *BNIP3*, *ANGPT1*, *MDK, NF-κB1*, *STAT5a*, *G6PD*, *PRKCD*, *S100A10*, *S100A6* as NF-κB target genes were seen to be downregulated. Therefore, a SEAP-driven NF-κB reporter cell line was used to prove a possible role for aloe-emodin. Indeed, aloe-emodin induced a dose-dependent inhibition on NF-κB transcriptional activity (**Figure 4.119.**). Triptolide treatment (1 μM) for 1 h served as positive control.
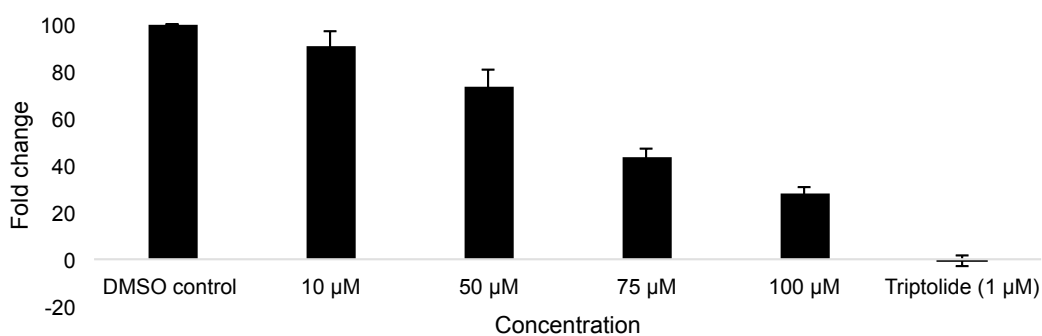
Figure 4.119. Inhibition of transcriptional activity of NF-κB by aloe-emodin in a SEAP-driven NF-κB reporter cell line. Mean values ± SD of three independent experiments are shown.

4.14   Molecular Docking

The results of the pathway analysis of microarray data, motif analysis and reporter assay indicate that we commented that aloe-emodin may have a connection with NF-κB signaling. We further proved this hypothesis with molecular docking analysis (**Tables 4.45.** and **4.46.**).

We analyzed the binding of aloe-emodin to several proteins involved in NF-κB activation, *i.e*. IκK, NEMO, p50, p65 and p52ReIB. **Figures 4.120.**, **4.123.**, **4.126.** and **4.129.** show overall proteins while **Figures 4.121.**, **4.124.**, **4.127.** and **4.130.** show aloe-emodin bindings on those proteins. Interestingly, aloe-emodin bound with high affinity to p52RelB and to the complexes of IκK-NEMO and p50-p65 (**Table 4.46.**). The lowest binding energies ranged from -7.57 to -9.58 kcal/mol and the pKi values from 0.563 (± 0.3) to 4.23 (± 2.44) μM. This indicates that aloe-emodin may inhibit NF-κB signaling by interfering with different targets of the NF-κB activation cascade. The binding of aloe-emodin was only modest to IκK (the lowest binding energy: -6.98 kcal/mol; pKi value: 7.69 (± 0.005) μM). Triptolide as known NF-κB inhibitor was used as positive control in the molecular docking analysis (**Figures 4.121.**, **4.125.**, **4.128.** and **4.131.**). Triptolide revealed good binding energy to the IκK-NEMO complex (the lowest binding energy: -9.58 kcal/mol) however with a fair pKi value (95.3 ± 0.61 μM) (**Table 4.46.**). The binding to the other proteins occurred with less activity than aloe-emodin, indicating that aloe-emodin might be a better NF-κB inhibitor than triptolide.

Table 4.45. Molecular docking of aloe-emodin and triptolide to NF-κB subunits (blind docking).

Blind docking Aloe-emodin	Lowest binding energy	Mean binding energy	Residues making hydrogen bonds	Residues involved in hydrophobic interactions	pKi
IκK	-5.49	-5.04	UNK1:H27 1	LEU312, SER313, GLN355, LEU361, TYR370, VAL371, ILE372, GLY384, ASP385, LEU386	135.035
IκK-NEMO	-6.52	-6.43	UNK1:H30 1	GLN86, GLU89, LYS90, LEU93, GLN86, ARG87, GLU89, LYS90	78.59
P50-p65 complex	-5.34	-5.08	1vkx:A:GLU282:HN1	GLU193, LEU194, LYS195, ILE196, CYS197, SER281, GLU282	198.18
P52ReIB	-7.00	-6.76	UNK1:H30 1	LYS210 LYS211 DA7 DT8 DT20 DC21 DC22	8.41

Table 4.46. Molecular docking of aloe-emodin and triptolide to NF-κB subunits (defined docking).

	Defined docking	Lowest binding energy	Mean binding energy	Residues forming hydrogen bonds	Residues involved in hydrophobic interactions	pKi
IκK	**Aloe-emodin**	-6.98	-6.97	UNK1:H27 1 UNK1:H24 1	LEU312 SER313 GLN355 LEU361 TYR370 VAL371 ILE372 GLY384 ASP385 LEU386	7.69 ± 0.005 μM
	Triptolide	-5.47	-5.42	-	LEU312 GLN355 TYR370 VAL371 ILE372 GLY384 ASP385 LEU386	115.17 ± 21.3 μM
IκK-NEMO	Aloe-emodin	-8.12	-8.09	UNK1:H27 1 UNK1:H30 1	GLN86 LYS90 GLN730 MET734 ARG87 GLU89 LYS90 LEU93	1.13 ± 0.03 μM
	Triptolide	-9.58	-9.57	UNK1:H37	MET734 GLN86 GLU89 LYS90 LEU93 GLN730 GLN86 ARG87 GLU89 LYS90	95.3 ± 0.61 μM
P50-p65 complex	**Aloe-emodin**	-7.57	-7.53	UNK1:H27 1 UNK1:H30 1 UNK1:H24 1 1vkxA:ILE196:HN 1 1vkxA:GLU282:HN 1	GLU193 LEU194 LYS195 ILE196 CYS197 SER281 GLU282	4.23 ± 2.44 μM
	Triptolide	-5.33	-5.12	UNK1:H37 1vkxA:ARG30:HE 1	ARG30 GLU193 GLN271 GLU279 LEU280 SER281 GLU282	4.37 ± 2.43 μM

Table 4.46. Molecular docking of aloe-emodin and triptolide to NF-κB subunits (defined docking, continued).

	Defined docking	Lowest binding energy	Mean binding energy	Residues forming hydrogen bonds	Residues involved in hydrophobic interactions	pKi
P52RelB	**Aloe-emodin**	-8.88	-8.86	UNK1:H27 1 UNK1:H30 1 UNK1:H24 P52RelB:B:LYS144:HN1	LYS143 LYS144 DT9 DC10 DA18 DT19 DT20	0.563 ± 0.3 μM
	Triptolide	-7.74	-7.74	UNK1:H30 1	DA7 DT8 DT20 DC21 DC22	2.23 ± 0.006 μM

Molecular docking analysis of aloe-emodin and triptolide to NF-κB subunits were shown below:
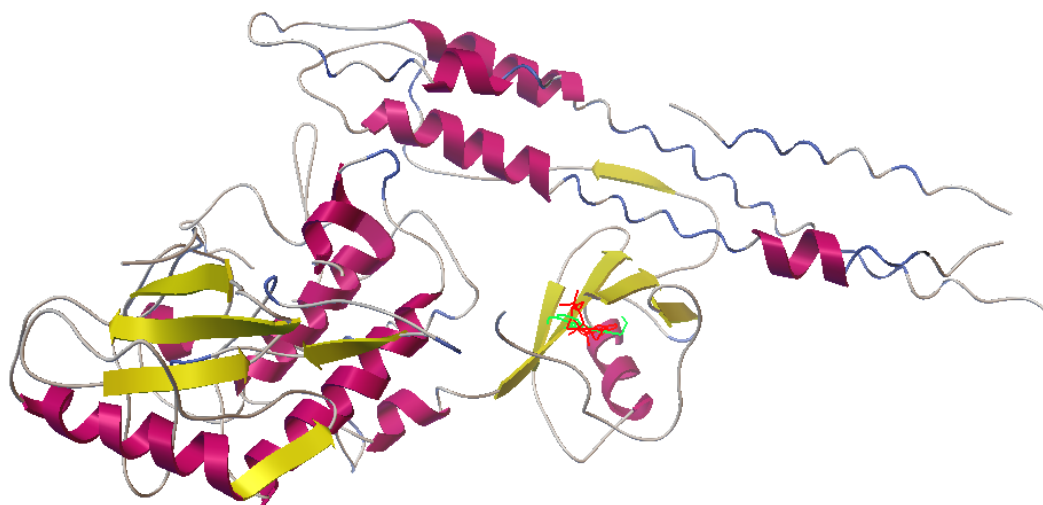
Figure 4.120. IκK as overall protein
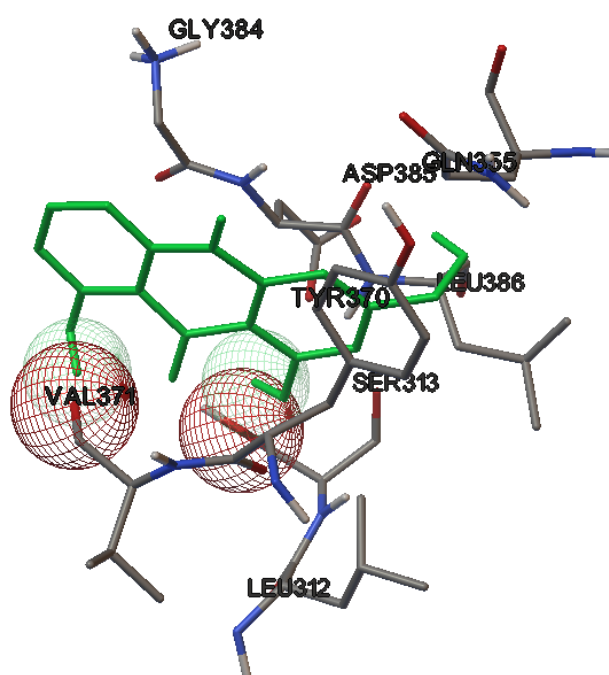
Figure 4.121. Aloe-emodin docking on IκK.
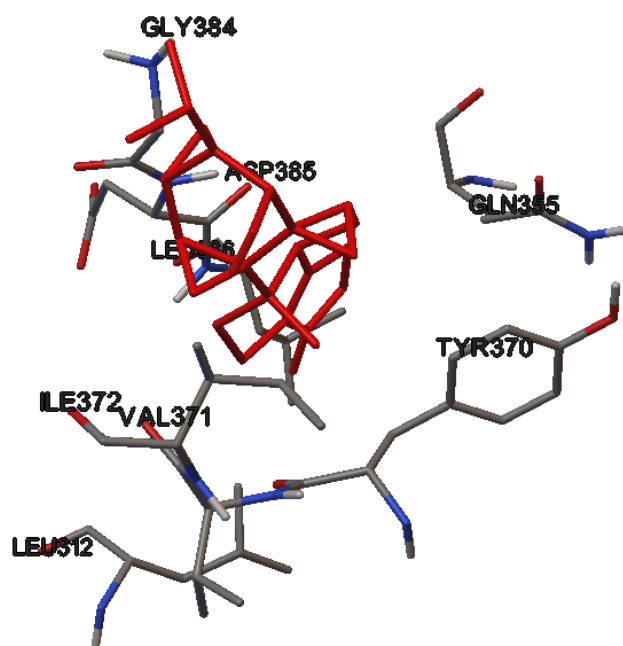
Figure 4.122. Triptolide docking on IκK.
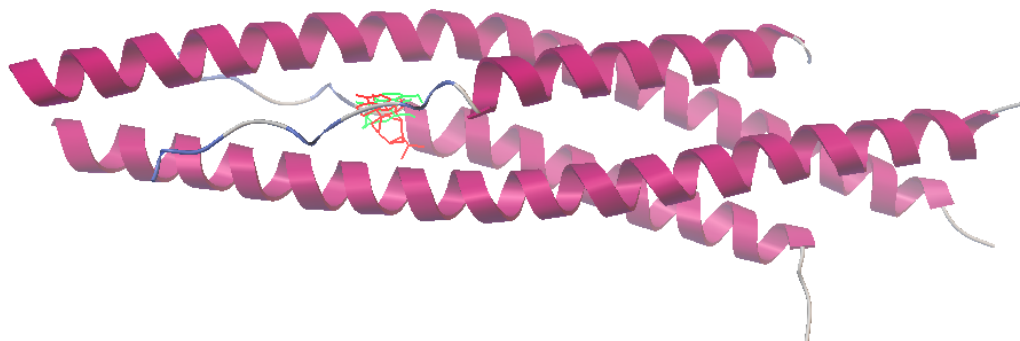
Figure 4.123. IκK NEMO as overall protein.
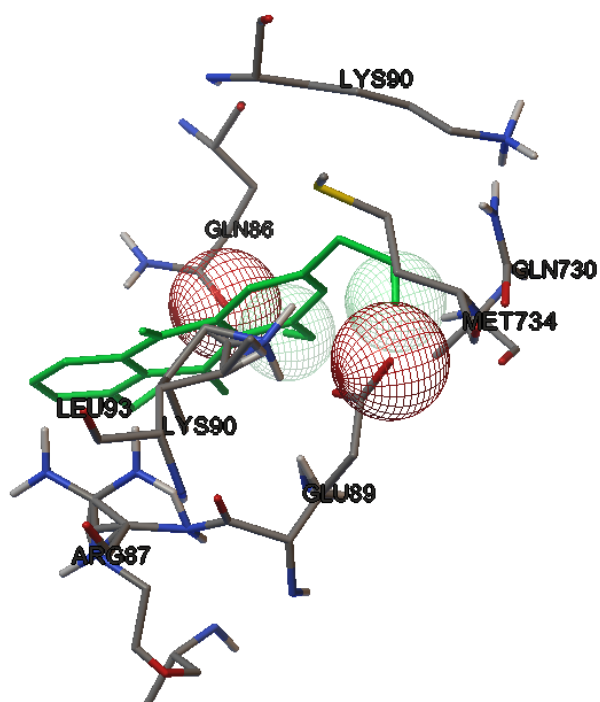
Figure 4.124. Aloe-emodin docking on IκK NEMO.
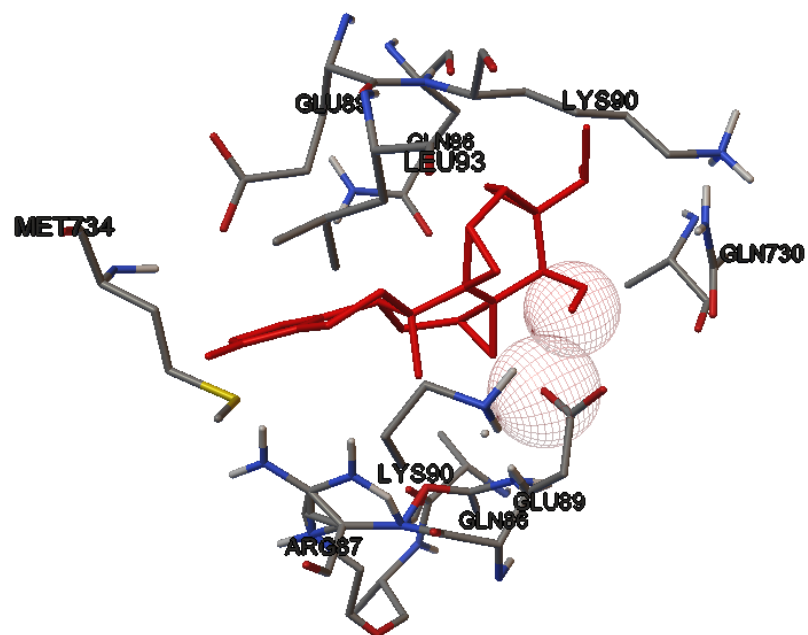
Figure 4.125. Triptolide docking on IκK NEMO.
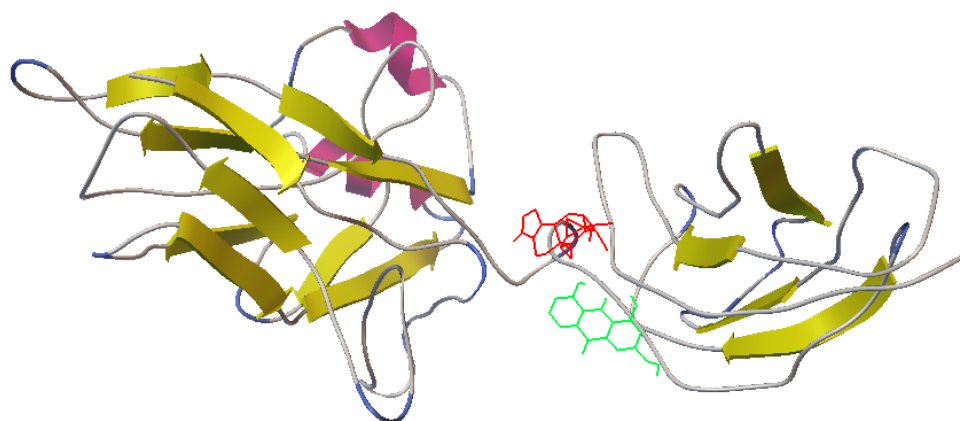
Figure 4.126. P50-p65 as overall protein.
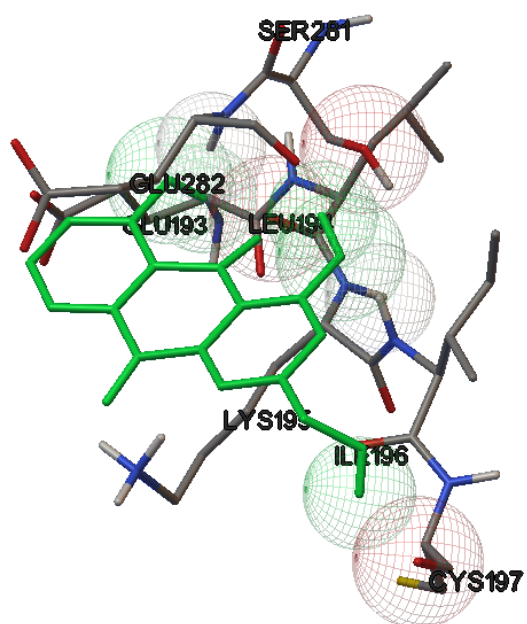
Figure 4.127. Aloe-emodin docking on p50-p65.
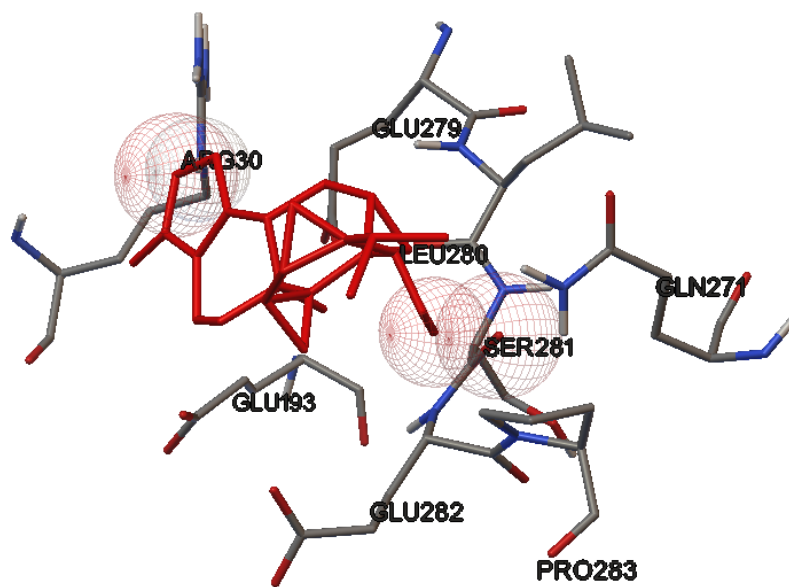
Figure 4.128. Triptolide docking on p50-p65.
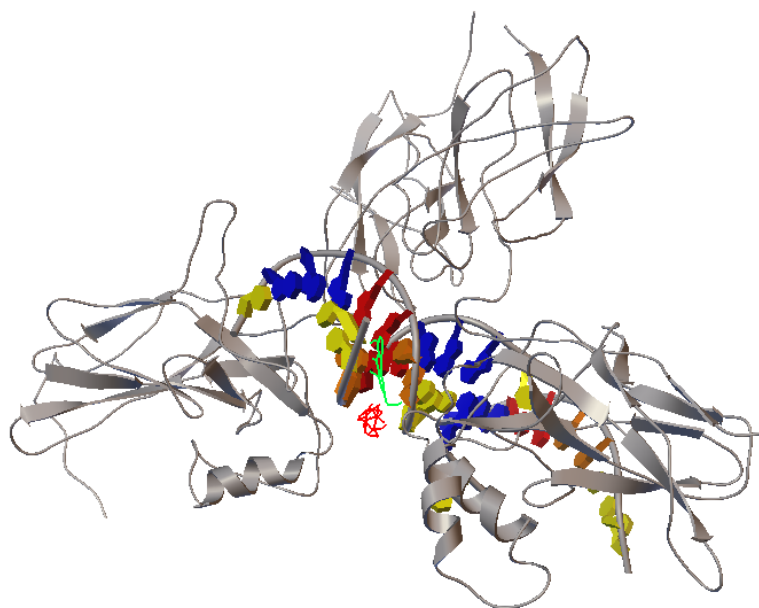
Figure 4.129. P52ReIB as overall protein.
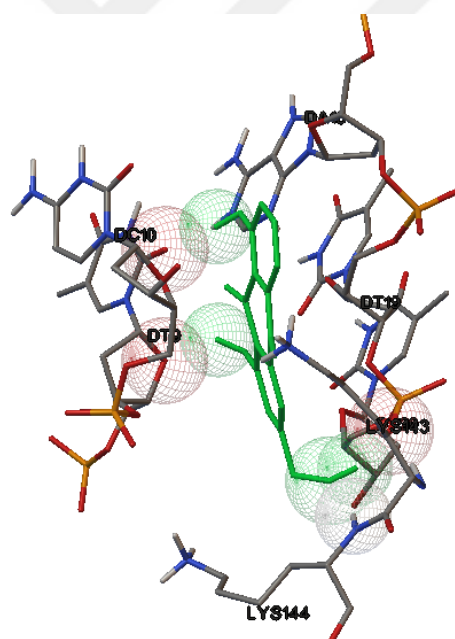
Figure 4.130. Aloe-emodin docking on p52ReIB.
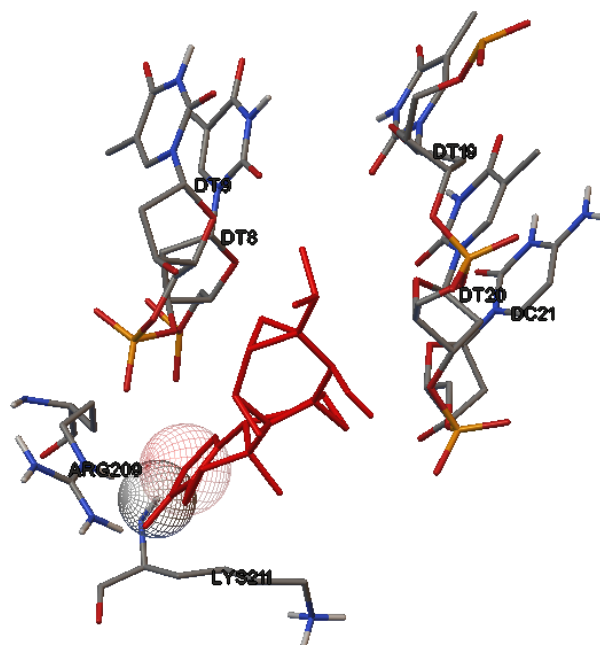
Figure 4.131. Triptolide docking on p52ReIB.

4.15   Enzyme Inhibition Assays

4.15.1 *α*-Amylase Enzyme Inhibition

Based on *α*-amylase enzyme inhibition assay, only ethanol extracts of both roots and herbs of *Rumex acetosella* inhibited *α*-amylase enzyme. IC_{50} value of ethanol extract of herbs were observed at around 500 µg/mL which was lower than that of positive control acarbose (728.55 µg/mL), while ethanol extract of roots (>1000 µg/mL) had higher than that of positive control acarbose (**Table 4.47.** and **Table 4.48.**). Acarbose inhibited *α*-amylase in dose dependent manner, which reached up to 56.2% at 1000 µg/mL.

Additionally, anthraquinone aglycons generally seemed to get modest inhibition on *α*-amylase enzyme (**Table 4.49.**). Their inhibition potentials didn't reach up to 50% in studied concentrations (**Figure 4.132.**). IC_{50} value of main anthraquinone aglycons as well as ethanol extract of roots (>1000 µg/mL) couldn't be detected as they required higher concentrations to be determined. Therefore, interpretation of structure-activity relationships (SARs) of the main anthraquinone aglycons is not a reasonable approach in *α*-amylase enzyme inhibition assay.

Table 4.47. *α*-amylase enzyme inhibitory activity % of positive control acarbose.

Acarbose	Concentration (µg/mL)					
	25 µg/mL	50 µg/mL	100 µg/mL	250 µg/mL	500 µg/mL	1000 µg/mL
% α-amylase inhibition	13.2 ± 1.40	16.4 ± 2.73	26.9 ± 4.39	38.06 ± 4.99	44.7 ± 4.03	56.2 ± 4.39

Table 4.48. *α*-amylase enzyme inhibitory activities % of ethanol extracts of *R. acetosella*.

Concentration (µg/mL)	Ethanol extracts of *R. acetosella*	
	Roots	**Herbs**
200	16.26 ± 1.78	-
400	26.27 ± 4.30	29.90 ± 2.57
500	33.50 ± 1.78	50.06 ± 2.83
1000	36.78 ± 1.75	52.60 ± 1.28

Table 4.49. *α*-amylase enzyme inhibitory activities % of main anthraquinone aglycones.

Concentration (µg/mL)	Main anthraquinone aglycons				
	Emodin	Aloe-emodin	Rhein	Chrysophanol	Physcion
10	14.81 ± 2.28	9.14 ± 1.61	2.45 ± 0.64	1.04 ± 1.48	-
50	17.52 ± 3.29	14.30 ± 0.14	12.88 ± 1.04	15.27 ± 1.94	8.10 ± 1.31
100	18.47 ± 1.51	16.72 ± 0.67	14.94 ± 1.33	22.68 ± 4.56	11.33 ± 2.24
200	19.03 ± 2.16	22.44 ± 0.08	28.17 ± 1.78	31.05 ± 3.61	29.32 ± 2.96
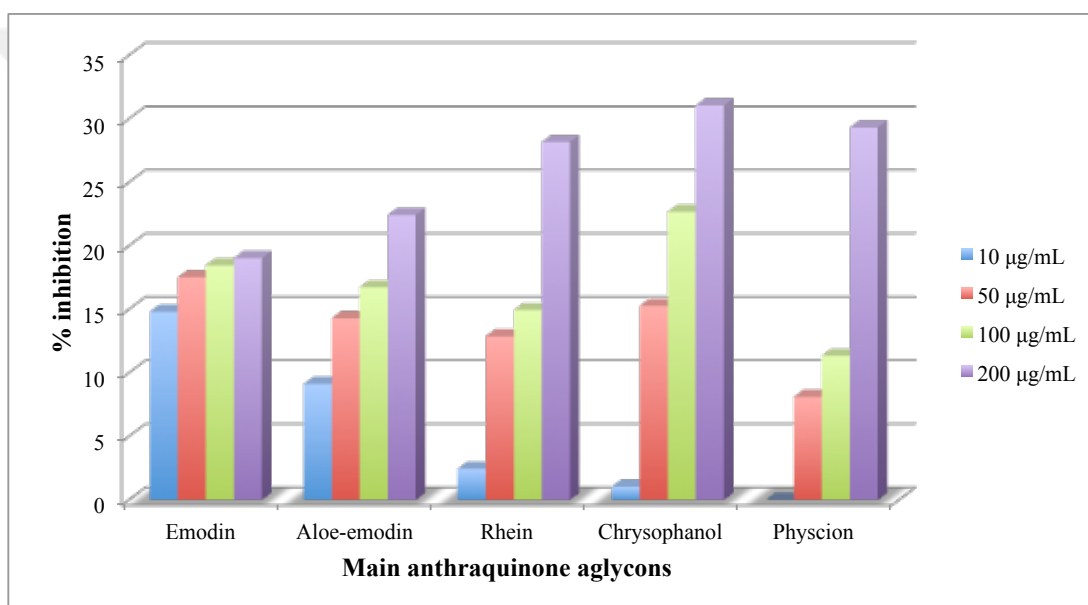
Figure 4.132. *α*-amylase enzyme inhibitory activities % of main anthraquinone aglycones.

4.15.2 *α*-Glucosidase Enzyme Inhibition

α-Glucosidase inhibitory activities of chloroform, methanol and 70% methanol, ethanol and 70% ethanol extracts of the roots and herbs of *Rumex acetosella* showed that almost all extracts had lower IC_{50} values and got better inhibition potential than positive control acarbose (**Tables 4.50.-4.52. and 4.54.**). Chloroform extracts of both *Rumex acetosella* roots and herbs displayed lower inhibition than other studied extracts. Ethanol extracts of roots and herbs of *R. acetosella* got the lowest IC_{50} (< 50 μg/mL) in all (**Table 4.54.**). Methanol, ethanol and 70% ethanol extracts of both herbs and roots reached over 90% inhibitory activities at higher concentrations (**Tables 4.50. and 4.51.**, **Figures 4.133. and 4.134.**). Additionally, main anthraquinone aglycons except for chrysophanol didn't show any inhibition on *α* glucosidase enzyme. Chrysophanol is the only compound in all anthraquinone aglycones with the IC_{50} value of 206.29 μg/mL, getting lower IC_{50} value than standard acarbose (**Tables 4.53. and 4.54.**).

When we evaluate of SARs of the main anthraquinone aglycons based on their *α*-glucosidase inhibitory activities, the 3rd and 6th positions of 1,8-dihydroxyanthraquinone molecule are expressed to be important. The 6th position should be nonsubstituted for enzyme inhibition. Besides, 1,8-dihydroxyanthraquinone molecule should contain a methyl group at the 3rd position. Polar groups at the 3rd position such as $-CH_2OH$ and $-COOH$ instead of $-CH_3$ cause loss of inhibitory activity.

Table 4.50. α-glucosidase enzyme inhibitory activities % of root extracts of *R. acetosella*.

Concentration (µg/mL)	Root extracts of *R. acetosella*				
	CHCl$_3$	CH$_3$OH	70% CH$_3$OH	C$_2$H$_5$OH	70% C$_2$H$_5$OH
50	-	2.05 ± 2.90	9.90 ± 4.24	78.85 ± 0.68	5.92 ± 3.64
100	-	30.935 ±1.22	11.45 ± 4.74	95.49 ± 0.32	43.84 ± 4.59
200	1.8 ± 0.09	63.5 ± 1.41	14.40 ± 2.83	97.33 ± 0.05	91.99 ± 0.32
400	17.2 ± 0.14	95.75 ± 1.63	66.64 ± 2.06	97.26 ± 0.05	92.82 ± 0.73
500	30.6 ± 0.12	96.25 ± 0.92	73.50 ± 0.71	97.33 ± 0.05	96.52 ± 0.05

Figure 4.133. α-glucosidase enzyme inhibitory activities % of root extracts of *R. acetosella*.

Table 4.51. *α*-glucosidase enzyme inhibitory activities % of herbal extracts of *R. acetosella.*

Concentration (μg/mL)	Herbal extracts of *R. acetosella*				
	CHCl$_3$	CH$_3$OH	70% CH$_3$OH	C$_2$H$_5$OH	70% C$_2$H$_5$OH
50	9.1 ± 0.14	42.4 ± 5.52	20.50 ± 0.57	80.84 ± 1.84	16.25 ± 1.22
100	12.9 ± 2.83	49.45 ± 2.05	38.40 ± 1.98	95.30 ± 0.18	60.14 ± 2.67
200	25.7 ± 4.24	57.75 ± 3.18	52.20 ± 3.25	95.41 ± 0.02	93.66 ± 0.02
400	38.7 ± 1.70	84.5 ± 2.83	59.40 ± 2.83	95.43 ± 0.41	93.90 ± 0.15
500	53.6 ± 1.98	91.7 ± 2.26	79.80 ± 3.54	95.43 ± 0.05	95.99 ± 0.13
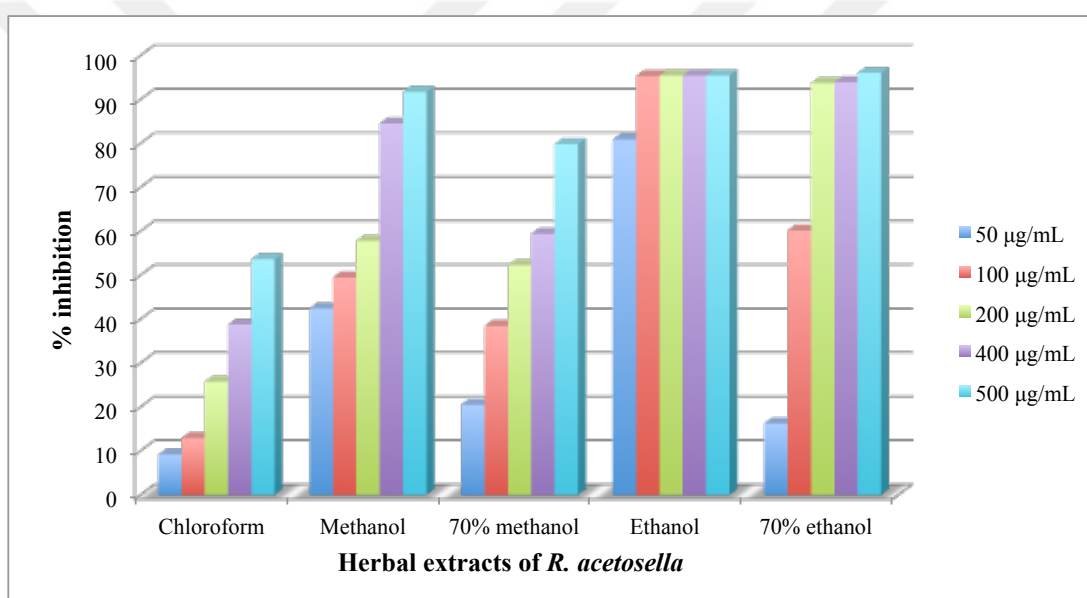
Figure 4.134. *α*-glucosidase enzyme inhibitory activities % of herbal extracts of *R. acetosella.*

Table 4.52. *α*-glucosidase enzyme inhibitory activity % of acarbose.

Acarbose	Concentration				
	250 µg/mL	**500 µg/mL**	**1000 µg/mL**	**2500 µg/mL**	**5000 µg/mL**
% α glucosidase inhibition	-	6.05 ± 5.44	19.36 ± 3.56	47.30 ± 1.75	67.61 ± 0.76

Table 4.53. *α*-glucosidase enzyme inhibitory activity % of chrysophanol.

Chrysophanol	Concentration		
	100 µg/mL	**250 µg/mL**	**500 µg/mL**
% α-glucosidase inhibition	28.60 ± 2.1	58.60 ± 3.05	71.10 ± 1.20

Table 4.54. The concentrations of *R. acetosella* extracts, chrysophanol and acarbose required for 50% inhibition (IC_{50}) of *α*-glucosidase enzyme.

Extracts	IC_{50} values of extracts, chrysophanol and acarbose (µg/mL)			
	Roots	**Herbs**	**Chrysophanol**	**Acarbose**
CHCl₃	> 500	475.84		
CH₃OH	158.54	106.63		
70% CH₃OH	336.29	184.06	206.29	2832.8
C₂H₅OH	< 50	< 50		
70% C₂H₅OH	112.80	88.45		

5. DISCUSSION

In recent years, incidences of cancer and diabetes have rapidly increased. Cancer is one of the leading cause of death worldwide. In 2012, 14.1 million patients were diagnosed (33) and new cases with cancer are predicted to increase by 70% over the next 20 years (34). Likewise, patients with diabetes mellitus have been 422 million nearly quadrupling since 1980 and inclined 1.5 million deaths in 2012 as indicated in WHO reports (51). These statistics have led us to investigate medicinal plants traditionally used for these diseases. *Rumex acetosella* have been used against cancer and diabet in folk medicine (13, 17-19, 44-47). In this thesis, cytotoxic and antidiabetic activities of *R. acetosella* were investigated.

Oxidative stress plays an important role in the etiology of many diseases. Therefore, primarily we examined antioxidant potentials of ethanolic, methanolic, 70% ethanolic, 70% methanolic and chloroform extracts of *R. acetosella* as preliminary studies. We performed DPPH, ABTS, NO radical scavenging acitivity assays as well as phosphomolybdate assay to test antioxidant capacities of the extracts. In general terms, specifically methanolic and ethanolic extracts could be evaluated as good antioxidants. Our results showed DPPH (RC$_{50}$ of the ethanolic extract of herbs and methanolic extract of roots are 59.66 and 67.94 μg/mL, respectively, while RC$_{50}$ of ascorbic acid is 15.89 μg/mL), ABTS (RC$_{50}$ of methanolic extract of herbs and roots are 65.57 and 70 μg/mL, respectively, while RC$_{50}$ of trolox is 6.21 μg/mL), NO (RC$_{50}$ of ethanolic extract of herbs and roots are 208.61 and 280 μg/mL, respectively, while RC$_{50}$ of ascorbic acid is >800 μg/mL) radical scavenging activities. In general terms, radical scavenging capacity of methanolic and ethanolic extracts were evaluated as fairly good. Total antioxidant capacities by phosphomolybdate assay showed that methanolic extract of the herbs and 70% ethanolic extract of the roots to have 324.03 and 422.6 mg AEE/g extract, respectively, which may be attributable the presence of phenolic substances.

There have not been extensive researches about phytochemical profile of *R. acetosella* till now. For the detailed investigation, we isolated the compounds from *R. acetosella* before proceeding activity assays related diabetes and cytotoxicity. Standard chromatographic methods such as Sephadex, normal and reverse phase

column chromatographies were used for the isolation of the compounds. The structures of these compounds were identified with spectroscopic data such as IR, NMR, MS and the measurement of optical rotations. 12 compounds isolated from the roots of *R. acetosella*. These compounds were identified a stilbene derivative (*E*)-piceid, an ethanone derivative and new compound ethanone,1-[2-(*β*-glucopyranosyloxy)-4-hydroxy-6-methylphenyl)] (named as acetoselloside), a naphthalene derivative nepodin-8-*O*-*β*-glucoside, a tannin derivative catechin, lignan derivatives lyoniside and isolariciresinol-9-*O*-*β*-xyloside and anthranoid derivatives rumejaposide G, rumejaposide H, emodin, emodin-8-*O*-*β*-glucoside, chrysophanol-8-*O*-*β*-glucoside and physcion-8-*O*-*β*-glucoside. Isolated compounds distinct from emodin and chrysophanol-8-*O*-*β*-glucoside were detected for the first time in the title plant. Additionally, compound 2 was identified as a new compound and named as acetoselloside.

Thousands of cytotoxic phytochemicals are present in medicinal plants; still most of them have not reached to the clinical stage. We need to find new substances which are more effective than established anticancer drugs and put them into treatment.

Phytochemical profile of *R. acetosella* mainly comprises anthraquinones, which are analogous to anthracyclines-clinically well known drugs. Preliminary cytotoxicity researches of the isolated compounds and commercial anthraquinone aglycones were conducted on CCRF-CEM cells (leukemia cells) by resazurin reduction assay because these cells are much more sensitive than other cell lines. However, the majority of the compounds did not displayed notable cytotoxicity towards leukemia cells (see **Table 4.40.**). Anthraquinones displayed stronger cytotoxicities than the other compounds and aloe-emodin showed the best cytotoxicity among anthraquinones (see **Figure 4.91.**). Detailed cytotoxicity studies on aloe-emodin were carried out in this thesis.

Our motivation to investigate the cellular and molecular mechanisms of aloe-emodin was its activity against diverse tumor cells. Aloe-emodin is not only outstanding to suppress tumor growth *in vivo* as previously demonstrated (489-491), but this compound is also able to kill tumor cells, which are resistant to standard anticancer agents as shown in the present study. The development of resistance to

anticancer drugs reduces the success of chemotherapy. For this reason, there is a high demand for novel compounds with activity against resistant tumors. Therefore, aloe-emodin may have the potential as a new drug, because it may be able to kill otherwise refractory tumors in the clinic.

We focused on resistance phenotypes, which are characterized by broad cross-resistance to many chemically and functionally different cytostatic drugs. These multiple drug resistance (MDR) phenomena can be mediated by drug efflux pumps of the ATP-binding cassette (ABC) type, oncogenes or tumor suppressor genes. We have chosen three ABC-transporters, P-glycoprotein (MDR1/ABCB1) and breast cancer resistance protein (BCRP/ABCG2) as well-known MDR-mechanisms and ABCB5 as a novel efflux transporter relevant in cancer stem-like cells. Oncogenes and tumor suppressor genes do not only drive carcinogenesis but also confer drug resistance (406). We have chosen the epidermal growth factor receptor (400) and the tumor suppressor gene p53 for our investigations.

Aloe-emodin's cytotoxicity was tested towards pairs lines from different tumor types by resazurin assay, as well. These cell lines were breast cancer cells (MDA-MB-231-pcDNA cells and a multidrug-resistant subline transfected with a *BCRP* cDNA (MDA-MB-231-BCRP clone 23), embryonic kidney cells (wild type HEK293 cells and a multidrug-resistant subline transfected with an *ABCB5* cDNA (HEK293-ABCB5)), colon cancer cells (HCT116 cells with wild-type TP53 tumor supressor gene (HCT116($p53^{+/+}$)) and (HCT116 knockout cells (HCT116($p53^{-/-}$)) and brain tumor cells (wild type U87.MG and a subline transfected with a deletion-activated *EGFR* cDNA (U87.MGΔEGFR)). We observed that aloe-emodin was mostly cytotoxic to the other cell lines; even collateral sensitive to HCT116($p53^{-/-}$). Collateral sensitivity in P-glycoprotein-overexpressing cells has been explained by futile cycles of ATP cleavage by the efflux transporter and transient depletion of cellular ATP stores ultimately leading to cell death (492). However, the underlying mechanisms of the collateral sensitivity in p53-knockout cells compared to p53 wildtype cells are not known yet. Further researches are needed to clarify background mechanism.

Aloe-emodin was detected as the most cytotoxic substance- specifically towards CCRF-CEM cells- in all. Following, protease viability marker assay was performed on CCRF-CEM cells to exclude the possibility that the cytotoxicity of aloe-emodin measured by the resazurin assay was artificially influenced by any non-intended interaction with aloe-emodin-induced ROS generation. Cytotoxicity determined by protease viability marker assay confirmed the outcomes of resazurin reduction assay.

We also investigated aloe-emodin's toxicity towards normal cells. Human peripheral mononuclear cells (PMNC) isolated from fresh blood samples of a healthy donor were tested against various concentrations of aloe-emodin ranging from 0.001-100 µM. Interestingly, it did not show cytotoxic activity towards the normal cells, presenting a good point to go further researches as non-toxic to normal cells.

The background mechanisms behind aloe-emodin's cytotoxicity were detected as ROS inducement, S-phase arrest, DNA damage, mitochondrial membrane potential breakdown, apoptosis and necrosis in aloe-emodin-treated CCRF-CEM cells.

The analysis of response of aloe-emodin towards resistant cell lines provided us first clues on the relevance of major mechanisms of drug resistance for aloe-emodin. However, cell lines of different tumor types may react differently, when treated with aloe-emodin according to their individual and tumor-type specific gene expression profiles. Therefore, we were interested to find out, which tumor types react more sensitive and which ones more resistant to aloe-emodin. To address this question, we performed COMPARE and hierarchical cluster analysis of transcriptome-wide microarray-based mRNA hybridizations in a panel of 60 tumor cell lines of the Developmental Therapeutics Program (DTP) of the National Cancer Institute (NCI, USA) (http: dtp.cancer.gov).

DTP has assessed more than 88,000 pure compounds and more than 34,000 crude extracts against the panel of human tumor cell lines till now and reported that even if the correlation of *in vitro* histology to clinical activity is poor, since they are only 60 in all cell lines, lacking in cytokines, hormones in their environment or possibility of having other cell types in a tumor. Still, these are model systems for drug analysis as applicable to an unlimited number of samples, consistent, highly

efficient and testable (493, 494). This approach has been frequently applied in the past years, as well (495-499). Here, we used it to identify genes, whose expression correlated with sensitivity or resistance of the cell lines to aloe-emodin.

An intriguing result in our study for hierarchical cluster analyses was that a set of only 40 genes out of the entire transcriptome was sufficient to determine, whether a cell line was sensitive or rather resistant to aloe-emodin. This is a remarkable result, because the IC_{50} values of the cell lines had not been prior included into the calculations for the cluster analyses. The implication of this result is that sensitivity or resistance of a drug in tumor cells can be predicted based on the gene expression profile alone. It can be speculated that such an approach is thought to be able to transfer clinical status to personalized treatment of cancer patients.

The following scenario can be envisaged: If a tumor is resistant to all standard treatment options, gene expression profiling could be applied to predict, which phytochemical is still active in this tumor. Before clinical treatment with aloe-emodin could be considered, the gene expression profile of the patient's tumor has to be determined to see, whether the tumor is sensitive to aloe-emodin. If the gene expression profile indicates that the tumor is resistant to this drug, we switch to other drugs. The present study opens the door for personalized medicine with aloe-emodin as the first step. Much more analyses are necessary before this concept can be realized in the clinics. Nevertheless, it is a proof-of-principle that natural products could be implemented in future treatment strategies.

Two conditions are necessary to realize this concept of individualized therapy: (1) existing phytochemicals should be numerous to choose the right compound for the right patient; (2) therapeutically relevant genes have to be separated from non-relevant genes in the gene expression profile. In the past few years, commercial low density arrays have been developed that carry only therapeutically relevant genes for standard treatment options. Although gene expression profiles have been generated in cell lines for many phytochemicals (500, 501), clinical validation has not been done yet. This represents an important prerequisite to establish natural product-based cancer therapy in the future.

Microarray hybridization results pointed out that the range of genes with different functions is remarkably diverse for aloe-emodin. Genes operating cell death

and survival, cellular growth and proliferation, cellular development, gene expression, cellular function and maintenance were shown to deregulated by aloe-emodin.

This raises the question, whether these genes may be commonly regulated by one or few master genes that are relevant for drug resistance. To solve this problem, we performed a search for transcription factor binding sites in the promoter regions of those genes we found by COMPARE analyses and included into the cluster analysis. A transcription factor that appeared in all promoter sequences of genes subjected to this binding motif analysis was NF-κB. The data indicated that NF-κB may have a role in the responsiveness of tumor cells to aloe-emodin by regulating the expression of genes with diverse functions. Our result may be supported by published data showing that NF-κB influences drug response not only by regulation of apoptosis and other cell death mechanisms but also by genes that are not directly related to drug resistance, *e.g.* inflammation and immune functions (502-504).

NF-κB activation starts with the activation of the inhibitor of IkB-kinase (IKK) complex, which consist of IKK1/IKK α, IKK2/IKK β and NEMO/IKK γ and isozymes. IKK2/IKK β phosphorylates the inhibitor of NF-κB (IkB) and targets the protein for subsequent degradation (505) causing the release and translocation of NF-κB factors p65 (Rel-A) and p50 (NF-κB1) dimers. As a consequence, the dimers move to the nucleus to exert its biological functions (505, 506). NF-κB is a known mechanism in anticancer drug response. We revealed that aloe-emodin may kill cancer cells by inhibition of NF-κB causing apoptosis and cell death. Molecular docking studies suggested that aloe-emodin supported NF-κB binding. Even though, reporter assay and molecular docking results confirmed NF-κB to be downregulated by aloe-emodin, western blot analysis should be performed on CCRF-CEM cells to clearly see if aloe-emodin affects total NF-κB, phosphorylated NF-κB or its regulator IκB. Then, this will provide a certain basis for aloe-emodin's effect on NF-κB.

Genes operating in signal transduction, apoptosis, nucleic acid metabolism and other pathways were identified by COMPARE analysis and seemed to be diverse. This gene expression profile resembles the architecture of cell lines that have not been pretreated with aloe-emodin. This approach is characteristic for primary resistance. While some tumors will respond to chemotherapy, others are

non-responsive, although they have never been pretreated with anticancer drugs.

In addition to primary resistance, an initially sensitive tumor can acquire resistance upon repeated chemotherapy applications, which was termed acquired or secondary resistance. Under laboratory conditions, it is possible to compare gene expression profiles of treated and non-treated cells. The resulting differentially expressed genes can be used to generate hypothesis on the molecular modes of action and determinants of resistance of cytotoxic compounds. This is supported by a large number of literature (507-511).

The results as well as the genes obtained by COMPARE and cluster analyses indicate that aloe-emodin acts by multiple mechanisms against cancer cells. The versatility of natural products is typical (512). Based on the multiplicity of affected genes, we generated a hypothesis on the modes of action of aloe-emodin with the intention to subsequently prove this hypothesis experimentally by independent methods. On the grounds of microarray data of differentially expressed genes between treated and non-treated cells, we assumed that aloe-emodin generates ROS, which leads to DNA damage and cell cycle arrest. As a consequence, the mitochondrial pathway of apoptosis was induced as shown by disruption of the mitochondrial membrane potential and annexin V/PI staining.

It has been determined by other authors that aloe-emodin damages the DNA. (513-515). A disruption of the cell cycle causing S and G2/M arrest and apoptosis have been reported upon aloe-emodin exposure (516). Findings of other authors confirm our point of view.

Although the use of *R. acetosella* as an anti-cancer seems to be explained by these findings, it should be kept in mind that the traditional use of *R. acetosella* as anticancer remedy cannot be explained by aloe-emodin alone and that presumably many other phytochemicals contribute to the bioactivity of this plant.

Several modes of action can be envisioned:

(1) One substance is the main active compound and other compounds in the plant support its actions,

(2) Several compounds affect one or several therapeutic targets. The substances mutually supplement each other in additive or synergistic manner.

(3) The main compound reveals not only activity against diseased cells and tissues but also against normal tissues leading to side effects. Concomitant compounds in the plant dampen the side effects.

Based on the results of the present investigation, further analyses are needed to elucidate which of these possibilities are realized in *R. acetosella*. The final goal should be to understand the full bioactivity of this plant to utilize its full potential for rationale phytotherapy of cancer.

R. acetosella is also used in diabetes in folk medicine in Turkey (44-47). Ethnobotanical investigations of natural sources should be followed with biological activity studies of those to create evidence for their known activities by indigenous people. Thus, investigation of antidiabetic effect of *R. acetosella* may be an important strategy to confirm its usage in folk medicine.

Nowadays, medicinal plants and plant-based medicines get interest in the prevention of diabetes. Plants having wide diversity may be significant sources for the development of more effective antidiabetic agents with slight or no side effects. In the past decades, acarbose and voglibose have been developed to control the hyperglycemia via natural sources (517-519). Medicinal plants and their constituents have been investigated to determine their hypoglycaemic activities till now. Majority of published researches on hypoglycaemic drugs have focused on polyphenols. Besides, various plants have been studied for their hypoglycaemic activity, as well. For instance, methanolic extracts of *Salsola* species including *S. soda*, *S. kali* and *S. oppositi* were shown to have a notable α-amylase inhibitory activities with an IC_{50} value ranging from 0.65 to 0.28 mg/mL (519, 520). Inhibitory activities of methanolic extract of *Marrubium* radiatum against both α-amylase (IC_{50}=61.1 μg/mL) and α-glucosidase (IC_{50}=68.8 μg/mL) (519, 521), acetone extract of *Pteronia divaricate* against α-glucosidase (IC_{50}=31.22 μg/mL) as well as acetone extracts of *Euclea undulata* and *Elaeodendrondron transvaalense* against α-amylase with IC_{50} values of 2.80 and 1.12 μg/mL, respectively (519, 522) were further reported. As it is seen, IC_{50} values of the extracts are diverse though they are expressed as strong inhibitors in each study. The reason for that may be different enzyme or substrate concentrations used as well as different conditions in the enzyme inhibition studies. Therefore, following the same protocol for each extract, substance or positive control

will be more reasonable to clearly evaluate inhibitory activities. Taken all, investigation of antidiabetic potential of *R. acetosella* and its constituents by means of α-amylase and α-glucosidase enzymes is a notable approach, since the title plant is traditionally used in diabetes.

DM may be otoimmmun-origined or idiopatic (Type I DM) as well as caused by insulin resistance or relative insulin deficiency (Type II DM). Patients with type II DM comprises large majority of the people (90-95%), while the rest of whom are suffering from type I DM whose treatment only depends on insulin uptake. Eyes, kidneys, hearts and vital organs of people living with long-lasting hyperglycemia are under risk (50). For this reason, it is important to control various enzymes such as α-amylase, and α-glucosidase to prevent hyperglycemia. In our study, *R. acetosella* extracts and the main anthraquinone aglycones were investigated by means of their *in vitro* α-amylase and α-glucosidase inhibitory activities.

We detected α-amylase inhibitory effects of ethanol extracts obtained from roots and herbs of *R. acetosella*. The IC_{50} value of ethanol extract of aerial parts of *R. acetosella* was found to be at around 500 µg/mL, which was better than the positive control acarbose (IC_{50}= 728.55 µg/mL), while the ethanol extract of roots (>1000 µg/mL) had less effect than acarbose and ethanol extracts of aerial parts. Anthraquinone aglycones were studied in the concentration ranges of 10 to 200 µg/mL and displayed moderate inhibitions % (for emodin ranging from 14.81 to 19.03 µg/mL, for aloe-emodin ranging from 9.14 to 22.44 µg/mL, for rhein ranging from 2.45 to 28.17 µg/mL, for chrysophanol ranging from 1.04 to 31.05 µg/mL. and for physcion no activity to 29.32 µg/mL) on the enzyme. Even if, they seemed to have modest inhibitions, higher concentrations of the aglycons are needed to be tested on the enzyme. Therefore, we can calculate IC_{50} values and compare those values with IC_{50} of acarbose. Our findings only present clear data about extracts, which indicates ethanol extract of aerial parts to display better inhibition potential than acarbose. This may form a ground for its use in DM by local people.

α-Glucosidase inhibitory activities of chloroform, methanol and 70% methanol, ethanol and 70% ethanol extracts of the roots and herbs of *R. acetosella* were determined. Nearly all extracts had lower IC_{50} values and displayed better inhibition potential than positive control acarbose (IC_{50}= 2832.8 µg/mL). Among the

anthraquinone aglycones, only chrysophanol had the lowest IC_{50} (206.29 μg/mL) and was observed to be more active than the standard acarbose. Ethanol extracts of roots and herbs of *R. acetosella* showed the lowest IC_{50} (< 50 μg/mL) in all extracts and aglycons. This might be because other substances in the plant support aglycons' effect on the enzyme and they can all behave in synergistic manner. This can be considered as an evidence for the use of the plant in DM in traditional medicine.

In this thesis, we examined biological activity studies on the extracts of *R. acetosella* as well as its containing compounds. The extracts and substances were investigated against diabetes and cancer; because the plant is traditionally used in these diseases. Initially, antioxidant assays were performed as preliminary studies that oxidative stress may take part in the etiology of many diseases. Generally, alcoholic exracts have shown to display good antioxidant potentials. Then, isolation studies were conducted to view phytochemistry profile of the plant. Because the plant is known to contain anthraquinones, which have similar structure to clinically used anticancer drugs. Therefore, the main anthraquinone aglycones and isolated compounds were examined to test their cytotoxicities. Aloe-emodin was displayed as the most effective compound and shown to be a potential drug candidate in cancer theraphy. Moreover, antidiabetic potentials of the extracts and anthraquinone aglycons were investigated by means of *α*-amylase and *α*-glucosidase enzyme inhibition properties. Especially, ethanol extracts might be evaluated as significant resources rather than substances in *R. acetosella* to prevent complications of diabetes, confirming the use of *R. acetosella* in DM by local people.

6.   CONCLUSIONS and SUGGESTIONS

In this thesis named "Isolation of Potential Drug Candidate Molecules from *Rumex acetosella* L. and *In Silico*, *In Vitro* Researches on Those Molecules", all the targets have been reached.

R. acetosella, growing in flora of Turkey and used against diabetes in Turkish folk medicine as well as against cancer in Canadian and American traditional medicine, was elaborated in terms of phytochemical studies and biological activities in this thesis.

Oxidative stress contributes to the formation of many diseases such as cancer and diabetes. Medicinal plants with their high phenolic contents may be the main sources of antioxidants. The radical scavenging capacities of methanolic and ethanolic extracts from *R. acetosella* were quite good.

In our study conducted on *R. acetosella*, total of 12 compounds in which one substance as a new structure (acetoselloside) were elucidated on the basis of spectroscopic data such as IR, NMR and mass spectrum. Structures of those compounds were elucidated as stilbene, ethanone, lignan, naphthalene, tannin and anthranoid derivatives, which were (*E*)-piceid (a stilbene derivative), a new compound named as acetoselloside ethanone, 1-[2-(*β*-glucopyranosyloxy)-4-hydroxy-6-methylphenyl)] (an ethanone derivative), nepodin-8-*O*-*β*-glucoside (a naphthalene derivative), catechin (a tannin derivative**)**, lyoniside and isolariciresinol-9-*O*-*β*-xyloside (lignan derivatives), a mixture of rumejaposide G and rumejaposide H, emodin, emodin-8-*O*-*β*-glucoside, a mixture of chrysophanol-8-*O*-*β*-glucoside and physcion-8-*O*-*β*-glucoside (anthranoid derivatives). There have not been extensive researches about phytochemical profile of *R. acetosella* till now. Isolated compounds distinct from emodin and chrysophanol-8-*O*-*β*-glucoside were detected for the first time in this plant.

Cytotoxicity of the isolated compounds as well as main anthraquinone aglycons were primarily investigated on leukemia cells (CCRF-CEM drug sensitive and multi-drug resistant P-glycoprotein-overexpressing CEM/ADR5000), because these cells are more sensitive than other cells. We substantially performed resazurin reduction assay to test the cytotoxicity. Most of the compounds did not display any cytotoxicity towards leukemia cells. Therefore, only aloe-emodin was selected to be taken for

further researches owing to getting the best cytotoxicity in all. Aloe-emodin was further performed on eight cell lines which were breast cancer cells (MDA-MB-231-pcDNA cells and a multidrug-resistant subline transfected with a *BCRP* cDNA (MDA-MB-231-BCRP clone 23), embryonic kidney cells (wild type HEK293 cells and a multidrug-resistant subline transfected with an *ABCB5* cDNA (HEK293-ABCB5), colon cancer cells (HCT116 cells with wild-type TP53 tumor supressor gene (HCT116(p53$^{+/+}$)) and HCT116 knockout cells (HCT116(p53$^{-/-}$)) and brain tumor cells (wild type U87.MG and a subline transfected with a deletion-activated *EGFR* cDNA (U87.MGΔEGFR)).

Aloe-emodin's toxicity was investigated on human peripheral mononuclear cells (PMNC). It is desirable that aloe-emodin didn't show any toxicity in heathy cells. On the contrary, it displayed cytotoxicity on drug-sensitive and drug-resistance leukemia cells at very low concentrations. This result suggests that the cytotoxicity of aloe-emodin may be tumor specific. Moreover, the cytotoxicity of aloe-emodin has been confirmed by protease viability marker assay due to the possibility of aloe-emodin to give false positive results by resazurin assay.

The researches for identification of cellular and molecular mechanisms determining cytotoxicity and acquired resistance by aloe-emodin were carried out. Upon treatment of CCRF-CEM cells with aloe-emodin, microarray-based expression profiles conceived and analyzed by IPA. The most pronounced molecular and cellular functions were: cell death and survival, cellular growth and proliferation, cellular development, gene expression, cellular function and maintenance.

According to the results of *in vitro* experiments performing to clarify mechanisms of aloe-emodin, generation of ROS, S-phase arrest, DNA damage, mitochondrial membrane potential breakdown as well as apoptosis and necrosis were observed in aloe-emodin-treated CCRF-CEM cells.

Motif analysis was performed to search transcription factor binding sites in the promoter regions of the genes we found by COMPARE analyses and included into the cluster analysis. Because the deregulated genes with different functions were various. This transcription factor was NF-κB, indicating NF-κB to have a possible role in the responsiveness of tumor cells to aloe-emodin by regulating the expression of genes with diverse functions.

NF-κB was shown to be downregulated by aloe-emodin in CCRF-CEM cells by several pathways, as well, indicating it could be a target for NF-κB pathway. Western blot analysis should be performed for NF-κB detection to prove this assumption certainly.

Aloe-emodin is not only outstanding to suppress tumor growth *in vivo* as previously demonstrated (489-491), but this compound is also able to kill tumor cells, which are resistant to standard anticancer agents as shown in the present studies. Drug resistance is a major handicap in cancer therapy. Therefore aloe-emodin may have the potential as a new drug, because of its property to kill otherwise refractory.

COMPARE and hierarchical cluster analysis of transcriptome-wide microarray-based mRNA hybridizations. Only 40 genes were detected as sufficient to determine aloe-emodin's response to normal cells.

In addition to the elucidation of mechanisms of action and determinants of resistance to aloe-emodin, our molecular pharmacological data substantiate the therapeutic application of *R. acetosella* against tumors in traditional medicine. The traditional use of the plant in cancer cannot be explained only by aloe-emodin and presumably other phytochemicals contribute to the bioactivity of this plant. Based on the results of the present investigation, further analyses are needed to clarify, which of these possibilities are realized in *R. acetosella*.

We investigated antidiabetic potential via evaluation of α-amylase and α-glucosidase inhibition of the extracts or single compounds. Because α-amylase and α-glucosidase inhibitors are known to reduce starch hidrolysis and retard glucose absorbtion, avoiding hyperglycemia, which may constitute risks for cardiac, nephrotic, neurotic diseases as well as vital organ damages. Taken together α-amylase and α-glucosidase inhibitors may have a notable role to prevent hyperglycemia- related diseases. The ethanol extract of *R. acetosella* was found to be a more effective antidiabetic source than the other extracts and pure anthraquinone aglycones.

In our study, ethanol extracts with inhibition potential on α-amylase and α-glucosidase enzymes confirm the traditional use of the plant as antidiabetic. Several compounds in *R. acetosella* may contribute to the biological activity. The

antidiabetic effects of the extracts can be explained by synergism. Further researches should be conducted to determine the substances account for the activity to obtain a more potent new substance from acarbose.

7. REFERENCES

1. Veeresham C. Natural products derived from plants as a source of drugs. J Adv Pharm Technol Res. 2012; 3 (4): 200-1.

2. Kassab A, Piwowar A. Cell oxidant stress delivery and cell dysfunction onset in type 2 diabetes. Biochimie. 2012; 94 (9):1837-48.

3. Matheus AS, Tannus LR, Cobas RA, Palma CC, Negrato CA, Gomes MB. Impact of diabetes on cardiovascular disease: an update. Int J Hypertens. 2013; 2013.

4. Valko M, Rhodes CJ, Moncol J, Izakovic M, Mazur M. Free radicals, metals and antioxidants in oxidative stress-induced cancer. Chem Biol Interact. 2006; 160 (1):1-40.

5. Pham-Huy LA, He H, Pham-Huy C. Free radicals, antioxidants in disease and health. Int J Biomed Sci. 2008; 4 (2): 89-96.

6. Hamel PB, Chiltoskey MU. Cherokee plants and their uses: a 400 year history: Herald Publishing Company; 1975.

7. Turner NJ, Bouchard R, Kennedy DID. Ethnobotany of the Okanagan-Colville Indians of British Columbia and Washington. Victoria: British Columbia Provincial Museum; 1980.

8. Moerman, D., Native American Ethnobotany. A database of foods, drugs, dyes and fibers of Native American peoples, derived from plants [Internet]. 2003 [Access date 5th September 2017]. Access address: http://naeb.brit.org

9. Turner NJ. The Ethnobotany of the Bella Coola Indians of British Columbia. Syesis 6: Economic Botany; 1973.

10. Gunther E. Ethnobotany of Western Washington. United States of America: University of Washington Press; 1973.

11. Cakilcioglu U, Turkoglu I. An ethnobotanical survey of medicinal plants in Sivrice (Elazig-Turkey). J Ethnopharmacol. 2010; 132 (1): 165-75.

12. Butură V. Romanian ethnobotany encyclopedia. Bucharest, Romania: The Scientific and Encyclopedic Publishing; 1979.

13. Vasas A, Orban-Gyapai O, Hohmann J. The Genus *Rumex*: Review of traditional uses, phytochemistry and pharmacology. J Ethnopharmacol. 2015; 175: 198-228.

14. Erdei A. Elődeink öröksége: békési és székelyföldi települések etnobotanikai értékelése [MSc dissertation]. Szeged: University of Szeged; 2011.

15. Amiri MS, Joharchi MR, TaghavizadehYazdi ME. Ethno-medicinal plants used to cure jaundice by traditional healers of mashhad, Iran. Iran J Pharm Res. 2014; 13 (1): 157-62.

16. Hartwell JL. Plants used against cancer. A survey.[Continued.]. Lloydia. 1970; 33: 97-194.

17.   Rao K, Ch S, Banji D. A study on the nutraceuticals from the genus *Rumex*. Hygeia J DMed. 2011; 3 (1): 76-88.

18.   Hartwell JL. Plants used against cancer. A survey. Lloydia. 1971; 34 (4): 386-425.

19.   Leonard SS, Keil D, Mehlman T, Proper S, Shi XL, Harris GK. Essiac tea: Scavenging of reactive oxygen species and effects on DNA damage. J Ethnopharmacol. 2006; 103 (2): 288-96.

20.   Eyong KO, Kuete V, Efferth T. Quinones and benzophenones from the medicinal plants of Africa. Medicinal Plant Research in Africa. Oxford: Elsevier; 2013.

21.   Seigler DS. Plant secondary metabolism. New York: Springer Science&Business Media; 2012.

22.   Zhang LS, Chang CJ, Bacus SS, Hung MC. Suppressed transformation and induced-differentiation of Her-2/neu-overexpressing breast cancer cells by emodin. Cancer Res. 1995; 55 (17): 3890-6.

23.   Cichewicz RH, Zhang YJ, Seeram NP, Nair MG. Inhibition of human tumor cell proliferation by novel anthraquinones from daylilies. Life Sci. 2004; 74 (14): 1791-9.

24.   Zhang L, Lau YK, Xia W, Hortobagyi GN, Hung MC. Tyrosine kinase inhibitor emodin suppresses growth of HER-2/neu-overexpressing breast cancer cells in athymic mice and sensitizes these cells to the inhibitory effect of paclitaxel. Clin Cancer Res. 1999; 5 (2): 343-53.

25.   Srinivas G, Anto RJ, Srinivas P, Vidhyalakshmi S, Senan VP, Karunagaran D. Emodin induces apoptosis of human cervical cancer cells through poly (ADP-ribose) polymerase cleavage and activation of caspase-9. Eur J Pharmacol. 2003; 473 (2-3): 117-25.

26.   Cha TL, Qiu L, Chen CT, Wen Y, Hung MC. Emodin down-regulates androgen receptor and inhibits prostate cancer cell growth. Cancer Res. 2005; 65 (6): 2287-95.

27.   Acevedo-Duncan M, Russell C, Patel S, Patel R. Aloe-emodin modulates PKC isozymes, inhibits proliferation, and induces apoptosis in U-373MG glioma cells. Int Immunopharmacol. 2004; 4 (14): 1775-84.

28.   Shieh DE, Chen YY, Yen MH, Chiang LC, Lin CC. Emodin-induced apoptosis through p53-dependent pathway in human hepatoma cells. Life Sci. 2004; 74 (18): 2279-90.

29.   Lin S, Fujii M, Hou DX. Rhein induces apoptosis in HL-60 cells via reactive oxygen species-independent mitochondrial death pathway. Arch Biochem Biophys. 2003; 418 (2): 99-107.

30.   Chen YC, Shen SC, Lee WR, Hsu FL, Lin HY, Ko CH, et al. Emodin induces apoptosis in human promyeloleukemic HL-60 cells accompanied by activation of caspase 3 cascade but independent of reactive oxygen species production. Biochem Pharmacol. 2002; 64 (12): 1713-24.

31.   Newman DJ, Cragg GM. Natural products as sources of new drugs over the last 25 years. J Nat Prod. 2007; 70 (3): 461-77.

32.   Kuete V, Saeed ME, Kadioglu O, Börtzler J, Khalid H, Greten HJ, et al. Pharmacogenomic and molecular docking studies on the cytotoxicity of the natural steroid wortmannin against multidrug-resistant tumor cells. Phytomedicine. 2015; 22 (1): 120-7.

33.   Ferlay J SI, Ervik M, Dikshit R, Eser S, Mathers C, Rebelo M, Parkin DM, Forman D, Bray F. Estimated Cancer Incidence, Mortality and Prevalence Worldwide in 2012 Lyon, France: International Agency for Research on Cancer, 2013.

34.   Cancer statistics. [Internet]. 2017 [21st February 2017]. Access address: https://www.cancer.gov/about-cancer/understanding/statistics.

35.   Efferth T. Resistance to Targeted ABC Transporters in Cancer. New York Springer; 2014.

36.   Efferth T, Grassmann R. Impact of viral oncogenesis on responses to anti-cancer drugs and irradiation. Crit Rev Oncog. 1999; 11 (2): 165-87.

37.   Efferth T, Volm M. Pharmacogenetics for individualized cancer chemotherapy. Pharmacol & Ther. 2005; 107 (2): 155-76.

38.   Wegiera M, Smolarz HD, Bogucka-Kocka A. *Rumex* L. species induce apoptosis in 1301, EOL-1 and H-9 cell lines. Acta Pol Pharm. 2012; 69 (3): 487-99.

39.   Duke JA. Handbook of biologically active phytochemicals and their activities. Boca Raton, Florida: CRC Press; 1992.

40.   Đurđević L, Gajić G, Jarić S, Kostić O, Mitrović M, Pavlović P. Analysis of benzoic and cinnamic acid derivatives of some medicinal plants in Serbia. Arch Biol Sci. 2013; 65 (2): 603-9.

41.   Fairbairn JW, El-Muhtadi FJ. Chemotaxonomy of anthraquinones in *Rumex*. Phytochemistry. 1972; 11 (1): 263-8.

42.   Munavu RM, Mudamba LO, Ogur JA. Isolation and Characterization of the Major Anthraquinone Pigments from *Rumex* abysinica. Planta Med. 1984; 50 (1): 111.

43.   Getie M, Gebre-Mariam T, Rietz R, Hohne C, Huschka C, Schmidtke M, et al. Evaluation of the anti-microbial and anti-inflammatory activities of the medicinal plants *Dodonaea viscosa*, *Rumex nervosus* and *Rumex abyssinicus*. Fitoterapia. 2003; 74 (1-2): 139-43.

44.   Kilic O, Bagci E. An ethnobotanical survey of some medicinal plants in Keban (Elazığ-Turkey). J Med Plants Res. 2013; 7 (23): 1675-84.

45.   Çakılcıoğlu U, Türkoğlu İ. Plants used to lower blood sugar in Elazığ central district. Acta Hortic. 2007; 826: 97-104.

46.   Cakilcioglu U, Khatun S, Turkoglu I, Hayta S. Ethnopharmacological survey of medicinal plants in Maden (Elazig-Turkey). J Ethnopharmacol. 2011; 137 (1): 469-86.

47.   Arıtuluk ZC, Ezer N. Halk arasında diyabete karşı kullanılan bitkiler-II. Hacettepe Pharm J. 2012; 32 (2): 179-208.

48.   Mentreddy SR. Medicinal plant species with potential antidiabetic properties. J Sci Food Agric. 2007; 87 (5): 743-50.

49.   Van De Laar FA, Lucassen PL. *α*-Glucosidase inhibitors for patients with type 2 diabetes. Diabetes Care. 2005; 28 (7): 1841-.

50.   Association AD. Diagnosis and classification of diabetes mellitus. Diabetes Care. 2014; 37 (1): 81-90.

51.   WHO. Global report on diabetes, Switzerland, WHO, 2016.

52.   Gray GM. Carbohydrate digestion and absorption - role of small-intestine. New Engl J Med. 1975; 292 (23): 1225-30.

53.   Cheng AYY, Fantus IG. Oral antihyperglycemic therapy for type 2 diabetes mellitus. Can Med Assoc J. 2005; 172 (2): 213-26.

54.   Goke B, Herrmann-Rinke C. The evolving role of alpha-glucosidase inhibitors. Diabetes Metab Rev. 1998; 14: S31-S8.

55.   Lebovitz HE. Alpha-glucosidase inhibitors as agents in the treatment of diabetes. Diabetes Rev. 1998; 6 (2): 132-45.

56.   Inzucchi SE. Oral antihyperglycemic therapy for type 2 diabetes - Scientific review. Jama-J Am Med Assoc. 2002; 287 (3): 360-72.

57.   Yanovski SZ, Yanovski JA. Drug therapy - Obesity. New Engl J Med. 2002; 346 (8): 591-602.

58.   Abrams LR, Ferris RS. An illustrated Flora of the Pacific States: Polygonaceae to Krameriaceae, buckwheats to kramerias. Stanford: Stanford University Press; 1923.

59.   Geven F, Bingöl Ü, Güney K. The revision of Polygonaceae family at Herbarium ANK and to prepare of the database. Kastamonu Uni J For Fac. 2008; 8 (1): 67-85.

60.   Tutin TG. Flora Europaea: Psilotaceae to Platanaceae. Cambridge: Cambridge University Press; 1993.

61.   Cullen J. *Rumex,* In: Davis PH, ed. Flora of Turkey and the East Aegean Islands. Edinburgh: Edinburgh University Press; 1972.

62.   TÜBİVES Turkish Plant Data Service [Internet]. 2017 [3rd August 2017]. Access address: http://naeb.brit.org

63.   Mohlenbrock RH, Thomson PM. Flowering plants: smartweeds to hazelnuts. USA: Southern Illinois University Press; 1987.

64.   Watt JM, Breyer-Brandwijk MG. The medicinal and poisonous plants of southern and eastern Africa: being an account of their medicinal and other uses, chemical composition, pharmacological effects and toxicology in man and animal. USA: E. & S. Livingstone; 1962.

65.   Moerman DE. Native American Ethnobotany. UK: Timber Press; 1998.

66.   Allen DE, Hatfield G. Medicinal plants in folk tradition: an ethnobotany of Britain & Ireland: Timber Press; 2004.

67.   Stopps GJ, White SN, Clements DR, Upadhyaya MK. The biology of Canadian weeds. 149. *Rumex acetosella* L. Can J Plant Sci. 2011; 91 (6): 1037-52.

78.   Baytop T. Türkiyede bitkiler ile bedavi (Geçmişte ve bugün). Istanbul: Nobel Tip Kitabevleri; 1999.

69.   Girma B, Yimer G, Makonnen E. Effect of *Rumex abyssinicus* on preneoplastic lesions in dimethylhydrazine induced colon carcinogenesis in rats. Bmc Complem Altern M. 2015; 15: 365.

70.   Temizer A, Onar A, Orbey M, Sener B, Basgul M. Determination of some naturally-occurring hydroxylated anthraquinones by differential pulse polarography. J Chem Soc Pakistan. 1988; 10 (4): 455-9.

71.   Wegiera M, Smolarz HD, Wianowska D, Dawidowicz AL. Anthracene derivatives in some species of *Rumex* L. genus. Acta Soc Bot Pol. 2007; 76 (2).

72.   Tamano M, Koketsu J. Isolation of hydroxyanthrones from the roots of *Rumex acetosa* Linn. Agr Biol Chem Tokyo. 1982; 46(7):1913-4.

73.   Demirezer LO, Kuruüzüm A, Özcan A, Işımer, A. HPLC studies on some *Rumex* species growing in Turkey. Hacettepe Pharm J. 1996; 16 (2): 67-72.

74.   Rodríguez de Vera BdC, Jiménez Díaz JF, Navarro García E, Alonso Díaz S, Trujillo Carreño J. Componentes fitoquímicos de las especies botánicas de *Rumex*, plantas de uso medicinal. Canar med quir. 2004; 48.

75.   Guo S, Feng B, Zhu R, Ma J, Wang W. Preparative isolation of three anthraquinones from *Rumex japonicus* by high-speed counter-current chromatography. Molecules. 2011; 16 (2): 1201-10.

76.   Demirezer ÖL, Kuruüzüm A. Rapid and simple biological activity screening of some Rumex species; evaluation of bioguided fractions of *R. scutatus* and pure compounds. Zeitschrift für Naturforschung C. 1997; 52 (9-10): 665-9.

77.   Sharma M, Rangaswami S. Chemical components of roots of *Rumex acetosa,* isolation of omega-acetoxyaloe-emodin, a new 1,8-dihydroxyanthraquinone derivative. Indian J Chem B. 1977; 15 (10): 884-5.

78.   Fassil Y, Bezabeh A, Abegaz B, Botta B, Monache GD, Monache FD. Anthracene derivatives from *Rumex abyssinicus*. J Nat Prod. 1985;48(1):148.

79.   Midiwo JO, Rukunga GM. Distribution of anthraquinone pigments in *Rumex* species of Kenya. Phytochemistry. 1985; 24 (6): 1390-1.

80.   Lee N-J, Choi J-H, Koo B-S, Ryu S-Y, Han Y-H, Lee S-I, et al. Antimutagenicity and cytotoxicity of the constituents from the aerial parts of *Rumex acetosa*. Biol Pharm Bull. 2005; 28 (11): 2158-61.

81.   Van den Berg A, Labadie R. The production of acetate derived hydroxyanthraquinones,-dianthrones,-naphthalenes and-benzenes in tissue cultures from *Rumex alpinus*. Planta Med. 1981; 41 (02): 169-73.

82.   Rada KH , Starhova H, Brazdova V. A study of anthraquinone derivatives in some *Rumex* species. Acta Facultatis Pharmaceuticae Universitatis Comenianae. 1974; 25: 153-75.

83.   Liyi H, Bizhu C, Peigen X. Botanical investigation and chemical analysis of Chinese Herbal Medicines derived from the genus *Rumex*. Acta Pharm Sin. 1981; 4: 008.

84.   Saleh NAM, El-Hadidi MN, Arafa RFM. Flavonoids and anthraquinones of some Egyptian *Rumex* species (Polygonaceae). Biochem Syst Ecol. 1993; 21 (2): 301-3.

85.   Zhang H, Guo Z, Wu N, Xu W, Han L, Li N, et al. Two novel naphthalene glucosides and an anthraquinone isolated from *Rumex dentatus* and their antiproliferation activities in four cell lines. Molecules. 2012; 17 (1): 843-50.

86.   Guo LH, Zhu R, Hui Y, L. W. Chemical constituents of *Rumex dictyocarpus*. Xj'an Yike Daxue Xuebao. 1990; 11 (4): 346-8.

87.   Demirezer LO. Anthraquinones from *Rumex gracilescens* Rech. Hacettepe Pharm J. 1995; 5 (2): 77-9.

88.   Liang H-X, Dai H-Q, Fu H-A, Dong X-P, Adebayo AH, Zhang L-X, et al. Bioactive compounds from *Rumex* plants. Phytochem Lett. 2010; 3 (4): 181-4.

89.   Yang Y, Yan Y-M, Wei W, Luo J, Zhang L-S, Zhou X-J, et al. Anthraquinone derivatives from *Rumex* plants and endophytic *Aspergillus fumigatus* and their effects on diabetic nephropathy. Bioorg Med Chem Lett. 2013; 23 (13): 3905-9.

90.   Rivero-Cruz I, Acevedo L, Guerrero JA, Martinez S, Bye R, Pereda-Miranda R, et al. Antimycobacterial agents from selected Mexican medicinal plants. J Pharm Pharmacol. 2005; 57 (9): 1117-26.

91.   Koyama J, Morita I, Kawanishi K, Tagahara K, Kobayashi N. Capillary electrophoresis for simultaneous determination of emodin, chrysophanol, and their 8-beta-D-glucosides. Chem Pharm Bull. 2003; 51 (4): 418-20.

92.   Abd el-Fattah H, Gohar A, el-Dahmy S, Hubaishi A. Phytochemical investigation of *Rumex luminiastrum*. Acta Pharm Hung. 1994; 64(3):83-5.

93.   Gusakova SO, Khomova TV, Al. G. Oxygenated acids in storage lipids of *Rumex paulsenianus*. Khim Prir Soedin. 1991; 6: 762-5.

94.   Kuruzum-Uz A. *Rumex patientia* L. Üzerinde Fitokimyasal Araştırmalar ve Biyolojik Aktivite Çalışmaları [Doctor of Philosophy Thesis]. Ankara: Hacettepe University; 1999.

95.   Yuan Y, Chen W, Zheng S, Yang G, Zhang W, Zhang H. Studies on chemical constituents in root of *Rumex patientia* L. Zhongguo Zhong yao za zhi= Zhongguo zhongyao zazhi= China Journal of Chinese Materia Medica. 2001; 26 (4): 256-8.

96.   Liu J, Xia Z, Zhou G, Zhang L, Kong L. Study on the chemical constituents of Rumex Patientia. Zhong yao cai= Zhongyaocai= Journal of Chinese Medicinal Materials. 2011; 34 (6): 893-5.

97.   Demirezer LÖ, Kuruüzüm-Uz A, Bergere I, Schiewe HJ, Zeeck A. The structures of antioxidant and cytotoxic agents from natural source: anthraquinones and tannins from roots of *Rumex patientia*. Phytochemistry. 2001; 58 (8): 1213-7.

98.   Zaghou M, El-Fattah H. Anthraquinones and flavonoids from *Rumex tingitanus* growing in Libya Zagazig. Pharm Sci. 1999; 8: 54-8.

99.   Litvinenko Y, Muzychkina R. Phytochemical investigation of biologically active substances in certain Kazakhstan *Rumex* species. Chem Nat Compd. 2003; 39 (5): 446-9.

100.   Al Easa HS, Rizk A-FM, Hussiney HA. Constituents of plants growing in Qatar, Part XXVI: Phytochemical investigation of *Rumex vesicarius*. 1995.

101.   Rai J, Thakar K. Chemical investigation of *Rumex vesicarius* Linn. Indian J Chem. 1970.

102.   Ciulei I, Istudor V. Chemical study of the species *Rumex wallichii*. Farmacia. 1973; 21 (2): 85-8.

103.   Kato T, Morita Y. Anthraquinone components in *Rumex acetosa* L. Shoyakugaku Zasshi. 1987; 41 (1): 67-74.

104.   Brazdova V, Hrochova V, Rada K, Starhova H. Anthracene derivatives in some species of the family *Rumex*. IV. Cesk Farm. 1969; 18 (7): 337-40.

105.   Souto AA. Process of obtainment of trans-resveratrol and/or emodin and nutraceuticcal compositions containing them. Germany Patent no. US 20100081724 A1, 2010.

106.   Sayed M, Balbaa S, Afifi M. Anthraquinone content of certain *Rumex* species growing in Egypt. Egypt J Pharm Sci. 1975; 15: 1-10.

107.   Erturk S, Imre M. Anthraquinone pigments from *Rumex cristatus*. Acta Pharm. Turc. 2001; 43 (1): 21-2.

108.   Wang ZY, Zhao HP, Zuo YM, Wang ZQ, Tang XM. Two new C-glucoside oxanthrones from *Rumex gmelini*. Chinese Chem Lett. 2009; 20 (7): 839-41.

109.   Ahmad S, Ullah F, Ayaz M, Sadiq A, Imran M. Antioxidant and anticholinesterase investigations of *Rumex hastatus* D. Don: potential effectiveness in oxidative stress and neurological disorders. Biol Res. 2015; 48.

110.   Jiang L, Zhang S, Xuan L. Oxanthrone C-glycosides and epoxynaphthoquinol from the roots of *Rumex japonicus*. Phytochemistry. 2007; 68 (19): 2444-9.

111.   Jang DS, Kim JM, Kim J, Yoo JL, Kim YS, Kim JS. Effects of compounds isolated from the fruits of *Rumex japonicus* on the protein glycation. Chem Biodivers. 2008; 5 (12): 2718-23.

112.   Jan S, Kamili AN, Parray JA, Bedi YS. Differential response of terpenes and anthraquinones derivatives in *Rumex dentatus* and *Lavandula officinalis* to harsh winters across north-western Himalaya. Nat Prod Res. 2016; 30 (5): 608-12.

113.   Gautam R, Karkhile KV, Bhutani KK, Jachak SM. Anti-inflammatory, cyclooxygenase (COX)-2, COX-1 inhibitory, and free radical scavenging effects of *Rumex nepalensis*. Planta Med. 2010; 76 (14): 1564-9.

114.   Liu S, Sporer F, Wink M, Jourdane J, Henning R, Li Y, et al. Anthraquinones in *Rheum palmatum* and *Rumex dentatus* (Polygonaceae), and phorbol esters in Jatropha curcas (Euphorbiaceae) with molluscicidal activity against the schistosome vector snails Oncomelania, Biomphalaria, and Bulinus. Trop Med Int Health. 1997; 2 (2): 179-88.

115.   Gunaydin K, Topcu G, Ion RM. 1,5-Dihydroxyanthraquinones and an anthrone from roots of *Rumex crispus*. Nat Prod Lett. 2002; 16 (1): 65-70.

116.   Başkan S, Daut-Özdemir A, Günaydın K, Erim FB. Analysis of anthraquinones in *Rumex crispus* by micellar electrokinetic chromatography. Talanta. 2007; 71 (2): 747-50.

117.   Ikan R. Natural products: a laboratory guide. San Diego, California: Academic Press; 2013.

118.   Kang Y, Wang Z, Li J, Liu L. Isolation and identification of two anthraquinones from *Rumex gmelini* Turcz. Zhongguo Zhong Yao Za Zhi. 1996; 21 (12): 741-2, 62.

119.   LO D. Quantitative determination of some *Rumex* species with regards of anthraquinone derivatives. Pharmazie. 1994; 49 (12):936-7.

120.   Yoon H-M, Park J-Y, Oh M-H, Kim K-H, Han J-H, Whang W-K. A new acetophenone of aerial parts from *Rumex aquatica*. Nat Prod Sci. 2005; 11 (2): 75-8.

121.   Kurkin VA, Zaitseva NV, Avdeeva EV, Daeva ED, Kadentsev VI. Anthraquinones and naphthalene derivatives of *Rumex confertus*. Chem Nat Compd. 2013; 49 (1): 135-6.

122.   Fan JP, Zhang ZL. Studies on the chemical constituents of *Rumex crispus*. Zhong Yao Cai. 2009; 32 (12): 1836-40.

123.   Kim J-M, Jang D-S, Lee Y-M, Lee G-Y, Kim J-S. Constituents of the fruits of *Rumex japonicus* with inhibitory activity on aldose reductase. J Appl Biol Chem. 2008; 51 (1): 13-6.

124.   Sharma M, Rangaswami S, Sharma P. Crystalline Chemical Components of Roots of *Rumex nepalensis* Wall. Indian J Chem B. 1978; 16 (4): 289-91.

125.   Annamalai T., Venkateswara Rao G, T. M. Pulmatin from the roots of *Rumex acetosa*. Der Pharmacia Lettre. 2013; 5 (5): 116-9.

126.   Cui HH, Wang ZY, Wang ZQ, Li RM, Kang YH. Study on the optimal harvesting time of *Rumex gmelini* by analyzing the contents of principal components. Zhongguo Zhong Yao Za Zhi. 2005; 30 (11): 808-11.

127.   Chen JM. Studies on chemical components of *Rumex gmelini* Turcz (Ⅳ) [Master Thesis]: Heilongjiang University of Traditional Chinese Medicine; 2008.

128.   Orban-Gyapai O, Liktor-Busa E, Kusz N, Stefko D, Urban E, Hohmann J, et al. Antibacterial screening of *Rumex* species native to the Carpathian Basin and bioactivity-guided isolation of compounds from *Rumex aquaticus*. Fitoterapia. 2017; 118: 101-6.

129.   Xie QC, Yang YP. Anti-proliferative of physcion 8-*O*-beta-glucopyranoside isolated from *Rumex japonicus* Houtt. on A549 cell lines via inducing apoptosis and cell cycle arrest. BMC Complement Altern Med. 2014; 14: 377.

130.   Mei R, Liang H, Wang J, Zeng L, Lu Q, Cheng Y. New seco-anthraquinone glucosides from *Rumex nepalensis*. Planta Med. 2009; 75 (10): 1162-4.

131.   Zhu JJ, Zhang CF, Zhang M, Bligh SW, Yang L, Wang ZM, et al. Separation and identification of three epimeric pairs of new C-glucosyl anthrones from *Rumex dentatus* by on-line high performance liquid chromatography-circular dichroism analysis. J Chromatogr A. 2010; 1217 (33): 5384-8.

132.   Khan AA. The isolation of 1,8-dihydroxy-3-methyl-9-anthrone from the root of *Rumex crispus* Linn. Can J Chem. 1963; 41 (6): 1622-3.

133.   Labadie RP, Scheffer JJ, Svendsen AB. An investigation of the anthracene derivatives in *Rumex hydrolapathum* Huds. I. Pharm Weekbl. 1972; 107 (34): 535-9.

134.   Lim TK. Edible Medicinal and Non Medicinal Plants: Volume 9, Modified Stems, Roots, Bulbs. Netherlands: Springer; 2014.

135.   Abu-Taleb AM, El-Deeb K, Al-Otibi FO. Assessment of antifungal activity of *Rumex vesicarius* L. and *Ziziphus spina-christi* (L.) Willd. extracts against two phytopathogenic fungi. Afr J Microbiol Res. 2011; 5 (9): 1001-11.

136.   Desta KT, Kim GS, Hong GE, Kim YH, Lee WS, Lee SJ, et al. Dietary-flavonoid-rich flowers of *Rumex nervosus* Vahl: Liquid chromatography with electrospray ionization tandem mass spectrometry profiling and in vitro anti-inflammatory effects. J Sep Sci. 2015; 38 (19): 3345-53.

137.   El-Hawary SA, Sokkar NM, Ali ZY, Yehia MM. A Profile of bioactive compounds of *Rumex vesicarius* L. J Food Sci. 2011; 76 (8): C1195-C202.

138.   Kato T, Morita Y. C-glycosylflavones with acetyl substitution from *Rumex acetosa* L. Chem Pharm Bull. 1990; 38 (8): 2277-80.

139.   Kawasaki M, Kanomata T, Yoshitama K. Flavonoids in the leaves of twenty-eight polygonaceous plants. The botanical magazine = Shokubutsu-gaku-zasshi. 1986; 99 (1): 63-74.

140.   Khan TH, Ganaie MA, Siddiqui NA, Alam A, Ansari MN. Antioxidant potential of *Rumex vesicarius* L.: *in vitro* approach. Asian Pac J Trop Biomed. 2014; 4 (7): 538-44.

141.   Pullaiah T, Ali Moulali D. Flora of Andhra Pradesh (India). India: Scientific Publishers; 1997.

142.   Kambhar S. *Rumex vesicarius* L. (Polygonaceae): An Overview. 2014; 11-4.

143.   Aritomi M, Kiyota I, Mazaki T. Flavonoid constituents in leaves of *Rumex acetosa* Linnaeus and *R. japonicus* Houttuyn. Chem Pharm Bull. 1965; 13 (12): 1470-1.

144.   Ferreres F, Ribeiro V, Izquierdo AG, Rodrigues MÂ, Seabra RM, Andrade PB, et al. *Rumex induratus* leaves: interesting dietary source of potential bioactive compounds. J Agr Food Chem. 2006; 54 (16): 5782-9.

145.   Wang X-L, Hu M, Wang S, Cheng Y-X. Phenolic compounds and steroids from *Rumex patientia*. Chem Nat Compd. 2014; 50 (2): 311-3.

146.   Mukhamedyarova M, Chumbalov T. Flavonoids of *Rumex confertus*. Khim Prir Soedin. 1979; 6: 853.

147.   Afifi M. A pharmacological study of certain species belonging to the families Polygonaceae and Cucurbitaceae growing in Egypt [Doctor of Philosophy Thesis]. Cairo, Egypt: Cairo University; 1972.

148.   Chumbalov TK, Kuznetsova LK, Taraskina KV. Catechins and flavonols of *Rumex rechingerianus* roots. Khimiya Prirodnykh Soedinenii. 1969; 5 (3): 181-2.

149.   Hänsel R, Hörhammer L. Phytochemisch-systematische Untersuchung über die Flavonglykoside einiger Polygonaceen. Arch Pharm. 1954; 287 (4): 189-98.

150.   Uzun M. *Rumex crispus* L. ekstreleri ve Sekonder Metabolitlerinin MMPS İnhibitör Aktiviteleri, Antioksidan Kapasiteleri ve SPF Değerlerinin Araştırılarak, Ciltteki Kollajen Dokuyu Onarıcı Fitokozmatik Ürün Geliştirilmesi [Doctor of Philosophy Thesis]. Ankara, Turkey: Hacettepe University; 2017.

151.   Horhammer L, Volz E. Isolation of hyperoside (quercetin-3-D-galactoside) from *Rumex acetosa*. Arch Pharm Ber Dtsch Pharm Ges. 1955; 288 (2):58-60.

152.   Cassileth BR, Lucarelli CD. Herb-drug Interactions in Oncology. USA: PMPH; 2003.

153.   Orban-Gyapai O, Raghavan A, Vasas A, Forgo P, Hohmann J, Shah ZA. Flavonoids isolated from *Rumex aquaticus* exhibit neuroprotective and neurorestorative properties by enhancing neurite outgrowth and synaptophysin. CNS Neurol Disord Drug Targets. 2014; 13 (8): 1458-64.

154.   Elkiey MA, Darwish S, Moustafa MA. Investigation of the flavonoid contents of certain *Rumex* species growing in Egypt. J Pharm Sci. 1964; 5: 197-208.

155.   Tiwari R, Sinha K. Chemical examination of *Rumex hastatus* D-Don. Indian J. Chem. 19B, 531–532.

156.   Ahmed A, Datta BK, Rouf AS. Anthraquinone, chromone and flavone derivative from *Rumex maritimus*. Pharmazie. 1991; 46(7): 548-9.

157.   Chumbalov T, Kuznetsova L, Taraskina K. Catechins and flavonols of the roots of *Rumex rechingerianus*. Chem Nat Compd. 1969; 5(3): 155-6.

158.   Volkhonskaya TA, Minaeva VG, Kiseleva AV, Gorbaleva GN. Flavonoids from cultivated *Rumex thyrsiflorus*. Oikorastushchei Flory Sib. 1970: 206-12.

159.   Li J, Zhang L. Chemical constituents of n-butyl alcohol extract from *Rumex hastatus* roots. Zhongguo Shiyan Fangjixue Zazhi. 2015; 21 (13): 46-9.

160.   Russell S, Dumas C. Sexual Reproduction in flowering plants. Academic Press, 1992.

161.   Wiermann R, Wollenweber E, Rehse C. "Yellow flavonols" as components of pollen pigmentation. Zeitschrift für Naturforschung C. 1981; 36 (3-4): 204-6.

162.   Hasan A, Ahmed I, Jay M, Voirin B. Flavonoid glycosides and an anthraquinone *from Rumex chalepensis*. Phytochemistry. 1995; 39 (5):1211-3.

163.   John K. Edible wild plants. Layton, Utah: Gibbs Smith; 2010.

164.   Bagrii OK, Kurmaz BV, Litvinenko VI. A new bioside of quercetin. Chem Nat Compd. 1966; 2 (2): 65-8.

165.   A. Ahmad M, Ghaleb Naji I, Jaradat N. Determination of rutin in selected Palestinian medicinal plants. USARJ. 2014; 2(1): 6-10.

166.   Rizk AM. The Phytochemistry of the flora of Qatar. Qatar: Scientific and Applied Research Centre, University of Qatar; 1986.

167.   Zhang L-S, Li Z, Mei R-Q, Liu G-M, Long C-L, Wang Y-H, et al. Hastatusides A and B: Two New Phenolic Glucosides from *Rumex hastatus*. Helv Chim Acta. 2009; 92 (4): 774-8.

168.   Zhu J, Zhang C, Zhang M, Wang Z. Studies on chemical constituents in roots of *Rumex dentatus*. Zhongguo Zhong yao za zhi= Zhongguo zhongyao zazhi= China journal of Chinese materia medica. 2006; 31 (20): 1691-3.

169.   Bhadoria B, Gupta R. Chemical investigation of *Rumex dentatus* Linn. Journal. 1977; 54 (12): 1200-1201.

170.   Tavares L, Carrilho D, Tyagi M, Barata D, Serra AT, Duarte CM, et al. Antioxidant capacity of Macaronesian traditional medicinal plants. Molecules. 2010; 15 (4): 2576-92.

171.   Orban-Gyapai O, Raghavan A, Andrea V, Forgo P, Shah Z, Hohmann J. Flavonoid-glycosides from *Rumex aquaticus* with neuroprotective activity. Planta Med. 2014; 80 (16).

172.   Yan XM, Joo MJ, Lim JC, Whang WK, Sim SS, Im C, et al. The effect of quercetin-3-*O*-β-D-glucuronopyranoside on indomethacin-induced gastric damage in rats via induction of mucus secretion and down-regulation of ICAM-1 expression. Arch Pharm Res. 2011; 34 (9): 1527.

173.   Mohamed NZ, Abd-Alla HI, Aly HF, Mantawy M, Ibrahim N, Hassan SA. CCl_4-induced hepatonephrotoxicity: protective effect of nutraceuticals on inflammatory factors and antioxidative status in rat. J. Appl Pharm Ssci. 2014; 4 (2): 87-100.

174.   Savran A, Zengin G, Aktumsek A, Mocan A, Glamoclija J, Ciric A, et al. Phenolic compounds and biological effects of edible *Rumex scutatus* and *Pseudosempervivum sempervivum*: potential sources of natural agents with health benefits. Food Funct. 2016; 7 (7): 3252-62.

175.   Guerra L, Pereira C, Andrade PB, Rodrigues MAn, Ferreres F, Pinho PGD, et al. Targeted metabolite analysis and antioxidant potential of *Rumex induratus*. J Agr Food Chem. 2008; 56 (17): 8184-94.

176.   Siddiqui AW, Ali M, Naquvi K, Sultana S. New flavanones from the seeds of *Rumex vesicarius* L. Nat Prod. 2014; 10 (6): 1-6.

177.   Siddiqui AW, Ali M, Naquvi KJ, Husain SS. New Aliphatic Ester, beta-sitosterol diglucoside and *Vesicaria* biflavones from the seeds of *Rumex vesicarius* L. Acta Pol Pharm. 2015; 72 (5): 965-71.

178. Zee OP, Kim DK, Kwon HC, Lee KR. A new epoxynaphthoquinol from *Rumex japonicus*. Arch Pharm Res. 1998; 21 (4): 485-6.

179. Mohamed G, Ibrahim S. Naturally occurring naphthalenes: chemistry, biosynthesis, structural elucidation, and biological activities. Phytochem Rev. 2015; 15 (2): 279–295.

180. Nishina A, Kubota K, Osawa T. Antimicrobial components, trachrysone and 2-methoxystypandrone, in *Rumex japonicus* Houtt. J Agr Food Chem. 1993; 41 (10): 1772-5.

181. Lee KH, Rhee KH. Antimalarial activity of nepodin isolated from *Rumex crispus*. Arch Pharm Res. 2013; 36 (4): 430-5.

182. Choi GJ, Lee S-W, Jang KS, Kim J-S, Cho KY, Kim J-C. Effects of chrysophanol, parietin, and nepodin of *Rumex crispus* on barley and cucumber powdery mildews. Crop Prot. 2004; 23 (12): 1215-21.

183. Nishina A, Kubota K, Kameoka H, Osawa T. Antioxidizing component, musizin, in *Rumex japonicus* houtt. J Am Oil Chem Soc. 1991; 68 (10): 735-9.

184. Gautam R, Srivastava A, Jachak SM. Simultaneous determination of naphthalene and anthraquinone derivatives in *Rumex nepalensis* Spreng. roots by HPLC: comparison of different extraction methods and validation. Phytochem Anal. 2011; 22 (2): 153-7.

185. Suri J, Dhar K, Atal C. Chemical constituents of *Rumex orientalis* Bernh. J Indian Chem Soc. 1978; 55 (3): 292-3.

186. Bagril OK, Kurnaz K. Hydroxy naphthalenes in some species of dock. Fenol'nye Soedin Ikh Biol Funkts MaterVsesSimp. 1969; 1: 89-93.

187. Yong Y, Shin SY, Lee Y, Kim SH, Lee YH, Lim Y. A compound isolated from *Rumex japonicus* induces apoptosis in heLa cells. J Korean Soc Appl Bi. 2010; 53 (5): 657-60.

188. Bowman R, Franklin C, King T, Falshaw C, Johnson A. 2-Acetyl-3-methylnaphthalane-1,8-diol and its 8-glucoside, constituents of broad-leaved dock, *Rumex obtusifolius*. J Chem Soc. 1963; 1340.

189. Zeng Y, Luo JJ, Li C. Chemical constituents from aerial part of *Rumex patientia*. Zhong Yao Cai. 2013; 36 (1): 57-60.

190. Demirezer O, Kuruuzum A, Bergere I, Schiewe HJ, Zeeck A. Five naphthalene glycosides from the roots of *Rumex patientia*. Phytochemistry. 2001; 56 (4): 399-402.

191. Kuruuzum A, Demirezer LO, Bergere I, Zeeck A. Two new chlorinated naphthalene glycosides from *Rumex patientia*. J Nat Prod. 2001; 64 (5): 688-90.

192. Cobzac S, Moldovan M, Olah N, Bobos L, Surducan E. Tannin extraction efficiency, from *Rubus idaeus*, *Cydonia oblonga* and *Rumex acetosa*, using different extraction techniques and spectrophotometric quantification. Ser F Chem. 2005; 8:5 5-9.

193. Bicker J, Petereit F, Hensel A. Proanthocyanidins and a phloroglucinol derivative from *Rumex acetosa* L. Fitoterapia. 2009;80(8):483-95.

194. Ventura MR, Castañón JIR, Pieltain MC, Flores MP. Nutritive value of forage shrubs: *Bituminaria bituminosa, Rumex lunaria, Acacia salicina, Cassia sturtii* and *Adenocorpus foliosus*. Small Ruminant Res. 2004; 52 (1): 13-8.

195. Nagarajan A, Rajkumar G, Sellamuhtu M, Venkataramegowda S, Anita M. Evaluation of *Basella rubra* L., *Rumex nepalensis* Spreng and *Commelina benghalensis* L. for antioxidant activity. Int J Phar and Pharmaceut Sci. 2012; 4: 714-20.

196. Beddou F, Bekhechi C, Ksouri R, Chabane Sari D, Atik Bekkara F. Potential assessment of *Rumex vesicarius* L. as a source of natural antioxidants and bioactive compounds. Food Sci Technol. 2015; 52 (6): 3549-60.

197. Buchalter L, Cole JR. Isolation of a potential antitumor fraction from *Rumex hymenosepalus* (Polygonaceae). II. Identification of the active fraction. J Pharm Sci. 1967; 56 (8): 1033-4.

198. Cole JR, Buchalter L. Isolation of a potential antitumor fraction from *Rumex hymenosepalus*. J Pharm Sci. 1965; 54 (9): 1376-8.

199. Molan AL, Faraj AM. The effects of condensed tannins extracted from different plant species on egg hatching and larval development of *Teladorsagia circumcincta* (Nematoda: Trichostrongylidae). Folia Parasitol (Praha). 2010; 57 (1): 62-8.

200. Mojab F, Kamalinejad M, Ghaderi N, Vahidipour H. Phytochemical Screening of Some Species of Iranian Plants. Iran J Pharm Res. 2010; 2 (2): 77-82.

201. Tanker N, Koyuncu M, Coşkun M, Güven A, Özgen U. Phytochemical screening of the specimens from İdris Mountain. FABAD J Pharm Sci. 1995; 20 (2): 41-8.

202. Demirezer LÖ, Kuruuzum A. A comparative chemotaxonomic study on eleven *Rumex* species growing in Turkey. FABAD. 1997; 22 (4): 153-8.

203. Sabahi M, Ramezanian M, Jaffari G, Heravi G, Bahaeddini F, Aynehchi Y. Survey of Iranian plants for saponins, alkaloids, flavonoids, and tannins. IV. The Plants of Kerman Province. Int. J. Crude Drug Res. 1985; 23 (4): 165-75.

204. Stöggl WM, Huck CW, Bonn GK. Structural elucidation of catechin and epicatechin in sorrel leaf extracts using liquid-chromatography coupled to diode array-, fluorescence-, and mass spectrometric detection. J Sep Sci. 2004; 27 (7-8): 524-8.

205. Kumar V, Sharma A, Bhardwaj R, Thukral AK. Polyphenol profiling in the leaves of plants from the catchment area of river beas, India. Int J Pharm and Bio Sci. 2015; 6 (4): 1005-12.

206. Desta KT, Lee WS, Lee SJ, Kim Y-H, Kim G-S, Lee SJ, et al. Antioxidant activities and liquid chromatography with electrospray ionization tandem mass spectrometry characterization and quantification of the polyphenolic contents of *Rumex nervosus* Vahl leaves and stems. J Sep Sci. 2016; 39 (8): 1433-41.

207. Gescher K, Hensel A, Hafezi W, Derksen A, Kühn J. Oligomeric proanthocyanidins from *Rumex acetosa* L. inhibit the attachment of herpes simplex virus type-1. Antivir Res. 2011; 89 (1): 9-18.

208.   Elzaawely AA, Xuan TD, Tawata S. Antioxidant and antibacterial activities of *Rumex japonicus* HOUTT. Aerial parts. Biol Pharm Bull. 2005; 28 (12): 2225-30.

209.   SA S, SS S, Khusnutdinov K. Comparative biological study of some *Rumex species* in a crop. Dokl Akad Nauk SSSR. 1971; 28 (4): 59-60.

210.   OK K, SM V. Antitumor activity of leucoanthocyanidins and catechins. Vopr Onkol. 1966; 12 (4): 61-4.

211.   Raez G, Fuzi J. The presence of leucoanthocyanins in herbs. Acta Pharm Hung. 1959; 29: 64-70.

212.   Yoshitama K, Hisada M, Ishikura N. Distribution pattern of anthocyanins in the Polygonaceae. J Plant Res. 1984; 97 (1): 31-8.

213.   Garciabilbao JL, Rodriguez B. Flavonones of *Rumex conglomeratus*. An Quim 1978; 74 (12): 1570-2.

214.   Aynehchi Y, Salehi Sormaghi MH, Amin GH, Khoshkhow M, Shabani A. Survey of Iranian plants for saponins, alkaloids, flavonoids and tannins. III. Int J Crude Drug Res. 1985; 23 (1): 33-41.

215.   Ahmad S, Ullah F, Ayaz M, Zeb A, Ullah F, Sadiq A. Antitumor and anti-angiogenic potentials of isolated crude saponins and various fractions of *Rumex hastatus* D. Don. Biol Res. 2016; 49: 18.

216.   Al-Sunafi SMY. Pharmacognostical Study of *Rumex nervosus* Vahl. family (Polygonaceae) growing in Yemen [Master Thesis]: Cairo University; 2016.

217.   Kasimala MB, Tukue M, Ermias R. Phytochemical screening and antibacterial activity of two common terresterial medicinal plants *Ruta chalepensis* and *Rumex nervosus*. Bali Med J. 2014; 3 (3).

218.   Jimoh F, Adedapo A, Afolayan A. Assessing the polyphenolic, nutritive and biological activities of acetone, methanol and aqueous extracts of *Rumex sagittatus* Thunb. Afr J Pharm Pharmaco. 2010; 4 (9): 630-5.

219.   Kerem Z, Regev-Shoshani G, Flaishman MA, Sivan L. Resveratrol and two monomethylated stilbenes from Israeli Rumex bucephalophorus and their antioxidant potential. J Nat Prod. 2003; 66 (9): 1270-2.

220.   Kerem Z, Bilkis I, Flaishman MA, Sivan L. Antioxidant activity and inhibition of alpha-glucosidase by trans-resveratrol, piceid, and a novel trans-stilbene from the roots of Israeli *Rumex bucephalophorus* L. J Agric Food Chem. 2006; 54 (4): 1243-7.

221.   Guo Z, Xu Y, Tan L, Wang J, Wu N. Method for extracting rhaponticin from *Rumex* plant, China Patent no. CN101475613 A; 2009.

222.   Agarwal J, Rastogi R, Srivastava O. *In vitro* toxicity of constituents of *Rumex maritimus* Linn. to ringworm fungi. Curr Sci India. 1976.

223.   Gusakova SD, Khomova TV, Glushenkova A. Lipids of the fruit of *Rumex paulsenianus*. Chem Nat Compd. 1990; 26 (5): 512-8.

224.   Ammar NM, Ayoub NA, El-Ahmady SH, El-Kassem LTA, Zeid EMA. Phytochemical and Cytotoxic Studies of *Rumex pictus* Forssk. and *Rumex vesicarius*

L. (Family Polygonaceae), growing in Egypt. European J Med Plants. 2015; 10 (3): 1-13.

225.   Orban-Gyapai O, Forgo P, Hohmann J, Vasas A. Phytochemical investigation of *Rumex thyrsiflorus* Fingerh. Acta Biol Hung. 2017; 68 (2): 232-6.

226.   Ladeji O, Okoye ZS. Chemical analysis of sorrel leaf (*Rumex acetosa*). Food Chem. 1993; 48 (2): 205-6.

227.   Elfotoh M, Shams K, Anthony K, Shahat A, Ibrahim M, Abdelhady N, et al. Lipophilic constituents of *Rumex vesicarius* L. and *Rumex dentatus* L. Antioxidants. 2013; 2 (3): 167.

228.   Sridhar R, Lakshminarayana G. Lipid classes, fatty acids, and tocopherols of leaves of six edible plant species. J Agr Food Chem. 1993; 41 (1): 61-3.

229.   Miyazawa M, Tanaka S, Kameoka H. The constituent of the essential oil from *Rumex japonicus* Houtt. Yakugaku Zasshi. 1981; 101 (7): 660-2.

230.   Ahmad S, Ullah F, Sadiq A, Ayaz M, Imran M, Ali I, et al. Chemical composition, antioxidant and anticholinesterase potentials of essential oil of *Rumex hastatus* D. Don collected from the North West of Pakistan. Bmc Complem Altern M. 2016; 16 (1): 29.

231.   Khomova T, Gusakova S, Glushenkova A. Lipids of *Rumex confertus.* Chem Nat Compd. 1989; 25 (2): 248-9.

232.   Daun JK, Tkachuk R. Fatty acid composition of oils extracted from Canadian weed seeds. J. Am. Soc. Brew. Chem.1976; 53 (10): 661-2.

233.   Avci E, Avci GA, Kose DA, Emniyet AA, Suicmez M. *In vitro* antimicrobial and antioxidant activities and GC/MS analysis of the essential oils of *Rumex crispus* and *Rumex cristatus*. Hacettepe J Biol Chem. 2014; 42 (2): 193-9.

234.   Vahedi H, Lari J, Asrabadi MN, Halimi M. Composition and extraction of essential oil from *Rumex chalepensis* using hydrodistillation. Chem Nat Comp. 2012; 48 (2).

235.   Ramesh L, Asha Tukappa NK. Pharmacognostical Evaluation and Comparative Phytochemical Screening of *Rumex vesicarius* L. Int J Phytomed. 2013;5(2):8.

236.   Nisa H, Kamili AN, Bandh SA, Amin S-u, Lone BA, Parray JA. Phytochemical screening, antimicrobial and antioxidant efficacy of different extracts of *Rumex dentatus* L. - A locally used medicinal herb of Kashmir Himalaya. Asian Pac J Trop Dis. 2013; 3 (6): 434-40.

237.   Wilkinson S. alpha-Picoline from *Rumex obtusifolius* L. Nature. 1958; 181 (4609): 636-7.

238.   Salama H. Diterpenoid alkaloids from *Rumex pictus* L. Egypt J Bot. 1997;37 (1): 85-92.

239.   Kim JM, Jang DS, Lee YM, Lee GY, Kim JS. Constituents of the fruits of *Rumex japonicus* with inhibitory activity on aldose reductase. J Appl Biol Chem. 2008; 51 (1): 13-6.

240.   Mithril C, Ove Dragsted L. Safety evaluation of some wild plants in the New Nordic Diet. Food Chem Toxicol. 2012; 50 (12): 4461-7.

241.   Cooper MR, Johnson AW. Poisonous plants in Britain and their effects on animals and man Eureka, CA: Mad River Press; 1984.

242.   Guil JL, Torija ME, Giménez JJ, Rodríguez-García I, Giménez A. Oxalic acid and calcium determination in wild edible plants. J Agr Food Chem. 1996; 44 (7): 1821-3.

243.   Kasai T, Okuda M, Sano H, Mochizuki H, Sato H, Sakamura S. Biological activity of the constituents in roots of Ezo-no-gishigishi (*Rumex obtusifolius*). Agr Biol Chem Tokyo. 1982; 46 (11): 2809-13.

244.   Sánchez-Mata MC, Cabrera Loera RD, Morales P, Fernández-Ruiz V, Cámara M, Díez Marqués C, et al. Wild vegetables of the Mediterranean area as valuable sources of bioactive compounds. Genet Resour Crop Evol. 2012; 59 (3): 431-43.

245.   Molnar P, Osz E, Zsila F, Deli J. Isolation and structure elucidation of anhydroluteins from cooked sorrel (*Rumex rugosus* Campd.). Chem Biodivers. 2005; 2 (7): 928-35.

246.   Kucekova Z, Mlcek J, Humpolicek P, Rop O, Valasek P, Saha P. Phenolic compounds from *Allium schoenoprasum*, *Tragopogon pratensis* and *Rumex acetosa* and their antiproliferative effects. Molecules. 2011; 16 (11): 9207-17.

247.   Kasai T, Okuda M, Sakamura S. 6-O-Malonyl-β-methyl-d-glucopyranoside from roots of *Rumex obtusifolius*. Phytochemistry. 1981; 20 (5): 1131-2.

248.   Khare CP. Indian Medicinal Plants: An Illustrated Dictionary. New York: Springer; 2008.

249.   Alfawaz MA. Chemical composition of hummayd (*Rumex vesicarius*) grown in Saudi Arabia. J Food Compos Anal. 2006; 19 (6): 552-5.

250.   Thomas R. The essiac report: The true story of a Canadian herbal cancer remedy and of the thousands of lives it continues to save: alternative treatment information network. Gig Harbor, WA, USA: Alternative Treatment Information Network, USA; 1993.

251.   Pereira C, Barros L, Carvalho AM, Ferreira IC. Use of UFLC-PDA for the analysis of organic acids in thirty-five species of food and medicinal plants. Food Anal Methods. 2013; 6 (5): 1337-44.

252.   Siener R, Hönow R, Seidler A, Voss S, Hesse A. Oxalate contents of species of the Polygonaceae, Amaranthaceae and Chenopodiaceae families. Food Chem. 2006; 98 (2): 220-4.

253.   Watanabe M, Miyagi A, Nagano M, Kawai-Yamada M, Imai H. Characterization of glucosylceramides in the Polygonaceae, *Rumex obtusifolius* L. injurious weed. Biosci Biotechnol Biochem. 2011; 75 (5): 877-81.

254.   Morales P, Ferreira IC, Carvalho AM, Sanchez-Mata MC, Camara M, Tardio J. Fatty acids profiles of some Spanish wild vegetables. Food Sci Technol Int. 2012; 18 (3): 281-90.

255.	Hanan EB, Spindler JW. Lectins in extracts of certain Polygonaceae seed precipitate animal and human serums. Science. 1968; 160 (3835): 1462-3.

256.	Ito H. Effects of the antitumor agents from various natural sources on drug-metabolizing system, phagocytic activity and complement system in sarcoma 180-bearing mice. Jpn J Pharmacol. 1986; 40 (3): 435-43.

257.	Zava DT, Dollbaum CM, Blen M. Estrogen and progestin bioactivity of foods, herbs, and spices. Proc Soc Exp Biol Med. 1998; 217 (3): 369-78.

258.	Culafic L, Tesevic V, Dokovic D, Kozomara B, editors. Endogenous cytokinins in flowers of male and female clones of *Rumex acetosella* L. Physiol. Biochem Cytokinins Plants, 1992; 381- 383.

259.	Jelic G, Culafic L, Kapor S, Neskovic M. Endogenous cytokinins in the vegetative and reproductive phases of development in the dioecious plant *Rumex acetosella* L. Plant Growth Regul. 1988; 7 (1): 53-8.

260.	Łuczaj Ł, Szymański WM. Wild vascular plants gathered for consumption in the Polish countryside: a review. Ethnobiol Ethnomed. 2007; 3 (1): 17.

261.	Łuczaj Ł, Köhler P, Pirożnikow E, Graniszewska M, Pieroni A, Gervasi T. Wild edible plants of Belarus: from Rostafiński's questionnaire of 1883 to the present. Ethnobiol Ethnomed. 2013; 9: 21.

262.	Luczaj L. Changes in the utilization of wild green vegetables in Poland since the 19th century: a comparison of four ethnobotanical surveys. J Ethnopharmacol. 2010; 128 (2): 395-404.

263.	Dogan Y, Baslar S, Ay G, Mert HH. The use of wild edible plants in Western and Central Anatolia (Turkey). Econ Bot. 2004; 58 (4): 684-90.

264.	Akaydin G, Şimşek I, Arituluk ZC, Yeşilada E. An ethnobotanical survey in selected towns of the Mediterranean subregion (Turkey). Turk J Bio. 2013; 37 (2): 230-47.

265.	Tukan SK, Takruri HR, al-Eisawi DM. The use of wild edible plants in the Jordanian diet. Int J Food Sci Nutr. 1998; 49 (3): 225-35.

266.	Pardo-de-Santayana M, Tardío J, Blanco E, Carvalho AM, Lastra JJ, San Miguel E, et al. Traditional knowledge of wild edible plants used in the northwest of the Iberian Peninsula (Spain and Portugal): a comparative study. J Ethnobiol Ethnomed. 2007; 3 (1): 27.

267.	Pareek A, Kumar A. *Rumex crispus* L.–A plant of traditional value. Drug Discov. 2014; 9 (20): 20-3.

268.	Mekonnen T, Urga K, Engidawork E. Evaluation of the diuretic and analgesic activities of the rhizomes of *Rumex abyssinicus* Jacq in mice. J Ethnopharmacol. 2010; 127 (2): 433-9.

269.	Tyler V. The Honest Herbal: A Sensible guide to the use of herbs and related remedies. Toledo, OH, USA: Pharmaceutical Products Press; 1993.

270.	Dénes A, Papp N, Babai D, Czúcz B, Molnár Z. Edible wild plants and their use based on ethnographic and ethnobotanical researches among Hungarian in the

Carpathian Basin. Dunántúli Dolgozatok (A) Természettudományi Sorozat. 2013; 13: 35-76.

271.   Harshaw, Nahar DL, Naser S-E, Vadla, Sarker S. Harshaw, D., Nahar, L., Saif-E-Naser, G. M., Vadla, B. and Sarker, S. D. Bioactivity of *Rumex obtusifolius* (Polygonaceae). A Biol. Sci. 2010; 62: 387-92.

272.   Vogl S, Picker P, Mihaly-Bison J, Fakhrudin N, Atanasov AG, Heiss EH, et al. Ethnopharmacological *in vitro* studies on Austria's folk medicine—An unexplored lore *in vitro* anti-inflammatory activities of 71 Austrian traditional herbal drugs. J Ethnopharmacol. 2013; 149 (3): 750-71.

273.   Çakılcıoğlu U, Şengün T, Turkoglu I. An ethnobotanical survey of medicinal plants of Yazikonak and Yurtbasi districts of Elazig province, Turkey. J Med Plants Res. 2010; 4 (7): 567-72.

274.   Polat R, Selvi S, Çakılcıoğlu U, Açar M. Investigations of ethnobotanical aspect of wild plants sold in Bingöl (Turkey) local markets. Bio Divers Conserv. 2012; 5 (3): 155-61.

275.   Kaval I, Behcet L, Cakilcioglu U. Ethnobotanical study on medicinal plants in Gecitli and its surrounding (Hakkari-Turkey). J Ethnopharmacol. 2014;155 (1): 171-84.

276.   Solomon T, Largesse Z, Mekbeb A, Eyasu M, Asfaw D. Effect of *Rumex steudelii* methanolic root extract on ovarian folliculogenesis and uterine histology in female albino rats. Afr Health Sci. 2010; 10 (4): 353-61.

277.   Jung J, Nam Y, Sohn UD. Inhibitory effects of ECQ on indomethacin-induced gastric damage in rats. Korean J Physiol Pharmacol. 2012; 16 (6): 399-404.

278.   Rouf AS, Islam MS, Rahman MT. Evaluation of antidiarrhoeal activity *Rumex maritimus* root. J Ethnopharmacol. 2003; 84 (2-3): 307-10.

279.   Ahmad M-u-D, Erum S, Wahid A. Exploring the medicinal plants wealth: a traditional medico-botanical knowledge of local communities in Changa Manga Forest, Pakistan. Middle East J Sci Res. 2014; 20 (12): 1772-9.

280.   Abbasi AM, Shah MH, Li T, Fu X, Guo X, Liu RH. Ethnomedicinal values, phenolic contents and antioxidant properties of wild culinary vegetables. J Ethnopharmacol. 2015; 162: 333-45.

281.   Rousseau J. Notes Sur L'ethnobotanique D'anticosti. Archives de Folklore. 1946; 1: 60-71.

282.   Tamokou JdD, Chouna JR, Fischer-Fodor E, Chereches G, Barbos O, Damian G, et al. Anticancer and antimicrobial activities of some antioxidant-rich Cameroonian medicinal plants. Plos One. 2013; 8 (2): e55880.

283.   Yuan ROC. The Illustration of Common Medicinal Plants in Taiwan. Taipei: Tah-Jinn Printing Co; 2009.

284.   Šťastná P, Klimeš L, Klimešová J. Biological flora of Central Europe: *Rumex alpinus* L. Perspect. Plant Ecol Evol Syst. 2010; 12 (1): 67-79.

285.   Jang H-S, Han JH, Jeong JY, Sohn UD. Protective effect of ECQ on rat reflux esophagitis model. Korean J Physiol Pharmacol. 2012; 16 (6): 455-62.

286. WHO. Medicinal Plants in Vietnam. Manila: WHO Regional Publications; 1990.

287. Shiwani S, Singh NK, Wang MH. Carbohydrase inhibition and anti-cancerous and free radical scavenging properties along with DNA and protein protection ability of methanolic root extracts of *Rumex crispus*. Nutr Res Pract. 2012;6(5):389-95.

288. Steiner RP, Washington DC. Folk medicine: The art and the science.Washington DC: The American Chemical Society; 1986.

289. Sahreen S, Khan MR, Khan RA. Ameliorating effect of various fractions of *Rumex hastatus* roots against hepato- and testicular toxicity caused by CCl_4. Oxid Med Cell Longev. 2013; 2013: 325406.

290. Gairola S, Sharma J, Bedi YS. A cross-cultural analysis of Jammu, Kashmir and Ladakh (India) medicinal plant use. J Ethnopharmacol. 2014; 155 (2): 925-86.

291. Zlatković BK, Bogosavljević SS, Radivojević AR, Pavlović MA. Traditional use of the native medicinal plant resource of Mt. Rtanj (Eastern Serbia): Ethnobotanical evaluation and comparison. J Ethnopharmacol. 2014; 151 (1): 704-13.

292. Lewis WH, Elvin-Lewis MPF. Medical botany: plants affecting human health. United States: Wiley; 2003.

293. Lajter I, Zupko I, Molnar J, Jakab G, Balogh L, Vasas A, et al. Antiproliferative activity of polygonaceae species from the Carpathian Basin against human cancer cell lines. Phytother Res. 2013; 27 (1): 77-85.

294. Tai J, Cheung S, Wong S, Lowe C. *In vitro* comparison of Essiac and Flor-Essence on human tumor cell lines. Oncol Rep. 2004; 11 (2): 471-6.

295. Ottenweller J, Putt K, Blumenthal EJ, Dhawale S, Dhawale SW. Inhibition of prostate cancer-cell proliferation by Essiac. J Altern Complement Med. 2004; 10 (4): 687-91.

296. Ahmad S, Ullah F, Zeb A, Ayaz M, Ullah F, Sadiq A. Evaluation of *Rumex hastatus* D. Don for cytotoxic potential against HeLa and NIH/3T3 cell lines: chemical characterization of chloroform fraction and identification of bioactive compounds. Bmc Complem Altern M. 2016; 16 (1): 308.

297. Kamal Z, Ullah M, Ahmad S, Ullah F, Sadiq A, Ayaz M, et al. Ex-vivo antibacterial, phytotoxic and cytotoxic, potential in the crude natural phytoconstituents of *Rumex hastatus* D. Don. Pak J Bot. 2015; 47 (SI): 293-9.

298. Jagdale P, Ambavade S, Bang S, Adkar P, Salavi N, Ambavade P. Saponins from *Rumex vesicarius* reduces acute and chronic inflammation and HDAC. J Pharm Res. 2014; 8 (2): 1074-81.

299. Wang Q, Wang Y, Xing Y, Yan Y, Guo P, Zhuang J, et al. Physcion 8-*O*-*β*-glucopyranoside induces apoptosis, suppresses invasion and inhibits epithelial to mesenchymal transition of hepatocellular carcinoma HepG2 cells. Biomed Pharmacother.2016; 83 (Supplement C): 372-80.

300.   Degirmenci I, Ustuner MC, Kalender Y, Kalender S, Gunes HV. The effects of acarbose and *Rumex patientia* L. on ultrastructural and biochemical changes of pancreatic B cells in streptozotocin-induced diabetic rats. J Ethnopharmacol. 2005; 97 (3): 555-9.

301.   Sedaghat R, Roghani M, Ahmadi M, Ahmadi F. Antihyperglycemic and antihyperlipidemic effect of *Rumex patientia* seed preparation in streptozotocin-diabetic rats. Pathophysiology. 2011; 18 (2): 111-5.

302.   Ahmed D, Mughal Q, Younas S, Ikram M. Study of phenolic content and urease and alpha-amylase inhibitory activities of methanolic extract of *Rumex acetosella* roots and its sub-fractions in different solvents. Pak J Pharm Sci. 2013; 26 (3): 553.

303.   Reddy NS, Sebbani V, Choday V. *In vitro* and *in vivo* antidiabetic activity of *Rumex vesicarius* leaves extract in streptozotocin induced diabetic albino wister rats. J Diabetes Metab. 2017; 8: 745.

304.   Ha BG, Yonezawa T, Son MJ, Woo JT, Ohba S, Chung U-I, et al. Antidiabetic effect of nepodin, a component of *Rumex* roots, and its modes of action *in vitro* and *in vivo*. Biofactors. 2014; 40 (4): 436-47.

305.   Lee S, Kim D, Yim D. Anti-inflammatory, analgesic and hepatoprotective effect of semen of *Rumex crispus*. Korean J Pharmacogn. 2007; 38 (4): 334-8.

306.   Traditional Chinese medicine composition for pediatric heat releasing and pain relieving. China Patent no. CN 105727011 A; 2016.

307.   Islam M, Rahman M, Rouf A, Nachname V. Evaluation of neuropharmacological effects of *Rumex maritimus* Linn. (Polygonaceae) root extracts. Pharmazie. 2003; 58 (10): 738-41.

308.   Süleyman H, Demirezer L, Kuruüzüm-Uz A. Analgesic and antipyretic activities of *Rumex patientia* extract on mice and rabbits. Pharmazie. 2001; 56 (10): 815-7.

309.   Traditional Chinese medicine ointment for treating allergic dermatitis and preparation method. China Patent no. CN 105687956 A; 2016.

310.   Kim J. Toothpaste Composition Containing *Curcuma longa* L. and Method of Manufacturing Same. China Patent no. US 20160303035 A1; 2016.

311.   Orbán-Gyapai O, Liktor-Busa E, Urbán E, Kúsz N, Jakab G, Stefkó D, et al. Antibacterial activity of *Rumex aquaticus* and *R. thyrsiflorus* extracts and isolation of the biologically active compounds. Planta Med. 2015; 81 (16).

312.   Alzoreky NS, Nakahara K. Antibacterial activity of extracts from some edible plants commonly consumed in Asia. Int J Food Microbiol. 2003; 80 (3): 223-30.

313.   Kustova T, Karpenyuk T, Goncharova A, Ross S. The phytochemical, antibacterial and antioxidant activity of wild plants growing in Kazakhstan against diabetic foot ulcer. J Biotech. 2014 (185): S98.

314.   Koochak H, Seyyednejad SM, Motamedi H. Preliminary study on the antibacterial activity of some medicinal plants of Khuzestan (Iran). Asian Pac J Trop Dis. 2010; 3 (3): 180-4.

315. Jeppesen AS, Soelberg J, Jager AK. Antibacterial and COX-1 Inhibitory Effect of Medicinal Plants from the Pamir Mountains, Afghanistan. Plants (Basel). 2012;1 (2): 74-81.

316. Mostafa H. Antioxidant and antibacterial activity of callus and adventitious root extracts from *Rumex vesicarius* L. J Med Plants Res. 2014; 8 (12): 479-88.

317. Degirmenci I, Kalender S, Ustuner MC, Kalender Y, Gunes HV, Unal N, et al. The effects of acarbose and *Rumex patientia* on liver ultrastructure in streptozotocin-induced diabetic (type II) rats. Drugs Exp Clin Res. 2002; 28 (6): 229-34.

318. Kasuko I, Nagayo O. Effects of vegetable drugs on pathogenic fungi I. Effect of anthraquinone-glycoside containing crude drugs upon the growth of pathogenic fungi. Bull Pharm Res Inst Jpn. 1951; 2: 23-9.

319. Johann S, Cisalpino PS, Watanabe GA, Cota BB, de Siqueira EP, Pizzolatti MG, et al. Antifungal activity of extracts of some plants used in Brazilian traditional medicine against the pathogenic fungus *Paracoccidioides brasiliensis*. Pharm Biol. 2010; 48 (4): 388-96.

320. Kim JC, Choi GJ, Lee SW, Kim JS, Chung KY, Cho KY. Screening extracts of *Achyranthes japonica* and *Rumex crispus* for activity against various plant pathogenic fungi and control of powdery mildew. Pest Manag Sci. 2004; 60 (8): 803-8.

321. Husein A, Al-Nuri MA, Zatar N, Jondi W, Ali-shtayeh MS. Isolation and Antifungal Evaluation of *Rumex cyprius* Murb Extracts. J. Chem. Eng. 2012; 6 (6): 547-50.

322. Basha S, Rekha R, Saleh S, Yemane S. Evaluation of in vitro anthelmintic activities of *Brassica nigra*, *Ocimum basilicum* and *Rumex abyssinicus*. Phcog J. 2011; 3 (20): 88–92.

323. Eguale T, Tadesse D, Giday M. In vitro anthelmintic activity of crude extracts of five medicinal plants against egg-hatching and larval development of *Haemonchus contortus*. J Ethnopharmacol. 2011; 137 (1): 108-13.

324. Ashab I, Lina SMM. *In vitro* phytochemical and anthelmintic activity of *Cocculus hirsutus* Linn. and *Rumex dentatus* Linn. S J Pharm Sci. 2011; 4 (2): 63-65.

325. Aggarwal PK, Kumar L, Garg SK, Mathur VS. Effect of *Rumex nepalensis* extracts on histamine, acetylcholine, carbachol, bradykinin, and PGs evoked skin reactions in rabbits. Ann Allergy. 1986; 56 (2): 177-82.

326. Aggarwal P, Garg S, Kumar L, Mathur V. Effect of *Rumex nepalensis* extracts on histamine, acetylcholine and carbachol evoked responses on isolated guinea pig ileum, frog rectus abdominis muscle, rabbit heart and blood pressure of dog. Indian J Exp Biol. 1985; 23 (8): 447.

327. Mulisa E, Asres K, Engidawork E. Evaluation of wound healing and anti-inflammatory activity of the rhizomes of *Rumex abyssinicus* J. (Polygonaceae) in mice. BMC Complement Altern Med. 2015; 15: 341.

328.   Sumitra S, Rupinder K, Surendra SK. Antinociceptive, antiinflammatory and antipyretic activities of *Rumex hastatus* D. don stem and roots. Der Pharm Sin. 2013; 4 (3): 95-102.

329.   Yeşilada E, Türköz S, Küsmenoğlu Ş, Şener B, Sezik E. Anti-inflammatory activity screening of some Turkish plants in mice. J Gazi Pharm. 1992; 9 (2): 115-23.

330.   Süleyman H, Demirezer LÖ, Kuruüzüm A, Banoğlu Z, Göçer F, Özbakir G, et al. Antiinflammatory effect of the aqueous extract from *Rumex patientia* L. roots. J Ethnopharmacol. 1999; 65 (2): 141-8.

331.   Jovin E, Simin N, Orcic D, Balog K, Beara I, Lesjak M, et al. Antioxidant and anti-inflammatory properties of *Rumex patientia* L. Planta Med. 2011; 77 (12): PM157.

332.   Krishna IV, Bag AK, Karimulla S. Anti-inflammatory activity of *Rumex vesicarius* L. leaves. International Journal of Research in Pharmaceutical Sciences. 2016; 6 (4): 339-43.

333.   Muganga R, Angenot L, Tits M, Frederich M. Antiplasmodial and cytotoxic activities of Rwandan medicinal plants used in the treatment of malaria. J Ethnopharmacol. 2010; 128 (1): 52-7.

334.   Clarkson C, Maharaj VJ, Crouch NR, Grace OM, Pillay P, Matsabisa MG, et al. *In vitro* antiplasmodial activity of medicinal plants native to or naturalised in South Africa. J Ethnopharmacol. 2004; 92 (2-3): 177-91.

335.   Wegiera M, Kosikowska U, Malm A, Smolarz HD. Antimicrobial activity of the extracts from fruits of *Rumex* L. species. Cent Eur J Biol. 2011; 6 (6): 1036-43.

336.   Akgunlu S, Sekeroglu N, Koca-Caliskan U, Ozkutlu F, Ozcelik B, Kulak M, et al. Research on selected wild edible vegetables: Mineral content and antimicrobial potentials. Ann Phytomed. 2016; 5 (2): 50-7.

337.   Ulukanli Z, Ulukanli S, Ozbay H, Ilcim A, Tuzcu M. Antimicrobial activities of some plants from the Eastern Anatolia region of Turkey. Pharm Biol. 2005; 43 (4): 334-9.

338.   Yildirim A, Mavi A, Kara AA. Determination of antioxidant and antimicrobial activities of *Rumex crispus* L. extracts. J Agric Food Chem. 2001; 49 (8): 4083-9.

339.   Coruh I, Gormez A, Ercisli S, Sengul M. Total phenolic content, antioxidant, and antibacterial activity of *Rumex crispus* grown wild in Turkey. Pharm Biol. 2008; 46 (9): 634-8.

340.   El-Shahaby O, El-Zayat M, Salih E, El-Sherbiny I, Reicha F. Evaluation of antimicrobial activity of water infusion plant-mediated silver nanoparticles. J Nanomed Nanotechol. 2013; 4:178.

341.   Nisa H, Kamili A, Amin S, Bandh S, Lone B, Gousia N. Antimicrobial and antioxidant activities of alcoholic extracts of *Rumex dentatus* L. Microb Pathog. 2013; 57:17-20.

342.   Panduraju T, Rao P, Kumar V. A study on antimicrobial activity of *Rumex vesicarius* Linn. Int J Pharm and Techn. 2009; 1 (1): 21-5.

343.   Porteka B, Mot A, Cimpoiu C, Hosu A, Bischin C, Damian G, et al. Selective protective effect of antioxidant-rich *Rumex acetosa* extracts. Revista de chimie. 2016; 67 (5): 833-7.

344.   Alzoreky N, Nakahara K. Antioxidant activity of some edible Yemeni plants evaluated by ferrylmyoglobin/ABTS*+ Assay. Food Sci Technol Res. 2001; 7 (2): 141-4.

345.   Kucekova Z, Mlcek J, Humpolicek P, Rop O. Edible flowers-Antioxidant activity and impact on cell viability. Cent Eur J Biol. 2013; 8 (10): 1023-31.

346.   Isbilir SS, Sagiroglu A. Total phenolic content, antiradical and antioxidant activities of wild and cultivated *Rumex acetosella* L. extracts. Biol Agric Hortic. 2013; 29 (4): 219-26.

347.   Sarikurkcu C, Targan S, Ozer MS, Tepe B. Fatty acid composition, enzyme inhibitory, and antioxidant activities of the ethanol extracts of selected wild edible plants consumed as vegetables in the Aegean region of Turkey. Int J Food Prop. 2017; 20 (3): 560-72.

348.   Ereifej KI, Feng H, Rababah T, Almajwal A, Alu'datt M, Gammoh SI, et al. Chemical composition, phenolics, anthocyanins concentration and antioxidant activity of ten wild edible plants. Food Nutr Sci. 2015; 6 (07): 581.

349.   Özen T. Antioxidant activity of wild edible plants in the Black Sea Region of Turkey. Grasas y aceites. 2010; 61 (1): 86-94.

350.   Maksimovic Z, Kovacevic N, Lakusic B, Cebovic T. Antioxidant activity of yellow dock (*Rumex crispus* L., Polygonaceae) fruit extract. Phytother Res. 2011; 25 (1): 101-5.

351.   Suh H-J, Lee K-S, Kim S-R, Shin M-H, Park S, Park S. Determination of singlet oxygen quenching and protection of biological systems by various extracts from seed of *Rumex crispus* L. J Photochem Photobiol. 2011; 102 (2): 102-7.

352.   Kilic I, Yesiloglu Y, Bayrak Y, Gülen S, Bakkal T. Antioxidant activity of *Rumex conglomeratus* P. collected from Turkey. Asian J Chem. 2013; 25 (17): 9683-7.

353.   Jaradat NA, Damiri B, Abualhasan MN. Antioxidant evaluation for *Urtica urens*, *Rumex cyprius* and *Borago officinalis* edible wild plants in Palestine. Pak J Pharm Sci. 2016; 29 (1): 325-30.

354.   Humeera N, Kamili AN, Bandh SA, Amin SU, Lone BA, Gousia N. Antimicrobial and antioxidant activities of alcoholic extracts of *Rumex dentatus* L. Microb Pathog. 2013; 57: 17-20.

355.   Sahreen S, Khan MR, Khan RA. Comprehensive assessment of phenolics and antiradical potential of *Rumex hastatus* D. Don. roots. Bmc Complem Altern M. 2014; 14 (1): 47.

356.   Dahmani F, Gnaouat H, El Hassouni H, El Hani S, Bouabid B, Sobh M, et al. To study the antioxidant extracts of plant foods *Malva sylvestris* L. et *Rumex palustris* Sm. Bio Technol. 2015; 11 (12).

357. Cetinkaya O, Silig Y, Cetinkaya S, Demirezer LO. The effects of *Rumex patientia* extract on rat liver and erythrocyte antioxidant enzyme system. Pharmazie. 2002; 57 (7): 487-8.

358. Lone IA, Kaur G, Athar M, Alam MS. Protective effect of *Rumex patientia* (English Spinach) roots on ferric nitrilotriacetate (Fe-NTA) induced hepatic oxidative stress and tumor promotion response. Food Chem Toxicol. 2007; 45 (10): 1821-9.

359. Dziedzic K, Kwolek D, Ślesak H. Superoxide dismutase activity in *Rumex thyrsiflorus* Fingerh. explants cultured *in vitro*–preliminary studies. New Biotechnol. 2016; (33): S154.

360. Litvinenko YA, Muzychkina R. New antioxidant phytopreparation from *Rumex thyrsiflorus* roots. III. Chem Nat Compd. 2008; 44 (2): 239-40.

361. Shah A, Singh T, Vijayvergia R. *In vitro* antioxidant properties and total phenolic and flavonoid contents of *Rumex vesicarius* L. Int J Pharm Pharm Sci. 2015; 7 (7): 81-84.

362. Worku N, Mossie A, Stich A, Daugschies A, Trettner S, Hemdan NY, et al. Evaluation of the *in vitro* efficacy of *Artemisia annua, Rumex abyssinicus*, and *Catha edulis* Forsk extracts in cancer and *Trypanosoma brucei* cells. ISRN Biochem. 2013; 2013.

363. Süleyman H, Demirezer L, Kuruüzüm-Uz A, Akcay F. Gastroprotective and antiulcerogenic effects of *Rumex patientia* L. extract. Die Pharmazie. 2002; 57 (3): 204-5.

364. Cos P, Hermans N, De BT, Apers S, Sindambiwe JB, Witvrouw M, et al. Antiviral activity of Rwandan medicinal plants against human immunodeficiency virus type-1 (HIV-1). Phytomedicine. 2002; 9 (1): 62-8.

365. El-Mekkawy S, Meselhy MR, Kusumote IT, Kadota S, Masao H, Namba T. Inhibitory effects of egyptian folk medicines oh human immunodeficiency virus (HIV) reverse transcriptase. Chem Pharm Bull. 1995; 43 (4): 641-8.

366. Taylor RS, Manandhar NP, Hudson JB, Towers GH. Antiviral activities of Nepalese medicinal plants. J Ethnopharmacol. 1996;52(3):157-63.

367. Orhan I, Deliorman-Orhan D, Özçelik B. Antiviral activity and cytotoxicity of the lipophilic extracts of various edible plants and their fatty acids. Food Chem. 2009; 115 (2): 701-5.

368. Kisangau D, Hosea K, V. M. Lyaruu H, C. Joseph C, H. Mbwambo Z, Masimba J, et al. Screening of traditionally used Tanzanian medicinal plants for antifungal activity. Pharm Biol. 2009; 47 (8): 708-16.

369. Suleyman H, Demirezer LO, Kuruuzum A, Buyukokuroglu ME, Gocer F, Banoglu ZN, et al. Effect of the aqueous extract of *Rumex patientia* on xylol and hyaluronidase induced capillary permeability compared to indomethacin. Pharmazie. 2001; 56 (1): 92-3.

370. Rao CV, Sivaramakrishna C, Mallikharjunarao C, Jayalakshmi R, Shaik DB, Subbaraju GV. Antimicrobial, antioxidant and cytotoxic constitutents from roots of *Rumex crispus* Linn. Asian J Chem. 2007; 19 (4): 2764.

371.   Rao K, Sunitha C, Banji D, Shwetha S, Krishna D. Diuretic activity on different extracts and formulation on aerial parts of *Rumex vesicarius* Linn. J Chem Pharm Res. 2011;3 (6): 400-8.

372.   Ahn MJ, Bae JY, Rhee YS, Kim HJ. Composition comprising ethanol extract of *Rumex acetosa* L. for improving gastrointestinal diseases. China Patent no. WO2013141573; 2013.

373.   Kwak HS, Park SY, Nguyen TT, Kim CH, Lee JM, Suh JS, et al. Protective effect of extract from *Rumex aquaticus* herba on ethanol-induced gastric damage in rats. Pharmacology. 2012; 90 (5-6): 288-97.

374.   Han JH, Khin PP, Sohn UD. Effect of *Rumex aquaticus* herba extract against *Helicobacter pylori*-induced inflammation in Gastric Epithelial Cells. J Med Food. 2016; 19 (1): 31-7.

375.   Suleyman H, Demirezer LO, Kuruuzum-Uz A. Effects of *Rumex patientia* root extract on indomethacine and ethanol induced gastric damage in rats. Pharmazie. 2004; 59 (2): 147-9.

376.   Kemper KJ. Sorrel (*Rumex acetosa* L.). Boston, MA: The Longwood Herbal Task Force; 1999.

377.   Fang F, Li Y, Ju X-h, Jiang X-m, Ma J-k. Effect of *Rumex japonicus* Houtt extract on immune function in thrombocytopenic purpura mice. China J Tradit Chin Med Pharm. 2012; 8:55.

378.   Ma J-k, Jiang Y-x, Ma H-b, Wang X-c, Chen Z-h, Lei J-t. Effect of *Rumex japonicus* Houtt extracts on hemopoietic system of model mice with thrombocytopenia. J Jilin Uni Med Edit. 2009; 35 (1): 82-86.

379.   Kanzik I, Şener B, Akar F, Şatiroğlu Ş, Karakoç H. Influence on some *Rumex* extracts on histamine and prostaglandin levels in rat gut. Int J Crude Drug Res. 1988; 26 (3): 173-7.

380.   Ghosh L, Arunachalam G, Murugesan T, Pal M, Saha BP. Studies on the psychopharmacological activities of *Rumex nepalensis* Spreng root extract in rats and mice. Phytomedicine. 2002; 9 (3): 202-6.

381.   Dzhumagalieva F, Scidakhanova T. Various aspects of the pharmacological action of preparations of polyphenol compounds. Akad Nauk Kaz SSR. 1971;16:33-8.

382.   Sun YY, Su XH, Jin JY, Zhou ZQ, Sun SS, Wen J, et al. *Rumex acetosa* L. induces vasorelaxation in rat aorta via activation of PI3-kinase/Akt- and Ca2+-eNOS-NO signaling in endothelial cells. J Physiol Pharmacol. 2015; 66 (6): 907-15.

383.   Orbán-Gyapai O, Lajter I, Hohmann J, Jakab G, Vasas A. Xanthine oxidase inhibitory activity of extracts prepared from Polygonaceae species. Phytother Res. 2015; 29 (3): 459-65.

384.   Scott I, Leduc R, Burt A, Marles R, Arnason J, Foster B. The inhibition of human cytochrome P450 by ethanol extracts of North American botanicals. Pharm Biol. 2006; 44 (5): 315-27.

385. Šežiene V, Baležentiene L, Maruška A. Identification and allelochemical activity of phenolic compounds in extracts from the dominant plant species established in clear-cuts of Scots pine stands. iForest. 2017; 10 (1): 309-14.

386. Cancer [Internet]. 2017 [Access date: 19th September 2017]. Access address: http://www.who.int/cancer/en/

387. Risk factors for cancer [Internet]. 2017 [Access date: 19th September 2017]. Access address: https://www.cancer.gov/about-cancer/causes-prevention/risk

388. Coleman WB, Tsongalis GJ, editors. The molecular basis of human cancer. New York, NY: Springer New York; 2017.

389. Surgery to treat cancer [Internet]. 2017 [Access date: 19th September 2017]. Access address: https://www.cancer.gov/about-cancer/treatment/types/surgery.

390. Radiation theraphy to treat cancer [Internet]. 2017 [Access date: 21st September 2017]. Access address: https://www.cancer.gov/about-cancer/treatment/types/radiation-therapy

391. Chemotheraphy to treat cancer [Internet]. 2017 [Access date: 21st September 2017]. Access address: https://www.cancer.gov/about-cancer/treatment/types/chemotherapy

392. Immunotheraphy to treat cancer [Internet]. 2017 [Access date: 21st September 2017]. Access address: https://www.cancer.gov/about-cancer/treatment/types/immunotherapy

393. Targeted cancer therapies [Internet]. 2017 [Access date: 24th September 2017]. Access address: https://www.cancer.gov/about-cancer/treatment/types/targeted-therapies/targeted-therapies-fact-sheet

394. Hormone theraphy to treat cancer [Internet]. 2017 [Access date: 22nd September 2017]. Access address: https://www.cancer.gov/about-cancer/treatment/types/hormone-therapy

395. Stem cell transplants in cancer treatment [Internet]. 2017 [Access date: 21st September 2017]. Access address: https://www.cancer.gov/about-cancer/treatment/types/stem-cell-transplant

396. Precision medicine in cancer treatment [Internet]. 2017 [Access date: 21st September 2017]. Access address: https://www.cancer.gov/about-cancer/treatment/types/precision-medicine

397. Targeted cancer therapies [Internet]. 2017 [Access date: 24th September 2017]. Access address: https://www.cancer.gov/about-cancer/treatment/types/targeted-therapies/targeted-therapies-fact-sheet

398. Holohan C, Van Schaeybroeck S, Longley DB, Johnston PG. Cancer drug resistance: an evolving paradigm. Nat Rev Cancer. 2013; 13 (10): 714-26.

399. Lackner MR, Wilson TR, Settleman J. Mechanisms of acquired resistance to targeted cancer therapies. Future Oncol. 2012; 8 (8): 999-1014.

400. Mattivi F, Reniero F, Korhammer S. Isolation, characterization, and evolution in red wine vinification of resveratrol monomers. J Agr Food Chem. 1995; 43 (7): 1820-3.

401. Szakacs G, Paterson JK, Ludwig JA, Booth-Genthe C, Gottesman MM. Targeting multidrug resistance in cancer. Nat Rev Drug Discov. 2006; 5 (3): 219-34.

402. Gillet JP, Efferth T, Remacle J. Chemotherapy-induced resistance by ATP-binding cassette transporter genes. Biochim Biophys Acta. 2007; 1775 (2): 237-62.

403. Wu Q, Yang Z, Nie Y, Shi Y, Fan D. Multi-drug resistance in cancer chemotherapeutics: mechanisms and lab approaches. Cancer Lett. 2014; 347 (2): 159-66.

404. Lage H. ABC-transporters: implications on drug resistance from microorganisms to human cancers. Int J Antimicrob Agents. 2003; 22 (3): 188-99.

405. Dean M, Rzhetsky A, Allikmets R. The human ATP-binding cassette (ABC) transporter superfamily. Genome Res. 2001;11 (7): 1156-66.

406. Hientz K, Mohr A, Bhakta-Guha D, Efferth T. The role of p53 in cancer drug resistance and targeted chemotherapy. Oncotarget. 2017; 8 (5): 8921-46.

407. Molecular genetics of cancer Part 4 [Internet]. 2017 [Access date: 26th September 2017]. Access address: http://what-when-how.com/acp-medicine/molecular-genetics-of-cancer-part-4/

408. Al-Lazikani B, Banerji U, Workman P. Combinatorial drug therapy for cancer in the post-genomic era. Nat Biotechnol. 2012; 30 (7): 679-92.

409. Ouyang L, Luo Y, Tian M, Zhang SY, Lu R, Wang JH, et al. Plant natural products: from traditional compounds to new emerging drugs in cancer therapy. Cell Prolif. 2014; 47 (6): 506-15.

410. Luckner M. Secondary metabolism in microorganisms, plants and animals. Heidelberg: Springer Berlin; 2013.

411. Demain AL, Vaishnav P. Natural products for cancer chemotherapy. Microbial biotechnol. 2011; 4 (6): 687-99.

412. Verdine GL. The combinatorial chemistry of nature. Nature. 1996; 384 (6604): 11-3.

413. Dumontet C, Jordan MA. Microtubule-binding agents: a dynamic field of cancer therapeutics. Nat Rev Drug Discov. 2010; 9 (10): 790-803.

414. Liu LF, Desai SD, Li TK, Mao Y, Sun M, Sim SP. Mechanism of action of camptothecin. Ann N Y Acad Sci. 2000; 922: 1-10.

415. Hartmann JT, Lipp HP. Camptothecin and podophyllotoxin derivatives: inhibitors of topoisomerase I and II - mechanisms of action, pharmacokinetics and toxicity profile. Drug Saf. 2006; 29 (3): 209-30.

416. Ovadje P, Roma A, Steckle M, Nicoletti L, Arnason JT, Pandey S. Advances in the research and development of natural health products as main stream cancer therapeutics. Evid Based Complement Alternat Med. 2015; 2015.

417. Pfisterer PH, Wolber G, Efferth T, Rollinger JM, Stuppner H. Natural products in structure-assisted design of molecular cancer therapeutics. Curr Pharm Des. 2010; 16 (15): 1718-41.

418. Shah B, Seth A. Textbook of Pharmacognosy and Phytochemistry - E-Book: Elsevier Health Sciences; 2012.

419. Jansen P, Cardon D, Lemmens R, Oyen L. Dyes and tannins. Technical Centre for Agricultural and Rural Cooperation; 2005.

420. McCreath SB, Delgoda R. Pharmacognosy: Fundamentals, Applications and Strategies: Academic Press; 2017.

421. Srinivas G, Babykutty S, Sathiadevan PP, Srinivas P. Molecular mechanism of emodin action: Transition from laxative ingredient to an antitumor agent. Med Res Rev. 2007; 27 (5): 591-608.

422. Kshirsagar A, V Panchal P, Harle U, K Nanda R, M Shaikh H. Anti-inflammatory and antiarthritic activity of anthraquinone derivatives in Rodents. Int J Inflam. 2014; (2014).

423. Davis RH, Agnew PS, Shapiro E. Antiarthritic Activity Of Anthraquinones found in aloe vera for podiatric medicine. J Am Podiatr Med Assoc. 1986; 76 (2): 1-8.

424. Yen G-C, Duh P-D, Chuang D-Y. Antioxidant activity of anthraquinones and anthrone. Food Chem. 2000; 70 (4): 437-41.

425. Shia C-S, Juang S-H, Tsai S-Y, Chang P-H, Kuo S-C, Hou Y-C, et al. Metabolism and pharmacokinetics of anthraquinones in *Rheum palmatum* in rats and *ex vivo* antioxidant activity. Planta Med. 2009; 75 (13): 1386-92.

426. Andersen DO, Weber ND, Wood SG, Hughes BG, Murray BK, North JA. In vitro virucidal activity of selected anthraquinones and anthraquinone derivatives. Antivir Res. 1991; 16 (2): 185-96.

427. Barnard DL, Huffman JH, Morris JLB, Wood SG, Hughes BG, Sidwell RW. Evaluation of the antiviral activity of anthraquinones, anthrones and anthraquinone derivatives against human cytomegalovirus. Antivir Res. 1992; 17 (1): 63-77.

428. Ali A, Ismail N, Mackeen M, Yazan L, Mohamed S, Ho A, et al. Antiviral, cyototoxic and antimicrobial activities of anthraquinones isolated from the roots of *Morinda elliptica*. Pharm Biol. 2000; 38 (4): 298-301.

429. Sittie A, Lemmich E, Olsen C, Hviid L, Kharazmi A, Nkrumah F, et al. Structure-activity studies: *in vitro* antileishmanial and antimalarial activities of anthraquinones from *Morinda lucida*. Planta Med. 1999; 65 (03): 259-61.

430. Wu Y-B, Zheng C-J, Qin L-P, Sun L-N, Han T, Jiao L, et al. Antiosteoporotic activity of anthraquinones from *Morinda officinalis* on osteoblasts and osteoclasts. Molecules. 2009;14 (1): 573-83.

431 Manojlovic NT, Solujic S, Sukdolak S. Antimicrobial activity of extract and anthraquinones from Caloplaca schaereri. The Lichenologist. 2002; 34 (1): 83-5.

432. Osman CP, Ismail NH, Ahmad R, Ahmat N, Awang K, Jaafar FM. Anthraquinones with antiplasmodial activity from the roots of *Rennellia elliptica* Korth.(Rubiaceae). Molecules. 2010; 15 (10): 7218-26.

433.   Lenta BN, Weniger B, Antheaume C, Noungoue DT, Ngouela S, Assob JC, et al. Anthraquinones from the stem bark of *Stereospermum zenkeri* with antimicrobial activity. Phytochemistry. 2007; 68 (11): 1595-9.

434.   Matsuda H, Shimoda H, Morikawa T, Yoshikawa M. Phytoestrogens from the roots of *Polygonum cuspidatum* (Polygonaceae): structure-requirement of hydroxyanthraquinones for estrogenic activity. Bioorg Med Chem Lett. 2001; 11 (14): 1839-42.

435.   Barbosa TP, Camara CA, Silva TM, Martins RM, Pinto AC, Vargas MD. New 1, 2, 3, 4-tetrahydro-1-aza-anthraquinones and 2-aminoalkyl compounds from norlapachol with molluscicidal activity. Bioorgan Med Chem. 2005; 13 (23): 6464-9.

436.   Wijnsma R, Go JTKA, van Weerden IN, Harkes PAA, Verpoorte R, Baerheim Svendsen A. Anthraquinones as phytoalexins in cell and tissue cultures of *Cinchona* spec. Plant Cell Rep. 1985; 4 (5): 241-4.

437.   Morimoto M, Tanimoto K, Sakatani A, Komai K. Antifeedant activity of an anthraquinone aldehyde in *Galium aparine* L. against *Spodoptera litura* F. Phytochemistry. 2002; 60 (2): 163-6.

438.   Comini L, Fernandez I, Vittar NR, Montoya SN, Cabrera J, Rivarola V. Photodynamic activity of anthraquinones isolated from *Heterophyllaea pustulata* Hook f.(Rubiaceae) on MCF-7c3 breast cancer cells. Phytomedicine. 2011; 18 (12): 1093-5.

439.   Jang DS, Lee GY, Kim YS, Lee YM, Kim C-S, Yoo JL, et al. Anthraquinones from the Seeds of *Cassia tora* with inhibitory activity on protein glycation and aldose reductase. Biol Pharm Bull. 2007; 30 (11): 2207-10.

440.   Foye WO, Vajragupta O, Sengupta SK. DNA-binding specificity and RNA polymerase inhibitory activity of bis (aminoalkyl) anthraquinones and bis (methylthio) vinylquinolinium iodides. J Pharm Sci. 1982; 71 (2): 253-7.

441.   Tosa H, Iinuma M, Asai F, Tanaka T, Nozaki H, Ikeda S, et al. Anthraquinones from *Neonauclea calycina* and their inhibitory activity against DNA topoisomerase II. Biol Pharm Bull. 1998; 21 (6): 641-2.

442.   Noro T, Noro K, Miyase T, Kuroyanagi M, Umehara K, Ueno A, et al. Inhibition of xanthine oxidase by anthraquinones. Chem Pharm Bull. 1987; 35 (10): 4314-6.

443.   Yun-Choi HS, Kim JH, Takido M. Potential inhibitors of platelet aggregation from plant sources, V. Anthraquinones from seeds of *Cassia obtusifolia* and related compounds. J Nat Prod. 1990; 53 (3): 630-3.

444.   WHO. Global status report on noncommunicable diseases 2014. Geneva: 2012.

445.   Mathers CD, Loncar D. Projections of global mortality and burden of disease from 2002 to 2030. Plos Med. 2006; 3 (11).

446.   Van de Laar FA, Lucassen PLBJ, Akkermans RP, Van de Lisdonk EH, Rutten GEHM, Van Weel C. Alpha-glucosidase inhibitors for type 2 diabetes mellitus (Review). Cochrane Database Syst Rev. 2005; 18 (2).

447. Hatano T, Edamatsu R, Hiramatsu M, Mori A, Fujita Y, Yasuhara T, et al. Effects of tannins and related polyphenols on superoxide anion radical, and on 1, 1-diphenyl-2-picrylhydrazyl radical. Chem Pharm Bull. 1989; 37: 2016-21.

448. Jensen SR, Gotfredsen CH, Harput US, Saracoglu I. Chlorinated iridoid glucosides from *Veronica longifolia* and their antioxidant activity. J Nat Prod. 2010; 73 (9): 1593-6.

449. Erel O. A novel automated direct measurement method for total antioxidant capacity using a new generation, more stable ABTS radical cation. Clin Biochem. 2004; 37 (4): 277-85.

450. Zhang J, Shen X, Wang K, Cao X, Zhang C, Zheng H, et al. Antioxidant activities and molecular mechanisms of the ethanol extracts of *Baccharis propolis* and *Eucalyptus propolis* in RAW64.7 cells. Pharm Biol. 2016; 54 (10): 2220-35.

451. Tsai P-J, Tsai T-H, Yu C-H, Ho S-C. Comparison of NO-scavenging and NO-suppressing activities of different herbal teas with those of green tea. Food Chem. 2007; 103 (1): 181-7.

452. Prieto P, Pineda M, Aguilar M. Spectrophotometric quantitation of antioxidant capacity through the formation of a phosphomolybdenum complex: specific application to the determination of vitamin E. Anal Biochem. 1999; 269 (2): 337-41.

453. O'brien J, Wilson I, Orton T, Pognan F. Investigation of the Alamar Blue (resazurin) fluorescent dye for the assessment of mammalian cell cytotoxicity. Eur J Biochem. 2000; 267 (17): 5421-6.

454. Kuete V, Tchakam PD, Wiench B, Ngameni B, Wabo HK, Tala MF, et al. Cytotoxicity and modes of action of four naturally occuring benzophenones: 2,2',5,6'-tetrahydroxybenzophenone, guttiferone E, isogarcinol and isoxanthochymol. Phytomedicine. 2013; 20 (6): 528-36.

455. Eberwine J, Yeh H, Miyashiro K, Cao Y, Nair S, Finnell R, et al. Analysis of gene expression in single live neurons. Proc Natl Acad Sci U S A. 1992; 89 (7): 3010-4.

456. Domercq M, Alberdi E, Sanchez-Gomez MV, Ariz U, Perez-Samartin A, Matute C. Dual-specific phosphatase-6 (Dusp6) and ERK mediate AMPA receptor-induced oligodendrocyte death. J Biol Chem. 2011; 286 (13): 11825-36.

457. Glare EM, Divjak M, Bailey MJ, Walters EH. beta-Actin and GAPDH housekeeping gene expression in asthmatic airways is variable and not suitable for normalising mRNA levels. Thorax. 2002; 57 (9): 765-70.

458. Cossarizza A, Ferraresi R, Troiano L, Roat E, Gibellini L, Bertoncelli L, et al. Simultaneous analysis of reactive oxygen species and reduced glutathione content in living cells by polychromatic flow cytometry. Nat Protoc. 2009; 4 (12): 1790-7.

459. Kuete V, Sandjo LP, Wiench B, Efferth T. Cytotoxicity and modes of action of four Cameroonian dietary spices ethno-medically used to treat cancers: *Echinops giganteus, Xylopia aethiopica, Imperata cylindrica* and *Piper capense.* J Ethnopharmacol. 2013; 149 (1): 245-53.

460.   Wu C-F, Klauck SM, Efferth T. Anticancer activity of cryptotanshinone on acute lymphoblastic leukemia cells. Arch Toxicol. 2016; 90 (9): 2275-86.

461.   Reers M, Smith TW, Chen LB. J-aggregate formation of a carbocyanine as a quantitative fluorescent indicator of membrane potential. Biochem. 1991; 30 (18): 4480-6.

462.   Paull KD, Shoemaker RH, Hodes L, Monks A, Scudiero DA, Rubinstein L, et al. Display and analysis of patterns of differential activity of drugs against human tumor cell lines: development of mean graph and COMPARE algorithm. J Natl Cancer Inst. 1989; 81 (14): 1088-92.

463.   Ooko E, Kadioglu O, Greten HJ, Efferth T. Pharmacogenomic Characterization and isobologram analysis of the combination of ascorbic acid and curcumin-two main metabolites of *Curcuma longa*-in cancer cells. Front Pharmacol. 2017; 8: 38.

464.   Liu T, Ortiz JA, Taing L, Meyer CA, Lee B, Zhang Y, et al. Cistrome: an integrative platform for transcriptional regulation studies. Genome Biol. 2011; 12 (8): R83.

465.   Seo EJ, Saeed M, Law BY, Wu AG, Kadioglu O, Greten HJ, et al. Pharmacogenomics of scopoletin in tumor cells. Molecules. 2016; 21 (4): 496.

466.   Morris GM, Huey R, Lindstrom W, Sanner MF, Belew RK, Goodsell DS, et al. AutoDock4 and AutoDockTools4: Automated docking with selective receptor flexibility. J Comput Chem. 2009; 30 (16): 2785-91.

467.   YinJun L, Jie J, YunGui W. Triptolide inhibits transcription factor NF-kappaB and induces apoptosis of multiple myeloma cells. Leuk Res. 2005; 29 (1): 99-105.

468.   Nampoothiri SV, Prathapan A, Cherian OL, Raghu K, Venugopalan V, Sundaresan A. *In vitro* antioxidant and inhibitory potential of *Terminalia bellerica* and *Emblica officinalis* fruits against LDL oxidation and key enzymes linked to type 2 diabetes. Food Chem Toxicol. 2011; 49 (1): 125-31.

469.   Bachhawat A, Shihabudeen M, Thirumurugan K. Screening of fifteen Indian Ayurvedic plants for alpha-glucosidase inhibitory activity and enzyme kinetics. Int J Pharm Pharm Sci. 2011; 3: 267-74.

470.   Teguo PW, Decendit A, Vercauteren J, Deffieux G, Mérillon J-M. Trans-resveratrol-3-*O*-*β*-glucoside (piceid) in cell suspension cultures of *Vitis vinifera*. Phytochem. 1996; 42 (6): 1591-3471.

471   Francis GW, Aksnes DW, Holt Q. Assignment of the 1H and 13C NMR spectra of anthraquinone glycosides from *Rhamnus frangula*. Magn Reson Chem. 1998; 36 (10): 769-72.

472.   Bouwstra JB, Kerekgyarto J, Kamerling JP, Vliegenthart JF. 1H- and 13C-NMR assignments for structural elements of xylose-containing N-linked oligosaccharides, using 1D-and 2D-NMR experiments. Carbohydr Res. 1989; 186 (1): 39-49.

473.   Dai SJ, Chen RY, Zhang PC, Yu DQ. A new compound from *Rhododendron anthopogonosides* Maxim. J Asian Nat Prod Res. 2005; 7 (4): 681-5.

474.   Szakiel A, Voutquenne-Nazabadioko L, Henry M. Isolation and biological activities of lyoniside from rhizomes and stems of *Vaccinium myrtillus*. Phytochem Lett. 2011; 4 (2): 138-43.

475.   Lundgren LN, Popoff T, Theander O. Dilignol glycosides from needles of *Picea abies*. Phytochem. 1981; 20 (8): 1967-9.

476.   L. Davis A, Cai Y, P. Davies A, Lewis J. 1H and 13C NMR Assignments of some green tea polyphenols. Magn Reson Chem. 1996; 34 (11): 887-90.

477.   Danielsen K, Aksnes DW, Francis GW. NMR study of some anthraquinones from rhubarb. Magn Reson Chem. 1992; 30 (4): 359-60.

478.   Cooke MS, Evans MD, Dizdaroglu M, Lunec J. Oxidative DNA damage: mechanisms, mutation, and disease. FASEB. 2003; 17 (10): 1195-214.

479.   Norbury CJ, Zhivotovsky B. DNA damage-induced apoptosis. Oncogene. 2004;23(16):2797-808.

480.   Kroemer G, Reed JC. Mitochondrial control of cell death. Nat Med. 2000; 6 (5): 513.

481.   Newmeyer DD, Ferguson-Miller S. Mitochondria: releasing power for life and unleashing the machineries of death. Cell. 2003; 112 (4): 481-90.

482.   Desagher S, Martinou J-C. Mitochondria as the central control point of apoptosis. Trends Cell Biol. 2000; 10 (9): 369-77.

483.   Wosikowski K, Schuurhuis D, Johnson K, Paull KD, Myers TG, Weinstein JN, et al. Identification of epidermal growth factor receptor and c-erbB2 pathway inhibitors by correlation with gene expression patterns. J Natl Cancer Inst. 1997; 89 (20): 1505-15.

484.   OMIM [Internet]. 2017 [Access date 24th May 2017]. Access address: https://www.ncbi.nlm.nih.gov/omim

485.   Gene Cards: The Human Gene Database [Internet]. 2017 [Access date 24th May 2017]. Access address: http://www.genecards.org

486.   Hoesel B, Schmid JA. The complexity of NF-κB signaling in inflammation and cancer. Mol Cancer. 2013; 12: 86.

487.   Karin M, Cao Y, Greten FR, Li Z-W. NF-[kappa]B in cancer: from innocent bystander to major culprit. Nat Rev Cancer. 2002; 2 (4): 301-10.

488.   Liu Z-g, Hsu H, Goeddel DV, Karin M. Dissection of TNF receptor 1 effector functions: JNK Activation is not linked to apoptosis while NF-κB activation prevents cell death. Cell. 1996; 87 (3): 565-76.

489.   Pecere T, Gazzola MV, Mucignat C, Parolin C, Vecchia FD, Cavaggioni A, et al. Aloe-emodin is a new type of anticancer agent with selective activity against neuroectodermal tumors. Cancer Res. 2000; 60 (11): 2800.

490.   Nesslany F, Simar-Meintières S, Ficheux H, Marzin D. Aloe-emodin-induced DNA fragmentation in the mouse *in vivo* comet assay. Mutat Res Genet Toxicol Environ Mutagen. 2009; 678 (1): 13-9.

491.   Liu K, Park C, Li S, Lee KW, Liu H, He L, et al. Aloe-emodin suppresses prostate cancer by targeting the mTOR complex 2. Carcinogenesis. 2012; 33 (7): 1406-11.

492.   Pluchino KM, Hall MD, Goldsborough AS, Callaghan R, Gottesman MM. Collateral sensitivity as a strategy against cancer multidrug resistance. Drug Resist Update. 2012; 15 (1-2): 98-105.

493.   Weinstein JN. Spotlight on molecular profiling: "Integromic" analysis of the NCI-60 cancer cell lines. Mol Cancer Ther. 2006; 5 (11): 2601-5.

494.   DTP Developmental Therapeutics Programme COMPARE Analysis [Internet]. 2017 [Access date 4th November 2017]. Access address: https://dtp.cancer.gov/databases_tools/compare.htm

495.   Szakács G, Annereau J-P, Lababidi S, Shankavaram U, Arciello A, Bussey KJ, et al. Predicting drug sensitivity and resistance: profiling ABC transporter genes in cancer cells. Cancer Cell. 2004; 6 (2): 129-37.

496.   Reinhold WC, Sunshine M, Liu H, Varma S, Kohn KW, Morris J, et al. CellMiner: a web-based suite of genomic and pharmacologic tools to explore transcript and drug patterns in the NCI-60 cell line set. Cancer Res. 2012; 72 (14): 3499-511.

497.   Abdelfatah SA, Efferth T. Cytotoxicity of the indole alkaloid reserpine from *Rauwolfia serpentina* against drug-resistant tumor cells. Phytomedicine. 2015; 22 (2): 308-18.

498.   Ooko E, Saeed ME, Kadioglu O, Sarvi S, Colak M, Elmasaoudi K, et al. Artemisinin derivatives induce iron-dependent cell death (ferroptosis) in tumor cells. Phytomedicine. 2015; 22 (11): 1045-54.

499.   Kadioglu O, Jacob S, Bohnert S, Nass J, Saeed ME, Khalid H, et al. Evaluating ancient Egyptian prescriptions today: Anti-inflammatory activity of *Ziziphus spina-christi*. Phytomedicine. 2016; 23 (3): 293-306.

500.   Fu Y, Kadioglu O, Wiench B, Wei Z, Gao C, Luo M, et al. Cell cycle arrest and induction of apoptosis by cajanin stilbene acid from *Cajanus cajan* in breast cancer cells. Phytomedicine. 2015; 22 (4): 462-8.

501.   Zamani M, Sadeghizadeh M, Behmanesh M, Najafi F. Dendrosomal curcumin increases expression of the long non-coding RNA gene MEG3 via up-regulation of epi-miRs in hepatocellular cancer. Phytomedicine. 2015; 22 (10): 961-7.

502.   Hellweg CE. The Nuclear Factor kappa B pathway: A link to the immune system in the radiation response. Cancer Lett. 2015; 368 (2): 275-89.

503.   Li R, Chen Y, Shi M, Xu X, Zhao Y, Wu X, et al. Gegen Qinlian decoction alleviates experimental colitis via suppressing TLR4/NF-kappaB signaling and enhancing antioxidant effect. Phytomedicine. 2016; 23 (10): 1012-20.

504.   Mitchell S, Vargas J, Hoffmann A. Signaling via the NFkappaB system. Wiley interdisciplinary reviews Systems Biology and Medicine. 2016; 8 (3): 227-41.

505.   Karin M, Ben-Neriah Y. Phosphorylation meets ubiquitination: the control of NF-[kappa]B activity. Ann Rev Immun. 2000; 18: 621-63.

506.   Bonizzi G, Karin M. The two NF-kappaB activation pathways and their role in innate and adaptive immunity. Trends Immunol. 2004; 25 (6): 280-8.

507.   Wesolowski R, Ramaswamy B. Gene expression profiling: changing face of breast cancer classification and management. Gene Expr. 2011; 15 (3): 105-15.

508.   Tsao AS, Papadimitrakopoulou V. The importance of molecular profiling in predicting response to epidermal growth factor receptor family inhibitors in non–small-cell lung cancer: focus on clinical trial results. Clin Lung Cancer. 2013; 14 (4): 311-21.

509.   Frank TS, Sun X, Zhang Y, Yang J, Fisher WE, Gingras MC, et al. Genomic profiling guides the choice of molecular targeted therapy of pancreatic cancer. Cancer Lett. 2015; 363 (1): 1-6.

510.   Lin Y, Kazlova V, Ramakrishnan S, Murray MA, Fast D, Chandra A, et al. Bone health nutraceuticals alter microarray mRNA gene expression: A randomized, parallel, open-label clinical study. Phytomedicine. 2016; 23 (1): 18-26.

511.   Wu C-F, Seo E-J, Klauck SM, Efferth T. Cryptotanshinone deregulates unfolded protein response and eukaryotic initiation factor signaling in acute lymphoblastic leukemia cells. Phytomedicine. 2016; 23 (2): 174-80.

512.   Efferth T, Koch E. Complex interactions between phytochemicals. The multi-target therapeutic concept of phytotherapy. Curr Drug Targets. 2011;12 (1): 122-32.

513.   Chen YY, Chiang SY, Lin JG, Yang JS, Ma YS, Liao CL, et al. Emodin, aloe-emodin and rhein induced DNA damage and inhibited DNA repair gene expression in SCC-4 human tongue cancer cells. Anticancer Res. 2010; 30 (3): 945-51.

514.   Lee HZ, Lin CJ, Yang WH, Leung WC, Chang SP. Aloe-emodin induced DNA damage through generation of reactive oxygen species in human lung carcinoma cells. Cancer Lett. 2006; 239 (1): 55-63.

515.   Muller SO, Eckert I, Lutz WK, Stopper H. Genotoxicity of the laxative drug components emodin, aloe-emodin and danthron in mammalian cells: topoisomerase II mediated? Mutation research. 1996; 371 (3-4): 165-73.

516.   Chen R, Zhang J, Hu Y, Wang S, Chen M, Wang Y. Potential Antineoplastic Effects of Aloe-emodin: A Comprehensive Review. Am J Chinese Med. 2014; 42 (2): 275-88.

517.   Toeller M. alpha-Glucosidase inhibitors in diabetes: efficacy in NIDDM subjects. Eur J Clin Invest. 1994; 24 (3): 31-5.

518.   Scheen A. Voglibose for prevention of type 2 diabetes mellitus. Lancet. 2009; 373 (9675): 1579-80.

519.   Tundis R, Loizzo MR, Menichini F. Natural products as alpha-amylase and alpha-glucosidase inhibitors and their hypoglycaemic potential in the treatment of diabetes: an update. Mini reviews in Med Chem. 2010; 10 (4): 315-31.

520. Tundis R, Loizzo M, Statti G, Menichini F. Inhibitory effects on the digestive enzyme *α*-amylase of three *Salsola* species (Chenopodiaceae) *in vitro*. Die Pharm-An Int J Pharm Sci. 2007; 62 (6): 473-5.

521. Loizzo MR, Saab AM, Tundis R, Menichini F, Bonesi M, Piccolo V, et al. *In vitro* inhibitory activities of plants used in Lebanon traditional medicine against angiotensin converting enzyme (ACE) and digestive enzymes related to diabetes. J Ethnopharmacol. 2008; 119 (1): 109-16.

522. Deutschländer M, Van de Venter M, Roux S, Louw J, Lall N. Hypoglycaemic activity of four plant extracts traditionally used in South Africa for diabetes. J Ethnopharmacol. 2009; 124 (3): 619-24.

8.   CURRICULUM VITAE

1. Personal Information

Name-Surname	**: Nadire ÖZENVER**
Place of birth- date	**: Karabük-01.01.1987**
Nationality	**: Turkish**
E-mail and tel	**:** nadire@hacettepe.edu.tr**, +90 312 305 1089**

2. Education

- **2012-2018** **:** Graduate education (PhD) in Hacettepe University, Institute of Health Sciences, Pharmacognosy Department.
- **2007-2011** **:** Undergraduate education in Hacettepe University Faculty of Pharmacy.
- **2006-2007** **:** Undergraduate education in Anadolu University Faculty of Pharmacy.
- **2001-2005** **:** High school education in Karabuk Mustafa Yazici High School (Foreign Language Oriented) .
- **1994-2001** **:** Primary education in Karabuk Yenisehir Ataturk Primary School.

3. Professional Experience

2012- : Research assistant in Hacettepe University Faculty of Pharmacy, Department of Pharmacognosy.

11.2015-11.2016 : Researcher in Johannes Gutenberg University, Institute of Pharmacy and Biochemistry, Department of Pharmaceutıcal Biology, Mainz, Germany.

4. Scientific Activities

- **3-7 September, 2017-** Attendance to **"**65th International Congress and Annual Meeting of the Society for Medicinal Plant and Natural Product Research (GA)" in Basel, Switzerland.

- **24–28 July, 2017-**Attendance to "International Conference on Science and Society 2017: 'Phytomedicine and Biopiracy' ICSS-2017" in Mainz, Germany.

- **16 November 2015-14 November 2016-** Studying about "Pharmacogenomic Studies on Natural Compounds" at Johannes Gutenberg University, Institute of Pharmacy and Biochemistry, Department of Pharmaceutıcal Biology, Mainz, Germany.

- **22 September 2016-** Attendance to "International Symposium on Streamlining Drug Discovery" in Basel, Switzerland.

- **7-10 August 2016-** Attendance to "The 3rd Annual Meeting of The Specialty Committee of Immunology of Traditional Chinese Medicine of the World Federation of Chinese Medicine Societies" in Mainz, Germany

- **24-27 July 2016-** Attendance to "9th Joint Natural Products Conference 2016" in Copenhagen, Denmark

- **7 June 2016-** Attendance to "Fit for Health 2.0- International Training for Horizon 2020 Applicants in Health, Demographic Change and Wellbeing" in Rome, Italy.

- **9-12 June 2015-** Attendance to "11th International Symposium on Pharmaceutical Sciences (ISOPS)" in Ankara University Faculty of Pharmacy, Turkey.

- **14 March 2015-** Attendance to "Scientific Publishing Course-III" conducted by Hacettepe University Institute of Health Sciences and *Acta Medica*.

- **18-21 September 2014-** Attendance to **"**Fourth International Meeting on Pharmacy & Pharmaceutical Sciences (IMPPS-4)" in Marmara University Faculty of Pharmacy, Istanbul with a poster presentation.

- **23-25 June 2014-** Attendance to "Trends in Natural Products Research A Young Scientists Meeting" in Olomouc, Czech Republic with two poster presentations.

- **27 May 2014-** Attendance to The Author Workshop conducted by Springer called "How to Publish a Scientific Journal Article".

- **1-3 November 2013-** Attendance to "Pharmacognosy and Phytotherapy Association Workshop-1; 1D, 2D NMR Techniques in the structure determination of natural compound: practical work" organized by FFD in Ankara University, Faculty of Pharmacy

- **1-5 September 2013-** Attendance to "61st International Congress and The Annual Meeting of The Society for Medicinal Plant and Natural Product Research (GA)" in Münster, Germany with a poster presentation.

- **20-22 February, 2013-** Attendance to "Course for Practical Molecular Modeling and Simulation Techniques in Drug Researches" in Hacettepe University Medicinal Chemistry Research, Development and Practice Center.

- **3 December 2012-** Education for introduction to clinical researches organized as a part of Hacettepe Technopolis Clinical Research Project.

- **19-20 September, 2012-** Attendance to "Membrane Bound Protein & Ligand Docking Workshop" in Sabanci University, Istanbul.

- **4 July-10 August, 2012-** Having a course about "*In silico* docking researches of natural compounds" with Prof. Ugur Sezerman in Sabanci University Faculty of Engineering and Natural Sciences.

- **31 May 2012**- Attendance to "From Plant to Drug-4" Joint meeting of FFD with ESCOP organized by FFD in Bezmialem Vakif University.

- **30 May 2012-** Attendance to symposium about "Membrane Structure and Interactions" organized by Acibadem University, Faculty of Medicine, Biophysics Department.

- **28 June- 6 August, 2010-** Training in Quality Control Units of Beta Lactam Products of Mustafa Nevzat Pharmaceuticals.

5. Publicatication, Book, Oral Presentation, Poster Presentation, Project and Scholarship

Original publications

1. Özenver N, Saeed M, Demirezer LÖ, Efferth T. Aloe-emodin as drug candidate for cancer therapy. Oncotarget. 2017. (Accepted)

2. Efferth T, Banerjee M, Paul NW, Abdelfatah S, Arend J, Elhassan G, Hamdoun S, Hamm R, Hong C, Kadioglu O, Naß J, Ochwangi D, Ooko E, Ozenver N, Saeed ME, Schneider M, Seo EJ, Wu CF, Yan G, Zeino M, Zhao Q, Abu-Darwish MS, Andersch K, Alexie G, Bessarab D, Bhakta-Guha D, Bolzani V, Dapat E, Donenko FV, Efferth M, Greten HJ, Gunatilaka L, Hussein AA, Karadeniz A, Khalid HE, Kuete V, Lee IS, Liu L, Midiwo J, Mora R, Nakagawa H, Ngassapa O, Noysang C, Omosa LK, Roland FH, Shahat AA, Saab A, Saeed EM, Shan L, Titinchi SJ. Biopiracy of natural products and good bioprospecting practice. Phytomedicine. 2016; 23(34):166-73.

3. Demirezer LO, Ozenver N, Uzun M, Yukselen O, Guvenalp Z, Sezerman OU. Molecular Docking of Anthranoids on Some Targeted Human Proteins. FABAD J. Pharm. Sci. 2016; 41: 1-16.

4. Demirezer LÖ, Gürbüz P, Kelicen Uğur EP, Bodur M, Özenver N, Uz A, Güvenalp Z. Molecular docking and ex vivo and in vitro anticholinesterase activity studies of *Salvia* sp. and highlighted rosmarinic acid. Turk J Med. 2015; 45(5):1141-1148.

Book Chapters

1. Özenver, N. and Demirezer LÖ *Rumex acetosa* L. Demirezer, L.Ö. Ersöz, T., Saraçoğlu, İ., Şener, B., Köroğlu, A., Yalçın, F. N. FFD Monografları- Bitkiler ve Etkileri. 3. Ankara: Akademisyen Kitabevi; 2017.

2. Özenver, N. and Demirezer LÖ. *Rumex acetosella* L. Demirezer, L.Ö. Ersöz, T., Saraçoğlu, İ., Şener, B., Köroğlu, A., Yalçın, F. N. FFD Monografları- Bitkiler ve Etkileri. 3. Ankara: Akademisyen Kitabevi; 2017.

Oral presentations

1. Ozenver, N., Saeed, M., Demirezer, L.O., Efferth, T. Aloe-emodin as drug candidate in cancer therapy. International Conference on Science and Society 2017: "Phytomedicine and Biopiracy" ICSS-2017, Mainz, Germany, 2017.

2. Ağar, O.T., Gönülalan, E.M., Özenver, N., Uzun, M., Demirezer, L.Ö. Sun protective potential and antioxidant capacity of *Rosa damascena* petal extracts. XXIst International Congress "Phytopharm 2017", Graz, Austria, 2017.

Poster presentations

1. Ozenver, N., Saeed M., Demirezer, L.O, Efferth, T. Cytotoxicity of aloe-emodin towards several drug sensitive cells and their resistant counterparts. 65th International Congress and Annual Meeting of the Society for Medicinal Plant and Natural Product Research (GA). Basel- Switzerland, 2017.

2. Ozenver, N., Saeed M., Demirezer, L.O, Efferth, T. Aloe-emodin's cytotoxicity against CCRF-CEM cells: NF-κB as a major player induces apoptosis . 65th International Congress and Annual Meeting of the Society for Medicinal Plant and Natural Product Research (GA). Basel- Switzerland, 2017.

3. Ozenver, N., Saeed, M., Kauhl, U., Guvenalp, Z., Demirezer, L.O., Opatz, T., Efferth, T. Structure determination and preliminary cytotoxicity researches of the compounds isolated from *Rumex acetosella* L. on leukemia cells. 65th International Congress and Annual Meeting of the Society for Medicinal Plant and Natural Product Research (GA). Basel, Switzerland, 2017.

4. Gonulalan, E.M., Ozenver, N., Demirezer, L.O. Sun Protection Factor (SPF) and antioxidant capacity of *Lavandula angustifolia* L. 65th International Congress and Annual Meeting of the Society for Medicinal Plant and Natural Product Research (GA). Basel, Switzerland, 2017.

5. Gonulalan, E.M., Uzun, M., Ozenver, N., Demirezer, L.O. Determination of Sun Protection Factor (SPF) and antioxidant capacity of *Tanacetum parthenium*. 65th International Congress and Annual Meeting of the Society

for Medicinal Plant and Natural Product Research (GA). Basel, Switzerland-2017.

6. Ozenver, N., Saeed, M., Demirezer, L.O., Guvenalp, Z., Efferth, T. Chrysophanol- and nepodin-8-O-*β*-D-glucopyranoside from *Rumex acetosell*a, the cytotoxicity towards drug sensitive and multi- drug resistant T leukaemia cancer cells. 9th Joint Natural Products Conference 2016, Copenhagen, Denmark.

7. Ozenver, N., Saeed M., Demirezer, L.O, Efferth, T. Cytotoxicity of main anthraquinone aglycons towards drug sensitive and multi drug resistant T leukaemia cancer cells. 9th Joint Natural Products Conference 2016, Copenhagen, Denmark.

8. Ozenver, N., Demirezer, L.O., Saeed, M., Efferth, T. *Rumex* Türlerinde Bulunan Bazı Antranoitlerin Kemoterapötiklere Duyarlı CCRF-CEM ve Çoklu İlaç Direnci Geliştiren Karşılığı CEM/ADR5000 T lösemi Hücrelerindeki Sitotoksisitesi. Bitkisel İlaç Hammaddeleri Toplantısı (BİHAT-2016), Trabzon, Turkey, 2016.

9. Ozenver N, Demirezer L.O. Alpha Glucosidase Inhibition and Antioxidant Potential of Some *Rumex acetosella* L. Extracts. 11th International Symposium on Pharmaceutical Sciences (ISOPS), Ankara, Turkey, 2015.

10. Demirezer, L.O., Ozenver, N., Bodur, M., Yerdelen, K.O., Yukselen, O., Guvenalp, Z., Sezerman, O.U. Molecular Docking of Anthranoids on Some Targeted Human Proteins; Rapid Natural Drug Discovery. 8th International Symposium on Computational Methods in Toxicology and Pharmacology Integrating Internet Resources, Chios Island, Greece, 2015.

11. Demirezer L.O., Ozenver, N., Bodur, M., Yerdelen, K.O., Guvenalp, Z. Determination of Phytoestrogenic Potential of Anthranoids by Molecular Docking Studies. 8th International Symposium on Computational Methods in Toxicology and Pharmacology Integrating Internet Resources, Chios Island, Greece, 2015.

12. Ozenver, N., Demirezer, L.O. Supression of Diabetic Retinopathy Formation via Alpha-Amylase and Glucosidase Inhibition Potential of *Rumex acetosella* L. Fourth International Meeting on Pharmacy & Pharmaceutical Sciences

(IMPPS-4), Istanbul, Turkey, 2014.

13. Ozenver, N., Sarikaya, M., Evcimen, N., Guvenalp, Z., Kuruuzum-Uz, A., Demirezer, L.O. *In silico* and *in vitro* researches of some anthraquinone compounds on alpha amylase and aldose reductase targets. Trends in Natural Products Research A Young Scientists Meeting in Olomouc, Czech Republic, 2014.

14. Ozenver, N., Sarikaya, M., Evcimen, N., Guvenalp, Z., Kuruuzum-Uz, A., Demirezer, L.O. Alpha amylase and aldose reductase inhibitory effect of *Rheum ribes* L. Trends in Natural Products Research A Young Scientists Meeting in Olomouc, Czech Republic, 2014.

15. Demirezer, L.O., Sezerman, U., Ozenver, N., Bodur, M., Yukselen, O., Kuruuzum-Uz, A. *In-silico* Docking Researches of Some Human Proteins with Anthranoids GA, Münster, Germany, 2013.

Project

1. *Rumex* türleri üzerinde fitokimyasal ve biyolojik aktivite çalışmaları (researcher), Hacettepe University Scientific Research Projects Coordination Unit, Project code: 014D01301003-485.

Scholarships

1. The Scientific and Technological Research Council of Turkey (TUBİTAK) 2211-C Scholarship Programme.

2. The Scientific and Technological Research Council of Turkey (TUBİTAK) 2214-A Scholarship Programme.